ACTA CHIMICA

ACADEMIAE SCIENTIARUM HUNGARICAE

ADIUVANTIBUS

L. ERDEY, K. POLINSZKY, G. SCHAY

AC

R. BOGNÁR, GY. BRUCKNER, Z. CSŰRÖS, T. ERDEY-GRÚZ, Z. FÖLDI, M. FREUND, Á. GERECS, GY. HARDY, J. HOLLÓ, M. KORACH, F. MÁRTA, F. NAGY, E. PUNGOR, Z. SZABÓ, P. TÉTÉNYI, L. VARGHA, K. VAS

REDIGIT

B. LENGYEL

TOMUS 59 FASCICULUS 1

AKADÉMIAI KIADÓ, BUDAPEST

1969

ACTA CHIM. ACAD. SCI. HUNG.

ACTA CHIMICA

A MAGYAR TUDOMÁNYOS AKADÉMIA KÉMIAI TUDOMÁNYOK OSZTÁLYÁNAK IDEGEN NYELVŰ KÖZLEMÉNYEI

SZERKESZTI

LENGYEL BÉLA

TECHNIKAI SZERKESZTŐK

DEÁK GYULA és HARASZTHY-PAPP MELINDA

Az Acta Chimica német, angol, francia és orosz nyelven közöl értekezéseket a kémiai tudományok köréből.

Az Acta Chimica változó terjedelmű füzetekben jelenik meg, egy-egy kötet négy füzetből áll. Évente átlag négy kötet jelenik meg.

A közlésre szánt kéziratok a szerkesztőség címére (Budapest 112/91 Műegyetem) küldendők.

Ugyanerre a címre küldendő minden szerkesztőségi levelezés. A szerkesztőség kéziratokat nem ad vissza.

Az Acta Chimica előfizetési ára kötetenként belföldre 120 Ft, külföldre 165 Ft. Megrendelhető a belföld számára az „Akadémiai Kiadó"-nál (Budapest V., Alkotmány utca 21. Bankszámla 05-915-111-46), a külföld számára pedig a „Kultúra" Könyv- és Hírlap Külkereskedelmi Vállalatnál (Budapest I., Fő utca 32. Bankszámla: 43-790-057-181) vagy annak külföldi képviseleteinél és bizományosainál.

Die Acta Chimica veröffentlichen Abhandlungen aus dem Bereiche der chemischen Wissenschaften in deutscher, englischer, französischer und russischer Sprache.

Die Acta Chimica erscheinen in Heften wechselnden Umfanges. Vier Hefte bilden einen Band. Jährlich erscheinen 4 Bände.

Die zur Veröffentlichung bestimmten Manuskripte sind an folgende Adresse zu senden:

Acta Chimica
Budapest 112/91 Műegyetem

An die gleiche Anschrift ist auch jede für die Redaktion bestimmte Korrespondenz zu richten.

Abonnementspreis pro Band: 165 Forint. Bestellbar bei dem Buch- und Zeitungs-Außenhandels-Unternehmen »*Kultúra*« (Budapest I., Fő utca 32. Bankkonto No. 43-790-057-181) oder bei seinen Auslandsvertretungen und Kommissionären.

ACTA CHIMICA

ACADEMIAE SCIENTIARUM HUNGARICAE

ADIUVANTIBUS

L. ERDEY, K. POLINSZKY, G. SCHAY

AC

R. BOGNÁR, GY. BRUCKNER, Z. CSŰRÖS, T. ERDEY-GRÚZ, Z. FÖLDI, M. FREUND, Á. GERECS, GY. HARDY, J. HOLLÓ, M. KORACH, F. MÁRTA, F. NAGY, E. PUNGOR, Z. SZABÓ, P. TÉTÉNYI, L. VARGHA, K. VAS

REDIGIT

B. LENGYEL

TOMUS 59

AKADÉMIAI KIADÓ, BUDAPEST

1969

ACTA CHIMICA

TOMUS 59

Fasciculus 1: 1969

Fasciculus 2: 1969

Fasciculi 3 — 4: 1969

INDEX

ALKONYI, I. und SÁNDOR, A.: Darstellung und Eigenschaften von δ-Oxogeraniumsäure. (The Preparation and Properties of δ-ketogeranic Acid) 397

AMBRÓ, I., FLÓRA, T. and BIRÓ, T.: Investigation of the Thermal Stability of the Resins VARION CH, Containing Imino Diacetic Acid Groups 249

BAJUSZ, S. s. MEDZIHRADSZKY, K.

BARTÓK, M. s. MOLNÁR, A.

BÁLINT-AMBRÓ, I.: The Dissociation of Varion CH Ion Exchange Resin 67

BÁNFI, D. s. ENGLER, R.

BEYER, H. s. FEJES, P.

BÉKÁSSY, S. and NÓGRÁDI, M.: Application of Gas-Liquid Chromatography to the Structural Elucidation of Natural Flavones 425

BIRÓ, T. s. AMBRÓ, I.

BOGNÁR, R., MAKLEIT, S. and MILE, T.: Conversions of Tosyl and Mesyl Derivatives of the Morphine Group. Synthesis of Acetylmercapto and Mercapto Derivatives. (Preliminary Communication) 161

BOGNÁR, R. and MAKLEIT, S.: Conversions of Tosyl and Mesyl Derivatives of the Morphine Group, III. Preparation of Azido- and Aminocodides 373

BOGNÁR, R., MAKLEIT, S. and MILE, T.: Conversions of Tosyl and Mesyl Derivatives of the Morphine Group, IV. Preparation of Azido- and Amidomorphides 379

BOGNÁR, R. s. MAKLEIT, S.

BOGNÁR, R. s. FARKAS, I.

Book Reviews 431

BÓR, G. s. VIZI-OROSZ, A.

BURGER, K. s. VÉRTES, A.

CYVIN, S. J. and VIZI, B.: Mean Amplitudes of Vibration for Diborane and Deuterodiborane 85

CSÁKVÁRI, B., JENEI, S., KNAUSZ, D. and MESZTICZKY, A.: The Reaction of Dichlorogallane with Ethyl Halides (Preliminary Communication) 225

CSŰRÖS, Z., DEÁK, GY., HARASZTHY-PAPP, M. and HOFFMANN, I.: Reactions Catalyzed by Strong Acids in Non-aqueous Media, II. The Sulphuric Acid and Boron Trifluoride Catalyzed Reaction of Aromatic Aldehydes with Aryl Acetonitriles Leading to Arylidene-bis Aryl Acetamide 119

CSŰRÖS, Z., DEÁK, GY., FENICHEL, L. and TÖRÖK-KALMÁR, A.: Nitration in the Presence of Boron Fluoride Catalyst 401

DEÁK, GY. s. CSŰRÖS, Z.

EGYED, C. L. s. VÉRTES, A.

ENGLER, J., BÁNFI, D. and HAJÓS, A.: Phenylethanolamine Derivatives, I. ^{14}C-Labeling of 1-(*m*-Aminophenyl)-2-Cyclopropyl-Aminoethanol Dihydrochloride, a Monoaminooxidase Blocking Agent 411

FARKAS, I., SZABÓ, I. F. und BOGNÁR, R.: Abbau und Reaktionen von Onsäureaziden, II. Ausdehnung der Curtius-Reaktion auf das Octaacetyl-Cellobionsäureazid. (Decomposition and Reactions of Onic Acid Azides, II. Extension of the Curtius Reaction to Octaacetylcellobionic Acid Azide) 419

FEJES, P. und BEYER, H.: Anwendungsmöglichkeiten mathematischer Verfahren zur Bestimmung von Geschwindigkeitskonstanten komplexer, heterogen-katalytischer Prozesse, unter Benutzung von elektronischen Rechenmaschinen, II. Prinzip und Anwendung der Gradientenmethode zur Auswertung kinetischer Versuchsergebnisse (On the possible application of mathematical Methods for the Determination of Rate Constants of Complex, Heterogeneous Catalytic Chemical Processes under Utilisation of Electronic Computers, II. Principles and Application of the Gradient Method for the Evaluation of Experimental Kinetic Data) 23

FENICHEL, L. s. CSŰRÖS, Z.

FÁY, L. s. MÜLLER, I.

FLÓRA, T. s. AMBRÓ, I.

GERGELY, A.: Equilibria of α-Amino Acid Complexes of Transition Metal Ions, I. Complexes of Glycine 309

GEYER, R. und ROTERMUND, U.: Oszillopolarographische Untersuchungen zinnorganischer Verbindungen. (Oscillopolarographic Investigation of Organotin Compounds) ... 201

GEYER, R. s. HENZE, G.

HAJÓS, A. s. ENGLER, J.

HARASZTHY-PAPP, M. s. CSŰRÖS, Z.

HARGITTAI, I.: Study of the Molecular Structure of Thionyl Chloride by the Electron Diffraction Sector Microphotometer Method 351

HENZE, G., GEYER, R. und HOLZBAUER, R.: Coulometrische Kobalttitration. (Cobalt Titration by Coulometry) 297

HOFFMANN, I. s. CSŰRÖS, Z.

HOLZBAUER, R. s. HENZE, G.

HUBAY, R. s. ZSADON, B.

HUN, GY. s. TÖRÖK, B.

ILLÉS, V.: The Pyrolysis of Gaseous Hydrocarbons, I. Kinetics of the Thermal Decomposition of *n*-Butane 35

ILLÉS, V.: The Pyrolysis of Gaseous Hydrocarbons, II. The Mechanism of the Thermal Decomposition of *n*-Butane 229

JENEI, S. s. CSÁKVÁRI, B.

KELEN, T. und TÜDŐS, F.: Kinetische Analyse einiger Folgereaktionen, III. Das konkurrente Folgereaktionssystem $A + A \rightarrow C$, $A + C \rightarrow E$. (Kinetical Discussion of a Few Consecutive Reactions, III. The Concurrent Consecutive Reaction System $A + A \rightarrow C$, $A + C \rightarrow E$) 323

KISFALUDY, L., PATTHY, A. and LŐW, M.: A Beta-elimination Reaction between Cysteine Derivatives Containing Free SH Group and Dicyclohexylcarbodiimide (Short Communication) 159

KNAUSZ, D. s. CSÁKVÁRI, B.

KOVÁCS, K. s. MOLNÁR, A.

KÖRMENDY, K. s. MÜLLER, A.

LÁNG, ZS. s. MEDZIHRADSZKY, K.

LŐW, M. s. KISFALUDY, L.

MAKLEIT, S. s. BOGNÁR, R.

MAKLEIT, S. and BOGNÁR, R.: Conversions of Tosyl and Mesyl Derivatives of the Morphine Group, V. A new Method for the Preparation of Isocodeine and Dihydroisocodeine (Short Communication) 387

MARKÓ, L.: Sulphur-containing Metal Carbonyls, X. Reactions of Cobalt Carbonyls with Aliphatic Thioethers and the Influence of Thioethers on the Catalytic Activity of Cobalt Carbonyls 389

MARKÓ, L. s. VIZI-OROSZ, A.

MEDZIHRADSZKY, K., BAJUSZ, S., S. VARGHA, H. und LÁNG, Zs.: Synthese des biologisch aktiven Fragments des β-lipotropen Hormons. (Vorläufige Mitteilung) (Synthesis of the Biologically Active Fragment of the β-lipotrophic Hormone).... 165

MESZTICKY, A. s. CSÁKVÁRI, B.

MILE, T. s. BOGNÁR, R.

MOLNÁR, A., BARTÓK, M. and KOVÁCS, K.: The Chemistry of 1,3-Bi-functional Compounds, II. Study of the Decomposition of the Quaternary Salts of 1,3-Aminoalcohols.... 133

MOHAI, M. s. VADOS, I.

MÜLLER, A., KÖRMENDY, K., RUFF, F. and VAJDA, M.: Ultraviolet Spectroscopic Investigation of Some 1-Hydroxyanthraquinons-9-monoimines 109

MÜLLER, A., KÖRMENDY, K., RUFF, F., SOHÁR, P. and VAJDA, M.: Infrared Spectroscopic Study of the Structure of 1-Hydroxy-anthraquinone-9-monoimines..... 99

MÜLLER, L.: The Adsorption of Uranium Hexafluoride, I..... 1

MÜLLER, L. and FÁY, L.: The Adsorption of Uranium Hexafluoride, II. Transport Processes in the Sorption of Uranium Hexafluoride 181

MÜLLER, L.: The Adsorption of Uranium Hexafluoride, III. 277

NAGY, F., SZABÓ, S. and TELCS, I.: Palladized Pd-Wire as a Hydrogenation Catalyst, I. Rate and Mechanism of Hydrogen Transport..... 359

NEMES, L.: Harmonic Force Field Refinement Calculations for Polyatomic Molecules, III. Normal Coordinate Analysis of the e" Species of Cyclopropane..... 75

NÓGRÁDI, M. s. BÉKÁSSY, S.

PAPP-MOLNÁR, E. s. VÉRTES, A.

PATTHY, A. s. KISFALUDY, L.

PUNGOR, E. s. WESER, A.

ROTERMUND, U. s. GEYER, R.

RUFF, F. s. MÜLLER, A.

SÁNDOR, A. s. ALKONYI, I.

SIMON, F.: Investigation of the Molecular Weight Distribution of Polyalkylmethacrylates by Adsorption Chromatography 57

SOHÁR, P. s. MÜLLER, A.

SZABÓ, S. s. NAGY, F.

SZABÓ, I. F. s. FARKAS, I.

TARNÓCZI, T. s. VÉRTES, A.

TELCS, I.: Kinetics of Hydrogen Adsorption on Platinum and Palladium Electrodes, II. The Volmer Reaction 263

TELCS, I. and JÁKY, M.: Kinetics of Hydrogen Adsorption on Platinum and Palladium Electrodes, III. The Tafel Reaction 271

TELCS, I. s. NAGY, F.

TÖRÖK, F. and HUN, GY.: On the Parameter Form of Force Constant Matrix, VIII. Calculation of all Mean Amplitudes of Vibration Compatible with the Normal Frequencies 303

TÖRÖK-KALMÁR, A. s. CSŰRÖS, Z.

TÜDŐS, E. s. KELEN, T.

ÚJHELYI, Cs.: On Solvolysis of "Alkylpyrophosphoric Acid Metal Solvent Extractants" 211

UPOR, E. s. VADOS, I.

VADOS, I., MOHAI, M. and UPOR, E.: Determination of Tantalum in Rocks by Neutron Activation Analysis 171

VAJDA, M. s. MÜLLER, A.

VARGHA, H. S. s. MEDZIHRADSZKY, K.

VÉRTES, A., BURGER, K., TARNÓCZI, T., PAPP-MOLNÁR, E. and EGYED, C. L.: On the Mössbauer Investigation and Magnetic Behaviour of Iron(III) Diethyldithiocarbamate (Short Communication) 15

VÉRTES, A., TARNÓCZI, T., EGYED, C. L., PAPP-MOLNÁR, E. and BURGER, K.: On the Mössbauer Investigation and Magnetic Behaviour of a few Iron(II) Complexes (Short Communication) 19

VIZI, B. and CYVIN, S. J.: Tentatively Standardized Symmetry Coordinates of Polyatomic Molecules, VIII. 91

VIZI-OROSZ, A., BÓR, G. and MARKÓ, L.: Preparation of Lead Cobalt Carbonyl and its Triphenylphosphine Derivative (Preliminary Note) 417

WESER, A. und PUNGOR, E.: Die Eignung von Perowskitphasen als Redoxindikatorelektroden. (On the Use of Perowskite Phases as Redox Indicator Electrodes) (Kurzmitteilung) 319

ZSADON, B., HUBAY, R.: On the Alkaloids of Amsonia Tabernaemontana Walt., cultivated in Hungary (Preliminary Communication) 157

Acta Chimica Academiae Scientiarum Hungaricae, Tomus 59 (1), pp. 1—13 (1969)

THE ADSORPTION OF URANIUM HEXAFLUORIDE, I

L. MÜLLER

(Mecsek Ore Mining Enterprise, Pécs)

Received December 21, 1967

The reversible sorption of uranium hexafluoride as adsorbate was measured on metal and plastics adsorbents.

The isotherms characterizing the examined pairs of adsorbent—adsorbate were established for the investigated adsorbents in the temperature range between 0 and 100 °C. It was found that the isotherms belong in all the cases to type I, and that they can be adequately described by the Freundlich isotherm equation in the domain which is of importance from the aspect of our further investigations.

It was attempted to describe the reversible equilibrium process of solid—gas systems with the aid of the available adsorption theories. The emerged difficulties which are unsurmountable from certain aspects are due of two reasons. On the one hand, the polymolecular adsorption mechanism which takes place on the surface of small-surface, unconventional and in respect of the energetical conditions of adsorption gases inhomogeneous adsorbents cannot be treated in a way analogous to the simplified methods evolved for conventional adsorbents. On the other hand, uranium hexafluoride as an adsorbate is a quite particular substance from the aspect of its macroscopic and molecular properties, and thus, not only the description of the adsorbed layer but also the determination of the fundamental physical constants (such as the surface requirement of the molecule) proved to be rather difficult.

The production of nuclear power sets steadily increasing requirements to the industry producing fissile materials in that greater amounts of power supplies prepared at possibly low costs are needed. However, during the operations in producing fissile materials, the physical adsorption process has not been utilized so far.

In the present series of papers, the results of researches into the adsorption of uranium hexafluoride (UF_6) are being summarized.

Sorption equilibrium of uranium hexafluoride on solid adsorbents

The adsorption transport processes of a solid—gas system lead in every case to a dynamical equilibrium. To study the operational adsorption unit, the primary concern is a thorough investigation of the equilibrium state.

The survey of the literature on adsorption equilibria (adsorption isotherms, isotherm equations) will be omitted here. It must be noted, however, that literature published up to about 1950 has been critically reviewed by BRUNAUER [1]. The Russian edition of this book supplemented by the results attained by the Russian research teams in the field of adsorption [2] is worth mentioning. A survey of the literature on equilibrium studies of the last 15 years is to be found in the papers of YOUNG and CROWELL [3], and of SZÉKELY [4].

In the investigations of the equilibrium of systems uranium hexafluoride—adsorbent those sorption theories are utilized which, according to our present knowledge, proved to be the most suitable ones for describing equilibrium data. Namely, the data of our measurements will be fitted to several adsorption theories. This is indispensable since, owing to the peculiar features of uranium hexafluoride as an adsorbate, special adsorbents (such as metals and plastics of small surface) are needed.

The field of application and the domains (pressure, temperature) of validity of the adsorption theories are rather well known for the conventional substances of the adsorption techniques applied in the industry (active carbon, silica gel etc., hydrocarbons, alcohols and solvents), and on the basis of preliminary considerations neither of the known theories could be preferred in the case of the systems investigated by us. However, on comparing the data of our measurements with several adsorption theories, the causes were examined which limited the validity of a given theory. In this way, with the aid of "negative proofs", it was attempted to obtain a fair view of the phenomena which take place at the interaction of a given pair of adsorbent—adsorbate.

The sorption processes of uranium hexafluoride are being investigated since more than two decades. The sorption of uranium hexafluoride on graphite and various active carbon preparations was examined by MAIRE *et al.* [5] who found that under low pressures and in the case of a slow sorption (on dosing the adsorbate in minute amounts), a reversible physical adsorption takes place on the surface. Under higher pressures ($P > 10$ Torr), in turn, the surface of the adsorbent undergoes "deformation" with the consequence that the adsorbate is bound irreversibly.

According to WILSON and SCHUMANN [6], the irreversible adsorption on carbon is due to the fact that traces of moisture are always retained by the surface of carbon. In the reaction of water with uranium hexafluoride, the latter undergoes decomposition, the formed fluorine and hydrogen fluoride react with carbon, converting this latter into carbon tetrafluoride.

However, this explanation is unsatisfactory, and contradicts to the experimental results of MAIRE.

The sorption of uranium hexafluoride on the surface of inorganic salts and oxides was studied by COLVIN and FORKOS [7, 8]. It was proved that uranium hexafluoride is bound by physical adsorption to the surfaces of calcium sulphate, calcium fluoride and alumina, though certain portions of the adsorbate (the amount of which depends on the purity of uranium hexafluoride and on the structure of the adsorbent, respectively) cannot be desorbed.

The mechanism of the binding of uranium hexafluoride on the surface of sodium fluoride has been cleared up by GATHERS and JOLLEY [9, 10] who claimed that complex formation took place on the surface. On raising the

temperature, the equilibrium pressure of uranium hexafluoride increases. Thus, at higher temperatures, the complex can be quantitatively decomposed. This effect has been utilized in a number of industrial processes for the preparation of fissile materials.

Description of the experimental equipment

In order to plot the isotherms, an equipment has been constructed to meet the requirements specified for operations with uranium hexafluoride.

1. *Measurement of the equilibrium pressure of the adsorbate*

Owing to the corrosive effect of uranium hexafluoride, no mechanical pressure meter or liquid manometer can be attached to the instrument. The equilibrium pressure corresponding to the single points of the isotherm curve is maintained by thermostating the adsorbate at a temperature calculated from the tension data of uranium hexafluoride. The equilibrium pressure of the adsorbate is checked with an α-chamber attached to the instrument.

2. *Determination of the adsorbed amount of substance*

The substances selected on the basis of the preliminary experiments at the surface of which the adsorption of uranium hexafluoride proved to be of an undoubtedly reversible process belonged all to the group of adsorbents of low specific surface (from 1 to 20 sq.m per gram). Owing to the nature of the applied adsorbate, the gas volumetric and gravimetric methods used conventionally to the isotherms of small-surface substances could not be applied. Thus, on establishing the isotherms, the equilibrium concentrations were determined by α-activity measurements.

3. *Preparation of uranium hexafluoride for establishing the isotherms*

Since uranium hexafluoride is rapidly decomposing on air and being extremely hazardous from the viewpoint of radiation biology, it should be transferred from the container through a pipeline under high vacuum directly into the separator of the measuring system, where the traces of HF are removed. Since the adsorbate is transferred and purified solely by varying the temperature of the container, of the measuring system and of the separator, completely excluding the effect of the atmosphere, the method seems to be well applicable for the preparation of readily decomposing radioactive substances for various physico-chemical measurements.

The scheme of the equipment is shown in Fig. 1.

The adsorption isotherms are measured as follows:

Container *(1)* containing uranium hexafluoride is heated to 60—70 °C, the experimental equipment is exposed to high vacuum, and separator *(3)* is cooled to —30 °C. On opening needle valve *(2)*, uranium hexafluoride condensates in the separator. After about 10 to 15 g of uranium hexafluoride condensated in the separator, valve *(2)* is closed, and the traces of HF present in the crystalline substance are removed by means of high vacuum. Small amounts of uranium hexafluoride were recovered by evaporates, and introduced into a soda-lime trap.

The adequately prepared adsorbent is placed into the adsorbent flasks *(8)*, thermostated to the required temperature, and the flasks are exposed to vacuum through tap *(6)*. The thermostate jacket of the separator *(3)* is adjusted to the temperature at which the tension of uranium hexafluoride attains the desired equilibrium pressure. After closing tap *(6)*, taps *(5, 9* and *7)* are opened, exposing thus the instrument to the required uranium hexafluoride pressure. The equilibrium pressure of uranium hexafluoride is measured by an ionization chamber *(10)*. Prior to the measurement the ionization chamber (Type DB-59) is filled with argon of 300 Torr pressure.

By varying the pressure of uranium hexafluoride in the adsorbent flasks, adsorbent samples in equilibrium with the given pressure are obtained.

By opening tap *(7)*, nitrogen gas saturated with ethanol vapours is introduced into the adsorbent flasks; uranium hexafluoride in gas phase is decomposed and rinsed off the system, by the gas stream. In order to determine the amount of adsorbate bound irreversibly to the surface, preparations are made from the saturated adsorbent samples and their activity was measured with an α-scintillator. The equilibrium amounts of adsorbed substance were calculated using preparations of known activity.

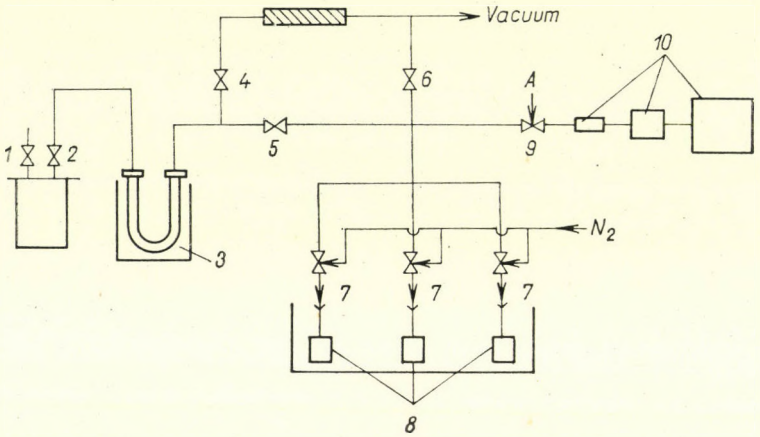


Fig. 1. Instrument for the measurement of adsorption isotherms

Preliminary investigations

For our experiments adsorbents binding uranium hexafluoride by reversible physical adsorption were needed. The following materials were tested:

1. Molecular sieves: Linde A5, Linde X13, NEVIKI 50KX
2. Adsorbents with a silicate skeleton: Silica gel with large pores, TCC catalyst, TCC coated with nickel
3. Active carbons: Nuxit BO, Nuxit AL
4. Metal catalysts: Nickel catalyst, Copper catalyst
5. Plastics foams: Polystyrene foam, Polyethylene foam, Teflon FO9 foam
6. Inorganic salts, oxides: Calcium fluoride, Alumina

The above classification of the adsorbents is quite arbitrary. It appears to be more favourable to divide them into a group of large-surface industrial adsorbents and a group of small-surface (1 to 20 sq.m per gram) adsorbents of high chemical resistance.

In our preliminary tests, the isotherms were established at 20 °C; adsorption and desorption isotherms were plotted separately. Sorption processes taking place on the surface of adsorbents were regarded as reversible ones when the adsorption and desorption isotherms, respectively, showed identical shapes, and when the points of the adsorption and desorption isotherms pertaining to $p = 0$ coincided.

Metal catalysts

In our earlier papers, the corrosion of uranium hexafluoride on various metals has been reported. The results of these investigations turned our attention to nickel and copper.

Nickel adsorbents denoted as Ni I and Ni II were prepared as follows.

Adsorbent Ni I [11]: From a hot solution of nickel nitrate, nickel hydroxide was precipitated by adding ammonium hydroxide. Nickel hydroxide was dried and reduced at 350 °C in a hydrogen current. The product had a specific surface of 18 sq.m per gram. A fraction of grain size adequate for our measurement was separated by sieving.

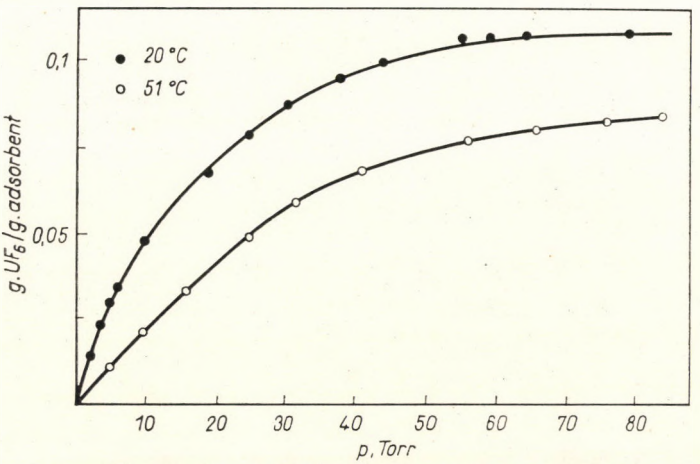


Fig. 2. Adsorption isotherms on adsorbent Ni I

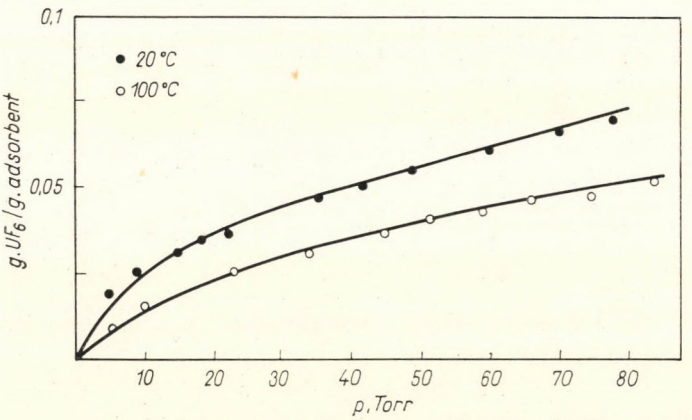


Fig. 3. Adsorption isotherms on adsorbent Ni II

Adsorbent Ni II: Nickel carbonate (A. R.) was ignited at 600 °C to oxide. Subsequently, nickel oxide was reduced at 350 °C in a hydrogen current. The adsorbent had a specific surface of 10 sq.m per gram.

Physical adsorption was measured also on the adsorbents Cu I and Cu II [11].

Adsorbent Cu I was prepared by the method specified for the adsorbent Ni I. The product had a specific surface of 3—4 sq.m per gram.

Cu II was prepared by activating "Cuprum metall reductum" (Reanal) at 350 °C in a hydrogen current. The specific surface of this adsorbent ranged from 2 to 3 sq.m per gram.

The isotherms established using adsorbents Ni I, Ni II, Cu I and Cu II are presented in Figs 2 to 5.

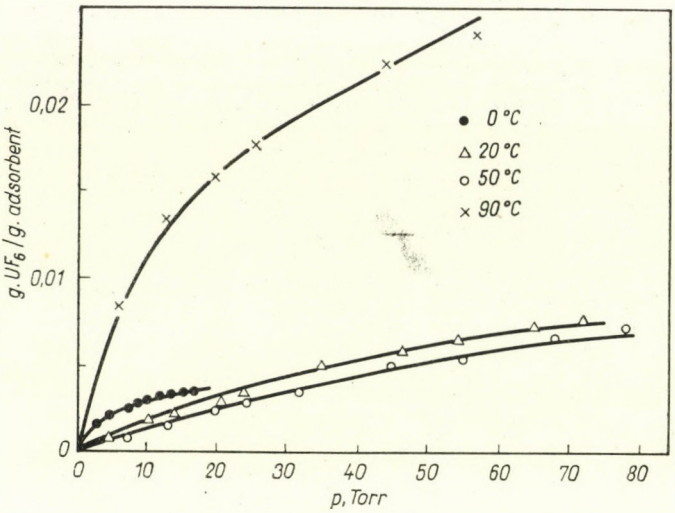


Fig. 4. Adsorption isotherms on adsorbent Cu I

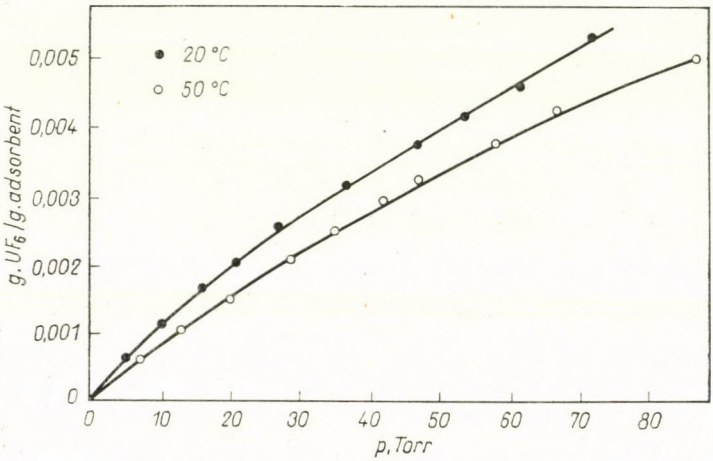


Fig. 5. Adsorption isotherms on adsorbent Cu II

Plastics adsorbents

Measurements were carried out with two different plastics foams.

Polyethylene plastics foam was prepared as follows. A solution of polyethylene in hot benzene was rapidly cooled and the solvent was removed by means of a vacuum pump. From the porous, granular substance obtained after the quickly performed suction a fraction of 0.5 to 0.1 mm grain size (amounting to about 30—40 per cent of the total quantity) was separated by sieving. The specific surface of the product varied from 15 to 30 sq.m per gram.

Fluoporak FO9 type polytetrafluoroethylenefoam was made available by the Central Research Institute for Chemistry of the Hungarian Academy of Sciences. The teflon foam had a specific surface of 1.5—2.0 sq.m per gram.

Reversible physical adsorption was measured on the surface of the polyethylene foam type Pth and of the teflon foam type FO9. The plotted isotherms are shown in Figs 6 and 7.

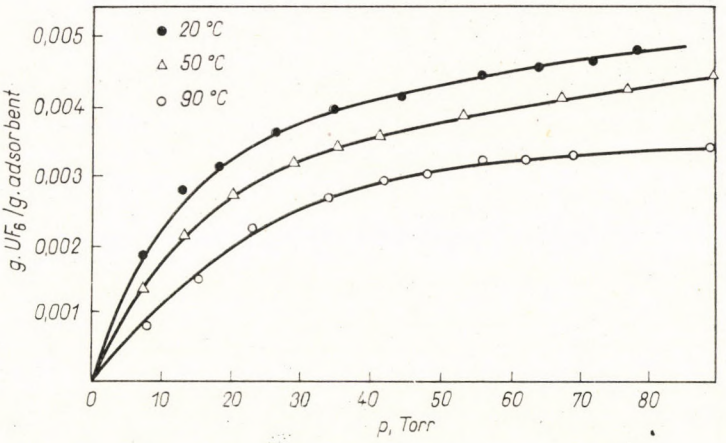


Fig. 6. Adsorption isotherms on adsorbent FO9

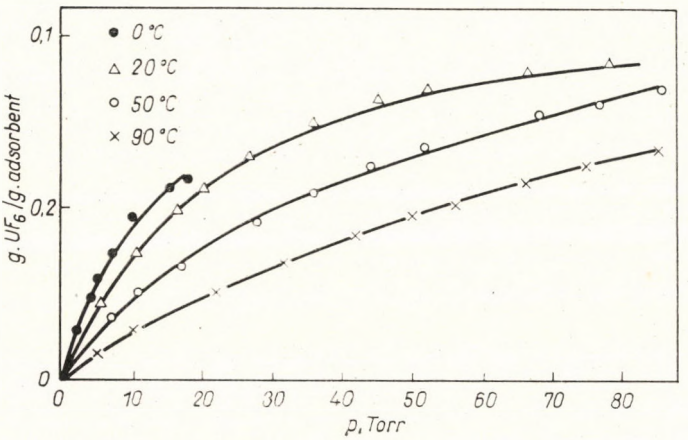


Fig. 7. Adsorption isotherms on adsorbent Pth

Discussion

The adsorption isotherms of uranium hexafluoride measured at various temperatures belong to type I.

The dependence on temperature of the isotherms established using nickel adsorbents and their comparison with known theoretical correlations appeared to be unequivocal.

This is not the case, however, with the copper adsorbents. It can be seen in Fig. 4 that the isotherm measured at 90 °C has a shape appreciably differing from that of equilibrium curves measured at lower temperatures. This is due to the activation of the adsorbent prior to measurement. Namely, it was

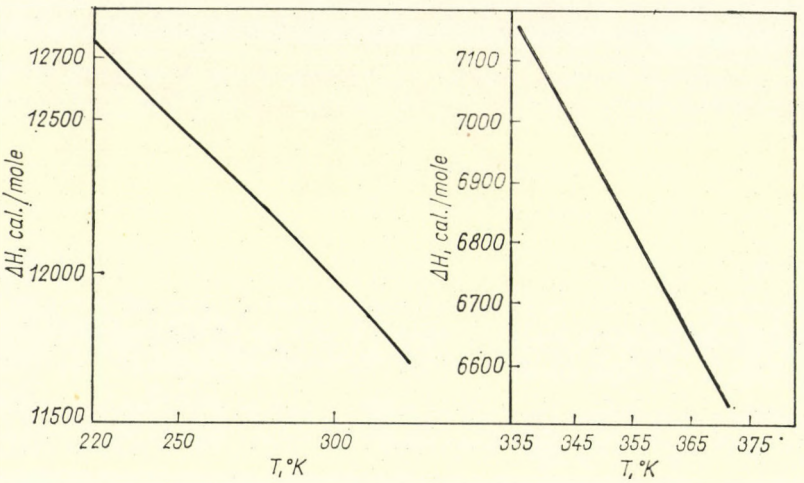


Fig. 8. Heats of sublimation and heats of evaporation of uranium hexafluoride plotted against temperature

Table I

Specific surfaces of the adsorbents

Adsorbent	Denotation	Specific surface sq.m per gram
Ni adsorbent	Ni I	18
	Ni II	10
Copper adsorbent	Cu I	3—4
	Cu II	2—3
Polyethylene foam	Pth	15—20
Polytetrafluoroethylene	FO9	1.5—2.0

found that in the case of copper adsorbents higher specific surfaces were obtained when, at temperatures above 60 °C, the surface was previously coated with the adsorbate measurements. This was proved by our control tests and also by the visually observable changes of the surface of adsorbent. In the activation period, only a small fraction of the total amount of adsorbed substance (not exceeding 1 per cent) was bound to the surface, having practically no influence on the experimental results.

From the shape of the isotherms established on plastics foams it can be concluded that a physical adsorption takes place. The surface of polyethylene foam is discoloured during the adsorption process.

It was found that a part of uranium hexafluoride adsorbed on the surface of plastics (not more than 0.5 per cent) is reduced to UF_5 and U_2F_9, respec-

tively. This process is due to the fact that on preparing the adsorbate, owing to the rapid removal of solvent, certain amounts of benzene are still retained in the inside of pore walls. These solvent traces undergo reaction with the adsorbate and lead to the decomposition of the latter [12].

This presumption is supported also by the observation that decomposition of a small extent takes place when the adsorbent is durably pretreated in high vacuum (at 100 °C). However, our attempts to eliminate this process by a prolonged treatment in high vacuum failed.

The obtained isotherms will be discussed here with the use of the Freundlich, Langmuir, BET and Dubinin equations and theories.

Domains of validity of the isotherm equations

The constants of the Freundlich, Langmuir and BET equations were determined graphically. The obtained data are listed in Table II.

Table II

Constants of equations calculated for various temperatures

Adsorbent type	Temperature, °C	Freundlich		Langmuir		BET	
		m	k	v_m	b	$v_m \cdot 10^3$	c
Ni I	4	0.960	$6.03 \cdot 10^{-3}$	0.1818	$0.234 \cdot 10^{-1}$	79.20	2.882
	20	0.608	$1.09 \cdot 10^{-2}$	0.1293	$0.593 \cdot 10^{-1}$	27.12	24.32
	50	0.842	$2.08 \cdot 10^{-2}$	0.1293	$0.234 \cdot 10^{-1}$	45.14	158.14
Ni II	20	0.457	$7.00 \cdot 10^{-3}$	0.0809	$0.494 \cdot 10^{-1}$	66.82	14.96
	100	0.508	$5.30 \cdot 10^{-3}$	0.0679	$0.278 \cdot 10^{-1}$	87.43	2.386
Cu I	0	0.506	$9.00 \cdot 10^{-4}$	$0.449 \cdot 10^{-2}$	0.1713	0.100	—
	20	0.683	$4.15 \cdot 10^{-4}$	0.0160	0.0120	3.467	6.343
	50	0.860	$1.81 \cdot 10^{-4}$	0.0290	0.0042	14.856	9.335
	90	0.420	$4.44 \cdot 10^{-4}$	0.0395	0.0337	30.933	132.15
Cu II	20	0.800	$1.79 \cdot 10^{-4}$	0.0156	0.00745	2.724	4.128
	50	0.880	$1.13 \cdot 10^{-4}$	0.0126	0.00661	9.241	5.610
Pth	6	0.710	$8.61 \cdot 10^{-3}$	0.0883	0.0944	51.95	5.23
	20	0.610	$8.20 \cdot 10^{-3}$	0.1113	0.0561	41.48	19.93
	50	0.616	$5.98 \cdot 10^{-3}$	0.1400	0.0219	92.75	17.62
	90	0.727	$2.54 \cdot 10^{-3}$	0.1333	0.0112	128.18	28.37
FO9	20	0.380	$1.00 \cdot 10^{-4}$	0.00547	0.0731	2.19	1.67
	50	0.480	$6.12 \cdot 10^{-4}$	0.00588	0.0459	4.11	1.59
	90	0.647	$2.60 \cdot 10^{-4}$	0.00414	0.0503	3.83	2.13

In the examined temperature range between 0.1 and 0.8 relative pressures, the measured values could be adequately described by the Freundlich isotherm equation. The deviation between the measured points and the theoretical data calculated by the isotherm equation did not exceed 5 per cent.

For the applicability of the Freundlich isotherm equation in a so wide interval the properties of the adsorbents must be responsible. In connection with the Freundlich isotherm which is generally considered as an empirical correlation, it was claimed by a number of authors that in the case of an adsorption on an inhomogeneous surface when the adsorption energy vs. density plot is exponential, the use of the Freundlich isotherm is also theoretically justified [18].

Since in the case of the examined adsorbents possessing small-surface inhomogeneous adsorption centres, it appears from the plots of heat of adsorption against surface coatedness calculated from the isobars that the presumed exponential function of energy against density is with a fair approximation correct, we attempted to find a correlation between the constants of the Freundlich equation of isotherms and the calculated data of sorption heats, utilizing TÓTH's analysis [19] of the Freundlich equation of isotherms. The comparison of the calculated values with the measured points does not afford any possibilities to draw unequivocal conclusions. This is due, in addition to the simplifications to be discussed later in detail, to the fact that the Freundlich equation as an empirical correlation lends itself well to the description of isotherms of type I.

It is impossible, however, to decide unequivocally the range of theoretical validity of the equation for a given pair of adsorbent—adsorbate.

The Langmuir equation of isotherms is suitable for the description of the experimental data in the range of 0.20—0.45 relative pressures. On taking into account the simplifying presumptions applied on deriving the Langmuir equation, *i.e.* monomolecular adsorption, energetically homogeneous surface, it is quite understandable why the validity of the equation is limited to a relatively narrow pressure range.

It is characteristic that in the case of the small-surface adsorbent FO9 of nearly uniform nature, the obtained value v_m may be considered as invariant in respect of temperature while in the case of the adsorbent Cu I of greater surface and an appreciable inhomogeneity, v_m changes in function of isotherm temperature, and also the availability of the value v_m determined for a given temperature is limited to a range of about 0.3 relative pressure.

The BET equation is unsuitable for the description of the measured isotherms. On carrying out the conventional linearization, a curve which was convex in respect of the pressure axle has been obtained. The v_m values calculated at various temperatures from the slope of the straight fitting best to the linearized BET curve and listed in the table, pertain, depending on the

experimental conditions, to different relative pressures, and show significant deviations from each other.

The unsuitability of the BET equation for the description of the experimental data can be attributed to the following causes.

1. A fundamental presumption of the BET equation is that the formation of the adsorbed phase in the first layer is a dynamical equilibrium process characterizable by the heat of adsorption while in the consecutive layers by the heat of condensation. On the examined adsorbents the energetical conditions of sorption are much more complicated.

2. The inhomogeneity of the surface is not taken into account in the BET equation.

On applying *A*, *B* and *C* equations of DUBININ for the description of the experimental data, the following statements can be made.

a) The *A* equation of DUBININ, a correlation derived by presuming a microporous adsorbent, is suitable for the description of the isotherm data in a narrow pressure range. This range does not exceed the domain of 0.3 relative pressure.

b) The *B* equation of DUBININ, a correlation derived for macroporous adsorbents, proved to be unsuitable for describing the experimental isotherms.

c) The *C* equation of DUBININ derived for adsorbent with mixed pore size described well the measured data.

As already mentioned in the introduction of that paper, our aim set to study the operational model of the adsorbent systems of uranium hexafluoride. Up to the present, equilibrium systems of uranium hexafluoride : adsorbent were investigated and adsorbents were chosen on which the sorption is reversible. It was found that the isotherms belong to type I, and that they can be described relatively well by the Freundlich isotherm equation.

In order to further elucidate the properties of the adsorbed phase, the differential values of heats of adsorption were calculated from the isotherms. The results are presented in Table III. The heats of phase change were calculated by means of the correlations given by KIRSHENBAUM [13], [14], WEINSTOCK *et al.* [15], BRAUNE *et al.* [16] and SIMON [17], affording the following data (see Fig. 8):

$$\Delta H_{evap.} = 2473.4 + 14.476 \cdot T - 0.390\ T^2 + 987670 \cdot T^{-1} \text{ cal/mole}$$

$$\Delta H_{subl.} = 20400 - 0.00521 \cdot T^3 + 0.3905\ T^2 - 98.66\ T$$

On comparing the data of Table III with the values of the heat of phase change, it appears that

$$[\Delta H] \text{ phase change} > [\Delta H] \text{ ads.}$$

Table III

Heat of adsorption and surface coatedness

Ni I		Ni II		Cu I		Cu II
Adsorbed amount, g of UF_6/g	Heat of sorption, cal/mole	Adsorbed amount, g of UF_6/g	Heat of sorption, cal/mole	Adsorbed amount, g of UF_6/g	Heat of sorption, cal/mole	Adsorbed amount, g of UF_6/g
0.01	7804.8	0.005	3763.6	0.002	4856.6	0.0005
0.02	7628.8	0.01	—	0.004	3801.8	0.0010
0.03	7561.2	0.015	3657.2	0.006	2905.4	0.0015
0.04	7467.8	0.02	3106.4	0.008	2378.4	0.0020
0.05	6579.3	0.025	2655.2	0.010	1891.1	0.0025
0.06	5887.7	0.030	2149.1	0.012	1628.7	0.0030
0.07	5784.8	0.035	1947.3	0.014	1194.4	0.0035
0.08	—	0.040	1831.1	0.016	1122.1	0.0040
		0.045	1761.1			0.0045
		0.050	1748.9			0.0050

Estimations based on the values of heat of adsorption calculated from the isotherms can be considered as orientative data. On taking into account the specific surface of adsorbents and calculating the surface requirement of the adsorbate molecule uranium hexafluoride from the saturation values of the isotherms established at 20 °C, the following data are obtained:

Ni I	10 Å^2
Ni II	10
Cu I	100
Cu II	50
Pth	10
FO9	25

It is quite clear from the above values that the isotherms cannot be interpreted in a simple way: the adsorption by the adsorbents Ni I, Ni II and Pth is by far not monomolecular but in the average a layer of the thickness of free molecules is formed. (The surface requirement of uranium hexafluoride is, calculated from the solid density, about 25—30 Å, but the real value is likely to be higher.)

List of symbols

a	=	adsorbed amount of substance,	g/g
p	=	equilibrium pressure,	Torr
p_0	=	equilibrium tension	Torr
T	=	temperature	°K

Cu II	FO9		Pth		CaF_2	
Heat of sorption, cal/mole	Adsorbed amount, g of UF_6/g	Heat of sorption, cal/mole	Adsorbed amount, g of UF_6/g	Heat of sorption, cal/mole	Adsorbed amount, g of UF_6/g	Heat of sorption, cal/mole
3223.8	0.0005	4322.1	0.01	5823.5	0.005	8586.2
2690.8	0.0010	3848.8	0.02	5700.1	0.010	7768.8
2197.7	0.0015	3611.9	0.03	5454.9	0.015	6550.3
1963.1	0.0020	3540.5	0.04	5368.2	0.020	6247.4
1919.8	0.0025	3480.1	0.05	5040.7	0.025	5400.6
1820.7	0.0030	3400.0	0.06	4776.9	0.030	4720.2
1768.3	0.0035	3370.0	0.07	4719.7	0.035	4062.3
1645.2	0.0040	3347.9	0.08	4460.1		
1552.5	0.0045	3255.1				
1168.3						

REFERENCES

1. Brunauer, S.: The Adsorption of Gases and Vapors. Princeton, 1954.
2. Brunauer, S.: Adsorpciya gazov i parov. Moscow, 1948.
3. Young Crowell: Physical Adsorption of Gases. London, 1962.
4. Székely, Gy.: A gőz-adszorpció mechanizmusáról (On the mechanism of vapour adsorption). Thesis 1963, Budapest.
5. Maire, J.: A (Conf. 15) P/326. 1958. Geneva.
6. Wilson, T., Schumann, S.: Kellex Corp. KZ 5585. 1946.
7. Colvin, W.: Union Carbide Co. Publ. No. 12315.
8. Forkos, J.: Wak Ridge Gaseous Diffusion Plant A 3604 Z. 1945.
9. Chaters, G.: Nucl. Sci. Eng. **2,** 768 (1957).
10. Chaters, G., Jolley, R.: Ind. Eng. Chem. **50,** 1709 (1958).
11. Tétényi, P., Király, J.: Magyar Kém. Foly. **64,** 439 (1958).
12. Katz, Rabinovich: Chemistry of Uranium. Vol. 1. p. 354.
13. Kirshenbaum, I.: Report A-753, 1943, from SAM.
14. Abstract from Report A 763, from SAB.
15. Weinstock, B., Weaver, E.: J. Inorg. Nucl. Chem. **11,** 104 (1959).
16. Braune, H., Pinnow, P.: Z. physik. Chem. **B-35,** 239 (1937).
17. Simon, F.: Report B 55. Mar. 1942.
18. Langmuir, I.: J. Amer. Chem. Soc. **40,** 1361 (1918); Zeldowitsch, J.: J. Acta Physicochim. URSS **1,** 961 (1934); Baly, E.: Proc. Roy. Soc. **A 160,** 465 (1937); Roginskii, S.: Acad. Sci. URSS **45,** 61 (1944); Roginskii, S.: Acad. Sci. URSS **45,** 194 (1944); Roginskii, S.: Acta Physicochim. URSS **21,** 519 (1946); Temkin, M., Pyzhev, V.: Acta Physicochim. URSS **12,** 327 (1940); Roginskii, S.: Adsorption and Catalysis on Heterogeneous Surfaces. Akad. Nauk. USSR, Moscow, 1949; Roginskii, S. *et al.*: Izvest. Akad. Nauk USSR, Otdel. Khim. Nauk. **59,** (1952); Halsey, G., Taylor, H.: J. Chem. Phys. **15,** 624 (1947); Fowler, R.: Statistical Mechanics. Cambridge Univ. Press, 1936; Halsey, G.: J. Chem. Phys. **16,** 935 (1948); Sips, R.: J. Chem. Phys. **18,** 1024 (1950).
19. Tóth, J.: Magyar Kém. Foly. **66,** 213, 398, 431 (1960).

László Müller; Pécs III. Páfrány u. 47, Hungary

Acta Chimica Academiae Scientiarum Hungaricae, Tomus 59 (1), pp. 15—18 (1969)

ON THE MÖSSBAUER INVESTIGATION AND MAGNETIC BEHAVIOUR OF IRON(III) DIETHYLDITHIOCARBAMATE

(SHORT COMMUNICATION)

A. VÉRTES,* K. BURGER,** T. TARNÓCZI,*** E. PAPP-MOLNÁR** and C. L. EGYED***

(Institute for Physical Chemistry and Radiology of the Loránd Eötvös University, Budapest; Institute for Inorganic and Analytical Chemistry of the Loránd Eötvös University, Budapest**; Central Research Institute for Physics of the Hungarian Academy of Sciences, Budapest***)*

Received March 27, 1968

In the investigation of the magnetic properties of several iron(III) dithiocarbamate complexes, CAMBI *et al.* [1, 2] showed the magnetic moment of the complexes to be influenced considerably by the substituents of the ligand. The magnetic moment of the complexes was decreased also by cooling. Recent investigations of WHITE *et al.* [3, 4] verified the findings of CAMBI, and explained the phenomenon by assuming that a thermal equilibrium is established in the complex between low spin and high spin iron(III) atom. Mössbauer investigations of WICKMAN and TROZZOLO [5] did not substantiate this interpretation, while data of FRANK and ABELEDO [6] seem to be consistent. Though these authors do not give the changes of the Mössbauer spectrum in function of temperature, they find that the exchange of the substituent changes both the magnetic moment and the Mössbauer spectrum of the complex. However, a spectrum indicating the simultaneous presence of iron in two kinds of electron configuration has not been found even in the case of complexes of medium magnetic moment. Therefore, their investigations cannot be considered as such unambiguous solution of the problem, as *e.g.* the Mössbauer investigation of the high spin → low spin transformation of iron(II) phenanthroline thiocyanate mixed complexes [7].

To complement published data, the Mössbauer spectrum of iron(II) diethyldithiocarbamate was recorded at liquid nitrogen temperature and the temperature dependence of the magnetic moment of the complex was measured in the temperature range from −193 to 40 °C. For comparison, also the magnetic behaviour of Fe(III) diisopropyl dithiophosphate, possessing a similar co-ordination sphere as the diethyldithiocarbamate complex, has been investigated.

The dependence of the reciprocal magnetic susceptibility on temperature of the dithiocarbamate complex is shown in Fig. 1. It can be seen from the diagram and from the values of calculated magnetic moment that the

magnetic moment is dependent on temperature (at 116 °K 2.54 B.M., at 311 °K 4.42 B.M.), while the diisopropyl dithiophosphate complex strictly follows the Curie law (Fig. 2). Its magnetic moment is 5.97 B.M., corresponding to the spin-only value of the high spin iron(III) atom (5.92 B.M.).

Values of the Mössbauer parameters of the diethyldithiocarbamate complex at the temperature of liquid air (Fig. 3) are: isomer shift 0.53 mm/sec

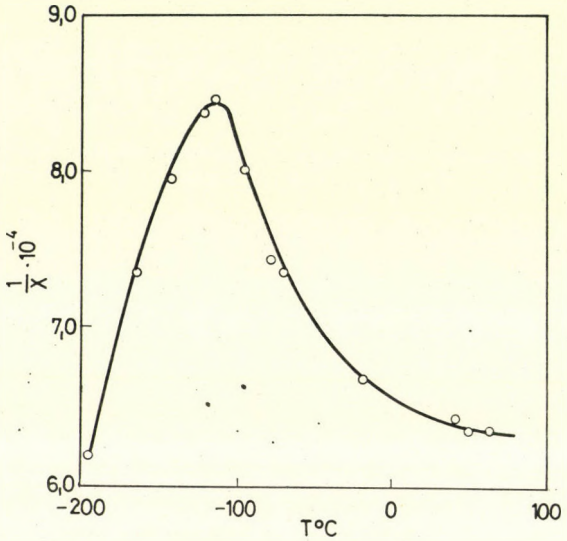


Fig. 1. Temperatrure dependence of the reciprocal magnetic susceptibility of iron(III) diethyldithiocarbamate

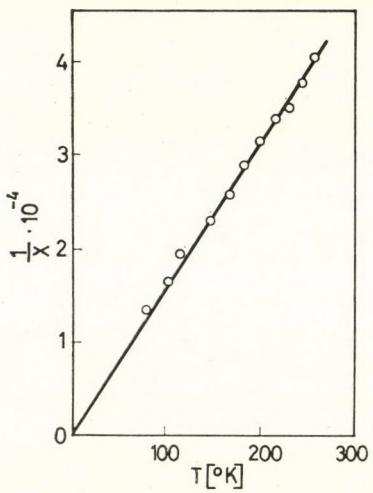


Fig. 2. Temperature dependence of the reciprocal magnetic susceptibility of iron(III) diisopropyl dithiophosphate

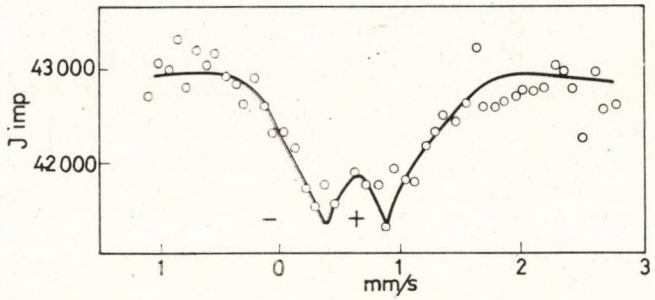


Fig. 3. Mössbauer spectrum of iron(III) diethyldithiocarbamate

quadrupole splitting 0.53 mm/sec. On comparing this latter values with the quadrupole splitting measured by FRANK and ABELEDO [6] at room temperature (0.25 mm/sec), it can be seen that quadrupole splitting is increased substantially on cooling. A comparison of the isomer shift with that of iron diisopropyl dithiophosphate (0.62 mm/sec) [8] shows the former complex to be more covalent.

Thus, our investigations showed the iron(III) diisopropyldithiophosphate complex to possess a high spin electron configuration throughout the whole temperature interval. The anomalous magnetic behaviour of iron(III) diethyldithiocarbamate can be ascribed presumably to an equilibrium of high spin and low spin electron structures. Cooling shifts the equilibrium towards the low spin electron structure. The higher value of quadrupole splitting at low temperatures is caused by the transformation of the nearly spherical symmetrical electron configuration $t_{2g}^3 e_g^2$, predominant at room temperature, cooling into t_{2g}^5 electron configuration of higher field gradient. It is a natural phenomenon that the covalency of low spin complexes (with strong ligand field) is greater than that of high spin complexes (with weak ligand field).

Experimental part

Magnetic susceptibilities were determined by the Faraday method. Essentially, this is based on the measurement of force, acting on the sample in inhomogeneous magnetic field. The advantage of this method over the Gouy method, which is also often used, is that it requires a considerably smaller quantity of material and, moreover, it can be used also for the investigations of substances, the magnetic susceptibility of which is dependent on the applied field.

For the measurements an automatic vacuum balance Model DAM B-60, and an electromagnet manufactured by KFKI have been used [9].

The sensitivity and accuracy of the balance was ± 0.05 mg, and the strength of the magnetic field applied 10^4 Oe. Pd of spectroscopical purity was used as standard.

When using a sample of 50 mg, the relative measuring error for a susceptibility of $5 \cdot 10^{-6}$ e.m.u/g, or greater, was ± 1.6 per cent, while reproducibility was ± 0.8 per cent.

Mössbauer spectra were recorded on a Mössbauer spectrometer connected to a multichannel analyser, described in a previous publication [10]. A Co-57 isotope, diffused in stain

less steel, was used as radiation source. The line width of the source, measured with $K_4Fe(CN)_6$ as adsorber, was 0.4 mm/sec. Absolute measuring error was ± 0.05 mm/sec.

*

The authors thank Mrs. L. SUBA for her conscientious work in carrying out the measurements.

REFERENCES

1. CAMBI, L., SZEGŐ, L.: Chem. Ber. **64,** 2591 (1931); **66,** 2067 (1937).
2. CAMBI, L., MALATESK, L.: Chem. Ber. **70,** 2067 (1937).
3. WHITE, A. H., KOKOT, E., ROPER, R., WATERMANN, H., MARTIN, R. L.: Austral. J. Chem. **17,** 294 (1964).
4. EWALD, A. H., MARTIN, R. L., ROSS, I. G., WHITE, A. H.: Proc. Roy. Soc. (London) A **280,** 235 (1964).
5. WICKEMAN, H. H., TROZZOLO, A. M.: Phys. Rev. Letters **15,** 156 (1965).
6. FRANK, E., ABELEDO, C. R.: Inorg. Chem. **5,** 1453 (1966).
7. DÉZSI, I., MOLNÁR, B., TARNÓCZI, T., TOMPA, K.: J. Inorg. Nucl. Chem. **28,** 1001 (1966).
8. KORECZ, L., BURGER, K., JÖRGENSEN, C. K.: Helv. Chim. Acta **51,** 211 (1968).
9. PÁL, L., TARNÓCZI, T., ZSIGMOND, GY.: under print.
10. BURGER, K., VÉRTES, A., PAPP-MOLNÁR E.: Acta Chim. Acad. Sci. Hung. **57,** 257 (1968).

Attila VÉRTES
Kálmán BURGER
Tivadar TARNÓCZI
Etelka PAPP-MOLNÁR
C. László EGYED

Budapest VIII. Múzeum krt. 4/b

Acta Chimica Academiae Scientiarum Hungaricae, Tomus 59 (1), pp. 19—22 (1969)

ON THE MÖSSBAUER INVESTIGATION AND MAGNETIC BEHAVIOUR OF A FEW IRON(II) COMPLEXES

(SHORT COMMUNICATION)

A. VÉRTES,* T. TARNÓCZI,*** C. L. EGYED,*** E. PAPP-MOLNÁR** and K. BURGER**

*(*Institute for Physical Chemistry and Radiology of the Loránd Eötvös University, Budapest; **Institute for Inorganic and Analytical Chemistry of the Loránd Eötvös University, Budapest; ***Central Research Institute for Physics of the Hung. Acad. Sci.)*

Received March 27, 1968

It is well known that in the Mössbauer spectra of high spin ($t_{2g}^4 e_g^2$) iron(II) compounds the great electric field gradient at the iron nucleus, produced by *d* electrons, results in a strong quadrupole splitting. Depending on the covalency and symmetry of the iron(II) compound, the (ΔE) value of quadrupole splitting ranges generally between 1.6 and 3.6 mm/sec, while the isomer shift (δ) changes depending on covalency between 1.2 and 1.6 mm/sec.* In our earlier investigations, we found in the Mössbauer spectra of several high spin iron(II) complexes lower values for the Mössbauer parameters than those mentioned above, *i.e.* 0.4—1.6 mm/sec for ΔE, and 0.4—1.0 mm/sec for δ[1]. Since this phenomenon was met only with iron(II) complexes having ligands of π-acceptor ability, its appearance was interpreted by back-coordination, resulting in a metal → ligand electron transfer [1]. Back-coordination may effect the transformation of the $t_{2g}^4 e_g^2$ electron configuration of the central atom into an almost spherical-symmetrical electron configuration $t_{2g}^3 e_g^2$, similar to that of high spin iron(II) atom. Such transformation results in a considerable decrease of the field gradient at the iron nucleus. This may be one of the causes of the lower values in quadrupole splitting.

The anomalous Mössbauer spectrum may be produced also by other effects. The possibility that the smaller quadrupole splitting is caused by the oxidation of the central atom, was excluded by the measurement of the magnetic moment of the complexes at room temperature. However, owing to the low Debye temperature of the complexes, Mössbauer measurements had to be undertaken at liquid air temperature. Thus, the possibility that cooling caused those changes in the electron structure of the central iron(II) atom which resulted in the anomalous Mössbauer spectrum, could not be excluded. Such change is to be expected for example as a result of high spin → low spin electron structure transformation. To clear this problem, the magnetic susceptibility of the

* Referred to cobalt-57 source, diffused in stainless steel.

complexes iron(II) salicylaldoxime, iron(II) thionalide and iron(II) malonate was determined in the temperature range from −193 °C to 20 °C (Fig. 1). Mössbauer spectra of the complexes, recorded at the temperature of liquid air, are shown in Figs 2—4.

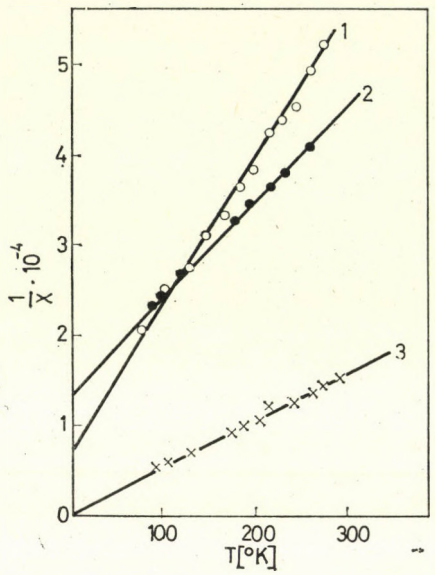


Fig. 1. Temperature dependence of the reciprocal magnetic susceptibility of iron(II) thionalide *(1)*, iron(II) salicylaldoxime *(2)* and iron(II) malonate *(3)*

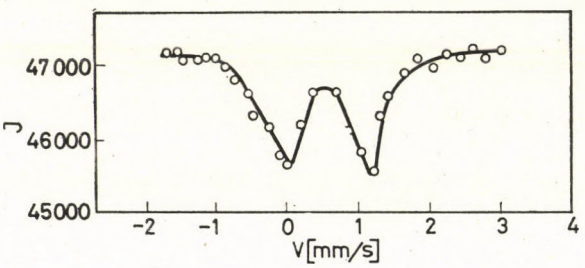


Fig. 2. Mössbauer spectrum of iron(II) salicylaldoxime at the temperature of liquid air

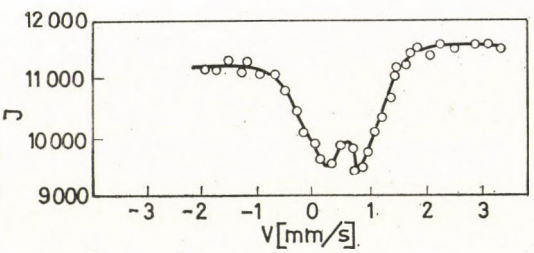


Fig. 3. Mössbauer spectrum of iron(II) thionalide at the temperature of liquid air

It can be seen from Fig. 1 that cooling did not produce any change in the number of unpaired electrons. Magnetic moments calculated from the measured magnetic susceptibilities [iron(II) salicylaldoxime: 5.19 B.M.; iron(II) thionalide: 4.94 B.M.; iron(II) malonate: 4.88 B.M.], indicated the presence of high spin iron(II) central atoms in all three complexes. [The spin only value for 4 unpaired electrons, characteristic of iron(II), is 4.90 B.M., while for 5 unpaired

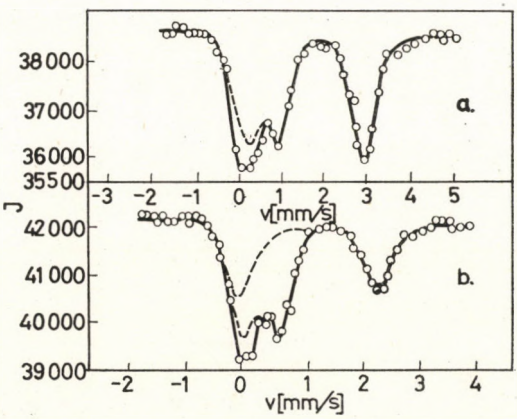


Fig. 4. Mössbauer spectra of iron(II) malonate *(a)* at the temperature of liquid air, *(b)* atroom temperature

electrons, characteristic of iron(III), 5.92 B.M.]. The Mössbauer parameters of iron(II) salicylaldoxime ($\delta = 0.68$ mm/sec, $\Delta E = 1.4$ mm/sec) and of iron(II) thionalide ($\delta = 0.52$ mm/sec, $\Delta E = 0.54$ mm/sec) correspond approximately to an electron configuration $t_{2g}^3 e_g^2$, while the Mössbauer spectrum of iron(II) malonate ($\delta = 1.78$ mm/sec, $\Delta E = 2.70$ mm/sec) refers to configuration $t_{2g}^4 e_g^2$.*

As mentioned earlier, a change in spin number caused by the decrease in temperature must be excluded for all the three complexes on the basis of magnetic measurements. Therefore, the Mössbauer parameters of iron(II) salicylaldoxime and iron(II) thionalide can be explained only by back-coordination. This is in agreement with the circumstance that the molecular structure of these two

* The above values of the Mössbauer parameters were measured at liquid air temperature. However, in the case of iron(II) malonate, the Mössbauer spectrum was recorded also at room temperature (Fig. 4b), to give the following values: $\delta = 1.35$ mm/s, $\Delta E = 2.53$ mm/s. It should be mentioned that a spectrum indicative of the presence of an iron(III) compound is superponed on the spectrum of iron(II) malonate (see Figs 4a and 4b). Presumably, this is due to the fact that in a few hours elapsing between the preparation of iron(II) malonate and the measurement a part of the substance was oxidized by air. This assumption was substantiated by the finding that in the spectrum recorded at room temperature — taken about 4 hours after the measurement at low temperature — the intensity of that part of the spectrum, which was characteristic of iron(III) compounds, increased as compared to the previous measurement. Actually, the Mössbauer spectrum, of a three-day-old sample indicated only the presence of the iron(III) compound (Fig. 5). Parameters measured for this compound at room temperature were: $\delta = 0.56$ mm/s, $\Delta E = 0.56$ mm/s.

compounds permits a back-coordination (in the case of salicylaldoxime to the N=C antibonding orbitals and in that of thionalide to the empty d_π orbitals of the donor sulfur atom). In the case of iron(II) malonate, there exists no possibility for back-coordination.

Instruments used for the measurements were described in an earlier publication [2]. Magnetic susceptibility was determined by the Faraday method.

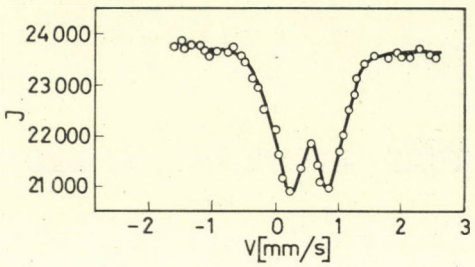


Fig. 5. Mössbauer spectrum of oxidized iron(II) malonate at room temperature

When using a sample of a mass of 50 mg, for susceptibilities of $5 \cdot 10^{-6}$ e.m.u./g or more, the relative measuring error was $\pm$ 1.6 per cent, while reproducibility was $\pm$ 0.8 per cent.

In the recording of the Mössbauer spectra, cobalt-57, diffused into stainless steel was used as radiation source. The absolute error in Mössbauer parameters was $\pm$ 0.05 mm/sec.

*

The authors wish to thank Mrs. L. SUBA for her conscientious work.

REFERENCES

1. BURGER, K., KORECZ, L., MANAUBA, I. B. A., MAG, P.: J. Inorg. Nucl. Chem. **28,** 1673 (1966).
2. VÉRTES, A., BURGER, K., TARNÓCZI, T., PAPP-MOLNÁR, E.: Acta Chim. Acad. Sci. Hung. **59,** 59, 15 (1969)

Attila VÉRTES
Tivadar TARNÓCZI
C. László EGYED
Etelka PAPP-MOLNÁR
Kálmán BURGER
Budapest VIII. Múzeum krt. 4/b

Acta Chimica Academiae Scientiarum Hungaricae Tomus 59 (1), pp. 23—33 (1969)

ANWENDUNGSMÖGLICHKEITEN MATHEMATISCHER VERFAHREN ZUR BESTIMMUNG VON GESCHWINDIGKEITSKONSTANTEN KOMPLEXER, HETEROGEN-KATALYTISCHER PROZESSE UNTER BENUTZUNG VON ELEKTRONISCHEN RECHENMASCHINEN, II

PRINZIP UND ANWENDUNG DER GRADIENTENMETHODE ZUR AUSWERTUNG KINETISCHER VERSUCHSERGEBNISSE

P. FEJES und H. BEYER

(Zentralforschungsinstitut für Chemie der Ungarischen Akademie der Wissenschaften, Budapest)

Eingegangen am 20. Januar 1968

Nach kurzer Darstellung der grundlegenden Prinzipien der Gradientenmethode, insbesondere der Wahl der Fehler- bzw. Zielfunktion, wird anhand einer hypothetischen katalytischen Modellreaktion des Typs $A \rightleftharpoons B$ erörtert, auf welche Weise dieses Rechenverfahren, bei Kenntnis des Reaktionsmechanismus, die Geschwindigkeitskonstanten der einzelnen Teilschritte eines katalytischen Prozesses und experimentell nicht zu bestimmende Größen (z. B. Oberflächenkonzentrationen und Anzahl der freien Sorptionszentren im Verlaufe der Reaktion) zu optimalisieren gestattet. Die Eindeutigkeit der so erhaltenen Ergebnisse wird diskutiert. Die Leistungsfähigkeit der Methode wird anhand von Ergebnissen derartiger für die gewählte Modellreaktion und die *n*-Butenisomerisierung durchgeführten Optimalisierungen von — vorläufig allerdings nur zwei — freien Parametern (Geschwindigkeitskonstanten) demonstriert.

Die in der vorangegangenen Mitteilung [1] behandelte Methode der kleinsten Fehlerquadrate ist nicht anwendbar, wenn die Differentialgleichung bzw. das Differentialgleichungssystem unmittelbar nicht zu bestimmende Größen (wie z. B. Oberflächenbedeckungen, Anzahl der aktiven Zentren usw.) enthält. In solchen Fällen muß zur Lösung der Aufgabe von einem sich von der Methode der kleinsten Fehlerquadrate grundsätzlich unterscheidenden, Gradienten-Methode genannten Optimalisierungsverfahren [2] Gebrauch gemacht werden, das bei Einführung geeigneter Zielfunktionen auch auf kinetische Messungen anwendbar ist.

a) Prinzip der kinetischen Aufgaben angepaßten Gradientenmethode

Es ist bekannt, daß eine Funktion von zwei unabhängigen Veränderlichen

$$z = f(x,y),$$

die in einem bestimmten Bereich der x,y-Koordinaten definiert ist, im dreidimensionalen Koordinatensystem eine Fläche darstellt. Diese Fläche kann

für ein gegebenes Wertesystem $\{C_i\}$, mit Hilfe der Kurven $C_i = f(x,y)$ bzw. $y = g(x,C_i)$, auf der x,y-Ebene in Form von Niveaulinien dargestellt werden. Es ist allgemein bekannt, daß der Gradientenvektor grad f auf der x,y-Ebene die Richtung der am ausgewählten Punkt senkrecht zu den Niveaulinien verlaufenden sog. orthogonalen Trajektorie angibt. Bei entsprechender Wahl des Vorzeichens erreicht man beim Schreiten entlang grad f früher oder später ein — eventuell nur lokales — Minimum der Fläche $z = f(x,y)$.

Wir nehmen, um beim einfachsten Fall zu bleiben, eine Geschwindigkeitsgleichung der Gestalt

$$\frac{dy}{dx} = f(x, y; k_1, k_2)$$

an. Die den Anfangsbedingungen gerecht werdende Lösungsfunktion sei

$$y = g(x; k_1, k_2).$$

An experimentellen Ergebnissen soll die Konversionskurve

$$\bar{y} = \bar{g}(x)$$

zur Verfügung stehen.

Die Abweichung $\varrho(y,\bar{y})$ zwischen y und $\bar{y}$ in einem gegebenen Intervall der unabhängigen Variablen $[x_1, x_p]$ definieren wir durch

$$\varrho(y,\bar{y}) = \int_{x_1}^{x_p} | g(x; k_1, k_2) - \bar{g}(x) | \, dx$$

oder, da es rechentechnische Vorteile mit sich bringt, durch

$$\varrho(y,\bar{y}) = \| y - \bar{y} \| = \left(\int_{x_1}^{x_p} | y - \bar{y} |^2 \, dx \right)^{\frac{1}{2}}$$

wobei das Symbol $\| y - \bar{y} \|$ für die Norm der Differenz von zwei im L_2 Funktionsraum definierten Funktionen verwendet wird.

Führen wir nun eine Fehlerfunktion $H = H[\varrho(y,\bar{y})] = H(k_1, k_2)$ ein, von der wir bestimmte Eigenschaften fordern (Monotonie, Eindeutigkeit), so ist offensichtlich, daß die Optimalisierung der Funktion $H(k_1, k_2)$ im obigen Sinne durchgeführt werden kann.

Wenn es gelingt, ein solches Rechenverfahren auszuarbeiten, bei dem die, von einem Anfangswert $\mathbf{k}_0$ des Vektors $\mathbf{k}$

$$\mathbf{k} = \left\| \begin{matrix} k_1 \\ k_2 \end{matrix} \right\|$$

ausgehend, nacheinander gebildeten Differenzenvektoren gleich oder annähernd gleich der Gradientenrichtung sind

$$\mathbf{k}_j - \mathbf{k}_{j-1} \cong \operatorname{grad} H,$$

so führt die Berechnung in mehreren Schritten zu einem k*-Vektor, mit dessen Komponenten k_1^* und k_2^*, die die unbekannten Geschwindigkeitskonstanten sind, die Fehlerfunktion $H = H[\varrho(y,\bar{y})]$ ein Minimum erreicht.

Es ist zweckmäßig, die Definition

$$H = \varrho(y, \bar{y})$$

zu verwenden, da dann nämlich nach einem bekannten Satz aus der Bedingung

$$H = \varrho(y,\bar{y}) = 0 = \int_{x_1}^{x_p} | g(x; k_1^*, k_2^*) - \bar{g}(x) | \, dx$$

für die im Argument des Integrals stehende stetige Funktion die Identität

$$\left.\begin{array}{r} | g(x; k_1^*, k_2^*) - \bar{g}(x) \equiv 0 \\ \text{bzw.} \\ g(x; k_1^*, k_2^*) \equiv \bar{g}(x) \end{array}\right\} (x_1 \leq x \leq x_p)$$

folgt.

Diese Definition der Fehler- bzw. Zielfunktion bringt den weiteren Vorteil mit sich, daß die Minima der Fläche $H = \varrho(y,\bar{y}) = H(k_1, k_2)$ bedeutend flacher und Höhenunterschiede weniger schroff sind, als bei anderen (z. B. $H = \log [\varrho(y,\bar{y})]$), und deshalb zur Minimalisierung der Zielfunktion weniger Schritte ausgeführt werden müssen.

Aus dem Vorangegangenen geht nicht deutlich hervor, in welcher Hinsicht die Gradientenmethode gegenüber der Methode der kleinsten Fehlerquadrate wesentliche und prinzipiell neue Wege eröffnende Fortschritte mit sich bringen kann. Diese Frage soll anhand eines Modells, nämlich einer nach der für katalytische Prozesse denkbar einfachsten Reaktionsgleichung

$$A \rightleftharpoons B$$

verlaufenden hypothetischen Reaktion, erörtert werden, an dem auch die Leistungsfähigkeit unserer Programme getestet wurde.

Nach einer Reaktionsgleichung dieses einfachsten Typs verlaufen ausschließlich Isomerisierungen, z. B. die Umlagerung von Cyclopropan in Propylen [3]

$$\begin{array}{c} CH_2 \\ \diagup \quad \diagdown \\ CH_2 - CH_2 \end{array} \longrightarrow CH_3 - CH = CH_2$$

oder die reversible katalytische Isomerisierung von Methylacetylen zu Propadien [4]

$$CH_3 - C \equiv CH \rightleftharpoons CH_2 = C = CH_2 .$$

Bei allen diesen Reaktionen muß man natürlich annehmen, daß der Reaktionsablauf in einer Reihe elementarer Schritte erfolgt, wobei auch die mit X bezeichnete Anzahl der aktiven Zentren des Katalysators eine Rolle spielt. Folgende Vorstellungen über den Reaktionsmechanismus sollen dem zu untersuchenden Modell zugrunde liegen:

Der erste Teilschritt der katalytischen Umwandlung sei die Sorption der Komponente A an den aktiven Zentren nach

$$A + X \underset{\overleftarrow{k_A}}{\overset{\overrightarrow{k_A}}{\rightleftharpoons}} (A)_a ,$$

wobei $(A)_a$ das Symbol für die sorbierte Komponente A ist. Darauf soll die Oberflächenreaktion

$$(A)_a \underset{\overleftarrow{k}}{\overset{\overrightarrow{k}}{\rightleftharpoons}} (B)_a$$

folgen. Der letzte Schritt sei die Desorption der sorbierten Komponente $(B)_a$ unter Rückbildung der freien aktiven Zentren

$$(B_a) \underset{\overleftarrow{k_B}}{\overset{\overrightarrow{k_B}}{\rightleftharpoons}} B + X.$$

Werden für die abhängigen Variablen die Symbole

$y_1(x)$ = Molenzahl der Komponente A in der Gasphase

$y_2(x)$ = Molenzahl der Komponente A in der Sorptionsphase

$y_3(x)$ = Molenzahl der Komponente B in der Gasphase

$y_4(x)$ = Molenzahl der Komponente B in der Sorptionsphase

$y_5(x)$ = Molenzahl der freien aktiven Zentren X des Katalysators und für die Zeit das Symbol x eingeführt, so ist für eine nach diesem Mechanismus in einem geschlossenen System (z. B. in einer Zirkulationsapparatur) ablau-

fende katalytische Reaktion folgendes Differentialgleichungssystem aufzustellen:

$$\begin{aligned}
\frac{dy_1}{dx} &= -\vec{k}_A y_1 y_5 + \overleftarrow{k}_A y_2 \\
\frac{dy_2}{dx} &= \vec{k}_A y_1 y_5 - (\overleftarrow{k}_A + \vec{k}) y_2 + \overleftarrow{k} y_4 \\
\frac{dy_3}{dx} &= \vec{k}_B y_4 - \overleftarrow{k}_B y_3 y_5 \qquad (1) \\
\frac{dy_4}{dx} &= \overleftarrow{k}_B y_3 y_5 - (\vec{k}_B + \overleftarrow{k}) y_4 + \vec{k} y_2 \\
\frac{dy_5}{dx} &= \frac{dy_1}{dx} + \frac{dy_3}{dx}
\end{aligned}$$

Wenn keine zu Vereinfachungen dieses Differentialgleichungssystems führenden Annahmen gemacht werden können, so kann, wie ohne weiteres ersichtlich ist, das aus 5 nichtlinearen Gleichungen bestehende System mit analytischen Methoden nicht gelöst werden. Eine weitere Schwierigkeit besteht darin, daß von den 5 abhängigen Veränderlichen nur die Molenzahlen des Ausgangsstoffes A und des Endproduktes B in der Gasphase experimentell bestimmt werden können und somit auch nur die Ableitungen dieser Variablen nach der Zeit dy_1/dx und dy_3/dx zur Verfügung stehen. Dieser Umstand schließt die Anwendung der Methode der kleinsten Fehlerquadrate aus, da für diese die Kenntnis des Kurvenverlaufs aller Variablen unbedingte Voraussetzung ist, stellt jedoch kein prinzipielles Hindernis für die Anwendung der Gradientenmethode dar.

Die numerische Integration des Differentialgleichungssystems (1) ergibt mit einem Anfangswert des Vektors **k**, dessen Komponenten innerhalb vernünftiger Grenzen beliebig gewählte Werte für die Geschwindigkeitskonstanten sind, für die Variable ein Wertesystem $\{y_1(x_i), y_2(x_i). \ldots y_5(x_i)\}$ $(i = 1, 2, \ldots p)$.

Bezeichnen $\bar{y}_1(x)$ und $\bar{y}_3(x)$ die experimentell bestimmten Konzentrationen der Komponenten A und B in der Gasphase, dann können mit einer für die numerische Integration geeigneten Methode (z. B. mit der Simpson-Methode) die Normen

$$\| y_1 - \bar{y}_1 \| \text{ und } \| y_3 - \bar{y}_3 \|$$

gebildet werden. Mit Hilfe dieser Normen läßt sich eine Fehlerfunktion z. B. mit der Definitionsgleichung

$$H = \| y_1 - \bar{y}_1 \| + \| y_3 - \bar{y}_3 \|$$

aufstellen, die die bei der Berechnung der Kurven $y_1(x)$ und $y_3(x)$ infolge der Wahl falscher Werte für die Geschwindigkeitskonstanten auftretenden Fehler zum Ausdruck bringt.

Um eine höchstmögliche Eindeutigkeit zu gewährleisten, soll als Prinzip gelten, alle experimentell zu bestimmenden Funktionen der Variablen (in dem erörterten Beispiel sind es mit den Komponenten A und B in der Gasphase gerade zwei) in den Vergleich einzubeziehen, *eventuell auch derart, daß man die Normen entsprechend der Zuverlässigkeit der in ihnen enthaltenen Meßdaten mit Gewichten versieht.*

Bei Verwendung von Digitalrechenmaschinen kann das die Zielfunktion H berechnende Funktionsverfahren, das als Ausgangsdaten den Anfangswert des Vektors **k**, das Anfangswertesystem der Funktionen $y_j(x)$ sowie eine die Meßdaten enthaltende Matrix **M** verwendet, variiert und den Gegebenheiten angepaßt werden. Die Optimalisierung beschränkt sich nämlich nicht nur auf den Vektor **k**, sondern es können auch, wenn es notwendig ist, einige Ausgangswerte der Funktionen y_j [z. B. die Zahl der aktiven Zentren, d. h. deren Anfangswert $y_5(0)$] unter die zu optimalisierenden Konstanten aufgenommen werden.

Bevor auf die bisher mit der Gradientenmethode bei der Lösung kinetischer Aufgaben gemachten Erfahrungen eingegangen wird, müssen wir noch auf ein prinzipielles Problem hinweisen, nämlich auf die Frage nach der Eindeutigkeit der mit dieser Methode erhaltenen Lösung. Es kann nämlich nicht von vornherein ausgeschlossen werden, daß derartige Berechnungen zur Auffindung von nur lokalen Minima führen. Unseres Wissens steht die theoretische Bearbeitung dieses Problems noch aus. Es kann deshalb zum jetzigen Zeitpunkt nicht mit Sicherheit gesagt werden, ob die mit Digitalrechenmaschinen ausgeführten Optimalisierungen der Geschwindigkeitskonstanten in allen Fällen die besten Werte für diese liefern. Es besteht jedoch eine Möglichkeit, die auf diese Weise erhaltenen Resultate zu erhärten, nämlich die Optimalisierung nicht nur mit den Funktionen y_j, sondern auch mit ihren Ableitungen dy_j/dx durchzuführen.

Wir können annehmen, daß in der Umgebung des bei der Optimalisierung erhaltenen Lösungsvektors **k*** ein Bereich $\mathscr{T}^*$ vorhanden ist, für dessen Punkte der Fehler unter einem bestimmten, noch als annehmbar zu bezeichnenden Wert liegt. Ein entsprechend definierter Bereich $\mathscr{U}^*$ wird bei der mit den Ableitungen durchgeführten Optimalisierung erhalten. Wenn beide Bereiche nicht überlappen,

$$\text{d. h.} \qquad \mathscr{U}^* \cap \mathscr{T}^* = 0\,,$$

so ist die Richtigkeit der Lösung in Zweifel zu ziehen. Liegt dagegen eine Überlappung beider Bereiche vor, so ergeben alle in dem Überlappungsbereich $\mathscr{V}^* = \mathscr{U}^* \cap \mathscr{T}^* \neq 0$ liegenden Punkte P_i

$$P_i \in \mathscr{V}^* \tag{2}$$

sowohl für die Funktionen als auch für die Ableitungen eine innerhalb der angenommenen Fehlergrenzen liegende Näherung. Natürlich ist (2) für die Eindeutigkeit nur eine notwendige, aber keine ausreichende Bedingung. Mit der Eindeutigkeit der Lösung nichts zu tun hat die theoretisch zu begründende Tatsache, daß bei Verwendung einer mit den Normen der Ableitungen definierten Zielfunktion die Optimalisierung einfacher und genauer auszuführen ist.

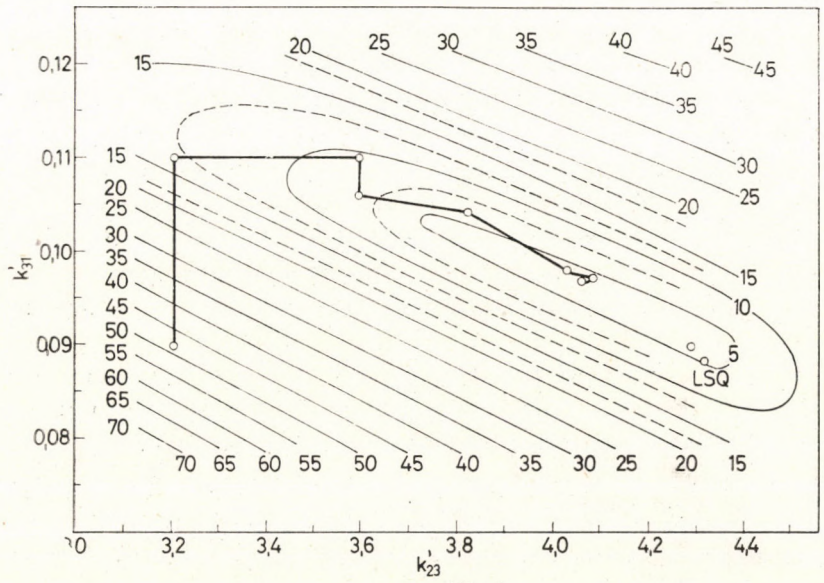


Abb. 1

b) Ergebnisse und Diskussion

In Abb. 1 ist das Resultat einer auf die in der vorangegangenen Mitteilung erörterte kontaktkatalytische Isomerisierung von Buten-1 angewandten Optimalisierungsberechnung dargestellt. Die die Niveaulinien charakterisierenden Zahlen geben den Wert der Fehlerfunktion

$$H \equiv \varrho(y, \bar{y}) = \int_{x_1}^{x_p} | g(x; k'_{23}, k'_{31}) - \bar{g}(x) | \, dx$$

in 10^{-4}-Einheiten an. Im Verlauf der Optimalisierung geht der Fehler in 7 Schritten vom Anfangswert $4{,}8 \cdot 10^{-3}$ bei $\mathbf{k}(3{,}2;\ 0.09)$ auf $3{,}9 \cdot 10^{-4}$ bei einem Endwert des Vektors $\mathbf{k}^*(4{,}07;\ 0.097)$ zurück, nimmt also um etwa eine Größenordnung ab. Die Meßfehler der dieser Optimalisierung zugrunde liegenden Konversionskurven sind zwar gering, aber immerhin so groß, daß eine Näherung über einen Wert der Fehlerfunktion von etwa $5 \cdot 10^{-4}$ hinaus sinnlos ist. Somit sind in diesem speziellen Fall alle Geschwindigkeitskonstanten als »innerhalb der Meßgenauigkeit liegend« zu betrachten, die in dem von der

Niveaulinie (Isofehlerkurve) $5 \cdot 10^{-4}$ umgrenzten Gebiet liegen. Selbstverständlich sind auch die mit der Methode der kleinsten Fehlerquadrate erhaltenen, in Abb. 1 mit LSQ bezeichneten Geschwindigkeitskonstanten (siehe vorangehende Mitteilung [1]) als »gut« anzusehen. Obwohl die Molenbrüche der experimentell bestimmten Komponenten mit Fehlern von höchstens $\pm 2 \cdot 10^{-3}$ behaftet sind, könnnen die Konstanten, wie aus dem ziemlich großen, von der Niveaulinie $5 \cdot 10^{-4}$ begrenzten Gebiet zu ersehen ist, nur relativ ungenau angegeben werden. Dies steht in vollem Einklang mit der bekannten, jedoch auf so deutliche Weise bisher vielleicht noch nicht zum Ausdruck gebrachten Tatsache, daß man auch anhand sehr zuverlässiger Messungen nicht in der Lage ist, die Geschwindigkeitskonstanten »genau« zu bestimmen.

Die eigentliche Aufgabe ist jedoch, mit der Gradientenmethode nicht solche relativ einfache, sondern komplizierte, nichtstationäre bzw. nichtquasistationäre kinetische Probleme zu lösen, für die zur Zeit keine anderen Lösungsmethoden zur Verfügung stehen. Inwieweit unsere Programme solche Aufgaben erfüllen können, wurde am Beispiel der erwähnten hypothetischen Modellreaktion $A \rightleftharpoons B$ untersucht.

Als »Meßdaten« dienten die bei geeigneter Wahl der 6 in Betracht kommenden Geschwindigkeitskonstanten und der Ausgangswerte der Funktionen $y_j(x)$ durch numerische Integration des Differentialgleichungssystems (1) nach der Methode von Runge-Kutta erhaltenen Kurven. Folgende Werte wurden für die Geschwindigkeitskonstanten angenommen:

$$\vec{k}_A = 0{,}1 \text{ m-mol}^{-1} \text{ min}^{-1}$$

$$\overleftarrow{k}_A = 0{,}1 \text{ min}^{-1}$$

$$\vec{k} = 0{,}1 \text{ min}^{-1}$$

$$\overleftarrow{k} = 0{,}1 \text{ min}^{-1}$$

$$\vec{k}_B = 0{,}05 \text{ min}^{-1}$$

$$\overleftarrow{k}_B = 0{,}1 \text{ m-mol}^{-1} \text{ min}^{-1}$$

Die Anfangswerte der Funktionen $y_j(x)$ waren:

$$y_1(0) = 2 \text{ m-mol}$$

$$y_2(0) = 0 \text{ m-mol}$$

$$y_3(0) = 0 \text{ m-mol}$$

$$y_4(0) = 0 \text{ m-mol}$$

$$y_5(0) = 0{,}25 \text{ m-mol}$$

Für die Optimalisierung wurden natürlich nur die Funktionen $\bar{y}_1(x)$ (Komponente A in der Gasphase) und $\bar{y}_3(x)$ (Komponente B in der Gasphase) verwendet, da bei tatsächlicher Durchführung einer katalytischen Reaktion dieses Typs die anderen Funktionen experimentell nicht erhalten werden können. Von den Konstanten wurden zunächst nur die beiden Geschwindigkeitskonstanten $\vec{k}$ und $\overleftarrow{k}$ als freie Parameter behandelt.

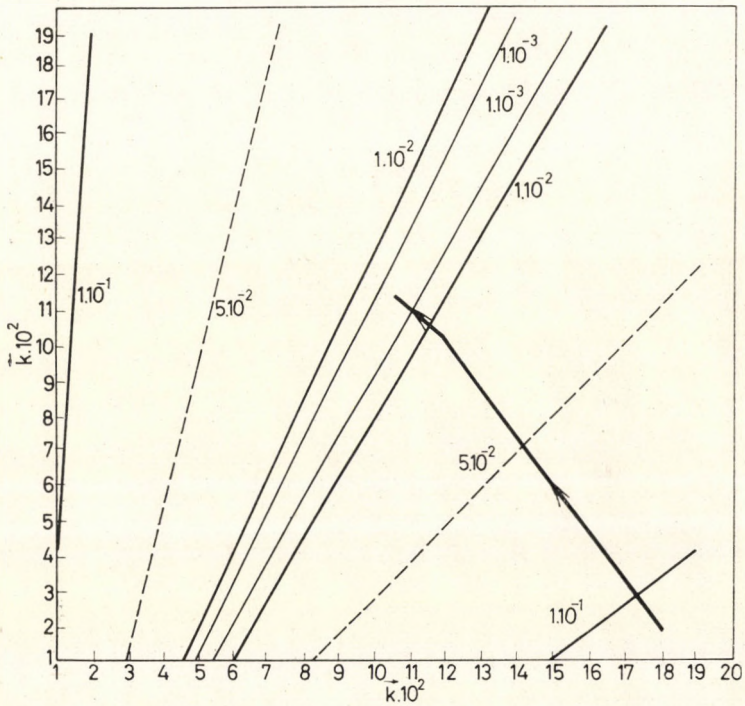


Abb. 2

Mit der Zielfunktion

$$H = \|y_1 - \bar{y}_1\| + \|y_3 - \bar{y}_3\|$$

erhält man die in Abb. 2 dargestellte Fehlerfläche. Wie aus dieser Abbildung zu ersehen ist, erhält man bei der Optimalisierung von $\vec{k}$ und $\overleftarrow{k}$, ausgehend vom Punkt **k**(0,18; 0,02), in zwei Schritten den Lösungsvektor **k***(0,106; 0,113). Daß die Näherung bereits nach dem 2. Schritt abgebrochen wird, liegt am Profil der Fehlerfläche, die in diesem Falle die Form eines diagonal verlaufenden Tales aufweist.

Die mit der die Ableitungen enthaltenden Zielfunktion

$$H = \left\| \frac{dy_1}{dx} - \frac{\overline{dy_1}}{dx} \right\| + \left\| \frac{dy_3}{dx} - \frac{\overline{dy_3}}{dx} \right\|$$

in der positiven Viertelebene der Variablen $\vec{k}$ und $\overleftarrow{k}$ dargestellte Fehlerfläche zeigt dagegen kein talartiges Profil, sondern das eines elliptischen Paraboloids (s. Abb. 3). Diese Form der Fehlerfläche macht verständlich, daß in diesem Fall die Optimalisierung, ausgehend von einem nur unwesentlich veränderten Anfangswert (0,19; 0,01) des Vektors **k** in 11 Schritten zum Punkt **k*** (0,099; 0,098) führt, der den in die Methode gesetzten Erwartungen in jeder Hinsicht gerecht wird.

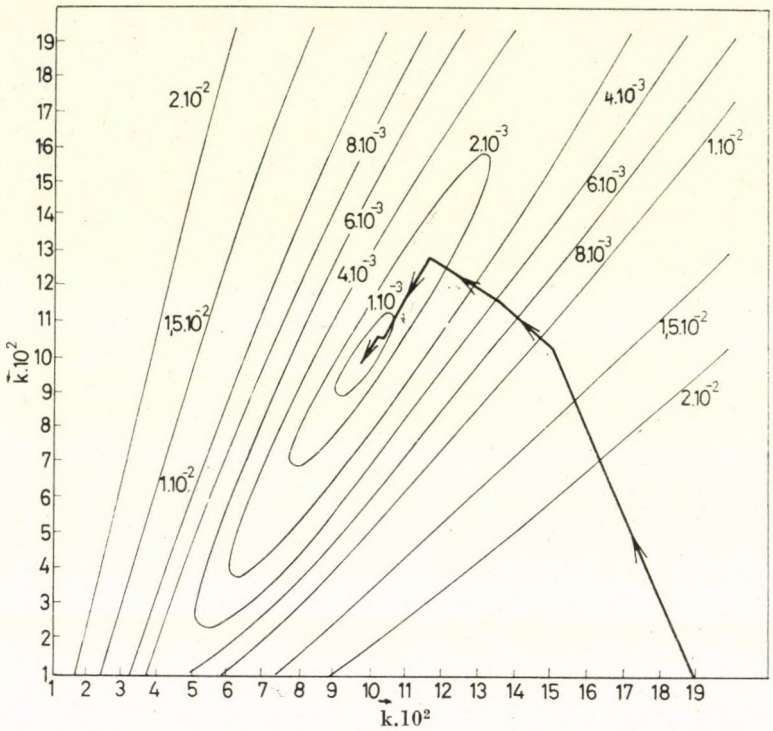


Abb. 3

Selbstverständlich wird eine solche Genauigkeit bei den mit Meßfehlern behafteten, experimentell bestimmten Konversionskurven nicht zu erreichen sein, um so mehr, als eigentlich alle in Frage kommenden Geschwindigkeitskonstanten (in unserem Modellbeispiel also 6) als freie Parameter zu behandeln sind. Nach unseren bisherigen Erfahrungen nimmt die für die Berechnung notwendige Zeit proportional mit der Zahl der zu optimalisierenden freien Parameter zu. Steht z. B. eine Digitalrechenmaschine vom Typ Gier, die pro Sekunde 15 000 Operationen ausführt, zur Verfügung, so beansprucht im Falle unserer Modellreaktion die Optimalisierung von 2 freien Parametern etwa 20—25 Minuten, die von 6 freien Parametern etwa 90 Minuten. Da die Genauigkeit der Annäherung auch dann nicht wesentlich abnimmt, wenn die Zahl der freien

Parameter erhöht wird, ist zu erwarten, daß in Fortführung dieser Arbeit kompliziertere, bis jetzt nicht auf andere Weise zu bearbeitende kinetische Probleme mit Hilfe der Gradientenmethode mit Erfolg gelöst werden können.

LITERATUR

1. FEJES, P., BEYER, H.: Acta Chim. Acad. Sci. Hung. **58**, 439 (1968).
2. COURANT, R.: Bull. Amer. Math. Soc. **49**, 1 (1943).
CURRY, H. D.: Qu. Appl. Math. **2**, 258 (1944).
ROSENBROCK, H. H.: Computer J. **3**, 175 (1960).
3. ROBERTS, R. M.: J. Phys. Chem. **63**, 1400 (1959).
4. CORDES, J. F., GÜNZLER, H.: Zeitschr. f. Naturforscher **15b**, 682 (1960); Chem. Ber. **92**, 1055 (1959).

Pál FEJES; Budapest XII. Konkoly Thege M. út
Hermann BEYER; Budapest II. Pusztaszeri út 59/67

Acta Chimica Academiae Scientiarum Hungaricae, Tomus 59 (1), pp. 35—55 (1969)

THE PYROLYSIS OF GASEOUS HYDROCARBONS, I

KINETICS OF THE THERMAL DECOMPOSITION OF *n*-BUTANE

V. ILLÉS

(Hungarian Oil and Gas Research Institute, Veszprém)

Received July 10, 1967

The kinetics of the thermal decomposition of *n*-butane have been investigated in a continuous tube reactor, at a total pressure of 1 atm, in the temperature range between 600 and 820 °C. The description of the experimental equipment and measuring methods is given. It was shown that, in the temperature range and within the reaction period usual for industrial pyrolysis reactors, expansion in function of conversion can be characterized independently of temperature by a "single-curve". Based on the expansion, a method has been developed for the calculation of the actual reaction time, and for the determination of the conversion-dependent factor replacing the ratio of the stoichiometric coefficients in the rate equation. On the basis of this method, kinetic relationships in function of fictive and actual reaction time were obtained, which are suitable for the calculation of the rate constants and of the conversion curves. It was established that the overall decomposition rate of *n*-butane cannot be described by a simple first order kinetic relationship. Two methods have been presented for the description of the conversion curves. In one of them the deviation from first order kinetics was taken into account by the introduction of an empirical constant representing the restraining effect of the reaction products. According to the other method the changing of the order of the reaction with temperature was taken into consideration in the calculations.

Introduction

Unsaturated hydrocarbons with carbon atom number C_2—C_4, constituting the most important basic materials of industrial chemical syntheses, are prepared by the thermal decomposition (pyrolysis) of gaseous and liquid hydrocarbons. In view of this industrial importance of pyrolysis, the studying of thermal decomposition reactions and the development of industrial processes is the subject of intensive research all over the world.

This topic is of interest also from the theoretical aspect, as several problems concerning the mechanisms and the kinetics of thermal decomposition are not yet cleared or only partly solved. Thus for example the question, whether the thermal decomposition of hydrocarbons proceeds according to a pure free radical chain mechanism, or is a simultaneous process of chain and molecular reactions, has been still much discussed recently. The earlier conception, according to which the overall decomposition reaction can be represented by a first order kinetics is also widely open to discussion. Here the difficulty lies in the complex nature of the reaction, owing to which also the overall stoichiometry of the reaction changes when the degree of decomposition is increased.

Besides the mentioned incertitudes of primarily theoretical character, the practical use of data published in literature is rendered difficult by several cir-

cumstances. One of these circumstances, resulting in a great difference in the numerical values of kinetical and yield data, is the fact that various authors use different measuring and analytical methods. Moreover, a great part of the data published involves but a narrow region of temperature and reaction time.

Our work, in which the pyrolysis of *n*- and isobutane and of propane has been investigated, had the double objective to study the pyrolysis process, and to establish relationships required in the design of industrial reactors. In accordance with this aim, measurements were carried out in the temperature range from 600 to 820 °C, important from the point of view of the operation of industrial reactors, in a continuous tubular reactor, under isothermic and isobaric conditions [10].

In our present paper the apparatus is presented and the kinetical relationships for the description of the overall decomposition rate of *n*-butane are described.

Apparatus and procedure

The schematic diagram of the apparatus is shown in Fig. 1. The principal parts of the apparatus are: the feeder, the preheater, the furnace, the quartz reactor with condenser, and the thermocouple for measuring the temperature in the reaction zone.

Hydrocarbon gases were fed from a steel pressure cylinder through a differential mercury manometer into the reactor. The flow rate of the gas was adjusted with a pressure reducer and a needle valve to the required value.

For the preheating of gases an electrically heated metal capillary was used, which was connected through a metal connection head to the silica reactor. The gas-tight joining of the silica reactor and the connection head was ensured by silicone rubber sealing.

The furnace was equipped with four electrical heating elements of different length, each having an individual temperature regulation. The electrical heating filaments, run through ceramic beads, were arranged in slots cut into the external shell of a heat-resistant metal block. The metal block holding the heating filaments is surrounded by a ceramic tube, which, besides providing thermal insulation, serves also as terminal of the electric heating filaments. This heating core was surrounded by a cylindrical metal jacket. The annular space between the ceramic tube and the metal jacket was insulated with slag wool. The high heat capacity of the metal block holding the heating filament, and that of the whole furnace permitted to maintain an adequate section of the reactor tube for hours at constant temperature (ensuring the conditions of an isothermal reactor). The heating elements of the tubular furnace were adjusted to the required value by manual regulation of toroidal transformers. Power was supplied by a 220 V stabilized a.c. source.

The quartz reactor of 8 mm internal diameter and 110 cm length was introduced into the boring of the metal block holding the heating filament. A water condenser, serving for the rapid cooling of the reaction mixture (for quenching the reaction) was soldered to the bottom of the quartz reactor. A quartz capillary of 2 mm external diameter is running along the axis of the reactor tube and the water-cooled condenser. The capillary is soldered to the bottom of the reactor (below the condenser), while a silicone rubber seal is used at the top joining. The capillary houses the Pt-Rh-Pt thermocouple for measuring the temperature in the reaction zone. (There was no contact between the thermocouple and the gas flowing in the reactor tube.) The two branches of the thermocouple, including an angle of 180°, fit into the notches of the bakelite discs fastened to the bottom and the top of the reactor oven, and can be moved before the millimeter scale arranged on the external jacket of the reactor oven. This arrangement permitted to measure the actual temperature of the reaction zone along the whole length of the reactor tube with the same thermocouple. The thermocouple was joined to a temperature reading (millivoltmeter) instrument of system Deprez, equipped with a mirror scale, graduated into 0.5 divisions. The mirror scale ensured a reading accuracy of ± 0.2 mm, corresponding to an accuracy of ± 2 °C.

The pyrolysis experiments were performed at constant reaction temperatures and with different reaction periods. The change in reaction period could be attained by changing the feed-rate. In the adjustment of the reactor temperature we tried to obtain a temperature distribution in the reaction zone approximating the temperature distribution of an ideal isothermic reactor tube.

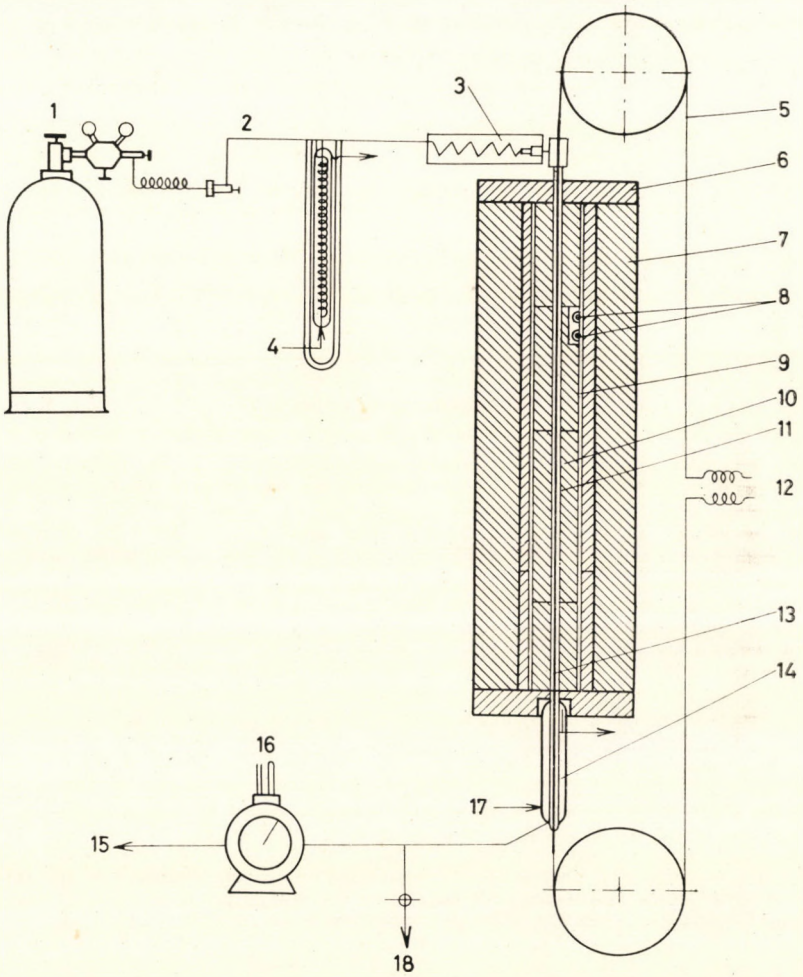


Fig. 1. Pyrolysis equipment for laboratory experiments. *1* — Gas pressure bottle, *2* — Needle valve, *3* — Preheater, *4* — Differential manometer, *5* — Pt-Rh-Pt thermocouple, *6* — Asbestos, *7* — Glass wool, *8* — Electric heating spiral, *9* — Corundum tube, *10* — Metal block holding the heating filaments, *11* — Quartz reactor, *12* — Temperature reading instrument, *13* — Thermocouple case, *14* — Condenser, *15* — Pyrolysis gas, *16* — Gas meter, *17* — Water, *18* — Gas sample

Fig. 2 shows the temperature distribution curves measured during the experiments in series No. 116 of *n*-butane pyrolysis. On recording the 11 successive curves, the feed rate was increased by an order of magnitude. (The value of fictive reaction time was 2.62 sec for No. 116/1, and 0.25 sec for No. 116/11.) The shape of the curves and their relative position shows that the case of an ideal isothermal reactor tube could be well approximated, and that the isothermal section of the temperature distribution curves could be brought into full

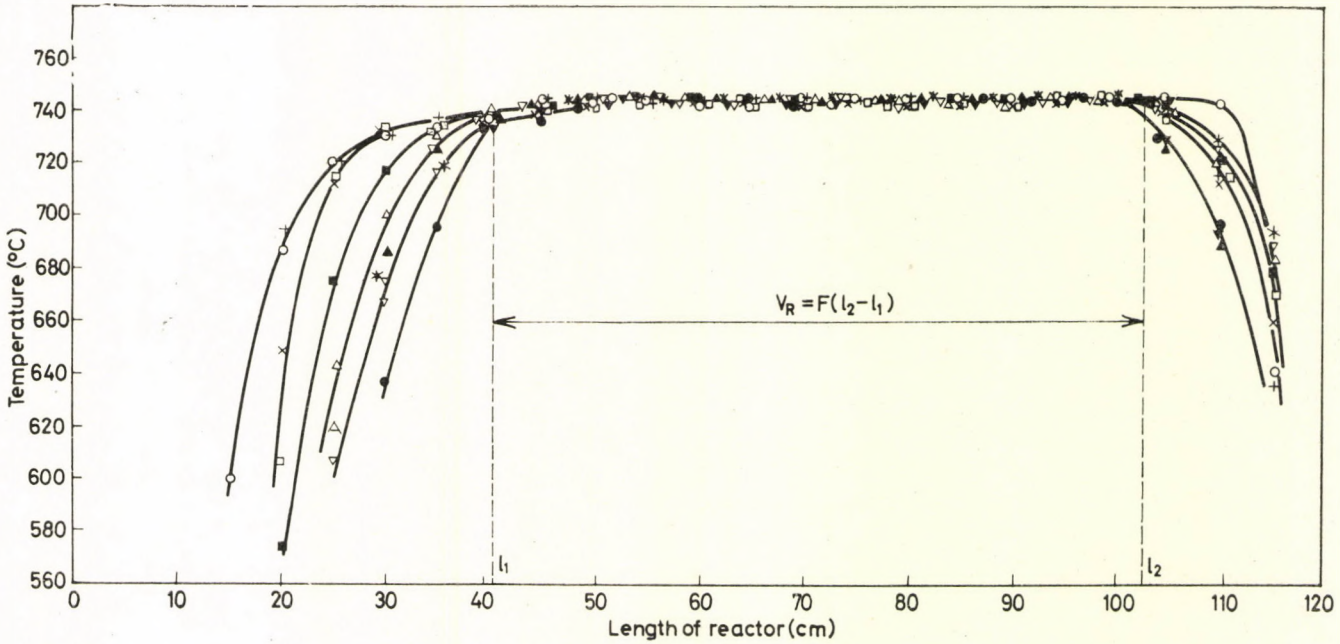


Fig. 2. The change of reaction temperature in dependence of the length of the reactor in the measuring series No. of 116 *n*-butane ○ 116/1; + 116/2; × 116/3; □ 116/4; ■ 116/5; △ 116/6; ▲ 116/7; ▽ 116/8; ▼ 116/9; * 116/10; ● 116/11

coverage in measurements belonging to various feeding rates. The volume of the reactor (V_R) was determined separately for each measurement on the basis of the corresponding temperature distribution curve, by marking the limits of the isothermal reaction zone, as shown in Fig. 2.

Actual measurements were performed after the fine-adjustment of temperature. During the measurements, the hydrocarbon gas was flowing through a regulating valve and a differential manometer into the preheater, and was heated to 170—180 °C. From here, it passed through the connection head into the vertical silica reactor, in which, after covering a distance of 25—40 cm, in dependence of its flow rate, the hydrocarbon was heated to the required temperature, and its decomposition started. The rapid quenching of the reaction mixture took place in the condenser soldered to the bottom of the reactor tube. The gas mixture leaving the condenser was lead through a wet gas meter into the free air. Gas samples for analysis were collected in a Dewille flask. Samples were taken during the whole measuring process. Gas samples were taken before the gas meter, so that the sample could not become contaminated by the gas of the preceding measurement. Depending on the feed rate, the single measurements took 10—30 minutes.

Depending on the circumstances of the measurements, more or less coke was deposited on the internal wall of the reactor tube and the external surface of the thermocouple casing. This was removed by burning off with air or with an oxygen—nitrogen mixture.

The gas mixture in the pyrolysis of the hydrocarbons consisted of hydrogen, saturated and unsaturated C_1—C_4 hydrocarbons, and of a small amount of aromatic hydrocarbons. The qualitative and quantitative composition of the gas mixtures was determined by gas chromatography, using the method developed by SIMON, SZEPESY and FÁY [26].

The quantity of hydrogen, air and methane was determined at 20 °C with a chromatograph, type Janák, in a column of 0.8 m length, packed with active carbon. The quantity of ethane, ethylene, propane and propylene was determined at 40 °C with a gas chromatograph Carlo Erba Model B/f, equipped with a detector on heat conductivity principle, in a column of 1 m length, packed with alumina. The quantity of butanes, butenes, butadiene and heavier (aromatic) components was determined at 40 °C with the same chromatograph, using a 4 m column, packed with 35 per cent dimethylsulfolane impregnated alumina. The chromatograph comprised also an integrator. The quantitative evaluation of the chromatograms was made with the aid of calibration curves plotted for the pure gases.

Kinetics of the thermal decomposition of *n*-butane

The thermal decomposition of hydrocarbons is a process proceeding with an increase in the mole number. The kinetical equations given by BENTON [1], HULBURT [2] and HOUGEN and WATSON [3] for gas reactions accompanied by a change in mole number, contain a constant calculated from the stoichiometric coefficients. Owing to secondary reactions, in the thermal decomposition of hydrocarbons the overall stoichiometry of the reaction is changing with the degree of conversion. Therefore, the cited equations cannot be applied directly for the calculation of the rate of these reactions. The fact that no exact method is known for the calculation of the actual reaction time of reactions proceeding in continuous reactor tubes under a change in volume, constitutes a further difficulty. Therefore, generally the so-called fictive reaction time calculated on the basis of the feed rate, or its reciprocal, the space velocity is used for technological calculations [4].

To eliminate these difficulties, PANCHENKOV and BARANOV [5] use instead of the stoichiometric coefficients the average value of the change in mole number for the calculation. HIRSH *et al.* [6] consider the effect of the change in mole number in function of the change in the specific volume of the reaction mixture,

assuming its linear change with conversion. Both methods permit only approximative calculations.

On the basis of the expansion of the reaction mixture a method has been developed by us for the calculation of the actual reaction time, and for the determination of the conversion-dependent factor, to replace the ratio of the stoichiometric coefficients [7, 8, 9, 10]. On the basis of this method, kinetic relationships in function of the fictive and actual reaction times, suitable for the calculation of the rate constants and the conversion curves, were obtained.

Determination of the composition of the reaction mixture under consideration of the expansion

The decomposition of the individual hydrocarbons can be represented by the following overall reaction scheme:

$$A_1 + S_1 \rightarrow v_1 R_1 + v_2 R_2 + v_3 R_3 + \ldots + S_1 \tag{1}$$

where:

A_1 is a hydrocarbon,
S_1 is an inert substance,
$R_{1,2}$ is the symbol of reaction products,
$v_{1,2}$ is the quantity of the products (stoichiometric coefficient) formed from 1 mole of hydrocarbon.

The inert substance (*e.g.* water vapour) does not participate in the reaction, it influences, however, the composition of the reaction mixture in the reactor and therefore must be considered in the rate equation. To describe a correct rate equation, first of all the composition of the reaction mixture must be determined.

The number of moles and the volume of the mixture fed into the reactor in unit time (assuming that the coefficient of the compressibility of the mixture is 1) are:

$$\Sigma n^0 = n_1^0 + S_1 = n_1^0 (1 + s_1) \tag{2}$$

$$B_0 = n_1^0 \frac{RT}{P} (1 + s_1) \tag{3}$$

where:

n_1^0 mole/sec is the quantity of hydrocarbon A_1,
S_1 mole/sec is the quantity of the inert substance,
$s = S_1/n_1^0$ is the relative quantity of the inert substance,
B_0 ml/sec is the volume velocity of the mixture fed into the reactor at temperature T and pressure P.

The number of moles and volume of the mixture leaving the reactor in unit time at a conversion x of the initial hydrocarbon A_1:

$$\Sigma n = n_1 + \Sigma m_i + S_1 = n_1^0 [(1 - x) + \Sigma v_i x + s_i] \tag{4}$$

$$B = n_1^0 \frac{RT}{P} [1 + s_1 + (\Sigma v_i - 1) x] = \\ = B_0 + n_1^0 \frac{RT}{P} [\Sigma v_i - 1] x \tag{5}$$

where:

n_1 mole/sec	is the quantity of hydrocarbon A_1 in the mixture leaving the reactor,
m_i mole/sec	is the quantity of reaction product R_i in the mixture leaving the reactor,
$\Sigma v_i = v_1 + v_2 + \ldots$	is the sum of the stoichiometrical coefficients of the products,
B ml/sec	is the volume velocity of the mixture leaving the reactor at a reactor temperature of T and a pressure of P.

In gas reactions occurring with a change in mole number, the volume of the reaction mixture changes with the proceeding of the reaction. This change is expressed by the ratio of the mole number of the mixture leaving the reactor and fed into the reactor, and in case of an isothermal, isobaric reactor by the ratio of the volume of this mixture. This ratio is called expansion, and is denoted by E. The change of the expansion in function of the conversion of the starting hydrocarbon is described by the following equation [7]:

$$E = \frac{\Sigma n}{\Sigma n^0} = \frac{B}{B_0} = \frac{n_1^0 \frac{RT}{P} (1 + s_1) + n_1^0 \frac{RT}{P} [\Sigma v_i - 1] x}{n_1^0 \frac{RT}{P} (1 + s_1)} = \\ = 1 + (E_v - 1) x \tag{6}$$

where E_v is the value of expansion for the conversion $x = 1$ (the total decomposition of 1 mole of the initial hydrocarbon A_1), which is given by the following relationship:

$$E_v = 1 + \frac{\Sigma v_i - 1}{1 + s_1} \tag{7}$$

According to equation (6), the expansion changes linearly with the conversion, if E_v is constant. This condition is fulfilled only with simple reactions pro-

ceeding according to a given stoichiometric equation, where the value of E_v can be calculated, if the stoichiometric coefficients and the quantity of the inert substance are known, and in knowledge of these values the expansion can be given as an explicit function of conversion.

In the pyrolysis of *n*-butane, the overall stoichiometry of the reaction — due to secondary reactions — is dependent on conversion. Therefore the value

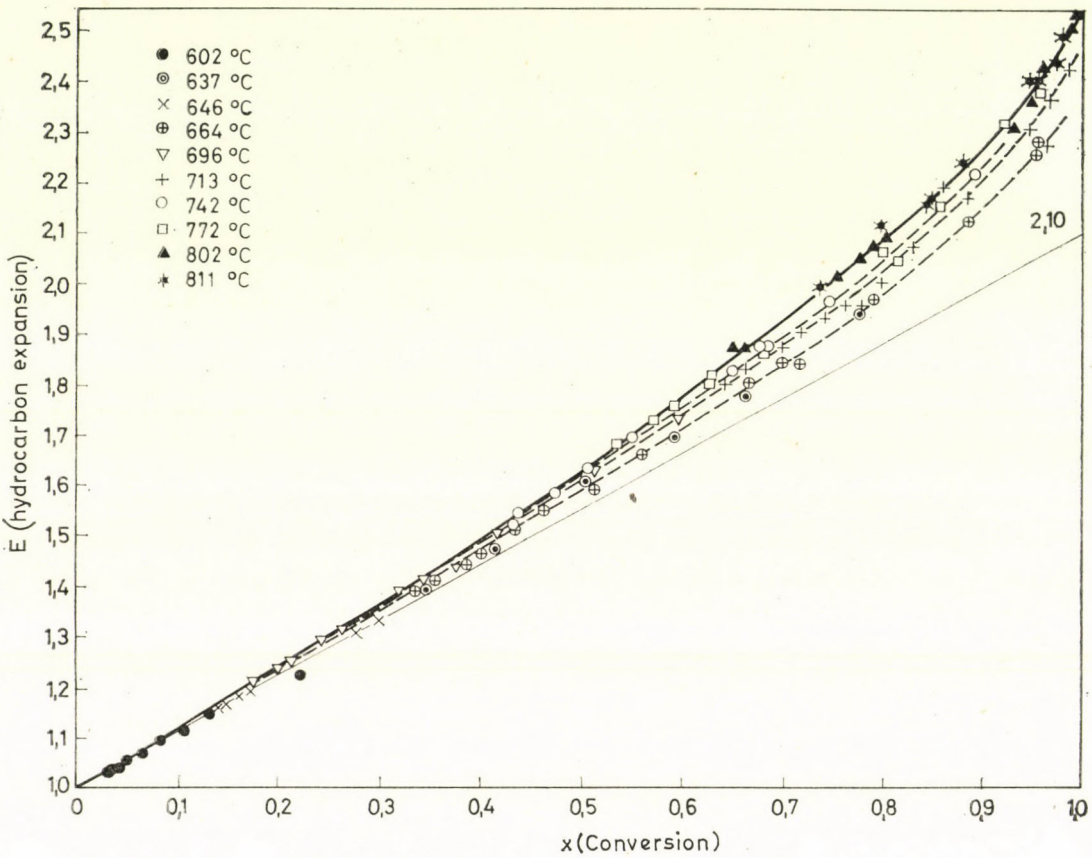


Fig. 3. The change of hydrocarbon expansion with conversion in the pyrolysis of *n*-butane

of E_v is not constant, and neither is the function $E(x)$ linear. However, it can be seen from Fig. 3, showing the function $E(x)$, that the expansion is highly independent of temperature. In the conversion range $0 < x < 0.4$ values plotted for various temperatures scatter within $\pm$ 1.5 relative per cent. The deviation increases with an increase in temperature, however, the deviation of the expansion values appertaining to 637 °C and 812 °C is even for $x = 0.95$ not greater than 5 per cent.

It can be established on the basis of Fig. 3 and Fig. 5 that, under the conditions applied for industrial pyrolysis (*i.e.* a temperature range of 600—820 °C

and reaction times of 0.5—1 sec), the change of the expansion of *n*-butane in dependence of conversion can be described by the "single curve" drawn in full line. Actually, a deviation from the single curve exceeding $\pm$ 1.5 relative per cent occurs at the various temperatures at such conversion values, the attainment of which at the given temperature requires a substantially longer reaction time than 1 sec.

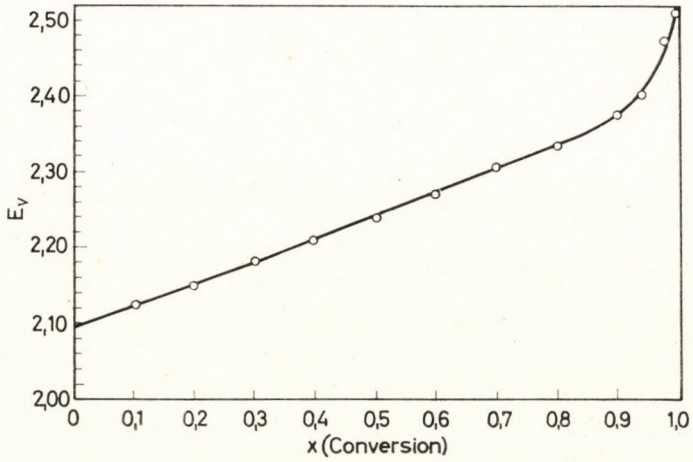


Fig. 4. The change of E_v with conversion in the pyrolysis of *n*-butane

Moreover, it can be established from Fig. 3 that the initial section of the $E(x)$ curve is linear, so that at low conversion values the primary decomposition reactions predominate. The slope of the curve $E(x)$ in the point $x = 0$ (the intercept on the vertical straight line drawn in point $x = 1$) gives the sum of the stoichiometric coefficients of the products formed in the primary decomposition reaction. If there would be no secondary reactions during decomposition, expansion would change along the straight line defined by the tangent appertaining to zero conversion. The actual $E(x)$ curves deviate upwards from the straight line, due to the increase in mole number and volume, caused by the secondary processes mentioned. (For a detailed discussion of the secondary reactions see our next communication.)

In knowledge of the expansion, the value of E_v appertaining to the given conversion x and comprising the overall stoichiometric coefficients, can be calculated from the following relationship:

$$E_v = \frac{E - 1}{x} + 1 \tag{8}$$

The change of the E_v value, calculated from (8) and from the "single curve" in Fig. 3, in function of the conversion is shown in Fig. 4.

From the presented relationships and the curves $E(x)$ and $E_v(x)$, the concentration of the single components in the mixture fed into the reactor and in that leaving the reactor can be calculated.

The molar concentration (the number of moles in unit volume) of the initial hydrocarbon A_1 in the mixture fed into the reactor is:

$$C_1^0 = \frac{n_1^0}{B_0} = \frac{P}{RT(1 + s_1)} \tag{9}$$

The molar concentration of the starting hydrocarbon A_1 in the mixture leaving the reactor at a conversion x is:

$$C_1 = \frac{n_1}{B} = \frac{n_1^0 (1 - x)}{n_1^0 \frac{RT}{P} [1 + s_1 + (\Sigma v_i - 1)\, x]} =$$

$$= \frac{C_1^0 (1 - x)}{1 + (E_v - 1)\, x} \tag{10}$$

The mole concentration of the product R_i in the mixture leaving the reactor at a conversion x of A_1 is:

$$C_{R_i} = \frac{m_i}{B} = \frac{n_1^0 v_i x}{n_1^0 \frac{RT}{P} [1 + s_1 + (\Sigma v_i - 1)\, x]} =$$

$$= \frac{C_1^0 v_i x}{1 + (E_v - 1)\, x} \tag{11}$$

The rate equation of the decomposition reaction; the change of conversion in time

In knowledge of the actual concentration of A_1, the rate of the conversion, according to the reaction scheme (1), can be written in the following form:

$$r = kC_1^n = k \left[\frac{C_1^0 (1 - x)}{1 + (E_v - 1)\, x} \right]^n \tag{12}$$

where:

r mole ml^{-1} sec^{-1} is the rate of the reaction, expressed as the quantity of A_1 decomposing in unit time in unit volume of the reactor,

n is the exponent determining the order of the overall reaction, and

k is the rate constant, dependent on temperature.

On the other hand, in a tube reactor of stationary operation, the rate of the reaction is determined by the change in mole number occurring in unit time in the volume element dV_R of the reactor [4, 11, 12]. Under consideration of the fact that no accumulation of substance can take place in the volume element dV_R, we have:

$$r\,dV_R = -\,dn_1 \tag{13}$$

From expression (10), $n_1 = (B/E)\,C_1^0\,(1-x) = B_0C_1^0\,(1-x)$, representing the quantity in moles of A_1 entering in unit time the volume element dV_R of the reactor. From this, $dn_1 = -\,B_0C_1^0\,dx$, which substituted into (13), gives the known fundamental equation of flow reactors:

$$\frac{dV_R}{B_0} = d\,\omega = C_1^0\,\frac{dx}{r} \tag{14}$$

If no change in volume (in mole number) occurs during the reaction, the volume flow rate is constant, and its value is the same as that of the feed rate B_0 (in an isothermic, isobar reactor). In this case, the ratio V_R/B_0 (the dimension of which is time), gives the average sojourn time of the particles in the reactor.

If the reaction is accompanied by a change in mole number, the volume of the reaction mixture and the volume flow rate will change in function of the conversion. In this case, the value of the ratio V_R/B_0 will not be identical with the average sojourn time of the particles and, therefore, it is called fictive reaction time. The fictive reaction time is denoted by ω.

When the volume of the reactor and feed parameters are known, the fictive reaction time can be calculated. Therefore, in chemical engineering practice measured data (the conversion curves) are generally plotted as a function of the fictive reaction time, or its reciprocal, the space velocity [4]. As will be seen in the following, also the rate equation written as a function of fictive reaction time yields exact expressions suitable for the calculation of rate constants and conversion curves.

The actual (average) reaction time for gas reactions proceeding under a change in mole number, can be expressed by the ratio of the volume of the isothermal reactor zone and the average volume velocity prevailing in this reactor zone:

$$\tau = \frac{V_R}{\bar{B}} \tag{15}$$

where:

τ sec is the actual (average) reaction time,

V_R ml is the volume of the isothermal reactor zone, and

$\bar{B}$ ml/sec is the average volume velocity of the reaction mixture in the reactor.

To calculate generally the average volume velocity calculated from the arithmetic mean value of the volume velocities, prevailing at the inlet and outlet of the reactor, are used [13]:

$$\bar{B} = \frac{B_0 + B}{2} \tag{16}$$

A more exact value is obtained for $\bar{B}$, if it is expressed from equation (6), by the average expansion: $\bar{B} = B_0\bar{E}$. The average expansion is determined by the graphical integration (planimetration) of curve $E(x)$.

To establish the relationship between the fictive (ω) and the actual (τ) reaction time, we started from the equation describing linear velocity. According to this, the linear velocity of the reaction mixture at a given section of the tube reactor is:

$$u = \frac{dl}{d\tau} \tag{17}$$

where:

l is the distance covered by the reaction mixture in time τ (assuming plug flow).

Writing this equation in terms of volume velocity, and introducing the relationship $B = B_0E$ from Equ. (6), the following differential equation is obtained for the actual reaction time:

$$d\tau = \frac{dV_R}{B_0 E} = \frac{d\omega}{E} \tag{18}$$

The actual reaction time is obtained by the integration of the differential equation (18):

$$\tau = \int_0^{\omega} \frac{d\omega}{E} \tag{19}$$

Since analytically the function $E(\omega)$ is unknown, the actual reaction time corresponding to a fictive reaction time is determined graphically or by a numerical method from ω and E values obtained experimentally.

Figs 5 and 6 show for various temperatures the change of *n*-butane conversion in function of the fictive and the actual reaction time, respectively. With an increase in temperature, the reaction rate of the decomposition increases rapidly and, consequently, a substantially shorter reaction time is required to attain the same conversion. Conversion curves approach the value $x = 1$ asymptotically, therefore a considerably longer reaction time is needed to

attain a conversion of $x > 0.95$. Long reaction times are favourable for the undesirable secondary reactions. To suppress secondary reactions, in industrial practice pyrolysis is carried out until a conversion of 0.9—0.94 is reached.

Now, the rate equation can be written both as a function of the fictive and the actual reaction time. On substituting the reaction rate, as given by Equ. (12), into the fundamental equation of flow reactors (14), for the change of

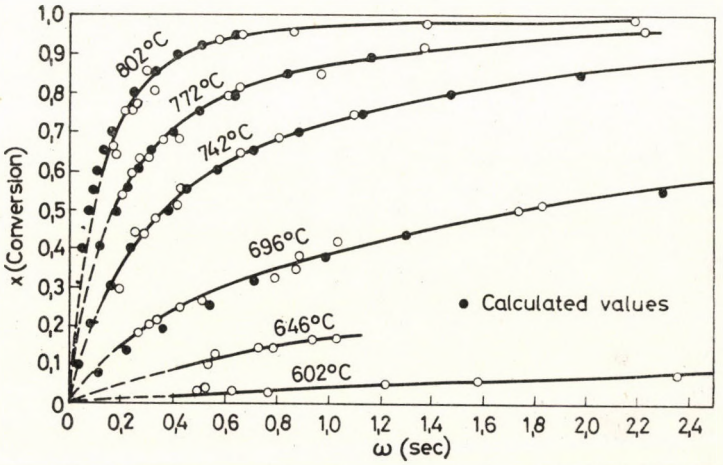


Fig. 5. The change of the conversion of *n*-butane in function of the fictive reaction time

the conversion in dependence of the fictive reaction time the following expression is obtained:

$$\frac{dx}{d\omega} = \frac{k}{C_1^0}\left[\frac{C_1^0(1-x)}{1+(E_v-1)x}\right]^n \tag{20}$$

Equation (20), from Equ. (18) gives for the change of the conversion in function of the actual reaction time the following expression:

$$\frac{dx}{d\tau} = \frac{k}{C_1^0}\left[\frac{C_1^0(1-x)}{1+(E_v-1)x}\right]^n [1+(E_v-1)x] \tag{21}$$

For the determination of the overall decomposition rate (the description of the conversion curves), we can start both from the differential equation (20) written in function of the fictive reaction time, and the differential equation (21) written in function of the actual reaction time. The experimental results were evaluated from both equations.

According to the general view in earlier publications [14, 15, 16], the thermal decomposition of hydrocarbons under the conditions of pyrolysis can

be treated with good approximation as a first order reaction.

Rearranging Equ. (20) for the condition $n = 1$ gives:

$$d\omega = \frac{1 + (E_v - 1)\,x}{k_1\,(1 - x)}\,dx \tag{22}$$

The integration (for E_v = constant) yields

$$k_1\omega = E_v \ln \frac{1}{1 - x} - (E_v - 1)\,x \tag{23}$$

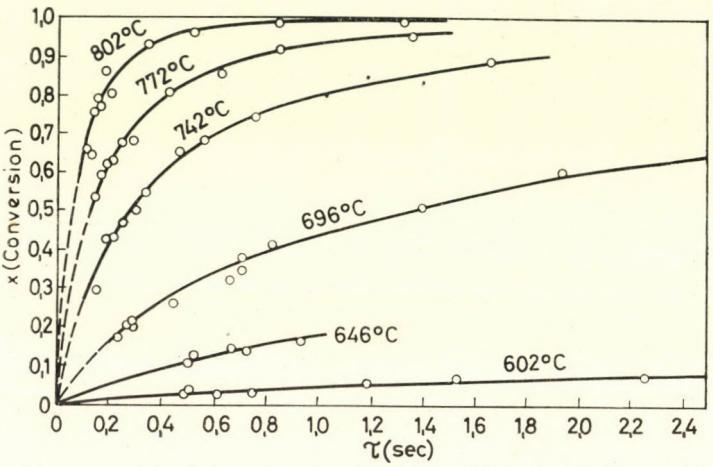


Fig. 6. The change of the conversion of *n*-butane in function of the actual reaction time

Equ. (23) corresponds to the relationships obtained by BENTON [1], HULBURT [2], and HOUGEN and WATSON [3] for $n = 1$ by different approaches, with the difference that Equ. (23) is of more general validity, as it takes also into consideration that the inert diluting substance changes the concentration (included in the value of E_v according to Equ. (7)).

From Equ. (21) for the condition $n = 1$ the following differential equation is obtained:

$$d\tau = \frac{dx}{k_1\,(1 - x)} \tag{24}$$

Performing the integration:

$$k_1\tau = \ln \frac{1}{1 - x} \tag{25}$$

This relationship is conform to the equation of first order reactions valid for static reactors. The difference lies only in the mode of determination of the reaction time. The actual reaction time necessary to attain the given conversion

x can be determined for a continuous tube reactor on the basis of the expansion of the reaction mixture from Equ. (19).

Assuming an overall decomposition reaction of first order, the value of the rate constants can be calculated from the integrated equations (23) and (25). (Equation (23) gives exact values only if the condition E_v = constant is fulfilled.) Rate constants calculated using the two equations show a good agreement.

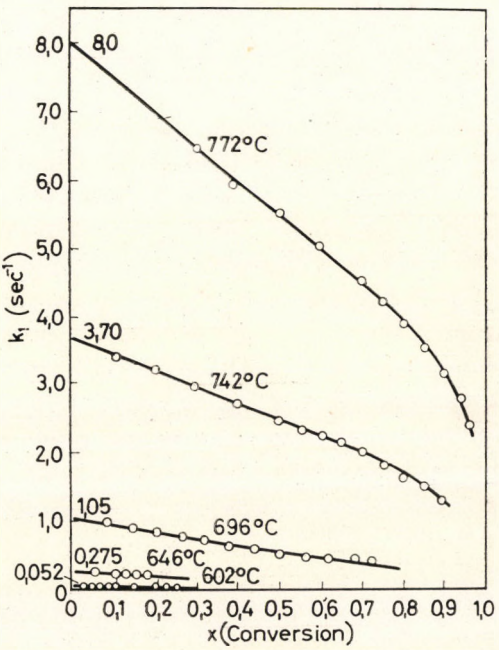


Fig. 7. The change of the rate "constants" of the decomposition of *n*-butane in dependence of conversion

In Fig. 7 the k_1 values, calculated from Eq. (25), are plotted in function of the conversion for the pyrolysis of *n*-butane at various temperatures. It can be seen from the diagram that the value of the "rate constants", calculated on the basis of first order kinetic relation, decreases with increasing conversion. The degree of the decrease (the slope of the straight lines) is temperature dependent.

This phenomenon can be explained in two different ways. According to one explanation, the change of the rate constants with conversion is to be ascribed to the fact that the condition $n = 1$ is not fulfilled and, therefore, the overall decomposition reaction cannot be considered as a first order reaction. According to the other explanation, the decrease of the rate constants of decomposition is due to the restraining action of the reaction products. In the

pyrolysis of ethane and propane, DINCES and FROST [17] were the first to point out that the value of the rate constants, calculated from the first order kinetic relationship, descreases with the increase of the conversion of the initial hydrocarbon. They draw the conclusion that the reaction products, primarily propylene, inhibit the decomposition of the initial hydrocarbon. In the rate equation, this inhibiting action was taken into consideration by the introduction of an empirical factor. Since then, HINSHELWOOD [18], LAIDLER [16, 19], STJEPUHOVICH [20], VOJEVODSKIJ [21], PURNELL [22] and several other authors have investigated this restraining action in the pyrolysis of various hydrocarbons. It was established that out of the reaction products primarily propylene and isobutylene exert such restraining action. (The decomposition reaction is inhibited very strongly also by the presence of NO.) The above experiments were performed with the primary aim to study the reaction mechanism of thermal decomposition and to clear whether after complete inhibition the so-called residual reaction proceeds as molecular decomposition or according to a chain mechanism.

Therefore, the expressions (23) and (25) are not suitable in their present form for the calculation of the rate constants of the decomposition, or for the description of the change of conversion with time. By introducing the empirical constants taking into account the restraining effect of the reaction products, equations suitable for solving the above tasks are obtained. Namely, on the basis of Fig. 7 the following expression can be written:

$$k_1^0 = \frac{2.303}{\tau} \log \frac{1}{1-x} + \beta x \tag{26}$$

where:

k_1^0 is the rate constant extrapolated at the given temperature for zero conversion,

β is the "restraining coefficient", representing the inhibitive effect of the reaction products on the decomposition of the starting hydrocarbon.

Both constants are temperature dependent. Their values were determined on the basis of experimental data, plotted in Fig. 7.

The rearrangement of Equ. (26) gives for the relationship between actual reaction time and conversion the following expression:

$$\tau = - \frac{2.303 \ \log \ (1-x)}{k_1^0 - \beta x} \tag{27}$$

For the determination of the temperature dependence of k_1^0, the logarithm of the rate constants extrapolated for zero conversion was plotted against the reciprocal of the reaction temperature in °K (Fig. 8). With good approximation,

a straight line may be drawn through the experimental points, from the slope of which the overall activation energy of the primary decomposition reaction, and from its intersection the value of the pre-exponential factor can be calculated.

The equation obtained reads:

$$\log k_1^0 = 11.806 - \frac{52\,200}{4.576\,T} \tag{28}$$

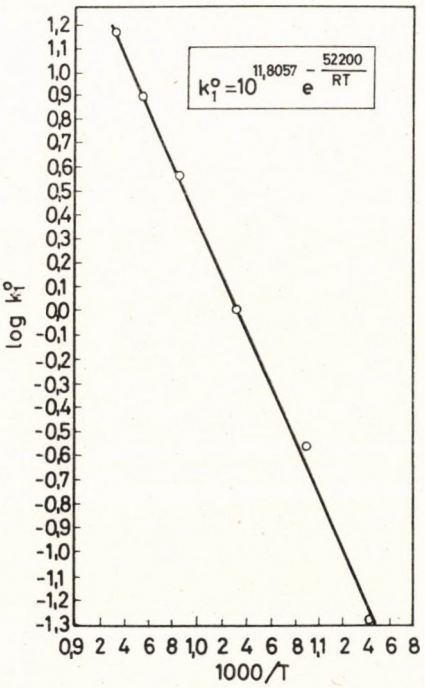


Fig. 8. The dependence of the rate constants of the decomposition of *n*-butane on temperature

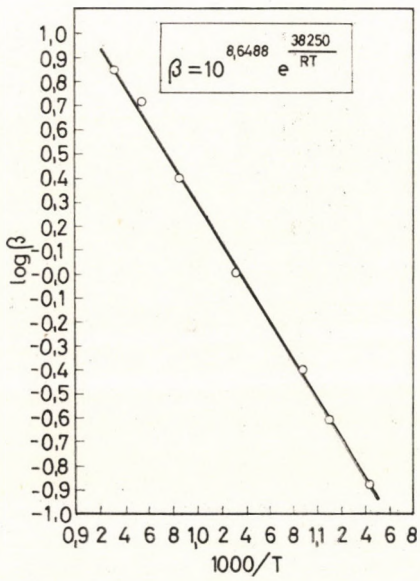


Fig. 9. The dependence of the "restraining coefficient" on temperature in the pyrolysis of *n*-butane

Kinetic data published in the literature show great differences. STEACIE and PUDDINGTON [23] obtained for the pyrolysis of *n*-butane in a static reactor in the temperature range from 550 to 650 °C an activation energy of 59 000 cal/mole, SANDLER and YU-HO-CHUNG [24] in a flow reactor in the temperature range from 700 to 900 °C 43 000—47 000 cal/mole, YUI-LOONG WANG *et al.* [25], similarly in a flow reactor, in the temperature range from 460—560 °C 55 000—57 000 cal/mole.

In Fig. 9 the logarithm of the "restraining coefficients" is plotted against the reciprocal of the reaction temperature in °K. Through the experimental points a straight line can be drawn with good approximation. From the slope

and the intersection, the following expression can be written for the temperature dependence of the restraining coefficient β:

$$\log \beta = 8.6488 - \frac{38\,250}{4.576\,T} \tag{29}$$

The rapid increase of the restraining coefficient with an increase in temperature can be explained probably by the fact that at higher temperatures also the rate of the reactions, proceeding between the olefine hydrocarbons and the

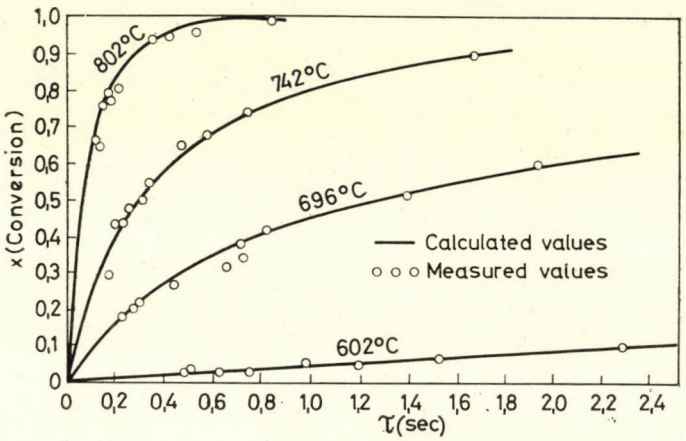


Fig. 10. The conversion curves of *n*-butane plotted for data calculated from the relationship (27) and for data measured

chain propagating active radicals, being responsible for the restrain, is substantially accelerated.

From the relationships (28) and (29) the values of k_1^0 and β can be determined for a given temperature. On substituting these constants into Equ. (27), the conversion curve for the given temperature can be calculated. To illustrate the performance of this method, conversion curves measured for *n*-butane at 602, 696, 742 and 802 °C and those calculated for the same temperatures by the method described are presented in Fig. 10. (The solid curve represents the calculated values.) Values calculated and found show a good agreement.

In the following, the kinetical relationship describing the overall decomposition reaction without taking into account the self-inhibiting effect shall be investigated. This investigation was carried out on the basis of differential equation (20), describing the dependence of conversion on fictive reaction time. The logarithmic form of Equ. (20) is the following:

$$\log\left(\frac{dx}{d\omega}\right) = \log\left(\frac{k}{C_1^0}\right) + n \log\left[\frac{C_1^0\,(1-x)}{1+(E_v-1)\,x}\right] \tag{30}$$

$(dx/d\omega)$ values characteristic of the rate of the decomposition reaction were determined by graphical differentiation of the conversion curves presented in Fig. 5. The value of the actual concentration belonging to conversion x was calculated under consideration of the expansion from Equ. (10).

The relationship (30) for the pyrolysis of *n*-butane is shown in Fig. 11. It can be seen that measuring points belonging together give with good approximation a straight line. The slope of the straight lines, giving the order of the overall decomposition reaction, is a number ranging between one and two, its value decreasing with the increase in temperature.

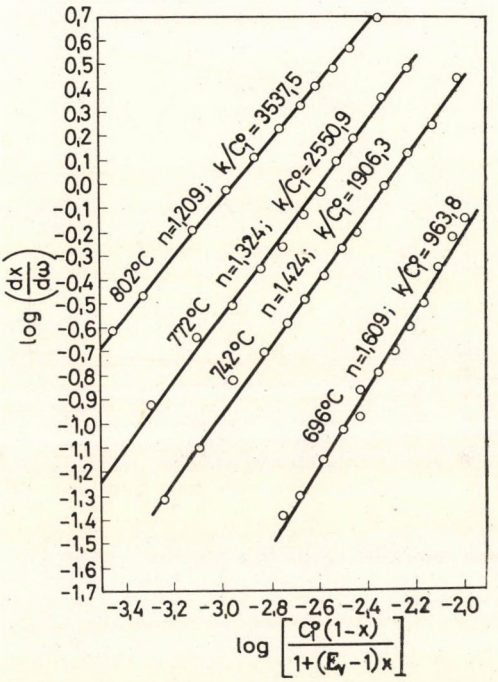


Fig. 11. The relationship $\log\left(\frac{dx}{d\omega}\right) = \log\left(\frac{k}{C_1^0}\right) + n \log\left[\frac{C_1^0 (1-x)}{1+(E_v-1)\,x}\right]$ for the pyrolysis of *n*-butane

After separation and integration, also the differential equation (20) gives a relationship suitable for the calculation of design data of the reactor:

$$\omega = \frac{C_1^0}{k} \int_0^x \left[\frac{1+(E_v-1)\,x}{C_1^0\,(1-x)}\right]^n dx \tag{31}$$

For the use of Equ. (31), the values of n and k belonging to the required temperature must be determined. This determination is made on the basis of Fig. 11, plotted for relationship (30).

For comparison with measured data, these calculated values of the conversion curve, marked by crosses, were plotted on Fig. 5. As may be seen, the agreement with the curves drawn for measured data is satisfactory, which proves the usability of the method described.

Out of the two methods presented for the description of the conversion curves, the method based on the first order kinetic relationship, complemented by the restraining coefficient, is more advantageous from the practical point of view. Namely, the temperature dependent constants k_1^0 and β, figuring in Equ. (27), can be easily determined on the basis of Fig. 7, while the determination of the constants in Equ. (30) requires graphical differentiation. The occurrence of reactions giving rise to restrain can be readily interpreted on the basis of radical mechanism. These reactions will be treated in detail in our next communication.

*

I wish to thank the Leaders of the Hungarian Oil and Gas Research Institute and L. SZEPESY, head of department, for the supporting of my work, and I. PLESZKÁTS for his help in the construction of the experimental apparatus, further Mrs. F. SIMON, directing analytical works.

REFERENCES

1. BENTON, A. F.: J. Am. Chem. Soc. **53,** 2987 (1931).
2. HULBURT, H. M.: Ind. Eng. Chem. **36,** 1012 (1944).
3. HOUGEN, O. A., WATSON, K. M.: Chemical Process Principles. Part III. John Wiley, New York, 1947. p. 834.
4. ERDEY-GRÚZ, T. and SCHAY, G.: Elméleti fizikai kémia (Theoretical physical chemistry). Vol. II. Tankönyvkiadó, Budapest, 1954. p. 433.
5. PANCHENKOV, G. M., BARANOV, V. Y.: Kinetika i Kataliz. Akad. Nauk. SSSR. **1,** 188 (1960).
6. HIRSCH, I. H., GRAWFORD, C. L., HOLLOWAY, C.: Ind. Eng. Chem. **38,** 885 (1946).
7. ILLÉS, V.: Magy. Kém. Foly. **71,** 319 (1965).
8. ILLÉS, V., PLESZKÁTS, I.: Magy. Kém. Foly. **71,** 323 (1965).
9. ILLÉS, V., PLESZKÁTS, I., SZEPESY, L.: Conference on some Aspects of Physical Chemistry. Fundamentals of Physical Chemistry I. No. 1. p. 31. Budapest, April 25—27, 1966.
10. ILLÉS, V.: Szénhidrogének pirolízise laboratóriumi csőreaktorban (The pyrolysis of gaseous hydrocarbons in a tubular laboratory reactor). Thesis, Veszprém, 1967.
11. BENEDEK, P., LÁSZLÓ, A.: A vegyészmérnöki tudomány alapjai (Fundamentals of chemical engineering science). Műszaki Könyvkiadó, Budapest, 1964. p. 328.
12. FROST, A. A., PEARSON: Kinetics and Mechanism. A Study of Homogeneous Chemical Reactions. New York, London, 1953. p. 183.
13. EGLOFF, G., THOMAS, C. L., LINN, C. B.: Ind. Eng. Chem. **28,** 1283 (1936).
14. SACHANEN, A. N.: Conversion of Petroleum. Reinhold Publ. Corp., New York, 1948. p. 17.
15. STEACIE, E. W. R.: Free Radical Mechanism. Reinhold Publ. Corp., New York, 1946. p. 70.
16. LAIDLER, K. J.: Chemical Kinetics. McGraw-Hill, New York, Toronto, London, 1950. pp. 255, 234.
17. DINCES, A. J., FROST, A. V.: Dokl. Akad. Nauk. SSSR. **3,** 510 (1934); Zh. Obshch. Himii **3,** 747 (1933).
18. STUBBS, F. J., HINSHELWOOD, F. R. S.: Proc. Roy. Soc. **A 200,** 458 (1950).
19. SAGERT, N. H., LAIDLER, K. J.: Canad. J. Chem. **41,** 848 (1963).
20. STJEPUHOVICH, A. D., CHAJKIN, A. M.: Zhurn. Fiz. Him. **27,** 1737 (1953).
21. VOJEVODSKIJ, V. V., POLTORAK, V. A.: Dokl. Akad. Nauk. SSSR. **9,** 585, 589 (1953).
22. PURNELL, J. H., QUINN, C. P.: Nature **189,** 656 (1961).

23. STEACIE, E. W. R., PUDDINGTON, J. E.: Can. J. Res. **16,** 176 (1938).
24. SANDLER, S., YU-HO CHUNG: Ind. Eng. Chem. **53,** 391 (1961).
25. YUI-LOONG WANG, RINKER, R. G., CORCORAN, W. H.: Ind. Eng. Chem. Fundamentals **2,** No. 3, 161 (1963).
26. SIMON, F., SZEPESY, L., FÁY, L.: Paper read on the Conference on the Chemistry and Chemical Technology of Petroleum and Natural Gas. Budapest, September 29—October 3, 1965.

Vendel ILLÉS; Veszprém, Wartha V. u. 2—4, Hungary

Acta Chimica Academiae Scientiarum Hungaricae, Tomus 59 (1), pp. 57—66 (1969)

INVESTIGATION OF THE MOLECULAR WEIGHT DISTRIBUTION OF POLYALKYLMETHACRYLATES BY ADSORPTION CHROMATOGRAPHY

F. SIMON

(Hungarian Oil and Gas Research Institute, Veszprém)

Received September 15, 1967

A method has been developed for the determination of the molecular weight distribution of the active component in polymer lubricating oil additives, by means of adsorption chromatography.

The separation of the polymer part from the diluent oil and its fractionation according to molecular weights were carried out in two steps, using silica gel as the adsorbent.

The method can be applied as a qualifying examination in research and industry.

Introduction

The effectivity of high molecular weight polymers used as additives in lubricating oils and the change of effectivity with time depend considerably on the average molecular weight and the distribution of the molecular weight of the active component. In lubricating oils containing components of excessively high molecular weight, degradation due to mechanical and thermal stresses, when the oils are used in recirculation lubrication systems, may give rise to a rapid decrease of the initial high viscosity and viscosity index, with a corresponding deterioration of the quality of the oil. The data obtainable by the methods of measuring mechanical stability (shear proofness) are satisfactory from the point of view of lubrication technique, but they are not applicable to exact theoretical investigations.

Alkyl methacrylate polymer additives are usually marketed diluted with lubricating oils of low viscosity. The percentage and molecular weight of the active component are usually unknown, thus, regarding quality, besides viscosity data we have to rely exclusively on the results of mechanical tests.

For the separation of the polymer, oil, and the inactive part, an adsorption chromatographic method has been developed by VÁMOS and SIMON [1, 2], based on the selective separating power, according to molecular weights, of silica gel having a suitable pore structure.

There are many publications in the literature dealing with the separation of organic polymers into fractions of different molecular weights. GEISELER et al. have published data concerning the adsorption fractionation and investigation of the molecular weight distribution of polyethylene [3, 4] and polypropylene [5]; by chromatography and subsequent measurements of the molecular

weights, carried out on polymers in the range of molecular weights from 500 to 3000, the integral and differential curves of mass distribution were determined. The molecular weight distribution in silicones was studied by BANNISTER, PHILLIPS and WILLIAMS [6] on a column of active charcoal, by a method using gradient elution. LOSSIKOV, KAVERINA and FEBANTZEVA [7] fractionated polyisobutylenes, using active charcoal and silica gel adsorbents. Methods have been developed for the fractionation by precipitation chromatography, and for the determination of the molecular weight distribution of polystyrene by BAKER and WILLIAMS [8]; the same work was done by WEAKLY, WILLIAMS and WILSON [9] for polymethylmethacrylate, and by MOCHEL, NICHOLS and MIGHTON for neoprene [10]. There are several papers reviewing this field [11, 12].

The methods available for the determination of the average molecular weights of the respective fractions supply data of either the number average, or weight average, or viscosity average molecular weights. According to Staudinger's law, a direct relation can be found between the molecular weight and the viscosity of dilute solutions of macromolecules. The average molecular weight measured by this method is the so-called viscosity average.

Among the wide-spread methods, there are such that are applicable to wide ranges and yield a high accuracy [9, 13, 14], and quick ones, suitable for relative comparison.

Among these latter, PATOLOFSKY's [15] method is especially suitable for measurements related to examinations of molecular weight distribution, calculating the molecular weight from the viscosity determined in toluene solutions of the polymer. His empirical relation gives results of satisfactory exactness in the molecular weight range of 1000 to 100 000:

$$\overline{M}_v = \frac{\left(\frac{v}{v_0} - 1\right) \cdot 10^3}{3 \cdot 436 \cdot C} \tag{1}$$

Experiments and results

Method

The determination of the molecular weight distribution in the active part of polymer additives diluted with lubricating oils, requires three different operations:

(1) Separation of the polymer component of the additive from the diluent oil and impurities.
(2) Fractionation of the polymer according to molecular weights.
(3) Measurement of the molecular weights of the different fractions.

In our experiments, the fractionation by adsorption chromatography, as the first part of the determination of the molecular weight distribution, was carried out by gradient elution.

The apparatus used is shown in Fig. 1.

At the beginning of the operation, the solvents are filled in the charging funnel and the blending vessel, respectively. Simultaneously with the setting-on

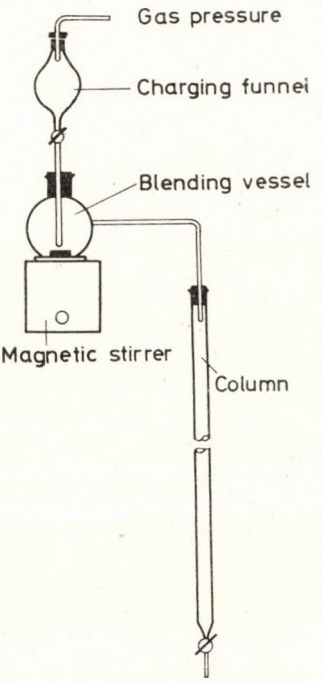


Fig. 1. Gradient elution chromatographic apparatus

of the stream from the mixer into the column, the mixer and the charging funnel are connected, and the magnetic stirrer is then put into motion. The changes in concentration of the solvent mixture entering the chromatographic column are expressed by Eq. (2) [16]:

$$C_e = C_2 - (C_2 - C_1) \cdot e^{-\frac{v}{V}} \tag{2}$$

In our case, $C_1 = 0$ and $C_2 = 100$.

The procedure of separation is the following: 110 g of activated wide-pored silica gel foith a particle size of 0.18—0.58 mm is poured into a glass column having an inside diameter rf 1.1—1.2 cm, and it is shaken to obtain a compact bed, which is then wetted with gasoline wee of aromatics. 5 g of the polymer is dissolved in 30 ml of aromatic-free gasoline and poured on top of the column. The blending vessel is connected with the column and filled up to the brim with the same gasoline. At the same time, 300 ml of benzene is filled into the charging fun-

nel, the stopcock separating the two vessels is opened, and the mixer is put into motion. The flow velocity of the eluate is adjusted to a value of 2 ml/min, by means of controlling the gas pressure. When the benzene has run out from the charger, it is refilled with 400 ml of methanol. The eluate leaving the column is collected by fractions of 20 ml each, then the solvent is gently evaporated on a water-bath in the presence of an inert gas, and the residue is weighed.

The trend of change of the eluent concentration as a function of the volume leaving the blending vessel is shown in Fig. 2.

The determination of the molecular weights of the solvent-free fractions was carried out in toluene solution, by viscosity measurements [15]. The kinematic viscosities of the solutions having a polymer concentration of 5—6 g/l, were measured using a modified Ostwald viscosimeter, at 50 °C, and the average molecular weight was calculated from Eq. (1).

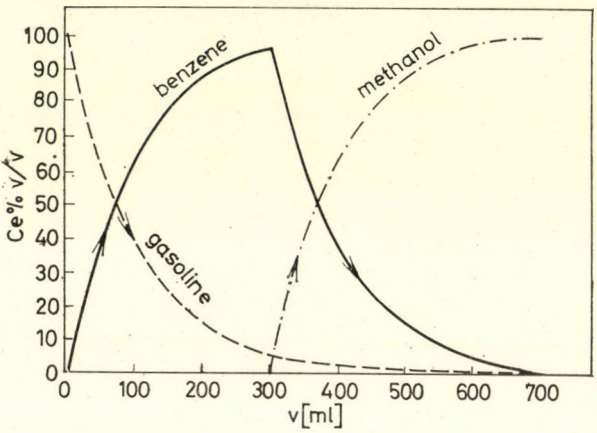


Fig. 2. Changes in the concentration of the eluent

From the average molecular weight of the fractions — in the knowledge of their weight— an integral distribution curve can be plotted. By graphical derivation, a differential distribution curve can be drawn from it, whose maximum gives the most probable value of the average molecular weight. The peak-width measured at the half-maximum of the differential distribution curve, the so-called "half-maximum width value", $M_{v1/2}$, is characteristic of the molecular weight homogeneity of the polymer, and of the molecular weight distribution, and it can be used as a qualifying index.

Model substances

In the course of the experiments, preliminary polycetylmethacrylate block polymers, prepared in the laboratory without diluent oil, were examined by the method described above. The molecular weight distribution was determined and the reproducibility of the test examined.

The data of one of the tests on a polymer product denoted by E_1 are shown in Table I. The integral and the differential molecular weight distribution curves can be seen in Figs 3a and 3b.

The average molecular weights and the half-maximum width values determined from 3 examinations by means of the differential distribution curves and the data characteristic of the reproducibility are contained in Table II.

Table I

Molecular weight distribution of block polymer E_1

Weight: 5.4997 g

No.	Weight [g] of fraction	Percentage [w%] of fraction	v_0 [cSt/50°]	C [g/ml]	v [cSt/50°]	$\bar{M}_v$	$\bar{M}_v^*$	$M_{v1/2}$
4.	0.9256	16.8		0.0053	1.2403	76 050		
5.	1.2305	22.4		0.0053	1.1830	70 048		
6.	1.1583	21.1		0.0053	1.1093	62 247		
7.	0.8193	14.9		0.0057	1.1321	60 863		
8.	0.2624	4.7	0.5179	0.0053	0.9973	50 463	67 500	19 000
26—28.	0.1000	1.8		0.0053	0.6332	12 111		
29—30.	0.1135	2.1		0.0053	0.6028	8 892		
31.	0.3159	5.8		0.0053	0.5524	3 600		
32.	0.2344	4.2		0.0053	0.5482	3 164		
Total	5.1599	93.8						

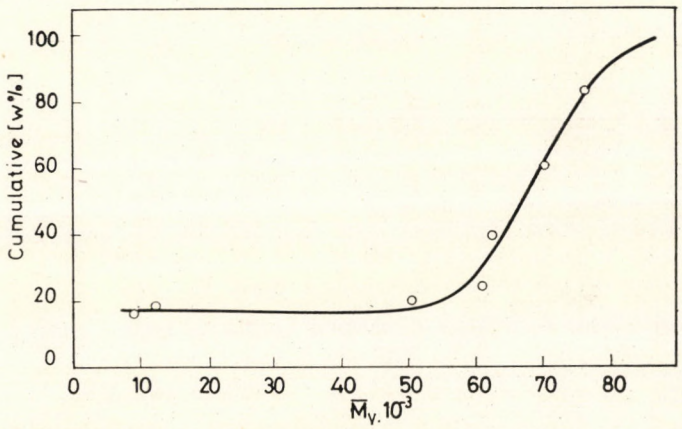


Fig. 3a. Integral molecular weight distribution of block polymer E_1

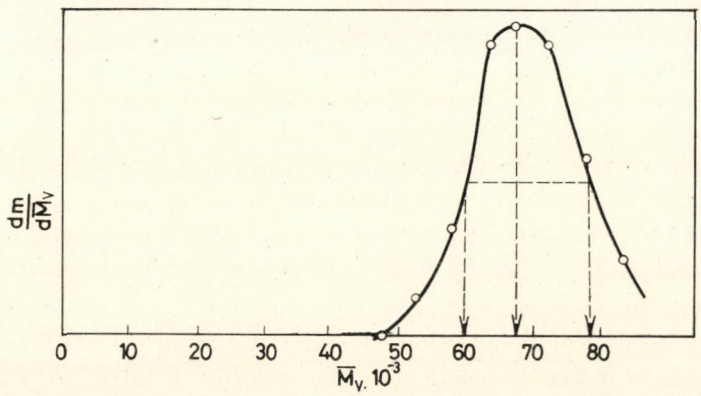


Fig. 3b. Differential molecular weight distribution of block polymer E_1

Table II

Reproducibility of the testing method

M_v 1/2	Average	Maximum deviation from mean value	$M_{v1/2}$	Average	Maximum deviation from mean value
70 000			21 500		
67 500	67 666	2334	19 000	20 000	1500
65 500			19 500		

The reproducibility of the average molecular weight measurement is $\pm$ 3—4%, and of the determination of the half-maximum width value $\pm$ 7—8%.

The fractionation data as well as the results of the determination of the molecular weight distribution for the block polymer E_2 are contained in Table III. The distribution curves are shown in Figs 4a and 4b.

Table III

Molecular weight distribution of block polymer E_2

Weight: 5.5426 g

No.	Weight [g] of fraction	Percentage [w%] of fraction	ν_0 [cSt/50°]	C [g/ml]	ν [cSt/50°]	$\bar{M}_v$	$\bar{M}_v^*$	$M_{v1/2}$
1—3.	0.1537	2.8		0.0053	0.7030	19 460		
4.	1.7652	31.8		0.0054	0.7005	19 047		
5.	1.3676	24.7		0.0061	0.7158	18 347		
6.	0.6413	11.5		0.0062	0.7123	17 581		
7.	0.1721	3.1		0.0053	0.6740	16 556		
8—11.	0.0745	1.3	0.5179	0.0048	0.5707	6 160	18 625	500
21.	0.1017	1.9		0.0052	0.5676	5 278		
22.	0.0706	1.3		0.0054	0.5645	4 769		
23.	0.0957	1.7		0.0053	0.5546	3 831		
24.	0.0862	1.5		0.0055	0.5553	3 809		
25—26.	0.1153	2.1		0.0053	0.5497	3 331		
27.	0.6580	11.9		0.0053	0.5275	983		
Total	5.3019	95.6						

After polymerization, this polymer was dissolved in petroleum ether, and the highest molecular weight fraction was precipitated by refrigeration, in order to study its effect on the distribution curve, for checking the sensitivity of the method. As shown in Fig. 4b, as it was expected, the resulting distribution is in a narrower range and asymmetrical.

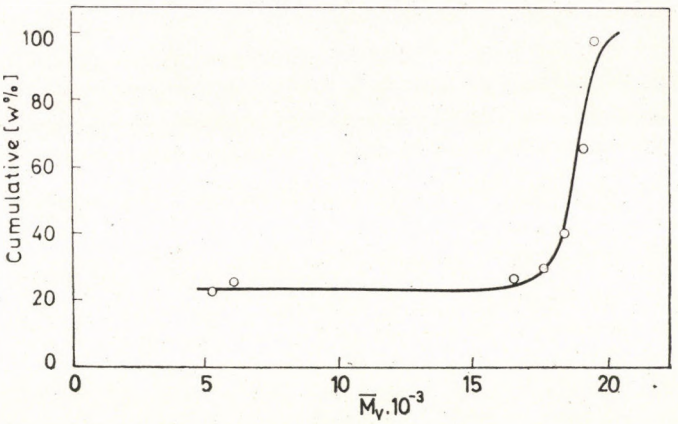


Fig. 4a. Integral molecular weight distribution of block polymer E_2

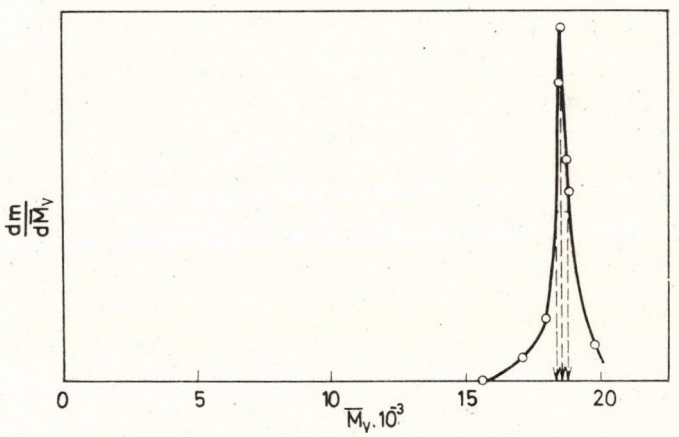


Fig. 4b. Differential molecular weight distribution of block polymer E_2

Lubricating oil additives

For the determination of the molecular weight distribution in the polymer part of commercial lubricating oil additives, the method discussed above needs certain amendments. The polymer product diluted with oil is separated into three parts by the method described in previous publications [1, 2], these parts being the oil, the polymer fractions and impurities (monomer+oligomers+unreacted substances). The polymer fractions are combined and fractionated according to molecular weight, using the method described in this paper, and the average molecular weights of the fractions are determined by viscosity measurements in toluene solution.

By this method we investigated the molecular weight distribution in the active matter of commercial polycetylmethacrylate additives. The integral and differential distribution curves for two additives can be seen in Figs 5a, 5b and 6a, 6b. Compared with the block polymer, the molecular weight distribu-

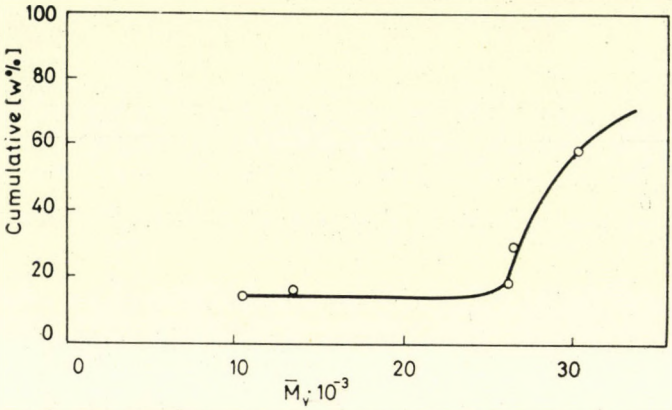


Fig. 5a. Integral molecular weight distribution of additive *A*

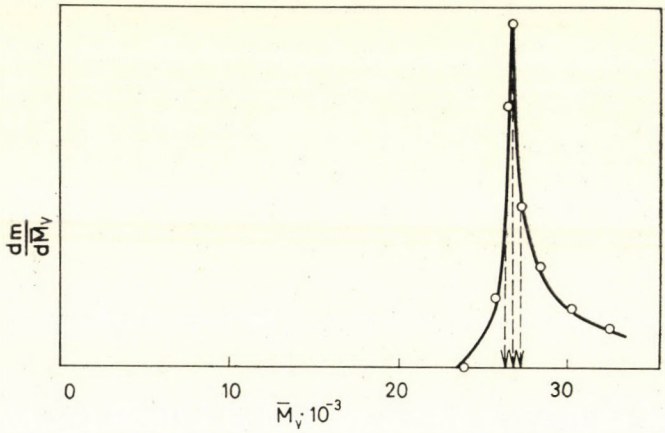


Fig. 5b. Differential molecular weight distribution of additive *A*

tion in these two polymers is narrower, which shows the essential difference between the polymerization in block and in solution.

Discussion

Based on earlier experiences [1] obtained in the chromatography of polymers, we concluded that, under suitable circumstances, silica gel adsorbent might also be useful to effect separations according to molecular weights. The

difference in the adsorption activities of polymer molecules being negligibly small, significant results could not be expected from this type of interactions. However, using silica gel of suitable particle and pore sizes, we succeeded, at

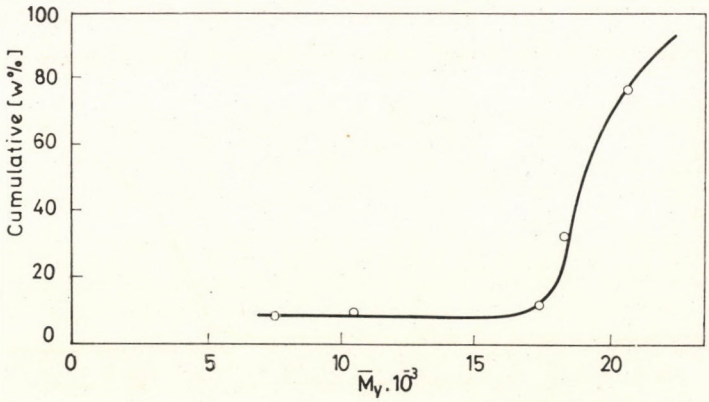


Fig. 6a. Integral molecular weight distribution of additive *B*

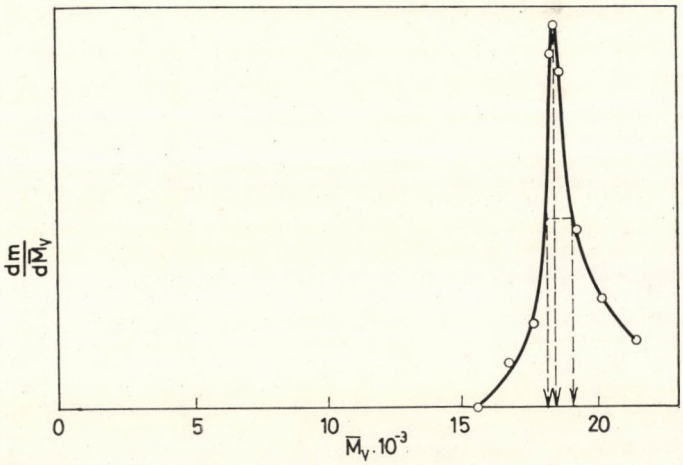


Fig. 6b. Differential molecular weight distribution of additive *B*

a given dilution and flow rate, to obtain fractions of different average molecular weights.

In the order of elution, the fractions show decreasing molecular weights of their polymer contents. This suggests that in the process of separation a phenomenon resembling the action of molecular sieves is involved. The influence of gradient elution manifests itself by the fact that the use of solvent mixtures of gradually increasing eluting power causes the broadening of the front of the lower molecular weight components, which diffuse into the pores, and the front develops only at a moderate velocity.

The separation will be the combined result of a "molecular sieve" action and elution chromatography; for this reason, compared with the widely used solvent precipitation method [17], the fractionation is faster and better.

*

The author wishes to express his thanks to Professor M. FREUND, director of the Institute, for his readiness to help in this work.

List of symbols

C	concentration of the polymer in the solution, [g/ml]
C_e	concentration of the eluent placed into the charging funnel, in the mixture leaving the blending vessel, at a given moment, [% *v/v*]
C_1	initial concentration of the stronger eluent in the blending vessel, [% *v/v*]
C_2	initial concentration of the stronger eluent in the charging funnel, [% *v/v*]
$\overline{M}_v$	viscosity average molecular weight
$M_v{}^1/_2$	peak-width at the half-maximum of the differential distribution curve
$\overline{M}_v^*$	the most probable value of the average molecular weight from the differential distribution curve
v	volume of the mixture which has left the blending vessel, up to a given moment, [ml]
V	volume of the blending vessel, [ml]
v_0	kinematic viscosity of toluene, [cSt/50 °C]
ν	kinematic viscosity of the solution, [cSt/50 °C]

REFERENCES

1. VÁMOS, E., SIMON, F.: Acta Chim. Acad. Sci. Hung. **27,** 335 (1961).
2. VÁMOS, E., SIMON, F.: Papers of Hungarian Oil and Gas Research Institute **4,** 28 (1964).
3. GEISELER, G., HEROLD, H., RUNGE, F.: Erdöl u. Kohle **7,** 357 (1954).
4. GEISELER, G., JUNGHANS, W.: Erdöl u. Kohle **8,** 786 (1955).
5. GEISELER, G., BAUMANN, H. P.: Z. Elektrochem. **62,** 209 (1958).
6. BANNISTER, D. W., PHILLIPS, C. S. G., WILLIAMS, R. J. P.: Analyt. Chem. **26,** 1451 (1954).
7. LOSSIKOV, B. V., KAVERINA, N. I., FEBANTZEVA, A. A.: Khim. i Tekhnol. Topliv i Masel **3,** 51 (1956).
8. BAKER, C. A., WILLIAMS, R. J. P.: J. Chem. Soc. **1956,** 2352.
9. WEAKLY, T. J. R., WILLIAMS, R. J. P., WILSON, J. D.: J. Chem. Soc. **1960,** 3963.
10. MOCHEL, W. E., NICHOLS, J. B., MIGHTON, C. J.: J. Am. Chem. Soc. **70,** 2185 (1948).
11. SCHNEIDER, N. S.: Analyt. Chem. **33,** 1829 (1961).
12. SAMSONOV, G. V.: Usp. Khim. **30,** 1410 (1961).
13. STAUDINGER, H.: Organische Kolloidchemie, 3rd Ed., Vieweg, Braunschweig, 1950. p. 137.
14. CHIEN JEN JUAN, SHIH LIANG HO: Z. phys. Chem. **207,** 60 (1957).
15. PATOLOVSKY, L. A.: Examination of Polymers. (Documentation of the VNIINP) Moscow, 1958.
16. BOCK, M. R., LING NAN SING: Analyt. Chem. **26,** 1543 (1954).
17. FLORY, P. J.: Principles of polymer chemistry, Cornell University Press, New York, 1953. p. 342.

Ferenc SIMON; Veszprém, Wartha V. u. 1, Hungary

Acta Chimica Academiae Scientiarum Hungaricae, Tomus 59 (1), pp. 67—73 (1969)

THE DISSOCIATION OF VARION CH ION EXCHANGE RESIN

I. BÁLINT-AMBRÓ

(Research Institute for the Heavy Chemical Industry, Veszprém)

Received December 30, 1967

The dissociation properties of Varion CH ion exchange resin were studied by infrared spectroscopy. It was attempted to determine the ionic forms which participate in the dissociation equilibrium caused by the moisture content of the air-dried resin, by analyzing the positions of the antisymmetric stretching vibration bands of the carbonyl groups in the Na and H forms of the resin.

Some recent communications on ion exchange resins have discussed, in addition to the use and application, the dissociation properties of resins having a structure similar to that of Varion CH (aminopolycarboxylic resins) [1, 2]. The equilibrium dissociation constants were determined either potentiometrically [1], or by isotope analytical methods in systems of aqueous solutions.

Our investigation of the thermal properties and stability of Varion CH resins [3] indicated a considerable moisture content in the air-dried resin. A fraction of this water is very strongly bound; the H form of Varion CH will lose the last molecule of water (calculated per ion exchange group) only at 250°. The loss of this water is preceded by the loss of a considerable quantity of water bound adsorptively or by capillary forces within the pores, this quantity being dependent on the moisture content of the ambient air and on the temperature. An air-dried resin may contain, on the average, 10—16% of moisture. The work to be described below is based on the assumption that this moisture content may lead to electrolytic dissociation of the resin; an attempt was made to determine the various dissociated forms, that is to detect the ionic forms which participate in the dissociation equilibrium.

The skeleton of Varion CH resin is a styrene–divinylbenzene copolymer containing $-CH_2-N=(CH_2-COOH)_2$ ion exchange groups. Fig. 1 shows the possible dissociation process and the resulting ionic forms, R being the resin matrix. It appears from Fig. 1 that the COOH group may participate in the dissociation process, and the nitrogen is protonated. It is obvious that an acid medium will promote protonation and repress the dissociation of the carboxyl groups, whereas alkaline pH favours the dissociation of the latter. In air-dried resins, the limited moisture content gives rise to a relatively concentrated solution, in which dissociation may be suppressed. In fact, the system should be regarded as a gel which must not be disturbed by the examination of the dissociation forms, therefore, a test method is required which will not upset dissocia-

tion equilibrium. Infrared spectroscopy seemed to be a suitable method, provided the dissociation forms can be recognized from change in the spectrum. Buffering, as used in the examination of dissociation processes, had to be omitted in this case. Instead of this, the exchangeable ion of the resin was altered in a way to obtain a possibly simple dissociation process in the "solution" formed with the counter-ion. In these experiments Varion CH was used in the H or Na form,

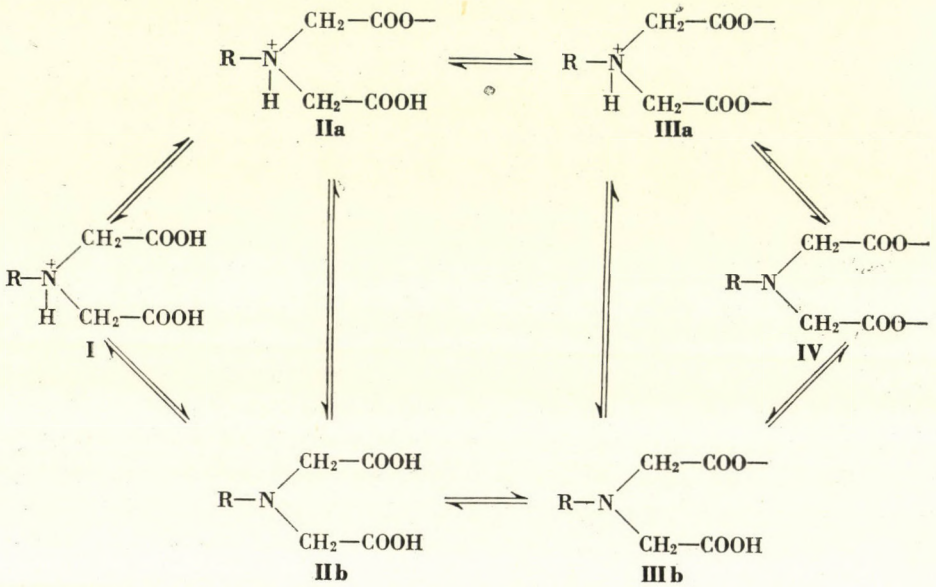


Fig. 1. Dissociation of Varion CH ion exchange resin

in other words the carboxyl groups were present as COOH, or COONa, respectively.

It is expected that the dissociation processes shown in Fig. 1 may cause changes in the parts of the spectrum due to the carboxyl groups, mainly in the position of the stretching vibration band of the CO group, whose high molar absorption coefficient is well known. The assessment of the dissociation forms from the spectra is hindered by the six possible dissociation forms of the iminodiacetic acid group, several of which may be simultaneously present in a certain dissociation equilibrium. By shifting the dissociation equilibrium in the direction of one or other ionic form, it is possible to assess the bands assigned to the extreme ionic forms (Fig. 1, **I** and **IV**). In these experiments, the resin in the Na form was considered as one of the extremes, where, as a result of the hydrolysis of the —COONa-group, the pH will be higher than 10, and a spectrum characteristic of ionic carboxyl may be expected. Examination of the resin in the

H form is hindered by the fact that at lower pH values the dissociation of the COOH group and the protonation of N are associated processes.

BUSCH and BAILAR [4, 5] studied the dissociation properties of aminopolycarboxylic acids by means of infrared spectrophotometry. From the infrared spectrophotometric patterns of ethylenediamine tetraacetic acid and its complexes, they worked out a method for the determination of both the ligand dissociation and the number of ligands coordinated to the central atom. They determined the dissociation form from the position of the antisymmetric stretching vibration band of the carbonyl group. The method is based on the observation that the position of ν_{as}CO depends on the ionic character of the bond between the carbonyl group and the counter-ion. BUSCH *et al.* found that un-ionized and un-coordinated COO groups can be distinguished from the free ionized COO groups in the spectra of the compounds under investigation: ν_{as}CO for the un-ionized and un-coordinated COO lies in the range between 1750 and 1700 cm^{-1}, whereas for coordinated COO this band is in the range 1650—1590 cm^{-1}. The position of the band depends also on the coordinated metal, which finally determines the ionic character of the bond.

In a study of the dissociation of iminodiacetic acid and nitrilotriacetic acid by the method of BUSCH and BAILAR [4, 5], NAKAMOTO succeeded in assigning the spectra to the corresponding dissociation forms. NAKAMOTO [6, 7] used solutions of iminodiacetic acid in D_2O in this infrared spectrophotometric studies to avoid interference from water in the higher wavenumber region of the spectrum. As NAKAMOTO's results have been used in the present work we wish to describe his experimental conditions in greater detail, since iminodiacetic acid, in first approximation, may be considered analogous to the ion exchange group of our resin.

NAKAMOTO adjusted the pH of the solutions to six values: 0.4, 1.1, 2.2, 4.1, 7.5 and 10.9. The spectra of these solutions showed a shift of the wavenumber of ν_{as}CO as a function of the pH. With increasing pH, the band was shifted in the direction of the lower wavenumbers, and in the pH range where ionic and associated carboxyl might be present together two bands appeared in the spectrum. At extreme pH values the intensities of these bands had a maximum and minimum value, respectively. The spectrum of the pH 10.9 solution had only one band in the 1800—1500 cm^{-1} range. Solutions with lower pH showed this band with gradually decreasing intensity, and shifted higher frequencies. The band indicating the presence of undissociated carboxyl was absent even in the spectrum of the solution of pH 4.1, and appeared only at pH 2.2. The intensity of this band gradually increases as the pH is decreased and shifted higher frequencies can be observed. BUSCH [4] claims that products containing hydrogen bands between the undissociated COOH groups may also cause a certain absorption, whereas according to NAKAMATO [7] protonation of the nitrogen results in a further shift of the position of the ν_{as}CO band, since the $[>\overset{+}{N}-CH_2COO]$ group

absorbs in the 1630—1620 cm^{-1} range, and the [$>NH-CH_2-COO$] group (with non-protonated N) between 1585 and 1575 cm^{-1}.

On the analogy of NAKAMOTO's results obtained for iminodiacetic acid, we attempted to determine the dissociation forms and equilibria which correspond to Fig. 1, by the infrared spectra of the H and Na forms of Varion CH resin. This approach seemed to be reasonable, since the dissociation constant of iminodiacetic acid is quite close to that of Dowex AI resin which has a structure analogous to Varion CH ($pK_a = 2.54$ and 2.30, respectively [1, 2]).

Experimental

Varion CH ion exchange resin was prepared in the Research Institute for Plastics Industry, Budapest, by their own method [8]. The matrix of the bead resin is a styrene–divinylbenzene copolymer. The capacity of the resin, determined partly from its nitrogen content and partly from complex formation with Cu(II) ions, was found to be 2.35 mmoles/g. The resin was treated first with dilute hydrochloric acid, then with sodium hydroxide, followed by thorough washing with water deionized by ion exchange, dried to constant weight at 105°, and allowed to cool in a desiccator. Samples of 8—10 mg were compressed to tablets with 800 mg of potassium bromide for infrared spectrophotometry. The spectra were taken with a Zeiss IR-10 recording spectrophotometer.

Discussion

Fig. 2 shows the infrared spectra of the resin. Spectrum *1* is that of the resin matrix, polystyrene, which was recorded for the identification of the bands due to the matrix. Spectra *2* and *3* are those of the H and Na forms of Varion CH. These two latter spectra could not be evaluated beyond 1800 cm^{-1}, because of the absorption caused by the moisture content of the sample. There is a considerable difference between the two spectra in the range between 1800 and 1400 cm^{-1}. This range includes the stretching vibration bands of the CO group ($\nu_s CO$ and $\nu_{as} CO$).

In the spectrum of the Na form (Fig. 2 Spectrum *3*) three relatively intense and broad absorption bands appear in the range between 1800 and 1200 cm^{-1}, namely at about 1600, 1555 and 1400 cm^{-1}. The first two are of identical intensity; the third is due to a somewhat more intense absorption. A comparison with the spectrum of the matrix shows that the band due to the monosubstituted aromatic ring (δCH) is to be expected in this region, at about 1600 cm^{-1}. In Varion CH resin this band appears with increased width towards the region of wavenumbers higher than 1600 cm^{-1}, as a result of the absorption due to the dissociated ion exchange group $-\overset{+}{N}H-CH_2-COO-$, containing a protonated nitrogen. This is in agreement with NAKAMOTO's findings with iminodiacetic acid.

The absorption at 1555 cm^{-1} corresponds, when BUSCH's method is used, to the antisymmetric stretching vibration band of CO ($\nu_{as} CO$), in the dissociated

carboxyl group, while the band at 1400 cm^{-1} is the symmetric stretching vibration band of the carbonyl group ($\nu_s CO$). If undissociated carboxyl were present this would be indicated by an absorption band at 1700 cm^{-1}.

The above facts seem to indicate the presence of dissociated carboxyl and protonated nitrogen under the experimental conditions used. Without attempting to draw conclusions on the concentration of the various ionic forms in the dissociation equilibrium, such an equilibrium may be assumed between the

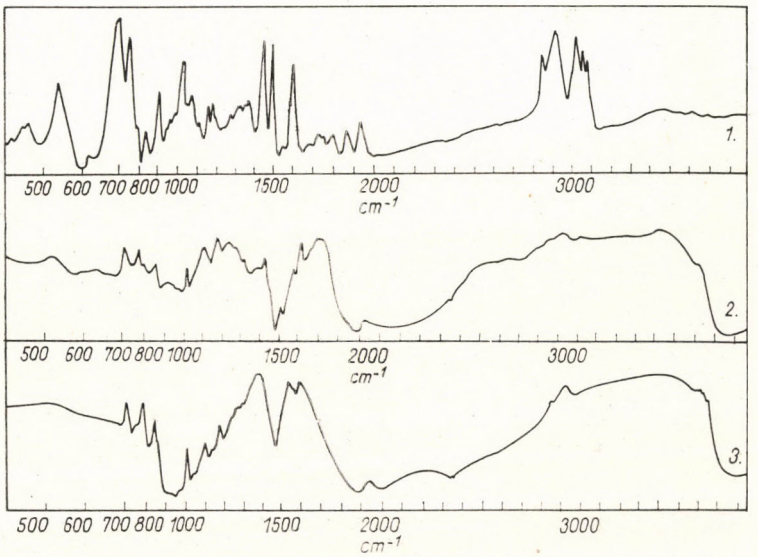


Fig. 2. Infrared spectra: (1) polystyrene (matrix); (2) Varion CH resin, H form; (3) Varion CH resin, Na form

states **IIIa** and **IV** in Fig. 1 in the case of the air-dried Na-form Varion CH resin. Comparing this with NAKAMOTO's results on iminodiacetic acid, a similarity may be detected to the dissociation equilibrium observed at pH > 10.

In the region below 1800 cm^{-1} in the spectrum of the H form of Varion CH it is the band in the vicinity of 1700 cm^{-1} which provides some important information on the dissociation of the carboxyl groups. According to BUSCH [4], the absorption of undissociated carboxyl groups and of the hydrogen bonds between these groups occurs in the wavenumber range below 1800 cm^{-1}, thus the absorption at 1700 cm^{-1} should be attributed to undissociated COOH groups.

Comparing the position intensity of the relatively weak absorption band at 1615 cm^{-1} with the spectrum of the matrix, a slight shift may be observed. The presence of protonated nitrogen and dissociated COO^- would have caused a broader band, thus the presence of $\overset{+}{N}H-CH_2-COO^-$ is not confirmed, but the band could perhaps be assigned to the deformational and stretching vibra-

tions of the matrix. The band at 1578 cm^{-1} may perhaps be assigned to the iminodiacetic acid groups with non-protonated nitrogen, but containing dissociated carboxyl groups.

Presumably due to substitution, the band at 1513 cm^{-1} is slightly shifted compared to its position in the matrix spectrum (1495 cm^{-1}). Aromatic deformational vibrations (δCH) also give rise to an absorption at 1455 cm^{-1} in the spectrum of the matrix which is, however, masked by the ν_sCO vibration of the substituting group on the resin. In the spectrum of the H form only a slight shoulder appears at this wavenumber.

The bands assigned to the dissociated forms are listed in Table I together with NAKAMOTO's data on iminodiacetic acid and the values obtained by BUSCH and BAILAR [4] for EDTA, in view of the fact that the ion exchange groups of Varion CH are analogous to half a molecule of EDTA.

When considering the dissociated forms of Varion CH in the H form in air-dried condition one may assume equilibrium between states **IIb** and **IIIb** in Fig. 1. It was concluded from the results of the experiments with iminodiacetic acid [6, 7] that while iminoacetic groups with protonated and dissociated N could be detected, in addition to the undissociated COOH groups, at lower pH's (pH < 2.2) in the spectrum of iminoacetic acid, in our case the band indicated that the non-dissociated COOH groups may be accompanied by non-protonated, but dissociated groups.

Table I

The position of ν_{as} CO in the infrared spectra of Varion CH resin, iminodiacetic acid and ethylenediamine tetraacetic acid

Substance	—COOH (cm^{-1})	—COO (cm^{-1})	Dissociation form	Ref.
Varion CH	1730			
H form	1690	1578	IIb—IIIb	
Na form	—	1555	IIIa—IV	
Iminodiacetic acid				
pH 0.4	1733	1619		6
pH 2.2	1721	1619		6
pH 4.1	—	1619		6
pH 7.5	—	1619		6
pH 10.9		1575		6
EDTA				
H_4Y	1697			4
Na_2H_2Y	1668	1637		4
Na_4Y		1597		4

Note: Y stands for the acid residue of EDTA.

NAKAMOTO attributed the increasing bond order of CO to the inductive effect of the positive charge of the protonated nitrogen atom, resulting in a shift of the band to higher frequencies. When estimating the bond order of CO in the COOH group of ion exchange resins, the influence of the matrix must also be considered: as a non-polar macromolecule or macro-radical, the matrix may cause a decrease in the bond order of CO, and thus a shift of the position of ν_{as}CO to lower wavenumbers. This may explain the position of ν_{as}CO of the Na-form resin at 1555 cm^{-1}, a wavenumber lower than that of ν_{as}CO in iminodiacetic acid (1575 cm^{-1}) though the latter group is in analogous dissociation state.

The band assigned to the undissociated carboxyl group has a lower wavenumber in the case of the Varion CH resin in the H form in the case of iminodiacetic acid; this again may be attributed to the influence of the resin matrix.

*

The experiments described here were carried out in the Institute of Special Analyses of the Technical University of Dresden, G.D.R. I should like to thank the Head of the Institute, Prof. Dr. habil. E. STEGER for permitting this work and for his interest and support in the evaluation of the spectra.

I wish to thank also Dr. J. MIKES and Dr. J. SZÁNTÓ, both of the Research Institute for the Plastics Industry, Budapest, for preparing the resin samples.

REFERENCES

1. LEYDEN, D. E., UNDERWOOD, A. L.: J. Phys. Chem. **68,** 2093 (1964).
2. MARINSKY, J. A., KRASNER, J.: Radioisotopes in the Physical Sciences and Industry, IAEA, Vienna, 1962. p. 503.
3. AMBRÓ, I.: "On the swelling of a chelate-forming ion exchange resin". Paper presented at the 3rd Transdanubian Analytical Conference, Szombathely, August 10, 1967 (In Hungarian); Magyar Kémikusok Lapja, **1968,** 250 (In Hungarian).
4. BUSCH, D. H., BAILAR, J. C.: J. Am. Chem. Soc. **78,** 716, 5178 (1956).
5. BUSCH, D. H.: J. Am. Chem. Soc. **75,** 4574 (1953).
6. NAKAMOTO, K.: J. Am. Chem. Soc. **84,** 2081 (1962).
7. NAKAMOTO, K.: Infrared Spectra of Inorganic and Coordination Compounds, John Wiley and Sons, Inc. New York, London, 1963. p. 160.
8. SZÁNTÓ, J., MIKES, J.: Kolorisztikai Értesítő, **1964,** 239 (In Hungarian).

Irén BÁLINT-AMBRÓ; Veszprém, Wartha Vince út 1—3, Hungary

Acta Chimica Academiae Scientiarum Hungaricae, Tomus 59 (1), pp. 75—83 (1969)

HARMONIC FORCE FIELD REFINEMENT CALCULATIONS FOR POLYATOMIC MOLECULES, III

NORMAL COORDINATE ANALYSIS OF THE e'' SPECIES OF CYCLOPROPANE

L. NEMES

(Central Research Institute for Chemistry of the Hungarian Academy of Sciences, Budapest)

Received January 15, 1968

Force field calculations are reported for the e'' species normal vibrations of cyclopropane and d_6-cyclopropane, utilizing the Coriolis ζ constants derived from gas-phase Raman band contours by MATHAI *et al.* It is concluded that of the two alternative values for ζ^z_{14}, —0.29 and —0.86, the former should be rejected, while the latter seems to be acceptable. It is shown that both the vibrational forms and the force field are very sensitive to the Coriolis ζ constants. Refinement calculated ζ constants are reported for C_3D_6.

Introduction

There have been several attempts at the determination of the molecular force field of cyclopropane. Thus SAKSENA [1], GÜNTHARD, LORD and MCCUBBIN [2], and CYVIN [3] have all reported the force field analysis of this molecule. Precise structural data have recently become available from high resolution Raman spectroscopy of C_3H_6 and C_3D_6, reported by MATHAI, SHEPHERD and WELSH [4], and later by JONES and STOICHEFF [5]. BASTIANSEN and TRAETTEBERG also reported structural data obtained from gas-phase electron diffraction [6]. In the present paper we report normal coordinate calculations for the solely Raman active e'' species of cyclopropane and d_6-cyclopropane. These calculations utilize normal frequency data as well as Coriolis ζ constants in the e'' species obtained for C_3H_6 by MATHAI, SHEPHERD and WELSH [4].

Molecular geometry

The data reported by JONES and STOICHEFF [5] were used in our calculations. These are the following: $r(C-C) = 1.514$ Å; $r(C-H) = 1.082$ Å; and $\sphericalangle HCH = 116.5°$.

The matrix elements of G and C^z were calculated using CYVIN's programmes [7].*

Coordinates and vibrational data

In the present study we have adopted the D_{3h} symmetry coordinates proposed by CYVIN [3]. For the e'' species these are shown in Table I.

* The author would like to acknowledge here the private communications of Professor S. J. CYVIN concerning the optimum choice of Cartesian coordinates in the calculations of C^z.

Table I

Symmetry coordinates for species e″

$$S_{12a} = \frac{1}{\sqrt{12}}(2r_1 - r_2 - r_3 - 2r_1 + r_2' + r_3')$$

$$S_{12b} = \frac{1}{2}(r_2 - r_3 - r_2' + r_3')$$

$$S_{13a} = \frac{1}{\sqrt{2}}\sqrt{RD}\,(\theta_2 - \theta_3)$$

$$S_{13b} = \frac{1}{\sqrt{6}}\sqrt{RD}\,(-2\theta_1 + \theta_2 + \theta_3)$$

$$S_{14a} = \frac{1}{\sqrt{6}}\sqrt{RD}\,(2\xi_1 - \xi_2 - \xi_3)$$

$$S_{14b} = \frac{1}{\sqrt{2}}\sqrt{RD}\,(\xi_2 - \xi_3)$$

In this table R and D stand for the equilibrium values of the bond lengths C—H (C—D) and C—C, respectively. The two angle-deformation coordinates, θ and ξ, are two of the four types introduced by WILSON *et al.* [8], and are related to the coordinates α_{ij} in the following manner:

$$\theta_i = \frac{1}{2}(\alpha_{i1} - \alpha_{i2} - \alpha_{i3} + \alpha_{i4}) \text{ (torsion)}$$

$$\xi_i = \frac{1}{2}(\alpha_{i1} + \alpha_{i2} - \alpha_{i3} - \alpha_{i4}) \text{ (rocking)}$$

The valence coordinates are depicted in Fig. 1.

The vibrational assignment and Coriolis ζ constants used here are taken from the work of MATHAI, SHEPHERD and WELSH [4]. The fundamental frequen-

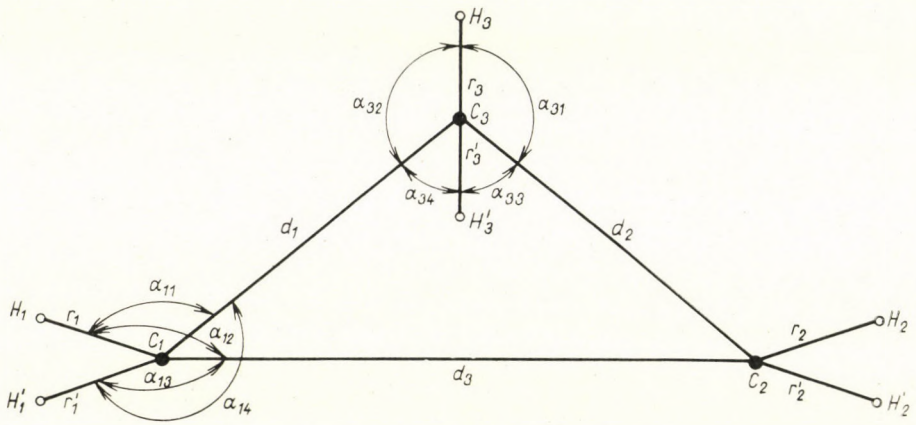


Fig. 1. Valence coordinates for C_3H_6 molecule and axis convention

cies were corrected for anharmonicity by CYVIN [3] using the DENNISON method [9]. Table II contains frequency and Coriolis ζ data. The uncertainties indicated in Table II were used in the normal coordinate analysis. These calculations were done using a general force field refinement programme utilizing least-squares principles, as described in Part I of this series [10].

Table II

Frequency values and Coriolis ζ constants

	C_3H_6	C_3D_6
ν_{12}	3082.2 ± 31	2329.0 ± 23
ν_{13}	1188.0 ± 12	956.8 ± 10
ν_{14}	738.8 ± 7	528.0 ± 5
ω_{12}	3220.8 ± 10	2407.3 ± 10
ω_{13}	1212.2 ± 5	972.5 ± 5
ω_{14}	749.9 ± 5	533.6 ± 5
ζ^z_{12}	0.29 ± 0.05	—
ζ^z_{13}	0.63 ± 0.05	—
ζ^z_{14}	−0.86 / −0.29 ± 0.05	—

Vibrational analysis

The basic goal of these calculations has been to determine which of the two choices for ζ^z_{14} is substantiated by normal coordinate analysis results.

The Coriolis ζ constants in Table II were obtained by gas-phase contour calculations by MATHAI *et al.* [4]. These authors reported that neither of these values gives a good fit to the theoretical symmetric top Coriolis ζ sum rule, since the latter gives −0.027 (this follows from the values of the rotational constants; for C_3H_6: $A'' = 0.4199$ cm^{-1}, $B'' = 0.6696$ cm^{-1}), while one obtains 0.06 and 0.63 for the sum by using the alternative values −0.86 and −0.29, respectively; it is however very probable that the right choice is closer to −0.86. (The alternative values for ζ^z_{14} come from a positive or negative sign choice for $\Delta\nu^{PR}$, the separation of the ^PQ and ^RQ branch maxima.) As we shall see later, the p^{r}esent calculation unequivocally substantiates the choice of $\zeta^z_{14} = -0.86$.

We have tried four possibilities in the normal coordinate analysis, according to the four basic combinations:

Case (*a*): anharmonic/fundamental frequencies, $\zeta^z_{14} = -0.29$
Case (*b*): harmonic/normal frequencies, $\zeta^z_{14} = -0.29$
Case (*c*): anharmonic frequencies, $\zeta^z_{14} = -0.86$
Case (*d*): harmonic frequencies, $\zeta^z_{14} = -0.86$.

Earlier calculations indicated that in order to secure reasonable speed of convergence, either $F_{12,14}$ or $F_{13,14}$ should be constrained to zero. (In fact, utilizing the automatic force field model modification feature built in the programme [10], $F_{13,14}$ is automatically constrained when no oscillation damping is applied.) All the calculations reported here were damped runs using a damping constant

Table III

Converged force field data, errors of the calculated frequencies and Coriolis ζ constants (exp.-calcd.)

Case (*a*)

mdyn/Å	$F_{12,12}$:	5.117 ± 0.383
	$F_{12,13}$:	—0.197 ± 0.392
	$F_{12,14}$:	0 ± 0 (constrained)
	$F_{13,13}$:	0.366 ± 0.063
	$F_{13,14}$:	—0.023 ± 0.042
	$F_{14,14}$:	0.278 ± 0.050

	C_3H_6	C_3D_6
$\Delta\nu_{12}$	—24.2 cm^{-1}	5.76 cm^{-1}
$\Delta\nu_{13}$	— 2.1	1.76
$\Delta\nu_{14}$	— 2.1	1.53
$\Delta\zeta^z_{12}$	0.265	—
$\Delta\zeta^z_{13}$	0.284	—
$\Delta\zeta^z_{14}$	0.284	—

Table IV

Converged force field data, errors of the calculated frequencies and Coriolis ζ constants (exp.-calcd.)

Case (*b*)

mdyn/Å	$F_{12,12}$:	5.366 ± 0.415
	$F_{12,13}$:	—0.425 ± 0.391
	$F_{12,14}$:	—0.192 ± 0.305
	$F_{13,13}$:	0.393 ± 0.078
	$F_{13,14}$:	0 ± 0 (constrained)
	$F_{14,14}$:	0.309 ± 0.046

	C_3H_6	C_3D_6
$\Delta\omega_{12}$	6.79 cm^{-1}	—9.46 cm^{-1}
$\Delta\omega_{13}$	—3.10	5.21
$\Delta\omega_{14}$	—0.43	—1.07
$\Delta\zeta^z_{12}$	0.236	—
$\Delta\zeta^z_{13}$	0.305	—
$\Delta\zeta^z_{14}$	0.292	—

Table V

Converged force field data, errors of the calculated frequencies and Coriolis ζ constants (exp.-calcd.)

Case (*c*)

mdyn/Å	$F_{12,12}$:	5.252 ± 0.058
	$F_{12,13}$:	—0.997 ± 0.062
	$F_{12,14}$:	0 ± 0 (constrained)
	$F_{13,13}$:	0.763 ± 0.049
	$F_{13,14}$:	—0.066 ± 0.007
	$F_{14,14}$:	0.175 ± 0.017

	C_3H_6	C_3D_6
$\Delta\nu_{12}$	—48.60 cm^{-1}	34.09 cm^{-1}
$\Delta\nu_{13}$	7.10	6.13
$\Delta\nu_{14}$	— 0.60	0.42
$\Delta\zeta^z_{12}$	0.122	—
$\Delta\zeta^z_{13}$	0.084	—
$\Delta\zeta^z_{14}$	0.057	—

Table VI

Converged force field data, errors of the calculated frequencies and Coriolis ζ constants (exp.-calcd.)

Case (*d*)

mdyn/Å	$F_{12,12}$:	5.629 ± 0.093
	$F_{12,13}$:	—1.015 ± 0.133
	$F_{12,14}$:	0 ± 0 (constrained)
	$F_{13,13}$:	0.679 ± 0.106
	$F_{13,14}$:	—0.069 ± 0.016
	$F_{14,14}$:	0.217 ± 0.042

	C_3H_6	C_3D_6
$\Delta\omega_{12}$	—19.65 cm^{-1}	28.20 cm^{-1}
$\Delta\omega_{13}$	10.94	—13.07
$\Delta\omega_{14}$	— 1.26	1.78
$\Delta\zeta^z_{12}$	0.133	—
$\Delta\zeta^z_{13}$	0.057	—
$\Delta\zeta^z_{14}$	0.073	—

value: $x = 400$ or 800. From general considerations it seems more preferable to constrain $F_{12,14}$, as it is the interaction term between the antisymmetric CH_2 stretching and CH_2 rocking coordinates; therefore, except for case (*b*), the constraint $F_{12,14} = 0$ was applied in all calculations. In case (*b*), the constraint relation was: $F_{13,14} = 0$. Tables III, IV, V and VI summarize the main results

of the calculations for cases (a)—(d). The $(L^{-1})'$ matrices, characteristic of the vibrational form, are given in Tables VII and VIII, while Table IX shows the comparison of the experimental and calculated Coriolis ζ constants.

Table VII

Comparison of the $(L^{-1})'$ matrices in species e″ for C_3H_6 [a.m.u.]$^{+1/2}$

	0.9452	0.2182	—0.0087
(a)	—0.0280	—0.2433	0.9826
	—0.0185	0.5502	0.2700
	0.9340	0.2602	0.0332
(b)	—0.0680	—0.2202	0.9861
	—0.0564	0.5552	0.2539
	0.9527	—0.0517	0.1752
(c)	—0.1830	0.7073	0.7012
	—0.0078	—0.3286	0.5176
	0.9528	—0.0937	0.1567
(d)	—0.1720	0.5655	0.8223
	—0.0096	—0.4196	0.4470

Table VIII

Comparison of the $(L^{-1})'$ matrices in species e″ for C_3D_6 [a.m.u.]$^{+1/2}$

	1.2510	0.5152	—0.0260
(a)	—0.0244	—0.3422	1.3583
	—0.0461	0.6689	0.4349
	1.2282	0.5672	0.0312
(b)	—0.0777	—0.3333	1.3585
	—0.0955	0.6695	0.4260
	1.2943	—0.2816	0.2764
(c)	—0.2272	0.8699	1.0744
	—0.0239	—0.4247	0.6766
	1.2911	—0.3332	0.2301
(d)	—0.2150	0.7129	1.1867
	—0.0283	—0.5152	0.6103

Discussion

The comparison of the converged force field data for cases (a)—(d) shows that the field significantly depends on the value of ζ^z_{14}. (These are, of course, reflected in the corresponding Jacobian matrix elements, but to save space these

Table IX

Comparison of the calculated and experimental Coriolis ζ constants in species e″ for C_3H_6

	Exp. [4]	(a)	(b)	(c)	(d)
ζ^z_{12}	0.29	0.0248	0.0539	0.1679	0.1572
ζ^z_{13}	0.63	0.3460	0.3246	0.5461	0.5728
ζ^z_{14}	—0.29	—0.5741	—0.5818		
	—0.86			—0.9173	—0.9333

are not reported here.) In the case of anharmonic frequencies, *e.g.* $F_{13,13}$ is doubled when the value —0.86 is used instead of —0.29 for ζ^z_{14}. From the point of arriving at an acceptable set of force constants it is obviously crucial to use the right value for this Coriolis ζ constant. Considering the data in Table IX, the conclusion can be drawn that a reasonable fit to the experimental data can only be obtained if $\zeta^z_{14} = -0.86$ is used in the refinement. This means that *the alternative choice* $\zeta^z_{14} = -0.29$ *should be rejected.* This conclusion is all the more important since Tables VII and VIII show that the (L^{-1}) matrices are also very sensitive to the Coriolis ζ constants. Actually the sensitivity of the force field is the result of the differences brought about in the vibrational forms, as both the root-Jacobian and the Coriolis-Jacobian elements are derived from the L matrix by first-order perturbation calculations [11]. In the case of the C_3H_6 molecule, *e.g.*, when the calculations are fitted to $\zeta^z_{14} = -0.29$, such an (L^{-1}) matrix is obtained which shows strong mixing between the antisymmetric CH_2 stretching and the CH_2 rocking deformation coordinates, while the mixing between the former and the CH_2 torsion coordinate is negligible. Even more interesting is the observation that while for $\zeta^z_{14} = -0.29$ the assignments seem to be reversed for Q_{13} and Q_{14}, $\zeta^z_{14} = -0.86$ leads to the right assignments, although it is obvious that in both normal modes both CH_2 deformation coordinates are heavily mixed. Similar conclusions can be reached for C_3D_6 from Table VIII.

In all the four different calculations ($a \rightarrow d$) the sum of the calculated Coriolis ζ constants is in almost perfect agreement with the theoretical value obtained from the experimental rotational constants, according to the following sum rule:

$$\sum_i \zeta^z_i = \frac{B''}{2A''} - 1.$$

The comparison is shown in Table X.

The very good agreement above is, of course, no guarantee for the correctness of the calculated individual Coriolis ζ constants, it only indicates that the calculations are formally correct.

Table X

Coriolis ζ sum rule values for species e″

C_3H_6		C_3D_6	
Calcd.	Theor.	Calcd.	Theor.
—0.2033	—0.2027	—0.2798	—0.2793

The further question emerges whether a force field derived from the anharmonic or the harmonic frequency data should be accepted as more dependable. Since up till now there is neither experimental nor theoretical proof for the acceptability of the anharmonic corrections, we find it more appropriate to choose case (*c*) as the best alternative (see Table V). This field is not very different, on the first glance, from that given by CYVIN [3], in as much as the diagonal terms are similar in both fields, and $F_{13,14}$ is a small negative quantity in both cases. (CYVIN used only frequency data in his calculations.) We find it significant, however, that our calculations show $F_{13,14}$ to be a relatively large negative quantity as opposed to CYVIN's field for which it is assumed to be zero. We would also like to point out that the force field calculated by GÜNTHARD *et al.* [2] can only be regarded as a rough approximation, since these authors calculated only a diagonal force field. In our opinion, the comparison bears out the role played by the use of the Coriolis ζ constants in the more exact (or at least more satisfactory) determination of the interaction force constants.

From the point of view of further investigations, it is evident that it would be a significant step in the vibrational analysis of cyclopropane if the Coriolis ζ constants in the *e″* species of C_3D_6 could be established from vapour phase Raman studies. According to the present calculations, the Coriolis constants for C_3D_6 are those shown in Table XI.

Table XI

Coriolis ζ constants calculated by the refinement treatment of species e″ for C_3D_6

S_{12}	S_{13}	S_{14}
0.1383	—0.3336	—0.2274
Sym.	0.5260	—0.0574
		—0.9441

REFERENCES

1. Saksena, B. D.: Proc. Indian Acad. Sci. **10A**, 449 (1939).
2. Günthard, Hs. H., Lord, R. C., McCubbin, Jr., T. K.: J. Chem. Phys. **25**, 768 (1956).
3. Cyvin, S. J.: Spectrochim. Acta **16**, 1022 (1960).
4. Mathai, P. M., Shepherd, G. G., Welsh, H. L.: Can. J. Physics **34**, 1448 (1956).
5. Jones, W. J., Stoicheff, B. P.: Can. J. Physics **42**, 2259 (1964).
6. Bastiansen, O., Traetteberg, M.: Tetrahedron **17**, 147 (1962).
7. Brunvoll, J., Cyvin, S. J.: Acta Polytechn. Scand. *Ma 11*, Trondheim, 1964
8. Wilson, E. B. Jr., Decius, J. C., Cross, P. C.: Molecular Vibrations. McGraw-Hil London, 1955.
9. Dennison, D. M.: Revs. Modern Phys. **12**, 175 (1940).
10. Nemes, L., Kemenczy, M.: Acta Chim. Acad. Sci. Hung. **53**, 359 (1967).
11. Mills, I. M.: J. Mol. Spectry. **5**, 334 (1960).

László Nemes; Budapest II. Pusztaszeri út 57—69

Acta Chimica Academiae Scientiarum Hungaricae, Tomus 59 (1), pp. 85—90 (1969)

MEAN AMPLITUDES OF VIBRATION FOR DIBORANE AND DEUTERODIBORANE

S. J. CYVIN and B. VIZI

(Technical University of Norway, Trondheim, and University for Chemical Industries, Veszprém)

Received April 22, 1968

A normal-coordinate analysis has been performed for isotopic diboranes. The developed harmonic force field was used to calculate the mean amplitudes of vibration for some isotopic species of diborane. These results were compared with electron-diffraction values of mean amplitudes, and some significant discrepancies are pointed out.

I. Introduction

Evidence for the ethylene-like, bridged molecular structure of diborane, B_2H_6, was given for the first time by PRICE [1] in his infrared work, and supported by the gaseous electron-diffraction work of HEDBERG and SCHOMAKER [2]. Recently BARTELL and CARROLL [3] have reinvestigated the molecule by electron diffraction, and included a study of the deuterated compound. In this work [3] the mean amplitudes of vibration [4] for diboranes were reported for the first time.

In the present work we have calculated the mean amplitudes of vibration from spectroscopic data. Such calculations have not been performed previously, although some normal-coordinate analyses of diboranes have been reported [5, 6]. Our normal-coordinate analysis is based on the symmetry coordinates specified in the previous article [7]. This set contains no redundants and seems to be more convenient than the sets of symmetry coordinates proposed previously [5, 8].

II. Structural and spectral data

In the present calculations we have used the following values as equilibrium parameters, the same for B_2H_6 and B_2D_6:

$$B - H_b = 1.336\,\text{Å}, \qquad B - H_t = 1.197\,\text{Å},$$
$$\angle H_b BH_b = 96.9°, \qquad \angle H_t BH_t = 121.3°.$$

The subscripts b and t refer to 'bridged' and 'terminal', respectively. The above values were obtained by averaging data from BARTELL and CARROLL [3]. In

this process we have disregarded the distinction between r_g (mean distance) and r_e (equilibrium distance) as immaterial.

The most complete spectroscopic work concerning the assignment of vibrational frequencies is due to LORD and NIELSEN [9], and it was therefore used as the source for experimental frequencies in our calculations (*cf.* Table II). The work [9] summarizes a complete vibrational assignment for $^{11}B_2H_6$ and $^{10}B_2D_6$ and a partial assignment for $^{10}B_2H_6$, according to a reinvestigation by the authors and previous work. A quotation of data on $^{11}B_2D_6$ is also included from PRICE [1] and others [10].

III. Force field

A harmonic force field was produced to make a best possible fit to the observed, uncorrected frequencies for $^{11}B_2H_6$ and $^{10}B_2D_6$. It seems to be of no interest to describe here the several steps of an iteration process during these computations. The final symmetrized F matrix elements are shown in Table I;

Table I

F matrix elements for diborane (mdyne/Å)

A_g	3.642			
	−0.126	2.353		
	−0.646	0.149	0.886	
	0.142	0.108	0.220	0.879
B_{1g}	0.140	B_{2g}	3.483	
			0.013	0.391
B_{3g}	1.672		A_u	0.295
	0.124	0.363		
B_{1u}	4.135			
	−0.168	1.568		
	−0.625	0.003	0.910	
B_{2u}	1.410			
	−0.065	0.447		
B_{3u}	3.494			
	−0.109	0.247		
	−0.024	−0.076	0.123	

they pertain to the symmetry coordinates specified elsewhere [7]. We have also evaluated the corresponding valence force-constants. Among these the B—H stretching force constants are those of greatest interest. Our result is:

$$f(\mathrm{B}-\mathrm{H}_b) = 2.715 \text{ mdyne/Å},$$

$$f(\mathrm{B}-\mathrm{H}_t) = 2.724 \text{ mdyne/Å}.$$

Table II

Observed and calculated frequencies for isotopic species of diborane (cm^{-1} units)

	$^{11}B_2H_6$		$^{11}B_2D_6$		$^{10}B_2H_6$		$^{10}B_2D_6$	
	Obs.	Calcd.	Obs.	Calcd.	Obs.	Calcd.	Obs.	Calcd.
A_g	2524	2517	1860	1847	—	2524	1860	1865
	2104	2073	1509	1524	—	2081	1511	1534
	1180	1170	—	920	—	1181	929	939
	794	827	710	690	820	854	726	698
B_{1g}	1012	1022	—	723	—	1022	730	723
B_{2g}	2591	2591	1960	1955	—	2609	1980	1980
	(920)	919	—	729	(930)	932	(740)	741
B_{3g}	1768	1767	1269	1269	—	1770	1273	1273
	(1035)	1036	—	849	(1044)	1054	(870)	869
A_u	829	833	—	589	729	833	592	589
B_{1u}	2525	2486	1850	1856	2528	2499	1845	1876
	1602	1641	1203	1174	1606	1643	1205	1177
	1177	1189	876	868	1181	1193	881	872
B_{2u}	1915	1908	—	1450	1920	1923	1465	1469
	973	986	722	716	977	989	728	719
B_{3u}	2612	2614	1994	1973	2625	2632	1999	1997
	(950)	957	—	696	—	961	(705)	700
	368	368	—	262	368	368	262	262

Table II shows the calculated frequencies for all the four mentioned isotopic species of diborane, along with the experimental values. The agreement seems to be satisfactory.

IV. Interatomic distances and mean-square amplitudes of vibration

In a diborane-type molecule (symmetry D_{2h}) there are nine types of interatomic distances, which we shall identify by the following numbering:

1. B—H_t; terminal B—H.
2. B—H_b; bridged B—H.
3. B . . . H; nonbonded B . . . H_t.
4. B—B.
5. H_b . . . H_b; between the two bridged H atoms.

6. $H_b \ldots H_t$; between one bridged and one terminal H atom.
7. *com* (H . . . H); between two terminal H atoms attached to the same B.
8. *cis* (H . . . H); between two terminal H atoms in a *cis* position.
9. *tr* (H . . . H); between two terminal H atoms in *trans* position.

The following symmetric structures have been derived by standard group-theoretical methods [4] for the different types of distances listed above.

$$\Gamma_1 = \Gamma_3 = A_g + B_{2g} + B_{1u} + B_{3u},$$

$$\Gamma_2 = A_g + B_{3g} + B_{1u} + B_{2u}, \quad \Gamma_4 = \Gamma_5 = A_g,$$

$$\Gamma_6 = A_g + B_{1g} + B_{2g} + B_{3g} + A_u + B_{1u} + B_{2u} + B_{3u},$$

$$\Gamma_7 = A_g + B_{1u}, \quad \Gamma_8 = A_g + B_{3u}, \quad \Gamma_9 = A_g + B_{2g}.$$

These equations give us information about the types of normal modes which contribute to the mean amplitude of vibration of a given distance [4]. This information may be helpful in discussions about the reliability of the calculated mean amplitudes.

Some of the mean-square amplitudes of vibration can easily be evaluated into simple expressions in terms of the Σ matrix [4] elements. The results for four of the distance types are given below; the σ subscripts refer to the numbers of the above survey of distances.

$$\sigma_1 = \frac{1}{4}\left[\Sigma_{22}(A_g) + \Sigma_{11}(B_{2g}) + \Sigma_{22}(B_{1u}) + \Sigma_{11}(B_{3u})\right],$$

$$\sigma_2 = \frac{1}{4}\left[\Sigma_{11}(A_g) + \Sigma_{11}(B_{3g}) + \Sigma_{11}(B_{1u}) + \Sigma_{11}(B_{2u})\right],$$

$$\sigma_4 = \Sigma_{11}(A_g)\cos^2 A - 2^{-1/2}\Sigma_{13}(A_g)\sin 2A + \frac{1}{2}\Sigma_{35}(A_g)\sin^2 A,$$

$$\sigma_5 = \Sigma_{11}(A_g)\sin^2 A + 2^{-1/2}\Sigma_{13}(A_g)\sin 2A + \frac{1}{2}\Sigma_{33}(A_g)\cos^2 A.$$

Here the Σ matrix elements pertain to the symmetry coordinates proposed in the aforementioned work [7], which should be consulted for further explanations of the symbols adopted here. The mean-square amplitudes for the remaining five types of distances can be evaluated in a similar way in terms of Σ matrix elements; those expressions, however, would not be quite so simple. We do not find it necessary to work out all these expressions, because they are not actually needed in the numerical computations of mean amplitudes of vibration.

V. Mean amplitudes of vibration

Table III shows the calculated mean amplitudes of vibration from the present work, along with observed values from electron diffraction [3]. There is satisfactory agreement only for the B—B distance in B_2D_6, and also quite good for the same distance in B_2H_6; this type of distances seems to be the most suitable one for an accurate determination of the mean amplitude from electron diffraction, as can be judged from the radial distribution curve [3]. For the other distances, the observed mean amplitudes seem to be systematically somewhat too low. It does not seem feasible to improve this discrepancy appreciably by small refinements of the force constants. For $^{11}B_2H_6$ we have calculated an alternative set of mean amplitudes (given in parentheses in Table III), which

Table III

Mean amplitudes of vibration for isotopic diboranes from electron diffraction [3] (E.D.) and present calculations (Spectr.)

(Å units)

Distance	Spectr. $^{11}B_2H_6$ $T = 0$	Spectr. $^{11}B_2H_6$ 298 °K		Spectr. $^{10}B_2H_6$ 298 °K	E. D. B_2H_6
1	0.0919	0.0920	(0.0922)	0.0921	$0.073_4 \pm 0.006$ (B — Ht)
2	0.0950	0.0951	(0.0949)	0.0953	$0.085_7 \pm 0.009$ (B — Hb)
3	0.1264	0.1332	(0.1340)	0.1335	$0.117_8 \pm 0.005$ (B . . . H)
4	0.0565	0.0573	(0.0584)	0.0585	$0.060_8 \pm 0.002$ (B — B)
5	0.1196	0.1198	(0.1199)	0.1199	
6	0.1521	0.1535	(0.1539)	0.1535	
7	0.1480	0.1482	(0.1486)	0.1482	
8	0.2227	0.2515	(0.2520)	0.2515	
9	0.1430	0.1440	(0.1442)	0.1441	
Distance	$^{11}B_2D_6$ $T = 0$	$^{11}B_2D_6$ 298 °K		$^{10}B_2D_6$ 298 °K	B_2D_6
1	0.0786	0.0787		0.0790	$0.064_3 \pm 0.005$ (B — Dt)
2	0.0815	0.0818		0.0821	$0.075_6 \pm 0.006$ (B — Db)
3	0.1091	0.1202		0.1205	$0.104_9 \pm 0.005$ (B . . . D)
4	0.0560	0.0570		0.0582	$0.059_5 \pm 0.002$ (B — B)
5	0.1011	0.1015		0.1015	
6	0.1283	0.1316		0.1317	
7	0.1246	0.1257		0.1258	
8	0.1879	0.2331		0.2331	
9	0.1214	0.1237		0.1238	

are consistent with force constants slightly different from those in Table I, but adjusted to fit exactly the observed frequencies.

BARTELL and CARROLL [3] have also discussed the ratios of mean amplitudes l_b/l_t, for which they found 1.17 ± 0.06 (B_2H_6) and 1.18 ± 0.05 (B_2D_6). They also report this ratio to be 1.12 ± 0.01 from a rough theoretic estimate. According to our more rigorous spectroscopic calculations l_b/l_t is 1.03 for B_2H_6 and 1.04 for B_2D_6.

REFERENCES

1. PRICE, W. C.: J. Chem. Phys. **15,** 614 (1947); **16,** 894 (1948).
2. HEDBERG, K., SCHOMAKER, V.: J. Am. Chem. Soc. **73,** 1482 (1951).
3. BARTELL, L. S., CARROLL, B. L.: J. Chem. Phys. **42,** 1135 (1965).
4. CYVIN, S. J.: Molecular Vibrations and Mean Square Amplitudes. Universitetsforlaget, Oslo, and Elsevier, Amsterdam, 1968.
5. VENKATESWARLU, K., THIRUGNANASAMBANDAM, P.: Proc. Indian Acad. Sci. **A48,** 344 (1958).
6. VENKATESWARLU, K., RADHAKRISHNAN, M.: Proc. Indian Acad. Sci. **B55,** 161 (1962).
7. VIZI, B., CYVIN, S. J.: Acta Chim. Acad. Sci. Hung. (in the press).
8. NAGARAJAN, G.: Bull. soc. chim. Belg. **71,** 370 (1962).
9. LORD, R. C., NIELSEN, E.: J. Chem. Phys. **19,** 1 (1951).
10. WEBB, A. N., NEU, J. T., PITZER, K. S.: J. Chem. Phys. **17,** 1007 (1949).

Sven Josef CYVIN; Trondheim, Norway
Béla VIZI; Veszprém, Schönherz Z. u. 12, Hungary

Acta Chimica Academiae Scientiarum Hungaricae, Tomus 59 (1), pp. 91—98 (1969)

TENTATIVELY STANDARDIZED SYMMETRY COORDINATES OF POLYATOMIC MOLECULES, VIII

MODELS OF DIBORANE, CYCLOPROPANE AND CYCLOHEXANE TYPES

B. VIZI and S. J. CYVIN

(University for Chemical Industries, Veszprém and Technical University of Norway, Trondheim)

Received April 22, 1968

Symmetry coordinates for molecular vibrations are specified for the following models: *(i)* Bridged $X_2Y_2Z_4$ model (symmetry D_{2h}) of the diborane type, *(ii)* trigonal symmetrical $(XY_2)_3$ model (symmetry D_{3h}) of the cyclopropane type, and *(iii)* the puckered-ring $X_6Y_6Z_6$ model (symmetry D_{3d}) of the cyclohexane type.

In Part V [1] of this series of papers we have treated three six-atomic models, which are of relevance in studies of molecular vibrations for cyclohexane, cyclopropane and diborane. Here we wish to specify the symmetry coordinates for models actually applicable to these molecule types.

I. Bridged $X_2Y_2Z_4$ model

Fig. 1 shows the bridged $X_2Y_2Z_4$ model of symmetry D_{2h}. The normal modes of vibration are found to be distributed among the symmetry species according to:

$$\Gamma(Q) = 4A_g + B_{1g} + 2B_{2g} + 2B_{3g} + A_u + 3B_{1u} + 2B_{2u} + 3B_{3u}.$$

This symmetric structure pertains to the orientation of Cartesian axes as shown in Fig. 1. With a different orientation the species designation may change. In particular if the X and Y axes are exchanged, also the subscripts 1 and 3 of the B species must be interchanged.

The valence coordinates are explained in Fig. 1 and its legend. They have been used to construct a complete set of symmetry coordinates without redundants, which are specified below.

$$S_1(A_g) = \frac{1}{2}(r_1 + r_2 + r_3 + r_4)$$

$$S_2(A_g) = \frac{1}{2}(s_1 + s_2 + s_3 + s_4)$$

$$S_3(A_g) = t$$

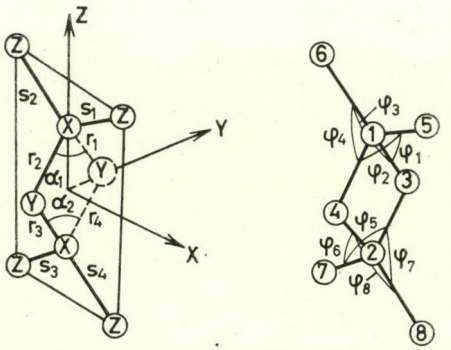


Fig. 1. The bridged $X_2Y_2Z_4$ model; symmetry D_{2h}. R and S are used to denote the equilibrium XY and XZ distances, respectively. The equilibrium YXY and ZXZ angles are $2A$ and $2B$, respectively.

The coordinate t is defined by

$$t = 2^{-1/2} R(\alpha_1 + \alpha_2).$$

On the separate drawing (right) the numbering of atoms and definition of φ (YXZ) bendings are given.

The ring deformation coordinate τ is defined in terms of Cartesian displacements by

$$R\tau = x_1 + x_2 - x_3 - x_4$$

$$S_4\,(A_g) = 8^{-1/2}\,(RS)^{1/2}\,(\varphi_1 + \varphi_2 + \varphi_3 + \varphi_4 + \varphi_5 + \varphi_6 + \varphi_7 + \varphi_8)$$

$$S(B_{1g}) = 8^{-1/2}\,(RS)^{1/2}\,(\varphi_1 - \varphi_2 - \varphi_3 + \varphi_4 - \varphi_5 + \varphi_6 + \varphi_7 - \varphi_8)$$

$$S_1\,(B_{2g}) = \frac{1}{2}\,(s_1 - s_2 + s_3 - s_4)$$

$$S_2\,(B_{2g}) = 8^{-1/2}\,(RS)^{1/2}\,(\varphi_1 + \varphi_2 - \varphi_3 - \varphi_4 + \varphi_5 + \varphi_6 - \varphi_7 - \varphi_8)$$

$$S_1\,(B_{3g}) = \frac{1}{2}\,(r_1 - r_2 + r_3 - r_4)$$

$$S_2\,(B_{3g}) = 8^{-1/2}\,(RS)^{1/2}\,(\varphi_1 - \varphi_2 + \varphi_3 - \varphi_4 - \varphi_5 + \varphi_6 - \varphi_7 + \varphi_8)$$

$$S(A_u) = 8^{-1/2}\,(RS)^{1/2}\,(\varphi_1 - \varphi_2 - \varphi_3 + \varphi_4 + \varphi_5 - \varphi_6 - \varphi_7 + \varphi_8)$$

$$S_1\,(B_{1u}) = \frac{1}{2}\,(r_1 + r_2 - r_3 - r_4)$$

$$S_2\,(B_{1u}) = \frac{1}{2}\,(s_1 + s_2 - s_3 - s_4)$$

$$S_3\,(B_{1u}) = 8^{-1/2}\,(RS)^{1/2}\,(\varphi_1 + \varphi_2 + \varphi_3 + \varphi_4 - \varphi_5 - \varphi_6 - \varphi_7 - \varphi_8)$$

$$S_1\,(B_{2u}) = \frac{1}{2}\,(r_1 - r_2 - r_3 + r_4)$$

$$S_2(B_{2u}) = 8^{-1/2}\ (RS)^{1/2}(\varphi_1 - \varphi_2 + \varphi_3 - \varphi_4 + \varphi_5 - \varphi_6 + \varphi_7 - \varphi_8)$$

$$S_1(B_{3u}) = \frac{1}{2}(s_1 - s_2 - s_3 + s_4)$$

$$S_2(B_{3u}) = R\tau$$

$$S_3(B_{3u}) = 8^{-1/2}(RS)^{1/2}(\varphi_1 + \varphi_2 - \varphi_3 - \varphi_4 - \varphi_5 - \varphi_6 + \varphi_7 + \varphi_8)$$

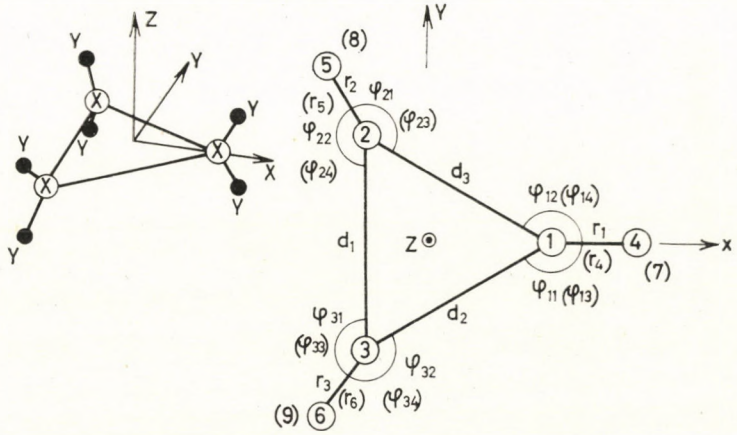


Fig. 2. The trigonal symmetrical X_3Y_6 model; symmetry D_{3h}. R and D are used to denote the equilibrium XY and XX distances, respectively, and the equilibrium YXY angle is $2A$. The symbols in parentheses refer to atoms and valence coordinates below the XY plane

II. Trigonal symmetrical $(XY_2)_3$ model

Consider the X_3Y_6 model of symmetry D_{3h} shown in Fig. 2. The normal modes of vibration are distributed according to

$$\Gamma(Q) = 3A_1' + A_2' + 4E' + A_1'' + 2A_2'' + 3E''.$$

The stretching coordinates and the twelve φ-type bendings are explained in Fig. 2. In order to construct the symmetry coordinates, we firstly form the intermediate combinations (for $i = 1, 2, 3$):

$$\zeta_i = \frac{1}{2}(\varphi_{i1} + \varphi_{i2} + \varphi_{i3} + \varphi_{i4});\ \text{scissoring},$$

$$\eta_i = \frac{1}{2}(\varphi_{i1} - \varphi_{i2} + \varphi_{i3} - \varphi_{i4});\ \text{wagging},$$

$$\theta_i = \frac{1}{2}(\varphi_{i1} - \varphi_{i2} - \varphi_{i3} + \varphi_{i4});\ \text{twisting},$$

$$\xi_i = \frac{1}{2}(\varphi_{i1} + \varphi_{i2} - \varphi_{i3} - \varphi_{i4}); \text{ rocking.}$$

A suitable set of symmetry coordinates is specified in the following.

$$S_1(A_1') = 6^{-1/2}(r_1 + r_2 + r_3 + r_4 + r_5 + r_6)$$
$$S_2(A_1') = 3^{-1/2}(d_1 + d_2 + d_3)$$
$$S_3(A_1') = 3^{-1/2}(RD)^{1/2}(\zeta_1 + \zeta_2 + \zeta_3)$$
$$S(A_2') = 3^{-1/2}(RD)^{1/2}(\eta_1 + \eta_2 + \eta_3)$$
$$S_{1a}(E') = 12^{-1/2}(2r_1 - r_2 - r_3 + 2r_4 - r_5 - r_6)$$
$$S_{2a}(E') = 6^{-1/2}(2d_1 - d_2 - d_3)$$
$$S_{3a}(E') = 6^{-1/2}(RD)^{1/2}(2\zeta_1 - \zeta_2 - \zeta_3)$$
$$S_{4a}(E') = 2^{-1/2}(RD)^{1/2}(\eta_2 - \eta_3)$$
$$S_{1b}(E') = \frac{1}{2}(r_2 - r_3 + r_5 - r_6)$$
$$S_{2b}(E') = 2^{-1/2}(d_2 - d_3)$$
$$S_{3b}(E') = 2^{-1/2}(RD)^{1/2}(\zeta_2 - \zeta_3)$$
$$S_{4b}(E') = 6^{-1/2}(RD)^{1/2}(-2\eta_1 + \eta_2 + \eta_3)$$
$$S(A_1'') = 3^{-1/2}(RD)^{1/2}(\theta_1 + \theta_2 + \theta_3)$$
$$S_1(A_2'') = 6^{-1/2}(r_1 + r_2 + r_3 - r_4 - r_5 - r_6)$$
$$S_2(A_2'') = 3^{-1/2}(RD)^{1/2}(\xi_1 + \xi_2 + \xi_3)$$
$$S_{1a}(E'') = \frac{1}{2}(r_2 - r_3 - r_5 + r_6)$$
$$S_{2a}(E'') = 6^{-1/2}(RD)^{1/2}(-2\theta_1 + \theta_2 + \theta_3)$$
$$S_{3a}(E'') = 2^{-1/2}(RD)^{1/2}(\xi_2 - \xi_3)$$
$$S_{1b}(E'') = 12^{-1/2}(2r_1 - r_2 - r_3 - 2r_4 + r_5 + r_6)$$
$$S_{2b}(E'') = 2^{-1/2}(RD)^{1/2}(\theta_2 - \theta_3)$$
$$S_{3b}(E'') = 6^{-1/2}(RD)^{1/2}(2\xi_1 - \xi_2 - \xi_3)$$

III. Puckered-ring $X_6Y_6Z_6$ model

The puckered-ring $X_6Y_6Z_6$ model of symmetry D_{3d} is shown in Fig. 3. The Y atoms are usually referred to as *axial*, while the Z atoms are termed as *equa-*

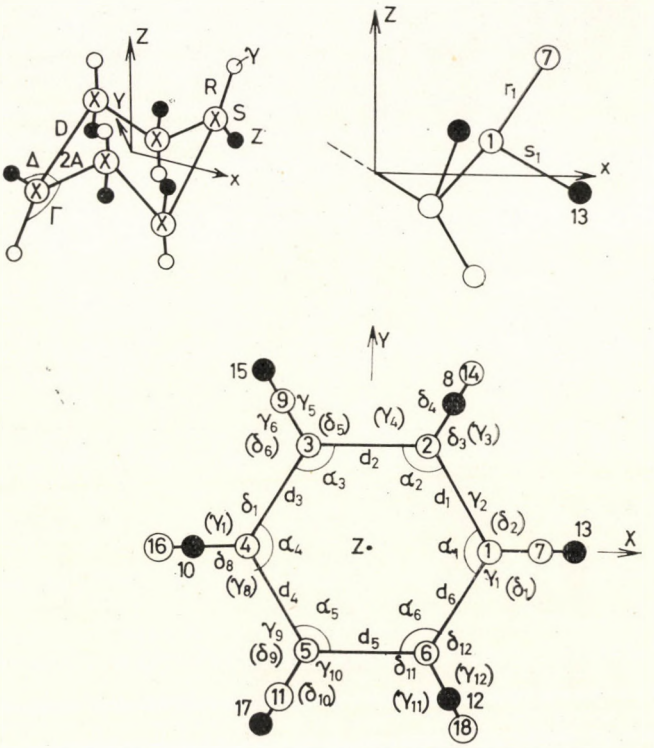


Fig. 3. The puckered-ring $X_6Y_6Z_6$ model; symmetry D_{3d}. D, R and S denote the equilibrium XX, XY and XZ distances, respectively. The equilibrium XXX angle is $2A$, while the XXY and XXZ angles at equilibrium may be identified by Γ and Δ, respectively. In the upper-left drawing, the small white circles represent the Y atoms; the black circles represent Z. In the lower-right drawing the system is different. The Y atoms are those with numbers 7—12; the white and black circles indicate an upward and downward tilting of the respective XY bonds. This system was also used in drawing the Z atoms, which run from 13 to 18. Valence coordinates: d and α pertain to the X_6 ring and are shown on the lower-right drawing. The r_i and s_i ($i = 1, 2, \ldots, 6$) are XY and XZ stretchings, respectively, and exemplified by r_1 and s_1 on the upper-right drawing. The γ_i and δ_i coordinates (see lower-right) are XXY and XXZ bendings, respectively

torial. The normal modes of vibration are distributed according to the symmetric structure:

$$\Gamma(Q) = 6A_{1g} + 2A_{2g} + 8E_g + 3A_{1u} + 5A_{2u} + 8E_u .$$

Before constructing the symmetry coordinates, it is expedient to form the intermediate combinations of γ and δ bendings (see Fig. 3) as shown below.

$$\beta_1 = 2^{-1/2}(\gamma_1 + \gamma_2), \qquad \varepsilon_1 = 2^{-1/2}(\delta_1 + \delta_2)$$
$$\beta_2 = 2^{-1/2}(\gamma_3 + \gamma_4), \qquad \varepsilon_2 = 2^{-1/2}(\delta_3 + \delta_4)$$
$$\beta_3 = 2^{-1/2}(\gamma_5 + \gamma_6), \qquad \varepsilon_3 = 2^{-1/2}(\delta_5 + \delta_6)$$

$$\beta_4 = 2^{-1/2}(\gamma_7 + \gamma_8), \qquad \varepsilon_4 = 2^{-1/2}(\delta_7 + \delta_8)$$
$$\beta_5 = 2^{-1/2}(\gamma_9 + \gamma_{10}), \qquad \varepsilon_5 = 2^{-1/2}(\delta_9 + \delta_{10})$$
$$\beta_6 = 2^{-1/2}(\gamma_{11} + \gamma_{12}), \qquad \varepsilon_6 = 2^{-1/2}(\delta_{11} + \delta_{12})$$

and

$$\xi_1 = 2^{-1/2}(\gamma_1 - \gamma_2), \qquad \eta_1 = 2^{-1/2}(\delta_1 - \delta_2)$$
$$\xi_2 = 2^{-1/2}(\gamma_3 - \gamma_4), \qquad \eta_2 = 2^{-1/2}(\delta_3 - \delta_4)$$
$$\xi_3 = 2^{-1/2}(\gamma_5 - \gamma_6), \qquad \eta_3 = 2^{-1/2}(\delta_5 - \delta_6)$$
$$\xi_4 = 2^{-1/2}(\gamma_7 - \gamma_8), \qquad \eta_4 = 2^{-1/2}(\delta_7 - \delta_8)$$
$$\xi_5 = 2^{-1/2}(\gamma_9 - \gamma_{10}), \qquad \eta_5 = 2^{-1/2}(\delta_9 - \delta_{10})$$
$$\xi_6 = 2^{-1/2}(\gamma_{11} - \gamma_{12}), \qquad \eta_6 = 2^{-1/2}(\delta_{11} - \delta_{12})$$

A complete set of symmetry coordinates has been constructed, and is specified in the following.

$$S_1(A_{1g}) = 6^{-1/2}(d_1 + d_2 + d_3 + d_4 + d_5 + d_6)$$
$$S_2(A_{1g}) = 6^{-1/2}D(\alpha_1 + \alpha_2 + \alpha_3 + \alpha_4 + \alpha_5 + \alpha_6)$$
$$S_3(A_{1g}) = 6^{-1/2}(r_1 + r_2 + r_3 + r_4 + r_5 + r_6)$$
$$S_4(A_{1g}) = 6^{-1/2}(s_1 + s_2 + s_3 + s_4 + s_5 + s_6)$$
$$S_5(A_{1g}) = 6^{-1/2}(RD)^{1/2}(\beta_1 + \beta_2 + \beta_3 + \beta_4 + \beta_5 + \beta_6)$$
$$S_6(A_{1g}) = 6^{-1/2}(SD)^{1/2}(\varepsilon_1 + \varepsilon_2 + \varepsilon_3 + \varepsilon_4 + \varepsilon_5 + \varepsilon_6)$$
$$S_1(A_{2g}) = 6^{-1/2}(RD)^{1/2}(\xi_1 + \xi_2 + \xi_3 + \xi_4 + \xi_5 + \xi_6)$$
$$S_2(A_{2g}) = 6^{-1/2}(SD)^{1/2}(\eta_1 + \eta_2 + \eta_3 + \eta_4 + \eta_5 + \eta_6)$$
$$S_{1a}(E_g) = \frac{1}{2}(d_1 - d_3 + d_4 - d_6)$$
$$S_{2a}(E_g) = \frac{1}{2}D(-\alpha_2 + \alpha_3 - \alpha_5 + \alpha_6)$$
$$S_{3a}(E_g) = \frac{1}{2}(-r_2 + r_3 - r_5 + r_6)$$
$$S_{4a}(E_g) = \frac{1}{2}(-s_2 + s_3 - s_5 + s_6)$$
$$S_{5a}(E_g) = \frac{1}{2}(RD)^{1/2}(-\beta_2 + \beta_3 - \beta_5 + \beta_6)$$
$$S_{6a}(E_g) = \frac{1}{2}(SD)^{1/2}(-\varepsilon_2 + \varepsilon_3 - \varepsilon_5 + \varepsilon_6)$$

$$S_{7a}(E_g) = 12^{-1/2}(RD)^{1/2}(2\xi_1 - \xi_2 - \xi_3 + 2\xi_4 - \xi_5 - \xi_6)$$

$$S_{8a}(E_g) = 12^{-1/2}(SD)^{1/2}(2\eta_1 - \eta_2 - \eta_3 + 2\eta_4 - \eta_5 - \eta_6)$$

$$S_{1b}(E_g) = 12^{-1/2}(-d_1 + 2d_2 - d_3 - d_4 + 2d_5 - d_6)$$

$$S_{2b}(E_g) = 12^{-1/2}D(2\alpha_1 - \alpha_2 - \alpha_3 + 2\alpha_4 - \alpha_5 - \alpha_6)$$

$$S_{3b}(E_g) = 12^{-1/2}(2r_1 - r_2 - r_3 + 2r_4 - r_5 - r_6)$$

$$S_{4b}(E_g) = 12^{-1/2}(2s_1 - s_2 - s_3 + 2s_4 - s_5 - s_6)$$

$$S_{5b}(E_g) = 12^{-1/2}(RD)^{1/2}(2\beta_1 - \beta_2 - \beta_3 + 2\beta_4 - \beta_5 - \beta_6)$$

$$S_{6b}(E_g) = 12^{-1/2}(SD)^{1/2}(2\varepsilon_1 - \varepsilon_2 - \varepsilon_3 + 2\varepsilon_4 - \varepsilon_5 - \varepsilon_6)$$

$$S_{7b}(E_g) = \frac{1}{2}(RD)^{1/2}(\xi_2 - \xi_3 + \xi_5 - \xi_6)$$

$$S_{8b}(E_g) = \frac{1}{2}(SD)^{1/2}(\eta_2 - \eta_3 + \eta_5 - \eta_6)$$

$$S_1(A_{1u}) = 6^{-1/2}(d_1 - d_2 + d_3 - d_4 + d_5 - d_6)$$

$$S_2(A_{1u}) = 6^{-1/2}(RD)^{1/2}(-\xi_1 + \xi_2 - \xi_3 + \xi_4 - \xi_5 + \xi_6)$$

$$S_3(A_{1u}) = 6^{-1/2}(SD)^{1/2}(-\eta_1 + \eta_2 - \eta_3 + \eta_4 - \eta_5 + \eta_6)$$

$$S_1(A_{2u}) = 6^{-1/2}D(\alpha_1 - \alpha_2 + \alpha_3 - \alpha_4 + \alpha_5 - \alpha_6)$$

$$S_2(A_{2u}) = 6^{-1/2}(r_1 - r_2 + r_3 - r_4 + r_5 - r_6)$$

$$S_3(A_{2u}) = 6^{-1/2}(s_1 - s_2 + s_3 - s_4 + s_5 - s_6)$$

$$S_4(A_{2u}) = 6^{-1/2}(RD)^{1/2}(\beta_1 - \beta_2 + \beta_3 - \beta_4 + \beta_5 - \beta_6)$$

$$S_5(A_{2u}) = 6^{-1/2}(SD)^{1/2}(\varepsilon_1 - \varepsilon_2 + \varepsilon_3 - \varepsilon_4 + \varepsilon_5 - \varepsilon_6)$$

$$S_{1a}(E_u) = \frac{1}{2}(d_1 - d_3 - d_4 + d_6)$$

$$S_{2a}(E_u) = 12^{-1/2}D(2\alpha_1 + \alpha_2 - \alpha_3 - 2\alpha_4 - \alpha_5 + \alpha_6)$$

$$S_{3a}(E_u) = 12^{-1/2}(2r_1 + r_2 - r_3 - 2r_4 - r_5 + r_6)$$

$$S_{4a}(E_u) = 12^{-1/2}(2s_1 + s_2 - s_3 - 2s_4 - s_5 + s_6)$$

$$S_{5a}(E_u) = 12^{-1/2}(RD)^{1/2}(2\beta_1 + \beta_2 - \beta_3 - 2\beta_4 - \beta_5 + \beta_6)$$

$$S_{6a}(E_u) = 12^{-1/2}(SD)^{1/2}(2\varepsilon_1 + \varepsilon_2 - \varepsilon_3 - 2\varepsilon_4 - \varepsilon_5 + \varepsilon_6)$$

$$S_{7a}(E_u) = \frac{1}{2}(RD)^{1/2}(-\xi_2 - \xi_3 + \xi_5 + \xi_6)$$

$$S_{8a}(E_u) = \frac{1}{2}(SD)^{1/2}(-\eta_2 - \eta_3 + \eta_5 + \eta_6)$$

$$S_{1b}(E_u) = 12^{-1/2}(d_1 + 2d_2 + d_3 - d_4 - 2d_5 - d_6)$$

$$S_{2b}(E_u) = \frac{1}{2} D(\alpha_2 + \alpha_3 - \alpha_5 - \alpha_6)$$

$$S_{3b}(E_u) = \frac{1}{2}(r_2 + r_3 - r_5 - r_6)$$

$$S_{4b}(E_u) = \frac{1}{2}(s_2 + s_3 - s_5 - s_6)$$

$$S_{5b}(E_u) = \frac{1}{2}(RD)^{1/2}(\beta_2 + \beta_3 - \beta_5 - \beta_6)$$

$$S_{6b}(E_u) = \frac{1}{2}(SD)^{1/2}(\varepsilon_2 + \varepsilon_3 - \varepsilon_5 - \varepsilon_6)$$

$$S_{7b}(E_u) = 12^{-1/2}(RD)^{1/2}(2\xi_1 + \xi_2 - \xi_3 - 2\xi_4 - \xi_5 + \xi_6)$$

$$S_{8b}(E_u) = 12^{-1/2}(SD)^{1/2}(2\eta_1 + \eta_2 - \eta_3 - 2\eta_4 - \eta_5 + \eta_6)$$

REFERENCE

1. VIZI, B., CYVIN, S. J.: Acta Chem. Scand. (in the press).

Béla VIZI; Veszprém, Schönherz Z. u. 12, Hungary
Sven Josef CYVIN; Trondheim, Norway

Acta Chimica Academiae Scientiarum Hungaricae Tomus 59 (1), pp. 99—107 (1969)

INFRARED SPECTROSCOPIC STUDY OF THE STRUCTURE OF 1-HYDROXYANTHRAQUINONE-9-MONOIMINES

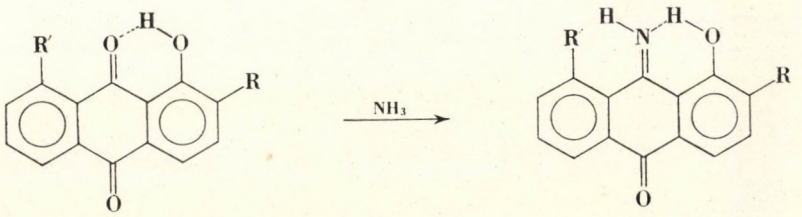
A. MÜLLER†, K. KÖRMENDY, F. RUFF, P. SOHÁR* and M. VAJDA

*(Institute of Organic Chemistry, L. Eötvös University, Budapest and *Pharmaceutical Research Institute, Budapest)*

Received January 22, 1968

The infrared spectra of the compounds formed in the reaction of hydroxy- and alkoxy-substituted anthraquinones with alcoholic ammonia were investigated for the purpose of structural investigation. It could be shown by assignment of the $\nu_{C=O}$ and $\nu_{C=N}$ bands that the 9-carbonyl group is converted to an imino group. Examination of the ν_{CO}, ν_{NH}, ν_{CN} and ν_{OH} bands made it possible to draw conclusion on the various hydrogen bonds formed in the imines. Further proof of the structure was obtained from the infrared and NMR spectra of acyl derivatives of some imines.

If 1-hydroxyanthraquinone or its 2- or 8-alkoxy or hydroxy derivatives **(I)** are treated with alcoholic ammonia, deep red, nitrogen-containing compounds are formed [1, 2]. Chemical behaviour of the compounds shows that these products are not simple ammonium salts of the parent hydroxyanthraquinones, and the 1-hydroxy group is not replaced by an amino group. It seems probable that a condensation occurs between the 9-carbonyl group (which is hydrogen-bonded to the 1-hydroxy group forming a chelate) and ammonia, to give compounds of the type of 1-hydroxy-anthraquinone-9-monoimine **(II)**.



I **II**

(R.R'= H. OH. OCH_3. $OCH_2C_6H_5$)

Recent investigations have shown [2] that the presence of an intramolecular hydrogen bond is not a prerequisite of the reaction, as 1-methoxyanthraquinone also yields a 9-imino derivative.

To obtain further evidence on the structures of the compounds, infrared and UV spectroscopic investigations were made. The UV spectra — which are discussed in detail in another paper [3] — showed that the chromophoric system of the new compounds is of the same type as that of the parent anthra-

quinones. Further proof of the structure could be obtained by the assignment of the infrared bands of the C=N double bond, the carbonyl groups, the OH and NH groups, as reported in the following.

Results and discussion

In addition to the spectra of the anthraquinone-imines, the IR spectra of the parent anthraquinones were recorded. The spectra of the two types of compounds are very similar in the region below 1500 cm^{-1}, the bands of the imines being shifted in analogous directions with the bands of the anthraquinone having the same R and R' substituents. We did not attempt the assignment of these bands. The bands appearing between 1600 and 1500 cm^{-1} were assigned to the NH deformation and aromatic ring vibrations (Table I), and the region between 3600 and 1600 cm^{-1}, which was the most important from the structural point of view, was studied in detail.

Table I

Assignment of the bands of the anthraquinone and anthraquinone-9-monoimine derivatives between 1500—1700 cm^{-1}

Substituent of the anthraquinone	$\nu_{C=O}$ intermolecular H bond	$\nu_{C=O}$ intramolecular H bond	$\nu_{C=N}$	Bands of aromatic rings	δ_{NH}
—	1685	—	—	1598 1590	—
1-Methoxy	1668	—	—	1585	—
1-Methoxy-9-monoimine	1671	—	1590	1590	1590
1-Hydroxy	1672	1640	—	1591	—
1-Hydroxy-9-monoimine	1668	—	1610	1592	1570
1-Hydroxy-2-methoxy	1665	1640	—	1590 1580	—
1-Hydroxy-2-methoxy-9-monoimine	1654	—	1612	1592	1565
1-Hydroxy-2-benzyloxy	1668	1638	—	1595	—
1-Hydroxy-2-benzyloxy-9-monoimine	1658	—	1615	1597	1568
1,2-Dihydroxy	1662	1632	—	1586	—
1,2-Dihydroxy-9-monimine	1623	—	1623	1590	1565
1-Hydroxy-2-glucosyloxy	1675	1638	—	1600 1585	—
1-Hydroxy-2-glucosyloxy-9-monoimine	1663	—	1622	1602	1570
1-Hydroxy-8-benzyloxy	1666	1630	—	1602 1580	—
1-Hydroxy-8-benzyloxy-9-monoimine	1660	—	1608	1585	1525

Bands of the C=O and C=N stretching vibrations

Evidence for the substitution of the carbonyl group in the 9 position could be obtained by the assignment of the $\nu_{C=O}$ and $\nu_{C=N}$ bands.

The assignment of the carbonyl bands in the anthraquinone derivatives was first accomplished by FLETT [4]. According to his results, the bands due to the two carbonyl groups appear at the same frequency in the spectra of anthraquinone and symmetrically substituted anthraquinones, because there is no coupling between the vibrations of the quinone carbonyl groups. Asymmetrically substituted anthraquinones also show only one carbonyl band, if the substituent is not a hydroxy or amino group. The inductive effect of the substituent influences the frequency of the carbonyl band in the expected manner. If the anthraquinone is α-substituted by a hydroxyl or amino group, the two carbonyl bands appear separately, because an intramolecular hydrogen bond is formed between the carbonyl and the hydroxyl or amino group, which lowers the frequency of the hydrogen-bonded carbonyl group.

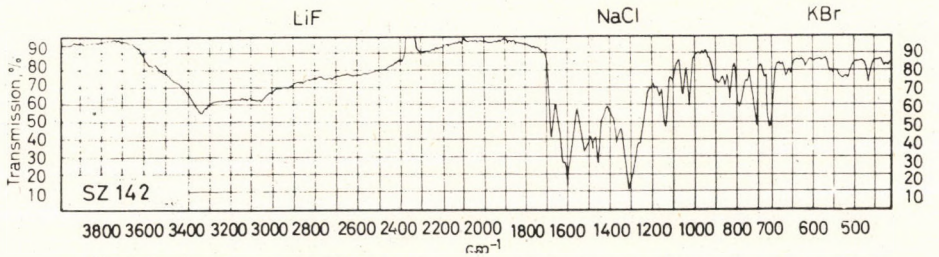


Fig. 1. Spectrum of 1-hydroxyanthraquinone-9-monoimine (in KBr disc)

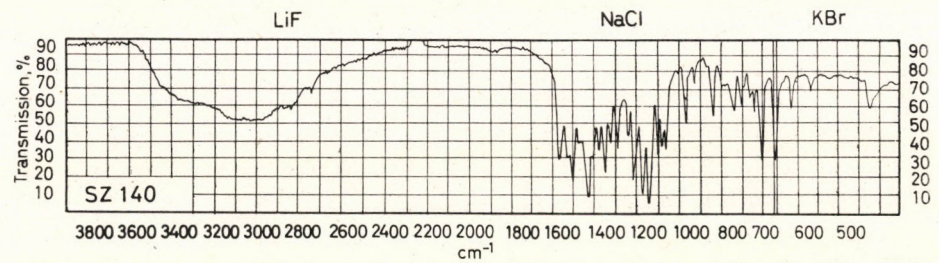


Fig. 2. Spectrum of 1-hydroxy-2-methoxyanthraquinone-9-monoimine (in KBr disc)

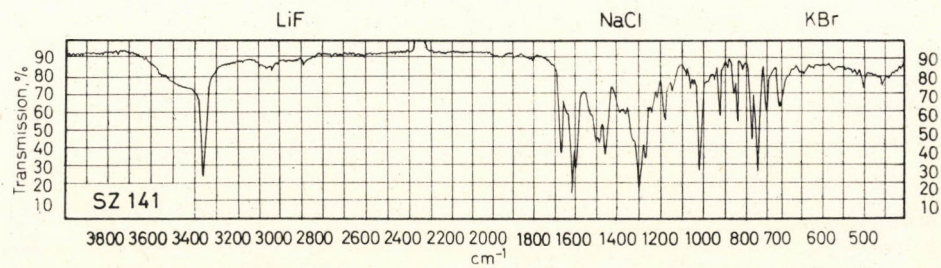


Fig. 3. Spectrum of 1-hydroxy-8-benzyloxyanthraquinone-9-monoimine (in KBr disc)

These findings of FLETT were corroborated by the investigations of HADZI and SHEPPARD [5]; our own results (Table I) are also in agreement with those of the above-mentioned authors.

The solid phase spectra of the anthraquinone-imines investigated (Spectra 1, 2, 3) usually show one band above 1625 cm^{-1}, namely between 1670 and 1650 cm^{-1}. (Alizarinimine is an exception. The spectrum of this compound will be discussed later on.) This band can be assigned to the C=O group in position 10, because the band of the hydrogen-bonded C=O in the 9 position always appears at frequencies 25—30 wave numbers lower in the spectra of the corresponding anthraquinones. The band occurring between 1625 and 1605 cm^{-1} must, therefore, be assigned to the C=N double bond of the imine, formed at the 9 position. Existing data on the C=N group are

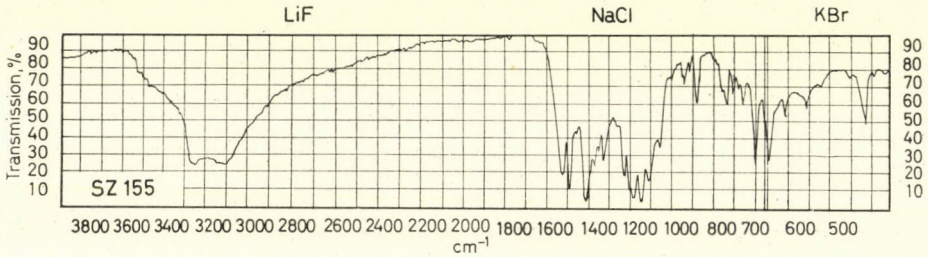
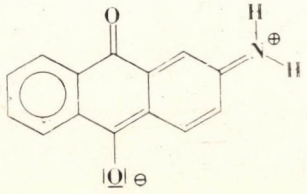


Fig. 4. Spectrum of 1,2-dihydroxyanthraquinone-9-monoimine (in KBr disc)

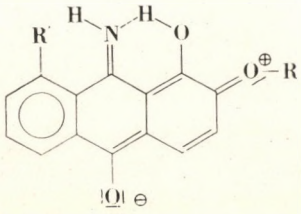
in accord with this assignment. RAO [6*a*] and others [7, 8] always found the absorption band corresponding to the C=N stretching vibration between 1610 and 1630 cm^{-1} in the spectra of aromatic Schiff bases. The slight lowering (about 10 wave numbers) of the frequencies of the carbonyl band at the 10 position can also be explained by the formation of the imino group at the 9 position. Namely, the electronegativity of the nitrogen in position 9 in the anthraquinone-imines is smaller than that of the oxygen in the corresponding anthraquinone, and therefore the polarity of the carbonyl in the 10 position is slightly enhanced.

The IR spectrum of alizarinimine must be discussed separately. The UV spectrum [3] shows conclusively that this compound has a chromophoric system which is identical with that of other anthraquinone-imines. Elemental analysis has shown that it contains one nitrogen atom, and alizarin can be regenerated from it by acid hydrolysis. Therefore, its structure must correspond to **II** (R=OH, R′=H). In the IR spectrum, on the other hand (Spectrum 4), the two bands do not occur near 1665 and 1615 cm^{-1}, but only one higher intensity band can be observed at 1623 cm^{-1}, which obviously contains both the C=O and C=N vibrations. No such shift of the 10-carbonyl group can be observed in alizarin or 2-hydroxyanthraquinone. FLETT [4] found a similar shift in the spectrum of 2-aminoanthraquinone, the two carbonyl bands of

which are found at 1676 and 1625 cm^{-1}. FLETT assigned the band at 1625 to the 10-carbonyl, and explained the lowering of the frequency with the higher probability of limiting structure **III**. Although the lowering of the carbonyl frequency of alizarinimine can partly also be due to the enhancement of the contribution of a limiting formula (**IV**; R=R′=H) analogous to **III** (this is shown by the shift of the carbonyl frequency in the 2-alkoxy derivatives, which is in the same direction but smaller), we think the main reason for the shift is the intermolecular association of the 2-hydroxyl group and the 10-carbonyl group, which in itself lowers the C=O band order (and therefore the $\nu_{C=O}$ frequency).



III



IV

Unfortunately, no evidence could be obtained by comparison of solution and solid state spectra, as the alizarin-9-monoimine is insoluble in the usua- solvents. Even its solubility in alcohol is much less than that of other anthrai quinone-imines, which incidentally also points to strong intermolecular association.

Bands of the NH and OH stretching vibrations

Intramolecular hydrogen bonds can form between the 1-hydroxyl group and the nitrogen of the imino group, or between the imino hydrogen and an ether or hydroxyl group in the 1-position. The hydrogen bond between the hydroxylic hydrogen and the imino nitrogen is a chelate-type bond (*cf.* [6*b*, 10]), which differs from that of 1-hydroxy-anthraquinones only in that one of the bridge-head atoms is a nitrogen. FLETT [4] could not find the ν_{OH} band in the solid phase spectra of 1-hydroxyanthraquinone, according to his paper published in 1948. BLOOM *et al.* obtained similar results [9]. HADZI and SHEPPARD [5] showed that the band appears between 3200 and 2600 cm^{-1} in solution spectra, with a maximum between 3000 and 2850 cm^{-1} but with a low intensity, while in solid phase spectra it vanishes under the curved base line due to the light scattering of the sample. The first reports on hydrogen bonds between chelated C=N and OH groups are due to KAZITSINA and MISHCHENKO [7] and FREEDMAN [8]. They also reported that the ν_{OH} band is very broad and drawn out with a maximum between 2800—2600 cm^{-1}, but its intensity seems to be larger than in the case of 1-hydroxyanthra-

quinone. The enhanced intensity can be explained by the difference in the charge of the bridge-head atoms.

The hydrogen bond between the 10-carbonyl group and the hydrogen atom of the imino group can only be intermolecular.

In the solid phase spectrum (KBr disc) (Spectrum 5) of 1-methoxy-anthraquinone-9-monoimine one band is found in the NH stretching region at 3325 cm^{-1}. The NH band is sharp, its half-band width is only 20 wave-numbers, so that it cannot be due to a chelate hydrogen bond. This band does not shift if the spectrum of the compound is taken in dichloromethane solution.

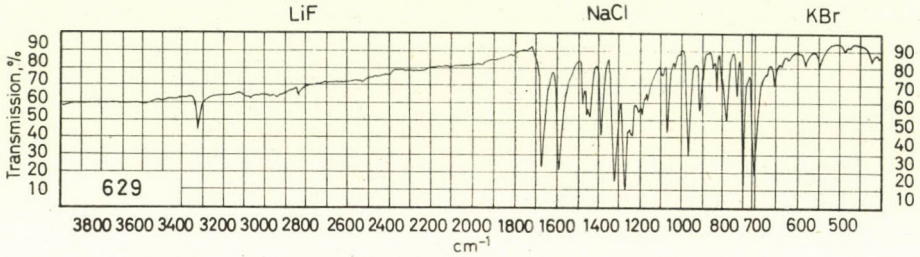
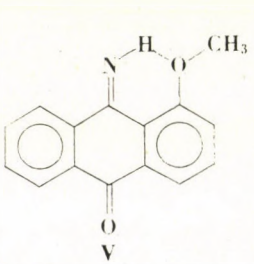
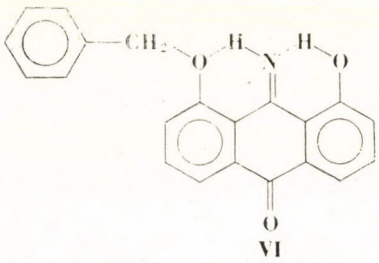


Fig. 5. Spectrum of 1-methoxyanthraquinone-9-monoimine (in KBr disc)

This shows that a weak intramolecular hydrogen bond is formed between the imino hydrogen and the oxygen of the methoxy group (**V**). The weakness of the hydrogen bond can be explained by the fact that the hydrogen of the imino group is less acid than that of a phenolic hydroxyl group, and therefore the strong hydrogen bond necessary for the formation of the chelate cannot be formed.



V



VI

The infrared spectrum shows the formation of a similar hydrogen bond in 1-hydroxy-8-benzyloxyanthraquinone-9-monoimine (Spectrum 3) between the NH group and the ethereal oxygen in the 8-position (**VI**). The ν_{NH} band appears at 3360 cm^{-1} in both liquid and solid phase spectra. The chelate band due to the hydrogen bond between the 1-hydroxyl and the imino-N atom cannot be identified in spectra taken in KBr discs, and it appears as a very broad, drawn-out, low-intensity band in CCl_4 solution with a maximum between 2600 and 2500 cm^{-1}.

The spectra are slightly more complex if the imino hydrogen cannot form an intramolecular hydrogen bond. In these cases intermolecular hydrogen bonds are formed between the NH group and the carbonyl group in position 10. These compounds are rather insoluble even in polar solvents, so that spectra could only be taken in the solid phase (KBr disc).

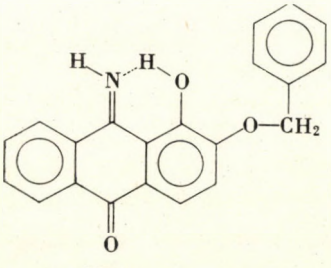
In the spectrum of 1-hydroxyanthraquinone-9-monoimine (Spectrum 1) a diffuse absorption appears between 3400 and 2200 cm^{-1}, and two smaller bands are superimposed on this at 3060 and 3340 cm^{-1}. The 3060 cm^{-1} band can be assigned to the stretching vibrations of the protons of the benzene rings, while the 3340 cm^{-1} band belongs to the NH group. Thus in 1-hydroxyanthraquinone-9-monoimine a chelate type hydrogen bond is formed between the 1-hydroxyl group and the imino nitrogen, the chelate band having a fairly high intensity with a maximum at about 2700 cm^{-1}.

In the spectra of 1-hydroxy-2-alkoxyanthraquinone-9-monoimines (*e.g.*, Spectrum 2) the OH and NH stretching vibrations appear together between 3400 and 2200 cm^{-1} with a maximum of about 3050 cm^{-1}. In these cases the NH band cannot be separated, contrary to the case of the 1-hydroxy derivative. This can be interpreted by assuming that the intermolecular hydrogen bond of the NH group is probably stronger, therefore the ν_{NH} band is more diffuse and shifts to lower wave numbers. The formation of a stronger intermolecular hydrogen bond is favoured by the polarization of the 10-carbonyl group by the 2-alkoxy group, thereby enhancing its ability to form hydrogen bonds. As already mentioned, the frequency of the ν_{CO} band of 1-hydroxy-2-alkoxyanthraquinone-9-monoimines is always lower than that of 1-hydroxyanthraquinone-9-monoimine.

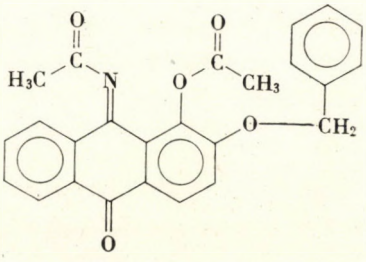
In the spectra of alizarinimine (Spectrum 4) a band appears at 3300—3350 cm^{-1}, which is due to the intramolecularly bonded hydroxyl group in the 2-position.

Structure of the acyl derivatives

Further proof for the above conclusions concerning the structures of the imines was obtained by the preparation and IR spectroscopic investigation



VII



VIII

of acyl derivatives. Compound **VIII** obtained by the acetylation of 2-benzyl-alizarin-9-monoimine (**VII**) shows four bands in the double bond region (Spectrum 6). The highest frequency band appears at 1770 cm^{-1} and is undoubtedly due to the carbonyl group of the phenolic ester formed from the 1-hydroxy group. The other three bands (1672, 1660, 1645 cm^{-1}) can be assigned to the carbonyl at carbon 10, the amide carbonyl, and the C=N groups (Table II). Similar results were obtained with the benzoyl derivatives of alizarin-(2)-benzyl ether 9-monoimine and alizarin-9-monoimine; the spectral data of these compounds are also shown in Table II.

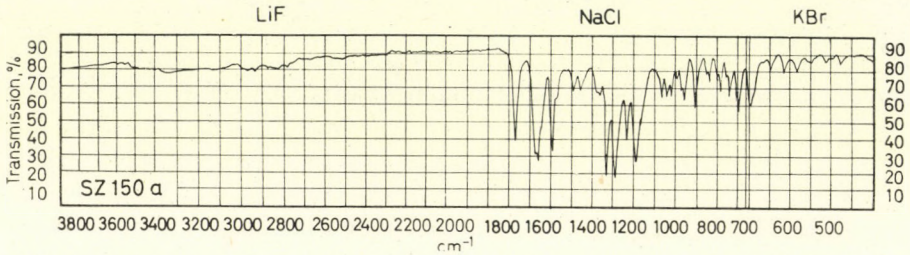


Fig. 6. Spectrum of N-acetyl-1-acetyl-2-benzylalizarin-9-monoimine (in KBr disc)

Table II

Assignment of the important bands of the acylated anthraquinone-imines

Compound	$\nu_{C=O}$			$\nu_{C=N}$
	phenol ester	amide	10-carbonyl	
N-acetyl-1-acetyl-2-benzyl-alizarin-9-monoimine	1770	1660	1672	1645
N-benzoyl-1-benzoyl-2-benzylalizarin-9-monoimine	1742	1660	1670	1645
N-benzoyl-1,2-dibenzoylalizarin-9-monoimine	1750	1648	1673	1648

Thus the investigation of the acyl derivatives has afforded further evidence for the structure of the compounds formed in the reaction of hydroxy-

Table III

NMR data of N-acetyl-2-benzylalizarin-9-monoimine

Group	Chemical shift (δ) ppm (TMS = 0 ppm)	Multiplicity	Number of protons from integration
CH_3CON	2.15	none	3
CH_3COO—	2.30	none	3
—O—CH_2—Ph	5.25	none	2

The multiplet signals of the aromatic protons appear between 7.10 and 8.50 ppm. The sum of their intensities indicates 11 protons.

anthraquinones and alcoholic ammonia, as the appearance of the phenol ester $\nu_{C=O}$ band proves that the OH group has not been replaced by an amino group, and the 1645 cm^{-1} band in the spectra shows the presence of the C=N group. Further confirmation of the structure has been obtained from the NMR spectrum of compound **VIII**, which shows all proton signals with the expected chemical shifts and with the expected integrated intensities (Table III).

Experimental

The anthraquinone-imines and their derivatives were prepared as reported in our previous papers [1, 2] and their purity was checked by microanalysis. Infrared spectra were recorded on a Zeiss UR 10 double-beam recording spectrophotometer. Solid phase spectra were obtained in KBr disc. The NH stretching region of the spectrum of 1-methoxyanthraquinone-9-monoimine and 1-hydroxy-8-benzyloxyanthraquinone-9-monoimine were also obtained in dichloromethane solution (concentration 1/10 mole/l) using a 0.1 mm NaCl cell, or in saturated carbon tetrachloride solution in a 40-mm infrasil cell.

The NMR spectrum was recorded with a JEOL J-NM-C-60 type 60 Mc instrument in $CDCl_3$ solution at room temperature.

REFERENCES

1. MÜLLER, A.: Ber. **64,** 1410 (1931).
2. MÜLLER, A., KÖRMENDY, K., Ruff, F.: Acta Chim. Acad. Sci. Hung. **58,** 465 (1968).
3. MÜLLER, A., KÖRMENDY, K., RUFF, F., VAJDA, M.: Acta Chim. Acad. Sci. Hung. **59,** 109 (1969).
4. FLETT, M. St. C.: J. Chem. Soc. **1948,** 1441.
5. HADZI, D., SHEPPARD, N.: Trans. Faraday Soc. **50,** 911 (1954).
6. RAO, C. N. R.: Chemical application of infrared spectroscopy. Academic Press, New York, London, Toronto, 1963 *(a)* p. 267; *(b)* p. 185.
7. KAZITSINA, L. A., MISHCHENKO, N. V.: Doklady Akad. Nauk. SSSR **150,** 555 (1963).
8. FREEDMAN, H. H.: J. Am. Chem. Soc. **83,** 2900 (1961).
9. BLOOM, H., BRIGGS, L. H., CLEVERLEY, B.: J. Chem. Soc. **1959,** 178.
10. SOHÁR, P.: Magyar Kém. Foly. **71,** 415 (1965).

Károly KÖRMENDY
Ferenc RUFF
Miklós VAJDA
} Budapest VIII. Múzeum krt. 4/b
Pál SOHÁR; Budapest IV. Szabadságharcosok útja 47—49

Acta Chimica Academiae Scientiarum Hungaricae Tomus 59(1), pp. 109—118 (1969)

ULTRAVIOLET SPECTROSCOPIC INVESTIGATION OF SOME 1-HYDROXYANTHRAQUINONE-9-MONOIMINES

A. MÜLLER†, K. KÖRMENDY, F. RUFF and M. VAJDA

(Institute of Organic Chemistry, L. Eötvös University, Budapest)

Received January 22, 1968

An ultraviolet spectroscopic investigation was made to obtain data on the structures and electronic transitions of hydroxyanthraquinone-9-monoimine type compounds. Analysis of the solvent effects showed that the band occurring at about 520 nm in the spectra of these compounds belongs to an $n \rightarrow \pi^*$ transition, whereas the band near 400 nm can be assigned to an intramolecular charge transfer transition. The changes in the band intensities depending on the solvent are interpreted by interactions between the substituents and the solvent.

In our previous communications [1, 2] we reported chemical and IR spectroscopic evidence concerning the structure of 1-hydroxyanthraquinone-9-monoimines, which were formed in the reaction of 1-hydroxyanthraquinone, or its 2- and 8-hydroxy and alkoxy derivatives, with alcoholic ammonia. The UV spectra of these compounds were also recorded so as to obtain data on the chromophoric system and electronic transitions of these anthraquinone-9-monoimines, thereby adding to the structural evidence. The analysis of the spectra of the corresponding anthraquinones was also important for our purposes, therefore these spectra were also recorded.

A simple comparison of the spectra of anthraquinones and the corresponding anthraquinone-imines taken in alcoholic solution — as can be seen from the spectra of 1-hydroxyanthraquinone and 1-hydroxyanthraquinone-9-monoimine (Figs 1, 2) — indicates that the structural arrangement of the two types of compounds is analogous, and it would seem that the spectra of the anthraquinone-imine can be constructed by shifting the analogous bands of the anthraquinone spectrum. However, the possibility of such a simple analogy had to be excluded from data gained from the examination of solvent effects.

Various authors have investigated the UV spectra of anthraquinone and its derivatives [3, 4, 5, 6, 7], and attempts have been made to assign bands to the quinonoid and benzenoid moieties of the molecule. The contribution of NAGAKURA and KUBOYAMA [7] is especially important, as they investigated the assignment of the various spectral bands of anthraquinone to definite electronic transitions on the basis of solvent effects [8]. They established that the bands appearing at 250 and 320 nm are due to $\pi \rightarrow \pi^*$ transitions while the absorption around 385 nm is due to an $n \rightarrow \pi^*$ transition. The assignment

of the first two bands was further substantiated by calculations of KUBOYAMA [9] using the MO method. According to these calculations, the 320 nm band can belong to several transitions of nearly identical energy, and electron donor groups in the molecule can influence the energy of these transitions in various ways. Due to these different effects, the 320 nm band shows a bathochromic shift and splits into several bands.

As anthraquinone-9-monoimines were not described previously, no direct data are available on the UV spectra of these compounds. MATSEN [10] mentions that the mono- and diimines of benzoquinone are not yellow, but very pale yellow or white. As the yellow colour of benzoquinone is due to an absorption band of $n \rightarrow \pi^*$ transition, which falls into the visible region, he supposes that in the imines the lone electron pair on the nitrogen atom is tightly bound because of its considerable *s* character.

1-Hydroxyanthraquinone-9-monoimines show much structural similarity to *o*-hydroxycarbonyl-imines which have been studied extensively. KISS [11], HIRES [12, 13] and KAZITSINA and MISHCHENKO [14] state unanimously in their publications that a band appears around 400 nm if the spectra of the *o*-hydroxycarbonyl-imines are taken in hydroxylic solvents, and this band is probably due to an $n \rightarrow \pi^*$ transition. As KISS only found this band in the spectra of *o*- and *p*-hydroxycarbonyl-imines, he supposed that its appearance was connected with the enhanced probability of a quinonoid limiting structure. HIRES suggested that the appearance of the band was due to the formation of a complex with alcohol, as in the case of compounds he investigated, the band did not appear in the spectra taken in hexane solutions. KAZITSINA and MISHCHENKO found some compounds where the band in question also appeared in spectra taken in non-polar solvents, and therefore they rejected the possibility of complex formation, as suggested by HIRES. These authors also rejected the suggestion of KISS on the ground that no quinonoid structure was present according to the IR and NMR spectra. They also mentioned that measurement of dipole moments also failed to show the existence of dipolar limiting structures. KAZITSINA and MISHCHENKO do not attempt to give a specific reason for the appearance of the band, but only state that the conditions for its appearance are: strong intramolecular interaction, and strong intermolecular interaction with hydrogen bond or dipole-dipole character between solvent and solute.

Results and discussion

In our work the spectra of anthraquinone and anthraquinone derivatives were recorded in ethanol, chloroform, pyridine, dioxane and carbon tetrachloride. (Our choice of solvents was limited by the solubility of the anthraquinone-imines.) The results obtained are collected in Table I and they can be summarized as follows.

Our results with anthraquinone confirm those of other authors. The wave length of the band around 320 nm is lowered with diminishing polarity

Table I

Spectral data of anthraquinones

Compound Solvent	$\lambda_{max.}$ ε							
Anthraquinone								
Alcohol	253 48300	~263 17700		272 15300	326 5000	384 140		
Chloroform	254 51300	~262 21000		274 16900	327 5100	384 125		
Pyridine					327 5050	384 120		
Dioxan	252 46200	~263 18800		~270 13500	324 4700	386 100		
Carbon tetrachloride		263 19000		~272 18000	323 5300	394 100	411 83	439 47
1-Methoxyanthraquinone								
Alcohol	220 27000	254 25500		~268 16000	331 2200	387 5840		
Chloroform		256 26500		~271 16100	328 2170	383 5700		
Pyridine					329 2300	380 5700		
Dioxan		255 26000		~266 16400	330 2300	376 5600		
Carbon tetrachloride		256 25000		~268 15000	328 1070	375 5600		
1-Hydroxyanthraquinone[1]								
Alcohol	219 22000	253 24800		~272 15200	331 2470	~390 5270	406 5840	~423 5100
Chloroform	254 23600	~258 22600	271 18900	~278 17500	334 2500	~392 5300	408 5900	~423 5000
Pyridine					337 2500	~394 5200	408 5600	~424 4800
Dioxan		255 25300		~267 20300	329 2770	~392 5700	405 6100	~420 5200

[1] Insoluble in carbon tetrachloride
~ Shoulder

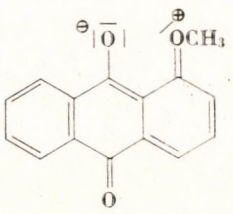
Table I (continued)

Compound Solvent	$\lambda_{max.}$ ε								
1-Hydroxy-2-methoxyanthraquinone[1]									
Alcohol	~231	248	~246		~278	~325	~409	429	~439
	19100	32000	2850		14500	3200	5500	6400	6000
Chloroform		249	~255	~261	278	327	~409	427	~440
		32000	30000	25400	15700	3200	5700	6600	6000
Pyridine						326	~411	428	~440
						3300	5400	6100	5800
Dioxan	~234	248	~255		~275	321		425	
	20400	33000	27700		14700	3250		6310	
1,2-Dihydroxyanthraquinone[1]									
Alcohol	~234	249	~260		~278	~327		438	
	18500	32000	24200		15500	3400		5600	
Chloroform		249	254	258	277	331	~414	425	
		29000	28000	25000	17000	3300	5100	5300	
Pyridine						329		440	
						3850		5600	
Dioxan	233	247			278	328		426	
	18200	30700			19700	3300		5300	
1-Hydroxy-8-benzyloxyanthraquinone									
Alcohol	224	255			~279			420	~427
	48900	24200			10900			10000	9800
Chloroform		256			278			420	~430
		28000			13800			10600	10400
Pyridine								420	~430
								10200	9800
Dioxan	224	256			~278		~396	415	~425
	44400	25000			11000		8500	10000	9600
Carbon tetrachloride		256	~274		~279		~404	416	~430
		23700	12500		10000		9300	10300	9800

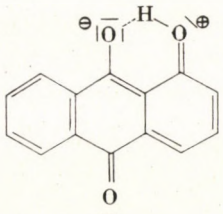
of the solvent, while the band near 250 nm shows no appreciable shift. These bands therefore belong to $\pi \rightarrow \pi^*$ transitions. The 380 nm low-intensity band, on the other hand, shows a bathochromic shift with diminishing solvent polarity, *i.e.* the polarity of the solvent has the opposite effect on this band compared with that at 320 nm. The 380 nm band, therefore, belongs to an $n \rightarrow \pi^*$ transition.

When a methoxyl group is introduced in the 1-position of anthraquinone, the following changes occur in the spectra. The intensity of the 250 nm band is reduced to half its previous value, and a higher intensity band appears at

about 380 nm which shows a hypsochromic shift with decreasing solvent polarity, therefore it cannot belong to an $n \rightarrow \pi^*$ transition. It can be supposed that it belongs to a transition where the donor character of the methoxyl group — as shown by limiting formula **I** — has an important role. Therefore, we think that we can call this transition an intramolecular charge transfer transition, as DILLING did in the case of hydroxybenzophenones [15].



I



II

In the spectra of 1-hydroxyanthraquinone the following changes can be observed compared with the spectra of the methoxy derivative. The longest wavelength band appears at 406 nm, *i.e* it is shifted by a further 20 nm to lower energies, and this band shows vibrational structure. Solvent effects, on the other hand, are less pronounced than in the case of 1-methoxyanthraquinone. The shift of the band of 1-hydroxyanthraquinone compared with that of 1-methoxyanthraquinone, can be explained by the fact that an intramolecular hydrogen bond (**II**) facilitates the charge transfer.

Similar results were obtained in the case of 1-hydroxy-2-methoxy-, 1,2-dihydroxy- and 1-hydroxy-8-benzyloxyanthraquinone, and it appears that a second electron donor group causes a further bathochromic shift of 20 nm on the longest wavelength band compared with that of 1-hydroxyanthraquinone.

From the spectra of the anthraquinone-9-monoimines (Table II) the following results were obtained:

The spectrum of 1-methoxyanthraquinone-9-monoimine does not show any significant difference from that of 1-methoxyanthraquinone. The two bands between 300 and 400 nm in the spectra of this imine are displaced by about 10 nm towards the shorter wavelengths compared with 1-methoxyanthraquinone. These bands shift to longer wavelengths with higher solvent polarity, so that they should also be assigned to intramolecular charge transfer transitions.

The spectrum of 1-hydroxyanthraquinone-9-monoimine is similar to that of 1-hydroxyanthraquinone, although the shifts of the bands are larger. If the spectra, taken in alcoholic solution, are compared, the bands at 330 and 408 nm in the 1-hydroxyanthraquinone spectrum appear to be shifted

Table II

Spectral data of anthraquinone-9-monoimines

Compound Solvent	$\lambda_{max.}$ ε								
1-Methoxyanthraquinone-9-monoimine[1]									
Alcohol	213		254	~270	324	373			
	26000		29000	14500	3400	4100			
Chloroform		237	256	~267	325	362			
		15300	30200	16300	3500	3900			
Pyridine					320	372			
					3500	3800			
Dioxan			254	~268	323	367			
			28500	14800	3900	3840			
1-Hydroxyanthraquinone-9-monoimine[2]									
Alcohol	221		250	276	320	409		519	
	17000		21900	14000	4500	2400		4500	
Pyridine						395		530	561
						3600		2200	1700
Dioxan	226	239	252	268	319	398	501	535	569
	19100	19600	19200	17300	3300	3900	730	840	660
1-Hydroxy-2-methoxyanthraquinone-9-monoimine[1]									
Alcohol		259		~290		391	507	535	565
		39000		7600		1500	8350	10300	7400
Chloroform		251	~262			421	510	536	575
		29500	27900			3100	4750	6000	4100
Pyridine						400	510	540	575
						2200	6400	8300	6000
Dioxan		248	~258	282		420	514	544	579
		29500	24300	10300		3300	3900	4800	3300
1,2-Dihydroxyanthraquinone-9-monoimine[3]									
Alcohol		236	260	~290		406	~514	544	575
		17000	38400	10500		2500	6200	7500	5550
Dioxan		251	264	283		406	519	544	577
		24500	28800	9730		2500	5100	6200	4300

to 409 and 520 nm (Figs 1, 2). The fact that the bands are not analogous and belong to different transitions was shown by the examination of solvent effects. The 520 nm band of the imine shows a bathochromic shift, and its intensity is decreased if the polarity of the solvent is lowered, while the 409 nm band shows a hypsochromic shift and its intensity is enhanced under these

Table II (continued)

1-Hydroxy-8-benzyloxyanthraquinone-9-monoimine									
Alcohol	218	249	283	372				519	
	33800	22300	9200	4100				5900	
Chloroform		250	283	368		~406		534	
		23600	10700	4500		3400		3800	
Pyridine				373		~398		539	~565
				4800		4400		2200	1800
Dioxan	216	~251	~278	368		~401	~514	544	~571
	35700	19400	10900	4800		4400	1330	1500	1200
Carbon tetrachloride			274	353	361	406	519	556	589
			12400	4500	4600	4700	770	820	590

[1] Insoluble in carbon tetrachloride
[2] Insoluble in carbon tetrachloride and chloroform
[3] Insoluble in carbon tetrachloride, chloroform and pyridine
~ Shoulder.

conditions. The 520 nm band can, therefore, be assigned to an $n-\pi^*$, the 409 nm band to an intramolecular charge transfer transition.

The spectra of 1-hydroxy-8-benzyloxy- and 1-hydroxy-2-methoxy-anthraquinone-9-monoimine show basically similar effects. In the case of

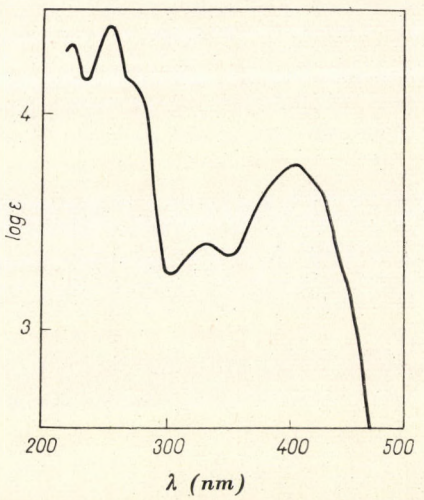


Fig. 1. Spectrum of 1-hydroxyanthraquinone in alcohol

the 1-hydroxy-2-methoxy derivative the lowering of the intensity of the 520 nm band is less than in the case of the 1-hydroxy derivative, and in the case of the 1-hydroxy-8-benzyloxy derivative the effect is quantitatively similar to the 1-hydroxy derivative. The intensity of the band at about 400 nm is enhanced with the lowering of solvent polarity in the spectra of both these substances, but the wavelength shift is less evident than in the case of the

1-hydroxy derivative. The reason for this is that several bands of varying intensity appear in this region and these bands coalesce, and the resultant band does not always give an unequivocal picture of the shifts of the component bands.

The spectra of alizarin-9-monoimine show no solvent effect.

Thus, anthraquinone-imines show spectral shifts with changing polarity of the solvents, similar to those observed in the spectra of *o*-hydroxycarbonyl-imines. In the following, we attempt to interpret these phenomena by correlation with the electronic transitions.

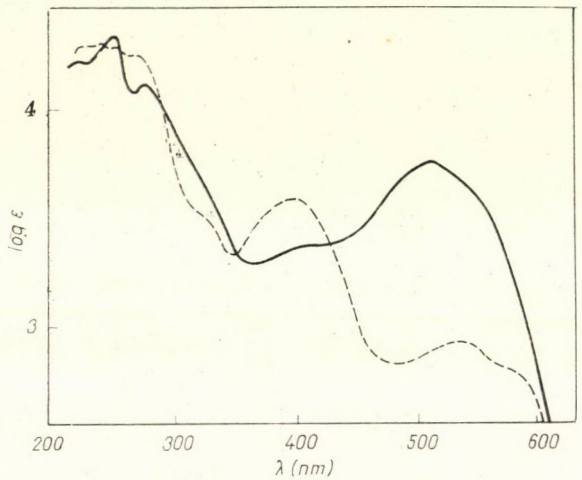


Fig. 2. Spectrum of 1-hydroxyanthraquinone-9-monoimine in alcohol (———) and in dioxan (— — —)

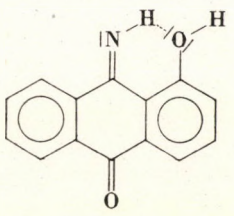
PORTER and SUPPAN [16] state that an $n-\pi^*$ transition enhances the positive charge on the atom having a lone electron pair. In the case of the imino compound this means that the $n-\pi^*$ transition will enhance the positive charge on the nitrogen atom. Nitrogen is less electronegative than oxygen, and this seems to account for the higher intensity of the $n-\pi^*$ transition band in the spectra of the imines. The charge density contribution of the electron which is promoted during excitation to the π^* orbital is defined by the wave function of the state in question. This wave function is not known, and because of the complicated structure of our compounds its calculation was not practicable. However, taking into account that an $n-\pi^*$ transition is only observed if there is an *ortho*, or according to KISS a *para*, hydroxyl group in the system, we can suppose that the higher electron density occurs in this position in the excited state. An electron-attracting group will stabilize this charge distribution, thereby enhancing the stability of the excited state and the probability of the transition. The hydroxyl group, of course, cannot be simply taken as an electron-attracting group as it exhibits both a $-I$ and a

$+T$ effect, and generally $+T$ has the larger absolute value. However, if the solvent contains a hydroxyl group or if it has high polarity, hydrogen bonding or solvent-solute interaction may fix the lone electron pairs to the oxygen atom to a considerable extent, thereby diminishing the tautomeric effect, so the $-I$ effect may become prevalent. This seems to account for the fact that the intensity of the $n-\pi^*$ band is enhanced in hydroxylic or strongly polar solvents.

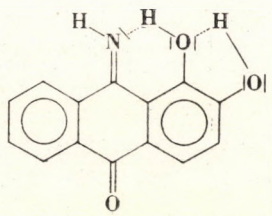
In non-polar solvents, interaction between the solute molecules or further electron-attracting groups in the molecule (*e.g.* the carbonyl group in the 10 position) may also exert a stabilizing influence. We suppose that this is the reason for the appearance of an $n-\pi^*$ transition band in the spectra of some of the compounds even if they are taken in non-polar solvents.

If the $+T$ effect of hydroxyl groups predominates — in non-polar or moderately polar solvents — this is favourable for the appearance of the intramolecular charge transfer band. The electron transfers involved are probably of the type shown in limiting formula **II.**

The above considerations seem to account for the appearance of the $n-\pi^*$ band (around 520 nm) in the spectra of 1-hydroxy-, 1-hydroxy-2-methoxy- and 1-hydroxy-8-benzyloxyanthraquinone-9-monoimine, taken in alcoholic solution, and also for the lowering of the intensity of this band with diminishing polarity of the solvent. They also account for the appearance of the charge transfer band (400 nm) in the less polar solvents. The probable reason why the intense $n-\pi^*$ transition band does not appear in the spectra of 1-methoxyanthraquinone-9-monoimine, is that it has structure **III.** This structure is in accord with infrared spectroscopic evidence [2].



III



IV

The hydrogen bond in this structure (**III**) does not cause transfer of the lone electron pair to an sp^3 hybrid orbital, therefore it retains its *s* character and is more difficult to excite, similarly to the phenomenon observed with benzoquinone-imines. The reason for the slight lowering of the wavelength of the charge transfer band (ca. 10 nm) compared with that of 1-methoxyanthraquinone, is probably the hydrogen bond between the imino and methoxy groups. This bond is unfavourable for the formation of limiting structure **II.**

The independence of the spectrum of alizarin-9-monoimine from the solvent is probably due to an intramolecular hydrogen bond between the 2- and 1-hydroxyl groups (**IV**).

EXPERIMENTAL

Anthraquinone-9-monoimines were prepared as reported in our previous communication [1]. The spectra were recorded with a UNICAM SP 700 spectrophotometer in 10^{-4} molar solution using cells from 1—40 mm. Data on the maxima and in figures have been converted to wavelengths.

REFERENCES

1. MÜLLER, A., KÖRMENDY, K., Ruff, F.: Acta Chim. Acad. Sci. Hung. **58,** 465 (1968).
2. MÜLLER, A., KÖRMENDY, K., RUFF, F., SOHÁR, P., VAJDA, M.: Acta Chim. Acad. Sci. Hung. **59,** 99 (1969).
3. MORTON, R. A., EARLAM, W. T.: J. Chem. Soc. **1941,** 159.
4. PETERS, R. H., SUMMER, H. H.: J. Chem. Soc. **1953,** 2101.
5. YOSIMOTHO, T.: Nippon Kagaku Zasshi **84,** 733 (1963).
6. HAYASHI, T., TOKUMITSU, T.: Bull. Chem. Soc. Japan **35,** 1500 (1962); **38,** 916 (1963).
7. NAGAKURA, S., KUBOYAMA, A.: J. Am. Chem. Soc. **76,** 1003 (1954).
8. MCCONNEL, H.: J. Chem. Phys. **20,** 700 (1952).
9. KUBOYAMA, A.: Bull. Chem. Soc. Japan **31,** 752 (1958).
10. MATSEN, F. A.: Application of the theory of electron spectra in "Technique of Organic Chemistry, IX". Interscience Publishers Inc. New York, 1956, p. 697.
11. KISS, A., AUER, J.: Z. Phys. Chem. **A 189,** 344 (1941).
12. HIRES, J.: Acta Phys. et Chem. Szeged **4,** 120 (1958).
13. HIRES, J., HACKEL, L.: Acta Phys. et Chem. Szeged **5,** 19 (1959).
14. KAZITSINA, L. A., MISHCHENKO, V. V.: Zhur. Org. Himii **1,** 617 (1965).
15. DILLING, W. L.: J. Org. Chem. **31,** 1045 (1966).
16. PORTER, G., SUPPAN, P.: Proc. Chem. Soc. **1964,** 191.

Károly KÖRMENDY
Ferenc RUFF
Miklós VAJDA

Budapest VIII. Múzeum krt. 4/b

Acta Chimica Academiae Scientiarum Hungaricae Tomus 59 (1), pp. 119—131 (1969)

REACTIONS CATALYZED BY STRONG ACIDS IN NON-AQUEOUS MEDIA, II*

THE SULPHURIC ACID AND BORON TRIFLUORIDE CATALYZED REACTION OF AROMATIC ALDEHYDES WITH ARYL ACETONITRILES LEADING TO ARYLIDENE-BIS(ARYL ACETAMIDE)

Z. CSŰRÖS, Gy. DEÁK, M. HARASZTHY-PAPP and I. HOFFMANN

(Department of Organic Chemical Technology, Polytechnical University, Budapest, and Research Group for Organic Chemical Technology of the Hungarian Academy of Sciences, Budapest)

Received April 3, 1968

Benzylidene-bis(phenylacetamide) and 17 new substituted derivatives have been prepared by reacting aromatic aldehydes with benzyl cyanide and its ring-substituted derivatives, in acetic acid, in the presence of boron trifluoride or sulphuric acid. It has been established that the amide group is not formed during the work-up procedure, but in a direct reaction while the organic acid is converted to its anhydride. There is an optimum amount of added catalyst above which the hydration of benzyl cyanide to phenylacetamide becomes predominant.

It has been reported [1] that the Claisen-Schmidt condensation of benzaldehyde with acetophenone leading to benzylideneacetophenone can be carried out in absolute acetic acid in the presence of boron trifluoride catalyst. When the reaction was studied with benzyl cyanide, a compound with an active methylene group, in the presence of a stoichiometric amount of BF_3, a white crystalline solid (m.p. 221—223 °C) was obtained in 22% yield instead of the expected α-phenylcinnamonitrile. The product was sparingly soluble in hot alcohol, soluble in hot acetic acid, bromobenzene, and dimethylformamide. The IR spectrum did not show the presence of the nitrile group, but the C=O and N—H stretching frequencies characteristic for amides did appear at 1660 and 3270 cm^{-1}, respectively. It was concluded that under the conditions of the experiment the primarily formed α-phenylcinnamonitrile had been hydrated to the corresponding amide. The product, however, was not α-phenylcinnamamide, and, therefore, we attempted to determine its structure. A direct determination of the molecular weight (Rast, ebullioscopic method) was impossible owing to the low solubility. Therefore, an indirect method was used. When the reaction was carried out with *p*-chlorobenzaldehyde or *p*-chlorobenzylcyanide, 8.9% and 16.4% chlorine was found in the product, respectively. This indicated that the product had been formed from 1 mole of aldehyde and 2 moles of the nitrile. The hydrolysis of the compound in glycerol with alkali or in acetic acid with BF_3, in the presence of the calculated amount of water led to phenylacetamide, while hydrolysis with mineral acids

* Part I: CSŰRÖS, Z., DEÁK, GY., HOFFMANN, I.: Acta Chim. Acad. Sci. Hung. 55, 125 (1968).

yielded phenylacetic acid. Reduction with nascent hydrogen in absolute ethanol also gave phenylacetamide. The same product was obtained from benzaldehyde and benzyl cyanide in absolute propionic acid. Although more slowly, the reaction also took place with catalytic amounts of boron trifluoride. The same product was obtained in the absence of a solvent when the aldehyde was first saturated with boron trifluoride, resulting in the formation of a solid complex, which was then treated with benzyl cyanide.

On the basis of the above results we have established that the compound is benzylidene-bis(phenylacetamide) [$C_6H_5CH(NHCOCH_2C_6H_5)_2$], first prepared by GUPTA [2] by heating molten phenylacetamide with benzaldehyde at 160 °C for 2 hours.

Compounds of the bis-amide type were first prepared by HEPP and SPIESS [3] from benzonitrile and acetamide in concentrated sulphuric acid. Sulphuric acid has since been used as the catalyst either alone [4—6] or in acetic acid [7, 8], formic acid [9], and chloroform [3] solutions. The temperature was usually below 50 °C, except with formic acid where the solution was heated to 100 °C. Hydrochloric acid [9, 10] as well as *p*-toluenesulphonic acid, ethylsulphuric acid and boron trifluoride [9] have been used as catalysts instead of sulphuric acid.

Benzonitrile [3, 8] and its substituted derivatives [4, 6, 8], benzyl cyanide and its substituted derivatives [6, 7, 10], as well as aliphatic nitriles [6, 7, 9] have been used as the nitrile components. Aldehydes not containing α-hydrogens are most satisfactory, since they do not undergo acid-catalyzed side reactions. The reactions of formaldehyde, as well as those of its precursor — trioxane — were studied recently [6, 9], because polyamides can be prepared from dinitriles by this method.

Since the preparation of benzylidene-bis(phenylacetamide) from benzyl cyanide has not yet been reported, and this type of reaction has not been thoroughly studied, we made a further investigation of the above reaction.

First, several substituted derivatives of the parent compound were prepared (Table I).

The data in Table I indicate that regardless of the fact that the yields of the derivatives do not differ significantly, electron-withdrawing substituents (nitro-, chloro-) in the *p*-position of the aromatic benzaldehyde ring increase, while electron-repelling substituents (methyl, methoxyl) decrease the yield. The yields shown in Table I refer to reactions that were carried out under identical conditions. It is remarkable that no product can be obtained from anisaldehyde under these conditions. The yield does not reach that obtainable with the parent compound even if the reaction time is doubled, indicating that the rate of the reaction is strongly decreased by methoxy-substitution.

Our first objective was to study the possibilities of increasing the rather low yield of benzylidene-bis(phenylacetamide). We observed that there was

Table I

Reactions of aromatic aldehydes with aryl acetonitriles in absolute acetic acid at 25°C, in the presence of boron trifluoride catalyst

$R_1—C_6H_4—CH(NH—CO—CH_2—C_6H_4—R_2)_2$

R_1	R_2	Crude yield** %	Product m. p., °C	Purified yield, %	Product m. p., °C	Formula	Analysis Calcd./Found C %	H %	N %
H	H	25	221	20	231 (EtOH, DMF*)	$C_{23}H_{22}N_2O_2$	77.09 77.16	6.14 6.20	7.82 7.90
p-NO_2	H	37	235	35	237 (EtOH, DMF)	$C_{23}H_{21}N_3O_4$	68.48 68.05	5.13 5.10	10.42 10.40
m-NO_2	H	20	214	18	216 (EtOH, DMF)	$C_{23}H_{21}N_3O_4$	68.48 68.06	5.13 5.34	10.42 10.70
o-NO_2	H	11	224	10	234 (EtOH, DMF)	$C_{23}H_{21}N_3O_4$	68.48 68.43	5.13 5.36	10.42 10.55
p-Cl	H	33	240	30	246 (EtOH, DMF)	$C_{23}H_{21}N_2O_2Cl$	70.40 70.36	5.61 5.32	7.14 7.12
o-Cl	H	26	214	24	217 (EtOH, DMF)	$C_{23}H_{21}N_2O_2Cl$	70.40 70.23	5.61 5.36	7.14 6.84
p-CH_3	H	21	231	16	237 (EtOH)	$C_{24}H_{24}N_2O_2$	77.41 77.13	6.45 6.52	7.52 7.32
p-CH_3	H	14***	235	10	240 (EtOH)	$C_{24}H_{24}N_2O_3$	74.18 74.16	6.24 6.36	7.23 7.29
H	*p*-Cl	25	232	21	245 (EtOH, DMF)	$C_{23}H_{20}N_2O_2Cl_2$	64.64 64.80	4.71 4.83	6.55 6.70
Naphthylidene-bis-phenylacetamide		28	240	21	245 (DMF : H_2O = 3:1)	$C_{27}H_{24}N_2O_2$	79.41 79.39	5.89 6.10	6.86 6.70

* DMF: Dimethylformamide.
** Reaction time: 24 hrs.
*** Reaction time: 48 hrs.

an optimum for the amount of catalyst added (Fig. 1). If less than the optimum amount of boron trifluoride is added, the yield is low even with long reaction times. Above the optimum, phenylacetamide formation becomes predominant. If the reaction is run at 60 °C instead of 25 °C, the product is less pure. When the reaction mixture was boiled, a brown oil was obtained from which no bis-amide could be isolated. Since the changing of different parameters did not improve the results, the BF_3 catalyst was replaced by mineral acids.

Sulphuric acid dissolved in absolute acetic acid was found to increase the yield from about 20% to 75%, using the optimum amount of catalyst.

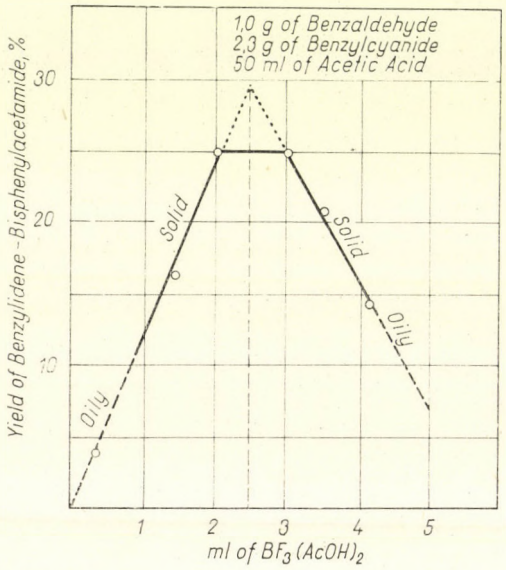


Fig. 1. Dependence of the amount and appearance of the product on the catalyst concentration in the reaction of benzaldehyde with benzyl cyanide in the presence of boron trifluoride

The bis-amides prepared by the sulphuric acid method are listed in Table II.

The *p*-nitrobenzyl cyanide derivative could only be prepared in very low yield due to poor solubility. No product was obtained from phenylacetaldehyde, acetophenone, and pyridinealdehyde.

Since the substituent in the aromatic ring is isolated from the nitrilo group, theoretical considerations suggest approximately the same yield for the compounds shown in Table II. The small conversion of the methoxy-substituted substrates can be explained theoretically (see below), but in the cases of the alkyl- and halogen-substituted derivatives the yields differ presumably because of losses occurring during work-up. In this procedure, the acetic acid solution was poured into water after it had been allowed to stand for 24 hours,

then the precipitated raw product was filtered off and washed with water and organic solvents (alcohol, acetone) to remove any acid, aldehyde, and nitrile.

Owing to the different solubilities, the products dissolved to varying extents during this procedure. This is supported by the observation that after pouring the solution into water and steam-distilling the raw product, better purity and higher yields were obtained when only water was used to wash the raw product on the filter.

Table II

The reaction of benzyl cyanide and its ring-substituted derivatives with benzaldehyde catalyzed by sulphuric acid, in acetic acid, at 25 °C

$C_6H_5—CH(NH—CO—CH_2—C_6H_4—R)_2$

R	Crude yield, %	Product m. p., °C	Purified product m. p. (°C) (recrystallized)	Formula	Analysis Calcd./Found C %	H %	N %
					77.52	6.77	7.24
o-CH_3	81	236—238	248 (DMF*)	$C_{25}H_{26}N_2O_2$	77.41	6.71	7.40
					77.52	6.77	7.24
m-CH_3	43	200—205	216 (DMF)	$C_{25}H_{26}N_2O_2$	77.66	6.89	7.38
					77.52	6.77	7.24
p-CH_3	66	220—225	235 (DMF)	$C_{25}H_{26}N_2O_2$	77.60	6.80	7.23
					64.64	4.71	6.55
p-Cl	74	218—220	240 (DMF)	$C_{23}H_{20}N_2O_2Cl_2$	65.10	4.80	6.30
					70.03	5.11	7.09
p-F	56	217—220	233 (EtOH:DMF = 1:1)	$C_{23}H_{20}N_2O_2F_2$	70.00	5.39	7.17
					71.75	6.26	7.69
p-OMe	traces	195—198	215 (EtOH:DMF = 1:1)	$C_{25}H_{28}N_2O_4$	71.66	6.32	6.90

* DMF: dimethylformamide.

Another reason for the varying yields is the full or partial precipitation of the products from the acetic acid solution as a result of differing solubilities. This means that the equilibrium is shifted toward the products to various degrees.

In order to throw light on the role of acetic acid, the reaction was carried out in different solvents. From among the solvents that had been tested, carbon tetrachloride and chlorobenzene were found suitable but the best results were obtained in nitrobenzene (a maximum yield of 55%). The results with different solvents are shown in Table III.

It was observed that the yield of the raw product increased with increasing amounts of sulphuric acid reaching a limiting value above which no solid product could be obtained. The amount of the bis-amide in the raw product was determined after removing phenylacetamide by extraction with

Table III

The reaction of benzaldehyde with benzyl cyanide in different solvents

Solvent	Catalyst	Crude yield, %	Product m. p., °C
Absolute acetic acid	boron trifluoride	19	224—22
Absolute acetic acid	100% sulphuric acid	75	219—2254
Nitrobenzene	100% sulphuric acid*	55	215—216
Chlorobenzene	100% sulphuric acid*	38	194—196
Carbon tetrachloride	100% sulphuric acid*	38	206—208

* With the optimum amount of acetic acid (see Table V).

water. After evaporation of the aqueous extraction to dryness the residue was phenylacetamide. The results are shown in Table IV and Fig. 2. It can be seen that when higher than the optimum amount of sulphuric acid is used the yield of the bis-amide decreases, the formation of phenylacetamide becoming predominant.

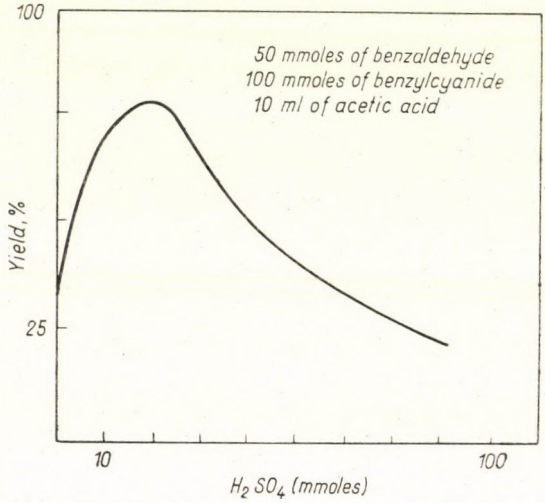


Fig. 2. Dependence of the yield on the catalyst concentration in the reaction of benzaldehyde with benzyl cyanide catalyzed by sulphuric acid

An interesting feature of the reaction catalyzed by sulphuric acid is that in the presence of small amounts of H_2SO_4 well-developed white crystals separate after a reaction time of 4—5 hours, and the mixture soon becomes a crystalline pulp. A similar phenomenon was observed in nitrobenzene as solvent. It is obvious that one molecule of water is also necessary for the formation of the bis-amide:

$$C_6H_5CHO + 2\ C_6H_5CH_2CN + H_2O \longrightarrow C_6H_5CH(NHCOCH_2C_6H_5)_2$$

The question arises whether the crystalline product obtained in anhydrous media is an intermediate which is converted into the product when poured into water, or the product is directly formed in the reaction. To answer the question, the crystals were isolated with the exclusion of moisture, filtered off and washed with dry acetone. The product obtained in this procedure was found to be benzylidene-bis(phenylacetamide).

Table IV

The reaction of benzaldehyde (0.05 mole) with benzyl cyanide (0.1 mole) in absolute acetic acid in the presence of sulphuric acid catalyst, at 25 °C

H_2SO_4 (mmoles)	Crude product (g)	m.p., °C	Phenyl-acetamide (g)	Benzylidene-bis-(phenylacet-amide) (g)	Yield, %
1	7.0	227	—	7.0	39.1
2.5	10.0	227	—	10.0	56.0
5.0	12.2	226	—	12.2	68.2
7.5	13.2	225	—	13.2	73.6
10.0	13.8	221	—	13.8	77.0
15.0	12.5	220	—	12.5	70.0
20.0	12.8	220	2.8	10.0	70.0
30.0	12.6	215	5.1	7.5	42.0
40.0	13.0	210	9.0	4.0	22.3
50.0	oil	—	—	—	—

Since no crystal separation occurs when the reaction is catalyzed by boron trifluoride, a different procedure was selected to study the problem in this case. After the reaction had gone to completion, acetic acid, the unchanged benzaldehyde, and benzyl cyanide were removed by distillation under reduced pressure. A viscous, non-solidifying oil was obtained. Since the syrupy liquid was shown to contain boron trifluoride, but BF_3 was completely absent in the distillate, we assumed that the whole amount of the catalyst was bound in the reaction product. Upon mixing the oil with dry ether a white, solid crystal-pulp formed. The analysis of the volatile components removed by distillation [11] showed that boron trifluoride had gone into the distillate as an ether complex. This experiment has proved that the reaction product is benzylidene-bis(phenylacetamide) also in the case when BF_3 is used as the catalyst.

On the basis of the experimental results it can be assumed that acetic acid is not merely a solvent, but participates in the reaction. This is supported by the results of ZIL'BERMAN [12] who studied reactions between nitriles

carboxylic acids, and hydrogen halides at low temperatures, in which amides were formed. ZIL'BERMAN has established that the amide hydrochloride is formed from the nitrile, the necessary amount of water being supplied by the carboxylic acid which is converted to the anhydride.

In order to determine whether acetic acid plays such a part in the reaction under consideration experiments were performed in nitrobenzene solution. The yield of benzylidene-bis(phenylacetamide) was found to depend on the amount of the acetic acid added (see Table V).

Table V

The yield of benzylidene-bis(phenylacetamide) as a function of the amount of acetic acid used in the reaction of benzaldehyde with benzyl cyanide in nitrobenzene catalyzed by sulphuric acid

Benzaldehyde:	25 mmoles	In 10 ml of nitrobenzene
Benzyl cyanide:	50 mmoles	25 °C, 24 hours
100% Sulphuric acid:	10 mmoles	

Acetic acid (mmoles)	Yield		m. p., °C
	(g)	%	
4	1.3	22	197—200
25	2.0	33	174—177
50	4.0	66	207—209
100	2.7	45	210—212

The yield was optimum when benzaldehyde and acetic acid were added in equimolar quantities. The results shown in Table V support the assumption that acetic acid is converted to acetic anhydride. The IR spectrum of the nitrobenzene solution obtained after isolating the product offers a means to clarify the problem. Acetic anhydride has characteristic bands at 1824 and 1748 cm^{-1} the observation of which is not obstructed by nitrobenzene. The spectrum obtained in the presence of sulphuric acid was not susceptible of evaluation, therefore it was necessary to neutralize the sample with solid sodium hydrocarbonate. A blank experiment indicated, however, that acetic anhydride was decomposed under such conditions. Since benzoic anhydride remains practically unchanged under the above experimental conditions, a test has been made to find out if the bis-amide is formed in the presence of benzoic acid. The product was found to crystallize from nitrobenzene solution, although the yield was lower. After filtration and neutralization, the benzoic anhydride bands at 1730 and 1790 cm^{-1} were easily detected in the IR spectrum, thus confirming that the reaction took place according to the following equation:

$$C_6H_5CHO + 2\ C_6H_5CH_2CN + AcOH \rightleftharpoons C_6H_5CH(NHCOCH_2C_6H_5)_2 + Ac_2O$$

Further, it has been established by the spectroscopic method that, in agreement with ZIL'BERMAN's experiments [12] performed under different conditions, the characteristic band of benzoic anhydride can also be detected when benzyl cyanide alone is dissolved in acetic acid which contains sulphuric acid. These results indicate two possible routes leading to the bis-amide: *(1)* benzyl cyanide is first converted to phenylacetamide which then reacts with benzaldehyde; *(2)* benzaldehyde reacts with benzyl cyanide to form an intermediate presumably also containing a bonded molecule of the organic acid, this step being followed by the conversion of the intermediate to the product.

When benzyl cyanide was treated with acetic acid containing a small amount of H_2SO_4, under conditions identical to those used in the preparation of the bis-amide, only traces of phenylacetamide could be isolated. Taking into account the mechanism proposed by ZIL'BERMAN [12], in the presence of sulphuric acid the reaction can be pictured in the following way:

$$R-C\equiv N+H_2SO_4 \rightleftharpoons R-\underset{\underset{OSO_3H}{|}}{C}=NH \rightleftharpoons R-\underset{\underset{OSO_3^-}{|}}{C}=\overset{+}{N}H_2$$

$$R-\underset{\underset{OSO_3^-}{|}}{C}=\overset{+}{N}H_2+AcOH \rightleftharpoons R-\underset{\underset{OAc}{|}}{C}=NH_2\cdot HSO_4^- + AcOH \rightleftharpoons R-\underset{\underset{OH}{|}}{C}=NH_2^+ HSO_4^- + Ac_2O$$

The above reaction sequence involving reversible steps explains why the use of less than stoichiometric amounts of sulphuric acid results in poor conversions to the amide. This, however, does not rule out the possibility that the bis-amide is formed from phenylacetamide. If benzaldehyde were capable of reacting with the small amounts of phenylacetamide produced, the reaction sequence would be shifted to the right to give bis-amide. According to our experiments, the product benzylidene-bis(phenylacetamide) does not form a salt with sulphuric acid, therefore, the released H_2SO_4 could convert another nitrile group.

As it has been mentioned, increasing amounts of sulphuric acid decrease the yield of the bis-amide and higher amounts of phenylacetamide can be isolated from the crude product. This may be explained by the distribution of sulphuric acid in the acetic acid solution of phenylacetamide, between the amide and the amphoteric acetic acid, the latter being present in considerably higher molar concentration:

$$CH_3COOH\cdot H_2SO_4 + C_6H_5CH_2CONH_2 \rightleftharpoons CH_3COOH + C_6H_5CH_2CONH_2\cdot H_2SO_4$$

Only the unprotonated amide is capable of reacting with the aldehyde. Increasing amounts of sulphuric acid result in the separation of more and more protonated amide from the solution. This is the source of phenylacetamide obtained in the subsequent procedure.

The very low yield of products with methoxy-substituted components is due to similar reasons. The oxygen of the methoxyl-group is more basic than the nitrogen in the nitrile, therefore it ties up a significant part of sulphuric acid, thus rendering it ineffective. Increasing amounts of sulphuric acid lead to the above mentioned effect, *i.e.* the nitrile is converted to an amide salt.

However, it is also possible that the reaction takes place according to the mechanism proposed by MOWRY and RINGWALD [9] for the reaction of azelaonitrile with formaldehyde:

$$Ar'CHO + H^+ \rightleftharpoons Ar'\overset{+}{C}HOH$$

$$ArCH_2C{\equiv}N + Ar'\overset{+}{C}HOH \rightleftharpoons ArCH_2\overset{+}{C}{=}N{-}\underset{\displaystyle OH}{\underset{|}{CH}}{-}Ar'$$

$$ArCH_2\overset{+}{C}{=}N{-}\underset{\displaystyle OH}{\underset{|}{CH}}{-}Ar' + OSO_3H^- \rightleftharpoons ArCH_2C{=}N{-}\underset{\displaystyle OSO_3H}{\underset{|}{CH}}{-}\underset{\displaystyle OH}{\underset{|}{CH}}{-}Ar'$$

$$ArCH_2C{=}N{-}\underset{\displaystyle OSO_3H}{\underset{|}{CH}}{-}\underset{\displaystyle OH}{\underset{|}{CH}}{-}Ar' + H^+ \rightleftharpoons ArCH_2C{=}N{-}\underset{\displaystyle OSO_3H}{\underset{|}{\overset{+}{C}H}}{-}Ar' + H_2O$$

$$ArCH_2C{=}N{-}\underset{\displaystyle OSO_3H}{\underset{|}{\overset{+}{C}H}}{-}Ar' + ArCH_2C{\equiv}N \rightleftharpoons ArCH_2C{=}N{-}\underset{\displaystyle OSO_3H}{\underset{|}{CH}}{-}\underset{\displaystyle Ar'}{\underset{|}{N{=}\overset{+}{C}{-}CH_2Ar}}$$

$$ArCH_2C{=}N{-}\underset{\displaystyle OSO_3H}{\underset{|}{CH}}{-}\underset{\displaystyle Ar}{\underset{|}{N{=}\overset{+}{C}{-}CH_2Ar}} + OSO_3H^- \rightleftharpoons$$

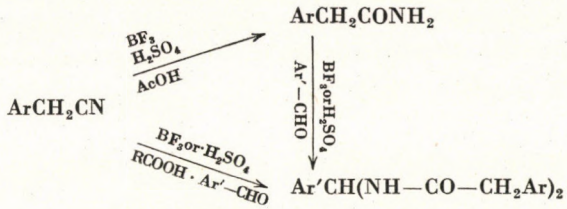
$$\rightleftharpoons Ar'CH\begin{cases} N{=}\underset{\displaystyle OSO_3H}{\underset{|}{C}}{-}CH_2Ar \\ N{=}\underset{\displaystyle OSO_3H}{\underset{|}{C}}{-}CH_2Ar \end{cases}$$

The bis-amide would then be formed from I, according to the process described above.

According to this mechanism, unprotonated nitrile is required for the reaction: the protonated form gives the amide, as described above, which, in turn, reacts with the aldehyde to yield the bis-amide.

It was established in preparative experiments that the bis-amide formed also when benzyl cyanide was replaced by phenylacetamide. The separation of the crystalline product began earlier, indicating that the reaction is faster with phenylacetamide than with benzyl cyanide.

As it has already been mentioned, the reaction may take place via one of the following routes, or simultaneously, involving parallel paths:



If Reactions (1) and (3) are actually faster than (2) the bis-amide probably forms via the amide. Further studies including kinetic measurements are in progress to obtain additional information about these reactions.

Experimental

Preparation of benzylidene-bis(phenylacetamide) with BF_3 catalyst

(a) 3 ml (30 mmoles) of benzaldehyde was saturated with boron trifluoride while cooling. To the solid complex that formed 6.6 ml (60 mmoles) of benzyl cyanide was added. A homogeneous solution was obtained. After 7 days it was mixed with saturated aqueous sodium acetate, then the unchanged reaction components were removed by steam distillation. The solid residue was filtered off, washed with water and dried to yield 0.12 g (1.1%) of benzylidene-bis(phenylacetamide), m.p. 220—225 °C.

(b) 10 ml (0.1 mole) of benzaldehyde was poured into 50 ml of absolute acetic acid, then 23 ml (0.2 mole) of benzyl cyanide and 20 ml of boron trifluoride—acetic acid complex was added. The reaction mixture became slightly warm and had a yellow colour. After 24 hrs. the mixture was poured into a fivefold volume of ice-water. The solid product was filtered off and washed with water and methanol. 14.3 g of a raw product was obtained which after recrystallization from 60 ml of dimethylformamide yielded 4.79 g (13%) of crystalline product (m.p. 224—225 °C).

A further 2.2 g (6%) of the same product with identical melting point was obtained after evaporating the mother liquors.

(c) 10 mmoles of benzaldehyde was allowed to react with 20 mmoles of benzyl cyanide under the above conditions in 5 ml of absolute acetic acid. After 24 hrs., the mixture was diluted with water and neutralized with Na_2CO_3. Unchanged benzaldehyde and benzyl cyanide were removed by steam distillation. Crystallization of the crude product (1.8 g) from ethanol gave 0.7 g (20%), m.p. 227—228 °C.

Preparation of benzylidine-bis(phenylacetamide) with sulphuric acid catalyst

5 ml (0.05 mole) of benzaldehyde was poured into 10 ml of absolute acetic acid and 1 ml of 100% H_2SO_4 was added while cooling in water. The solution turned slightly yellow. After about 10 minutes, 11.5 ml (0.1 mole) of benzyl cyanide was added. In about 1 hr. crystal separation started, and the homogeneous solution changed to a crystal pulp. After 24 hrs. it was diluted with water, filtered off, washed with acetone, dilute aqueous ammonia, water, and finally with acetone, to obtain 12.7 g (75%) of the product, m.p. 220—224 °C. When necessary, the compound can be recrystallized from dimethylformamide.

Preparation of benzylidene-bis(phenylacetamide) in nitrobenzene solution

2.5 ml (25 mmoles) of benzaldehyde was dissolved in 10 ml of nitrobenzene, and 2.8 ml (50 mmoles) of absolute acetic acid, then 0.1 ml (10 mmoles) of conc. H_2SO_4 were added, while cooling in water. After 10 minutes, 5.7 ml (50 mmoles) of benzyl cyanide was added. The separated substance was filtered off after standing for 3 days, and washed with acetone to yield 4.6 g (55%) of the product, m.p. 215°C.

Preparation of benzylidene-bis(phenylacetamide) under anhydrous conditions

(a) To 24 ml of absolute acetic acid there were added 10 ml of boron trifluoride—acetic acid complex, 5 ml (50 mmoles) of benzaldehyde, and 12 ml (0.1 mole) of benzyl cyanide. After 24 hrs. the volatile components were evaporated under reduced pressure on a bath with a maximum temperature of 70°C. The viscous oily residue solidified when it was triturated with absolute ether (20 ml). The white, powder-like product was filtered off and washed with ether to obtain 4.3 g of product (m.p. 180—185 °C) giving no m.p. depression when mixed with pure benzylidene-bis(phenylacetamide).

(b) 2.5 ml (25 mmoles) of benzaldehyde was dissolved in 10 ml of nitrobenzene and 2.8 ml (50 mmoles) of absolute acetic acid, 0.5 ml of 100% H_2SO_4, and 5.7 ml (50 mmoles) of benzyl cyanide were added. The crystals that separated on standing overnight were filtered off, washed with anhydrous benzene and petroleum ether, and dried in a vacuum desiccator to obtain 4 g of a crude product, m.p. 207—209°C. Recrystallization from dimethylformamide gave m.p. 227—228 °C.

Preparation of benzylidene-bis(phenylacetamide) in nitrobenzene in the presence of benzoic acid

2.5 ml (25 mmoles) of benzaldehyde was dissolved in 20 ml of nitrobenzene and 4.8 g (50 mmoles) of benzoic acid and 0.5 ml (10 mmoles) of 100% H_2SO_4 were added while cooling in water. After 10 min, the separated crystals were filtered off and the nitrobenzene solution was neutralized with anhydrous Na_2CO_3 and filtered. The IR spectrum was recorded using a 0.01 mm NaCl cell.

Hydrolysis of benzylidene-bis(phenylacetamide) by boron trifluoride

A mixture of 0.3 g of the bis-amide, 0.2 ml of water, and 2 g of $BF_3(AcOH)_2$ was heated for 10 min on a liquid bath at 120 °C. After neutralizing the cold solution with 10 ml of 5 N NaOH, brown flakes precipitated which sublimed above 100 °C and melted at about 145 °C. On sublimation the product was obtained in the form of plates which shrank at about 140 °C and melted at 157°C. No m.p. depression was observed with added phenylacetamide.

Hydrolysis of benzylidene-bis(phenylacetamide) with sulphuric acid

2.5 g of the bis-amide was boiled in 5 ml of 50% H_2SO_4 for 5 min. A solution was obtained from which 1.0 g of solid product with a benzaldehyde-like odour precipitated after cooling. Crystallization from water gave a product melting at 76 °C, which showed no depression of the m.p. with phenylacetic acid.

Reduction of benzylidene-bis(phenylacetamide) with nascent hydrogen

20 g of finely powdered bis-amide was suspended in 240 ml of absolute ethanol with constant stirring, and 20 g of metallic sodium was added in small portions over a period of 30 min. Ammonia was evolved and the solid gradually dissolved. The solution was boiled for 40 min. The unchanged bis-amide (5 g) separated from the solution on cooling. The solution was filtered, the filtrate neutralized with HCl, and extracted with benzene. The benzene extract was evaporated to yield an oily substance (2 g) which was distilled in vacuum. On the basis of its index of refraction and its reaction with copper + KOH (styrene), the distillate (b.p. 63—65 °C at 0.1 torr) was identified as β-phenylethyl alcohol. In the case of shorter reaction times phenylacetamide could also be isolated from the aqueous phase.

REFERENCES

1. CSŰRÖS, Z., DEÁK, GY.: Acta Chim. Acad. Sci. Hung. **17,** 439 (1958).
2. GUPTA, B. M.: J. Chem. Soc. **119,** 298 (1921).
3. HEPP, E., SPIESS, G.: Ber. **9,** 1424 (1876).
4. BATT, R. F., WOODCOCK, D.: J. Chem. Soc. **1948,** 2322.
5. GRADSTEN, M. A., POLLOCK, M. W.: J. Am. Chem. Soc. **70,** 3079 (1948).
6. MAGAT, E. E., FARIS, B. F., REITH, J. E., SALISBURY, L. F.: J. Am. Chem. Soc. **73,** 1028 (1951).

7. HEPP, E.: Ber. **10,** 1649 (1877).
8. THIESING, H.: J. prakt. Chem. [2] **44,** 570 (1891).
9. MOWRY, D. T., RINGWALD, E. L.: J. Am. Chem. Soc. **72,** 4439 (1950).
10. RIEDEL, F.: J. prakt. Chem. [2] **54,** 533 (1896).
11. CSŰRÖS, Z., DEÁK, GY., FENICHEL, L., TÖRÖK-KALMÁR, A.: Acta Chim. Acad. Sci. Hung. **50,** 63 (1966).
12. ZIL'BERMAN, E. N.: Zh. Obsch. Khim. **30,** 1277 (1960).

Zoltán CSŰRÖS
Gyula DEÁK
Melinda HARASZTHY-PAPP
István HOFFMANN

Budapest XI. Műegyetem rkp. 3

Acta Chimica Academiae Scientiarum Hungaricae, Tomus 59 (1), pp. 133—156 (1969)

THE CHEMISTRY OF 1,3-BIFUNCTIONAL COMPOUNDS, II

STUDY OF THE DECOMPOSITION OF THE QUATERNARY SALTS OF 1,3-AMINOALCOHOLS

A. MOLNÁR, M. BARTÓK and K. KOVÁCS

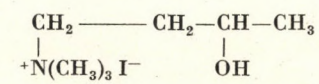
(Institute of Organic Chemistry, A. József University, Szeged)

Received October 30, 1967

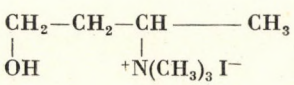
In the course of a study of the chemistry of 1,3-bifunctional compounds, the chemical transformations in the presence of bases, of quaternary salts of such 1,3-aminoalcohols have been investigated in which the two functional groups are connected to carbon atoms of different order [3-hydroxybutyl-2-trimethylammonium iodide (**I**), 4-hydroxybutyl-2-trimethylammonium iodide (**II**), (3-hydroxy-3-methyl)-butyltrimethylammonium iodide (**III**), and (2-hydroxy-2-methyl)-amyl-4-trimethylammonium iodide (**IV**)]. The directions of the decompositions of these four compounds and the overall rates of the processes have been studied. The principal primary directions of the reactions have been found to be the following: Hofmann elimination, demethylation, fragmentation, ring closure, and 1,3-rearrangement. The relative importance of these reactions depends upon the structure of the initial substance; the products are unsaturated alcohols, aminoalcohols and their methyl ethers, olefins and oxo compounds, oxetanes and oxo compounds. As the order of the carbon atom holding the trimethylammonium group becomes higher, Hofmann elimination and fragmentation become preponderant, while demethylation, as well as ring-closure together with rearrangement, become less important. The decomposition rates of the four compounds decrease in the following order: **IV** > **II** > **I** > **III**. On the basis of the experimental results, conclusions have been drawn concerning the mechanism of the reactions.

Introduction

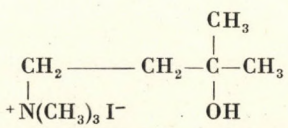
In Part I of this series [1] we have reported on the decomposition, in the presence of alkali, of the quaternary salts of 2-mono- and 2,2-dialkyl-1,3-aminoalcohols. In the present paper results will be discussed which refer to systems in which the two functional groups, the ammonium and the hydroxyl, are attached to carbon atoms of different orders. As models, the following compounds were chosen:



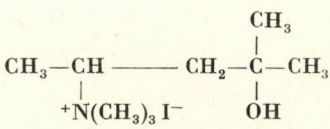
I



II



III



IV

Our purpose was to elucidate how the order of the carbon atom carrying the substituents affects the way of decomposition and the overall rate of the reaction. The decomposition of the four compounds was carried out in alkaline media, under the conditions of the Hofmann elimination.*

Experimental results and their evaluation

The decomposition of the quaternary derivatives, prepared with methyl iodide, of 4-dimethylaminobutan-2-ol and 3-dimethylaminobutan-1-ol (**I** and **II**) gave the products shown in Table I.

The main process is Hofmann elimination which produces vinylmethylcarbinol and crotyl-alcohol; demethylation gives rise to the methyl-ether of the corresponding aminoalcohol in the case of both initial compounds; the same product, 2-methyltrimethylene oxide, is the result of ring closure; and rearrangement produces butyraldehyde first, and *n*-butanol in a subsequent secondary reaction. During the decomposition of 4-hydroxybutyl-2-trimethylammonium iodide (**II**) fragmentation also occurs to give formaldehyde and propylene.

The two other compounds, each containing a tertiary hydroxyl group, namely the methiodide of 1-dimethylamino-3-methylbutan-3-ol, and 2-dimethylamino-4-methylpentan-4-ol (**III** and **IV**), decomposed in basic medium to give the products listed in Table II.

Compared with the preceding compounds (**I** and **II**), here the difference between the share of the Hofmann elimination and demethylation is still greater. A comparison of the respective percentage values suggests the following conclusions (*cf.* Tables II and III).

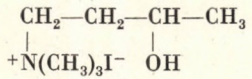
The increased proportion of trimethylamine has the obvious consequence of decreased demethylation. There is a significant difference in the proportion of Hofmann elimination. If the quaternary ammonium group is affixed to a secondary carbon atom (**II** and **IV**), the cleavage of the proton may occur from two carbon atoms. One of these is in a favoured position, exposed to collisions at the end of the chain; thus it is understandable that in such cases more of the unsaturated alcohol will be formed than in the cases of **I** or **III**, where the mobility of the hydrogens, thus their removal by hydroxide anions, is impeded by the positive inductive effect of the adjacent methyl groups, and by their steric hindrance.

Similar conclusions can be drawn when compounds with increasing order of the hydroxyl group are compared (Table IV).

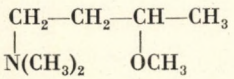
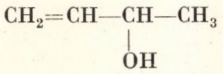
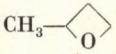
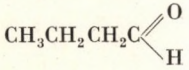
Thus, it can be stated that when quaternary salts of 1,3-aminoalcohols containing a primary ammonium group are decomposed in alkaline medium,

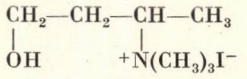
* The relative extents of the variously directed decompositions were determined by means of gas-liquid chromatography.

Table I



I

Demethylation	Hofmann elimination	Ring closure	Rearrangement	Rearrangement and secondary reaction
				
27%	46%	2%	5%	10%



II

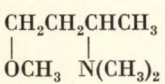
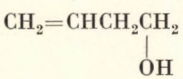
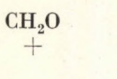
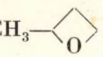
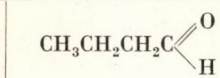
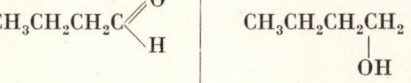
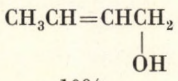
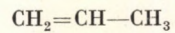
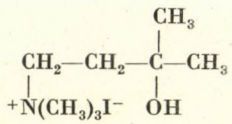
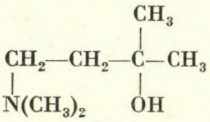
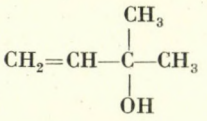
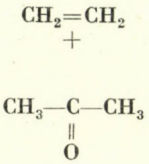
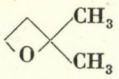
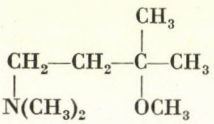
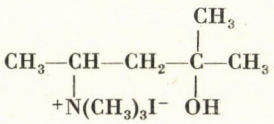
Demethylation	Hofmann elimination	Fragmentation	Ring closure	Rearrangement	Rearrangement and secondary reaction
					
2%	59%				
					
	10%	14%	1%	2%	1%

Table II

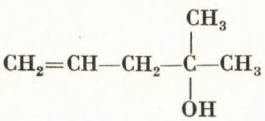
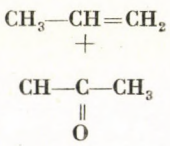
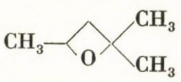


III

Demethylation	Hofmann elimination	Fragmentation	Ring closure
 42%			
 17%	26%	5%	4%



IV

Hofmann elimination	Fragmentation	Ring closure
 94%	 3%	 3%

the share of Hofmann elimination decreases owing to a lesser mobility of protons due to the inductive effect of, and steric hindrance by, the alkyl substituents. At the same time, the share of demethylation increases.

On the basis of the experimental data shown in the Tables of this and our preceding paper [1], the following conclusions seem to be justified.

Table III

	$CH_3—CH(OH)—CH_2—CH_2I(CH_3)_3N^+$ I		$CH_3—CH(N^+(CH_3)_3I^-)—CH_2—CH_2OH$ II	
Demethylation (ether)	27		2	
Hofmann elimination	46		69	
Fragmentation	—		14	
Ring closure	2	27	1	5
Rearrangement	5		2	
Rearrangement and secondary reaction	20		2	
$(CH_3)_3N$	73		98	

Table IV

	VIII $CH_2(N^+(CH_3)_3I^-)—CH_2—CH_2OH$		I $CH_2(N^+(CH_3)_3I^-)—CH(OH)—CH_3$		III $CH_2(N^+(CH_3)_3I^-)—C(CH_3)(OH)—CH_3$	
Demethylation (alcohol)	4	10	—	27	42	59
Demethylation (ether)	6		27		17	
Hofmann elimination	60		46		26	
Fragmentation	—		—		5	
Ring closure	4	30	2	27	4	4
Rearrangement	—		5		—	
Rearrangement and secondary reaction	26		20		—	
$(CH_3)_3N$	90		73		41	

1. The share of Hofmann elimination increases when the order of the carbon atom that carries the nitrogen is higher, and decreases with a higher order of the hydroxyl group, if the compound contains the quaternary ammonium group attached to a primary carbon atom.

2. De-quaternization (demethylation in this instance) increases with the order of the hydroxyl group, and decreases when the order of the carbon atom that carries the trimethylamino group becomes higher: *i.e.* it proceeds in inverse proportion to Hofmann elimination.

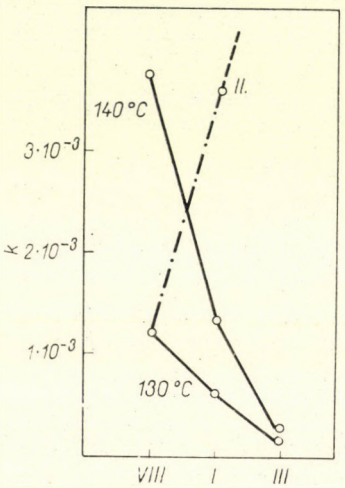


Fig. 1. Rate constants of the decomposition of quaternary ammonium salts of 1,3-amino-alcohols, in basic medium, at 130 and 140 °C

3. The higher the order of the carbon atom carrying the trimethylamino group, the greater the share of fragmentation, in the case of molecules containing primary and secondary hydroxyl groups.

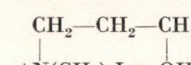
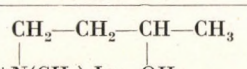
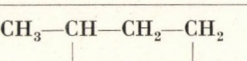
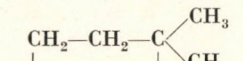
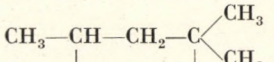
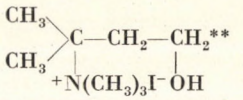
4. The combined proportion of ring closure and rearrangement is reduced when the order of the carbon atom carrying the trimethylamino group is lower.

The overall reaction rate constants also increase in proportion with the Hofmann elimination (*cf.* Table V and Fig. 1).* According to the relative rate constants, the compounds studied may be arranged in the sequence **IV** > **II** > > **VIII** > **I** > **III**. Thus compounds that carry the trimethylamino group attached to a secondary carbon atom decompose at the highest rate.

With the increase of the order of the hydroxyl group (*cf.* Fig. 1) the main process, *i.e.* Hofmann elimination, declines, and the reaction rate decreases in a direct proportion. The dotted line section of the function shows the rate growth

* Measurements concerning the reaction kinetics were carried out as described in our former communication [1].

Table V

No.	Compound		°C	$k \cdot 10^3$ $l \cdot \text{mole}^{-1} \cdot \text{min}^{-1}$	$\frac{k}{k_{III}}$
1.		VIII	130	1.23	10
2.			140	3.70	
3.		I	130	0.63	5
4.			140	1.36	
5.		II	120	1.20	28
6.			130	3.60	
7.		III	130	0.13	1
8.			140	0.24	
9.		IV	110	1.25	70
10.			120	3.68	
11.			130	9.14	
12.					

Note: Concentration of the quaternary salt: 0.1 mole per litre; [OH^-], 1 mole per litre.

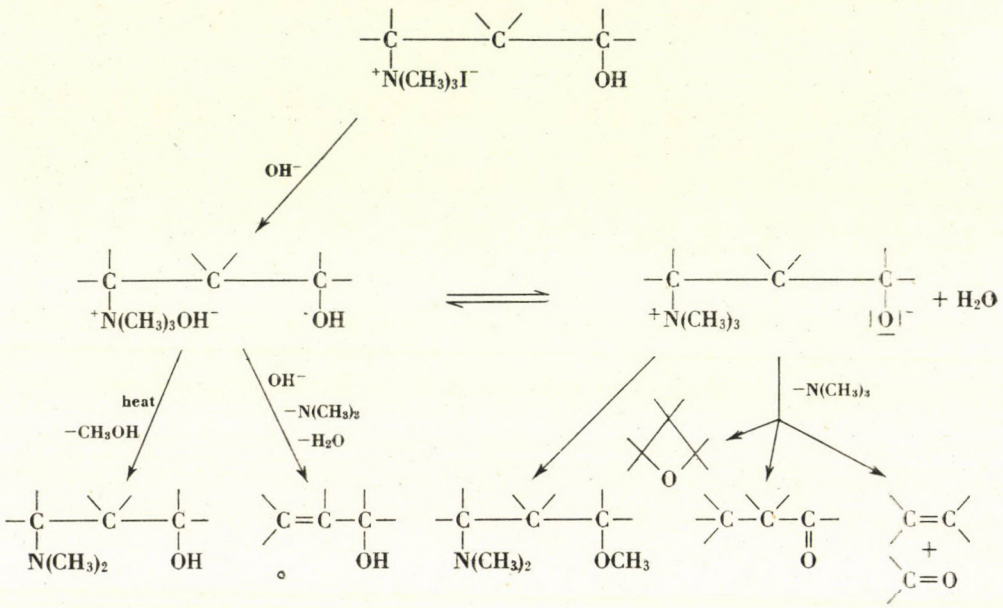
** Owing to its unstable character, attempts at the synthesis of this compound were unsuccessful.

which is due to the increase in the order of the carbon atom carrying the trimethylamino group. In contrast to the former three compounds — where the cause of rate decrease has been the diminution of the share of Hofmann elimination — the increase of rate is here only in part attributable to higher rates of elimination. The other cause of the rate increase should be sought in the occurrence of fragmentation. (A dashed line in the Figure indicates the trend of the rate constant of the decomposition of the compound which carries a trimethylamino group on a tertiary carbon atom. Attempts at a synthesis of this compound, however, failed, because the compound is unstable.)

The mechanism of the processes

An interpretation of our experimental findings and our conclusions concerning the mechanism of the reactions are given below.

In the presence of alkali, quaternary ammonium iodides containing a hydroxyl group are converted into the ammonium base at very high rates. Heat brings about the direct de-quaternization of ammonium bases to yield amino-alcohols, or, in the presence of excess alkali, ammonium bases decompose in a Hofmann elimination to yield unsaturated alcohols. De-quaternization to aminoalcohol methyl ether, fragmentation, ring closure, and rearrangement suggest the existence of the following equilibrium:



When the temperature is decreased to a certain level, this equilibrium is shifted towards the formation of the γ-alkoxyammonium ion, thus the amount of compounds formed *via* this intermediary state may relatively increase when the temperature is lowered. At higher temperatures, and with the shift of this equilibrium to the left, Hofmann elimination tends to increase.

As stated in a former communication [1], in the decomposition of 3-dimethylaminopropanol-1-methiodide, the reaction followed first order kinetics with respect to the concentration of the quaternary salt; however, as a function of the concentration of the alkali, the kinetic order was less than unity. The cause of this is the fact that several processes take place side by side, and the overall order of the reaction is the result of their combined effects. Therefore, we studied the mechanism of the Hofmann elimination on a model compound, (2-hydroxy-2-methyl)-amyl-4-trimethylammonium iodide (**IV**), that reacts almost exclusively in this way, as the trimethylammonium group is attached to a secondary carbon atom. On the basis of the differential method according to

van't Hoff, we have found that this is a first order reaction as a function of the concentration of the alkali (Fig. 2).

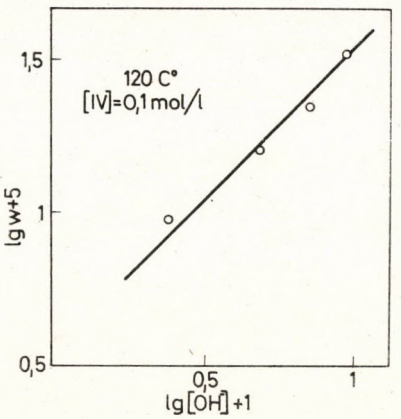


Fig. 2. The effect of $[OH^-]$ on the rate of decomposition (w) of **(IV)**

In the cases of trimethyl-n-butylammonium iodide **(V)** and of trimethyl-t-butylammonium iodide **(VI)**, as of instances of compounds carrying a nitrogen on a primary and a tertiary carbon atom, respectively, we found unity as the partial order of reaction with respect to the concentration of the alkali (*cf.* Table VI and Figs 3 and 4).

Table VI

No.	Compound	°C	$k \cdot 10^3$ $l \cdot mole^{-1} \cdot min^{-1}$	$\frac{k}{k_V}$
1	**V**	130	0.17	1
		140	0.46	
2	**VI**	120	5.30	68
		130	11.30	
3	**VII****	130	0.91	5
		140	2.20	

** Table VI also shows the rate constants, as determined by us, of the Hofmann elimination of trimethyl-sec-butylammonium iodide **(VII)**, to allow a comparison with the other two isomers. On the basis of the rates of Hofmann eliminations, these compounds can be arranged in the following order: **VI** $\gg$ **VII** $>$ **I**.

On the basis of our experiments, the 1,2-elimination occurring in the alkaline decomposition of the quaternary salts of 1,3-aminoalcohols proceeds according to an *E2* mechanism.

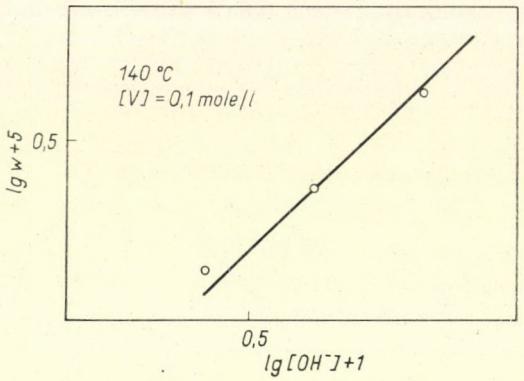


Fig. 3. Effect of $[OH^-]$ on the rate of decomposition of trimethyl-n-butylammonium iodide (**V**)

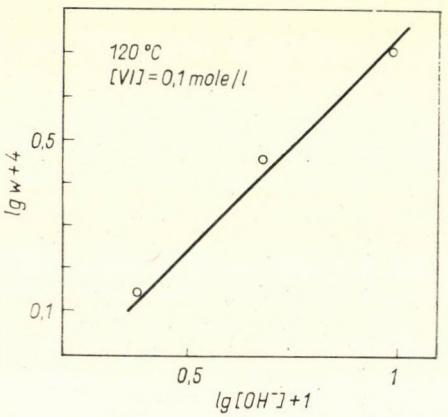
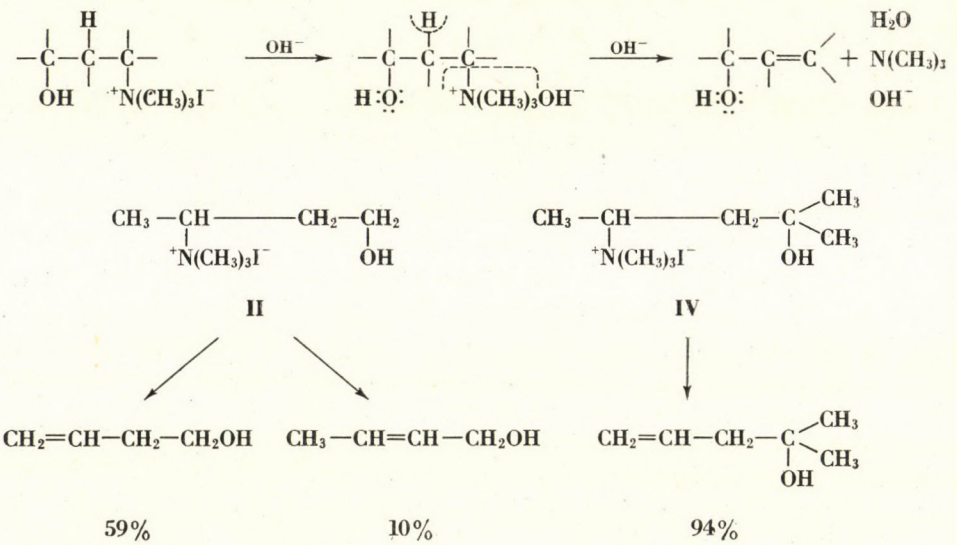


Fig. 4. Effect of $[OH^-]$ on the rate of decomposition of trimethyl-t-butylammonium iodide (**VI**)



In the first step, a momentary ion reaction effected by the alkali produces a quaternary ammonium hydroxide. In the course of the elimination by an *E2* type mechanism, a second hydroxide ion splits off a proton in β-position, and at the same time the trimethylamino group is also removed.

The elimination products of the two compounds in the above scheme throw light upon the effects that affect the prevalence of the Hofmann rule.

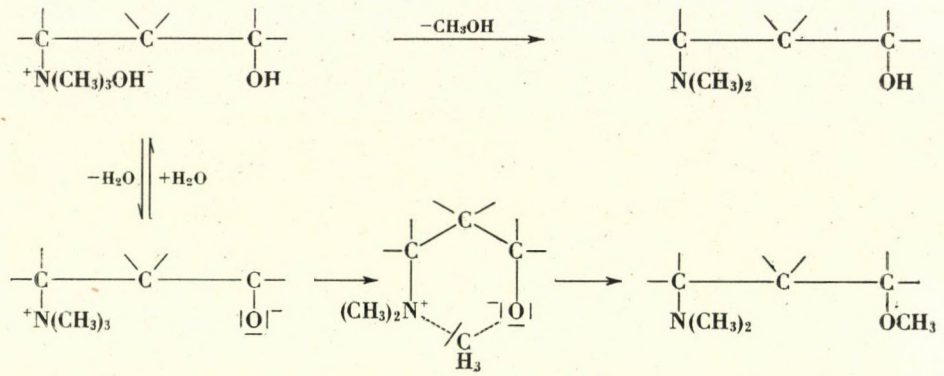
Three factors must be considered in both cases: the thermodynamic stability of the products formed, the probability of a collision of the base and one of the hydrogens attached to the two carbon atoms at β-position (this is the kinetic factor), and the mobility of the hydrogens.

In the first compound **(II)**, formation of crotyl alcohol, a direction opposite to the Hofmann rule, is thermodynamically more probable than the formation of allyl carbinol; in the former compound the double bond is conjugated with the hydroxyl group, and the hyperconjugative effect of the methyl group also favours the formation of crotyl alcohol. However, from a point of view of collisions, a collision of the base with a hydrogen of a terminal carbon atom is favoured as compared with a methylene in midposition. As a resultant of these effects, mainly the product in conformity with the Hofmann rule is formed, but the formation of compounds due to a contrary direction can also be observed.

In the second compound **(IV)**, the thermodynamic factor can be estimated similarly to the case of **II**. However, collision with a terminal methyl group is more probable than in the former instance, because the voluminous substituent adjacent to the second carbon in β-position obstructs an attack of the hydroxide anion at this point; at the same time, the mobility of the hydrogens of this carbon atom is low owing to the inductive effect of the methyl groups. Accordingly, in this instance the elimination proceeds according to a super Hofmann orientation.

The formation of aminoalcohol in the course of demethylation is explained by the single-step decomposition of the quaternary ammonium hydroxide. However, to explain ether formation, an intermediary six-membered ring structure must be supposed; in this ring one methyl group of the quaternary ammonium ion is also attached to the alcoholate anion. This bonding is probable because of the great bulk of the quaternary ammonium group, and the thermodynamic stability of the six-membered ring. The stabilization of this intermediary cyclic structure is responsible for the formation of the methyl ether of the aminoalcohol.

It seems appropriate to raise the question, what determines the ratio of the two main products of demethylation. As a first approximation, and prompted by the well-known rules of ether formation, one would think that the order of the hydroxyl group is decisive, meaning that an increase of this order should cause the decline of ether formation. Experimental findings contradict this



insofar that the share of de-quaternization does not change unequivocally with a higher order of the hydroxyl group. This contradiction can be resolved, however, by supposing the equilibrium discussed before, the reality of which is supported just by ether formation.

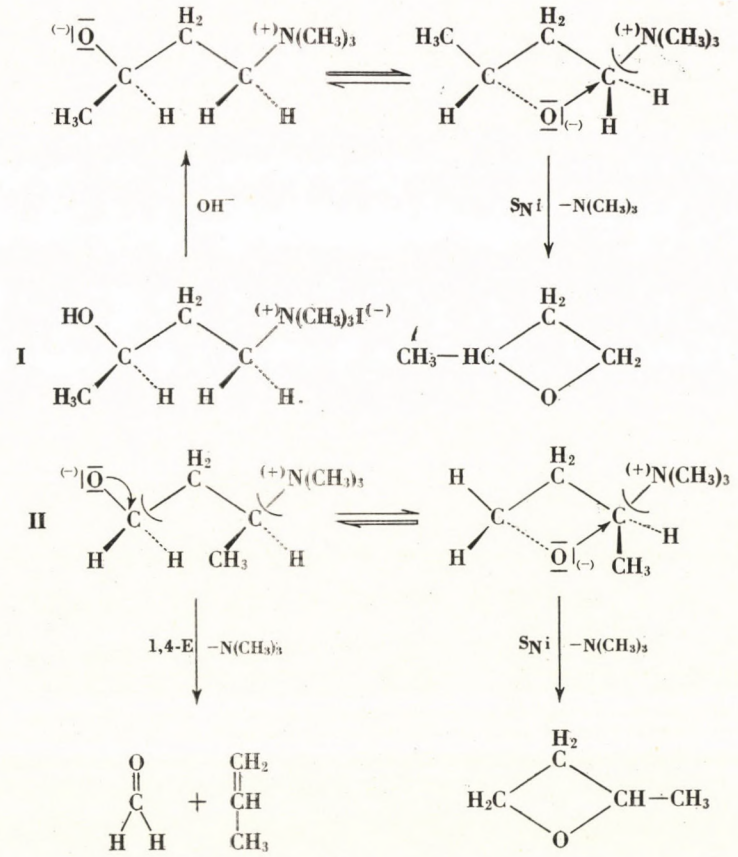
Thus, if the parent substance has a structure that obstructs the removal by hydroxide anions of protons at the β, or β'-positions, *i.e.* the occurrence of Hofmann elimination, the equilibrium γ-hydroxyammonium hydroxide $\rightleftarrows$ γ-alkoxyammonium ion $+H_2O$ is shifted towards the right hand side. This explains the direction of de-quaternization leading to ether formation. In compounds containing a tertiary hydroxyl group, this group obstructs shifting of the equilibrium towards the alkoxyammonium ion, and this is the reason why the amount of aminoalcohol increases.

The formation of the oxacyclobutane skeleton, the course of fragmentation, and the 1,3-rearrangement process can also be interpreted by means of this transition state.

The formation of cyclic ethers is due to an intramolecular attack of the alcoholate anion, *i.e.* to an S_Ni process. A conformation favourable to such a reaction is present when the quaternary ammonium group is attached to a primary carbon atom (as in **I** and **III**). In the opposite case (*e.g.* **II**), the spatially close methyl group hinders the intramolecular attack of the alcoholate anion, and thus promotes the emergence of a conformation with spatially distant functional groups, favourable to fragmentation. Accordingly, the latter compound is decomposed in 14% in the direction of fragmentation, whereas this reaction does not take place with the former compound.

When the formation of the cyclic ether alone is considered, what has been said does not seem to be valid. However, another process, rearrangement, must be taken into account which, in our opinion, proceeds *via* the same transition state and should thus be affected by the same factors.

(The formation of butyraldehyde can be explained with the 1,3-migration of the hydride anion.)



Accordingly, if accurate conclusions concerning the conformations are to be drawn, the sum of the percentages of the products yielded by all the three processes (ring-closure, rearrangement, and subsequent secondary processes) must be taken into account; in this case great deviations are, indeed, found (for **I** and **II**, 27% and 5% respectively). (Process 2 has not been detected.)

Finally, we wish to draw attention to the following. A comparison of the corresponding rate constants shown in Tables V and VI points to a substantially increased rate of decomposition in alkaline medium, other conditions being the same, when a hydroxyl group is introduced into tetraalkylammonium iodides. *E.g.:*

$$CH_3-CH_2-CH_2-CH_2-{}^{+}N(CH_3)_3\,I^- \quad k_1 = 0.00017$$

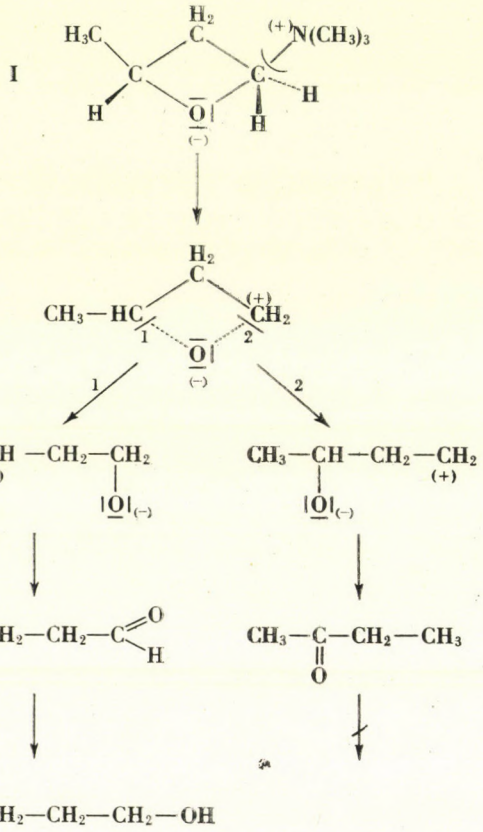
$$CH_3-CH(OH)-CH_2-CH_2-{}^{+}N(CH_3)_3\,I^- \quad k_2 = 0.00063$$

$$\frac{k_2}{k_1} = 3.7$$

$CH_3-CH(^+N(CH_3)_3\ I^-)-CH_2-CH_3$ $\quad k_3 = 0.00091$

$CH_3-CH(^+N(CH_3)_3\ I^-)-CH_2-CH_2OH$ $\quad k_4 = 0.0036$

$$\frac{k_4}{k_3} = 4$$



Thus, comparing the rate constants, the change in favour of the compounds which contain a hydroxyl group is fourfold. The presence of a hydroxyl in γ-position causes this rate change by opening up new ways of reactions, whose proportion, in our opinion, increases up to a certain limit with the decrease of temperature, in contrast to the Hofmann elimination which changes in direct proportion to the temperature.

Experimental

4-Dimethylaminobutan-2-one

This compound was prepared as described in the literature [2], with the modification that a stirred mixture of acetone (200 ml; 2.72 moles), paraformaldehyde (28 g; 0.93 mole),

and dimethylamine hydrochloride (64 g; 0.784 mole) was kept at 80 °C for 7 hrs. The base was liberated from the obtained hydrochloride with sodium hydroxide (50 g), to obtain 43 g (47%) of the product, b.p. 78—95 °C (45 mm Hg); $n_D^{21} = 1.4240$. (Lit. [2] b.p. 72—74 °C (40 mm Hg); $n_D^{20} = 1.4240$.)

4-Dimethylaminobutan-2-ol

A solution of 4-dimethylaminobutan-2-one (43 g; 0.374 mole) in abs. ether (300 ml) was added by drops to an ice-cold, stirred solution of lithium aluminium hydride (10 g; 0.264 mole) in abs. ether (300 ml). After warming on a water bath for 30 min, water (20 ml), and then an aqueous NaOH solution (13 g in 20 ml) were added under ice cooling. The usual work-up and fractional distillation gave 35 g (80%) of the product, b.p. 71—81 °C (40 mm Hg); $n_D^{21} = 1.4296$. (Lit. [3] b.p. 75—79 °C (50 mm Hg); $n_D^{25} = 1.4290$.)

3-Hydroxybutyltrimethylammonium iodide (I)

4-Dimethylaminobutan-2-ol (6 g; 0.0513 mole) was quaternized [1] in the presence of ethanol (6 ml) with methyl iodide (11 g; 0.0777 mole), to yield 10 g (70%) of **I**. The substance was recrystallized from ethanol, m.p. 136—139 °C (hygroscopic). (Lit. [4] m.p. 119 °C.)

$C_7H_{18}ONI$. Calcd. C 32.45, H 7.00, N 5.41. Found C 32.10, H 6.40, N 5.11%.

Ethyl-β-dimethylaminobutyrate

This compound was prepared [5] as follows. Crotonic acid ethyl ester (88 g; 0.77 mole) and dimethylamine (36 g; 0.80 mole) were allowed to stand in ethanol (50 ml) for 2 weeks. Distillation of this mixture gave 104 g (83%) of the substance, b.p. 96—105 °C (40 mm Hg); $n_D^{20} = 1.4248$. (Lit. [5] b.p. 178—180 °C.)

3-Dimethylaminobutanol

To a stirred, ice-cold solution of lithium aluminium hydride (4 g; 0.105 mole) in abs. ether (100 ml) there was added, by drops, a solution of ethyl β-dimethylaminobutyrate (26 g; 0.163 mole) in abs. ether (100 ml). The mixture was warmed on a water bath for 1 hr., then cooled in ice, and water (7 ml) was added followed by an aqueous solution of NaOH (10 g in 15 ml). The usual work-up yielded 14 g (73%) of the product, b.p. 91—97 °C (38 mm Hg); $n_D^{27} = 1.4374$. (Lit. [6] b.p. 78 °C (14 mm Hg); n_D^{20} [7] 1.4408.)

4-Hydroxybutyl-2-trimethylammonium iodide (II)

3-Dimethylaminobutanol (5 g; 0.0427 mole) in ethanol (8 ml) was treated with methyl iodide (9 g; 0.0634 mole), to obtain 7 g (63%) of **II**, m.p. 267—269.5 °C (from EtOH) (hygroscopic). (Lit. [8] m.p. 242 °C.)

$C_7H_{18}ONI$. Calcd. C 32.45, H 7.00 N 5.41. Found C 32.56, H 7.27, N 5.54%.

1-Dimethylamino-3-methylbutan-3-ol

1-Chloro-3-hydroxy-3-methylbutane (15 g; 0.135 mole) and liquid dimethylamine (45 g; 1 mole) in benzene (30 ml) were allowed to stand for 2 weeks. Dimethylamine hydrochloride was filtered off, the filtrate evaporated, and the residue distilled to yield 10 g (62%) of the product, b.p. 75—85 °C (40 mm Hg); $n_D^{20} = 1.4276$. (Lit. [9] b.p. 52—56 °C (15 mm Hg); $n_D^{20} = 1.4284$).

(3-Hydroxy-3-methyl)-butyltrimethylammonium iodide (III)

1-Dimethylamino-3-methylbutan-3-ol (5 g; 0.0381 mole) in ethanol (10 ml) was quaternized with methyl iodide (8 g; 0.0563 mole) to obtain 7.9 g (76%) of **III**, m.p. 159—162 °C (from EtOH). (Lit. [9] m.p. 165—169 °C.)

$C_8H_{20}ONI$. Calcd. C 35.17, H 7.38, N 5.13. Found C 35.62, H 7.27, N 5.01%.

2-Dimethylamino-4-methylpentan-4-ol

A Grignard mixture was prepared from magnesium (18.2 g; 0.775 mole) and methyl iodide (107 g; 0.754 mole) in abs. ether (100 ml). The mixture was stirred and cooled in a salt and ice bath, and ethyl β-dimethylaminobutyrate (48 g; 0.302 mole) in abs. ether (200 ml) was added by drops. After warming for 4 hrs., the mixture was cooled in an ice and salt mixture, and mixed with 1 : 1 HCl (240 ml). The aqueous phase was extracted with ether continuously for 3 days. The combined organic extracts gave on fractional column a product boiling between 60 and 73 °C (12 mm Hg), $n_D^{22} = 1.4260$. (Lit. [10] b.p. 168—170 °C.)

(2-Hydroxy-2-methyl)-amyl-4-trimethylammonium iodide (IV)

2-Dimethylamino-4-methylpentan-4-ol (8.6 g; 0.0593 mole) in ethanol (10 ml) was made to react with methyl iodide (12 g; 0.0845 mole). After recrystallization from ethanol, the m.p. of the substance was 174.5—176.5 °C.

$C_9H_{22}ONI$. Calcd. C 37.64, H 7.72, N 4.88. Found C 37.24, H 7.72, N 5.02%.

Dimethyl-n-butylamine

A mixture of *n*-butyl chloride (23.14 g; 0.25 mole) and dimethylamine (33 ml; 0.5 mole) was kept at 60 °C for 24 hrs. in a Carius tube. The dimethylamine hydrochloride which separated was filtered off, washed, the filtrate evaporated, and the residue distilled at atmospheric pressure to obtain a product (17 g; 67%) boiling between 85 and 95 °C; $n_D^{25} = 1.3965$. (Lit. [11] b.p. 94.7—95.2 °C (749 mm Hg); $n_D^{20} = 1.3970$.)

Trimethyl-n-butylammonium iodide (V)

Dimethyl-*n*-butylamine (1.7 g; 0.0168 mole) in ether (5 ml) was quaternized with methyl iodide (8 g; 0.0563 mole). After recrystallization from ethanol the yield was 1.9 g (46%) of **V**, m.p. 232—234 °C. (Lit. [12] m.p. 230—231 °C.)

$C_7H_{18}NI$. Calcd. C 34.58, H 7.46, N 5.76. Found C 34.39, H 7.09, N 5.78%.

Dimethyl-sec-butylamine

This compound was prepared by heating a mixture of *sec*-butyl chloride (23.14 g; 0.25 mole) and dimethylamine (33 ml; 0.5 mole) at 85 °C for 7 days in a Carius tube. The dimethylamine hydrochloride formed was filtered off, and the filtrate distilled at atmospheric pressure, to yield 4 g (16%), b.p. 89 °C; $n_D^{24} = 1.4004$. (Lit. [13] b.p. 93—93.5 °C; $n_D^{25} = 1.4000$.)

Trimethyl-sec-butylammonium iodide (VII)

Dimethyl-*sec*-butylamine (1.6 g; 0.0158 mole) in ether (3 ml) was quaternized with methyl iodide (3.5 g; 0.0246 mole). After recrystallization from ethanol the yield was 1.9 g (46%) of **VII**, m.p. 257—259 °C. (Lit. [13] m.p. 258—259 °C.)

t-Butylamine

It was prepared according to the literature [14]. *t*-Butylurea, needed for this synthesis, was made as described in the literature [15], in 41% yield. This product (48 g; 0.41 mole) was reacted with a mixture of sodium hydroxide (41 g; 1.025 mole), water (52 ml) and ethylene glycol (152 ml), to give *t*-butylamine (14 g; 47%), b.p. 45.5 °C. (Lit. [14] b.p. 44—46 °C.)

Trimethyl-t-butylammonium iodide (VI)

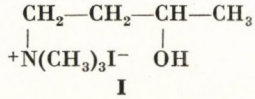
t-Butylamine (3 g; 0.041 mole) was allowed to react in the presence of acetone (3 ml) with methyl iodide (18 g; 0.127 mole). After standing overnight, this mixture was heated for 1 hr. The precipitate was collected and dissolved in a solution of NaOH (2 g) in water (25 ml). The insoluble phase was recrystallized from ethanol to give 1.1 g (15%) of the substance. In determinations of the m.p., the crystals turned yellow and began to decompose at 240 °C, then they became dark brown andmpose decod between 248 and 251 °C without melting (Lit. [16] m.p. 258 °C (decomp.), and [17] m.p. 240—241 °C (decomp.).)

$C_7H_{18}NI$. Calcd. C 34.58, H 7.46, N 5.76. Found C 34.20, H 7.22, N 5.62%.

The decomposition reactions of compounds **I, II, III, IV, V, VI** and **VII** were studied according to the method described in a former communication [1].

Results of measurements

t = time (minute)
x = quaternary ammonium iodide transformed up to time t, mole per litre
k = second-order rate constant ($l \cdot mole^{-1} \cdot min^{-1}$)



I

130 °C
[I] = 0.1 mole/litre
$[OH^-]$ = 0.95308 mole/litre

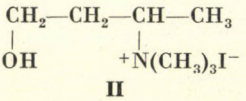
	t	x	$k \cdot 10^3$
1.	40	0.00309	0.82472
2.	105	0.00634	0.65690
3.	170	0.00992	0.64091
4.	230	0.01298	0.63875
5.	290	0.01585	0.62984
6.	350	0.01853	0.61890
7.	410	0.02101	0.61070

k_2—k_7 average = $0.63 \cdot 10^{-3}$

140 °C
[I] = 0.1 mole/litre
$[OH^-]$ = 0.95308 mole/litre

	t	x	$k \cdot 10^3$
1.	12	0.00278	2.4679
2.	40	0.00570	1.5442
3.	70	0.00872	1.3741
4.	100	0.01217	1.3708
5.	130	0.01553	1.3741
6.	160	0.01874	1.3751
7.	200	0.02233	1.3425
8.	240	0.02587	1.3280

k_3—k_8 average = $1.36 \cdot 10^{-3}$



II

120 °C
[II] = 0.1 mole/litre
$[OH^-]$ = 0.95308 mole/litre

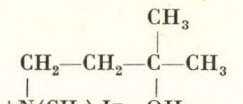
	t	x	$k \cdot 10^3$
1.	62	0.00416	0.72063
2.	100	0.00823	0.90517
3.	135	0.01221	1.0189
4.	170	0.01583	1.0729
5.	210	0.02055	1.1626
6.	247	0.02528	1.2556
7.	290	0.02864	1.2408
8.	340	0.03298	1.2586
9.	385	0.03661	1.2690
10.	440	0.04068	1.2753

k_3—k_{10} average = $1.20 \cdot 10^{-3}$

130 °C
[II] = 0.1 mole/litre
$[OH^-]$ = 0.95308 mole/litre

	t	x	$k \cdot 10^3$
1.	30	0.00501	1.8024
2.	45	0.01030	2.5491
3.	58	0.01456	2.8695
4.	73	0.01965	3.1789
5.	86	0.02401	3.3952
6.	100	0.02826	3.5410
7.	115	0.03299	3.7221
8.	128	0.03765	3.9576
9.	143	0.04169	4.0564
10.	160	0.04552	4.0915

k_3—k_{10} average = $3.60 \cdot 10^{-3}$



III

130 °C
[III] = 0.1 mole/litre
$[OH^-]$ = 0.95308 mole/litre

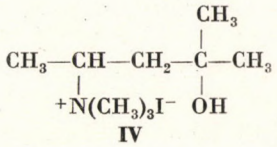
	t	x	$k \cdot 10^3$
1.	100	0.00255	0.27131
2.	200	0.00355	0.18992
3.	320	0.00458	0.15413
4.	440	0.00552	0.13584
5.	560	0.00657	0.12775
6.	680	0.00757	0.12196
7.	800	0.00898	0.12401

k_3—k_7 average = $0.13 \cdot 10^{-3}$

140 °C
[III] = 0.1 mole/litre
$[OH^-]$ = 0.95308 mole/litre

	t	x	$k \cdot 10^3$
1.	60	0.00285	0.50663
2.	135	0.00431	0.34315
3.	215	0.00588	0.29670
4.	300	0.00736	0.26843
5.	390	0.00881	0.24920
6.	480	0.01019	0.23627
7.	570	0.01154	0.22715
8.	660	0.01281	0.21945

k_4—k_8 average = $0.24 \cdot 10^{-3}$



IV

110 °C
[IV] = 0.1 mole/litre
$[OH^-]$ = 0.95308 mole/litre

	t	x	$k \cdot 10^3$
1.	30	0.00260	0.92236
2.	55	0.00561	1.1044
3.	80	0.00857	1.1807
4.	105	0.01137	1.2138
5.	130	0.01418	1.2434
6.	155	0.01694	1.2683
7.	180	0.01960	1.2852
8.	210	0.02261	1.2970

k_3—k_8 average = $1.25 \cdot 10^{-3}$

120 °C
[IV] = 0.1 mole/litre
$[OH^-]$ = 0.95308 mole/litre

	t	x	$k \cdot 10^3$
1.	17	0.00359	2.2534
2.	25	0.00665	2.8983
3.	34	0.00996	3.2554
4.	43	0.01331	3.5107
5.	52	0.01642	3.6522
6.	61	0.01943	3.7565
7.	70	0.02233	3.8353

k_4—k_7 average = $3.68 \cdot 10^{-5}$

130 °C
[IV] = 0.1 mole/litre
$[OH^-]$ = 0.95308 mole/litre

	t	x	$k \cdot 10^3$
1.	30	0.01057	3.9306
2.	48	0.02766	7.1894
3.	74	0.04518	8.7544
4.	104	0.05942	9.4417
5.	130	0.06753	9.4820
6.	160	0.07385	9.2402
7.	190	0.07795	8.8026

k_2—k_7 average = $9.14 \cdot 10^{-3}$

$$CH_3—CH_2—CH_2—CH_2—{}^+N(CH_3)_3I^-$$

V

130 °C
[V] = 0.1 mole/litre
$[OH^-]$ = 0.95308 mole/litre

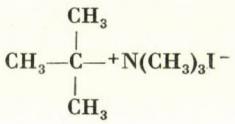
	t	x	$k \cdot 10^3$
1.	120	0.00152	0.11136
2.	240	0.00357	0.15913
3.	345	0.00519	0.16260
4.	441	0.00683	0.16889
5.	530	0.00821	0.17033
6.	620	0.00979	0.17530
7.	710	0.01115	0.17574

k_2—k_7 average = $0.17 \cdot 10^{-3}$

140 °C
[V] = 0.1 mole/litre
$[OH^-]$ = 0.95308 mole/litre

	t	x	$k \cdot 10^3$
1.	160	0.00597	0.40494
2.	280	0.01140	0.45641
3.	340	0.01405	0.47083
4.	401	0.01658	0.47873
5.	460	0.01887	0.48191
6.	520	0.02112	0.48438

k average = $0.46 \cdot 10^{-3}$



VI

120 °C
[VI] = 0.1 mole/litre
$[OH^-]$ = 0.95308 mole/litre

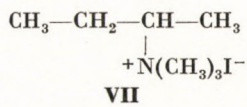
	t	x	$k \cdot 10^3$
1.	20	0.00246	1.3093
2.	38	0.01189	3.5180
3.	51	0.01987	4.6073
4.	66	0.02807	5.3216
5.	80	0.03513	5.7923
6.	95	0.04153	6.0745
7.	110	0.04741	6.3058

k_2—k_7 average = $5.30 \cdot 10^{-3}$

130 °C
[VI] = 0.1 mole/litre
$[OH^-]$ = 0.95308 mole/litre

	t	x	$k \cdot 10^3$
1.	26	0.01029	4.4067
2.	37	0.02149	6.9438
3.	45	0.03127	8.9002
4.	53	0.04015	10.403
5.	63	0.05000	11.897
6.	75	0.05936	12.773
7.	90	0.06817	13.946
8.	105	0.07432	14.273

k_2—k_8 average = $11.30 \cdot 10^{-3}$



VII

130 °C
[VII] = 0.1 mole/litre
$[OH^-]$ = 0.95308 mole/litre

	t	x	$k \cdot 10^3$
1.	62	0.00402	0.69581
2.	114	0.00804	0.77483
3.	160	0.01200	0.84396
4.	205	0.01548	0.86822
5.	250	0.01902	0.89474
6.	300	0.02252	0.90365
7.	360	0.02673	0.92020
8.	410	0.02994	0.92624
9.	470	0.03372	0.93608
10.	530	0.03738	0.94694

k_3—k_{10} average = $0.91 \cdot 10^{-3}$

140 °C
[VII] = 0.1 mole/litre
$[OH^-]$ = 0.95308 mole/litre

	t	x	$k \cdot 10^3$
1.	25	0.00428	1.8400
2.	46	0.00856	2.0505
3.	65	0.01213	2.1011
4.	86	0.01649	2.2187
5.	106	0.02014	2.2513
6.	126	0.02394	2.3095
7.	145	0.02693	2.3051
8.	168	0.03057	2.3133
9.	190	0.03366	2.3156
10.	215	0.03736	2.3327

k average = $2.20 \cdot 10^{-3}$

Reaction rate measurements for the determination of the part-orders according to the van't Hoff equation.

Δc = quaternary ammonium salt and hydroxide ion, respectively (in mole per litre), transformed during time Δt

$$\lg w = \lg\left(-\frac{\Delta c}{\Delta t}\right)$$

120 °C
[IV] = const. = 0.1 mole/litre
$[OH^-]$ = 0.95308 mole/litre

	t	Δc	$\lg w + 5$
1.	17	0.00359	1.32464
2.	25	0.00306	1.58263
3.	34	0.00331	1.56559
4.	43	0.00335	1.57080
5.	52	0.00311	1.53852
6.	61	0.00301	1.52433
7.	70	0.00290	1.50816

$[OH^-]$ = 0.71481 mole/litre

	t	Δc	$\lg w + 5$
1.	25	0.00525	1.32222
2.	45	0.00340	1.23045
3.	64	0.00440	1.36470
4.	80	0.00357	1.34855
5.	98	0.00402	1.34896
6.	117	0.00462	1.38589
7.	133	0.00386	1.38247

$[OH^-]$ = 0.47654 mole/litre

	t	Δc	$\lg w + 5$
1.	30	0.00228	0.88081
2.	55	0.00418	1.22324
3.	75	0.00357	1.25164
4.	100	0.00416	1.22115
5.	120	0.00325	1.21085
6.	140	0.00305	1.18327
7.	160	0.00293	1.16584

$[OH^-]$ = 0.23827 mole/litre

	t	Δc	$\lg w + 5$
1.	30	0.00279	0.96848
2.	60	0.00311	1.01564
3.	90	0.00317	1.02394
4.	125	0.00348	0.99751
5.	155	0.00286	0.97925
6.	185	0.00267	0.94939
7.	215	0.00258	0.93450
8.	250	0.00284	0.90925

$[OH^-]$	$\lg [OH^-] + 1$	$\lg w + 5$
0.95308	0.97913	1.51638
0.71481	0.85419	1.34046
0.47654	0.67810	1.20933
0.23827	0.37707	0.97224

140 °C

[V] = const. = 0.1 mole/litre

$[OH^-]$ = 0.95308 mole/litre

	t	Δc	$\lg w + 5$
1.	160	0.00597	0.82558
2.	280	0.00543	0.65562
3.	340	0.00265	0.64510
4.	401	0.00253	0.61779
5.	460	0.00229	0.58899
6.	520	0.00225	0.57363

$[OH^-]$ = 0.47654 mole/litre

	t	Δc	$\lg w + 5$
1.	150	0.00345	0.36299
2.	210	0.00150	0.39794
3.	270	0.00138	0.36173
4.	330	0.00139	0.36486
5.	390	0.00136	0.35539
6.	450	0.00140	0.36798
7.	510	0.00131	0.33912

$[OH^-]$ = 0.23827 mole/litre

	t	Δc	$\lg w + 5$
1.	150	0.00209	0.14406
2.	226	0.00104	0.14780
3.	315	0.00127	0.15441
4.	405	0.00134	0.17286
5.	495	0.00116	0.11022
6.	585	0.00128	0.15297
7.	675	0.00115	0.10646

[OH⁻]	lg [OH⁻] + 1	lg w + 5
0.95308	0.97913	0.65112
0.47654	0.67810	0.36428
0.23827	0.37707	0.14125

120 °C
[VI] = const. = 0.1 mole/litre
[OH⁻] = 0.95308 mole/litre

	t	Δc	lg w + 4
1.	20	0.00246	0.08991
2.	38	0.00943	0.71924
3.	51	0.00798	0.78806
4.	66	0.00820	0.73772
5.	80	0.00706	0.70267
6.	95	0.00640	0.63009

[OH⁻] = 0.47654 mole/litre

	t	Δc	lg w + 4
1.	30	0.00832	0.45700
2.	49	0.00776	0.61111
3.	70	0.00741	0.54760
4.	90	0.00636	0.50234
5.	110	0.00559	0.44638
6.	130	0.00520	0.41497
7.	150	0.00443	0.34537
8.	180	0.00607	0.30602

[OH⁻] = 0.23827 mole/litre

	t	Δc	lg w + 4
1.	30	0.00500	0.22185
2.	60	0.00478	0.20231
3.	90	0.00537	0.25285
4.	135	0.00831	0.26639
5.	175	0.00899	0.35170
6.	220	0.00675	0.17609
7.	260	0.00515	0.10975

[OH⁻]	lg [OH⁻] + 1	lg w + 4
0.95308	0.97913	0.71556
0.47654	0.67810	0.45396
0.23827	0.37707	0.22585

REFERENCES

1. BARTÓK, M., MOLNÁR, Á., KOVÁCS, K.: Acta Chim. Acad. Sci. Hung. (In the press).
2. KOSZT, A. N., ERSOV, V. V.: Zsurn. Obschej Him. **27,** 1722 (1957).
3. STECK, E. A., BRUNDAGE, R. P.: J. Am. Chem. Soc. **81,** 6511 (1959).
4. LICHTENBERGER, J., LICHTENBERGER, R.: Bull. soc. chim. France **1948,** 1002.
5. ADAMSON, D. W.: J. Chem. Soc. **1950,** 885.
6. MANNICH, C., HORKHEIMER, P.: Arch. Pharm. **264,** 177 (1926).
7. BRECKPOT, R.: Bull. soc. chim. Belge **32,** 417 (1923).
8. MANNICH, C., HORKHEIMER, P.: Arch. Pharm. **264,** 176 (1926).
9. GROB, C. A., OSTERMAYER, F.: Helv. Chim. Acta **45,** 1119 (1962).
10. BEILST. **4,** III, 813.
11. BROWN, H. C., BONNER, W. H.: J. Am. Chem. Soc. **75,** 14 (1953).
12. GUSTUS, E. L., STEVENS, P. G.: J. Am. Chem. Soc. **55,** 378 (1923).
13. COPE, A. C., LEBEL, N. A., LEE, H. H., MOORE, W. R.: J. Am. Chem. Soc. **79,** 4720 (1957).
14. PEARSON, D. E., BAXTER, J. F., CARTER, K. N.: Org. Synth. **29,** 21 (1949).
15. SMITH, L. I., EMERSON, O. H.: Org. Synth. **29,** 19 (1949).
16. BORTNICK, N., LUSKIN, L. S., HURWITZ, M. D., CRAIG, W. E., EXNER, L. J., MIRZA, J.: J. Am. Chem. Soc. **78,** 4039 (1956).
17. SPIALTER, L., PAPPALARDO, J.: J. Org. Chem. **22,** 840 (1957).

Árpád MOLNÁR
Mihály BARTÓK
Kálmán KOVÁCS
Szeged, Beloiannisz tér 8, Hungary

Acta Chimica Academiae Scientiarum Hungaricae, Tomus 59 (1), pp. 157—158 (1969)

ON THE ALKALOIDS OF AMSONIA TABERNAEMONTANA WALT. CULTIVATED IN HUNGARY

(PRELIMINARY COMMUNICATION)

B. ZSADON and R. HUBAY

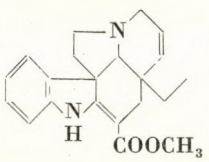
(Department of Chemical Technology, L. Eötvös University, Budapest, and Research Institute for Medicinal Plants, Budapest)

Received May 6, 1968

The alkaloids of *Amsonia tabernaemontana* Walt. acclimatized and cultivated in Hungary, were studied. (—)-Tabersonine (1.05%) was isolated from the ripe seeds, and (+)-1,2-dehydroaspidospermidine (0.18—0.20%) and (—)-quebrachamine (0.01%) from the green parts (shoots and leaves) of the plant.

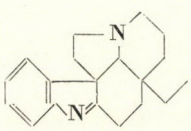
At the Department of Chemical Technology, L. Eötvös University, investigations have been made to isolate the main alkaloids of the plant *Amsonia tabernaemontana* Walt. acclimatized and cultivated by the Research Institute for Medicinal Plants, Budapest.

From the ripe seeds of the plant 1.05% (—)-*tabersonine* **(I)** was isolated in the form of its hydrochloric salt (fine needles from dilute hydrochloric acid), m.p. 195—197 °C (decomp.), $[\alpha]_D$ —300° (methanol, c = 0.5). UV spectrum (in methanol): λ_{max} (lg ε) = 226 (3.98), 298 (4.00), 328 (4.16). R_f = 0.38 (thin-layer alumina/benzene).



(I)

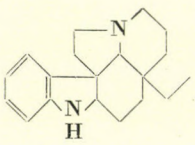
From the dried green parts (shoots and leaves) of the plant 0.18—0.20% (+)-1,2-*dehydroaspidospermidine* **(II)** was isolated. (The plant material was harvested in September 1967, after the seeds had been gathered separately.) The alkaloid **(II)** purified by chromatography was a colorless viscous oil, turning yellow on air at room temperature; $[\alpha]_D$ + 265° (ethanol, c = 0.5). UV spec-



(II)

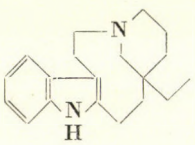
trum (in methanol): λ_{max} (lg ε) = 222 (4.57), 228$_s$ (4.45), 263 (3.99). R_f = 0.11 (thin-layer alumina/benzene) and 0.62 (thin-layer alumina/benzene—methyl-ethyl-ketone 95 : 5).

The alkaloid **(II)** was identified by conversion into two well-known derivatives. Reduction with lithium-aluminium-hydride in ether solution, or with sodium-borohydride in ethanolic solution at 0 °C, gave (+)-*aspidospermidine* **(III)** in good yields (80—90%), m.p. 120—121 °C (plates from isopropanol), $[\alpha]_D$ +17° (methanol, c = 1.5). UV spectrum (in methanol): λ_{max} (lg ε) = 244 (3.81), 297 (3.46). R_f = 0.20 (thin-layer alumina/benzene—methyl-ethyl-ketone 95 : 5).



(III)

The alkaloid **(II)** could be transformed into (—)-*quebrachamine* **(IV)** by reducing it with sodium borohydride in boiling ethanolic solution (yield: 80%).



(IV)

(—)-Quebrachamine (0.01%) could also be isolated from the dried green parts of the plant and identified with the alkaloid **(IV)** produced by transforming the alkaloid **(II)**. M. p. 147 °C (plates from n-heptane), $[\alpha]_D$ — 103° (chloroform, c = 0.5). UV spectrum (in methanol): λ_{max} (lg ε) = 228 (4.53), 286 (3.84), 293 (3.83). R_f = 0.30 (thin-layer alumina/benzene) and 0.94 (thin-layer alumina/benzene—methyl-ethyl-ketone 95 : 5).

The elemental analyses (C, H, N, O) and the physical constants of these alkaloids (I, II, III, IV) were consistent with the calculated values and with the data of M. HESSE's "Indolalkaloide in Tabellen" (Springer 1964), respectively.

The authors are obliged to Prof. Á. GERECS (Department of Chemical Technology, L. Eötvös University) for his advice and help in these investigations; to Director P. TÉTÉNYI (Research Institute for Medicinal Plants, Budapest) for directing the botanical works; and to Miss É. EGRY and Miss M. SÁRKÖZI for their participation in the chemical experiments.

Béla ZSADON; Budapest VIII. Múzeum krt. 6/8
Róbert HUBAY; Budapest XII. Dániel út 40

Acta Chimica Academiae Scientiarum Hungaricae, Tomus 59 (1), pp. 159—160 (1969)

A BETA-ELIMINATION REACTION BETWEEN CYSTEINE DERIVATIVES CONTAINING FREE SH GROUP AND DICYCLOHEXYLCARBODIIMIDE*

(SHORT COMMUNICATION)

L. KISFALUDY, A. PATTHY and M. LŐW

(Research Laboratory, Chemical Works of Gedeon Richter Ltd., Budapest)

Received June 13, 1968

The reactions of the SH group of cysteine have been thoroughly studied in recent years, especially with respect to problems encountered in the synthesis of insulin. In this paper we report a β-elimination reaction of a cysteine derivative that takes place under mild conditions, when the amino and carboxyl groups of cysteine are protected. Namely, N-*p*-chlorobenzyloxycarbonyl-cysteine methyl ester has been found to react with dicyclohexylcarbodiimide (DCC) in an organic solvent, resulting in the nearly quantitative formation of a crystalline compound that was identified by elemental analysis as dicyclohexylthiourea. This compound was compared with the product of the reaction of DCC with hydrogen sulphide. The two compounds were shown to be identical by their IR-spectra and mixed melting point determination. The dehydroalanine *i.e.* acrylic acid derivative remaining in the mother liquor were identified after saponification and compared with the condensation product of pyruvic acid and *p*-chlorobenzylurethane [1].

This reaction seems to be applicable for the degradation of cysteine peptides and the preparation of dehydroalanine derivatives.

Experimental

(a) 3.03 g (0.01 mole) of N-*p*-chlorobenzyloxycarbonyl-L-cysteine methyl ester (m.p. 54—56 °C; Calcd. C 47.4; H 4.6; O 21.1; N 4.7; S 10.6; Cl 11.7. Found C 47.4; H 4.8; O 21.0; N 4.8; S 10.4; Cl 11.7%) prepared by reductive cleavage of the corresponding cystine derivative, was dissolved in 14 ml of peroxide free dry dioxane, then 2.06 g (0.01 mole) of DCC was added. The crystals that separated on standing overnight, were filtered off and washed to obtain 2.09 g (88%) of dicyclohexylthiourea, m.p. 170—175 °C. Recrystallization from 12 ml of ethanol gave 1.89 g of the pure product, m.p. 177—179 °C. (Calcd. C 65.5; H 9.4; S 13.4; N 11.8. Found C 65.0; H 10.0; S 13.3; N 11.7%.)

(b) Hydrogen sulphide was bubbled through a solution of 2.06 g (0.01 mole) of DCC in 14 ml of dry dioxane for 15 min to obtain 2.3 g (96%) of a crystalline solid, m.p. 176—177 °C. The IR-spectra of the products prepared according to (a) and (b) were identical, with characteristic bands at 3.05, 3.45, 3.55, 6.42, 6.65 and 10.15 μ.

(c) An aliquot of the dioxane mother liquor from Reaction (a) was saponified with 2*N* NaOH and, after isolation, the N-*p*-chlorobenzyloxycarbonyldehydroalanine was recrystallized from toluene, m.p. 126 °C.

* Abstracted from the paper presented at the Chemical Conference organized by the Hungarian Chemical Society, September 2—4, 1965, Sopron.

(d) 8.3 g (0.045 mole) of *p*-chlorobenzylurethane and 13.2 g (0.15 mole) of pyruvic acid were converted into 2,2-di(*p*-chlorobenzyloxycarbonylamino)propionic acid [2], which, after boiling in acetic acid, gave 0.86 g of N-*p*-chlorobenzyloxycarbonyldehydroalanine, m.p. 126—127 °C. (Calcd. C 51.8; H 3.9; N 5.4; Cl 13.8. Found C 51.5; H 4.1; N 5.6; Cl 13.4%.)

The IR-spectra of the compounds described under (c) and (d) were identical, with characteristic bands at 3.0, 3.9, 5.82, 5.96, 6.15 and 9.2 μ.

REFERENCES

1. KISFALUDY L., DUALSZKY S.: Acta Chim. Acad. Sci. Hung. **24**, 301 (1960).
2. WIELAND TH., OKNACKER G., ZIEGLER W.: Ber. **90**, 194 (1957).
FRANKEL M., REICHMANN M. E.: J. Chem. Soc. **1952**, 289.

Lajos KISFALUDY
Ágnes PATTHY
Miklós LŐW
Budapest X. Gyömrői út 19—21

Acta Chimica Academiae Scientiarum Hungaricae, Tomus 59 (1), pp. 161—164 (1969)

CONVERSIONS OF TOSYL AND MESYL DERIVATIVES OF THE MORPHINE GROUP

SYNTHESIS OF ACETYLMERCAPTO AND MERCAPTO DERIVATIVES

(PRELIMINARY COMMUNICATION)

R. BOGNÁR, S. MAKLEIT and T. MILE

(Institute for Organic Chemistry of the Lajos Kossuth University, Debrecen)

Received July 31, 1968

During a systematic investigation of the possible conversions of tosyl and mesyl derivatives of the morphine group, effected with various nucleophilic agents [1], the 6-desoxy-6-acetylmercapto and the 6-desoxy-6-mercapto derivatives of morphine, codeine, dihydromorphine and dihydrocodeine have been synthesized for the first time, using potassium thiolacetate [2].

No attempt to prepare the acetylmercapto derivatives is known to the authors, while the synthesis of morphine derivatives containing the free mercapto group, was tried by PSCHORR [3] without positive results.

Only the preparation and investigation of the thioether derivatives, starting with halogen codides, have been reported in the literature [4].

The compounds prepared by us, and the outlines of the syntheses are shown in Figs 1 and 2.

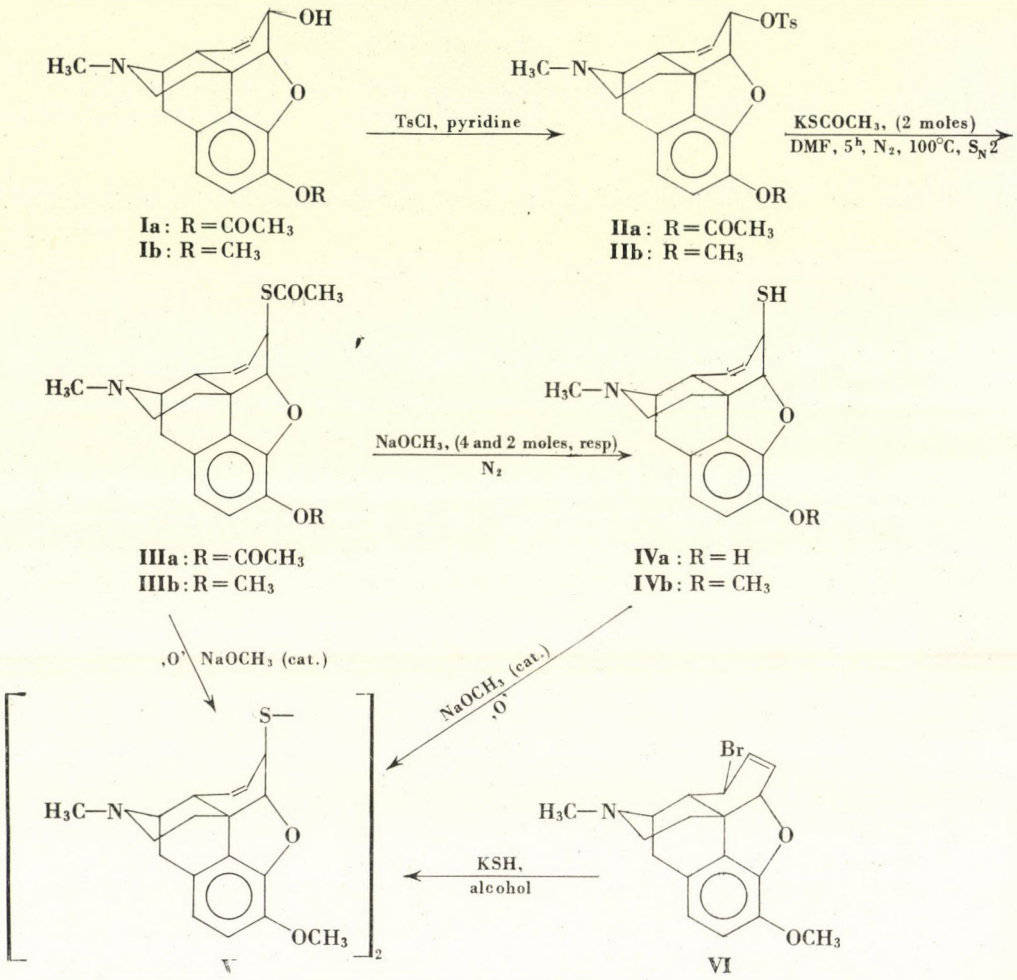
Ia: 3-O-acetylmorphine; **Ib:** codeine; **IIa:** 3-O-acetyl-6-O-tosylmorphine; **IIb:** 6-O-tosylcodeine [5]; **IIIa:** 3-O-acetyl-6-desoxy-6-acetylmercapto-α-isomorphine* (3-O-acetyl-6-desoxy-6-acetylmercaptoisomorphine); **IIIb:** 6-desoxy-6-acetylmercaptoisocodeine; **IVa:** 6-desoxy-6-mercapto-α-isomorphine (6-desoxy-6-mercaptoisomorphine); **IVb:** 6-desoxy-6-mercaptoisocodeine; **V:** bis-thiocodide [3], 6,6'-didesoxy-6,6'-isocodeine disulfide; **VI:** bromocodide [6]; **VIIa:** 3-O-acetyl-6-O-tosyldihydromorphine; **VII:b** 6-O-mesyldihydrocodeine; **VIIIa:** 3-O-acetyl-6-desoxy-6-acetylmercaptodihydro-α-isomorphine; (3-O-acetyl-6-desoxy-6-acetylmercaptodihydroisomorphine); **VIIIb:** 6-desoxy-6-acetylmercaptodihydroisocodeine; **IXa:** 6-desoxy-6-mercaptodihydro-α-isomorphine (6-desoxy-6-mercaptodihydroisomorphine); **IXb:** 6-desoxy-6-mercaptodihydroisocodeine.

The following data are characteristic of the new compounds.**

* For recommendations concerning the nomenclature of the compounds, see in our earlier publications.

** All compounds gave proper analytical results; thin-layer chromatography (benzene/methanol = 8 : 2, Silicagel G, Dragendorff) showed them to be homogeneous, with the exception of compound **IV**; the infrared spectra of the compounds were consistent with the structures given.

IIIa: $C_{21}H_{23}O_4NS$; m.p. 131.5 °C (abs. alcohol); yield 43%; $[\alpha]_D = -7.7°$ (abs. alcohol, 0.516); **IIIb:** $C_{20}H_{23}O_3NS$; m.p. 137—138 °C (abs. alcohol); yield 57.3%; $[\alpha]_D = -34.7°$ (chloroform, 0.459); **IVa:** $C_{17}H_{19}O_2NS$; m.p. 170—171 °C; yield 42%; $[\alpha]_D = +66.4°$ (abs.alcohol, 0.512). (This compound contains



a small amount of disulfide as impurity. Various purification processes, such as recrystallization or preparative thin-layer chromatography, failed to give satisfactory results on account of the instability of the compound.)

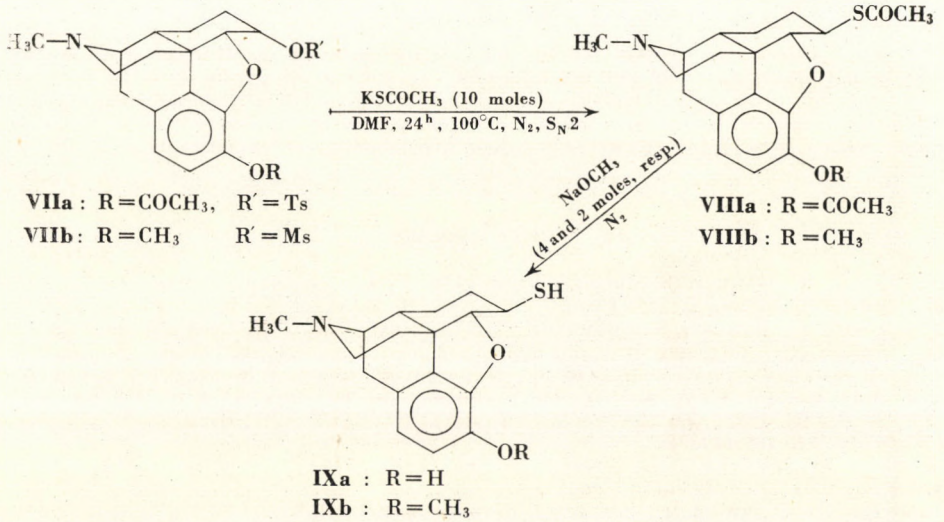
IVb: $C_{18}H_{21}O_2NS$; m.p. 160—161 °C (abs. alcohol); yield 38.5%; $[\alpha]_D = -36.6°$ (chloroform, 0.6).

VIIIa: $C_{21}H_{25}O_4NS$; m.p. 129—130 °C (abs. ether — *n*-hexane); yield 22% $[\alpha]_D = -123.4°$ (chloroform, 0.567).

VIIIb: $C_{20}H_{25}O_3NS$; m.p. 159—160 °C (abs. ether); yield 42%; $[\alpha]_D = -139.4°$ (chloroform, 0.509).

IXa: $C_{17}H_{21}O_2NS$; m.p. 220—221 °C; yield 95%; $[\alpha]_D = -166.6°$ (chloroform, 0.15).

IXb: $C_{18}H_{23}O_2NS$; m.p. 155—157 °C (abs. alcohol); yield 91%; $[\alpha]_D = -171.8°$ (chloroform, 0.64).



VIIa : R = $COCH_3$, R' = Ts
VIIb: R = CH_3 R' = Ms

VIIIa : R = $COCH_3$
VIIIb : R = CH_3

IXa : R = H
IXb : R = CH_3

Concerning the chemical reactions shown in Figs 1 and 2, the following theoretical considerations are to be mentioned:

The alcoholic 6-O- tosyl derivatives of unsaturated morphine and codeine react with potassium thiolacetate, without allyl migration, in an S_{N^2} reaction to yield the corresponding acetylmercapto derivatives (**IIIa, IIIb**).

Tosyloxy and mesyloxy groups react, namely, when acted by $SCOCH_3$ ions, under suitable experimental conditions, generally by inversion [7]; the absence of allyl migration (*i.e.* the absence of the reaction of type S_{N^2}') is further substantiated by the fact that both **IIIb** and **IVb** could be converted into **V**, which compound (Pschorr's bis-thiocodide) is, in our opinion, best represented by the formula given, on the basis of known conversions of bromocodide with nucleophilic agents [8].

We think that the absence of allyl migration in the present case and its occurrence in other cases [1] can be accounted for partly by taking into con-

sideration the quantitative value of the nucleophilic activity of the agent used [9].

The absence of an S_{N1} reaction can be explained by the reaction conditions [1], the stereochemical properties of the molecule, and by electrical factors [10].

The correctness of the structural and stereo-structural formulas has also been confirmed by NMR investigations.

It is hoped that details of this work will be published in Acta Chim. Acad. Sci. Hung.

*

The authors wish to thank the Chemical Department of the Hungarian Academy of Sciences and Alkaloida Chemical Works, Tiszavasvári, for supporting this work, Dr. L. RADICS for the recording and evaluation of the NMR spectra, the Analytical Laboratory of our Institute for the analyses and for recording the infrared spectra, and undergraduate S. NAGY, and technicians G. KISS and E. KERTÉSZ for their assistance in the experiments.

REFERENCES

1. BOGNÁR, R., MAKLEIT, S.: Chem. and Ind. **1956,** 1239. — BOGNÁR, R., MAKLEIT, S.: Arzneimittel-Forschung **8,** 323 (1958). — BOGNÁR, R., MAKLEIT, S.: Acta Univ. Debr. **5,** 225 (1958). — MAKLEIT, S., BOGNÁR, R.: M.T.A. Kém. Tud. Oszt. Közl. **30,** 289 (1968) — BOGNÁR, R., MAKLEIT, S.: Acta Chim. Acad. Sci. Hung. **58,** 203 (1968) — BOGNÁR, R., MAKLEIT, S.: Acta Chim. Acad. Sci. Hung. (in the press). — BOGNÁR, R., MAKLEIT, S.: Magyar Kém. Foly. **74,** 523 (1968) — BOGNÁR, R., MAKLEIT, S., MILE, T.: Acta Chim. Acad. Sci. Hung. (in the press). — BOGNÁR, R., MAKLEIT, S., MILE, T.: Magyar Kém. Foly. **74,** 526 (1968).
2. COX, J. M., OWEN, L. N.: J. Chem. Soc. **1967,** 1121.
3. PSCHORR, H.: Ber. **39,** 3130 (1906).
4. MORRIS, D. E., SMALL, L.: J. Am. Chem. Soc. **56,** 2159 (1934).
5. KARRER, P., WIDMARK, G.: Helv. Chim. Acta **34,** 34 (1951).
6. RAPOPORT, H., PAYNE, G. B.: J. Org. Chem. **15,** 1093 (1950).
7. OWEN, L. W., RAGG, P. L.: J. Chem. Soc. **1966,** 1291.
8. SMALL, L. F.: Chemistry of the opium alkaloids. United StatesGovernment Printing Office, Washington, 1932. — BENTLEY, K. W. The chemistry of the morphine alkaloids. Clarendon Press, Oxford, 1954. — MANSKE, R. H. F., HOLMES, H. L.: The Alkaloids, Vol. II. Academic Press Inc., New York, 1952. — MANSKE, R. H. F.: The alkaloids, Vol. VI. Academic Press, New York, London, 1960.
9. SWAIN, C. G., SCOTT, C. B.: J. Am. Chem. Soc. **75,** 141 (1953). — HAWTHORNE, M. F., HAMMOND, G. S., GRAYBILL, B. M.: J. Am. Chem. Soc. **77,** 486 (1955).
10. STORK, G., CLARKE, F. H.: J. Am. Chem. Soc. **78,** 4619 (1956).

Rezső BOGNÁR
Sándor MAKLEIT
Teréz MILE
Debrecen, 10, Hungary

Acta Chimica Academiae Scientiarum Hungaricae, Tomus 59 (1), pp. 165—168 (1969)

SYNTHESE DES BIOLOGISCH AKTIVEN FRAGMENTS DES β-LIPOTROPEN HORMONS

(VORLÄUFIGE MITTEILUNG)

K. MEDZIHRADSZKY, S. BAJUSZ, H. S.-VARGHA und Zs. LÁNG

(Institut für Organische Chemie der L. Eötvös Universität, Budapest und Institut für Arzneimittelforschung, Budapest)

Eingegangen am 18. November 1968

Vor einigen Jahren haben LI und Mitarbeiter [1, 2] aus Schafshypophyse ein aus 90 Aminosäureresten aufgebautes, lipoidmobilisierendes Polypeptid isoliert und auch seine Aminosäuresequenz ermittelt. Es ist recht auffallend, daß der mittlere Sequenzbereich dieses als β-lipotropes Hormon (β-LPH) bezeichneten Polypeptids einigen Sequenzbereichen anderer Hypophysenhormone sehr ähnlich ist. So enthalten alle bekannten Corticotropine (ACTH) [3] und melanocitstimulierenden Hormone (MSH) [4] die -Met-Glu-His-Phe-Arg--Trp-Gly-* Heptapeptidsequenz des Bereiches 47—53 vom β-LPH, und der Sequenzbereich 41—58 ist sogar mit der Vollsequenz des β-MSH aus Rinderhypophyse identisch, desgleichen auch der Sequenzbereich 37—58 — mit Ausnahme des an Stelle 42, bzw. 48 stehenden Serins bzw. Lysins — mit der Vollsequenz des menschlichen β-MSH.

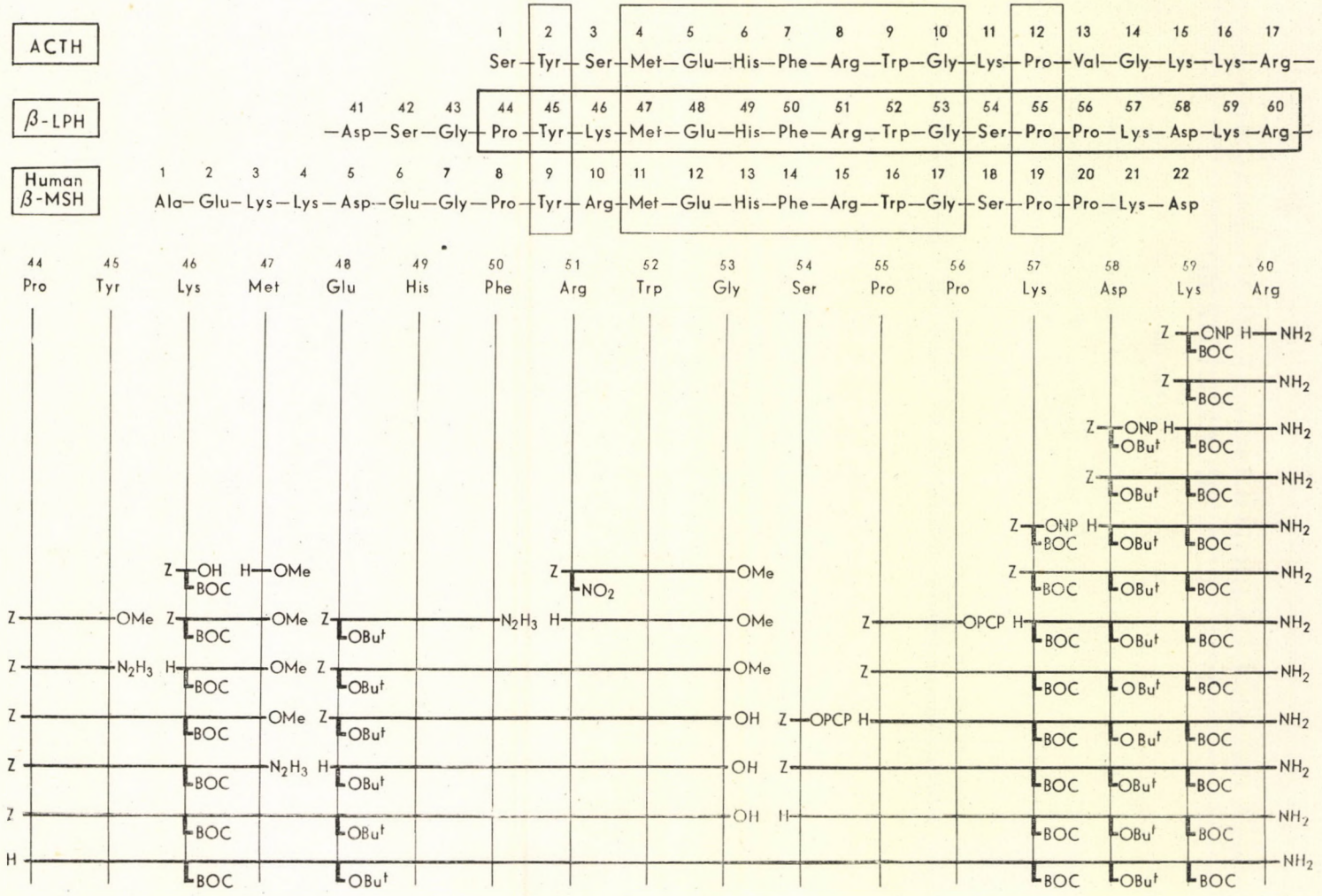
Auf Grund dieser Strukturbeziehungen war zu vermuten, daß das β-LPH außer der lipoidmobilisierenden Aktivität auch eine melanocitstimulierende und vielleicht auch eine corticotrope Wirkung zeigen dürfte. Auch war zu erwarten, daß zur Ausübung dieser Wirkungen nicht unbedingt das ganze Molekül, sondern auch seine Fragmente fähig sind, die die oben angeführten Sequenzen enthalten. Zur Überprüfung der Richtigkeit dieser Vermutung haben wir die Synthese des Heptadekapeptidamids angestrebt, das dem Sequenzbereich 44—60 des β-LPH entspricht (vgl. den dick eingerahmten Teil in Abb. 1). Unsere Wahl fiel deshalb auf diesen Sequenzbereich, weil er dem N-terminalen 1—17 Sequenzbereich der Corticotropine, dessen erhebliche lipoidmobilisierende Wirkung unlängst an Hand des synthetisierten 1—17 Fragments gezeigt werden konnte [5], äußerst ähnlich ist.

Die Synthese des Heptadekapeptidamids ist in Abb. 2 skizziert** und wird im folgenden kurz geschildert.

Zwecks Synthese des der Teilsequenz 44—47 entsprechenden, geschützten Tetrapeptidhydrazids wurde zuerst Z-Lys(BOC)-OH [6] mit Methionin-

* Die Abkürzungen richten sich nach den Vorschlägen der Commission on Biochemica Nomenclature (J. Biol. Chem. **241**, 527 (1966)).

** Über diese Synthese haben wir zuerst an einer in Pécs im September 1967 gehaltenen Konferenz des Vereins Ungarischer Chemiker ganz kurz berichtet.


ACTH
β-LPH
Human β-MSH
1 2 3 4 5 6 7 8 9 10 11 12 13 14 15 16 17
Ser—Tyr—Ser—Met—Glu—His—Phe—Arg—Trp—Gly—Lys—Pro—Val—Gly—Lys—Lys—Arg—
41 42 43 44 45 46 47 48 49 50 51 52 53 54 55 56 57 58 59 60
—Asp—Ser—Gly—Pro—Tyr—Lys—Met—Glu—His—Phe—Arg—Trp—Gly—Ser—Pro—Pro—Lys—Asp—Lys—Arg—
1 2 3 4 5 6 7 8 9 10 11 12 13 14 15 16 17 18 19 20 21 22
Ala—Glu—Lys—Lys—Asp—Glu—Gly—Pro—Tyr—Arg—Met—Glu—His—Phe—Arg—Trp—Gly—Ser—Pro—Pro—Lys—Asp
44 45 46 47 48 49 50 51 52 53 54 55 56 57 58 59 60
Pro Tyr Lys Met Glu His Phe Arg Trp Gly Ser Pro Pro Lys Asp Lys Arg
Z OH H OMe
BOC
Z OMe
Z N2H3 H OMe
BOC
Z OMe
BOC
Z N2H3 H
BOC
Z
BOC
H
BOC
Z OMe
Z OMe
BOC
Z OBut
Z OBut
Z OBut
Z OBut
OBut
Z N2H3
OBut
Z NO2
OMe
Z OMe
Z OMe
Z OH
Z OH
OH H
Z OPCP H
Z OPCP H
Z
Z
Z
Z
Z
Z
Z
BOC
Z ONP H
BOC
Z
BOC
Z ONP H
OBut
BOC
Z
OBut
BOC
Z ONP H
BOC
OBut
BOC
Z
BOC
OBut
BOC
NH2
BOC
OBut
BOC

methylester durch Anwendung der Carbodiimid-Methode zum geschützten Dipeptid Z-Lys(BOC)-Met-OMe (Schmp.: 98—100°. — $C_{25}H_{39}O_7N_3S$: 525.7. — Ber. C 57,1; H 7,6; N 8,0; S 6,1% Gef. C 57,2; H 7,6; N 8,0; S 6,2%) umgesetzt, aus diesem durch in Gegenwart von Triäthylamin durchgeführte Hydrogenolyse [7] der Dipeptidester H-Lys(BOC)-Met-OCH_3 hergestellt und dessen Acetat (R_F^1 0,85)*** wegen seiner Labilität gleich mit aus Z-Pro-Tyr-OMe [8] bereitetem Z-Pro-Tyr-N_2H_3 (Schmp.: 198—199°. — $C_{22}H_{26}O_5N_4$: 426,5. — Ber. C 61,7; H 6,1; N 13,1; Hydrazid-N 6,5%. — Gef. C 61,4; H 6,3; N 12,8; Hydrazid-N [9] 6,6%) bzw. aus diesem hergestellten Azid zum Z-Pro-Tyr-Lys(BOC)-Met-OMe (Schmp.: 107—108°. — $C_{39}H_{55}O_{10}N_5S$: 785,9. — Ber. C 59,5; H 7,05; N 8,9; S 4,1% Gef. C 59,0; H 7,1; N 9,05; S 4,15%) gekoppelt. Dieses Produkt ließ sich mit Hydrazinhydrat zum Hydrazid Z-Pro-Tyr-Lys(BOC)-Met-N_2H_3 (Schmp.: 180—182°. — $C_{38}H_{55}O_9N_7S$: 785,9. — Ber. C 58,1; H 7,05; N 12,5; S 4,1; Hydrazid-N 3,6%.— Gef. C 58,4; H 7,5; N 12,1; S 3,95; Hydrazid-N 3,6%) umsetzen.

Zwecks Synthese des der Sequenz 48—53 entsprechenden Hexapeptids haben wir das von GEIGER und Mitarbeiter [10] beschriebene Z-Arg(NO_2)-Trp-Gly-OMe hydrogenolysiert und das gewonnene Tripeptidacetat (R_F^1 0,15) mit dem Azid, das aus dem bereits bekannten [5,11] Peptidhydrazid Z-Glu(OBu^t)-His-Phe-N_2H_3 bereitet worden war, acyliert. Der erhaltene, geschützte Hexapeptidester Z-Glu(OBu^t)-His-Phe-Arg(NO_2)-Trp-Gly-OMe ließ sich auf chromatographischem Weg reinigen (R_F^1 0,40. — Aminosäureanalyse: His 1,12; Glu 1,02; Phe 1,03; Arg 0,97; Gly 0,82). Diese Verbindung haben SCHWYZER und Mitarbeiter [12] anders aufgebaut. Die Verseifung dieses Esters [12] und eine darauf folgende Hydrogenolyse ergaben das Hexapeptidderivat H-Glu(OBu^t)-His-Phe-Arg-Trp-Gly-OH (R_F^2 0,17).

Durch Acylierung des oben beschriebenen Hexapeptidderivats mit dem aus dem Hydrazid Z-Pro-Tyr-Lys(BOC)-Met-N_2H_3 bereiteten Tetrapeptidazid konnte das Dekapeptidderivat Z-Pro-Tyr-Lys(BOC)-Met-Glu(OBu^t)-His-Phe-Arg-Trp-Gly-OH gewonnen werden; das Produkt ließ sich durch Ausfällen aus seiner Lösung in Dimethylformamid mit absol. Essigester reinigen (R_F^1 0,38. — Aminosäureanalyse: Pro 1,07; Tyr 0,98; Lys 0,94; Met 0,89; Glu 1,00; His 0,95; Phe 0,94; Arg 1,02; Gly 1,07).

Die Acylierung des Amids H-Arg(NO_2)-NH_2 mit Hilfe des aktiven Esters Z-Lys(BOC)-ONP führte zum kristallinen Dipeptidderivat Z-Lys(BOC)-Arg(NO_2)-NH_2 (Schmp.: 178°. — $C_{25}H_{40}O_8N_8$: 580,6. — Ber. C 51,7; H 6,9; O 22,05; N 19,3%. — Gef. C 51,6; H 7,0; O 22,0; N 19,3%). Aus diesem konnte durch Hydrogenolyse das Acetat H-Lys(BOC)-Arg-$NH_2 \cdot 2CH_3COOH$ (R_F^1 0,15) gewonnen werden, das dann mit dem aktiven Ester Z-Asp(OBu^t)-ONP zum Tripeptidderi-

*** Die bei der Dünnschichtchromatographie angewandten Lösungsmittel waren: 1. Essigester—Pyridin—Eisessig—Wasser: 60 : 20 : 6 : 11; 2. Butanol—Pyridin—Eisessig—Wasser: 30 : 20 : 6 : 24.

vat Z-Asp (OBu^t)-Lys(BOC)-Arg-NH_2 · CH_3COOH umgesetzt wurde; dieses Produkt ließ sich mittels Säulenchromatographie reinigen (R_F^1 0,65). Nach hydrogenolytischer Abspaltung der Carbobenzoxygruppe wurde das gewonnene Tripeptid-diacetat (R_F^1 0,36) mit dem aktiven Ester Z-Lys(BOC)-ONP zum Tetrapeptidderivat Z-Lys(BOC)-Asp(OBu^t)-Lys(BOC)-Arg-NH_2 · CH_3COOH gekoppelt, das sich auf chromatographischem Weg in einheitlichem Zustand isolieren ließ (R_F^1 0,85). Nachdem die terminale Aminogruppe dieses Tetrapeptidderivats durch Hydrogenolyse freigesetzt wurde, konnte das gewonnene Diacetat (R_F^1 0,20) mit Hilfe des kristallinen Pentachlorphenylesters Z-Pro-Pro-OPCP (Schmp.: 103—105°. — $C_{24}H_{21}O_5N_2Cl_5$: 594,7. — Ber. C 48,5; H 3,6; O 13,45; N 4,7; Cl 29,8%. — Gef. C 48,5; H 3,55; O 13,5; N 4,7; Cl 29,8%) zum Z-Pro-Pro-Lys(Boc)-Asp(OBu^t)-Lys(BOC)-Arg-NH_2 · CH_3COOH umgesetzt und dieses auf chromatographischem Weg gereinigt werden (R_F^1 0,75. — $C_{54}H_{88}O_{14}N_{12}$ · CH_3COOH: 1189,3. — Ber. C 56,6; H 7,8; O 21,5; N 14,1%. — Gef. C 56,25; H 7,9; O 21,3; N 14,1%). Nach hydrogenolytischer Entcarbobenzoxylierung ließ sich das N-terminal freie Hexapeptid-amid-diacetat (R_F^1 0,15) mit dem aktiven Ester Z-Ser-OPCP zum geschützten Hexapeptidamid Z-Ser-Pro-Pro-Lys(BOC)-Asp(OBu^t)-Lys(BOC)-Arg-NH_2 umsetzen, das nach chromatographischer Reinigung und darauf folgender Gefriertrocknung als Monoacetat anfiel (R_F^1 0,65.— $C_{57}H_{93}O_{16}N_{13}$ · CH_3COOH · H_2O: 1294,5. — Ber. C 54,7; H 7,7; O 23,5; N 14,1%. — Gef. C 54,7; H 7,8; O 23,5; N 14,05%). Nach Freisetzen der terminalen Aminogruppe durch Hydrogenolyse wurde das Heptapeptidderivat in sein Hydrochlorid übergeführt (R_F^1 0,10 — Aminosäureanalyse; Ser 0,90; Pro 1,90; Lys 2,00; Asp 1,00; Arg 0,94).

Die Koppelung des oben beschriebenen C-terminal freien Dekapeptidderivats und des N-terminal freien Heptapeptidderivats zum geschützten Heptadekapeptidamid Z-Pro-Tyr-Lys(BOC)-Met-Glu(OBu^t)-His-Phe-Arg-Trp-Gly-Ser-Pro-Pro-Lys(BOC)-Asp(OBu^t)-Lys(BOC)-Arg-NH_2 erfolgte mit Dicyclohexyl-carbodiimid in Gegenwart von überschüssigem Triäthylamin und Pentachlorphenol. Das Rohprodukt ließ sich durch Säulenchromatographie reinigen (R_F^1 0,30). Nach Abspaltung sämtlicher Schutzgruppen durch Hydrogenolyse bzw. durch Einwirkung von Trifluoressigsäure und darauf folgendem Ionenaustausch wurde das dem Sequenzbereich 44—60 des β-LPH entsprechende Heptadekapeptidamid in Form seines Acetats als einheitliches Produkt gewonnen (R_R^2 0,49 — Aminosäureanalyse: Pro 2,83; Tyr 0,86; Lys 3,07; Met 0,81; Glu 1,00; His 1,02; Phe 0,97; Arg 1,97; Gly 1,09; Ser 0,78; Asp 1,00).

Das auf oben geschilderte Art synthetisierte Heptadekapeptidamid wies die erwartete biologische Aktivität auf: seine molare lipoidmobilisierende Wirkung entsprach der des β-lipotropen Hormons, d.h. die minimale effektive Dosis betrug am Kaninchen-Fettgewebe getestet $7 \times 10^{-\frac{\mu g}{ml}}$ ****. LOHMAR und LI

**** Die Testung der biologischen Aktivität hat Herr Dr. Gy. CSEH (Institut für Arzneimittelforschung) durchgeführt, wofür wir auch an dieser Stelle bestens danken.

[13] haben die biologische Wirkung des β-LPH mit der des Schafscorticotropins (α_S-ACTH) verglichen und dabei gefunden, daß das β-LPH am Ratten- bzw. Kaninchen-Fettgewebe getestet nur ein Tausendstel bzw. ein Zehntel-Fünftel der lipoidmobilisierenden Wirkung des α_S-ACTH aufweist; die MSH-Wirkung, weiterhin die corticotrope Wirkung des β-LPH beträgt nur die Hälfte bzw. ein Zehntel im Vergleich zu diesen Wirkungen des α_S-ACTH. Zwecks Ermittlung des aktiven Zentrums des β-LPH haben die genannten Forscher eine selektive Spaltung mit Bromcyan durchgeführt. Sie gelangten auf diese Weise zu Fragmenten, die noch eine lipoidmobilisierende Wirkung aufwiesen. Hierbei zeigte sich, daß das Fragment 1—65, das auch die Sequenz des von uns jetzt synthetisierten Heptadekapeptidamids enthält, die gleiche lipoidmobilisierende Wirkung hat wie das unversehrte Hormon selbst, während diese Wirkung des Fragments 48—90, das nur einen Teil der Sequenz des erwähnten Heptadekapeptidamids enthält, nur ein Zehntel der des unversehrten Hormons beträgt. Nun konnten LOHMAR und LI die Möglichkeit nicht ausschließen, daß diese an sich sehr niedrigen lipoidmobilisierenden Wirkungen nicht von den Fragmenten selbst herrühren, sondern von ihrem Corticotropingehalt, den sie als Verunreinigung enthalten dürften. Wir glauben, daß unsere Untersuchungen nun eindeutig beweisen, daß die lipoidmobilisierende Wirkung der aus dem Naturprodukt (β-LPH) erhältlichen Fragmente eine Folge ihrer eigenen Struktur ist. Auch haben unsere synthetischen Untersuchungen das aktive Zentrum des lipoidmobilisierenden Hormons enger eingegrenzt.

LITERATUR

1. LI, C. H., BARNAFI, L., CHRETIEN M., CHUNG, D.: Proc. Sixth Pan-American Congrsse of Endocrinol., 1965, Excerpta Med. Int. Congress Series No. **112**. p. 349.
2. LI, C. H., BARNAFI, L., CHRETIEN, M., CHUNG, D.: Nature **208**, 1093 (1965).
3. SCHRÖDER, E., LÜBKE, K.: The Peptides, Vol. 2. p. 195. Academic Press, 1966.
4. SCHRÖDER, E., LÜBKE, K.: The Peptides, Vol. 2. p. 162. Academic Press, 1966.
5. BAJUSZ, S., MEDZIHRADSZKY, K.: Peptides, p. 209. eds. H. C. Beyerman et al. North-Holland, Amsterdam, 1967.
6. SCHWYZER, R., RITTEL, W.: Helv. Chim. Acta **44**, 159 (1961).
7. MEDZIHRADSZKY-SCHWEIGER, H., MEDZIHRADSZKY, K.: Acta Chim. Acad. Sci. Hung. **50**, 339 (1965).
8. ISELIN, B.: Helv. Chim. Acta **44**, 61 (1961).
9. MEDZIHRADSZKY-SCHWEIGER, H.: Acta Chim. Acad. Sci. Hung. **34**, 213 (1962).
10. GEIGER, R., STURM, K., SIEDEL, W.: Chem. Ber. **96**, 1080 (1963).
11. MEDZIHRADSZKY, K., BAJUSZ, S., KISFALUDY, L., LÖW, M., PAULAY, Z.: Acta Chim. Acad. Sci. Hung., im Druck.
12. SCHWYZER, R., ISELIN, B., KAPPELER, H., RINIKER, B., RITTEL, W., ZUBER, H.: Helv. Chim. Acta **46**, 1975 (1963).
13. LOHMAR, P., LI, C. H.: Endocrinology **82**, 898 (1968).

Kálmán MEDZIHRADSZKY; Budapest VIII. Múzeum körút 4/b
Sándor BAJUSZ; Budapest IV. Szabadságharcosok útja 47/49
Helga S.-VARGHA; Budapest VIII. Múzeum körút 4/b
Zsuzsa LÁNG; Budapest IV. Szabadságharcosok útja 47/49

INDEX

INORGANIC AND ANALYTICAL CHEMISTRY — ANORGANISCHE UND ANALYTISCHE CHEMIE — НЕОРГАНИЧЕСКАЯ И АНАЛИТИЧЕСКАЯ ХИМИЯ

MÜLLER, L.: The Adsorption of Uranium Hexafluoride, I 1

VÉRTES, A., BURGER, K., TARNÓCZI, T., PAPP-MOLNÁR, E., EGYED, C. L.: On the Mössbauer Investigation and Magnetic Behaviour of Iron(III) Diethyldithiocarbamate (Short communication) 15

VÉRTES, A., TARNÓCZI, T., EGYED, C. L., PAPP-MOLNÁR, E., BURGER, K.: On the Mössbauer Investigation and Magnetic Behaviour of a Few Iron(II) complexes (Short communication) 19

PHYSICAL CHEMISTRY — PHYSIKALISCHE CHEMIE — ФИЗИЧЕСКАЯ ХИМИЯ

FEJES, P., BEYER, H.: Anwendungsmöglichkeiten mathematischer Verfahren zur Bestimmung von Geschwindigkeitskonstanten komplexer, heterogen-katalytischer Prozesse unter Benutzung von elektronischen Rechenmaschinen, II 23

ILLÉS, V.: The Pyrolysis of Gaseous Hydrocarbons, I. Kinetics of the Thermal Decomposition of *n*-Butane 35

SIMON, F.: Investigation of the Molecular Weight Distribution of Polyalkylmethacrylates by Adsorption Chromatography 57

BÁLINT-AMBRÓ, I.: The Dissociation of Varion CH Ion Exchange Resin 67

NEMES, L.: Harmonic Force Field Refinement Calculations for Polyatomic Molecules, III. Normal Coordinate Analysis of the e'' Species of Cyclopropane 75

CYVIN, S. J., VIZI, B.: Mean Amplitudes of Vibration for Diborane and Deuterodiborane 85

VIZI, B., CYVIN, S. J.: Tentatively Standardized Symmetry Coordinates of Polyatomic Molecules, VIII 91

ORGANIC CHEMISTRY — ORGANISCHE CHEMIE — ОРГАНИЧЕСКАЯ ХИМИЯ

MÜLLER, A., KÖRMENDY, K., RUFF, F., SOHÁR, P., VAJDA, M.: Infrared Spectroscopic Study of the Structure of 1-Hydroxyanthraquinone-9-Monoimines 99

MÜLLER, A., KÖRMENDY, K., RUFF, F., VAJDA, M.: Ultraviolet Spectroscopic Investigetion of Some l-Hydroxyanthraquinone-9-monoimines 109

CSŰRÖS, Z., DEÁK GY., HARASZTHY-PAPP, M., HOFFMANN, I.: Reactions Catalyzed by Strong Acids in Non-Aqueous Media, II 119

MOLNÁR, A., BARTÓK, M., KOVÁCS, K.: The Chemistry of 1,3-Bifunctional Compounds, II. Study of the Decomposition of the Quaternary Salts of 1,3-Aminoalcohols 133

ZSADON, B.: HUBAY, R.: On the Alkaloids of Amsonia tabernaemontana Walt. Cultivated in Hungary (Preliminary communication) 157

KISFALUDY, L., PATTHY, A., LŐW, M.: A Beta-elimination Reaction between Cysteine Derivatives Containing Free SH Group and Dicyclohexylcarbodiimide (Short communication) 159

BOGNÁR, R., MAKLEIT, S., MILE, T.: Conversions of Tosyl and Mesyl Derivatives of the Morphine Group. Synthesis of Acetylmercapto and Mercapto Derivatives. (Preliminary communication) 161

MEDZIHRADSZKY, K., BAJUSZ, S., S.-VARGHA, H., und LÁNG, ZS.: Synthese des biologisch aktiven Fragments des β-lipotropen Hormons (Vorläufige Mitteilung) 165

Printed in Hungary

A kiadásért felel az Akadémiai Kiadó igazgatója — Műszaki szerkesztő: Farkas Sándor

A kézirat nyomdába érkezett: 1968. X. 8. — Terjedelem: 15 (A/5) ív, 75 ábra

69.66414 Akadémiai Nyomda, Budapest — Felelős vezető: Bernát György

ACTA CHIMICA

ТОМ 59 — ВЫП 1

РЕЗЮМЕ

Изучение адсорбции шестифтористого урана, I

Л. МЮЛЛЕР

Настоящая серия сообщений посвящена изучению исследованиям по диффузии и адсорбции UF_6.

В первом сообщении рассматриваются вопросы выбора адсорбентов, вопросы измерения адсорбционных равновесий и их разрешение, а также приводятся экспериментальные данные по измерению фазовых равновесий систем UF_6-адсорбент и их оценка.

После краткого обзора литературы описывается технология изготовления выбранных на основе предварительных опытов адсорбентов, из пластмассовой пены или металлов, а также приводятся основные параметры адсорбционных исследований. Рассматриваются технические вопросы измерения рановесий систем UF_6-адсорбент. Описывается радиометрическая установка для определения адсорбционных изотерм. Приводятся обратимые изотермы, снятые в интервале температур 20—100° С, которые формально оцениваются с точки зрения классических теорий адсорбции.

Применение электронных счетных машин для определния констант скоростей сложных гетерогенных каталитических процессов, II.

Принцип метода градиента и его использование для оценки данных кинетических исследований

П. ФЕЙЕШ и Г. БЕЙЕР

Приводится краткое описание теоретических основ метода градиента, с особым вниманием к выбору функции для погрешности и целевой функции. Далее, на примере гипотетической модельной реакции типа $A \rightleftharpoons B$, авторами демонстрируется применение этого метода для определения констант скоростей каталитических процессов и других параметров, не поддающихся экспериментальному определению (как напр., покрытие поверхности, число активных центров и т. д.) и в тех случаях, когда другие методы, как напр., метод наименьших квадратов, даже принципиально не пригодны. Обсуждается вопрос однозначности «оптимальных» параметров, обеспечивающих наилучшее согласие между измеряемыми и расчетными кривыми конверсии. О возможностях данного метода можно судить по расчету, произведенному для определения двух (пока) неизвестных параметров для случая вышеупомянутой модельной реакции и изомеризации норм. бутена.

Пиролиз углеводородных газов, I. Кинетика термического разложения н.-бутана

В. ИЛЛЕШ

Кинетика термического разложения н.-бутана изучалась в проточном трубчатом реакторе при общем давлении 1 атм. и в интервале температур от 600 до 820° С. Описывается экспериментальная установка и метод измерений.

Было установлено, что экспансия в зависимости от конверсии — в интервале температур и времени реакции, применяемых в промышленных реактора пиролиза — характеризуется «одной кривой», не зависящей от температуры. На основе экспансии был

разработан метод расчета истинного времени реакции и определения фактора, заменяющего отношение с техиометрических коэффициентов в уравнении скорости и зависящего от конверсии. На основе этого метода были получены кинетические уравнения, в зависимости от кажущегося и истинного временей реакции, пригодны для расчета констант скоростей и кривых конверсии. Было установлено, что общая скорость разложения н.-бутана не описывается однозначно уравнением скорости первого порядка.

Для описания кривых конверсии было разработано два метода. Согласно первому методу отклонение от кинетики первого порядка принимается во внимание с помощью эмпирической постоянной, учитывающей тормозящее влияние продукта реакции. Согласно второму методу, учитывалось влияние температуры на порядок реакции. Оба метода оказались пригодными для описания общей-скорости разложения н.-бутана.

Изучение распределения по молекулярным весам полиалкилметакрилатов с помощью адсорбционной хроматографии

Ф. ШИМОН

Автором был разработан метод адсорбционной хроматографии для изучения распределения по молекулярным весам полимерных добавок к смазочным маслам.

Отделение полимера от масла-растворителя и фракционирование его по молекулярным весам проводилось в две ступени на силикагельном адсорбенте.

Данный метод может быть использован, как в научных исследованиях, так и в промышленности для исследований квалифицирования.

Данные по диссоциации искусственной ионообменной смолы Varion CH

И. БАЛИНТ-АМБРО

Проводились ик-спектроскопические исследования диссоциационных свойств искусственной ионообменной смолы VARION CH. Из фотометрических спектров смол с формами Na и H и на основе положения полос антисимметричных валентных колебаний карбонильных групп определялись ионные формы, участвующие при данных экспериментальных условиях в диссоциационном равновесии, наступающем при увлажнении воздушно-сухих смол.

Уточненный расчет гармонического поля для многоатомных молекул, III

Анализ нормальных колебаний циклопропана, тина e″

Л. НЕМЕШ

Настоящая работа посвящана расчету молекулярного силового поля циклопропана, типа e″, с помощью тех констант Кориолиса ζ, которые были определены Матаи и сотр. на основе контурного анализа полос спектра комбинационного рассеивания газообразного C_3H_6. Было установлено, что среди двух предложенных этими авторами возможных величин для ζ значение —0,86 кажется вполне приемлемым, в то время как значение —0,29 должно отбросить. Было также установлено, что, как форма колебаний, так и элементы силового поля очень чувствительны к значению ζ. Приводятся константы Кориолиса, рассчитанные для молекулы C_3D_6.

Средние амплитуды колебаний диборана и дейтеродиборана

С. И. СИВИН и Б. ВИЗИ

Проводился нормально-координатный анализ изотопных дибораноп. Рассчитанное гармоническое силовое поле использовалось для расчета средних амплитуд колебаний для некоторых изотопов диборана. Эти результаты сравнивались с величинами средних амплитуд, полученными методом электронной диффракции. Указываются некоторые значительные расхождения.

Пробная стандартизация координат симметрии многоатомных молекул, VIII

Модели тина диборана, циклопропана и циклогексана

Б. ВИЗИ и С. И. СИВИН

Координаты симметрии молекулярных колебаний специфированы для следующих моделей: 1) Мостиковая модель $X_2Y_2Z_4$ (симметрия D_{2h}) типа диборана, 2) Модель с тригональной симметрией $(XV_2)_3$ (симметрия D_{3h}) типа циклопропана и 3) Модель неплоских колец $X_6Y_6Z_6$ (симметрия D_{3d}) типа циклогексана.

Изучение структуры 1-окси-антрахинон-9-моноимина с помощью ик-спектроскопии

А. МЮЛЛЕР†, К. КЁРМЕНДИ, Ф. РУФФ, П. ШОХАР и М. ВАЙДА

С целью определения структуры соединений, образующихся под влиянием спиртового раствора аммиака на гидрокси- и алкокси-замещенные антрахинона, проводились ик-спектроскопические исследования. На основе ассигнации полос поглощения было установлено, что карбонильная группа антрахинонного кольца, находящаяся в положении 9, замещается в течение реакции на иминогруппу. Из исследований полос OH, NH и C = O была определена структура водородных связей в иминосоединениях. Предположенная структура иминов подтверждалась также ик- и ямр-спектрами их ацил-производных.

Изучение 1-окси-антрахинон-9-моноиминов с помощью уф-спектроскопии

А. МЮЛЛЕР†, К. КЁРМЕНДИ, Ф. РУФФ и М. ВАЙДА

Проводились уф-спектроскопические исследования для изучения структуры и переходов электронов в случае соединений типа 1-гидрокси-антрахинон-9-моноимин. На основе изучения влияния растворителя было установлено, что полоса поглощения этих соединений при 520 нм относится к $n \rightarrow \pi^*$, а при 400 нм к переходу внутримолекулярного переноса заряда. Изменения интенсивностей полос под влиянием растворителя объяснялись на основе взаимодействия заместителей с растворителем.

Изучение реакций, катализированных сильми кислотами, в неводных средах, II

Взаимодействие ароматических альдегидов с арил-ацетонитрилами, катализированное трехфтористым бором или серной кислотой, приводящее к образованию арилиден-бис (арилацетамида)

Э. ЧЮРЁШ, ДЬ. ДЕАК, М. ХАРАСТИ-ПАПП и И. ГОФФМАНН

При взаимодействии ароматических альдегидов с бензилцианидом или с его замещенными в кольце производными в среде уксусной кислоты, в присутствии трехфтористого бора или серной кислоты были получены бензилиден-бис-фенилацетамид и его 17 новых замещенных производных. Было установлено, что кислотно-амидная группа образуется не в процессе обработки, а непосредственно в результате реакции, в то время как органическая кислота превращается в ангидрид кислоты. С точки зрения реакции количество катализатора обладает оптимумом, при превышении которого преобладает гидратация бензилцианида в фенилацетамид.

Химия 1,3-бифункциональных соединений, II

Изучение разложения четвертичных солей 1,3-аминоспиртов

А. МОЛНАР, М. БАРТОК и К. КОВАЧ

В ходе изучения химии 1,3-бифункциональных соединений исследовалось разложение четвертичных солей 1,3-аминоспиртов в присутствии щелочей. В исследованных соединениях две функциональные группы связаны с углеродными атомами различных порядков замещенности: иодистые 3-гидроксибутил-триметиламмоний (I), -4-гидроксибутил-2-триметиламмоний (II), -(3-гидрокси-3-метил)бутил-триметиламмоний (III) и -(2-гидрокси-2-метил)амил-триметиламмоний (IV). Изучались направления разложения этих четырех соединений и общая скорость процессов. Основными направлениями этих реакций являются следующие: элиминация Гофманна, деметилирование, фрагментирование, циклизация и 1,3-перегруппировка. В результате этих процессов — степень протекания которых зависит от строения исходного соединения — образуются ненасыщенные спирты, аминоспирты и их метиловые эфиры, олефины и оксетаны, а также оксосоединения. С увеличением замещенности углеродного атома, содержащего аммонийную группу, увеличивается степень элиминации Гофманна и фрагментации, а совокупная мера деметилирования, циклизации и перегруппировки уменьшается. Скорость разложения четырех соединений изменяется в следующем порядке: $IV > II > I > III$. На основе экспериментальных данных были сделаны заключения о механизме протекающих процессов.

The Acta Chimica publish papers on chemistry in English, German, French and Russian.

The Acta Chimica appear in volumes consisting of four parts of varying size, 4 volumes being published a year.

Manuscripts should be addressed to

Acta Chimica
Budapest 112/91 Műegyetem

Correspondence with the editors should be sent to the same address.

The rate of subscription is 165 forints a volume. Orders may be placed with "*Kultúra*" Foreign Trade Company for Books and Newspapers (Budapest I., Fő utca 32. Account No. 43-790-057-181) or with representatives abroad.

Les Acta Chimica paraissent en français, allemand, anglais et russe et publient des mémoires du domaine des sciences chimiques.

Les Acta Chimica sont publiés sous forme de fascicules. Quatre fascicules seront réunis en un volume (4 volumes par an).

On est prié d'envoyer les manuscrits destinés à la rédaction à l'adresse suivante:

Acta Chimica
Budapest 112/91 Műegyetem

Toute correspondance doit être envoyée à cette même adresse.

Le prix de l'abonnement est de 165 forints par volume.

On peut s'abonner à l'Entreprise pour le Commerce Extérieur de Livres et Journaux «*Kultúra*» (Budapest I., Fő utca 32. Compte-courant No. 43-790-057-181) ou à l'étranger chez tous les représentants ou dépositaires.

«*Acta Chimica*» издают трактаты из области химической науки на русском, французском, английском и немецком языках.

«*Acta Chimica*» выходят отдельными выпусками разного объема. 4 выпуска составляют один том. 4 тома публикуются в год.

Предназначенные для публикации рукописи следует направлять по адресу:

Acta Chimica
Budapest 112/91 Műegyetem

По этому же адресу направлять всякую корреспонденцию для редакции.

Подписная цена «*Acta Chimica*» — 165 форинтов за том. Заказы принимает предприятие по внешней торговле книг и газет «*Kultúra*» (Budapest I., Fő utca 32. Текущий счет № 43-790-057-181) или его заграничные представительства и уполномоченные.

66,— Ft

Reviews of the Hungarian Academy of Sciences are obtainable at the following addresses:

ALBANIA
Ndermarja Shtetnore e Botimeve
Tirana

AUSTRALIA
A. Keessing
Box 4886, GPO
Sydney

AUSTRIA
Globus Buchvertrieb
Salzgries 16
Wien I

BELGIUM
Office International de Librairie
30, Avenue Marnix
Bruxelles 5
Du Monde Entier
5, Place St. Jean
Bruxelles

BULGARIA
Raznoiznos
1, Tzar Assen
Sofia

CANADA
Pannonia Books
2. Spadina Road
Toronto 4, Ont.

CHINA
Waiwen Shudian
Peking
P. O. B. 88

CZECHOSLOVAKIA
Artia
Ve Smečkách 30
Praha 2
Poštovná Novinová Služba
Dovoz tisku
Vinohradská 46
Praha 2
Mad'arská Kultura
Václavské nám. 2
Praha I
Poštová Novinová Služba
Dovoz tlače
Leningradská 14
Bratislava

DENMARK
Ejnar Munksgaard
Nörregade 6
Copenhagen

FINLAND
Akateeminen Kirjkauppa
Keskuskatu 2
Helsinki

FRANCE
Office International de Documentation et Librairie
48, rue Gay Lussac
Paris 5

GERMAN DEMOCRATIC REPUBLIC
Deutscher Buch-Export und Import
Leninstraße 16
Leipzig 701
Zeitungsvertriebsamt
Fruchtstrasse 3—4
1004 Berlin

GERMAN FEDERAL REPUBLIC
Kunst und Wissen
Erich Bieber
Postfach 46
7 Stuttgart S.

GREAT BRITAIN
Collet's Holdings Ltd.
Dennington Estate
London Rd.
Wellingborough, Northants.
Robert Maxwell and Co. Ltd.
Waynflete Bldg. The Plain
Oxford

HOLLAND
Swetz and Zeitlinger
Keizersgracht 471—487
Amsterdam C
Martinus Nijhof
Lange Voorhout 9
The Hague

INDIA
Current Technical Literature
Co. Private Ltd.
India House OPP
GPO Post Box 1374
Bombay I

ITALY
Santo Vanasia
Via M. Macchi 71
Milano
Libreria Commissionaria Sansoni
Via La Marmora 45
Firenze

JAPAN
Nauka Ltd.
92, Ikebukur O-Higashi 1-chome
Toshima-ku
Tokyo
Maruzen and Co. Ltd.
P. O. Box 605
Tokyo-Central
Far Eastern Booksellers
Kanda P. O. Box 72
Tokyo

KOREA
Chulpanmul
Phenjan

NORWAY
Johan Grundt Tanum
Karl Johansgatan 43
Oslo

POLAND
Ruch
ul. Wronia 23
Warszawa

ROUMANIA
Cartimex
Str. Aristide Briand 14—18
București

SOVIET UNION
Mezhdunarodnaya Kniga
Moscow G—200

SWEDEN
Almquist and Wiksell
Gamla Brogatan 26
Stockholm

USA
Stechert Hafner Inc.
31, East 10th Street
New York, N. Y. 10003
Walter J. Johnson
111, Fifth Avenue
New York, N. Y. 10003

VIETNAM
Xunhasaba
19, Tran Quoc Toan
Hanoi

YUGOSLAVIA
Forum
Vojvode Mišića broj 1
Novi Sad
Jugoslovenska Knjiga
Terazije 27
Beograd

19. II. 1969 Index: 26.007

ACTA CHIMICA

ACADEMIAE SCIENTIARUM HUNGARICAE

ADIUVANTIBUS

L. ERDEY, K. POLINSZKY, G. SCHAY

AC

R. BOGNÁR, GY. BRUCKNER, Z. CSŰRÖS, T. ERDEY-GRÚZ, Z. FÖLDI, M. FREUND, Á. GERECS, GY. HARDY, J. HOLLÓ, M. KORACH, F. MÁRTA, F. NAGY, E. PUNGOR, Z. SZABÓ, P. TÉTÉNYI, L. VARGHA, K. VAS

REDIGIT

B. LENGYEL

TOMUS 59 FASCICULUS 2

AKADÉMIAI KIADÓ, BUDAPEST

1969

ACTA CHIM. ACAD. SCI. HUNG.

ACTA CHIMICA

A MAGYAR TUDOMÁNYOS AKADÉMIA KÉMIAI TUDOMÁNYOK OSZTÁLYÁNAK IDEGEN NYELVŰ KÖZLEMÉNYEI

SZERKESZTI

LENGYEL BÉLA

TECHNIKAI SZERKESZTŐK

DEÁK GYULA és HARASZTHY-PAPP MELINDA

Az Acta Chimica német, angol, francia és orosz nyelven közöl értekezéseket a kémiai tudományok köréből.

Az Acta Chimica változó terjedelmű füzetekben jelenik meg, egy-egy kötet négy füzetből áll. Évente átlag négy kötet jelenik meg.

A közlésre szánt kéziratok a szerkesztőség címére (Budapest 112/91 Műegyetem) küldendők.

Ugyanerre a címre küldendő minden szerkesztőségi levelezés. A szerkesztőség kéziratokat nem ad vissza.

Az Acta Chimica előfizetési ára kötetenként belföldre 120 Ft, külföldre 165 Ft. Megrendelhető a belföld számára az „Akadémiai Kiadó"-nál (Budapest V., Alkotmány utca 21. Bankszámla 05-915-111-46), a külföld számára pedig a „Kultúra" Könyv- és Hírlap Külkereskedelmi Vállalatnál (Budapest I., Fő utca 32. Bankszámla: 43-790-057-181) vagy annak külföldi képviseleteinél és bizományosainál.

Die Acta Chimica veröffentlichen Abhandlungen aus dem Bereiche der chemischen Wissenschaften in deutscher, englischer, französischer und russischer Sprache.

Die Acta Chimica erscheinen in Heften wechselnden Umfanges. Vier Hefte bilden einen Band. Jährlich erscheinen 4 Bände.

Die zur Veröffentlichung bestimmten Manuskripte sind an folgende Adresse zu senden:

Acta Chimica
Budapest 112/91 Műegyetem

An die gleiche Anschrift ist auch jede für die Redaktion bestimmte Korrespondenz zu richten.

Abonnementspreis pro Band: 165 Forint. Bestellbar bei dem Buch- und Zeitungs-Außenhandels-Unternehmen »*Kultúra*« (Budapest I., Fő utca 32. Bankkonto No. 43-790-057-181) oder bei seinen Auslandsvertretungen und Kommissionären.

Acta Chimica Academiae Scientiarum Hungaricae, Tomus 59 (2), pp. 171—180 (1969)

DETERMINATION OF TANTALUM IN ROCKS BY NEUTRON ACTIVATION ANALYSIS

I. VADOS, M. MOHAI and E. UPOR

(Mecsek Ore Mining Enterprise, Pécs)

Received September 5, 1967

A method has been developed for the neutron activation analysis of tantalum in rocks. On the basis of the nuclear data, the 68 keV photo-peak of Ta^{182} has been selected. In order to compare the interference by individual elements, a characteristic number has been introduced which is based on the Clark value and nuclear data, with reference to a rock sample of average composition. The separation procedure consists of fusion with alkali, followed by leaching with water. The precipitated hydroxide is then dissolved, and the tantalum extracted as thiocyanate with methyl isobutyl ketone. The loss in tantalum is very low, therefore, its determination is unnecessary. The method has been successfully applied to the analysis of tungsten ores. The time required for an analysis is 30 minutes.

Introduction

The photometric determination of small amounts of tantalum is usually performed by means of Crystal Violet [1], Rhodamine 6-Zs [2], or fluorone derivatives [3, 4]. The sensitivity of these methods is 10^{-2}—10^{-4}%. Since the Clark value for tantalum is 10^{-4}—10^{-6}%, the above methods are not suitable for control purposes in geochemical studies [5]. Only methods based on neutron activation analysis [6—15] can be considered satisfactory. As a result of differing requirements, even these methods cannot all be regarded as highly sensitive. A sensitivity of 10^{-8} % for the determination of tantalum in quarz has been reported by GLEIT [8]. ATKINS [15], and SZABÓ *et al.* [9] determined tantalum in rocks with a sensitivity of 10^{-6} %. The rock samples are subjected to neutron activation after chemical separation in some of the methods [11, 13, 14]. In this case, the losses during chemical separation are not determined. In the other methods, the tantalum yields are as follows: 17—44% [8], 40—60% [15], 54—83% [10] and 90—95% [9]. The main step in chemical separation is ion exchange [6—8], or extraction with an oxygen-containing solvent [9, 10, 13, 14, 15], usually in hydrogen fluoride medium. The γ-spectrometric determination without separation is impossible when the samples contain small amounts of tantalum.

γ-spectrometry is widely used for the determination of the tantalum concentration [16—19, etc.], but total activity measurements may also be used if they can be combined with good radiochemical purification [20].

The γ-spectrometric analysis can be carried out using the area under the photo-peak, the number of counts corresponding to the photo-peak, or the result of measurements with relatively large energy-window [21]. The 68 keV photo-peak is usually selected for the determination of Ta^{182} [9, 10, 11, 13], but the spectral range between 1.12—1.23 MeV is also suitable [6].

Selection of the experimental method

Characteristic data for Ta^{182} are shown in Table I. It can be concluded from the Table that the measurement of β-activity is not practical owing to its relatively low energy. In spite of this, β-activity measurement has been used for the determination of tantalum in some cases [27].

Table I

Nuclear data for Ta^{182}

Half-life days	β-energy (MeV)	Yield (%)	γ-energy (MeV)	Yield (%)
112	0.514	48.4	0.068	30.0
	0.260	51.6	0.100	13.2
			0.114	2.9
			0.152	11.8
			0.179	5.4
			0.222	11.9
			1.122	33.9
			1.189	15.1
			1.222	32.1
			1.231	16.9

Both in the low and high energy ranges of the γ-radiation, there are photo-peaks that can be used in the measurements.

Measurements in the low-energy range usually give higher sensitivity with a given apparatus. At the same time, the interfering effects are stronger when the analysis is performed at such low energies.

Taking into account the possibilities of chemical separation and the conditions of the measurement, the analyses have been performed at the 68 keV photo-peak.

The isotopes which have photo-peaks in the energy range 48—88 keV are collected in Table II. In view of the time that elapsed between activation and measurement, isotopes with shorter half-lives have been disregarded. The activity values refer to 1 day of activation and 20 days of cooling.

The values in the last column of the Table give a direct possibility to compare the interfering effects of different elements, and to evaluate the requirements in respect of the chemical separation. (There is considerable disagreement in the literature data. As a precaution, the less favourable data have been used in all calculations. The γ-spectra of activated rock samples show that the safety was greater than necessary, since the Ta^{182} peaks were detected in all cases, but those of the interfering elements did not appear in a single case.)

It can be seen that the determination of tantalum at 68 keV may suffer, above all, from interference by Ho^{166}, Yb^{169}, Tm^{170}, Hf^{175}, Hf^{181}, Lu^{177}, Tb^{160}, and Eu^{155}.

The nuclear processes W^{182} (n, p)Ta^{182}, and Re^{185}(n, α)Ta^{182} may, in principle, be conflicting but they can be disregarded due to their low cross section [16, 22].

The measurements have been performed with a 100-channel amplitude analyzer, Type 1363 D. The detector was a 2×2 NaI(Tl) crystal, Type FH 421 A5. The energy resolution of the instruments with respect to the 661 keV line of Cs^{137} was approximately 7%.

In order to decrease interference effects usually present in the low-energy range, as well as to ensure homogeneity and identical geometry, and to simplify the chemical procedure, solution samples were used throughout the measurements.

Sensitivity and precision of the analyses

The minimum observable number of counts was used to establish the minimum concentration of Ta that can be determined. This is given by the following expression [6]:

$$\Delta N = k\sqrt{\frac{N_h}{t_h} + \sigma^2}\,(\text{cpm})$$

where N_h — the background,
t_h — time of the measurement,
σ — the mean statistical error of the background,
k — a constant (the probability is 68.26% if $k = 1$; 95.45% if $k = 2$; and 99.73% if $k = 3$).

In the present case:

$N_h = 80$ cpm
$t_h = 10$ min.
$\sigma = \pm 2.82$ cpm
$k = 3$

Therefore, the limit of observation is

$N = \pm 12$ cpm

Acta Chim. Acad. Sci. Hung. 59, 1969

Table II

1.	2.	3.	4.	5.	6.	7.	8.	9.	10.
Target nucleus	Abundance (%)	Cross section (barn)	Clark value (ppm)	Radioisotope	Half-life (days)	Energy (keV)	Yield (%)	Total activity (tpsec)	Activity of photo-peak
Ta-181	100	1.9*	0.4	Ta-182	112	68	30	149	45
Ho-165	100	6.0	1.5	Ho-166	30 y	80	14.3	195	28
Gd-160	21.9	0.8	1.6	Tb-161	6.88	49	6.8	135	9
						57	8.7	135	12
						75	12.2	135	16
Yb-168	0.14	1×10^{4}	4	Yb-169	32	63	42.8	28 400	12 180
Tm-169	100	1.18×10^{2}	0.3	Tm-170	127	51	3.12	6160	192
Hf-174	0.19	1.5×10^{3}	3.9	Hf-175	70	52	4.8	374	18
Pd-102	0.96	4.8	10^{-3}	Pd-103	17	53	2.1	0.5	0.01
Ru-102	31.5	1.44	5×10^{-3}	Ru-103	41	55	0.45	0.3	0.001
Hf-180	35.25	13	3.9	Hf-181	46	56	6.2	620	38
W-180	0.135	30	1.9	W-181	140	56	0.02	10	0.002
Te-126	18.71	0.09	0.02	Te-127	105	57	0.16	0.06	1×10^{-4}
Ba-132	0.097	7	500	Ba-133	7.7 y	57	5.2	0.2	0.01
						81	35.5		0.07
Dy-158	0.09	96	7.2	Dy-159	136	58	9.0	140	13
Os-184	0.018	200	0.001	Os-185	95	59	?	0.007	—
Sm-144	3.16	2	10	Sm-145	360	61	12.9	50	6
Sn-118	24.1	0.01	1.5	Sn-119	275	65	0.02	0.43	8×10^{-5}
Ir-191	38.5	700	0.001	Ir-192	74.4	65	0.02	70	0.014
Se-74	0.87	26	0.05	Se-75	127	66	1.0	4	0.04
Gd-152	0.2	125	10	Gd-153	236	70	5.35	248	13
Hg-202	29.8	3.8	0.05	Hg-203	45.8	70	0.02	18	0.0036
Lu-176	2.6	4000	1.2	Lu-177	6.75	72	0.63	5500	35
Tb-159	100	44	1.6	Tb-160	73	87	14.6	22 000	3200
Sm-154	22.53	5.5	1.6	Eu-155	1.7 y	86	39.8	75	30

* The values reported in the literature are 21 [26] and 19 [27, 28] too.

The following expression can be used to calculate the precision of the radiometric measurements:

$$\delta = \frac{\sqrt{\frac{N_m + N_h}{t_m} + \frac{N_h}{t_h}}}{N_m} \times 100\,(\%)$$

where N_m — the activity of the sample (cpm),
N_h — the activity of the background (cpm),
t_m — the time of the measurement with the sample (min),
t_h — the time of the background measurement (min),
δ — the relative error (%).

Under the conditions given above, the reliability at the lower limit of sensitivity is $\pm 35\%$.

The minimum detectable amount of tantalum in the case of the above activity is calculated from the following expression [28]:

$$m_0 = \frac{D_{\min} A\, e^{\frac{0.693 t'}{T}}}{\sigma \Phi f N_A \left(1 - e - \frac{0.693\, t}{T}\right)}\,(g)$$

and is equal to

$$T_{a_{\min}} = 6 \cdot 10^{-10}\, g$$

Explanation to Table II

"Abundance" is the natural abundance.
The total activity is calculated from the expression:

$$D = \sigma \Phi \frac{m f N_A}{A} (1 - e^{-\frac{0.639 t}{T}})\, e^{-\frac{0.639 t'}{T}}$$

where σ — cross-section
Φ — neutron flux ($1 \cdot 10^{13}$ n/cm²sec)
m — amount of the given element (in the present case the Clark value was taken into account)
f — fraction of natural abundance
N_A — Avogadro number (6×10^{23})
A — mass number of the target nucleus
t — time of activation
T — half-life
t' — time of cooling
The "activity of photo-peak" is the product of "total activity" and the "yield"/100.

Chemical separation of tantalum

According to the data in Table II, only holmium, ytterbium, thullium, lutetium, terbium, europium, gadolinium, dysprosium, samarium, and hafnium may interfere with the determination of tantalum in a rock sample of average composition.

Table III

Extraction of tantalum thiocyanate with methyl isobutyl ketone

Total volume of the aqueous phase: 30 ml; 8 ml of 3% tartaric acid + 6 ml of 15% $SnCl_2$ + x ml of HCl solution + y ml of KCNS solution. Ta^{182} with Nb-carrier. Extracted with 5 ml of methyl isobutyl ketone.

[HCl] (mole/l)	[KCNS] (mole/l)	Extraction (%)
3.1	0.2—0.3	70—75
5.2	0.2—0.3	75—80
1.5	0.6	98
4.0	0.6	98

Table IV

Extraction of the ions interfering with the measurement of the Ta^{182} γ-activity at 68 keV

Under the conditions given in Table III from a medium containing 4.0 mole/l HCl and 0.6 mole/l KCNS

Ion	Method of determination	Extraction (%)
Hf^{4+}	Labelled with Hf^{181}	<2
Lu^{3+}	Lu^{176}	<1
Tb^{3+}	Tb^{160}	<1
Sm^{3+}	Sm^{153}	<1
Yb^{3+}	Yb^{169}	<1
Sc^{3+}	Sc^{46}	0.9

The chemical similarity between niobium and tantalum suggest that successful separation could be achieved with the procedure used in the determination of small amounts of niobium [23]. According to this very simple method, the rock sample is fused with alkali, resulting in conversion to hydroxides which are then dissolved in tartaric acid. Niobium is extracted as thiocyanate, with methyl isobutyl ketone (hexone). It was expected that, similarly to niobium, it would be possible to extract tantalum quantitatively, thus determination of the yield, commonly performed with activation analyses, could

be avoided. It was necessary to carry out detailed studies, since the extraction procedure with niobium was well known. The results are shown in Table III.

As far as the requirements of trace analysis are concerned, at a KCNS concentration of 0.6 mole/l the extraction can be regarded as quantitative, and no changes are observed when the acid concentration is varied over a rather wide range.

Under these conditions, the extraction of the interfering elements resulted in complete separation from tantalum (Table IV).

The following comments are pertinent to the results and the planned scheme of analysis:

(1) The residue after fusion with alkali is leached with hot distilled water. Tantalum will be found quantitatively in the precipitate, therefore it is not necessary to determine the yield of tantalum separately.

(2) Scandium is not present among the elements that can potentially interfere according to Table I. However, it has been mentioned [24] that Sc^{46} has a characteristic γ-peak at 68 keV which is not described in the literature. (The existence of this peak is doubtless, since its height is comparable to those of peaks used in the determination of Sc^{46} even if the activated standard is prepared from reagent grade $Sc(NO_3)_3$. The fact that this peak originates from scandium has also been demonstrated by extraction with 0.01 mole/l HDBP from a hydrochloric acid–oxalic acid medium. The spectrum of the organic phase was identical to the original, therefore, the peak was not due to rare earth impurities which cannot be extracted from such a medium.)

Interference from scandium can, however, be completely eliminated by extracting the tantalum with thiocyanate.

(3) Similarly, good separation from hafnium and the rare earths has been obtained. In spite of this, it is advisable to wash the organic phase with the original aqueous solution. This does not lead to any loss of tantalum, and the extraction of hafnium and the rare earths will remain below the limit of detection (less than 0.1%).

(4) The methyl isobutyl ketone solution obtained from the rock sample is radiochemically pure. This is demonstrated by the identity of the spectra obtained with activated Ta_2O_5 and the solution (Fig. 1).

(5) The tantalum stock solution cannot be preserved even in the presence of tartaric acid. After a few days of standing irreversible hydrolysis takes place. It was found suitable to use niobium as a carrier to obtain more stable solutions. The application of this principle in the case of ions susceptible to hydrolysis is recommended by BABKO [25].

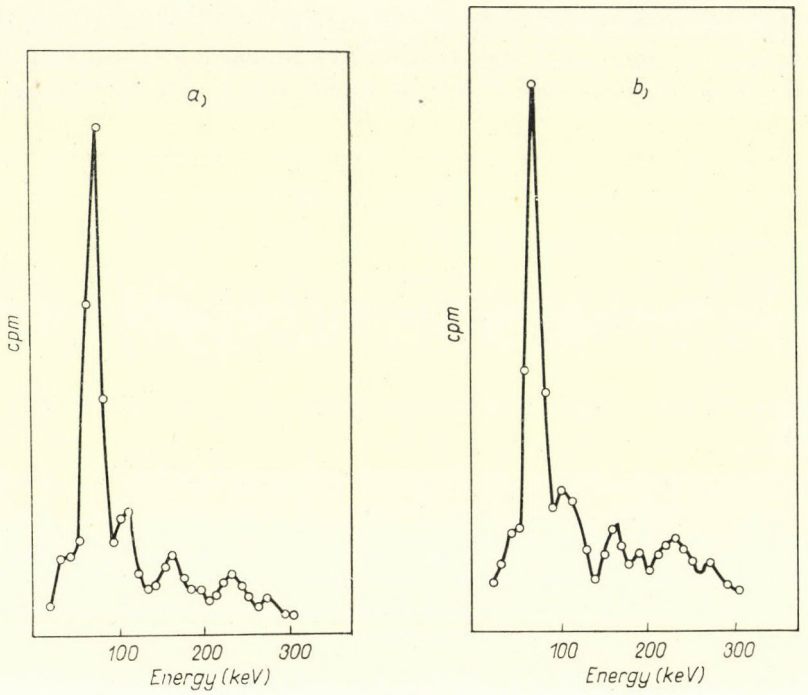


Fig. 1

Determination of small amounts of tantalum

Reagents: Ta_2O_5, G.R. or "Spectroscopic purity"; ("spec pure")
$K_2S_2O_7$ or $KHSO_4$, G.R.;
Nb_2O_5, G.R.;
NaOH, G.R.;
15% and 3% tartaric acid solutions, G. R.;
$SnCl_2$, G.R., 15 g of $SnCl_2 . 2H_2O$ dissolved in 30 ml of conc. HCl and diluted to 100 ml, conc. HCl, G.R.;
Washing solution: 8 ml of 3% tartaric acid + 6 ml of the $SnCl_2$ solution + 8 ml conc. HCl + 3 ml 20% KSCN; methyl isobutyl ketone, G.R.

Description of the procedure

0.2—0.5 g of the powdered rock sample (grain size: —100 μ) is weighed on a precision balance in a quartz vessel with a ground lid. The sample is irradiated for 24 hrs in a nuclear reactor using a neutron flux of 10^{13} n/cm^2. In order to decrease the radioactivity of the sample, the analysis is performed after 3 weeks of cooling.

The sample is transferred to a silver vessel and fused with 5—6 g of solid NaOH using a gas burner. After cooling, the sample is transferred to a beaker with hot water, and heated to boiling temperature. The hydroxide precipitate containing the tantalum is filtered off, washed with hot 1% NaOH, then transferred to a smaller beaker using a small volume of water.

10 ml of 15% tartaric acid solution is added, the solution is heated to 60—80 °C, transferred to a volumetric flask, and diluted to 50 ml with distilled water.

8 ml of the solution is pipetted into a separatory funnel, then 8 ml of 20% KSCN, 6 ml of 15% $SnCl_2$, and 8 ml of conc. HCl are added. After mixing 5 ml of methyl isobutyl ketone is added, and the solution extracted for 1/2 min. After the separation of the phases, the aqueous phase is discarded and then the organic phase washed with 15 ml of the washing solution.

The methyl isobutyl ketone solution containing the Ta^{182} is then poured into the measuring vessel and the radioactivity is determined at 68 keV.

An external standard is prepared together with the sample. Ta_2O_5 is fused with $KHSO_4$ in a platinum crucible, then it is dissolved in tartaric acid so that a 10 μg/ml solution is obtained. 0.5 and 1.0 ml portions of this solution are evaporated to dryness in quartz vials on a water bath, and activated together with the sample. This substance is dissolved in warm, 15% tartaric acid, the solution is diluted to 50 ml, and the γ-activity of a 10-ml sample is measured.

Less than 30 min is required to carry out an analysis.

Comments on the application of the method

Taking into account the nuclear data and the volumes of the solutions used in the analysis, the sensitivity of the method is $3 \cdot 10^{-7}$ %. This is by 2 orders of magnitude lower than the Clark value. It is, therefore. possible to decrease the error of the analysis significantly below the accepted $\pm 35\%$.

The losses of tantalum during the procedure do not exceed 2—3%. The separation from the interfering elements is complete. This makes the error of the analysis less than $\pm 10\%$.

Duplicated analyses have been performed on the standard rock samples prepared by the Berlin Institute of Geology, and the following results have been obtained:

Mudstone (TB)	$1.48 \cdot 10^{-4}\%$, $1.50 \cdot 10^{-4}\%$
Basalt (BM)	$2.04 \cdot 10^{-5}\%$, $2.06 \cdot 10^{-5}\%$
Granite (GM)	$1.51 \cdot 10^{-4}\%$, $1.39 \cdot 10^{-4}\%$.

The results calculated from the 68 keV radioactivity are in full agreement with those obtained from the total γ-activity.

A result is available for comparison for one sample.

The tantalum content of the M-1 sandstone sample was found to be $0.7 \cdot 10^{-4}\%$. With an earlier method [9] the result was $0.51 \cdot 10^{-4}\%$.

The method has been used in the analysis of different ores. The measurements on a tungsten ore (wolframite) are worth mentioning. Since W^{180} interferes in the analysis of Ta^{182}, the former had to be carefully separated. This was accomplished by repeating the precipitation with sodium hydroxide 3 times. The tantalum content of the tungsten ore was found to be $4 \cdot 10^{-2}\%$ in accordance with its higher niobium content (0.20%).

REFERENCES

1. Borovikova, A. L.: Izv. Kazakhst. n. i. in-ta mineral. syrya. 1961. vyp. 6. 196
2. Pavlova, N. N., Blum, I. A.: Zav. Lab. **28,** 1305 (1962)
3. Nazarenko, V. A., Shustova, M. B.: Method khim. analiza mineralnovo syrya. vyp. 5. 54. Gosgeoltekhizdat, Moscow, 1959
4. Gyhansky, V. D., Komusova, B. B.: Izv. Sib. otd. AN. SSSR. No 3. (1) 133—135
5. Rankama, K., Sahama, Th. G.: Geochemistry. Univ. of Chicago Press Chicago, 1950

6. MASTALKA, A.: Chem. listy **59,** 1446 (1965)
7. KRANZ, R., WÖLFLE, R.: Keramische Zeitschrift **17,** 19 (1965)
8. GLEIT, CH. E., BENSON, PH. A., HOLLAND, W. D.: Anal. Chem. **36,** 2067 (1964)
9. SZABÓ, E., ELEK, A., ÖRDÖGH, M., UPOR, E.: Központi Fizikai Kutató Intézet Közleményei **12,** 355 (1964).
10. KIMCHONG, K., MEINKE, W. W.: Anal. Chem. **35,** 2135 (1963)
11. RICQ, J. C., CAPITANT, M., TROLY, G.: C. r. Acad. Sci. **258,** 6486 (1964); Ref. Zh. Khim. 1965. 2 V 539
12. SCHILTZ, J. C., COQUEM, A. C.: Bull. Soc. franç. minéral. et cristallogr. **87,** 156 (1964); Ref. Zh. geol. 1965, 5 V 522.
13. RICQ. J. C., VIDAL, J. P., CAPITANT, M., TROLY, G.: Chim. Analyt. **47,** 77 (1965); Ref. Zh. Khim. 1965. 16 G. 94.
14. MORRIS, D. F. C., OLYA, A.: Talanta **4,** 194 (1960)
15. ATKINS, D. H. F., SMALES, A. A.: Anal. Chim. Acta **22,** 462 (1960)
16. DUGAIN, F., LAVERLOCHÈRE, J.: Anal. Chem. **37,** 998 (1965)
17. YULE, H. P.: Anal. Chem. **37,** 129, (1965)
18. GUIN, V. P., WAGNER, C. D.: Anal. Chem. **32,** 317 (1960)
19. GIRARDI, F., PIETRA, R.: Anal. Chem. **35,** 173 (1963)
20. HALVERSON, G., SHTASEL, A.: Anal. Chem. **33,** 1627 (1961)
21. Siemens Messtechnik, Eg-Berichte. Eg 5, No 14.
22. SCHULZE, W.: Neutronaktivierung als analytisches Hilfsmittel. F. Enke Verlag, Stuttgart, 1962
23. MOHAI, M., UPOR, E.: Magyar Kémiai Folyóirat **72,** 394 (1966)
24. MOHAI, M., UPOR, E., VADOS, I., ELEK, A.: Kőzetekben levő kismennyiségű tantál meghatározása neutronaktivizációs módszerrel. Lecture at the II. Analytical Conference (Dunántúl) Pécs, 1966
25. BABKO, A. K., GRUDCHINA, G. I.: Zav. Lab. **30,** 773, (1964)
26. Polevye jadernye geofizicheskie metody. A.N. SSSR. Izd. Nauka, Moscow, **1966**
27. BOWEN, H. J. M., GIBBONS, D.: Radioactivation Analysis. Clarendon Press Oxford **1963**
28. NAGY, A. GY., SZOKOLYI, L.: Neutronaktiválásos vizsgálatok (in Hungarian). Műszaki Könyvkiadó, Budapest, 1966

István VADOS; Pécs, III. Kőrösi Csoma út 9/b. Hungary
Magda MOHAI; Pécs, III. 39-es dandár út 4. Hungary
Endre UPOR; Pécs, III. 39-es dandár út 3/a. Hungary

Acta Chimica Academiae Scientiarum Hungaricae, Tomus 59 (2), pp. 181—200 (1969)

THE ADSORPTION OF URANIUM HEXAFLUORIDE, II

TRANSPORT PROCESSES IN THE SORPTION OF URANIUM HEXAFLUORIDE

I. MÜLLER and L. FÁY

(Mecsek Ore Mining Enterprise, Pécs and University of Chemical Industries, Veszprém)

Received December 21, 1967

Various diffusion-adsorptions are treated on the basis of the Damköhler's equation. In this concept, adsorption (boiling) is represented by static adsorption kinetics. The present communication discusses the results of adsorption-kinetic investigations.

First, the description of measuring equipment, developed for the investigation of UF_6 adsorber systems is presented, and the results are given. The obtained data show that kinetic equations which involve the condition of a linear isotherm, are unsuitable for the interpretation of the kinetics of interaction between UF_6 and the adsorbent. Therefore, new kinetic equations, under the assumption of a Freundlich-type isotherm have been derived. The resulting performance function is used for the description of the kinetic curves.

Sorption processes will be discussed in this paper on the basis of Damköhler's "continuity equation" [1] as the fundamental correlation. This equation was applied first by DAMKÖHLER for a general description on material transport occurring in operational units.

For an operational sorption unit, the equation of material transport reads as follows:

$$-\frac{\partial C_i}{\partial t} = \operatorname{div}[C_i \overline{V}] - \operatorname{div}(D \operatorname{grad} C_i) \pm \frac{\partial n_i}{\partial t} \tag{1}$$

In gas-solid transport processes the flowing substance is compressible, and there is an appreciable pressure gradient in the operational unit in the direction of convection. Consequently, the flow rate is a function of the local coordinates [2]. In this case, the kinetics of the process are described by Eq. (1) and by the Navier-Stokes equation for the streaming gas, when

$$\overline{V} \operatorname{grad} \overline{V} = -\frac{1}{\varrho} \operatorname{grad} P + \operatorname{div}(\operatorname{grad} \overline{V}) \tag{2}$$

(Eq. (2) is a special form of the "continuity equation" referring to the impulse current.)

The available mathematical apparatus precludes the possibility to find a general solution for the non-linear partial differential equation system

consisting of Eqs (1) and (2). In the determination of the inevitable model-simplifying conditions, the following aspects were taken into account:

(a) The equation describing the adsorption model includes the condition of a possibility of an explicit solution.

(b) The information obtained from the analysis of the solution function must be sufficient for the description of "in naturam" processes.

The general simplifying conditions applied by us were as follows:

1. In the operational unit of material transport, any material stream radial to the direction of the resultant material stream is negligible.

2. The streaming fluid is incompressible.

3. The thermal equilibrium of the system is not affected by transport processes.

On the basis of the above conditions of simplification, the equation describing the operational adsorption unit takes the form

$$-\frac{\partial C_i}{\partial t} = v_x \frac{\partial C_i}{\partial x} - D\frac{\partial^2 C_i}{\partial x^2} \pm \frac{\partial n_g}{\partial t} \tag{3}$$

where x is the coordinate of the preferred direction of material transport.

Let us now define Eq. (3) in words: convection — diffusion — (+) absorption (source) = local change = 0 stationary

$$\neq 0 \text{ unstationary} \tag{4}$$

Relation (4), which is well known from operation theory, establishes a connexion between the various adsorption processes. The possibilities offered by the equation of continuity are exploited when, in the following, the kinetics of transport processes occurring in the operational adsorption units will be investigated both individually and as a whole:

1. *Investigation of absorption (source)*

Static adsorption kinetics, according to the classical nomenclature of adsorption, belong to this group.

This process is described by the following equation:

$$\frac{\partial C}{\partial t} = KD\frac{\partial^2 C}{\partial x^2} + \frac{\partial n^x}{\partial t} \tag{5}$$

Condition:

$$\frac{\partial n^x}{\partial t} = 0 \tag{6}$$

2. *Investigation of stationary diffusion*

The process is described by the equation:

$$\frac{\partial C}{\partial t} = KD\frac{\partial^2 C}{\partial x^2} \tag{7}$$

Condition:

$$\frac{\partial C}{\partial t} = 0 \tag{8}$$

3. *Investigation of diffusion + absorption*

The process is described by the equation

$$\frac{\partial C}{\partial t} = KD\frac{\partial^2 C}{\partial x^2} - K\frac{\partial n}{\partial t} \tag{9}$$

Condition (in the case of a Freundlich isotherm):

$$\frac{\partial n_g}{\partial t} = K\frac{\partial n_g}{\partial C}\cdot\frac{\partial C}{\partial t} = K\bar{k}mC^{m-1}\frac{\partial C}{\partial t} \tag{10}$$

4. *Investigation of diffusion + convection*

The process is described by the equation:

$$\frac{\partial C}{\partial t} = KD\frac{\partial^2 C}{\partial x^2} - Kv_x\frac{\partial C}{\partial x} \tag{11}$$

5. *Diffusion + convection + absorption*

The general equation describing the process is:

$$\frac{\partial C}{\partial t} = -Kv_x\frac{\partial C}{\partial x} + \frac{\partial^2 C}{\partial x^2} + K\frac{\partial n}{\partial t} \tag{12}$$

where K is a constant which is, according to its sense, different in the various part-processes.

Investigation of the kinetics of physical adsorption (absorption source)

The concepts of the course of the sorption process against time have been defined by McBAIN [3] as follows: "Adsorption actually takes place almost instantaneously. The slowing down of the process is explained in each case either by the fact that longer periods are needed for the removal of the heat of sorption developed, or by the fact that the pores of the surface are with difficulty available to the molecules of the adsorbate in question."

It is, however, necessary to complement the original definition of McBAIN by adding that in the case of an activated adsorption, sorption is not an instantaneous, but rather a protracted process [4].

The abundant literature discussing the results of adsorption kinetics is mentioned here only superficially, reference being made to the data listed in the respective monographs [5].

From the aspects of operational theory, the description of adsorption kinetics can actually be reduced to a description of the transient state between the given initial conditions and the formation of the equilibrium state. In this presentation, the physico-chemical information relating to the equilibrium in a closer sense, can be obtained from the equation describing the kinetics of adsorption. It appears from an investigation of the equilibrium of sorption that the kinetical equations derived by presuming a linear equilibrium, which are at present available, are unsuitable for the description of the results of our measurement.

In order to overcome these difficulties, a kinetical equation has been derived for the case of a curved isotherm (which can be characterized by the Freundlich equation), presuming that the mechanism of adsorption is as follows:

1. The formation of adsorption equilibrium is the result of consecutive processes.

2. The approach of the adsorption surface is a process protracted in time, owing to diffusion taking place inside the adsorbent.

3. Binding on the surface, *i.e.* the actual adsorption, is a process faster by several orders of magnitude than diffusion through the pores (condition (6)).

4. The rate deforming diffusion takes place in a sphere.

5. For the description of the dynamical equilibrium, an isotherm equation is available which is valid in every point of the examined domain of pressures.

6. The inert, — pore — diffusion can be characterized as independent of concentration.

The presumed mechanism of adsorption is a greatly idealized form of the real adsorption process.

Equation adsorption kinetics in the case of a linear isotherm

In first approximation, let us examine the case when a linear isotherm is present, *i.e.* when the correlation between the adsorbed phase and the gaseous phase is independent of the concentration [6, 7].

The velocity of the process occurring in a particles of the adsorbent is described by Eq. (5), which reads, in the case of an adsorbent of spheric symmetry, as follows:

$$\frac{\partial C_a}{\partial t} = \frac{D}{r^2} \frac{\partial}{\partial r} \left(r^2 \frac{\partial C_g}{\partial t} \right) . \tag{13}$$

Let us substitute the condition for the linear isotherm; then for C_g, we have:

$$\frac{\partial C_g}{\partial t} = \frac{D}{H} \frac{1}{r^2} \frac{\partial}{\partial r} \left(r^2 \frac{\partial C_g}{\partial r} \right) . \tag{14}$$

The initial and boundary conditions of solving Eq. (14) are:

$$\begin{aligned} &\text{if } t = 0 \text{ and } 0 \leq r < R; && C_g = C(0) \\ &\text{if } 0 \leq t < \infty \text{ and } r = R; && C_g = C_0 \end{aligned}$$

On introducing the variable $u = rC_g$, Eq. (14) can be written as follows:

$$\frac{\partial u}{\partial t} = \frac{D}{H} \frac{\partial^2 u}{\partial r^2} , \tag{15}$$

and the initial conditions will be:

$$\begin{aligned} &\text{if } t \geq 0 \text{ and } r = R; && u = RC_0 \\ &\text{if } t \geq 0 \text{ and } r = 0; && u = 0 \\ &\text{if } t = 0 \text{ and } 0 \leq r < R; && u = rC(0). \end{aligned}$$

No difficulties are encountered in solving Eq. (15). The solution is a function, which, returning to the original variable, is the following:

$$C_g(r;t) = C_0 + \frac{2R}{\pi} [C(0) - C_0] \sum_{n=1}^{\infty} \frac{(-)^{n+1}}{n} \frac{1}{r} \sin \frac{n\pi r}{R} e^{-\frac{n^2\pi^2 D}{R^2 H} t} \tag{16}$$

while the function $C_a\,(r;t)$ reads, following from the conditions of the linear isotherm a:

$$C_a(r;t) = HC_g(r;t) .$$

In the experimental investigation of sorption kinetics, changes in time of the quantity of adsorbate adsorbed in the inside of the adsorbent or presented in gas phase are measured.

Considering equation (16) the total amount of adsorbate present in the inside of an adsorbent of spherical symmetry is calculated from the integral

$$n(t) = (H + 1) \int_0^R 4\pi r^2 C(r;t)\, dr \tag{17}$$

Substituting (16) into equation (17) and performing the required operations, we obtain ($H \gg 1$):

$$n(t) = \frac{4}{3} \pi R^3 H \left[C_0 + [C(0) - C_0] \frac{6}{\pi^2} \sum_{n=1}^{\infty} \frac{1}{n^2} e^{-\frac{n^2 D \pi^2}{R^2 H} t} \right] \tag{18}$$

When $C(0) = 0$, (*i.e.* the adsorption takes place on a surface free of adsorbate) and considering that $n(e) = 4/3\ \pi\ R^3\ HC_0$ is the specific adsorbate amount adsorbed in equilibrium, we obtain:

$$\vartheta = \frac{n(t)}{n(e)} = 1 - \frac{6}{\pi^2} \sum_{n=1} \frac{1}{n^2} e^{-\frac{n^2 D \pi^2}{HR^2} t} \tag{19}$$

Equation (19) described the kinetical curves of sorption with sufficient accuracy in the case of linear isotherms it cannot be used, however, in the case of adsorbent-adsorbate pairs with convex or concave equilibrium isotherms.

Equation of sorption kinetics in the case of Freundlich isotherm

In the knowledge of the adsorption isotherms of the systems uranium hexafluoride-adsorbent, we attempted to evolve an adsorption kinetical which can be characterized by Freundlich isotherms.

Namely, in the case of isotherms of Freundlich type, the substitution

$$C_a = \bar{k} C_g^m \tag{20}$$

is to be introduced into equation (13).

Then

$$\bar{k} \frac{\partial}{\partial t} C_g^m = \frac{D}{r^2} \frac{\partial}{\partial r} \left(r^2 \frac{\partial C_g}{\partial r} \right). \tag{21}$$

On applying variable $u = rC_g$ we obtain:

$$\bar{k} \frac{\partial}{\partial t} \left(\frac{u}{r} \right)^m = \frac{D}{r^2} \frac{\partial}{\partial r} \left(\frac{\partial u}{\partial r} r - u \right) \tag{22}$$

Deriving from (22) we may write:

$$\frac{\partial}{\partial t} u^m = \frac{D}{\bar{k}} r^{m-1} \frac{\partial^2 u}{\partial r^2} \tag{23}$$

The boundary conditions of equation (23) are as follows:

$$\begin{aligned} &\text{if } t = 0 \text{ and } 0 \leq r < R; && C_g = 0 \\ &\text{if } t \geq 0 \text{ and } r = R; && C_g = C_0 \end{aligned}$$

or, introducing variable u:

$$\begin{aligned} &\text{if } t = 0 \text{ and } 0 \leq r < R; && u = 0 \\ &\text{if } 0 \leq t < \infty \text{ and } r = R; && u = C_0 R, \end{aligned}$$

and

$$\text{if } t = 0 \text{ and } r = 0; \qquad u = 0.$$

Let us introduce the symbol

$$\frac{D}{\bar{k}} = A' \tag{24}$$

and let us define variable u by the function

$$u = w(r;t) + p(r) \tag{25}$$

On substituting condition (25) into equation (23) we obtain:

$$\frac{\partial}{\partial t} (w+p)^m = A' r^{m-1} \frac{\partial^2}{\partial r^2} (w+p). \tag{26}$$

On dividing and multiplying the left side by p^m, p^m can be anteposed since it is no function of t, and thus

$$p^m \frac{\partial}{\partial t} \left(1 + \frac{w}{p}\right)^m = A' r^{m-1} \frac{\partial^2}{\partial r^2} (w+p). \tag{27}$$

On applying to the left side of equation (27) the binomial approximation $(1 + x)^m \sim 1 + mx$ if $x \ll 1$) we obtain:

$$p^m \frac{\partial}{\partial t} \left(1 + m \frac{w}{p}\right) = A' r^{m-1} \frac{\partial^2}{\partial r^2} (w+p). \tag{28}$$

The condition of applying the binomial approximation is

$$\left|\frac{w}{p}\right| < \varepsilon \quad \text{or} \quad \left|\frac{u-p}{p}\right| < \varepsilon \text{ when } \varepsilon < 1. \tag{29}$$

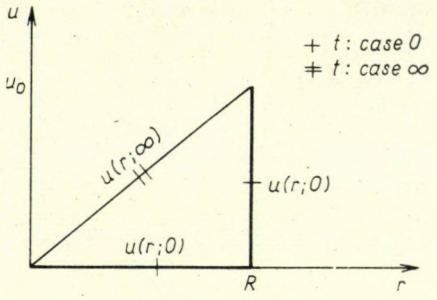


Fig. 1. Boundary solutions of Eq. (23)

From relation (29), the following two unequalities are derived:

$$-\varepsilon p < u - p \tag{30}$$

and

$$u - p < \varepsilon p \tag{31}$$

From these

$$p < \frac{u}{1-\varepsilon}$$
$$p > \frac{u}{1+\varepsilon} \tag{32}$$

In equilibrium, in the inside of the particles of the adsorbent, concentration C_0 will exist in the gas phase, independently of the local coordinate. On introducing variable u, its run will be linear in equilibrium. When $r = 0$, this straight will pass through the origo of the coordinate system u *vs* r, and at the site $r = R$, $u_0 = C_0 R$.

On plotting the function u pertaining to the values $t = 0$ and $t = \infty$, respectively, we obtain the diagram presented in Fig. 1.

Function $p(r)$ invariant in time must be chosen in a way that, on taking into account the unequality (32), the points of the function should be located in the surface range between the horizontal axis of coordinates and the function $u\ (r;\ \infty)$.

Now let us write the function $p(r)$, in first approximation, in the form

$$p(r) = \frac{1}{2}u(r;\infty) = 1/2\, u_0 \frac{r}{R} \tag{33}$$

Transforming equation (28)

$$\frac{\partial w}{\partial t} = \frac{A'}{m}\left(\frac{r}{p}\right)^{m-1}\frac{\partial^2}{\partial r^2}(w+p) \tag{34}$$

and applying variable u by adding to the left side the term $\frac{\partial p}{\partial t} = 0$, we obtain

$$\frac{\partial u}{\partial t} = \frac{A'}{m}\left(\frac{r}{p}\right)^{m-1}\frac{\partial^2 u}{\partial r^2} \tag{35}$$

On taking into account the considerations in respect to function p, and on substituting equation (33), we obtain

$$\frac{\partial u}{\partial t} = \frac{A'}{m}\left(\frac{r}{\frac{u_0 r}{2R}}\right)^{m-1}\frac{\partial^2 u}{\partial r^2} \tag{36}$$

Considering that $\frac{R}{u_0} = 1/C_0$, let us introduce the denotion

$$D' = \frac{D}{\bar{k}m}\left(\frac{C_0}{2}\right)^{1-m} \tag{37}$$

Then from equation (36) we obtain

$$\frac{\partial u}{\partial t} = D'\frac{\partial^2 u}{\partial r^2} \tag{38}$$

The solution of equation (38) on the basis of the initial and limit conditions is as follows:

$$C_g = C_0\left[1 + \frac{2}{\pi}\frac{R}{r}\sum_{n=1}^{\infty}\frac{(-1)^n}{n}\sin\frac{n\pi r}{R}e^{-\frac{n^2D'\pi^2}{R^2}t}\right] \tag{39}$$

while the concentration function of the adsorbed phase reads

$$C_a = \bar{k}\left\{C_0\left[1 + \frac{2}{\pi}\frac{R}{r}\sum_{n=1}^{\infty}\frac{(-1)^n}{n}\sin\frac{n\pi r}{R}e^{-\frac{n^2D'\pi^2}{R^2}t}\right]\right\}^m \tag{40}$$

In general, if $r > 0$; $t = 0$ in the initial condition the concentration is $C(0)$, the solution of equation (39) will be

$$C_g = C_0 + \frac{2R}{\pi r}(C_0 - C(0)) \sum_{n=1}^{\infty} \dots . \tag{41}$$

and, respectively,

$$C_a = \bar{k}\left\{C_0 + \frac{2R}{\pi r}[C_0 - C(0)] \sum_{n=1}^{\infty} \dots .\right\}^m \tag{42}$$

Utilizing the equations (39) and (40), the quantity of adsorbed substance is calculated by the correlation

$$n(t) = \int_0^R 4\pi r^2 (C_a + C_g)\, dr \tag{43}$$

On presuming that $C_a \gg C_g$, the term C_g in the parentheses can be neglected. Substituting the concentration function (40) into equation (43), we obtain

$$n(t) = 4\pi k C_0^m \int_0^R r^2 \left\{1 + \frac{2R}{\pi r} \sum_{n=1}^{\infty} \frac{(-1)^n}{n} \sin\frac{n\pi r}{R}\, e^{-\frac{n^2 D' \pi^2}{R^2}}\right\}^m dt \tag{44}$$

On carrying out the integration, the series

$$(1 + x)^\alpha = \sum_{i=0} \binom{\alpha}{i} x^i \tag{45}$$

is used for developing equation (44).

Let us consider the values of the integral (44) in the cases of $i = 0$; 1; 2 . . .

If $i = 0$

$$n(t)_0 = \frac{4}{3}\pi \bar{k} C_0^m \int_0^R r^2\, dr = \frac{4}{3}\pi \bar{k} C_0^m R^3 \tag{46}$$

If $i = 1$

$$n(t)_1 = \frac{4}{3}\pi \bar{k} C_0^m \int_0^R m \frac{2R}{\pi} r \sum_{n=1}^{\infty} \frac{(-1)^2}{n} \sin\frac{n\pi r}{R}\, e^{-n^2 \Theta t}\, dr \tag{47}$$

and, because

$$\int r \sin\frac{n\pi r}{R} = \frac{\sin\dfrac{n\pi r}{R}}{\left(\dfrac{n\pi}{R}\right)^2} - \frac{r\cos n\pi r}{\dfrac{n\pi}{r}}$$

$$\text{and } \sin n\pi = 0,$$

the integral can be written as

$$n(t)_1 = \frac{4}{3}\pi\bar{k}C_0^m R^3 \left(\frac{6}{\pi^2} m \sum_{n=1}^{\infty} \frac{1}{n^2} e^{-n^2\Theta t} \right) \tag{48}$$

If $i = 2$,

$$n(t)_2 = \frac{4}{3}\pi\bar{k}C_0^m \int_0^R r^2 \frac{m(m-1)}{2!} \cdot \frac{4R^2}{r^2\pi^2} \sum_{n=1}^{\infty} \frac{(-1)^{2n}}{n^2} \sin^2 \frac{n\pi r}{R} e^{-2n^2\Theta t} dr \tag{49}$$

and since

$$\int \sin^2 \frac{n\pi r}{R} = 1/2\, r - \frac{1}{\frac{4n\pi}{R}} \sin^2 \frac{n\pi r}{R}$$

to the analogy of equation (48),

$$n(t)_2 = \frac{4}{3}\pi\bar{k}C_0^m R^3 \frac{m(m-1)}{2!} \frac{6}{\pi^2} \sum_{n=1}^{\infty} \frac{1}{n^2} e^{-2n^2\Theta t} \tag{50}$$

If $i = 3$,

$$n(t)_3 = \frac{4}{3}\pi\bar{k}C_0^m \frac{m(m-1)(m-2)}{3!} \int_0^R 3 \frac{8R^3}{\pi^3} \frac{1}{r} \sum_{n=1}^{\infty} \frac{(-1)^{3n}}{n^3} \sin^3 \frac{n\pi R}{R} e^{-3n^2\Theta t} dr \tag{51}$$

If $i \geq 3$, difficulties are met in performing the integration. Namely, the determination of $\frac{\sin^m x}{x^n}$ leads to the analysis of the sinus integral function proper.

In the case of $i = 3$, the function $\int 1/r \sin^3 ar\, dr$ is to be sought. On applying the substitution $z = ar$,

$$\int_0^R \frac{1}{r} \sin^3 \frac{n\pi}{r} dr = \frac{3}{4} \mathrm{Si}(n\pi) - \frac{1}{4} \mathrm{Si}(3n\pi). \tag{52a}$$

On the basis of the numerical analysis, of the sinus integral function it was found that, if n is unit or a rational integer,

$$\frac{3}{4} \mathrm{Si}(n\pi) - \frac{1}{4} \mathrm{Si}(3n\pi) \sim \frac{\pi}{4}. \tag{52b}$$

Resubstituting conditions (53) into equation (51), we obtain

$$n(t)_3 = -\frac{4}{3}\pi\bar{k}C_0^m \frac{m(m-1)(m-2)}{3!}\frac{6}{\pi^2}\sum_{n=1}\frac{1}{n^2}e^{-3n^2\Theta_t} \tag{53a}$$

The solution function of (44), after full induction and rearrangement, reads as follows:

$$\vartheta = \frac{n(t)}{n(e)} = \sum_{i=0}^{\infty}(-1)^i\binom{m}{i}\frac{6}{\pi^2}\sum_{n=1}^{\infty}\frac{1}{n^2}e^{-\frac{n^2iD'\pi^2}{R^2}t} \tag{53b}$$

Now let us write function (53) if $m \approx 1$ (53). Instead of the solution function, we may write, due to the rapid convergence of the series:

$$\vartheta \cong 1 - \frac{6m}{\pi^2}\sum_{n=1}^{\infty}\frac{1}{n^2}e^{-\frac{n^2D'\pi^2}{R^2}t} \tag{54}$$

Finally, also the dimension of the complex term D' is to be discussed.

The term D' has been defined by equation (37). The dimensions of the term in correlation (37) are as follows

k : $[ML^{-3}]^{1-m}$
m : dimensionless
C : $[ML^{-3}]$
D : $[L^2T^{-1}]$

From these, the definition equation of D' reads:

$$D' = [L^2T^{-1}]\,[ML^{-3}]^{-(1-m)}\,[ML^{-3}]^{1-m} \tag{55}$$

and

$$D' = [L^2T^{-1}]$$

i.e. D' is the "virtual" diffusion constant.

Prior to searching some correlation between the solution function and the experimental kinetical curves, the followings can be stated, in general, of the solution function (53). No explicit kinetical equations are given in literature so far for systems of adsorbent-adsorbate which can be described by Freundlich isotherms. Results obtained by numerical methods cannot be built-up directly in the transport equation of the operational unit of adsorption (3). Thus, it appears that the application of the equation of continuity requires in the case of Freundlich isotherms the investigation of the possibilities of the explicit solutions of equation (13). Equation (53) is just the result of an attempt of this nature.

Solution function (53) undergoes simplification to an appreciable extent by a previous estimation of the conditions of convergence.

Experimental investigation of the sorption kinetics of systems of uranium hexafluoride adsorbent

a) *Apparatus*

Sorption kinetical investigations were carried out in an apparatus described in our previous papers, with the modification that a special measuring cell has been applied in place of the vessels serving as adsorbent tanks.

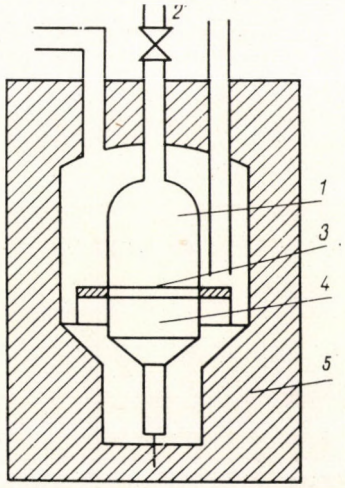


Fig. 2. Measuring cell for static adsorption kinetical measurements

The scheme of the measuring cell is presented in Fig. 2. In the course of the adsorption kinetical measurements, the adsorbent was placed in the adsorbent tank *1* equipped with a thermostated jacket. This tank was coupled to the measuring system by tap *2*. The lower surface of the adsorbent tank was sealed with a mica sheet of a thickness of 1—2 mg./sq.cm. This mica sheet was coated with a phosphor sensitive to α-radiation, as follows; a silicon-grease film was transferred onto the surface of the mica sheet, and to the ZnS(Ag) phosphor was sticked the silicon grease film. A photomultiplier (FEU 25 or Zeiss M12 Fs35) was connected to the scintillator through a photoconductor. The detector was surrounded by an opaque jacket, and placed in a lead column of 3 cm wall-thickness. The scintillation-type radiation detector was linked to an impulse counter. The amount of substance adsorbed under isotherm-isobar conditions, plotted against time, was calculated from the changes in activity recorded during the experiment.

The mica window of the measuring cell must be replaced by a new one after each series of measurements. Namely, the surface of mica is attacked by uranium hexafluoride, this latter being adsorbed on the surface. The effect of this process increases of background radiation. In order to check the contamination degree of the mica window, the instrument is maintained under a high vacuum after the termination of the desorption cycle, and the activity established.

In the measuring system, the gaseous radioactive substance gets into contact with the mica surface. Consequently, the measured activity is in fact the combined sum of the activity of the adsorbed phase plus that of the gas phase. Surplus activity which may be of a great extent at higher tension levels must be taken into account by using a correction value. On terminating the sorption cycle, the system is subjected to suction, and the desorption branch is examined. The rapid decrease of activity measured in the desorption cycle is due to two facts. On the one hand, the gaseous adsorbate is being removed by suction, and, owing to desorption, the concentration of the particles of adsorbent decreases. The activity increase due to the gaseous adsorbate is obtained from the value of the desorption curve extrapolated to time $t = 0$, plus the difference between that value and the saturation activity adsorption.

Table I

Experimental data of static sorption kinetics

Ni I					Ni II					Cu I				
	20 °C		50 °C			20 °C		50 °C			20 °C		50 °C	
t	$p = 16.9$	40.5	16.9	40.5	t	$p = 16.9$	40.5	16.9	40.5	t	$p = 16.9$	40.5	16.9	40.5
1	0.125	0.240	0.150	0.250	1	0.152	0.545	0.270	0.590	1	0.531	0.780	0.565	0.645
3	0.210	0.348	0.312	0.430	3	0.368	0.718	0.501	0.671	2	0.695	0.910	0.740	0.795
5	0.282	0.435	0.420	0.515	5	0.521	0.796	0.660	0.740	3	0.786	0.945	0.827	0.880
10	0.425	0.570	0.550	0.630	10	0.740	0.920	0.775	0.852	4	0.845	0.968	0.880	0.935
15	0.522	0.645	0.676	0.718	15	0.848	0.982	0.880	0.912	5	0.892	0.980	0.921	0.970
20	0.630	0.700	0.745	0.781	20	0.910	0.994	0.924	0.960	6	0.923	0.999	0.950	0.999
25	0.683	0.730	0.780	0.840	25	0.955	—	0.951	0.985	8	0.965	—	0.999	—
30	0.752	0.760	0.830	0.880	30	0.990	—	0.990	0.999	10	0.999	—	—	—

Cu II					Fo9					Pth			Pth		
	20 °C		50 °C			20 °C		50 °C			20 °C			50 °C	
t	$p = 16.9$	40.5	16.9	40.5	t	$p = 16.9$	40.5	16.9	40.5	t	$p = 16.9$	40.5	t	16.9	40.5
1	0.225	0.268	0.295	0.460	0.1	0.760	0.820	0.790	—	2	0.660	0.780	1	0.576	0.730
2	0.300	0.335	0.423	0.500	0.2	0.852	0.908	0.902	—	4	0.762	0.895	2	0.750	0.825
5	0.504	0.505	0.518	0.595	0.3	0.894	0.946	0.948	—	6	0.841	0.945	3	0.845	0.892
10	0.580	0.630	0.760	0.746	0.4	0.930	0.970	0.980	—	8	0.895	0.970	4	0.898	0.930
15	0.665	0.725	0.821	0.825	0.5	0.948	0.990	0.996	—	10	0.920	0.998	5	0.932	0.978
20	0.720	0.790	0.860	0.890	0.6	0.970	—	—	—	13	0.970	—	6	0.965	0.990
25	0.770	0.822	0.895	0.928	0.8	0.990	—	—	—	16	0.999	—	8	0.990	—
30	0.795	0.870	0.920	0.965	1.0	0.998	—	—	—	20	—	—	10	0.999	—

The technique of measurement was tested using instrument employed for establishing the points of equilibrium. The substance placed in the adsorbent tanks was allowed to be in contact for an adequate period with the adsorbate under isobar-isotherm conditions. Then samples were prepared from the adsorbate in the way specified at the equilibrium measurements and the quantities of uranium hexafluoride adsorbed were measured.

Differences in the points of measurement established by the two methods did never exceed 5 per cent.

b) *Results*

Kinetical measurements were carried out with six kinds of adsorbents at two different temperatures and two different pressures, respectively. The data are presented in Table 1.

c) *Discussion*

Let us examine the possibilities of employing equation (19) in processing the experimental results. On carrying out the Newton approximation it was found that in the initial period the experimental curves increased rather abruptly and later they had a transient section much sharper than those of the curves calculated by presuming a linear isotherm.

The correlation (53) derived by us on presuming the conditions of a Freundlich isotherm has been applied in processing the experimental data on the basis of the following considerations. Let us denote by Θ the exponent containing the physical constants of equation (53). Then we may write

$$\vartheta = \sum_{i=0}^{\infty} (-)^i \binom{m}{i} \frac{6}{\pi^2} \sum_{n=1}^{\infty} \frac{1}{n^2} e^{-n_2 i \Theta t} \tag{55a}$$

It is known that the Fourier series

$$\sum_{n=1}^{\infty} \frac{1}{n^2} e^{-n_2 i \Theta t}$$

shows a rather rapid convergence, and on establishing the total sum of the series the consideration of three or four members affords a sufficient accuracy even when the exponents are of a low value (<0.1). The same holds also for the series $\sum_{i=0}^{\infty}$ since the term $i!$ is present in the denominator.

Considering exponent t as an independent variable, equation (55a) can be solved in a general manner because the term Θ includes all the informations of the total sum of the series n plotted against the independent variable up to a value of $\varepsilon \leq 10^{-3}$ had been established. The term ε is defined by the formula

$$\varepsilon = \frac{\dfrac{1}{(k+1)^2} e^{-(k+1)^2 i \Theta t}}{\sum_{n=1}^{k} \dfrac{1}{n^2} 2^{-n^2 i \Theta t}} \leq 10^{-3}. \tag{56}$$

Table II

Function values calculated

	Ni I		Ni II		Cu I	
	20 °C	50 °C	20 °C	50 °C	20 °C	50 °C
0.1	0.4681	0.3734	0.5477	—	0.4347	0.3734
0.5	0.7270	0.6529	0.7788	—	0.7014	0.6529
1	0.8506	0.8040	0.8861	—	0.8349	0.8040
1.5	0.9134	0.8840	0.9345	—	0.9043	0.8840
2	0.9499	0.9302	0.9611	—	0.9426	0.9302
3	0.9815	0.9745	0.9861	—	0.9793	0.9745
4	0.9933	0.9907	0.9951	—	0.9923	0.9907
5	0.9975	0.9966	0.9982	—	0.9972	0.9966

The total sum of the series i has been established on taking into account sums of the series obtained in the above-given way. Since the binomial constant includes the Freundlich exponent, the resulting function has been referred to different m values, determined by static equilibrium measurements. The obtained functions t *vs.* ϑ are presented in Table II.

In the knowledge of the experimental data and of the solution of equation (55a), that value is to be found at which the kinetical curves plotted with experimental and calculated values, respectively, have identical shapes. It is rather simple to solve by a computer the classical function iteration task. In the followings, a graphic solution of the task is described.

The general kinetical curves (Table II) calculated by Eq. (53) do not include any limitations in respect to the adsorption parameters of the pair adsorbent-adsorbate. Concrete solutions can be derived by the linear formation of these functional relations. Thus, the determination of the constant Θ means at the same time also the determination of the adsorption constants of the system.

In a mathematical presentation, the theoretical function of the best approximation is as follows: find that value of Θ at which the function equilibrium

$$\int_0^t \frac{\partial \left(\vartheta_{\text{calculated}}(\Theta;t) - \vartheta_{\text{measured}}(t)\right)}{\partial t} \, dt \to \min \tag{57}$$

is of minimum value according to the integral definition. Let us this function against t for different values of Θ (choosing a range on investigation based on a preliminary estimation). On plotting now the graphical integral of the

on the basis of equation (53)

Cu II		Pth		Fo9		
20 °C	50 °C	20 °C	50 °C	20 °C	50 °C	Linear isotherm
0.3842	0.3622	0.4681	0.4681	0.6158	0.5462	0.3355
0.6653	0.6422	0.7270	0.7270	0.8156	0.7753	0.6103
0.8123	0.7958	0.8506	0.8506	0.9025	0.8798	0.7736
0.8893	0.8793	0.9134	0.9134	0.9450	0.9312	0.8644
0.9343	0.9278	0.9499	0.9499	0.9675	0.9587	0.9697
0.9758	0.9734	0.9815	0.9815	0.9855	0.9855	0.9697
0.9912	0.9912	0.9933	0.9933	0.9958	0.9947	0.9889
0.9968	0.9964	0.9975	0.9975	0.9984	0.9981	0.9959

correlation against Θ, a limit value is obtained which is at the same time the solution desired.

The sorption kinetical functions determined by the graphic method are listed in Table III.

The knowledge of the exponential exponent makes possible to draw further conclusions as regards the nature of the diffusion process.

According to the definition:

$$\Theta = \frac{D}{\bar{k}m}\left(\frac{C_0}{2}\right)^{1-m}\frac{\pi^2}{R^2} \tag{58}$$

On substituting into Equ. (58) the equilibrium concentration of the adsorbed phase

$$C_{\text{equil.}} = \bar{k}C_0^m \tag{59}$$

we obtain

$$\Theta = \frac{D}{m}\frac{C_0}{C_{\text{equil.}}}\frac{\pi^2}{R^2}\frac{1}{2^{1-m}} \tag{60}$$

Let us compare the exponential exponents of the kinetical equations derived by presuming a linear equilibrium (19), and Freundlich isotherm (53). Since in equation (19)

$\frac{1}{H} = \frac{C}{C_0}$, differences between the two exponents are limited to the multiplying factor $\frac{1}{m2^{1-m}}$.

The diffusion constant characteristic of the kinetical process is determined by means of the correlation (60). The obtained data are given in Table IV.

Table III

Calculated function values of static sorption kinetics

Ni I					Cu I					Cu II				
	20 °C		50 °C			20 °C		50 °C			20 °C		50 °C	
t	$p = 16.9$	40.5	16.9	40.5	t	$p = 16.9$	40.5	16.9	40.5	t	$p = 16.9$	40.5	16.9	40.5
1	0.123	0.260	0.151	0.280	1	0.600	0.780	0.595	0.645	1	0.180	0.220	0.296	0.360
5	0.210	0.433	0.430	0.513	2	0.702	0.906	0.723	0.794	2	0.290	0.340	0.421	0.470
10	0.276	0.570	0.596	0.610	3	0.781	0.939	0.825	0.875	3	0.446	0.500	0.570	0.560
15	0.522	0.627	0.670	0.704	4	0.816	0.970	0.880	0.920	4	0.592	0.638	0.700	0.746
20	0.610	0.700	0.730	0.768	5	0.853	0.986	0.921	0.950	5	0.660	0.710	0.817	0.850
25	0.635	0.728	0.780	0.820	6	0.902	0.996	0.940	0.976	6	0.700	0.770	0.860	0.910
30	0.670	0.760	0.820	0.872	8	0.970	—	0.980	0.980	8	0.765	0.815	0.840	0.940
					10	0.980	—	0.986	—	10	0.793	0.885	0.924	0.965

Pth					Fo9				
	20 °C		50 °C			20 °C		50 °C	
t	$p = 16.9$	40.5	t	$p = 16.9$	40.5	t	$p = 16.9$	40.5	16.9	40.5
2	0.660	0.780	1	0.640	0.730	0.1	0.762	0.818	0.800	
4	0.770	0.902	2	0.765	0.825	0.2	0.850	0.908	0.900	
6	0.826	0.952	3	0.845	0.930	0.3	0.896	0.946	0.948	
8	0.895	0.968	4	0.900	0.970	0.4	0.932	0.970	0.980	
10	0.922	0.985	5	0.925	0.980	0.5	0.950	0.982	0.994	
13	0.958	0.993	6	0.950	0.992	0.6	0.970	0.990	—	
16	0.980	—	8	0.970	—	0.8	0.990	—	—	
20	0.990	—	10	0.980	—	0.9	0.994	—	—	

Table IV

Diffusion constants of adsorbents

Type of adsorbent	R (cm)	D_{mean}, 20 °C	D_{mean}, 50 °C	$D_{K\,mean}$	Pore size, Å
Ni I	$1.5 \cdot 10^{-2}$	$1.205 \cdot 10^{-5}$	$1.263 \cdot 10^{-5}$	$1.320 \sqrt{\frac{T}{M}} \cdot 10^{-5}$	130—140
Ni II	$1.5 \cdot 10^{-2}$	$1.505 \cdot 10^{-5}$	$1.580 \cdot 10^{-5}$	1.649	170—180
Cu I	$2.0 \cdot 10^{-2}$	$1.281 \cdot 10^{-5}$	$1.342 \cdot 10^{-5}$	1.403	150
Cu II	$2.0 \cdot 10^{-2}$	$0.885 \cdot 10^{-5}$	$0.929 \cdot 10^{-5}$	0.970	100
Pth	$1.5 \cdot 10^{-2}$	$1.062 \cdot 10^{-5}$	$1.115 \cdot 10^{-5}$	1.164	120
Fo9	$1.5 \cdot 10^{-2}$	$1.771 \cdot 10^{-5}$	$1.771 \cdot 10^{-5}$	1.948	210

On the basis of the order of magnitude of the diffusion constant it was presumed that Knudsen diffusion is actually the rate-determining one. In order to check the correctness of this presumption, let us determine, from the diffusion constant, the mean dimension of a channel. Since the definition equation for D_K reads

$$D_K = \frac{2}{3} c_i \, r \, (\text{cm/sec}) \tag{61}$$

and the mean velocity of molecules is

$$c_i \simeq 14.551 \sqrt{\frac{T}{M}} \, (\text{cm/sec}) \tag{62}$$

and order of magnitude of 100 Å is obtained for the mean diameter of pores (*cf.* Table IV). On taking into account the dependence of the molecules on the free length of distance, on temperature and on pressure in the case of uranium hexafluoride:

$$L(\text{cm}) = \frac{200}{P} 6 \cdot 34 \, (1 + 4 \cdot 45/t \cdot 10^{-3}) + 3 \cdot 1 (t \cdot 10^{-3})^2 \cdot 10^{-6} \, . \tag{63}$$

From this:

$$L = 0.8 \cdot 10^{-4} \, (\text{at } 20° \text{ C}) .$$

This proves that the ratio L/r is greater than 10^2, proving the correctness of our presumption relating to Knudsen diffusion.

It must be noted that the mean diameter of channels employed above in place of the function of pore distribution idealizes the structure of the adsorbent to a great extent, and that the applied theoretical correlations are based on rough approximations. Therefore, this value of pore diameter cannot be used in calculations as an absolute value.

Processing experimental data in the presented way is in fact the first attempt to employ the kinetical equation (53). This equation proved to be suitable for describing the static kinetical data of the extreme systems of adsorbent-adsorbate examined in our present experiments. With respect to the special nature of our experimental data, no attempts could be made to examine the general applicability of the derived correlation.

On the basis of our present static adsorption kinetical experiments, some knowledge was obtained of the diffusion processes which take place in the inner spaces of adsorbents. It was found that the velocity of sorption kinetics is in fact determined by Knudsen diffusion. In the knowledge of the diffusion constants relating to systems of adsorbent—adsorbate, a possibility is offered for the determination of fundamental data required for further diffusion investigations.

Symbols

$A' = \dfrac{D}{k}$

C; C_0; $C(0)$ = concentration g/cu.cm mole/cu.cm
c_i = mean velocity of molecules sq.cm/sec
D = diffusion constant sqcm/sec

$D' = \dfrac{D}{km} \Big/ \dfrac{C_0^{1-m}}{2}$

D_K = Knudsen diffusion constant sq.cm/sec
k; m = constants of Freundlich equation
L = length of free distance of molecules cm
P = pressure
r = sphere symmetrical locate coordinate
R = radius of adsorbent particle cm
t = time sec; min.
$\bar{t}$ = temperature °C
T = temperature °K
$\bar{V}$; v_x = velocity cm/sec

$\vartheta = \dfrac{n(t)}{n(e)}$

$\Theta = \dfrac{D'\pi^2}{R^2}$

x = local coordinate

REFERENCES

1. DAMKÖHLER, G.: Z. Physik. Chem. **A 174,** 222 (1935)
2. NÉMETH, J.: Magyar Tud. Akad. Kémiai Tud. Oszt. Közl. **18,** No. 1. 23, (1962)
3. MCBAIN, J. W.: Trans. Faraday Soc. **14,** 202 (1919)
4. TAYLOR, S.: J. Am. Chem. Soc. **53,** 578 (1931)
5. BRUNAUER, S.: The adsorption of gases and vapors. Princeton, 1931; WICKE, E.: Kolloid Z. **86,** 167 (1939); **86,** 295 (1939); **90,** 156 (1940)
6. JOST, W.: Diffusion, p. 61. Verlag P. Steinkopf, 1957
7. CRANK, J.: Mathematics of diffusion, p. 84. Oxford, 1956

László MÜLLER; Pécs, III., Páfrány u. 47. Hungary
László FÁY; Veszprém, Schönherz Z. u. 12. Hungary

Acta Chimica Academiae Scientiarum Hungaricae, Tomus 59 (2), pp. 201—210 (1969)

OSZILLOPOLAROGRAPHISCHE UNTERSUCHUNGEN ZINNORGANISCHER VERBINDUNGEN

R. GEYER und U. ROTERMUND

(Institut für Analytische Chemie der Technischen Hochschule »Carl Schorlemmer«) Leuna—Merseburg, DDR)

Eingegangen am 2. Februar 1968

Die Verbindungen $BuSnCl_3$, Bu_2SnCl_2, $Bu_2Sn(OCOCH_3)_2$, Bu_3SnCl, $Bu_3SnOCOCH_3$, $Ph_3SnOCOCH_3$ und Bu_4Sn wurden mit der oszillopolarographischen Methode nach HEYROVSKY und FOREJT untersucht. Als Grundlösungen dienten Alkohol—Wasser—HCl-Gemische verschiedener Konzentration. Die Bestimmung der einzelnen Verbindungen ist bis auf das Bu_4Sn möglich. Die Acetate verhalten sich wie die Chloride, da Ionen des Typs $R_{4-n}Sn^{n+}$ vorliegen. Bu_3Sn^+ ist neben Bu_2Sn^{++} ab 0,005 Mol % erfaßbar. $BuSn^{+++}$ läßt sich komplexometrisch in Eisessig/$NaOCOCH_3$ gegen Brenzkatechinviolett neben Bu_2Sn^{++}, Bu_3Sn^+ und Bu_4Sn titrieren. Sn^{4+} wird dabei mit erfaßt.

Zinnorganische Verbindungen des Typs $R_{4-n}SnX_n$ (X = Halogen) sind an der Quecksilbertropfelektrode reduzierbar [1, 2, 3]. Außer gleichstrompolarographischen Arbeiten an zinnorganischen Verbindungen liegen Anwendungen der Breyerschen Wechselstrompolarographie auf die Analytik dieser Verbindungsklasse vor [4]. Oszillopolarographische Untersuchungen nach HEYROVSKY und FOREJT an diesen Verbindungen wurden bisher noch nicht beschrieben.

Die Polarität der Sn—Cl-Bindung (z. B. in Bu_2SnCl_2, Bu = Butyl) läßt sich nach PAULING zu 30% des Wertes einer Ionenbindung abschätzen (Dipolmoment: 4.2 D) [5]. Das Dipolmoment der Bu—Sn-Bindung beträgt dagegen nur 0,45 D. In dem polaren Lösungsmittel Wasser findet daher eine vollständige Dissoziation in solvatisierte Ionen des Typs $R_{4-n}Sn^{n+}$ statt. Ist der Substituent X nicht deformierbar, besteht bereits ein salzartiges Kristallgefüge. Dafür spricht z. B. der hohe Schmelzpunkt des Me_3SnF (Me = Methyl; 360 °C) [6].

Die Zinn-Kohlenstoff-Bindung ist eine der stabilsten Organometallbindungen. Es sind hier sogenannte $d\pi—p\pi$-Wechselwirkungen möglich. Es lassen sich einige bemerkenswerte Vergleiche zwischen der Sn—C ($d\pi—p\pi$) und der C = C ($p\pi—p\pi$)-Bindung ziehen. Die Sn—C-Bindung ist wie die C = C-Bindung befähigt Protonsäuren und Lewissäuren anzulagern. Im Unterschied zur elektrophilen Addition an die C = C-Bindung erfolgt danach Bindungsbruch, wobei auf Grund der vorhandenen Polarität ($Sn^+—\bar{R}$) sich das positive Ion der Säure mit dem negativen Substituenten verbindet. Die bekannten KOZESCHKOW-Reaktionen [7] stellen hiermit nur einen Spezialfall (Lewissäure =

$SnCl_4$) dar. Die Reaktionsfähigkeit der Sn—C-Bindung gegenüber Säuren steigt beim Vorhandensein von Alkylsubstituenten am C-Atom. Die Phenyl-Zinn-Bindung ist gegenüber Säuren instabiler als die Alkyl—Zinn-Bindung [8, 9]. Dieses Verhalten ist, wie bei den Olefinen, durch die Zunahme der Basizität der Sn—C-Bindung erklärbar. Die in wäßriger oder wäßrig-alkoholischer Lösung vorhandenen Ionen der Art RSn^{+++}, R_2Sn^{++} und R_3Sn besitzen in der obigen Reihenfolge eine steigende Elektronendichte am Zinnatom (+I-Effekt der Alkylgruppen). Es werden sich also in derselben Reihenfolge die polarographischen Halbstufenpotentiale (HSP) nach negativen Werten hin verschieben. Begünstigt wird diese Tatsache noch durch die sterische Hinderung am R_3Sn^+-Ion. Die Komplexbildung mit dem Lösungsmittel wird die Halbstufenpotentiale in gegenläufiger Richtung beeinflussen, da das Ion RSn^{+++} offensichtlich der stärkste Komplexbildner ist. Dieser Einfluß ist aber nicht dominierend, so daß die obige Reihenfolge der HSP-Werte erhalten wird.

1. Apparaturen und Reagenzien

Zur Untersuchung wurde ein Polaroskop P 576 der Fa. Křižik (Prag) benutzt. Die Quecksilbertropfelektrode bestand aus einer Kapillare mit einem Durchmesser von 0,1 mm und einer Länge von 13,8 cm. Die Niveaugefäßhöhe betrug 18,5 cm. Der Wert m dieser Kapillare hatte die Größe von 1,84 mg/s beim Tropfen in H_2O ohne Elektrolyse. Die Tropfdauer von 3 s wurde mit einem elektromechanischen Tropfenabreißer geregelt. Die Stromstärke des Wechselstroms von 50 Hz betrug 0,1 bis 0,6 mA. Als Gegenelektrode diente in jedem Falle Bodenquecksilber. Spitzenpotentiale (gegen G. K. E.) wurden unter der Voraussetzung berechnet, daß bei 0,6 mA in 1 *m* HCl $E_{H+} = -1{,}47$ V, $E_{Hg} = +0{,}02$ V und $E_{Tl^+} = -0{,}51$ V betragen [10]. Als Lösungsmittel dienten Alkohol/Wassergemische, als Leitelektrolyt meist HCl. Alkalische Grundlösungen waren schlecht geeignet, da sie die Tropfeigenschaften der Kapillare bei höheren Konzentrationen an zinnorganischen Verbindungen beeinträchtigten. Die angegebenen Leitelektrolytkonzentrationen beziehen sich auf das Gesamtvolumen. Es wurden die zinnorganischen Verbindungen Bu_2SnCl, Bu_2SnCl_2, $BuSnCl_3$, Bu_4Sn, $Bu_3SnOCOCH_3$, $Bu_2Sn(OCOCH_3)_2$ und $Ph_3SnOCOCH_3$ (Ph = Phenyl) untersucht.

Die Chloride und das Tetrabutylzinn stammten vom Elektrochemischen Kombinat Bitterfeld, die Butylzinnacetate wurden aus den Chloriden mit Silberacetat in Methanol dargestellt. Beim $Ph_3SnOCOCH_3$ handelte es sich um ein Präparat der Fa. Merck. Die Konstanten sämtlicher Verbindungen stimmten nach mehrfacher Reinigung mit den Literaturwerten überein.

2. Untersuchungen an Monobutylzinntrichlorid (MB)

Das Verhalten im System HCl/EtOH (Et = Äthyl)/H_2O zeigen die Oszillogramme *a* und *b* der Abb. 1. Es ergeben sich 2 kathodische und 2 anodische Einschnitte, die bei allen untersuchten Alkohol- (0,8—60 Vol %) und HCl-Konzentrationen (0,14—4,8 *n* HCl) reversibel sind. Der erste kathodische Einschnitt verschwindet bei Alkoholkonzentrationen von 20% EtOH oder 15% *i*-PrOH (Pr = Propyl). Bei höheren HCl-Konzentrationen (2,4 *n*—4,8 *n*) tritt bei 10% und 20% C_2H_5OH eine dritte kathodische Stufe auf, die auch bei Gelatinezugabe erhalten wird. Aus den Q-Werten in 1 *m* HCl ($Q_{1A} = Q_{1K} = 0{,}28$; $Q_{2A} = Q_{2K} = 0{,}43$) errechnen sich die Potentialwerte —0,39 V und

—0,61 V gegen die G. K. E. Die Stufe 2 (anodisch) spricht am empfindlichsten auf die Anwesenheit von $BuSn^{+++}$ an. Gleichzeitig liefert dieser peak bei 20% bis 40% EtOH in 0,14 *m* HCl die steilste Eichkurve zwischen $1 \cdot 10^{-5}$ und $1 \cdot 10^{-4}$ M/l MB. Bei zunehmender HCl oder Cl^--Konzentration werden die Verhältnisse ungünstiger. Die Einschnitte 2 (anod.) und 2 (kath.) durchlaufen

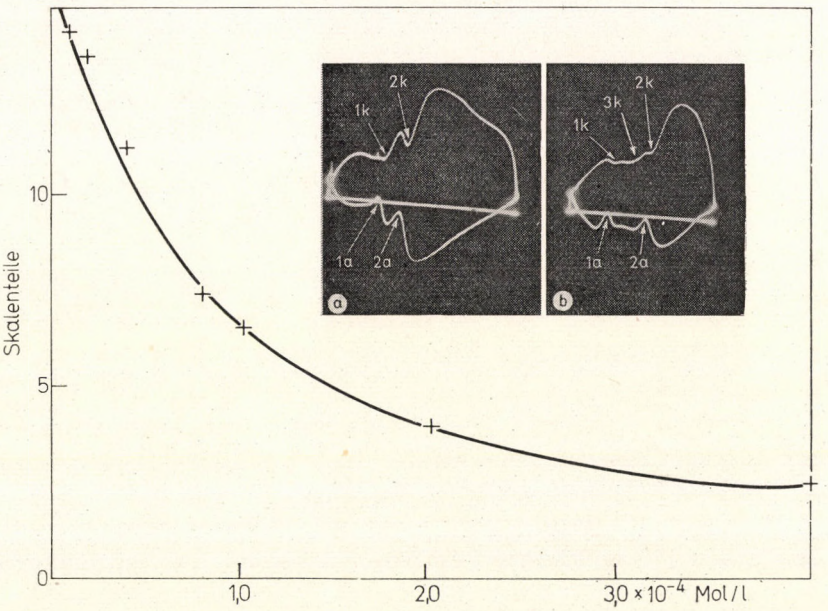


Abb. 1. Eichkurve zur Bestimmung von Monobutylzinntrichlorid (0,35 mA; Tropfzeit 2s) $Q_A = 0{,}48$; Auswertung des anodischen peaks Nr. 2; Grundlösung: 2,4 *m* HCl; 50% EtOH; Oszillogramme: a) 1.10^{-4} *m* MB; Grundlösung: 10 Vol% EtOH, 0,14 *m* HCl; b) $1{\cdot}10^{-4}$ *m* MB Grundlösung: 10% EtOH, 4,8 *m* HCl

in ihrer Empfindlichkeit bei wachsender Alkoholkonzentration ein Maximum, während die Stufe 1 (anod.) ihre Empfindlichkeit ungefähr beibehält, und der Einschnitt 1 (kath.) stetig unempfindlicher wird. Die Temperaturabhängigkeit, nach M. HEYROVSKY in einer thermostatisierten Zelle bestimmt, deutet auf diffusionsbedingte Wellen hin [11, 12]. Der Gelatineeinfluß läßt keine eindeutige Aussage zu.

Gleichstrompolarographisch treten ebenfalls 3 Stufen auf [13]. Auffallend ist die beobachtete Steigerung der Empfindlichkeit der Einschnitte 2 (anod. u. kath.) bei Alkoholzusatz. Die am Hg-Tropfen adsorbierte Alkoholschicht reichert wahrscheinlich die dem Einschnitt 2 entsprechenden Elektrolyseprodukte des $BuSn^{+++}$ an. Bei Erhöhung der Alkoholkonzentration macht sich die durchtrittshemmende Wirkung des Alkoholfilms bemerkbar. Diese Erscheinung ist auch beim Bu_2Sn^{++}, besonders stark aber beim Bu_3Sn^+ zu beobachten. Eine Eichkurve für MB zeigt die Abb. 1.

Zur Gehaltskontrolle der MB-Lösungen erwies sich die komplexometrische Titration mit Chelaplex III vorteilhaft. BÜRGER [8] fand, daß sich R_2Sn^+ und RSn^{3+}-Ionen mit Chelaplex III gegen Brenzkatechinviolett als Indikator in MeOH ohne pH-Puffer titrieren lassen. Unabhängig von den Autoren SPICHALE u. Mitarb. [14] wurde gefunden, daß auf Grund der größeren Komplexbildungstendenz des $BuSn^{+++}$ (s. o.) beim pH-Wert 3—4 nur noch das $BuSn^{+++}$ erfaßt wird.

Günstig für die Titration des MB neben DB, TB und Tetrabuthylzinn erwies sich das Arbeiten in Eisessig (mindestens 60 Vol %) [18], welcher mit Natriumacetat abgepuffert wurde. Als Indikator diente Brenzkatechinviolett. Auf diese Weise läßt sich der pH-Wert sehr leicht einstellen. In der Lösung mit vorhandenes $SnCl_4$ wird zwar mit erfaßt, stört aber die Bestimmung nicht, wogegen in wäßrig/alkoholischer Lösung auch Spuren Zinn(IV) die Indizierung unmöglich machen.

3. Untersuchungen an Dibutylzinndichlorid und -acetat (DB)

Wie oben dargestellt, dissoziieren die zinnorganischen Verbindungen des Typs $R_{4-n}SnX_n^{+}$ in Ionen. Dibutylzinndichlorid und -acetat verhalten sich daher auch völlig gleichartig bei der oszillopolarographischen Untersuchung. Das kann als weiterer Hinweis für das Vorliegen von Ionen angesehen werden. Das Verhalten des Bu_2Sn^{++} bei der oszillopolarographischen Untersuchung im System H_2O(EtOH)HCl zeigt Abb. 2. In alkoholarmer Lösung treten bei einer Konzentration $C_{Bu_2Sn^{++}} = 1 \cdot 10^{-4}$ M/1 3 Stufen auf. Die erste Stufe (in 0,6 *m* HCl $Q_A = 0{,}14$; $Q_K = 0{,}24$) zeigt mit ihrem anodischen peak in 0,6 *m* HCl noch eine Konzentration von $2 \cdot 10^{-6}$ M/1 Bu_2Sn^{++} an, wenn keine oberflächenaktiven Substanzen mit vorliegen. Mit steigender Alkoholkonzentration verschwindet die Stufe 1, mit steigender HCl-Konzentration wird der Elektrodenprozeß reversibel (Abb. 2c). Sowohl bei der gleichstrompolarographischen Untersuchung als auch bei der Wechselstrompolarographie nach Breyer tritt diese erste Welle nicht auf. Der Gelatine- und der Temperatureinfluß (Abb. 3) deuten auf einen vorgelagerten Prozeß und Adsorption hin. Es wird angenommen, daß die Welle 1 (anod.), die wesentlich empfindlicher Bu_2Sn^{++}-Ionen anzeigt als die Welle 1 (kath.), durch ein Artefakt hervorgerufen wird. Als Artefakt wird das $(Bu_2Sn)_2^{++}$-Ion angesehen, welches am Potential der Wasserstoffabscheidung durch Reduktion des Bu_2Sn^{++} entsteht. Eine Br_2-Zugabe vermindert die Empfindlichkeit der Stufe 1 (anod.) stark, da das Br_2 bekanntlich diese Dizinnverbindung äußerst leicht [15] oxydiert. Die Welle 1 (anod.) erscheint bei einem Potentialwert von $-0{,}18$ V (G. K. E.), der aus dem Q-Wert berechnet wurde. Dieser Einschnitt kann zur Bestimmung des DB in Gemischen verwendet werden. Bei Anwesenheit von MB und Tributylzinnchlorid (TB) vermindert sich die Empfindlichkeit des Einschnittes 1 (anod.) stark, aber die Bestimmung im Gemisch ist möglich. Eine Eichkurve und ein Oszillogramm zeigt die Abb. 4. Die durch die gegenseitige Beeinflussung der Wellen entstehenden Störungen können durch oszillopolarographische Titration nach JEZDINSKY [16] umgangen werden.

Die zweite, bei der oszillopolarographischen Untersuchung in 0,6 *m* HCl erhaltene Welle entspricht der ersten gleichstrompolarographischen und wech-

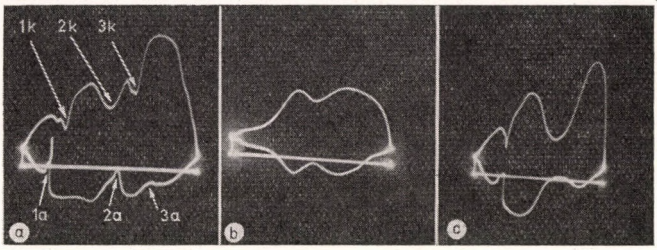


Abb. 2. Oszillogramme von Bu_2Sn^{++} ($1 \cdot 10^{-4}$ M/l) in HCl/EtOH/H_2O.
a) 1% EtOH; 0,6 *m* HCl; b) 80% EtOH; 0,6 *m* HCl; c) 10% EtOH; 7,2 *m* HCl

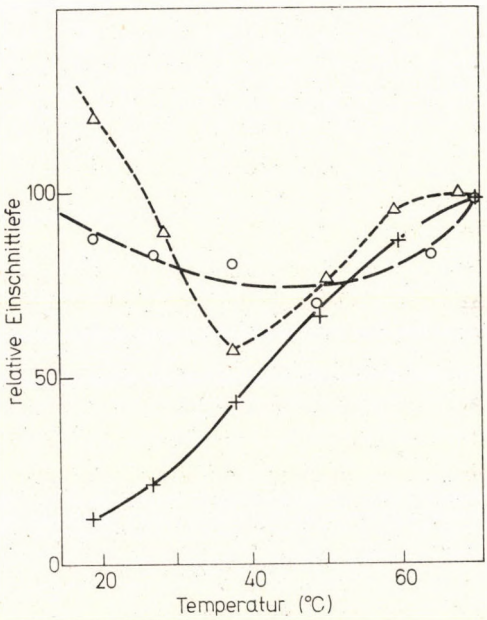


Abb. 3. Temperaturabhängigkeit der Einschnittiefen beim Bu_2Sn^{++} ($4 \cdot 10^{-5}$ M/l); Auswertungsmethode nach M. HEYROVSKY, ref. in (11) (Grundlösung: 0,5 *m* HCl, 1% *i*-PrOH; 0,15 mA; Tropfzeit 2s; Stufe 3 wurde bei einer Tropfzeit von 3s gemessen)
Stufe 1, anodisch: – – – △ – – –; Stufe 2, kathodisch; — — — ○ — — ; Stufe 3, kathodisch: ——— + ———

selstrompolarographischen Stufe. Es errechnete sich für 1 *m* HCl als Grundlösung ein Potentialwert von −0,62 V ($Q_{An} = Q_{Kath} = 0{,}45$) (gleichstrompol.: −0,593 V; wechselstrompol. (4): −0,60 V in 0,5 *m* KCl). Die Einschnitte sind sehr breit, und ihre Lage ist daher nicht genau bestimmbar. Mit steigender Alkoholkonzentration durchläuft die peak-Größe der Stufen 2 (kath. u. anod.) ein Maximum. Daraus folgt, daß die Bu_2Sn^{++}-Ionen in der alkoholhaltigen elektrischen Doppelschicht angereichert werden. Aus dem Temperatur- und dem Gelatineeinfluß folgt, daß die Stufe 2 (kath.) vermutlich durch einen Ein-

elektronenschritt (diffusionsbedingt) hervorgerufen wird (Abb. 3). Das stimmt mit dem von COSTA für die gleichstrompolarographische Reduktion angegebenen Mechanismus der Reaktion zum Radikal $R_2Sn^{+\cdot}$ überein [1]. Zur analytischen Auswertung der Stufe 2 (anod. u. kath.) eignet sich am besten als Grundlösung 0,6 *m* HCl und 50% bis 40% EtOH, da die übrigen DB-Stufen nicht erscheinen und die Empfindlichkeit durch den Alkohol verstärkt ist. Die Stufe 2 (anod. u. kath.) wird auch erhalten, wenn man das DB aus PVC-Folien bestimmt, da der Weichmacher nicht stört.

Die Stufe 3 (kath.) tritt nur bei längeren Tropfzeiten auf. Gleichstrompolarographisch wurde sie als zweite Welle bei −0,8 V (G. K. E.) beobachtet (1 *m* HCl).

Aus dem Q-Wert $Q_K = 0{,}58$ folgt in 1 *m* HCl ein Reduktionspotential von −0,81 V (G. K. E.). Bei Erniedrigung der Behälterhöhe des Hg-Niveaugefäßes vergrößert sich diese Welle sowohl bei gleichstrompolarographischer als auch bei oszillopolarographischer Messung. JEHRING u. MEHNER [4] beobachteten diese Welle bei der Breyerschen Wechselstrompolarographie nicht, vermutlich deshalb, weil sie nur eine kleine Tropfzeit (1 s) und eine andere Grundlösung (0,5 *m* KCl) anwendeten.

Auch oszillopolarographisch ist die Stufe 3 bei t = ls nicht zu beobachten. Die Temperaturabhängigkeit (Abb. 3) und die Abhängigkeit von Gelatinezusatz deuten auf den kinetischen Charakter dieser Welle hin. Es handelt sich wahrscheinlich um die Reduktion eines Folgeproduktes, das aus dem Radikal $Bu_2Sn^{+\cdot}$ entsteht. Analytisch ist die Stufe 3 schlecht verwertbar.

Allgemein muß noch festgestellt werden, daß bei steigender HCl- oder Cl^--Konzentration alle Stufen unempfindlicher werden. Mit den Grundlösungen

1) 20% *i*PrOH, 0,6 *m* HCl; 2) 0,4 *m* KCl, 0,04 *m* KOH; 3) 0,5 *m* KCl und Britton—Robinson-Puffer, pH 9,9; 4) 0,6 *m* HCl und 0,6 *m* LiCl

wurden keine Verbesserungen erzielt.

Das $Bu_2Sn(OCOCH_3)_2$ verhält sich auch bei höherer Alkoholkonzentration wie das Bu_2SnCl_2 (60% EtOH, 4,8 *m* HCl). Bei höherer DB-Konzentration (über 10^{-3} M/l) entstehen immer mehr neue Stufen, und das Kurvenbild wird unübersichtlich.

4. Untersuchungen an Tributylzinnchlorid und -acetat (TB)

Tributylzinnchlorid und -acetat verhalten sich, wie Dibutylzinnchlorid und -acetat, oszillopolarographisch gleich.

Im Grundlösungssystem EtOH (20—80%)/HCl (0,6—7,2 *m*)/H_2O erscheint nur eine reversible Welle. In alkoholarmer Lösung ist diese Welle bei $1 \cdot 10^{-4}$ *m* Bu_3Sn^+ kaum zu bemerken (Abb. 5a). Bei Alkoholzusatz werden die Einschnittiefen des anodischen und kathodischen Kurventeils ver-

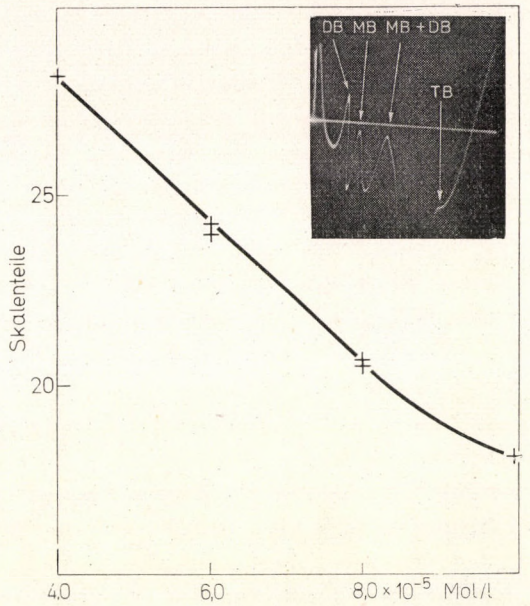


Abb. 4. Eichkurve zur Bestimmung von Bu_2Sn^{++} neben $BuSn^{+++}$, Bu_3Sn^+ und Bu_4Sn. ($C_{BuSn}{}^{+++} = 2{,}18 \cdot 10^{-4}$ M/l; $C_{Bu_3Sn}{}^{+} = 1{,}0 \cdot 10^{-5}$ M/l; $C_{Bu_4Sn} = 1 \cdot 10^{-5}$ M/l; 0,35 mA; Tropfzeit: 3s, Q = 0,14 in 0,6 *m* HCl). Oszillogramm: $C_{Bu_2Sn}{}^{++} = 1 \cdot 10^{-4}$ M/l

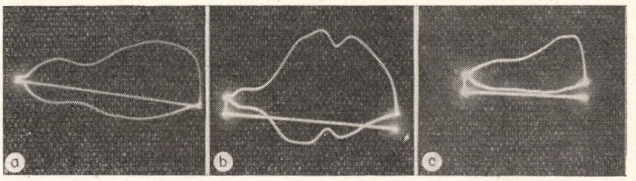


Abb. 5. Oszillogramme von $1 \cdot 10^{-4}$ M/l Bu_3Sn^+ in HCl/EtOH/H_2O-Gemischen: a) 1% EtOH; 0,6 *m* HCl; b) 20% EtOH; 0,6 *m* HCl; c) 20% EtOH; 7,2 *m* HCl

stärkt. Bei 20 Vol % *i*PrOH und 0,6 *m* HCl gelingt es, noch $6 \cdot 10^{-7}$ M/l Bu_3Sn^+ nachzuweisen. Das Bu_3Sn^+-Ion ist also in der alkoholhaltigen elektrischen Doppelschicht angereichert. Bei weiterer Erhöhung des Alkoholgehaltes geht die Empfindlichkeit des TB-Nachweises wieder zurück, da jetzt die Hemmung des Elektronendurchtritts erfolgt. In 1 *m* HCl mit 10% EtOH wurden die Q-Werte $Q_A = Q_K = 0{,}64$ bei 0,65 mA ermittelt. Daraus ergibt sich ein Potentialwert von $-0{,}93$ V (G. K. E.).

Die Verwendung von *tert.* Butylalkohol anstelle von Isopropylalkohol führte zu keiner Steigerung der Empfindlichkeit. Eine Erhöhung der HCl- oder Cl^--Konzentration verringerte die Einschnittiefen. Bei der Veränderung der Gleichstromkomponente wurde beobachtet, daß bei höheren Gleichstromwerten die Adsorption des Alkohols verstärkt wurde, da sich die Grundlösungs-

kurve erhöhte. Gleichzeitig wurde die Einschnitttiefe für das Bu_3Sn^+ mit vergrößert. Es ergab sich schließlich eine optimale Einstellbedingung zum TB-Nachweis in 0,6 *m* HCl, 20% *i*-PrOH am Polaroskop P 576: 0,1—0,15 mA; t = 3s; Q = 0,55 (Elektrode nicht voll polarisiert). Bei kurzen Tropfzeiten (t = 1s) ist die Empfindlichkeit stark herabgesetzt, da der Anreicherungsprozeß des Bu_3Sn^+ in der Doppelschicht erst bei größerer Tropfenoberfläche bemerkbar wird. Gelatineeinfluß und Temperaturabhängigkeit deuten auf einen kapazitiven Einschnitt hin. Es findet aber auch gleichzeitig ein Redoxprozeß statt. Der von COSTA für die gleichstrompolarographische Reduktion vorgeschlagene [1] Mechanismus (... über das Trialkylzinnradikal zum Hexaalkyldizinn) steht mit dem Verschwinden der oszillopolarographischen Einschnitte bei Gelatinezugabe nicht im Widerspruch.

In 0,5 *m* KCl mit Britton—Robinson-Puffer-Lösung (pH 9,9) und 30% *i*-PrOH erscheinen zwei Wellen $Q_{1A} = Q_{1K} = 0{,}43$; Q_{2K} (irreversibel) = 0,76, die auch von JEHRING und MEHNER mit der Breyerschen [4] Methode beobachtet wurden. Aus der Annahme, daß das positive Grenzpotential +0,03 V, das negative —1,85 V beträgt, lassen sich die Potentialwerte zu $E_1 = -0{,}80$ V (reversibel) und $E_2 = -1{,}40$ V (irrev.) näherungsweise berechnen.

JEHRING und MEHNER [4] erhielten in der gleichen Grundlösung die Werte —0,9 V und —1,4 V (G. K. E.).

Abgesehen von den allgemeinen Nachteilen der Verwendung alkalischer Grundlösungen übertrifft die Empfindlichkeit der Bestimmung des Bu_3Sn^+ im sauren Medium stark die Empfindlichkeit, die im alkalischen erreicht wird.

Die oben genannte Grundlösung von 20% Isopropylalkohol und 0,6 *m* HCl lieferte den empfindlichsten Nachweis (kath. Einschnitt). Die Eichkurve, die mit dieser Grundlösung erhalten wird, ist bei strenger Konstanthaltung des *i*-PrOH-Gehaltes gut reproduzierbar. Die Probelösung darf nicht zu lange bei geschlossenem Stromkreis über dem Bodenquecksilber stehen, da durch die Bildung von Kalomel der Widerstand des Bodenquecksilbers zu groß wird, und das Oszillogramm verzerrt erscheint.

Bestimmung des TB im Gemisch

Am elegantesten ist die Bestimmung des TB im Gemisch mit DB, MB und ¡Tetrabutylzinn, ohne vorherige Abtrennung des überschüssigen DB. Es lassen sich neben $3{,}6 \cdot 10^{-4}$ M/l MB noch $2 \cdot 10^{-6}$ M/l TB bestimmen. Weiterhin kann man (0,1 mA, 3s) $8 \cdot 10^{-7}$ M/l TB neben $1 \cdot 10^{-5}$ M/l DB erfassen. Eine Steigerung des DB-Überschusses ist nicht möglich. Das gleichzeitige Vorliegen von $1 \cdot 10^{-5}$ M/l DB und $1{,}45 \cdot 10^{-5}$ M/l MB und $1 \cdot 10^{-5}$ M/l Tetrabutylzinn behindert nicht die Sichtbarmachung des TB-peaks bei einer Konzentration des Bu_3Sn^+ von $8 \cdot 10^{-7}$ M/l (0,15 mA; 3s). Die Änderung der Größe des TB-Einschnittes mit wachsender Konzentration ist so groß, daß eine oszillopolarographische Titration gut möglich ist. So wurden auf diese Weise für 4,68 Gew. % TB in MB die Werte 4,9% und 4,5% wiedergefunden.

Bestimmt man das TB nach vorheriger Hydrolyse des DB, läßt sich der TB-Nachweis neben viel größeren Mengen an DB durchführen. In alkalischen Lösungen braucht keine Phasentrennung zu erfolgen, denn das TB kann auch bei Anwesenheit des DB-Niederschlags bestimmt werden. So wurden in 30% *i*-PrOH, Britton—Robinson-Pufferlösung (pH 9,9) und 0,5 *m* KCl $1 \cdot 10^{-4}$ M/l Bu_3Sn^+ neben $2 \cdot 10^{-2}$ M/l Bu_2Sn^{++} nachgewiesen (0,15 mA; 1,9s;

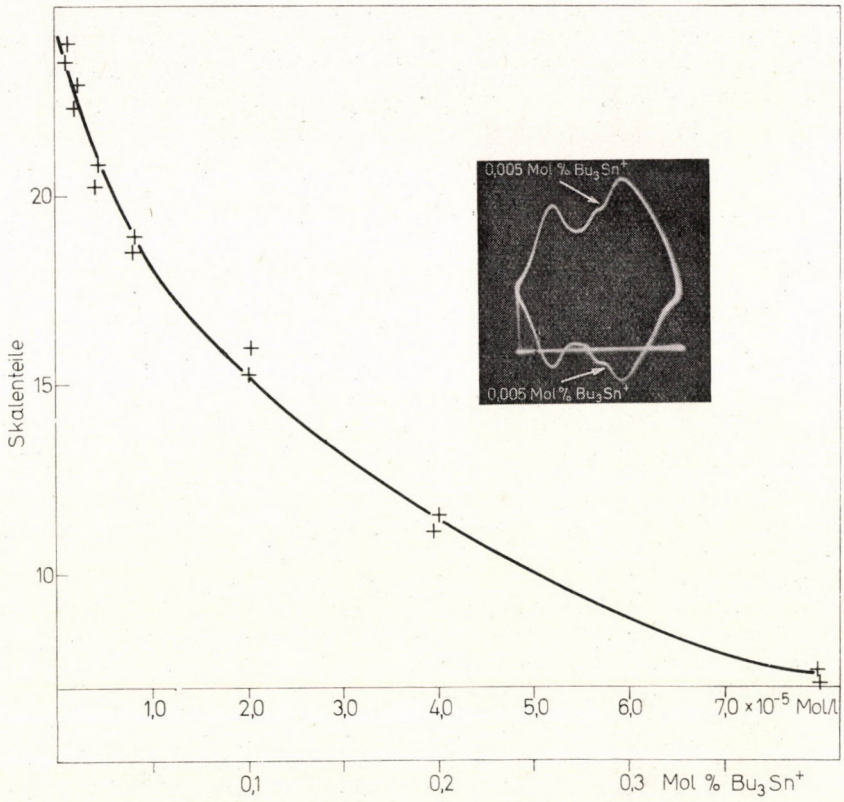


Abb. 6. Eichkurve zur Bestimmung von Bu_3Sn^+ nach hydrolytischer Abtrennung des Bu_2Sn^{++}. (Grundlösung: 20% *i*-PrOH, 0,6 *m* HCl; 0,1 mA; $C_{Bu_2Sn^{++}}$ vor der Abtrennung: $2 \cdot 10^{-2}$ M/l.) Oszillogramm: 0,005 Mol % Bu_3Sn^+ in Bu_2Sn^{++}

Behälterhöhe: 40 cm). Das DB wird nicht angezeigt. Fällt man das DB mit 0,04 *m* KOH, filtriert und säuert dann mit soviel konzentrierter Salzsäure an, daß die HCl-Konzentration 0,6 M/l beträgt, lassen sich noch 0,005 Mol % TB neben DB nachweisen. Die entstehende DB-Restwelle bleibt bei konstanten Fällungsbedingungen gleich. Maximal $4 \cdot 10^{-4}$ M/l MB können ebenfalls anwesend sein, und der TB-peak ist bei 0,05 Mol % TB (auf DB bezogen) noch sichtbar (Abb. 6). Die Eichkurve, in Abb. 6 dargestellt, ist bei konstanten Fällungsbedingungen des DB gut reproduzierbar. Liegt zusätzlich Tetrabutylzinn bereits in einer Suspension vor, wird das TB mit dem Tetrabutylzinn am Niederschlag des DB teilweise festgehalten, und die Bestimmung wird unmöglich.

Bestimmung des Triphenylzinnacetats

Triphenylzinnacetat stellt ein wichtiges Fungicid dar. Da es stark giftig ist, macht sich eine analytische Kontrolle erforderlich. In der Literatur sind nur ungenügende Methoden zur Bestimmung von Spuren $Ph_3SnOCOCH_3$ beschrieben. BÜRGER [8] z. B. entbindet das Benzol durch Protolyse unter gleichzeitiger Einwirkung von H_2 und bestimmt dieses. GORBACH und BOCK [19] veraschen auf nassem Wege das $Ph_3SnOCOCH_3$ und bestimmen das Sn^{4+} polarographisch.

Das Ph_3Sn^+-Ion wird wie das Bu_3Sn^+-Ion in der *i*-PrOH-haltigen elektrischen Doppelschicht am Hg angereichert und durch einen reversiblen Einschnitt angezeigt ($Q_{anod.} = Q_{kath.} = 0{,}46$ in 0,6 *m* HCl). Die Empfindlichkeit steigt ein wenig, wenn Benzylalkohol zugegen ist.

Es können $Ph_3SnOCOCH_3$-Konzentrationen ab $4 \cdot 10^{-6}$ M/l quantitativ bestimmt werden. Da zur Bestimmung 1 ml Meßvolumen ausreicht, kann man $1{,}6 \cdot 10^{-6}$ g noch erfassen. Sowohl Empfindlichkeit als auch Schnelligkeit und qualitative Sicherheit der Bestimmung übertreffen die in der Literatur beschriebenen Verfahren. In der verwendeten Grundlösung 0,6 *m* HCl, 20 Vol % *i*-PrOH und 4% Benzylalkohol wurde keine protolytische Zersetzung des $Ph_3SnOCOCH_3$ beobachtet.

5. Untersuchungen an Tetrabutylzinn

Bu_4Sn ist an der Quecksilbertropfelektrode nicht reduzierbar. Es wurde jedoch auch kein kapazitiver Einschnitt gefunden.

Bei der Bestrahlung im UV-Licht lassen sich oszillopolarographisch in Abhängigkeit von der Zeit zuerst TB und dann DB nachweisen. Leider erfolgt die Umsetzung undefiniert und ist analytisch nicht verwendbar. Die dünnschichtchromatographische Abtrennung und Zersetzung des Bu_4Sn mit H_2SO_4 conc./HNO_3 conc. zu Sn^{4+} [17] erfolgt zu langsam, um ein empfehlenswertes analytisches Verfahren zu ergeben.

LITERATUR

1. Costa, G.: Gazz. chim. ital. **80** (1950), 42—62
2. Allen, R. B.: "Dissertation Abstracts" **20** (1959), 897
3. Jehring, H. u. H. Mehner: Z. Chem. **3** (1963), 472
4. Jehring, H. u. H. Mehner: Z. Chem. **3** (1963), 34
5. Lorberth, J. u. H. Nöth: Chem. Ber. **98** (1965), 969
6. Kriegsmann, H. u. S. Pischtschan: Z. anorg. allg. Chem. **308** (1961), 212
7. Kozeschkow, K. A.: Ber. dtsch. chem. Ges. **62** (1929), 996
8. Bürger, K.: Z. Lebensmittel-Unters. u. Forschung **114** (1961), 1—8
9. Seyfert, D.: Naturw. **44** (1957), 34
10. Kalvoda, R.: »Die Technik oszillopolarographischer Messungen«. Verlag Steinkopff, Dresden—Leipzig, 1965
11. Heyrovsky, J. u. R. Kalvoda: »Oszillographische Polarographie mit Wechselstrom«. Akademie-Verlag, Berlin, 1960
12. Heyrovsky, M.: Diplomarbeit, Prag; referiert in [11]
13. Röske, P.: Diplomarbeit 1964, TH Merseburg
14. Spichale, W., J. Efer u. D. Quaas: Z. Chem. **10** (1965), 390
15. Gibbons, A. J., A. K. Sawyer u. A. Ross: J. org. Chemistry **26** (1961), 2304
16. Jezdinsky, R.: Chem. Zvesti **16** (1962), 295
17. Beydatsch, R.: Diplomarbeit 1965, Merseburg, TH f. Chemie »Carl Schorlemmer«
18. Rotermund, U.: Diplomarbeit 1965, Merseburg, TH f. Chemie »Carl Schorlemmer«
19. Gorbach, S. u. R. Bock,: Z. anal. Chem. **163**, 429 (1958)

R. Geyer, U. Rotermund; Institut für Analytische Chemie der Technischen Hochschule »Carl Schorlemmer« Leuna-Merseburg. DDR

Acta Chimica Academiae Scientiarum Hungaricae, Tomus 59 (2), pp. 211—223 (1969)

ON SOLVOLYSIS OF "ALKYLPYROPHOSPHORIC ACID METAL SOLVENT EXTRACTANTS"

Cs. ÚJHELYI

(Institute of Nuclear Research of the Hungarian Academy of Sciences, Debrecen)

Received June 27, 1967; in revised form August 5, 1968

The increase in the quantity of strong (primary) acid hydrogen during spontaneous solvolysis of the reaction products of phosphorus(V) oxide and an alcohol (*n*-butanol, or *n*-octanol) has been noted and interpreted as due to the alcoholysis or hydrolysis of the cyclic alkyltriphosphoric acid present among the reaction products.

It has been found that the mole ratio of weak (secondary) to strong acid hydrogen measured immediately after reaction in reaction products does not depend on the $n(\text{alcohol})/n(P_2O_5)$ mole ratio of the solution of reaction products.

Phosphoric acid, too, is formed in the hydrolysis of the so-called "dialkylpyrophosphoric acid extractants" (obtained by the reaction of phosphorus(V) oxide with an alcohol) used for the preparation of monoalkylorthophosphoric acid extractants. The formation of phosphoric acid is interpreted as due to the hydrolysis of the condensed alkylphosphoric acids containing more than two phosphorus atoms.

Introduction

For the extraction, and purification, of uranium and various other metals [1—6], "dialkylpyrophosphoric acid", obtained by the reaction of phosphorus (V) oxide with an alcohol, has found extensive application. The reaction between phosphorus(V) oxide, suspended in an inert diluent, and an alcohol at a mole ratio $R = n(\text{ROH})/n(P_2O_5) \sim 2$, can be represented according to LONG *et al.* [1], and GRINSTEAD *et al.* [4] as follows

$$2\text{ROH} + P_2O_5 \rightarrow \text{RO}-\underset{\underset{\text{OH}}{|}}{\overset{\overset{\text{O}}{\uparrow}}{\text{P}}}-\text{O}-\underset{\underset{\text{OH}}{|}}{\overset{\overset{\text{O}}{\uparrow}}{\text{P}}}-\text{OR} \qquad (1)$$

where ROH is an alcohol of 4 to 17 carbon atoms.

ZANGEN [7] claimed that "di-*n*-octylpyrophosphoric acid, OPPA" [1] is a mixture of seven unidentified components. In a comparison of uranium extractions from phosphoric acid with "OPPA" on the one hand, and with pure di-*n*-octylpyrophosphoric acid synthesized from phosphorus oxychloride, on the other, he found the extractive capacity of "OPPA" to be greater by two orders of magnitude.

SHIMA *et al.* [8] have identified the reaction products, at a mole ratio of $R \sim 100$, of dry ethanol with α-phosphorus(V) oxide: about 9% of the phosphorus is present in ortho-, 59% in pyro-, 12% in linear tri- (tripoly), 11% in cyclic tri-(trimeta)-phosphate and 4% in a highly polymerized poliphosphate form.

Hydrolytic cleavage of dialkylpyrophosphoric acid leads to the corresponding monoalkylorthophosphoric acids [4, 5, 6],

$$HO(RO)PO(O)PO(OR)OH + HOH \rightarrow 2(HO)_2PO(OR) \qquad (2)$$

Upon alcoholytic degradation, dialkylpyrophosphoric acid yields a mixture of monoalkyl- and dialkylorthophosphoric acids

$$(HO)_2(RO)_2P_2O_3 + ROH \rightarrow (HO)_2PO(OR) + (HO)PO(OR)_2 \qquad (3)$$

The reaction of phosphorus(V) oxide, used directly or suspended in ether, with an alcohol is given by the following equation [9a]

$$3\ ROH + P_2O_5 \rightarrow (HO)_2PO(OR) + (HO)PO(OR)_2 \qquad (4)$$

Eq. (4) is obtained by summarizing Eqs (1) and (3).

An approximate description of the partial alcoholysis of phosphorus(V) oxide is given [9b] by the following equations

$$2\ ROH + P_2O_5 \rightarrow (HO)_2(RO)_2P_2O_3$$
$$5\ ROH + 3\ P_2O_5 \rightarrow (HO)_3(RO)_2P_3O_5 + (HO)_2(RO)_3P_3O_5$$

Yields from 70 to 90% have been found [4, 5, 6] for monoalkylortophosphoric acid prepared according to Eq. (2). GRINSTEAD [5] claimed the presence of a substantial quantity of phosphoric acid in the aqueous phase (1 *M* for HCl) after hydrolysis. The formation of phosphoric acid cannot be explained by Eqs (1) and (2) because monoalkylorthophosphoric acids produced under the conditions of hydrolysis practically do not yield phosphoric acid [4, 5].

The present paper attempts to give an interpretation for the continuous increase of the primary acid hydrogen in reaction products prepared at various *R* mole ratios; and of the formation of phosphoric acid in the preparation of monoalkylorthophosphoric acids. This paper proves the approximate correctness of Eq. (4), in agreement with other authors [9a, 11, 12], and in disagreement with CHERNYAK and NAVTANOVICH [10].

Experimental

Chemicals. G.R. grade chemicals (REANAL Co., Budapest) were used throughout. The exceptions were phosphorus(V) oxide (from Établissements KUHLMANN, grade "léger"), and *n*-octanol (from FLUKA, purissimum grade). According to VAN WAZER [13a] commercially available phosphorus(V) oxide consists mainly of the hexagonal modification.

Preparation of the reaction products of phosphorus(V) oxide and *n*-butanol, or *n*-octanol

The reactions were carried out in beakers of 0.4 to 1 litre capacities, placed into melting ice. To phosphorus(V) oxide, vigorously stirred in carbon tetrachloride (1 g P_2O_5 in 3 to 11 ml) the alcohols were added. After stirring for 12 to 50 minutes, the undissolved residue was filtered off on an ice cooled G3 glass filter. In the solution of the reaction products obtained in our experiments the mole ratio R = [reacted and free alcohol]/[reacted phosphorus(V) oxide] was $2.3 \leq R \leq 7$. A considerable amount of the applied phosphorus(V) oxide did not dissolve under the experimental conditions. Data of a few typical experiments are listed in Table I. The temperature of the reaction products, within $\sim$ 15 minutes after the addition of the alcohol, fell to near 0 °C even after a maximum temperature of $\sim$ 70 °C.

Table I

Data on the preparation of reaction products

Experiment	$m^{init.}_{P_2O_5}$ [g]	t_{ROH} [min]	Max. temp. °C	$\frac{m^{react.}_{P_2O_5}}{m^{init.}_{P_2O_5}}$	g P_2O_5/litre	$\frac{n_{ROH}}{n_{P_2O_5}}$	t_0 [hour]	$\frac{v_1(0)}{v_1(t_{max})}$ [ml/ml]	Secondary/primary acid H mole ratios at times	
									$t = 0$	$t > t_{max}$
2/4 BuPa	71.0	1.5	76	0.83	194	2.4	0.5	0.91	0.15	0.23
2/5 BuPa	50.0	0.05	27	0.81	67	2.8	1.0	0.72	0.09	0.37
2/9 BuPa	35.5	1.0	64	0.81	196	2.7	0.5	0.90	0.16	0.47**
4/3 BuPa	75.2	90*	7	0.57	106	7.0	2.3	0.83	0.08	0.58
4/4 BuPa	50.2	0.05	28	0.97	78	4.1	0.6	0.84	0.07	0.55
2/1 OcPa	35.5	1.1	70	0.87	168	2.3	0.3	0.91	0.15	0.28
3/1 OcPa	35.9	1.5	71	0.93	152	3.2	0.4	0.87	0.16	0.60

BuPA = *n*-butylphosphoric acids; OcPA = *n*-octylphosphoric acids; t_{ROH} = time of the addition of the *n*-alcohol to the phosphorus(V) oxide suspended in carbon tetrachloride; Max. temp. = the maximum temperature noted during reaction, which significantly decreases within a few minutes; g P_2O_5/litre = the concentration of the solutions of the reaction products; t_0 = time elapsed between the start of alcohol addition and the start of the first titration; $t = 0$ = the point of time of the first titration of the reaction products cooled to about 0—4 °C after reaction; $t > t_{max}$ = point of time of the titration of reaction products kept at 60 °C for about 5 days.

* Manual agitation.

** This value is exceptionally high because the water content of the *n*-butanol used was higher than in other experiments *(cf.* Expt. 2/5 BuPA).

(In carbon tetrachloride solutions of *n*-butylphosphoric acids of $R < 3$ mole ratios, at concentrations below $\sim$ 200 g P_2O_5/litre, two phases were formed at 0 °C after the reaction had completed. The two phases could be homogenized by adding *n*-butanol. Since we intended to work with a homogeneous medium even at 0 °C, R was kept not lower than 2.4 in our experiments.)

It has been found that solutions at $2 < R < 3$ mole ratios, colourless immediately after preparation, turned yellow-brown within a certain period depending on temperature (one day at 60 °C). No colouration appeared in preparations at $R > 3$ mole ratios.

Aqueous extraction of the reaction products of *n*-butanol and phosphorus(V) oxide

When the carbon tetrachloride solutions of the reaction products at $2 < R < 3$ mole ratios were extracted with an equal volume of water, the upper phase was an emulsion which separated into two phases after some time. (The higher the mole ratio was, the faster the upper emulsified phase separated into two, because by increased butanol content the formation of emulsion decreased. In the cases of products at $R > 3$ mole ratios the upper aqueous phase did not separate into two.)

Hydrolysis, and alcoholysis, of the reaction products

In beakers of 0.6 to 1.0 litre capacities, under continuous vigorous stirring for 20 to 100 hours, in volumes 0.1 to 0.9 litre, 20 to 100 ml portions of the carbon tetrachloride solution of the reaction products were hydrolyzed with water at 70 to 90 °C, and 0.1 to 3 *N* primary acid hydrogen ion concentration. The evaporated water was intermittently replaced in order to maintain the initial 0.5 to 0.9 litre volume. It was found that under these conditions hydrolysis is practically complete and that splitting off of alcohol from the dialkyl- and from the monoalkyl-orthophosphoric acids formed does not exceed the limits of systematic errors of determinations.

The hydrolyzed reaction products were stirred and evaporated till one phase was produced. The homogeneous solution thus obtained was diluted with ethanol to 50 or to 100 ml and then titrated. (In order to reduce the viscosity of the residue a few ml octanol was added to octylphosphoric acids at the end of the evaporation.)

The alcoholysis of the reaction products was carried out at 60 °C in a thermostat. Care was taken that no water should contaminate the samples else the quantity of monoalkylorthophosphoric acid is increased considerably (*cf.* Expt. 2/9 BuPA, in Table I).

Determination of primary, secondary, and tertiary acid hydrogen in the presence of each other

From sodium hydroxide pellets an $\sim$ 50 wt % aqueous solution was prepared. This was centrifuged, and filtered through a G4 glass filter. The clear solution was diluted to obtain an $\sim$ 0.1 *N* sodium hydroxide solution. Bromo-cresol green and methyl orange indicator mixture, and a reference solution, were used for the determination of primary acid hydrogen. The volume of the solution titrated to the colour of sodium dihydrogen phosphate reference solution prepared in the same way was $\sim$ 80 ml and contained 2 drops of a 0.1% solution of bromo-cresol green in 20% ethanol (one drop per 40 ml of the titrated solution) and one drop of a 0.05% aqueous methyl orange solution (one drop per 80 ml). Deviation in titrations was $\sim$ 0.03 ml of 0.1 *N* sodium hydroxide.

Then, after addition of four drops of a 1% solution of phenolphthalein in 60 *v*/*v* % alcohol, (one drop per 20 ml), the solution was titrated to maximum colour intensity, for the determination of the secondary acid hydrogen. Deviation was $\sim$ 0.06 ml of 0.1 *N* sodium hydroxide.

For the determination of the tertiary acid hydrogen of phosphoric acid, the method of TILLMANS and BOHRMANN [14] was modified. To precipitate phosphate (PO_4^{3-}) 0.5 to 2.0 ml of a 6 *M* calcium chloride solution was added during shaking to $\sim$ 100 ml of the solution titrated to maximum phenolphthalein colour intensity. After the addition of 4 drops of phenolphthalein, the colourless solutions were titrated under vigorous stirring for $\sim$ 2 minutes (irrespective of their phosphoric acid content) to maximum colour intensity. (The solutions gradually lose their colour.) Deviation was $\sim$ 0.1 ml of 0.1 *N* sodium hydroxide.

The titration of the reactions products of phosphorus(V) oxide and *n*-butanol was carried out in the aqueous phase. To obtain clear phases the reaction mixture was diluted with water. In samples with lower free butanol contents ($2 < R < 3$) the addition of 0.5 to 1 ml of butanol might be necessary. Titrations of the products obtained with *n*-octanol were carried out in its aqueous ethanol solutions. In the $\sim$ 80 ml solutions present after the titrations of primary acid hydrogen, 40 to 50 vol % was the alcohol content. In titrations of reaction products with lower free octanol contents ($2 < R < 3$) the opalescence of the solution was stopped by the addition of 0.5 to 1.0 ml octanol.

Determination of the secondary/primary, and tertiary/primary acid hydrogen mole ratios

Let v_1, v_2, and v_3, respectively, stand for millilitres of 0.1 N sodium hydroxide consumed in the titration of the primary, the primary + secondary, and the primary + secondary + tertiary acid hydrogen ($10 < v_1 < v_2 < v_3 \leq \leq 50$ ml). The apparent secondary/primary and tertiary/primary acid hydrogen (H) mole ratios are given by the volume ratios $(v_2-v_1)/v_1$ and $(v_3-v_2)/v_1$.

The apparent secondary/primary acid H mole ratio $(v_2-v_1)/v_1$ for phosphoric acid is 1.02 ± 0.01, for monoalkylphosphoric acid this is 1.00 ± 0.01. From these values it follows that even in solutions of alkylphosphoric acids which contain phosphoric acid the apparent secondary/primary acid H mole ratio is equal within the limits of error with the true mole ratio.

The apparent tertiary/primary acid H mole ratios $(v_3-v_2)/v_1$ in pure solutions of phosporic acid and solutions of alkylphosphoric acids and phosphoric acid were the same within limits of error, and the $[(v_3-v_2)/v_1]_{H_3PO_4}$ value, at titrations performed in ~ 2 minutes, was 0.90 ± 0.03 instead of 1.00, which is the true mole ratio.

The true tertiary/primary acid H mole ratio for mixtures of phosphoric acid and alkylphosphoric acids is equal to the quotient

$$[(v_3 - v_2)/v_1]_{mixt.}/[(v_3 - v_2)/v_1]_{H_3PO_4}.$$

Calculation of the acid mole fractions of the orthocomponents from acid hydrogen mole ratios

The acid mole fraction $x(H_3PO_4)$ of phosphoric acid, derived exclusively from the acid components of HR_2PO_4, H_2RPO_4, and H_3PO_4, is given exactly by the true tertiary/primary acid H mole ratio of the reaction products solvolyzed to ortho form. (If the quantity of primary acid hydrogens in the titrated reaction products is less than the quantity found after complete alcoholysis or hydrolysis then this must be taken into account).

The secondary/primary acid H mole ratio gives the sum $x(H_2RPO_4) + + x(H_3PO_4)$ of the acid mole fractions of monoalkylorthophosphoric acid and phosphoric acid. The acid mole fraction of dialkylorthophosphoric acid is given by the equation $x(HR_2PO_4) + x(H_2RPO_4) + x(H_3PO_4) = 1$.

Results

Alcoholysis of the reaction products

Increase in the quantity of primary acid hydrogens — In the course of partial ($R < 3$), and complete ($R > 3$) spontaneous (non catalyzed) alcoholysis a steady increase in primary acid hydrogen content up to a constant value

was observed. Deviation from unity of the primary acid hydrogen ratio given as $v_1(0)/v_1(t_{max}) < 1$(see Table I) expresses the measure of total increase. The $v_1(0)$ volume of the sodium hydroxide solution consumed for primary acid hydrogens was determined immediately after the reaction in a portion of the filtrate obtained by filtering off the insoluble residue. The time of titration was arbitrarily chosen as $t = 0$. The $v_1(t_{max})$ values were determined in the reaction products kept at 60 °C for a few days. The values $v_1(0)$, and thus those of $v_1(0)/v_1(t_{max})$ too, greatly depend on the experimental conditions.

Maximum primary acid hydrogen increase noted for reaction products of $R < 3$ mole ratios was lower than the increase that occurred for complete alcoholysis after addition of alcohol ($R > 3$).

Increase in the secondary/primary acid hydrogen mole ratio — The secondary/primary acid H mole ratios measured in the reaction products at times $t = 0$ and $t > t_{max}$ are listed in Table I. Mole ratios measured at $t > t_{max}$ reached their maximum, practically constant, values.

Constancy of the secondary/primary acid hydrogen mole ratio in products immediately after the reaction of phosphorus(V) oxide and the alcohol

In the reaction products (in the filtrate obtained immediately after the, generally partial, dissolution of phosphorus(V) oxide, at $t = 0$) the values of secondary/primary acid H mole ratios are practically constant. The values of mole ratios depend mainly on the maximum temperature found during reaction, and are independent of the R values of the solutions of the reaction products. From the data of Table I it can be seen that in reaction products formed in the maximum temperature range from 64 to 76 °C the value of the mole ratio is ~ 0.15 while in the range from 7 to 28 °C it is ~ 0.08. (Of course, with lapse of time these values increase in consequence of alcoholysis. The rate of increase of mole ratios increases with the temperature and/or with the value of R.)

In contrary to our findings CHERNYAK and NAVTANOVICH [10] claimed that with an increase from 2 up to 6 of the value of R the weight fraction (0.12) of the monobutyl ester increases fivefold. In accordance with our results, SHIMA *et al.* [8] found $\sim 9\%$ of the converted phosphorus in the ortho form, even after reactions at rather high, $n(EtOH)/n(P_2O_5) \sim 100$, mole ratios.

Complete alcoholysis upon addition of alcohol of reaction products at $R < 3$ mole ratios

It has been found that in the $R < 3$ mole ratio reaction products, after the elapse of certain period, the secondary/primary mole ratio increases up to a constant value (*cf.* Table I), because the free alcohol concentration of the

reaction mixture is so low that no further alcoholysis can proceed. These various secondary/primary acid H mole ratios, each a function of the instantaneous value of $R < 3$ (*cf.* Table I), increase up to a constant value (~ 0.6) corresponding to complete alcoholysis, after the addition of alcohol ($R > 3$).

Hydrolysis of the reaction products

In Table II primary acid hydrogen ratios $[v_1(t \geq 0)/v_1(t_{max})]_{hydr.} \leq 1$ measured at times $t \geq 0$, and $t \geq t_{max}$ are listed. The $v_1(t \geq 0)$ ml sodium hydroxide consumption figures, for reaction products kept at 0° C, were determined prior to aqueous hydrolysis, $v_1(t_{max})_{hydr.}$ figures were determined after aqueous hydrolysis. The increase of primary acid hydrogens at hydrolysis was found to agree within 2 to 3% with the increase noted at complete alcoholysis in solutions of reaction products of mole ratios $R > 3$.

Table II

Data for the aqueous hydrolysis of reaction products

Experiment	$\frac{n_{ROH}}{n_{P_2O_5}}$	$\frac{v_1\,(t \geqq 0)}{v_1(t_{max})}$ [ml/ml] ($\sim \pm 0.01$)	Secondary/primary acid hydrogen mole ratios		Tertiary/primary acid hydrogen mole ratios	
			before	after	before	after
			($\sim \pm 0.005$)		($\sim \pm 0.01$)	
			hydrolysis			
2/4 BuPA	2.4	0.86	0.15	0.87	0.02	0.25
	5.1	1.00	0.56	0.57	0.02	0.02
2/9 BuPa	2.7	0.86	0.16	0.88	0.03	0.30
	2.7	0.96	0.47	0.80	0.03	0.10
2/1 OcPA	2.3	0.87	0.15	0.88	0.02	0.26
	2.3	0.96	0.28	0.82	0.02	0.14
3/1 OcPa	3.2	0.87	0.16	0.87	0.02	0.25
	3.2	1.00	0.60	0.64	0.02	0.03

Duration of hydrolysis was 20 to 60 hours, at 80 $\pm$ 5 °C and 0.2—1 *N* primary acid hydrogen content.

Increase in secondary/primary acid hydrogen mole ratio — Table II shows values of mole ratios before, and after, hydrolysis. (For data referring to the preparation of the reaction products, *cf.* Table I.)

At hydrolysis of the products, with low secondary/primary acid H mole ratio, obtained directly after reaction, the values of mole ratios increased in much higher degrees than at alcoholysis. At hydrolysis of the practically completely alcoholyzed reaction products the increase was generally 1 to 2% (*cf.* Expt. 2/4 BuPA). In Expt. 3/1 OcPA, the $\sim 7\%$ increase indicates the alcoholysis prior to hydrolysis being incomplete.

Increase in the tertiary/primary acid hydrogen mole ratio — In the hydrolysis of reaction products with low secondary/primary acid H mole ratio, the tertiary/primary acid H mole ratio increased considerably (see Table II).

A similar result was obtained at the aqueous extraction of the reaction products of phosphorus(V) oxide and butanol (*cf.* experimental part). In various experiments, in the aqueous phase of the first extraction immediately after reaction, 36 to 40 acid mole %, while in the aqueous phase of the second extraction 22 to 25 acid mole% of phosphoric acid were found after the hydrolysis of the reaction products extracted.

Decrease in pH of solutions of reaction products titrated to maximum phenolphthalein colour intensity

During the first few hours, a rapid decrease in pH values was noted in solutions titrated to maximum phenolphthalein colour intensity immediately after reaction (see Table III). Titration of reaction products, of mole ratios $R <$

Table III

Decrease in pH of solutions of reaction products titrated immediately after reaction to maximum phenolphthalein colour intensity
($t = 0$ is the point of time when titrations were terminated)

Experiment	$\frac{v_1(t \geq 0)}{v_1(t_{max})}$	$\left(\frac{v_2 - v_1}{v_1}\right)_{t \geq 0}$	pH values at 23 ± 2 °C				
2/5 BuPA	0.72	0.091	pH	9.9	2.8		
	0.90	0.106	pH	10.0	5.2		
			hour	0.02	1.7×10^4		
2/9 BuPa	0.90	0.162	pH	9.8	7.77	7.19	7.01
			hour	0.02	4.3	290	700
	0.92	0.178	pH	9.5	8.12	7.45	7.27
			hour	0.02	1.1	290	700
2/1 OcPA	0.91	0.153	pH	11.1	9.03	8.28	8.12
			hour	0.01	2.3	310	720
	0.93	0.157	pH	11.0	9.15	8.39	8.23
			hour	0.02	1.3	310	720
3/1 OcPA	0.87	0.156	pH	10.8	8.76	8.07	
			hour	0.02	3.5	330	
	0.89	0.165	pH	10.5	8.92	8.37	8.22
			hour	0.05	2.6	330	740

Na^+ concentration of the solutions titrated: 0.14 ± 0.03 mole/litre. The value of $v_1 (t \geq 0)/v_1 (t_{max})$ indicates the ratio of primary acid hydrogens in the reaction products, measured at time $t \geq 0$. The value of $[(v_2 - v_1)/v_1]_{t \geq 0}$ indicates the mole ratio of secondary to primary acid hydrogen at time $t \geq 0$.

In Expts. 2/1 and 3/1 OcPA the solutions titrated contain 45, 35, and 40 vol % ethanol.

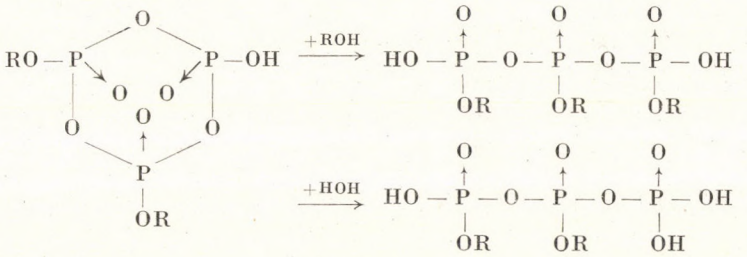
< 3, kept at room temperature for several years, revealed a decrease in pH values which was less than that found for solutions of reaction products titrated immediately after reaction.

The continuous decrease in pH of solutions of reaction products titrated to maximum phenolphthalein colour intensity points to a reaction which involves the liberation of hydrogen ions.

Discussion

Interpretation of the increase in primary acid hydrogens

SHIMA *et al.* [8] have stated that a cyclic ethyltriphosphoric acid is formed in the reaction of α-phosphorus(V) oxide and dry ethanol (*cf.* the introductory part). The increase in primary (strong) acid hydrogen content of the reaction products, can be ascribed to alcoholysis, or hydrolysis, of the cyclic mono- or dialkyltriphosphoric acid:



where R stands for an alkyl group.

The increase in primary acid hydrogens could be visualized also according to an interpretation given by CHERBULIEZ and WENIGER [11]. When titrating to methylorange end point the products of the reactions of phosphorus(V) oxide with aliphatic alcohols of 1—5 carbon atoms, these authors found that they could titrate 2 to 12% less phosphorus(V) oxide than had been introduced into the reaction. They attributed this "phosphorus loss", without experimental support, to the hydrolysis of a supposed trialkylpyrophosphoric acid,

$$(RO)_2PO(O)PO(OR)OH + HOH \rightarrow (HO)PO(OR)_2 + (HO)_2PO(OR)$$

This hypothesis is not tenable, since the rapid decrease in pH within a few hours in the solutions of reaction products titrated to maximum phenolphthalein colour intensity (pH 10 to 11) immediately after reaction (*cf.* Table III) cannot be interpreted by the hypothesis of CHERBULIEZ and WENIGER [11] because of the stability of pyrophosphoric acid (and chain phosphates generally), measured around pH 10 [13c].

Interpretation of the decrease in pH of solutions of reaction products titrated to maximum phenolphthalein colour intensity

According to VAN WAZER [13c] "splitting of the rings so as to form chains occurs quite rapidly in strongly basic solutions in which the chain phosphates are relatively very stable". Thus it seems to be obvious that in solutions of the reaction products titrated to maximum phenolphthalein colour intensity immediately after reaction the rapid decrease in pH is due in essence to the hydrolysis of cyclic alkyltriphosphoric acids (see Table III). Reaction products of $R < 3$ mole ratios were titrated after prolonged standing, too, when the secondary/primary acid H mole ratio had reached a constant value. A less pronounced decrease in pH of these solutions, is probably due to cyclic alkyltriphosphoric acid present in the reaction products after the termination of partial alcoholysis.

In solutions of *n*-butylphosphoric acids titrated to about pH 10 immediately after the reaction the pH value fell below the first equivalence point (pH $4._5$) that corresponds to primary acid hydrogens (see Expt. 2/5 BuPA, in Table III). This points to the fact that in the course of hydrolysis when cyclic butyltriphosphoric acid is converted into chain butyltriphosphoric acid also primary acid hydrogen is produced.

The rate of decrease in pH, observed in solutions of *n*-octylphosphoric acids titrated in aqueous ethanol immediately after the reaction to the equivalence point of primary acid hydrogens (pH $5._6$), cannot be interpreted on the basis of the lower rate of hydrolysis of trialkylpyrophosphoric acid, supposed by CHERBULIEZ and WENIGER [11].

Independence of the secondary/primary acid hydrogen mole ratio of the R mole ratio immediately after the reaction

Based upon results of SHIMA *et al.* [8] (*cf.* the introductory part), from the practically constant secondary/primary acid H mole ratio of the reaction products, measured immediately after reaction, it may be deduced that also in the reaction of *n*-butanol, or *n*-octanol, with phosphorus(V) oxide the products are formed in approximately the same ratio.

Interpretation of the formation of phosphoric acid at hydrolysis

Formation of phosphoric acid at complete hydrolysis of partially alcoholyzed reaction products can be explained by the presence of condensed alkylphosphoric acids containing more than two phosphorus atoms.

It could be observed that the sooner after the reaction of the phosphorus(V) oxide (*i.e.* at the lowest possible secondary/primary acid H mole ratios)

the reaction products are hydrolyzed the more phosphoric acid is formed. This might be interpreted on the basis that, after reaction (*i.e.* dissolving phosphorus(V) oxide), the conversion of condensed alkylphosphoric acids, that contain more than two phosphorus atoms, into dialkylpyrophosphoric acid proceeds at a steadily decreasing rate. Conversion is not complete even at higher secondary/primary acid H mole ratios, because even then phosphoric acid is formed (*cf.* data about Expts. 2/9 BuPA and 2/1 OcPA, in Table II).

In essence, the 2 to 3 acid mole % phosphoric acid produced at complete alcoholysis can be ascribed to the water content of phosphorus(V) oxide, and the water introduced in consequence of the preparation. This is supported by the fact that phosphoric acid content can be measured immediately after reaction. The incidental increase, during alcoholysis, of the phosphoric acid content fell within the limits of error of the determinations.

Losses in yield at the preparation of monoalkylorthophosphoric acid extractants

The reaction products, present in the solution filtered after dissolving phosphorus(V) oxide, were hydrolyzed immediately. Besides phosphoric acid the formation of HR_2PO_4 was observed, too (see Table IV). Irrespectively of R

Table IV

Acid mole fractions and mole ratios (calculated from data in Table II) of ortho acid components obtained after aqueous hydrolysis of the reaction products

Experiment	Acid mole fractions			$\frac{n_{H_2RPO_4}}{n_{HR_2PO_4}}$	$\frac{n_{H_2RPO_4}}{n_{H_3PO_4}}$	$\frac{n_{HR_2RPO_4}}{n_{H_3PO_4}}$
	$x_{HR_2PO_4}$	$x_{H_2RPO_4}$	$x_{H_3PO_4}$			
	($\sim \pm 0.01$)					
2/4 BuPA	0.13	0.62	0.25	4.8	2.5	0.5
	0.43	0.55	0.02			
2/9 BuPA	0.12	0.58	0.30	4.8	1.9	0.4
	0.20	0.70	0.10			
2/1 OcPA	0.12	0.62	0.26	5.2	2.4	0.5
	0.18	0.68	0.14			
3/1 OcPA	0.13	0.62	0.25	4.8	2.5	0.5
	0.36	0.61	0.03			

mole ratio, the acid mole fraction of the ortho components obtained after hydrolysis was approximately the same, because the start of hydrolysis immediately interrupts alcoholytic process. Acid mole % of HR_2PO_4 determined after hydrolysis was found to be approximately the same as the acid mole % of H_2RPO_4 present immediately after reaction (see Tables II, and IV). HR_2PO_4 is supposed to be present in the reaction products already before hydrolysis.

Deductions drawn from mole ratio figures of ortho acid components obtained after the solvolysis of the reaction products

The mole ratio figures of ortho acid components obtained from reaction products hydrolyzed immediately after reaction are approximately constant (see Table IV). (The deviations are due to the fact that the experiments could not be performed under identical conditions.)

The H_2RPO_4 content already present at the beginning of hydrolysis is taken into account in the $n(H_2RPO_4)/n(H_3PO_4)$ mole ratios (see Table IV). In view of this the average of the corrected values will be somewhat below two. (Even by reactions carried out at around 0 °C no reaction products could be obtained in which the secondary/primary acid *H* mole ratio would be near to zero (see Table I). Based upon communications of SHIMA *et al.* [8], it is supposed that secondary acid *H* content found after reaction derives mainly from monoalkylorthophosphoric acids.) These corrected values can be interpreted through the hydrolysis of cyclic dialkyltriphosphoric acid. The hydrolysis of cyclic dialkyltriphosphoric acid produces 2 moles of H_2RPO_4 and 1 mole of H_3PO_4, *viz.* the value of the $n(H_2RPO_4)/n(H_3PO_4)$ mole ratio is 2. The average value found somewhat less than two is may be due to the hydrolysis of the cyclic monoalkyltriphosphoric acid present in the reaction products. In the hydrolysis of cyclic monoalkyltriphosphoric acid 1 mole of H_2RPO_4 and 2 moles of H_3PO_4 are formed, *i.e.* the mole ratio is 0.5.

After complete alcoholysis carried out at mole ratios $R > 3$, constant mole ratios

$$n(H_2BuPO_4)/n(HBu_2PO_4) = 1.25 \pm 0.04$$

and

$$n(H_2OcPO_4)/n(HOc_2PO_4) = 1.51 \pm 0.05$$

were found instead of the $n(H_2RPO_4)/n(HR_2PO_4) = 1$ mole ratio according to Eq. (4). Thus Eq. (4) is only qualitatively correct. The experimental fact that $n(H_2BuPO_4)/n(HBu_2PO_4) < n(H_2OcPO_4)/n(HOc_2PO_4)$ can be explained, most likely, on the grounds that in a reaction of phosphorus(V) oxide with *n*-octanol relatively more cyclic monoalkyltriphosphoric acid is produced than in its reaction with *n*-butanol.

*

Addendum. — After our manuscript had been submitted we read the paper of ZANGEN *et al.* [15] wherein they reported the detection of cyclic dioctyl-, and monooctyltriphosphate among the reaction products of phosphorus(V) oxide and *n*-octanol.

The author wishes to express his thanks to Dr. S. SZALAY, Director of the Institute, for having made these studies possible, and to Mrs. E. ÚJHELYI for having carried out the experiments.

REFERENCES

1. LONG, R. S., ELLIS, D. A., BAILES, R. H.: Proc. 1st U. N. Int. Conf. P. U. A. E., Geneva, 1955; Vol. 8., p. 77.
2. LONG, R. S.: U. S. Pat. 2 866 680 (1958)
3. LEVINE, C. A., SKIENS, W. E., MOORE, G. R.: U. S. Pat. 2 947 774 (1960)
4. GRINSTEAD, R. R., SHAW, K. G., LONG, R. S.: Proc. 1st U. N. Int. Conf. P. U. A. E., Geneva, 1955, Vol. 8., p. 71.
5. GRINSTEAD, R. R.: U. S. Pat. 3 018 253 (1962)
6. BLACK, K. L., KOSLOV, J., MOORE, J. D.: Proc. 2nd U. N. Int. Conf. P. U. A. E., Geneva, 1958, Vol. 3., p. 488.
7. ZANGEN, M.: J. Inorg. Nucl. Chem., **16,** 165 (1960)
8. SHIMA, M., HAMAMOTO, K., UTSUMI, S.: Bull. Chem. Soc. (Japan), **33,** 1386 (1960)
9. KOSOLAPOFF, G. M.: "Organophosphorus Compounds", (a) p. 220, (b) p. 345. John Wiley and Sons, New York, 1950
10. CHERNYAK, A. S., NAVTANOVICH, M. L.: Zhur. Prikl. Khim. **33,** 85 (1960)
11. CHERBULIEZ, E., WENIGER, H.: Helv. Chim. Acta, **28,** 1584 (1945)
12. CESARANO, C., LEPSCKY, C.: J. Inorg. Nucl. Chem. **14,** 276 (1960)
13. VAN WAZER, J. R.: "Phosphorus and Its Compounds", Vol. I., (a) p. 269, (b) p. 276, (c) p. 680, 456, 454. Interscience Publishers, New York, 1958
14. KOLTHOFF, M., STENGER, V. A.: "Volumetric Analysis", Vol. II., 2nd ed. p. 137. Interscience Publishers, New York, 1947
15. ZANGEN, M., MARKUS, Y., BERGMANN, E. D.: Separ. Sci. **2** (2), 187 (1967)

Csaba ÚJHELYI; Debrecen 1, Pf 51, Hungary

Acta Chimica Academiae Scientiarum Hungaricae, Tomus 59 (2), pp. 225—227 (1969)

THE REACTION OF DICHLOROGALLANE WITH ETHYL HALIDES

(PRELIMINARY COMMUNICATION)

B. Csákvári, S. Jenei, D. Knausz and A. Meszticzky

(Department of General and Inorganic Chemistry, L. Eötvös University, Budapest)

Received July 31, 1968

The reactions of ethyl halides with dichlorogallane have been studied. It has been established that dichlorogallane reduces the ethyl halides to ethane. The temperature necessary for the reactions to take place increases in the order: ethyl chloride — ethyl bromide — ethyl iodide.

Schmidbaur and Klein [1] have prepared *n*-propylgallium dichloride by reacting allyl chloride with dichlorogallane. They suggested that the first step of this reaction is the reduction of allyl chloride by dichlorogallane, resulting in the formation of propylene:

$$HGaCl_2 + CH_2 = CH - CH_2Cl \rightarrow GaCl_3 + CH_2 = CH - CH_3 \qquad (1)$$

which is followed by the addition of dichlorogallane to the propylene formed in the first step:

$$HGaCl_2 + CH_2 = CH - CH_3 \rightarrow (CH_3)_2CHGaCl_2. \qquad (2)$$

We have studied the reaction between ethyl halides and dichlorogallane where no addition similar to (2) can take place.

Gallium trichloride has been prepared by the reaction of metallic gallium with dry chlorine gas, using an apparatus deoxygenated by flushing it with argon. The excess chlorine was removed with argon. Dichlorogallane was obtained according to Schmidbaur [1, 2], by the reduction of gallium trichloride with trimethylsilane:

$$(CH_3)_3SiH + GaCl_3 \rightarrow (CH_3)_3SiCl + HGaCl_2. \qquad (3)$$

The ethyl halide was added to the dichlorogallane containing chloromethylsilane. A gas burette was attached to the reaction vessel in order to collect, and measure the amount of the product gas. The gas formed in the reaction was shown to be pure ethane by gas chromatography. After the reaction had gone to completion as indicated by the cessation of gas evolution, chlorotrimethylsilane was removed from the mixture by distillation under reduced pressure.

According to gas chromatographic analysis, the distillate did not contain any other compound. After distillation, a crystalline product was found in the reaction mixture. A sample of this product was hydrolyzed with water. The ratio of halogens was determined by potentiometric titration in aqueous solution, using a silver iodide membrane indicator-electrode [3].

The experimental results are shown in Table I.

Table I

Ethyl halide	Ethane (%)	t_i	t_r	Cl/X
C_2H_5Cl	92—98	—10	0	—
C_2H_5Br	90—96	0	18	1.8—2.0
C_2H_5I	90—98	20	50	1.7—1.9

The first column shows the ethyl halides, and the second — the percentage of ethane actually formed calculated for the theoretical (ethane %). The initial temperature of the reaction mixture is given in the third column (t_i, °C).

The rate of gas evolution was measured during the reaction of ethyl chloride with dichlorogallane at 0°. The t_r values in the fourth column represent the temperatures at which the rates of gas evolution during the reaction of ethyl bromide and ethyl iodide were equal to that ethyl chloride at 0°, using identical initial amounts. It can be established that the temperature necessary for the reaction to take place increases in the order ethyl chloride — ethyl bromide — ethyl iodide.

The chlorine to halogen ratio (Cl/X) measured in the hydrolyzate of the crystalline product is shown in the fifth column.

As it is seen from the data in the Table, ethyl halides can be reduced to ethane by dichlorogallane, according to the following reaction:

$$C_2H_5X + HGaCl_2 \rightarrow C_2H_6 + \text{“}XGaCl_2\text{”} \qquad (4)$$

(where X = Cl, Br, I), with the formation of the corresponding gallium halides. The experimental results indicate that this reaction can be used for the preparation of “mixed gallium halides”. The preparation and investigation of the mixed halides, as well as a kinetic study of reaction (4) is in progress.

REFERENCES

1. SCHMIDBAUR, H., KLEIN, H. F.: Chem. Ber. **100**, 1129 (1967)
2. SCHMIDBAUR, H.: Angew. Chem. **77**, 170 (1965)
3. PUNGOR, E.: Anal. Chem. **39**, 28A (1967)
PUNGOR, E.: Kémiai Közlemények **30**, 1 (1968)
CSÁKVÁRI, B., MÉSZÁROS, K.: Hung. Sci. Instr. **11**, 9 (1968)

Béla CSÁKVÁRI
Sándor JENEI
Dezső KNAUSZ
Aranka MESZTICZKY

Budapest VIII., Múzeum krt. 6—8

Acta Chimica Academiae Scientiarum Hungaricae, Tomus 59 (2), pp. 229—247 (1969)

THE PYROLYSIS OF GASEOUS HYDROCARBONS, II

THE MECHANISM OF THE THERMAL DECOMPOSITION OF *n*-BUTANE

V. ILLÉS

(Hungarian Oil and Gas Research Institute)

Received July 10, 1967

The qualitative and quantitative distribution of the reaction products has been investigated at various temperatures in dependence on the conversion of *n*-butane. From the slope of the tangents, drawn to the initial section of the conversion curves (belonging to $x = 0$ conversion) the stochiometric coefficients of the reaction products, valid for the primary decomposition, were calculated. The product distribution obtained by this method showed a good agreement with the product distribution calculated on the basis of free radical chain theory, under assumption of a long reaction chain.

The quantitative distribution of the reaction products presented considerable changes with increasing conversion and temperature. The relative quantities of ethylene and hydrogen increased, those of propylene and methane decreased, as the conditions of pyrolysis became stricter. It was presumed that these changes were brought about — in accordance with the free radical chain theory — by the decomposition of the propylene and butylene molecules, caused by the chain propagating active radicals, by the isomerization, before decomposition, of the butyl radicals formed in the dehydrogenation from the initial hydrocarbon, and by the two directional reactions of the ethyl radicals formed in the chain process.

It was established that the yield of the reaction products in function of conversion can be characterized under the operational conditions of industrial pyrolysis reactors by a "single-curve", independent of temperature. Yield curves in function of conversion could be described with good approximation by third degree polynomials.

Several opinions appeared in the literature on the mechanism of the decomposition reactions of hydrocarbons. It was assumed earlier that the decomposition proceeds as a molecular process. Based on the work of RICE [1] and RICE and HERZFELD [2, 3], later the hypothesis of a free-radical chain-mechanism gained ground.

In the fifties, the so-called dualistic concept, based primarily on the research work of HINSHELWOOD *et al.* [4], was developed. This concept assumes the thermal decomposition of hydrocarbons to proceed by the simultaneous processes of free-radical chain-reaction and molecular decomposition.

Since then, the mechanism of thermal decomposition was studied by several authors [5—10]. Experimental results — particularly those obtained using deuterized and C-14 labelled hydrocarbons proved the thermal decomposition of hydrocarbons proceeding according to a free radical chain-mechanism. The mechanism and the kinetics of the primary decomposition reactions can be discussed satisfactorily by the RICE—HERZFELD theory.

The thermal decomposition of n-butane

According to the free radical chain-mechanism, the fundamental steps of the decomposition reaction are the following:

(1) $C_4H_{10} \rightarrow 2\,C_2H_5$

$C_4H_{10} \rightarrow CH_3 + C_3H_7$

(2) $C_4H_{10} + H \rightarrow H_2 + C_4H_9$

$C_4H_{10} + CH_3 \rightarrow CH_4 + C_4H_9$

$C_4H_{10} + C_2H_5 \rightarrow C_2H_6 + C_4H_9$

(3) $CH_3{-}CH_2{-}CH_2{-}CH_2 \rightarrow C_2H_4 + C_2H_5$

$CH_3{-}CH_2{-}CH{-}CH_3 \rightarrow C_3H_6 + CH_3$

$C_2H_5 \rightarrow C_2H_4 + H$

(4) $2C_2H_5 \rightarrow C_4H_{10}$

$2C_2H_5 \rightarrow C_2H_4 + C_2H_6$

$CH_3 + C_2H_5 \rightarrow C_3H_8$

$2CH_3 \rightarrow C_2H_6$

The first step is the splitting of the butane molecule into two ethyl or one methyl and one propyl radicals. The activation energy for both reactions is 83 kcal/mole [8].

In the reaction step (2), the chain-propagating radicals split off hydrogen atoms from the butane molecules, while hydrogen, methane, ethane and primary and secondary butyl radicals are formed. The activation energy of these reactions ranges between 8 and 10 kcal/mole [11]. In the reaction step (3) the primary butyl radicals split into ethylene and ethyl radicals, the secondary butyl radicals into propylene and methyl radicals. Both processes require an activation energy of 23 kcal/mole [12]. Also the decomposition of the ethyl radicals to ethylene and hydrogen atom, with an activation energy of 39.5 kcal/mole, belongs to this group of reactions [12]. It will become clear from data and figures presented later that the quantitative distribution of the reaction products is strongly influenced by this reaction. If this reaction would not take place, ethylene and ethane would be formed in identical quantities in the reaction chain. There is experimental proof that already in the primary decomposition reaction substantially more ethylene is formed than ethane, and with increasing butane conversion this ratio is shifted in favour of ethylene.

The activation energy of the recombination reactions (4) is less than 2 kcal/mole, so that their rate will be determined by the relative concentration of the radicals. According to PURNELL and QUINN [8], the recombination of the ethyl radicals to butane is the most probable process.

Thus, according to the radical mechanism, hydrogen, methane, ethane, ethylene and propylene form as chief products in the reaction chain in the thermal decomposition of *n*-butane. A small amount of propane may also form in the reaction of *n*-butane molecules with propyl radicals, formed in the dissociative reaction step, as well as in the recombination reaction of methyl and ethyl radicals. The reaction $C_4H_9 \rightarrow C_4H_8 + H$ proceeds with a very low rate (activation energy 40 kcal/mole), yielding butylene.

The free radical chain theory, permits to calculate only the primary products formed in the reaction chain and the relative quantity of the radicals, as the kinetic parameters of the single reaction steps are not exactly known. RICE and KOSSIAKOFF claimed the energy difference of the removal of primary and secondary hydrogen atoms being 2 kcal/mole [13]. According to this, the relative rate of the removal of hydrogen atoms in the reaction step (2) at 650 °C is as follows:

$$\log \frac{k_2}{k_1} = \frac{2000}{4.576 \cdot 923} = 0.474$$

and hence $k_2 = 2.98 \cdot k_1$. Taking into consideration that in the *n*-butane molecule six hydrogen atoms are linked to primary carbon atoms and four hydrogen atoms to secondary carbon atoms,

$6 \cdot 1 = 6.00$ 33.5 per cent of primary radicals, and $4 \cdot 2.98 = 11.92$ 66.5 per cent of secondary radicals are obtained.

According to this 0.335 mole of ethylene and ethyl radicals and 0.665 mole propylene and methyl radicals are formed in the decomposition of one mole of *n*-butane. Methyl radicals — with the exception of a very small part participating in the recombination reaction — are converted into methane in the dehydrogenation reaction (2). Ethyl radicals either participate in the dehydrogenation reaction (2) and are converted into ethane, or are decomposed according to (3) to ethylene and hydrogen. (A very small proportion of the ethyl radicals is recombined according to (4).)

The actual distribution of the products for the primary decomposition reaction is determined from the yield curves plotted in function of conversion. The yield curves of the main reaction products in function of the conversion of *n*-butane are shown in Figs 1—6.

Except for the relatively short initial linear section, the yield function does not give a straight line. In strictly stochiometric reactions (where no secondary reactions are present), yield data plotted against conversion, independently of the reaction temperature, always give a straight line. In the pyrolysis of hydrocarbons, owing to secondary reactions, the overall stoichiometry of the reaction changes both with the conversion and with the temperature. The interpretation of these changes will be discussed later.

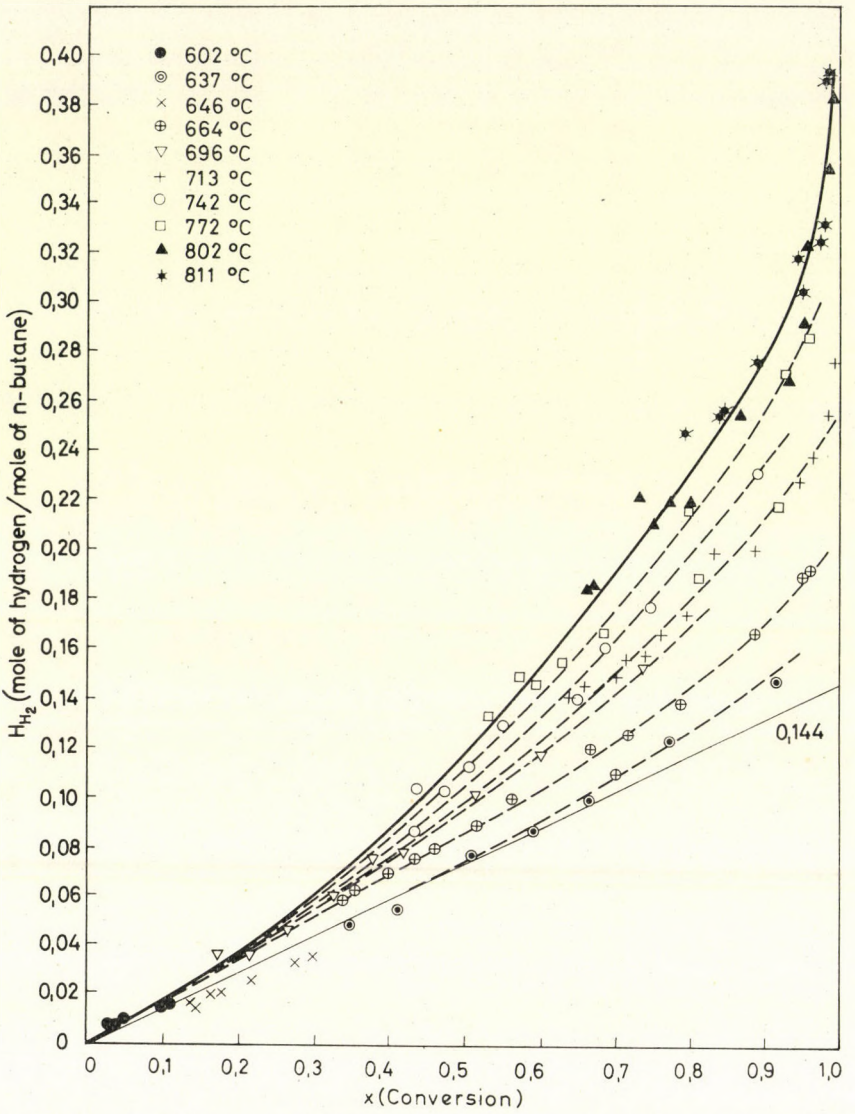


Fig. 1. The change of hydrogen yield in function of conversion in the pyrolysis of *n*-butane

On the basis of the yield curves plotted in function of conversion, the quantity of the single reaction products (their overall stoichiometric coefficient), referred to the decomposed butane, was determined by drawing a tangent to the point $x = 0$ of the conversion curve. The intersection of the tangent with the straight line drawn perpendicularly to point $x = 1$ (the slope of the tangent) gives the overall stoichiometric coefficient of the given reaction products, valid for the primary decomposition reaction. In Figs 1—6, tangent corresponding

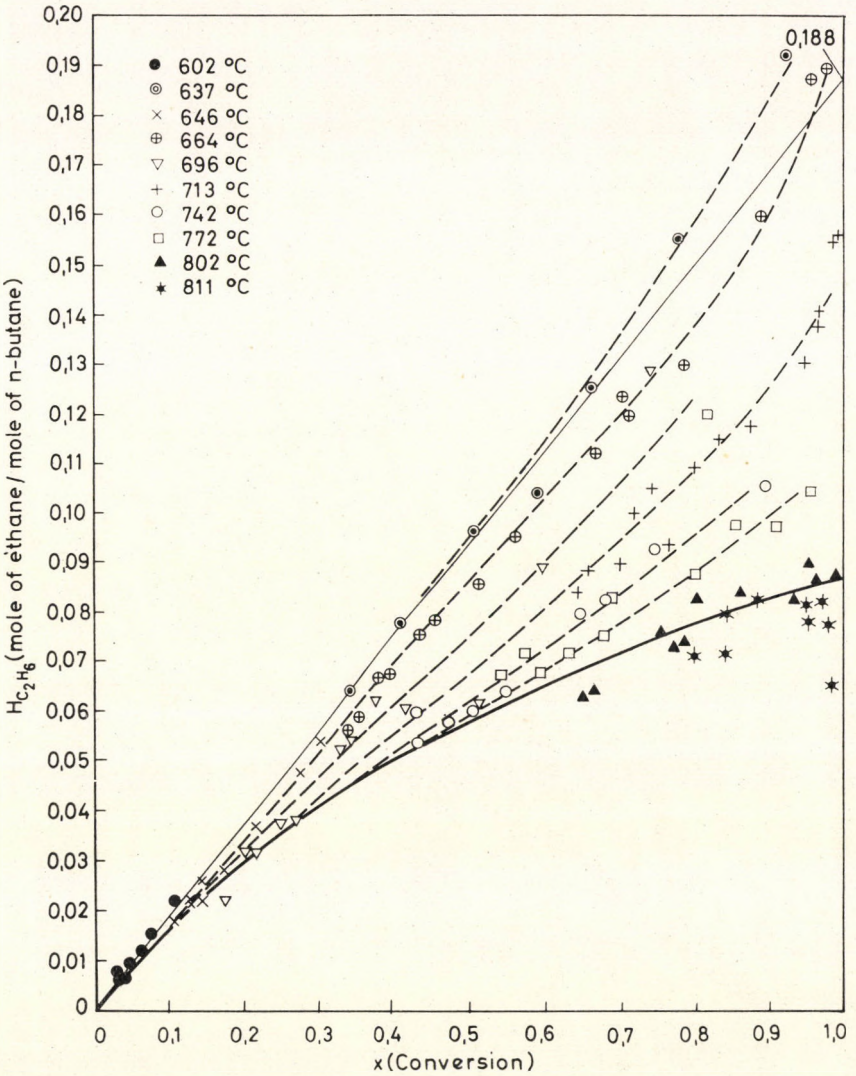


Fig. 2. The change of ethane yield in function of conversion in the pyrolysis of *n*-butane

to zero conversion are drawn with a thin line. Yield curves drawn with a thick continuous line, represent yield curves corresponding to the operating conditions (temperature, reaction time) of an industrial pyrolysis reactor.

In Table I the distribution of the reaction products, calculated by the RICE—KOSSIAKOFF theory, is compared with the distribution determined according to the described method, by extrapolation to zero conversion, for the primary decomposition reaction.

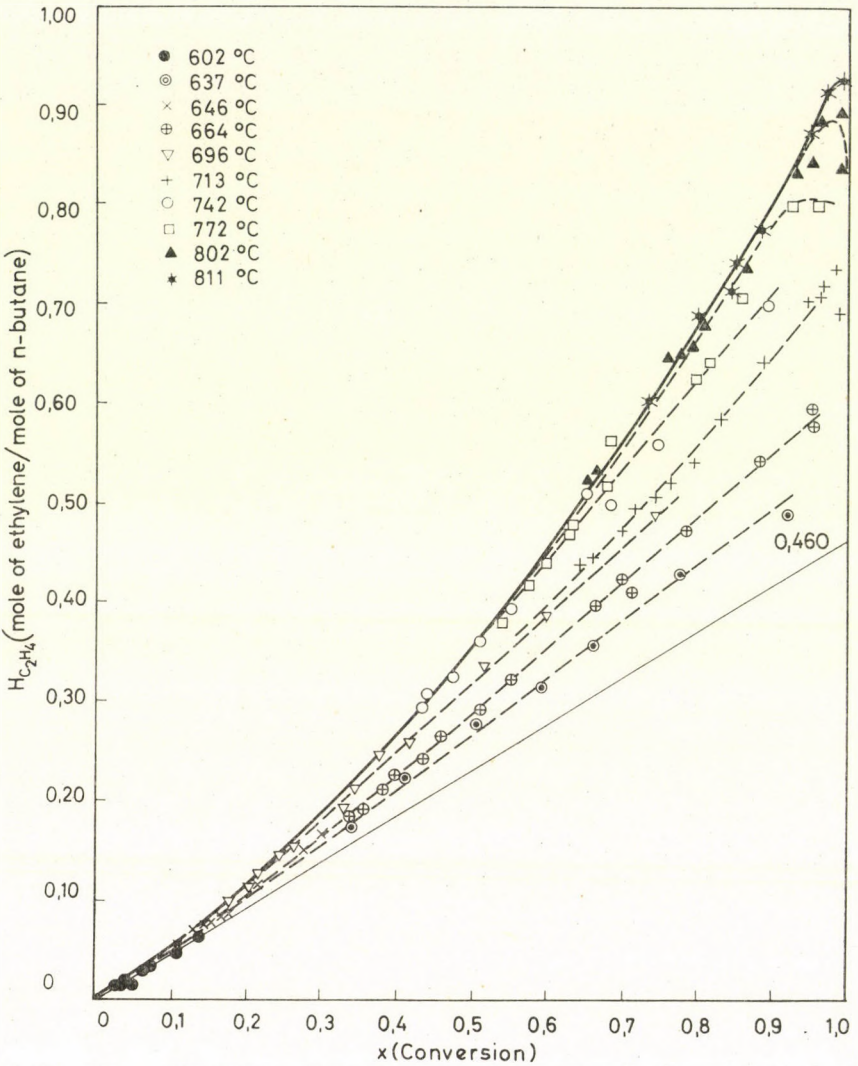


Fig. 3. The change of ethylene yield in function of conversion in the pyrolysis of *n*-butane

The calculated value of the ethyl radicals is the same as that of the calculated primary butyl radicals, since according to reaction step (3) primary butyl radicals decompose into ethylene and ethyl radicals. Ethyl radicals either participate in the dehydrogenation reaction (2) and are converted into ethane, or decompose into ethylene and hydrogen atom. Thus, the total quantity of ethane and hydrogen must be the same as the quantity of the ethyl radicals. Methyl radicals are converted into methane in the dehydrogenation reaction (2). Data in Table I, indicate a good agreement between calculated values and

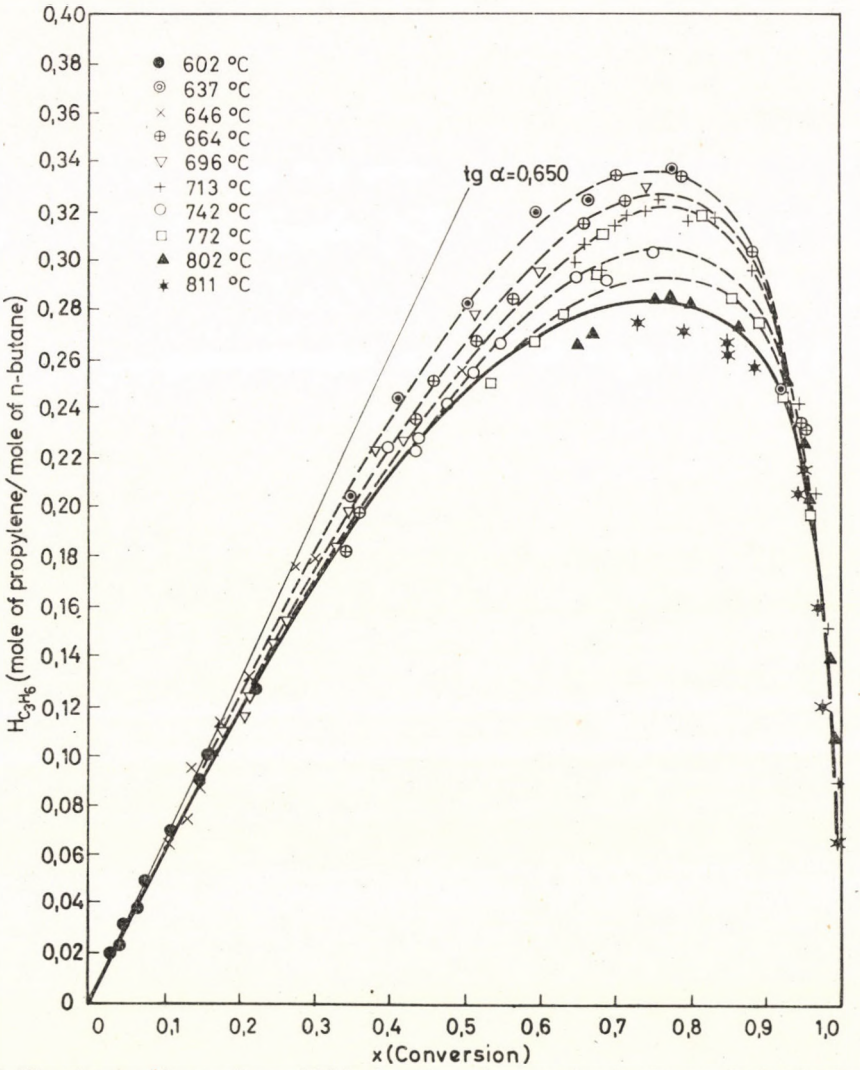


Fig. 4. The change of propylene yield in function of conversion in the pyrolysis of *n*-butan

those determined using the yield curves. The qualitative and quantitative distribution of the reaction products is in full accordance with the product distribution expected and calculated applying the free radical chain-mechanism.

The apparent length of the reaction chain was determined under consideration of the quantities of propylene, ethylene and hydrogen. Namely, the sum (propylene + ethylene — hidrogen) gives the approximate amount of *n*-butane decomposed in the chain process, while (1-sum) that decomposed in the dissociation reaction step. (The difference in the mole numbers of ethylene and hy-

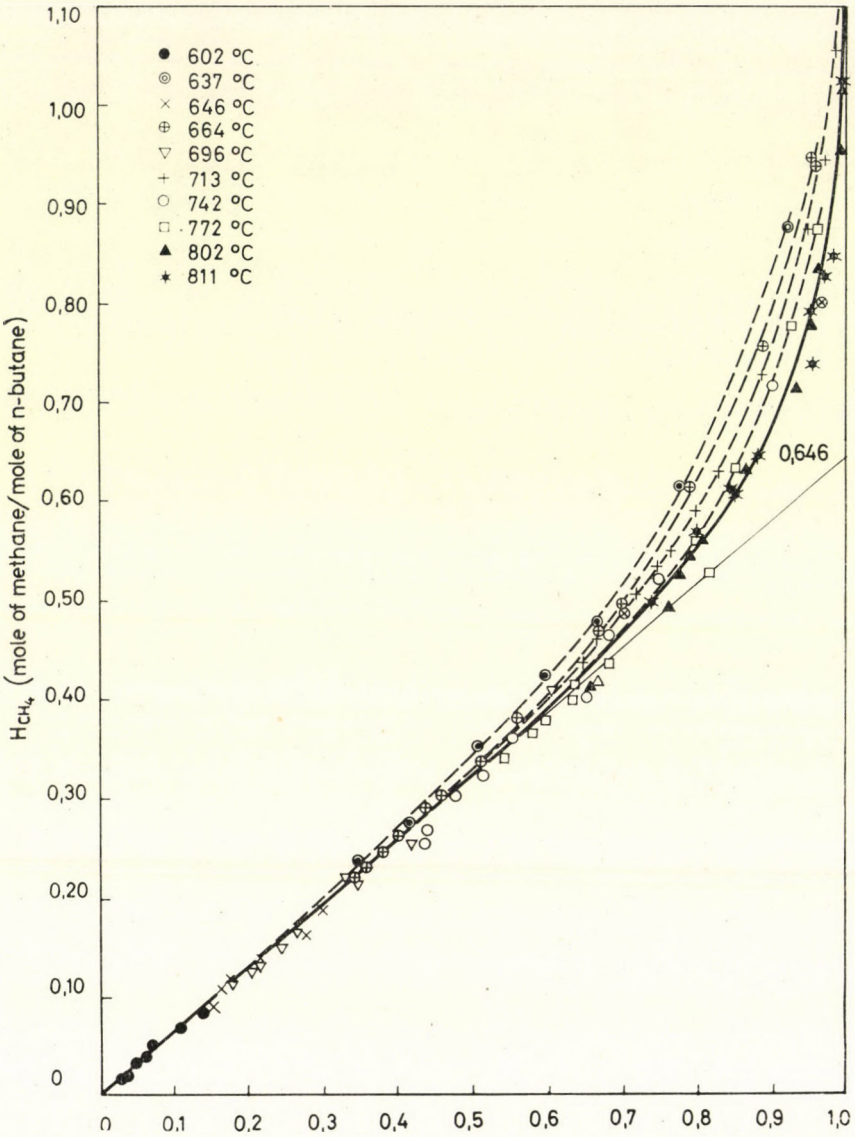


Fig. 5. The change of methane yield in function of conversion in the pyrolysis of *n*-butane

drogen is characteristic to the quantity of the primary radicals, while the mole number of propylene to the quantity of the secondary radicals.) Accordingly, in the decomposition of 1 mole of *n*-butane $0.650 + 0.460 - 0.144 = 0.966$ mole is decomposed in the chain process, and 0.034 mole in the dissociation step. The chain length is $0.966/0.034 = 28.4$. Thus, the assumption of a long reaction chain in the decomposition of *n*-butane is justified.

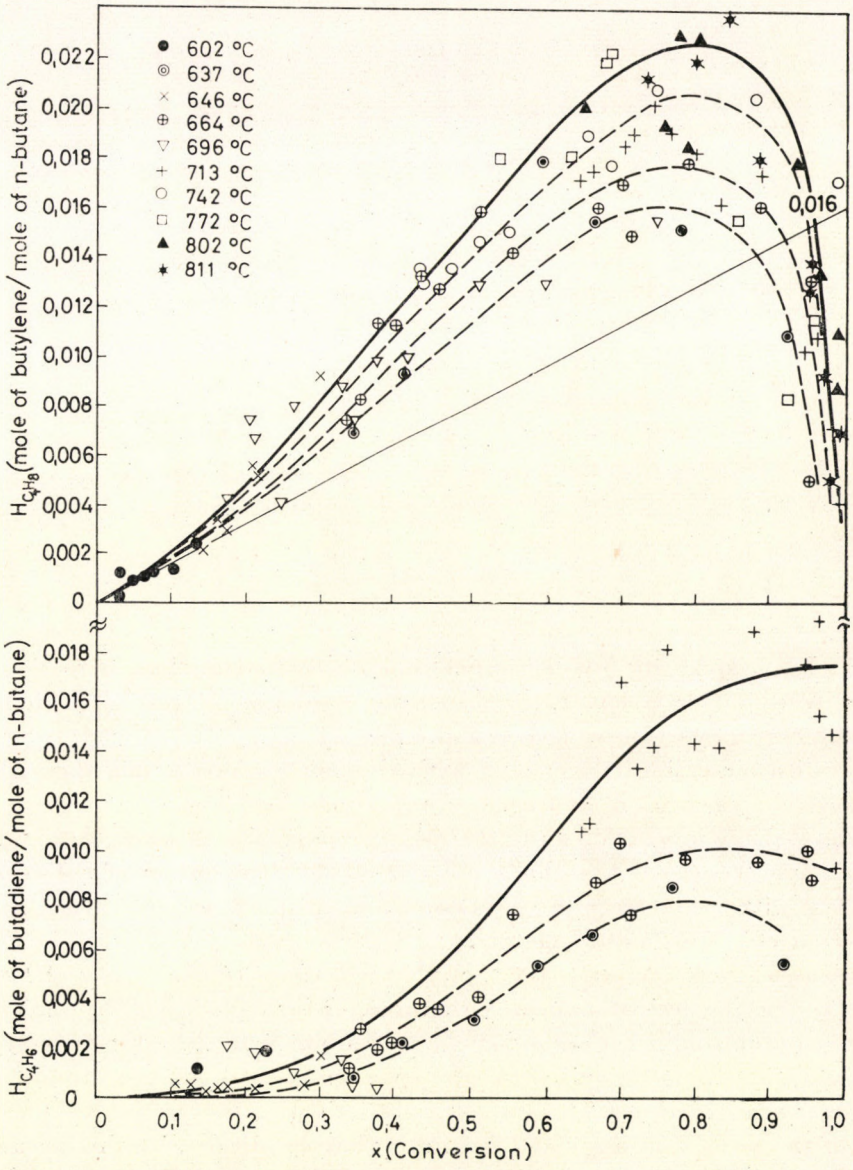


Fig. 6. The change of butylene and butadiene yield in function of conversion in the pyrolysis of *n*-butane

The relative quantity of the reaction products has changed considerably with the increase of butane conversion and with temperature, as can be seen from Figs 1—6.

The yield curves for hydrogen, methane and ethylene are located above the tangent drawn to the point of zero conversion, indicative of the fact that

Table I

Calculated and measured distribution of the reaction products in the primary decomposition of n-butane

Reaction products	v_i (mole of product/mole of decomposed *n*-butane)	
	calculated	found
H_2	—	0.144
C_2H_5	0.335	—
C_2H_6	—	0.188
C_2H_4	0.335	0.460
C_3H_6	0.665	0.650
CH_3	0.665	—
CH_4	—	0.646
C_3H_8	—	0.016
C_4H_8	—	0.016
		$E_v^0 = 2.120$

their relative quantity (overall stoichiometric coefficient) has increased with the increase of conversion. The yield curves of ethane and propylene lie below the tangent drawn to zero conversion, showing their relative quantity to decrease with increasing conversion. With the increase in reaction temperature the relative quantities of hydrogen, ethylene and butylene — for a given conversion — have increased, while the relative quantities of propylene and methane have decreased. The above changes in the distribution of the reaction products with an increase in conversion and temperature are caused by the combined effect of several factors.

One of these factors is the fact that according to the theory of RICE—KOSSIAKOFF, the activation energy required for the splitting off by radicals of hydrogen atoms linked to secondary carbon atoms is by 2 kcal/mole less, than the activation energy required for the splitting off of hydrogen atoms linked to primary carbon atoms. This difference in activation energy results in a slight shift of the ratio of primary and secondary butyl radicals with the increase of temperature. Namely, from primary butyl radicals ethylene and ethyl radicals, from secondary butyl radicals propylene and methyl radicals are formed. According to our earlier calculations, the ratio k_2/k_1 is 2.98 at 650 °C. At 750 °C this ratio is 2.68, from which the relative quantity of the primary radicals is 35.9 per cent instead of the 33.5 per cent calculated for 650 °C. Therefore, upon an increase in temperature by 100 °C, this factor would be expected to increase the quantity of ethylene and of ethane + hydrogen by 2—3 per cent, and to decrease the quantity of propylene and methane by 2—3 per cent.

A factor causing considerably greater changes in the composition of the reaction product is the fact that, with pyrolysis conditions becoming stricter, out of the two competing reactions $C_2H_5 + C_4H_{10} \rightarrow C_2H_6 + C_4H_9$ and $C_2H_5 \rightarrow C_2H_4 + H$, the latter, the decomposition reaction of the ethyl radicals becomes predominant. Though the activation energy of the dehydrogenation reaction of the ethyl radicals (10 kcal/mole) is substantially lower than the activation energy of decomposition (39.5 kcal/mole), butane concentration decreasing with increasing butane conversion, causes a decrease in the reaction rate of dehydrogenation. On the other hand, due to the greater temperature coefficient of the rate constant of the decomposition of the ethyl radicals, also the relative rate of the decomposition of ethyl radicals increases with increasing temperature. The above conclusions are strongly substantiated by measured data, plotted in Figs 1, 2 and 3. The relative quantity of ethane decreases with the increase of both conversion and temperature, while the relative quantities of hydrogen and ethylene increase with the increase of both parameters.

The following addition reactions proceeding between propylene, formed in the primary decomposition reaction, and the active radicals carrying the chain, resulted in the increase of the relative quantity of ethylene and methane, and simultaneously in a decrease of the relative quantity of propylene:

Reaction	Preexp. factor	Activation energy kcal/mole	Ref.
$C_3H_6 + H \rightarrow C_3H_7$	$10^{14.4}$	5.0	[14]
$C_3H_6 + CH_3 \rightarrow C_4H_9$	10^{11}	6 ± 1	[15]

In the initial phase of the decomposition reaction (at low conversions), these reactions play a subordinate role, due to the small concentration of propylene. However, with increasing conversion, the quantity of propylene in the reaction zone increases, which results in an increase of the decomposition rate of propylene. Measured data presented in Fig. 4. substantiate these observations, as the yield curves of propylene lie below the tangent drawn to zero conversion. Yield curves belonging to various temperatures give in the conversion range from 72 to 76 per cent a maximum. At the sites of these maximums the decomposition rate of propylene was the same as the rate of propylene formation. At higher conversions, the decomposition reaction of propylene was predominant, leading to a rapid decrease of the relative quantity of propylene.

In the above reactions of propylene and chain-propagating active radicals, *n*- and isopropyl radicals, and secondary butil radicals and isobutyl radicals may form. Normal-propyl radicals are decomposed to ethylene and methyl

radicals, the quantity of which is added to the quantities of ethylene and methane formed in the primary reaction. (Methyl radicals are converted namely in the dehydrogenation reaction (2) to methane.) In the decomposition of the isopropyl and secondary butyl radicals propylene and chain propagating active radicals are formed. Therefore, these reactions do not modify the composition of the product. The decomposition of the primary isobutyl radicals yields isobutylene and hydrogen (see later). The reaction mixture practically did not contain isobutylene, so that presumably only secondary butyl radicals were formed in the addition of the methyl radicals.

(Similarly to the above reaction, also ethylene can enter into a reaction with the chain propagating radicals. During these reactions, ethyl and *n*-propyl radicals are formed. The decomposition of these radicals yields ethylene and hydrogen atoms, and ethylene and methyl radical, respectively. Therefore, neither do these reactions influence the composition of the product.)

In the discussed reactions, the chain-propagating active radicals are converted to greater radicals of lower activity. This process results in a decrease of rate, an inhibition, of the chain reaction carrying the decomposition of the initial hydrocarbon.

The decomposition of propylene, proceeding as described above, is therefore accompanied by the simultaneous increase of the quantities of ethylene and methane. The quantity of methane, referred to decomposed butane, did not change up to a conversion of about 50 per cent (as shown by Fig. 5, the yield curve coincides with the tangent drawn to zero conversion), to increase from here on rapidly. This strong increase was a result of the decomposition of propylene. The decrease in the relative quantity of propylene could be observed already at substantially lower conversions (Fig. 7), however, this decrease did not go hand in hand with an increase in methane, at least, as evidenced on the basis of the overall product distribution. This phenomenon can be explained by presuming a reaction proceeding parallel with the methane-producing propylene decomposition, in the course of which the quantity of methane decreases, and up to a conversion of 50 per cent, these two processes approximately compensate each other. This reaction is assumed by us to be the isomerization of secondary butyl radicals into primary butyl radicals, which results in a decrease of the relative quantity of propylene and methyl radicals, and consequently in that of methane. (According to the reaction scheme (3), propylene and methyl radicals are formed in the decomposition of secondary butyl radicals.) Besides this experimental finding, substantiating the assumption of radical isomerization, it may be considered as further proof that the sum of the overall stoichiometric coefficients of hydrogen and ethane has increased with increasing conversion, owing to the increase of the relative quantity of primary butyl radicals. Ethane and hydrogen arise namely from the substitution and decomposition reactions of the ethyl radicals, while ethyl

radicals are formed during the decomposition of primary butyl radicals. According to McNesby, Drew and Gordon [16], the isomerization of primary and secondary butyl radicals does not take place under the conditions of pyrolysis. According to Kerr and Trotman-Dickenson [17], however, the two radicals isomerize readily. Purnell and Quinn [8] do not differentiate between the two radicals.

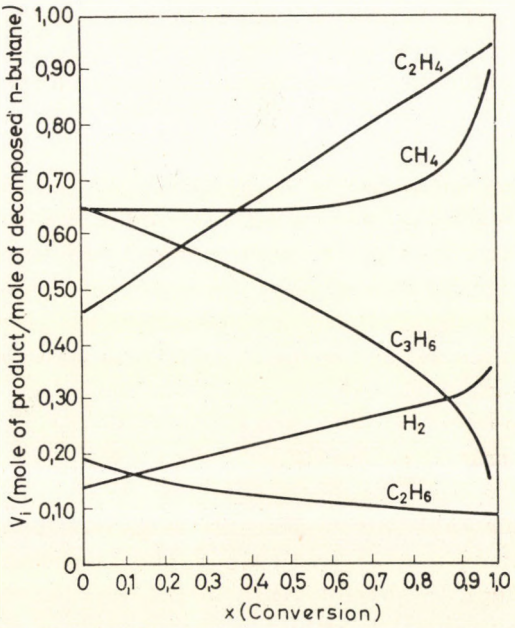


Fig. 7. The change of the "overall stoichiometric coefficients" of the principal reaction products in function of conversion in the pyrolysis of *n*-butane

Figs 4 and 5 show that both propylene yield and methane yield decrease with increasing temperature at a given conversion. This phenomenon can be explained by the fact that the temperature coefficient of the rate constants of reactions leading to the formation of primary butyl radicals (dehydrogenation and isomerization) is greater than that of reactions leading to the formation of secondary butyl radicals. Thus, with an increase in temperature the ratio primary/secondary radical will increase, and result in a decrease of the relative quantity of propylene and methane.

In the conversion region above 90 per cent also the ethylene yield curves belonging to different temperatures present a maximum (see Fig. 3). Maximum ethylene yields corresponding to higher reaction temperatures have a higher value. The increase in ethylene yield with increasing temperature for an identical conversion is brought about by the reactions discussed above (decompo-

sition of propylene, radical isomerization, decomposition of ethyl radicals). The maximum of the yield curves can be explained by the secondary reactions of ethylene (yielding butadiene and aromatic hydrocarbons). The temperature coefficient of the rate constants of these secondary reactions is namely lower than the temperature coefficients of the rate constants of the primary decomposition reactions. Consequently, the rate of the ethylene consuming reactions, as compared to that of the ethylene producing primary decomposition reactions, will decrease with increasing temperature. Moreover, a shorter reaction time is necessary at higher temperatures to attain the same conversion, so that a shorter time is available for the proceeding of the secondary reactions.

The yield curves of butylene and butadiene in function of the conversion are presented in Fig. 6.

In very low per cents, butylene was present also in the initial section of the decomposition reaction. Its quantity increased with the increase of conversion and temperature. This phenomenon is consistent with the difference in activation energy of the two ways of decomposition of the butyl radicals. The decomposition of the butyl radicals proceeds either according to the reaction scheme (3) with an activation energy of 23 kcal/mole, or according to the reaction $C_4H_9 \rightarrow C_4H_8 + H$ with an activation energy of 40 kcal/mole. The relative rate of this latter reaction increases with increasing temperature, due to the greater temperature coefficient.

As may be seen from Fig. 6, the yield curves of butadiene do not start from the origo. This substance appears at a conversion above 10 per cent in appreciable quantities in the product gas. Thus, butadien is not a primary decomposition product. Presumably, it is formed from butylene by dehydrogenation, or in the course of the combining of vinyl radicals and allyl and alkyl radicals.

The change of the yield of reaction products in ranges of temperature and reaction time usual with industrial reactors

The most important product of pyrolysis is ethylene. Operational conditions of industrial pyrolysis reactors are generally adjusted so as to give a high ethylene yield. To obtain a high ethylene yield, the hydrocarbon to be decomposed is heated quickly (applying a high temperature gradient), and the outlet temperature of the pipe still reaches in the pyrolysis of gases 810—830 °C. The average sojourn time of the molecules of the initial hydrocarbon, in the section of the reactor kept above 600 °C, varies between 0.6 and 1.0 sec. (Pipe stills of recent design are operated at an outlet temperature of 850 °C or more, and the average sojourn time of the hydrocarbon to be decomposed is about 0.5 sec. [18].) Under these operating conditions, a conversion of 90—95 per cent is attained in the pyrolysis of gaseous hydrocarbon in pipe stills.

The yield curve drawn out with a solid line in Fig. 3, gives the ethylene yield to be obtained under the operating conditions of an industrial tubular pyrolysis reactor. As can be seen, the yield curves belonging to different temperatures branch off from the yield curve drawn out with a solid line. The conversion range, in which yield data appertaining to various temperatures can be represented by a "single curve", increases with increasing temperature. Thus *e.g.* if a deviation of ± 3 relative percents is considered as permissible from the yield curve drawn with a solid line, the yield curves measured at 637 °C, 696 °C, 742 °C and 772 °C leave this band after 12, 34, 70 and 92 per cent conversion, respectively. To reach these conversion values, a reaction time of more than 0.6 sec is needed (see Fig. 4 in Part I (20)). Since the temperature of the hydrocarbon to be decomposed raises rapidly in industrial pipe stills when a high temperature gradient is present, the sojourn time of the molecules of the initial hydrocarbon in the section of lower temperatures (between 600 and 700 °C) of the reactor will be substantially shorter than the sojourn times given above. When the reactor is properly operated, the ethylene yield in dependence on conversion will change therefore along the curve drawn with a solid line, or within the band of ± 3 relative per cent of permissible scattering.

On the basis of the single-curve drawn with a solid line in Fig. 3, and Fig. 4 (in Part I), giving the relationship conversion *vs.* reaction time, optimum operating conditions, required to secure maximum yield in ethylene can be determined. Namely from the relationship ethylene yield *vs.* conversion it can be established for a given temperature, what is the maximum conversion to be attained, without exceeding the permissible deviation (*e.g.* 1, 2 or 3 per cent) from the single-curve drawn with a solid line. The reaction time belonging to this conversion value can be determined from Fig. 4 and Equ. (27) in Part I. In knowledge of the reaction time and the linear gas velocity, prevailing in the given section of the reactor, the length of the reactor necessary to attain the given temperature can be calculated. (It is to be checked by heat transfer calculations, whether the quantity of heat required to reach the given temperature can be introduced into the reactor.) Repeating this procedure for various temperatures, the optimum temperature distribution curve, ensuring maximum ethylene yield, can be determined.

If, owing to an incorrect design of the reactor, or an unadequate adjustment of the burners, the temperature of the substance to be decomposed is lower than that prescribed by this curve, the maximum yield of ethylene to be obtained will decrease.

On the basis of these considerations pertinent to the yield of ethylene, yield curves valid under the operational conditions of industrial pyrolysis reactors (permitting for a deviation of ± 3 rel. per cent) were drawn with a solid line also in Figs 1—6. Data for the yield curves represented by the continuous line are summarized in Table II. (In the table, the empirical formula C_8H_{10}

Acta Chim. Acad. Sci. Hung. 59, 1969

Table II

Yield of reaction products in dependence on conversion in the pyrolysis of n-butane

Components \ Conversion	0.10	0.20	0.30	0.40	0.50	0.60	0.70	0.80	0.90	0.94	0.98
H_2	0.0160	0.0360	0.0594	0.0860	0.1175	0.1512	0.1900	0.2300	0.2762	0.3030	0.3500
CH_4	0.0646	0.1292	0.1938	0.2584	0.3230	0.3920	0.4670	0.5550	0.6700	0.7450	0.8780
C_2H_6	0.0166	0.0296	0.0408	0.0500	0.0575	0.0647	0.0722	0.0784	0.0830	0.0852	0.0868
C_2H_4	0.0510	0.1120	0.1825	0.2626	0.3525	0.4530	0.5640	0.6810	0.8025	0.8600	0.9220
C_3H_8	0.0012	0.0024	0.0035	0.0045	0.0055	0.0063	0.0068	0.0071	0.0070	0.0069	0.0067
C_3H_6	0.0624	0.1190	0.1699	0.2120	0.2465	0.2706	0.2821	0.2810	0.2600	0.2340	0.1540
C_4H_8	0.0019	0.0048	0.0081	0.0117	0.0154	0.0188	0.0217	0.0226	0.0209	0.0182	0.0100
C_4H_6	0.0003	0.0007	0.0018	0.0036	0.0066	0.0103	0.0139	0.0160	0.1072	0.0174	0.0176
C_8H_{10}	0.0005	0.0007	0.0008	0.0021	0.0032	0.0043	0.0059	0.0106	0.0173	0.0154	0.0216
n-C_4H_{10}	0.9000	0.8000	0.7000	0.6000	0.5000	0.4000	0.3000	0.2000	0.1000	0.0600	0.0200
E	1.1145	1.2344	1.3606	1.4909	1.6277	1.7712	1.9236	2.0817	2.2541	2.3451	2.4667

represents the sum of the quantity of benzene, toluene, xylenes, ethylbenzene and styrene. These components were determined only in some of the measurements.) From the data of these yield curves, the overall stoichiometric coefficients of the reaction products were determined on the basis of the relationship $v_i = H_i/x$. The change of the overall stoichiometric coefficients in dependence on conversion is shown by Fig. 7. It can be easily seen that the relative quantity (overall stoichiometric coefficient) of ethylene and hydrogen increases with increasing conversion, while that of propylene and ethane decreases. The relative quantity of methane does not change up to a conversion of about 50 per cent, to increase then rapidly at higher conversion values. A detailed interpretation of the causes of these changes has been given already.

The following relationship exists between the yield curves and the expansion discussed in Part I of this communication: $E = \Sigma H_i$. The sum of the yield data belonging to conversion x gives the expansion corresponding to conversion x. (In summarizing, $H_{C_4H_{10}} = 1-x$.) When the overall stoichiometric coefficients in Fig. 7 are known, the value of E_v in the kinetic equations can be calculated from the following expression: $E_v = \Sigma v_i$.

The recognition that — under the operational conditions of industrial pyrolysis reactors — the yield of the reactin products in function of conversion can be characterized by a "single-curve", independently of temperature, renders it possible to treat the yield curves as mathematical functions. This gives relationships suitable for the design of pipe stills, and for the control of their operation. The yield curves can be represented with good approximation by a third degree polynomial, in which the conversion is the independent variable. The general form of the expression is as follows:

$$H_i = a_{i0} + a_{i1}\,x + a_{i2}\,x^2 + a_{i3}\,x^3.$$

The constants of the yield curves of ethylene, propylene, and butylene are summarized in Table III. The constants were calculated by the Section for Chemical Engineering Computation on an electronic computer Model GIER.

In Fig. 8, yield curves determined experimentally are compared with yield curves calculated with the described method. It can be seen that the third degree polynomial gives a satisfactory approximation.

Table III

Reaction products	Constants of the polynomial describing the yield curves			
	a_{i0}	a_{i1}	a_{i2}	a_{i3}
Ethylene	0.065	45.664	50.524	— 1.758
Propylene	1.818	41.006	47.786	—73.377
Butylene	0.400	— 3.075	18.582	—15.022

In our previous paper [20] kinetic relationships were given for the dependence of conversion on reaction time and temperature. Conversion values determined by reaction conditions (T, τ) and calculated from the referred relation-

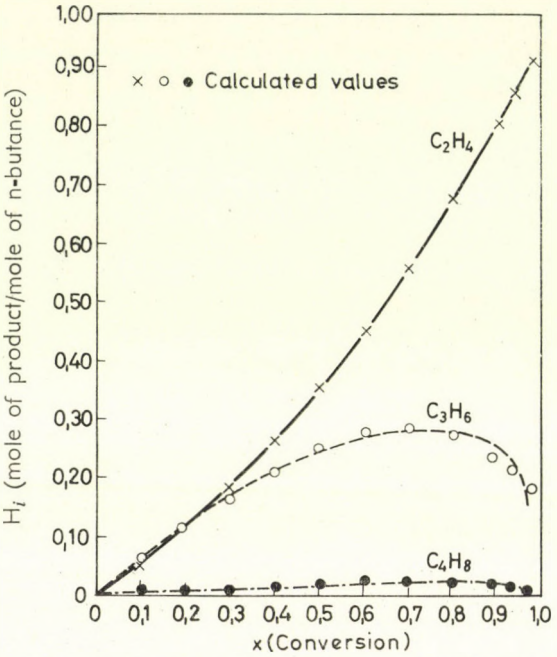


Fig. 8. The change of ethylene, propylene and butylene yield in function of conversion in the pyrolysis of *n*-butane

ships were substituted into the polynomials describing the yield curves. This permitted the calculation of the yields belonging to the given reaction conditions. Thus, the method described is suitable for the chemical engineering calculation of pyrolysis reactors, and for the control of the operation of industrial pyrolysis pipe stills.

REFERENCES

1. RICE, F. O.: J. Am. Chem. Soc. **53,** 1959 (1931)
2. RICE, F. O., HERZFELD, K. F.: J. Am. Chem. Soc. **56,** 284 (1934)
3. RICE, F. O., RICE, K. K.: The Aliphatic Free Radicals. Johns Hopkins University Press, Baltimore, 1935
4. STUBBS, F. J., HINSHELWOOD, F. R. S.: Discuss. Faraday Soc. **10,** 129 (1951)
5. RICE, F. O., VARNERIN, R. E.: J. Am. Chem. Soc. **74,** 324 (1954)
6. VOJEVODSKIJ, V. V., POLTORAK, V. A.: Doklad. Akad. Nauk SSSR **9,** 585, 589 (1953)
7. SEMJONOV, N. N.: A kémiai kinetika és a reakcióképesség néhány problémája (On Some Problems of Chemical Kinetics and Reactivity), p. 261. Akadémiai Kiadó, Budapest, 1961
8. PURNELL, J. H., QUINN, C. P.: Proc. Roy. Soc. **A 270,** 267 (1962)
9. LAIDLER, K. J.: Reaction Kinetics. Vol. I. Homogeneous Gas Reactions. Pergamon Press, Oxford, London, New York, Paris 1963

10. SZABÓ, Z., HUHN, P., BERGH, A.: Magy. Kém. Folyóirat **58,** 370 (1952)
11. SZABÓ, Z. G.: Fortschritte in der Kinetik der homogenen Gasreaktionen, p. 197. Dr. Dietrich Steinkopff Verlag, Darmstadt, 1961
12. SZABÓ, Z. G.: Fortschritte in der Kinetik der homogenen Gasreaktionen, p. 47. Dr. Dietrich Steinkopff Verlag, Darmstadt, 1961
13. KOSSIAKOFF, A., RICE, F. O.: J. Am. Chem. Soc. **65,** 590 (1943)
14. DARWENT, B. De B., ROBERTS, R.: Discuss. Faraday Soc. **14,** 55 (1953)
15. MANDELCORN, L., STEACIE, E. W. R.: Canad. J. Chem. **32,** 474 (1954)
16. MCNESBY, J. R., DREW, C. M., GORDON, A. S.: J. Chem. Soc. 1602 (1960)
17. KERR, J. A., TROTMAN-DICKENSON, S. F.: J. Chem. Soc. 1602 (1960)
18. Chemical Week, Novembre **13,** 70 (1965)
19. SCHUTT, A. C.: Chem. Eng. Progr. **55,** No. 1, 68 (1959)
20. ILLÉS, V.: On the pyrolysis of gaseous hydrocarbons, I. Acta Chim. Acad. Sci. Hung. **59,** 35 (1969)

Vendel ILLÉS; Veszprém, Wartha V. u. 2—4. Hungary

Acta Chimica Academiae Scientiarum Hungaricae, Tomus 59 (2), pp. 249—261 (1969)

INVESTIGATION OF THE THERMAL STABILITY OF THE RESINS VARION CH, CONTAINING IMINO DIACETIC ACID GROUPS*

I. AMBRÓ, T. FLÓRA and T. BIRÓ

(Research Institute for Heavy Chemical Industries, Veszprém)

Received 19 September, 1967

The thermal properties of the chelate-forming ion exchange resin Varion CH were investigated by derivatography. To follow the thermal process, the heating up of the samples had been interrupted at characteristic decomposition steps, and the residual substance was investigated by infrared spectrophotometry. These investigations were carried out also on the model substance of the matrix (styrene-divinylbenzene copolymer) and on EDTA-$Na_2 \cdot 2\,H_2O$, representing the model substance of the side chain. Kinetic data of the thermal decomposition were calculated from the DTG and TG curves of the derivatograms. The stability of the side chain was found to be increased considerably by the matrix. From one of the thermal decomposition steps of the resin, data verifying the composition were calculated.

Derivatographic investigations were undertaken to study the thermal stability of air-dry resins in hydrogen and sodium form. For the interpretation of the thermal processes, also polystyrene, forming the matrix, and EDTA-$Na_2 \cdot 2H_2O$, of a structure analogous to that of the side chain, were derivatographed under similar conditions as the resins: after the termination of the characteristic decomposition steps, derivatographic heating was interrupted, and the absorption spectrum of the residual products was recorded in the infrared region.

Data published on the thermal properties of ion exchange resins, generally concern conditions prevailing during their use, that is to say, the relationship between ion exchange ability and temperature in wet state. As is well known, higher temperatures favour many ion exchange processes, by increasing the selectivity in separation processes. However, operational temperature can not be increased too much without incurring the danger of damaging the ion exchange resin.

DANUSSO and POLIZOTTI [1] studied by differential thermal analysis the thermic properties of iso- and atactic polystyrene. During its pyrolysis in air, isotactic polystirene becomes crystalline at 80 °C, and the crystals melt between 210 and 220 °C. Two exothermic peaks occur at 250 and 300 °C, respectively, which, according to the authors, are due to the oxidation of the polymer. At 375 °C, indicated by a small endothermic peak, the depolymeri-

* Paper read at the III. Transdanubian Analytical Conference, Szombathely, 10 August 1967.

zation of the polymer took place, and subsequently monomers and oligomers distilled off. In their experiments undertaken in nitrogen atmosphere, the exothermic peak of the oxidation process at about 300 °C was absent, and two small endothermic effects were presented at this temperature, with a shift of the peak temperatures towards higher values.

With the atactic polystyrene, no endothermic effects, indicative of the crystalline state, were observed.

ANDERSON and FREEMAN [2] carried out their thermogravimetric investigation in the temperature range from 246 to 430 °C. In a vacuum of 1 torr, the decomposition of polystyrene begun at 320 °C. Up to 430 °C a loss in weight of 99 per cent took place, under formation of a carbonaceous residue of 1 per cent.

The kinetics of the decomposition was investigated by FREEMAN and CAROLL [3]. From the TG curves a zero order of the reaction was established up to a loss in weight of 10 per cent. The activation energy of the process was found to be 46 kcal/mole. In the weight-loss range from 15 to 95 per cent, decomposition proceeded according to a first order reaction, with an activation energy of 60 $\pm$ 5 kcal/mole. The first step of the decomposition occurred below 370 °C, the second above 370 °C.

Kinetic data, calculated the experiments carried out by JELLINEK [4] below 340 °C, and experiments carried out by MADORSKY [5] above 340 °C, are summarized in Table II, containing also the results of our own measurements.

To follow the decomposition process by infrared spectrophotometry, data published for polystyrene were used to identify in the infrared spectra of the resins the bands arising from the matrix. Complementary, the spectra of further compounds, thus that of Complexon III, sodium carbonate, sodium oxalate, were also recorded.

Instruments and compounds used

The derivatograms were recorded with a PAULIK—PAULIK—ERDEY [7] derivatograph Model GYEM 676, in nitrogen atmosphere. Heating up to the termination of the decomposition steps was also carried out in the derivatograph.

With the exception of styrene-divinylbenzene copolymer (matrix), Al_2O_3 was layered between the substances, to prevent foaming. The heating rate was 6° C/min.

Infrared spectra were recorded on a Zeiss UR-10 spectrophotometer. The powdered samples were tabletted with potassium bromide.

The ion exchange resin (trade name: Varion CH) was prepared in the Research Institute for Plastic Materials.

Experimental results

Derivatograms and infrared spectra are shown in Figs 1—8. Fig. 1 contains the DTG and TG curves of polystyrene (1), EDTA-$Na_2 \cdot 2H_2O$ (2), and Varion CH resin in the H-form (3) and in the Na-form (4). Fig. 2 shows the DTA curves of these samples.

In Figs 3—8, the infrared spectra are presented.

Thermal properties of the polistyrene matrix

The DTG and TG curves (Fig. 1, curve 1), present during heating two small steps at 100 and at 220 °C, indicating a loss in weight of 1.1 and 1.4 per cent, respectively. At this temperature, the sample looses its moisture content,

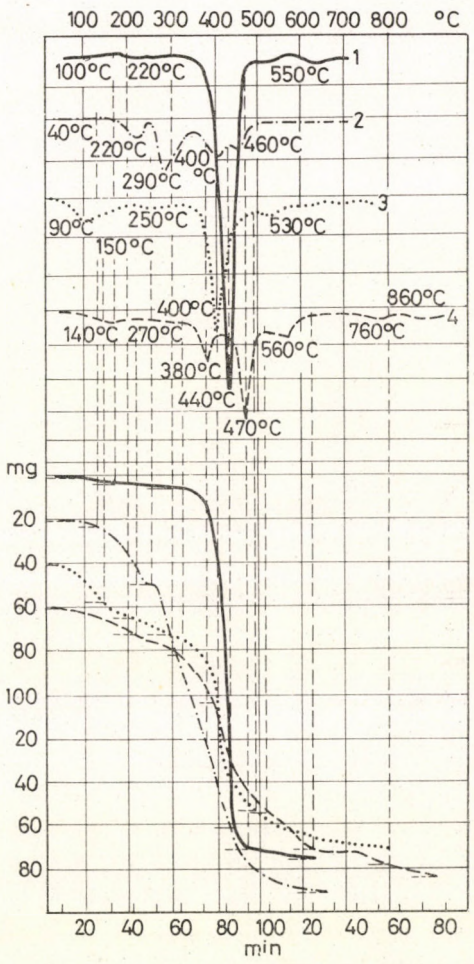


Fig. 1. The DTG and TG curves. 1. Styrene-divinylbenzene copolymer; 2. EDTA-$Na_2 \cdot 2\ H_2O$; 3. Varion CH resin in H-form; 4. Varion CH resin in Na-form

liberating water, bonded with different strength. The further loss in weight of the sample begins at 330 °C, to attain at 440 °C maximum velocity of the thermal decomposition. In this single step, the total loss in weight is 94.7 per cent, which, together with the two preceding decomposition steps amount to a loss in weight of 97.2 per cent. At 550 °C, a further small step occurs, corresponding to a loss in weight of 2.3 per cent, referred to the quantity

of the initial substance. Thus, the overall loss in weight is 99.5 per cent. As may be seen also from the derivatograms, heating has slightly exceeded 700 °C.

The section between 20 and 360 °C of the DTA curve (Fig. 2, curve 2) presents an arching, indicative to a change in thermal conductivity. Otherwise, its course is similar to that of the DTG curve.

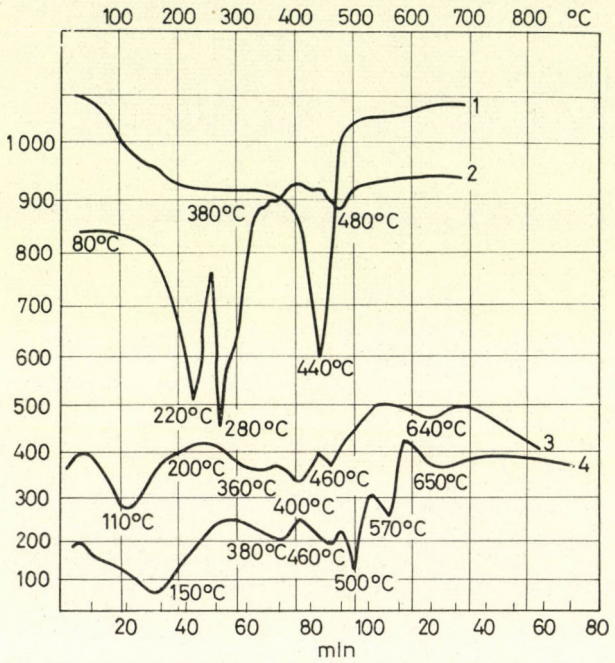


Fig. 2. DTA curves. The numeration of the curves is the same as in Fig. 1

Thus, the loss in weight of the sample during heating up occurred essentially in a single step, between 330 and 500 °C, if the decrease in weight arising from the liberation of moisture, indicated by the two small steps is disregarded. To find out, whether in this decrease in weight also other residual intermediate products participate, the decomposition of which coincides and is overlapping the process, in one instance heating up was interrupted after a loss in weight of 68 per cent, and IR spectrum of the residual sample was recorded. After the interruption, besides becoming slightly darker, no changes were observed on the sample, even its consistency remained the same, so that it preserved its original bead form. The infrared spectrum of this sample (Fig. 4) was the same as that of the starting bead polymer (Fig. 3) differences referring to structural changes were absent.

For the evaluation of the thermal properties of the matrix on the basis of the IR spectrum, the stretching frequencies of the CH_2, CH groups, and the bands arising from the monosubstituted benzene ring were used.

The infrared spectrum of polystyrene, corresponding to the matrix, was investigated by several authors. Thus LIANG and KRIMM [6] give the interpretation of about 30 bands on the basis of bands to be assigned to the mono-

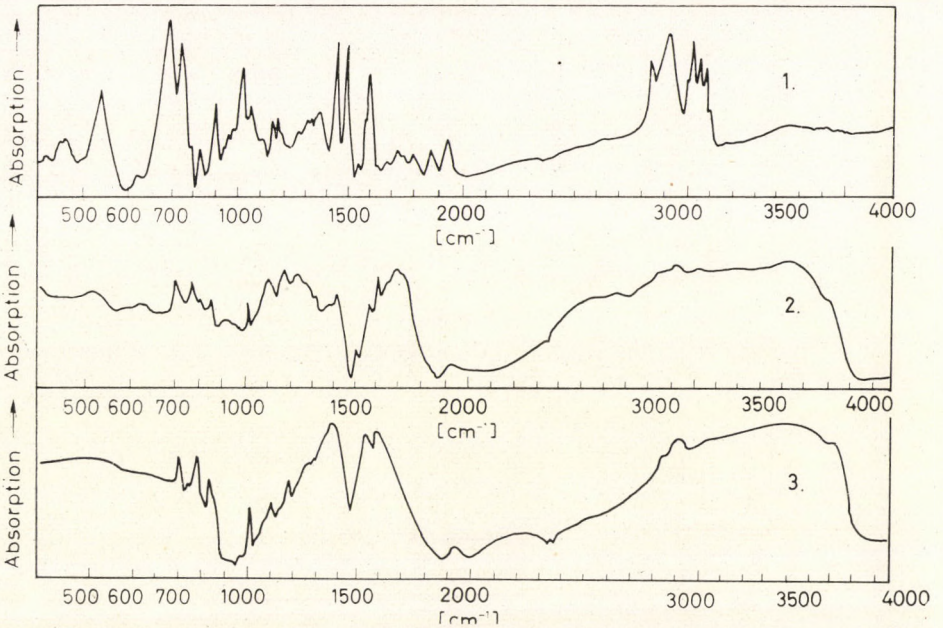


Fig. 3. Infrared absorption spectra. 1. Matrix (11.7 mg of polystyrene per 800 mg of KBr). 2. Varion CH resin in H-form. 3. Varion CH resin in Na-form

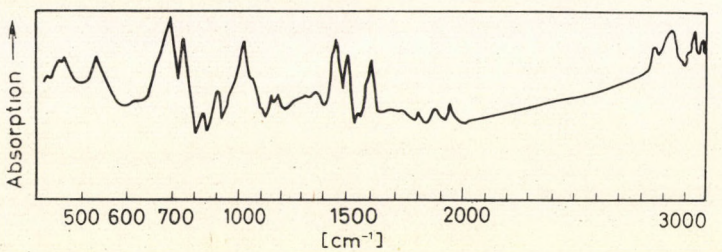


Fig. 4. The IR spectrum of the matrix after a loss in weight of 68 per cent

substituted benzene ring. On comparing spectral data published with the spectra recorded by us, there is an agreement concerning the number, intensity and location of the bands. Out of these, wave-numbers corresponding to the bands used for our evaluation are presented in Table I.

The infrared spectra of residual samples after a thermal treatment of the matrix resulting in a loss in weight of 68 per cent, presented no changes. This proves on the one hand that the chemical composition of the sample did not change, and on the other hand that decomposition did not yield new

Table I

Position of the bands used for the evaluation of the infrared spectra

	Polystyrene [6] cm^{-1}	Polystyrene cm^{-1}	Varion CH resin		Remarks
			H-form cm^{-1}	Na-form cm^{-1}	
ν_{as} CH_2	2923	2915	2920	2918	
ν_s CH_2	2851	2844	2850	2855	
δ CH_2	1450	1455	overlapped by 1425	ν_s C=O 1425	
γ_r CH_2	725	695	705	715	+substituent on the benzene ring
δ CH	1376	1380	overlapped by	ν_s C=O	
ϱ CH	1610	1605	1612	1606	
ν C—C	1070	1028	overlapped by	ν_s C=O	
δ C—C + C—H bending	1033	1028	1020	1015	for the evaluation of thermal behaviour of the matrix

Table II

Kinetic data on the thermal decomposition of polystyrene on the basis of derivatographic investigation

Order of reaction	Activation energy kcal/mole	Notes	Ref.
0	48	Under nitrogen atmosphere	Own measurements
0	46	Up to a weight loss of 10% below 370 °C	[3]
1	60 ± 5	Up to a weight loss of 15—95% above 370 °C	
0	44	Below 340 °C	[4]
0—1	58	Above 340 °C	[5]

compounds. The decrease in weight might be probably due to sublimation. However, no deposition of any sublimation product was observed.

Decomposition resulting in the formation of gaseous products, which volatilize without residue, is to be considered the most probable process. The determination of the order of the reaction and of the activation energy

of this decomposition from the DTG data of the derivatogram according to FREEMAN and CAROLL [3] and FLÓRA [9] gave zero order for the decomposition reaction, with an activation energy of 48 kcal/mole.

Kinetic data on the thermal decomposition of polystyrene have been summarized together with data published by other authors, in Table II.

Investigation of the thermal properties of EDTA-$Na_2 \cdot 2H_2O$

The thermal decomposition of Analar EDTA-$Na_2 \cdot 2H_2O$ proceeds in four distinctly separated steps (Curve 2, Fig. 1).

After the termination of the single decomposition steps, the heating up of the samples was interrupted, and the IR spectrum of the residual substance was recorded.

a) The first step, resulting in a loss in weight of 10 per cent, terminates at 220 °C. The IR-spectrum of the residual substance (Fig. 6) does not present any changes as compared to that of an untreated sample (Fig. 5). The decrease in weight corresponds to the loss of two moles of water. The liberation of water is not evidenced by the infrared absorption spectrum. Presumably the sample has taken up water again during its tabletting. Neither does the spectrum show other structural changes.

b) At the termination of the decomposition, characterized by a peak temperature of 290 °C, a loss in weight of 21.4 per cent was measured. During this process, intensive gas evolution, foaming, was observed. The residual sample after the termination of the process was a yellowish brown crumbling substance, which, upon the action of atmospheric humidity rapidly became sticky. The infrared spectrum of this residue presented substantial changes as compared to that of the original sample (Fig. 5). In the region from 1300 to 1400 cm^{-1}, the bands of the stretching and deformation vibrations of the CH_2-groups decreased strongly in comparison with the bands of the C=O stretching vibration, of known high molecular extinction coefficient. The spectral region of a wave number higher than 1800 cm^{-1} is rendered practically inevaluable by absorption due to the moisture content of the sample.

The spectrum is indicative of a change in the skeletal structure $N-CH_2-CH_2-N$. The band of the stretching vibration ($\nu C=O$) in the region from 1600 to 1700 cm^{-1} shows the carbonyl group belonging to the more thermostable part of the molecule.

c) The process appertaining to the third decomposition step took place at a peak temperature of 400 °C. The loss in weight measured was 21.1 per cent. The infrared spectra taken on samples after a loss in weight of 42.3 and 55 per cent, respectively (Figs 8 and 9) indicate the formation of carbonate through oxalate. An increase in the ratio of the COO-Na bonds can be observed in the neighbourhood of $\nu_s CO$ and $\nu_{as} CO$ at 1430 and 1620 cm^{-1}.

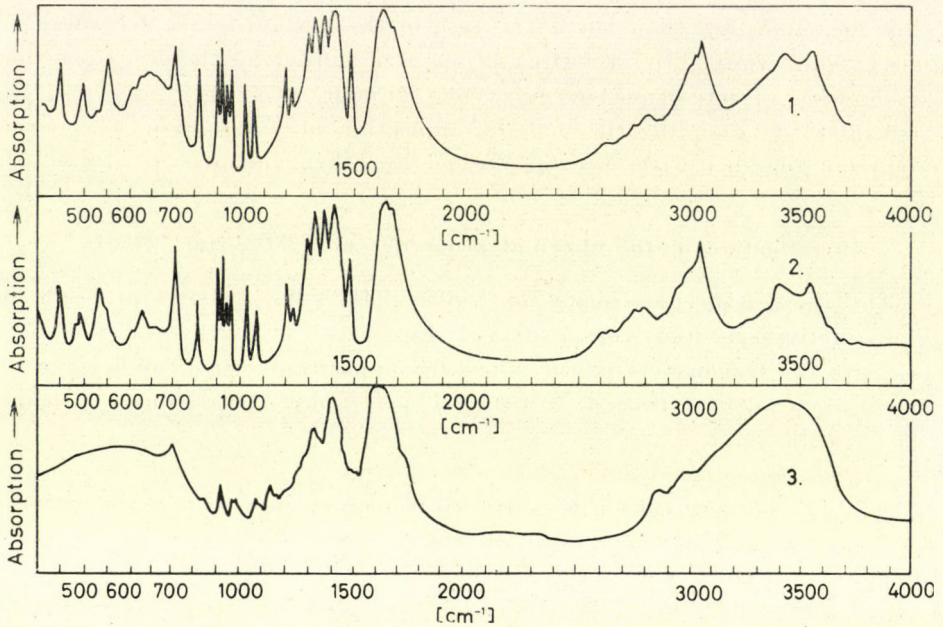


Fig. 5. IR spectra of EDTA-$Na_2 \cdot 2\ H_2O$. 1. Without heat treatment. 2. After heating, interrupted at 220 °C, loss in weight 11.4 per cent. 3. After heating, interrupted at 290 °C, loss in weight 14.4 per cent

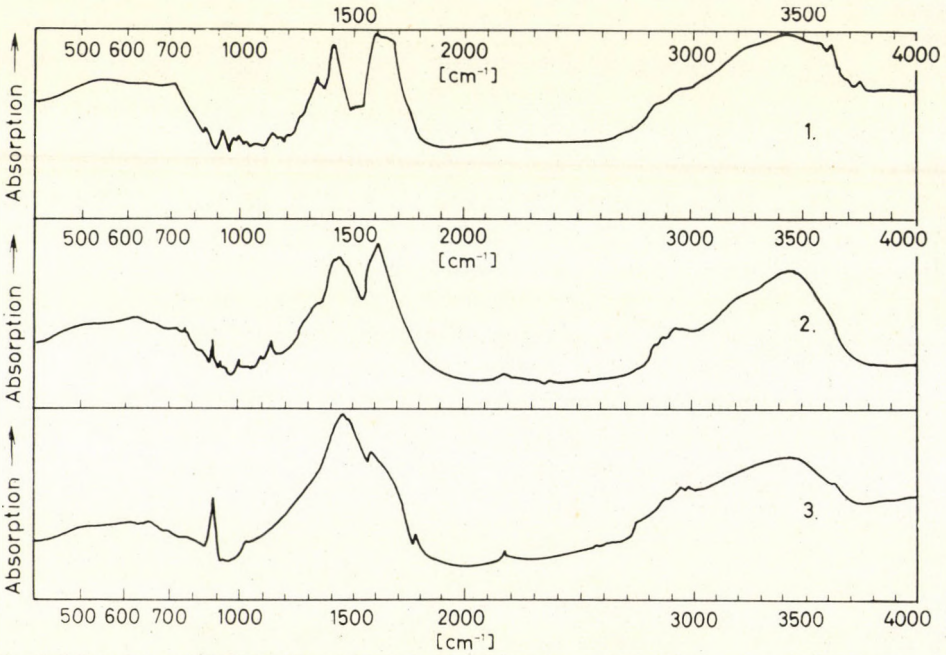


Fig. 6. IR spectra of EDTA-$Na_2 \cdot 2\ H_2O$. 1. Total loss in weight 42.3 per cent. 2. Total loss in weight 55.0 per cent. 3. Total loss in weight 64.0 per cent. (The decrease in weight is referred to the original substance)

d) Though derivatograms show distinctly separated decomposition steps, infrared spectra taken on samples from the two edges of the DTG peak at a loss in weight of 42.3 and 55 per cent respectively, show the gradual progress of the process.

To interpret the spectra of the residues after the beginning of this process (sample with 42.3 per cent of loss in weight) and before its termination (sample with 55 per cent of loss in weight), further of residues after the termination of the process (sample with 64 per cent of loss in weight), also the infrared spectra of sodium oxalate and sodium carbonate, and the derivatogram of sodium oxalate have been recorded.

In the spectrum of the sample having lost 55 per cent of its weight, the band occurring in the vicinity of 1620 cm^{-1} is indicative of an ionic carboxyl group, which is shifted in the spectrum of sodium oxalate to 1648 cm^{-1}. Bands observed in the vicinity of 885 cm^{-1} and 1450 cm^{-1} indicate the sodium carbonate content of this sample. The peak at about 1330 cm^{-1} to be expected in the presence of oxalate, is overlapped by the strong absorption due to the carbonate. The band in Fig. 6/2 at this place has only a shoulder. The presence of oxalate becomes more evident in the spectrum of the sample having suffered a loss in weight of 42.3 per cent (Fig. 6/1). A decrease in weight of 71.6 per cent would correspond to the process yielding as end product sodium carbonate, however, only a total loss in weight of 64 per cent was found. Nevertheless, the infrared spectrum of this sample (Fig. 6/3) is indicative almost exclusively of Na_2CO_3. The difference arises probably from carbonized components, formed upon the action of air impurity being in the nitrogen gas.

From derivatographic data, the activation energies and the order of reaction of the processes, corresponding to the separate decomposition steps, have been calculated. These data are presented in Table III.

Table III

Kinetic data on the thermal decomposition of EDTA-$Na_2 \cdot 2H_2O$ on the basis of derivatograms taken under nitrogen atmosphere

DTG peak temperature characteristic of the decomposition °C	Loss in weight (found) %	Loss in weight (calculated) %	Activation energy kcal/mole	Order of reaction
220	10	9.7	9.1	0
290	21.4	23.6	66.5	1.9
400	21.1	24.2	24.8	0.5
460	11.5	7.5		
	64.0	65.0		

Thermal properties of the ion exchange resins Varion CH

After the derivatographic and infrared spectrophotometric investigation of the matrix (styrene-divinylbenzene copolymer) and the model substance of the side chain, Varion CH resins in the H- and Na-form were studied.

Figs 1 and 2 contain the DTG, TG and DTA curves of these samples, too. Both samples present peaks showing the departure of the sorbed and absorbed water. In the case of the H-form resin, out of the peaks occurring at 90 and 150 °C, the latter may be caused by the departure of hydrochloric acid, held

Table IV

Kinetic data on the thermal decomposition of Varion CH resins on the basis of their derivatograms taken under nitrogen atmosphere

DTG peak temp. °C	Loss in weight %	Activation energy kcal/mole	Order of reaction	DTG peak temp. °C	Loss in weight %	Activation energy kcal/mole	Order of reaction
90	8.3	7.9	0.7				
150	3.9			140	6.3	5.5	0.5
250	4.4			270	6.0	1.7	0
	3.4			380	11.75	12.0	0.1
400	34.6	24.4	1.65	470	29.5	30.4	1
	9.2			560	9.5	7.7	0.13
				760	4.3		
				860	4.0		

back in the resin at the regeneration step. The derivatogram of the resin in the Na-form presents in this temperature range only one DTG peak at 140 °C, indicating the departure of water.

The decomposition of the resins begins at about 300 °C, but while the resin in the hydrogen form decomposes in two steps, characterized by the peak temperatures at 400 and 530 °C, respectively, the decomposition of the resin in the Na-form presents three steps with peak temperatures at 380, 470 and 500 °C. Kinetic data of the decomposition, calculated from the derivatograms, are presented in Table IV.

The decomposition of Varion CH resins was followed by infrared spectrophotometry. After each decomposition steps the residual samples were tested. In the evaluation, bands characteristic to the stretching and deformation vibrations of the CH and CH_2 groups were used for the evaluation of the skeleton structure, and bands arising from the stretching vibrations of the carbonyl group for that of the side chain.

Fig. 3/2 shows the infrared absorption spectrum of H-form Varion CH resin. Though we tried the remove adhering water from the sample by drying in a drying oven, the infrared spectrum showed above 1800 cm^{-1} intensive absorption, owing presumably to water content, taken up during pulverization and tabletting. At about 1700 cm^{-1}, a strong absorption band is exhibited, which is indicative of the formation of hydrogen bridges between the —COOH groups. At 1620 cm^{-1} the matrix, at 1425 cm^{-1} ν_s C=O produce relatively sharp absorption bands.

When heating up was interrupted at 300 °C, the spectrum (Fig. 7/1) did not present changes. The sample, the heating up of which has been interrupted at 420 °C (Fig. 7/2) exhibited changes concerning the carboxyl groups. The ratio of the band, indicative of the hydrogen bridges decreased, and also the decomposition of the aromatic skeleton can be presumed. The composition of the sample prepared by interruption of the heating at 520 °C (Fig. 7/3) could not be identified. This sample was a dark brown carbonaceous substance.

On interrupting the heating of the resin in sodium form (infrared spectrum: Fig. 3/3) at 400 °C, the residue exhibited the unchanged bands both of the matrix (1015, 1110, 1185) and of C=O (Fig. 8/1). As contrary to this, in the residual sample after interruption at 500 °C (Fig. 8/2), almost exclusively Na_2CO_3 was present (Fig. 8/3). Bands displayed at 1460 and 885 cm^{-1} are indicative of Na_2CO_3. In the IR spectrum of Na_2CO_3 (Fig. 8/3), out of the three the band appearing at 705 cm^{-1} is the weakest. This band is very weak for Na-Varion CH samples, the heating of which has been interrupted at 520 °C. Presumably, the presence of residual carbonaceous substances interfers.

A comparison with the model substances permits to draw the following conclusions on the thermal stability of the resins:

While the unsubstituted matrix departs in a single step, characterized by the peak temperature of 440 °C, in a reaction of zero order, and the skeleton of EDTA-$Na_2 \cdot 2H_2O$, of the model substance of the side chain, is decomposed at 290 °C, after the liberation of water (220 °C), the Varion CH resins do not show any decomposition at about 290 °C. After the liberation of water only a decrease in hydrogen bridges was observed. The decomposition of the resin at the points of interruption of heating begun simultaneously on the skeleton and on the side chain. The carboxyl groups of the side chain represent high termal stability. Decomposition takes place near the decomposition temperature of the unsubstituted matrix. Thus, the termal stability of the resin is determined primarily by the matrix, which stabilizes even the substituting imino acetic acid groups.

Presumably, also the increase in molecular weight has a stabilizing effect. Out of the Varion CH resins, that in Na-form showed higher thermal stability: it decomposed at a peak temperature of 470 °C, as compared to 400 °C, at which the H-form was decomposed.

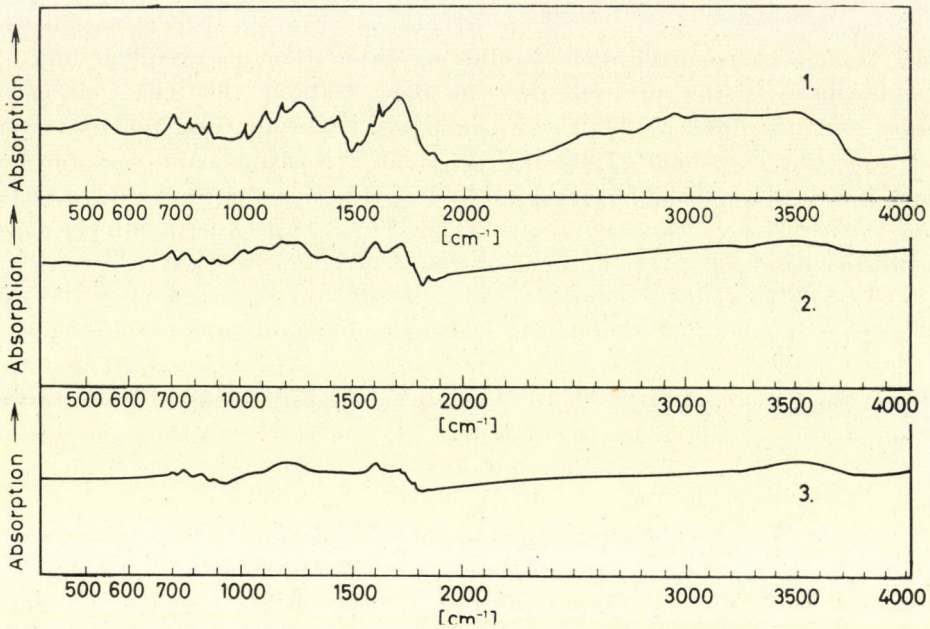


Fig. 7. IR spectra of the heat-treated Varion CH resins in H-form. Heating interrupted 1. at 300 °C 2. at 420 °C and 3. at 520 °C, respectively

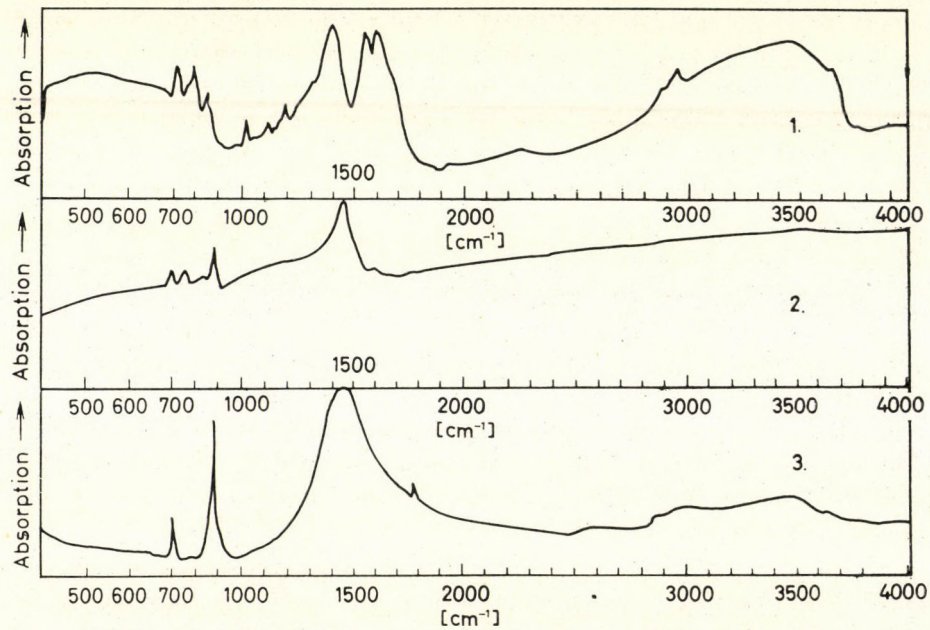


Fig. 8. IR spectra of the heat-treated Varion CH resins in Na-form. Heating interrupted 1. at 400 °C and 2. at 520 °C. 3. The IR spectrum of $Na_2CO_3.H_2O$

In the comparison of the peak temperatures of the decomposition steps, attention must be paid to the fact that Al_2O_3 was layered between the sample, to eliminate foaming during the heating up in the derivatograph, with the exception of polystyrene, where it was unnecessary. Presumably, the presence of Al_2O_3 shifts the decomposition peak on the DTG curve.

On the basis of the processes to be assigned to the single decomposition steps of Varion CH resins, conclusions may be drawn on their composition. One of these processes is the decomposition step of the H-form of Varion CH resin, characterized by a peak temperature of 250 °C. This step was assumed by us to correspond to the liberation of water. Assuming that this strongly bound water was linked to the substituent groups, and one imino diacetic acid group binds one molecule of water, a value of 2.92 mequv./g resin has been obtained for the capacity of the H-form resin. This value is in fairly good agreement with values obtained by other methods, thus *e.g.* with 2.55 mequv./g, obtained by capacity measurement on the basis of complex formation.

The other process, which similarly lends itself for capacity calculations, is the decomposition of the matrix, under the assumption, that on the side chains the beginning of the decomposition is retarded. The unsubstituted matrix is decomposed in a single decomposition step, characterized by a peak temperature of 440 °C. Assigning from the decomposition of the Na-form resin at a peak temperature of 470 °C on the basis of the behaviour of the matrix 94.7 per cent to the decomposition of the resin skeleton, the content in ion exchange group of the resin is 2.87 mequv./g, referred to the resin in H-form. This value is in fairly good agreement with the value of 2.92 mequv. per g of H-form resin, calculated on the basis of loss in water.

*

We wish to thank the Research Institute for Plastics Industry for the resin samples made available.

REFERENCES

1. Danusso, F., Polizotti, G.: Chimica e l'Industria **44**, 241 (1962)
2. Anderson, D. A., Freeman, S. S.: J. Polym. Sci. **54**, 253 (1961)
3. Freeman, E. S., Caroll, B.: J. Phys. Chem. **62**, 394 (1958)
4. Jellinek, H. H. G.: J. Polym. Sci. **4**, 13 (1949)
5. Madorsky, S. L.: J. Polym. Sci. **9**, 133 (1952)
6. Liang, C. Y., Krimm, S.: J. Polym. Sci. **27**, 241 (1958)
7. Paulik, F. and Paulik, J.: Termoanalízis (Thermoanalysis). Műszaki Könyvkiadó, Budapest 1963.
8. Szántó J., Mikes J.: Kolorisztikai értesítő **1964**, 239
9. Flóra, T.: Acta Chim. Acad. Sci. Hung. **48**, 225 (1966)
10. Náray-Szabó I.: Szervetlen Kémia (Inorganic Chemistry). Akadémiai Kiadó, Budapest 1962.

Irén Ambró
Teréz Flóra
Teréz Biró-Katkó
Veszprém, Wartha V.-u. 1. Hungary.

Acta Chimica Academiae Scientiarum Hungaricae, Tomus 59 (2), pp. 263—270 (1969)

KINETICS OF HYDROGEN ADSORPTION ON PLATINUM AND PALLADIUM ELECTRODES, II

THE VOLMER REACTION

I. TELCS

(Central Research Institute for Chemistry of the Hungarian Academy of Sciences.)

Received December 4, 1967

On platinum the Volmer reaction probably proceeds on several kinds of active sites, Eq. (1) being valid for all of these. The kinetics of the Volmer reaction can be measured during charging and discharging of the electrode on active sites with half-coverage equilibrium potentials $E_{0.5} > 0$, also known from adsorption equilibrium measurements. When hydrogen is eliminated from the electrode in a stationary process, kinetics of the Volmer reaction correspond to active sites with $E_{0.5} < 0$.

The possibilities of measurements during charging and discharging of the palladium electrode are less favourable, adsorption equilibrium cannot be measured, rates of adsorption can be measured only approximately. The tendency of the results, however, is so characteristic, that the presence of different kinds of active sites can be concluded with fair certainty. In stationary processes the Volmer reaction proceeds, according to observed kinetics, on other active sites, just as on platinum.

The conclusion seems reasonable that the Volmer reaction proceeds on all kinds of active sites with rate constants (exchange currents) not very different from each other. In the charging process, reaction is observed only on active sites with considerable coverages, *i.e.* $E_{0.5} > 0$. The Tafel reaction of hydrogen evolution and hydrogenation reactions proceed on active sites with $E_{0.5} < 0$. If these processes are investigated under stationary conditions, there is no charging process and the Volmer reaction is at equilibrium on active sites with $E_{0.5} > 0$. Thus the Volmer reaction becomes manifest on active sites with $E_{0.5} < 0$, which, on the other hand, are inoperative in the charging process.

In a previous communication [1] adsorption equilibrium of hydrogen on platinum electrodes was discussed. It was concluded that in acid solution hydrogen exists in at least four different states of adsorption, each of which can be described by a Langmuir isotherm of adsorption with haf-coverages in the potential range $E_e > 0$. The adsorption isotherm was there derived from the corresponding kinetic law of the Volmer reaction:

$$i = a_{H^+}^{\alpha}\left[k_+ \Theta e^{\frac{\alpha F}{RT}E} - k_-(1-\Theta)\, e^{-\frac{(1-\alpha)F}{RT}E}\right] \qquad (1)$$

where a_{H^+} is the activity of hydrogen ions, α a transmission coefficient, k_+ and k_- rate constants and E the electrode potential referred to a hydrogen electrode at 1 atm. overall pressure in the same solution as the electrode under examination. (Experiments were carried out in 1 N H_2SO_4 solution.)

From Eq. (1) immediately follows for the case of equilibrium, *i.e.* $i = 0$ the isotherm equation

$$\frac{\Theta}{1-\Theta} = \frac{k_-}{k_+} e^{-\frac{F}{RT}E_e} \tag{2}$$

The reverse relation, however, does not hold; the same isotherm can result from reactions with any different kinetics. As an example the possibility may be envisaged that adsorption takes place by the Volmer reaction according to Eq. (1) only on one kind of the several active sites while the others receive adsorbed atomic hydrogen by way of surface diffusion.

From the experiments to determine kinetics, the most sophisticated is that of BREITER [2] who carried out kinetic measurements by polarization with sinusoidal current. The experiment, complicated experimentally as well as computationally, in principle, simultaneously furnishes the hydrogen capacity C_a and the resistance R_V of the Volmer reaction as a function of the equilibrium potential E_e.

The course of C_a thus determined is similar to that known from the potential sweep method but lacking some of the finer details. Instead of peaks pointing to four kinds of active sites it revealed only two, which may point to a lesser sensitivity of the method.

The resistance R_V of the Volmer reaction is by definition

$$\frac{1}{R_V} = \left(\frac{di}{dE}\right)_{E \to E_e} \tag{3}$$

Applying this operation to Eq. (1) the following relation between R_V and E_e is obtained for a single kind of active sites:

$$\frac{1}{R_V} = k_+ \frac{F}{RT} a_{H^+}^{\alpha} \Theta e^{\frac{\alpha F}{RT}E_e} \tag{4}$$

where Θ may, if necessary, also be expressed by E_e from Eq. (2). The course of this function is similar to that of C_a: it is represented by a bell-shaped curve with a maximum at or near $E_e = E_{0.5}$ for $\Theta = 0.5$. The results of BREITER can indeed be represented by the superposition of two such curves which would signify that adsorption proceeds according to rate law 1 at least at two kinds of active sites simultaneously.

Because of the involved nature of the measurements and the relative insensitivity of the computation just with regard to changes of $1/R_V$, some doubt as to the reliability of the results is justified. It may be accepted as a fact, however, that in the case of freshly activated electrodes R_V is small over the entire range of measurement (60 mV $< E_e <$ 300 mV) and can be

neglected beside the resistance R_0 of the solution in series. It is seen from Eq. (4) that $1/R_V$ may be immeasurably small for small values of Θ, as Θ decreases more rapidly for positive values of $E_e - E_{0.5}$ as the exponential factor. This method, therefore, does not necessarily reveal all active sites on which the Volmer reaction may proceed.

Kinetics of the Volmer reaction have already been deduced much earlier in the range of negative potentials where this reaction does not perform the transient charging-discharging of the hydrogen capacity but the evolution of hydrogen gas, in series with the Tafel reaction. In this case the overall reaction is [3]

$$2\,H^+ + 2\,e^- \rightleftarrows 2\,H_a \rightleftarrows H_{2,s} \rightleftarrows H_{2,o} \tag{5}$$

and the corresponding rate equations are

$$\begin{aligned} i &= a_{H^+}^z\left[k_+\,\Theta e^{\frac{\alpha F}{RT}E} - k_-(1-\Theta)\,e^{-\frac{(1-\alpha)F}{RT}E}\right] = \\ &= 2\,Fk_T[(1-\Theta)^2 p_s - \Theta^2] = 2\,Fk_D\sqrt{n}\,(p_o - p_s) \end{aligned} \tag{6}$$

where k_D and k_T are the rate constants of diffusion and the Tafel reaction, respectively, p_o and p_s are the pressures in equilibrium with hydrogen dissolved in the bulk of the solution and the layer immediately adhering to the electrode surface, respectively. As may be seen, the Tafel reaction can only be accelerated by increasing Θ. In the range where the overall process is accelerated by potentials going in the negative direction, therefore, $\Theta \ll 1$ and the rate law of the Volmer reaction reduces to

$$i = -\,a_{H^+}^z\,k_-\,e^{-\frac{(1-\alpha)F}{RT}E}\,. \tag{7}$$

This rate law which in logarithmic representation gives

$$\log i = \text{const} - \frac{(1-\alpha)\,F}{RT}\,E \tag{8}$$

has been known for a long time [4].

As to the rate constant k_-, which, by the way, is identic with the more frequently cited exchange current i_0 in solutions of $p_H = 0$, views are rather divergent. In our judgement the highest values found in literature are the most reliable ones, as the most frequent errors, ageing of the electrode and the effect of the solution resistance tend to decrease the exchange current observed. Here we are only interested in the fact that this exchange current is relatively high and thus the overvoltage, *i.e.* the difference between E and E_e resulting from the Volmer reaction is quite negligible at pontentials not too far from 0 mV.

Consequently, in the case of the H_2 evolution reaction a Volmer reaction is observed which for $E_e < 0$ is accelerated in the direction of more negative values of E_e. The kind of active sites on which this reaction proceeds cannot, therefore, be among those which are demonstrated by measurements of either C_a or $1/R_V$ in the range of positive values of equilibrium potentials. Consequently, there must be assumed another kind of active sites on which half coverage is attained at negative equilibrium potentials $E_{0.5}$.

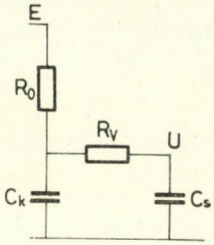


Fig. 1. Equivalent circuit of palladium electrode

In the following section conditions prevailing at the palladium electrode will be discussed. As far as known, hydrogen adsorption on the palladium electrode has not yet been measured because of the large, simultaneous absorption. This, however, does not prevent the determination of the kinetics of the adsorption reaction. The a.c. method employed in the case of platinum would be very complicated — if not entirely unmanageable — in this case, as periodic charging and discharging would involve absorption, too. The corresponding equivalent circuit is very complicated and even burdened with uncertainties. Measurements, therefore, were attempted by a simpler, though only approximate method.

The equivalent circuit under consideration is represented by Fig 1 where there appear besides the resistances R_0 and R_V, already introduced, the double layer capacity C_d and the sorption capacity C_s. The approximate nature of the assumption lies in the fact that C_s is taken as a simple capacity, as if hydrogen dissolved in the palladium were accessible without a resistance. According to diffusion coefficients quoted in literature [5] this resistance is indeed smaller by at least one order of magnitude than the investigated resistance R_V in the case of Pd layers 10^{-3} cm thick, as employed in the experiment. In the case of polarization by sinusoidal current the validity of this approximation is difficult to verify. Experiments, however, were carried out by a pulse technique giving simple and easily visualized results, so that any error committed would have been evident.

Measurements were carried out on α-phase palladium in the potential range 60—300 mV. The electrode was equilibrated by prolonged polarization at a fixed potential. Subsequently, polarization was switched to a constant

current and the change of potential with time observed on a crt. oscilloscope. Fig. 2 is a schematic drawing of a typical oscillogram. In the first, fast rising portion, the double layer is charged from the initial equilibrium potential E_e to the potential E, containing the overvoltage corresponding to current i. The subsequent slower rise originates from hydrogen depletion and, therefore, mainly from a change of E_e.

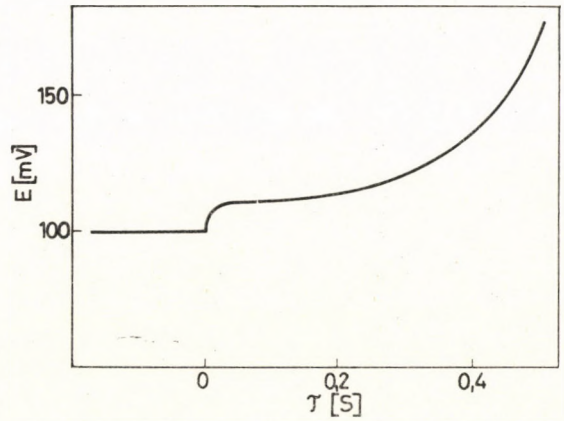


Fig. 2. Change of potential with ime on a hydrogen-containing palladium electrode after switching on of a constant (positive) current

If the slowly rising part of the curve is extrapolated to the instant of the switching on of the current — which can be done only approximately, of course — the potential E so determined gives — according to the assumption made — the overvoltage corresponding to i and the initial value of E_e. The difference $E - E_e$ is the potential drop on resistance R_V, *i.e.* the Volmer overvoltage. The quotient of i and $E - E_e$ gives $1/R_V$. This measurement can be carried out up to potentials of about 200 mV and gets uncertain at higher potentials.

The figure shows the justification of considering C_s as a single capacity, much larger than C_k. The relatively sharp break between the initial fast rise and the subsequent slower rise of potential can be explained only in this way. The same experiment does not lead to useful results in the case of platinum. The reason for this evidently is that with a comparable value for C_k, both C_s and R_V are much smaller for Pt than for Pd.

Fig. 3 schematically shows the change of $1/R_V$ with E_e on a palladium electrode. Values are only approximate as the relatively lengthy measurements can be carried out only on electrodes aged to an unknown degree. Still, it can be stated that $1/R_V$ is significantly smaller on Pd than on Pt, the difference being at least one order of magnitude. The weak change of $1/R_V$ in the interval extending up to about 200 mV would be hard to explain if conditions prevailing

on Pt were not known. Thus, however, the probable deduction is that this result points to the presence of several kinds of active sites in the case of Pd, too.

As in the case of platinum it may be investigated what information there can be derived from the hydrogen evolution process in the range of negative potentials. At very negative potentials relations (7) and (8) are valid for Pd,

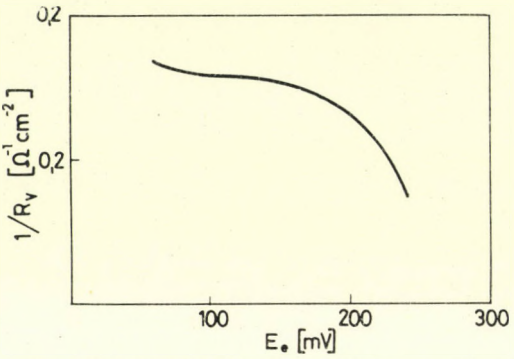


Fig. 3. Course of the reciprocal resistance $1/R_V$ of the Volmer reaction in the charging process of a palladium electrode

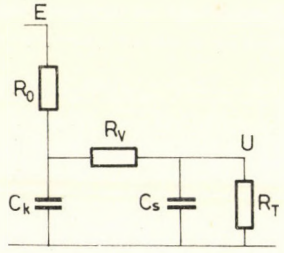


Fig. 4. Equivalent circuit of palladium electrode in the case of H_2 evolution reaction

too, with all the consequences ensuing. It is found, therefore, that on palladium, too, the Volmer reaction proceeds under conditions of H_2 evolution mostly, or entirely on such kinds of active sites on which half coverage equilibrium potentials are negative. In this range too, $1/R_V$ is smaller by at least one order of magnitude on Pd than on Pt.

In the case of palladium, investigation of the hydrogen evolution process is not restricted to the far negative end of the potential range, the so-called Tafel-line, for estimating kinetics of the Volmer reaction.

The method employed here is measurement of the potential after interruption of the polarizing current. While in the previous experiment the starting point was an equilibrium, here it is a stationary state. The corresponding equivalent circuit is shown in Fig. 4.

The new element of the circuit is R_T, the symbolic resistance of the Tafel reaction. In the stationary state U will differ from E. After cutting the current, the electrode potential, after a short transient, will revert to E_e, the value in equilibrium with the palladium surface. On ground of the foregoing it can be assumed in advance that $\Theta \ll 1$ and thus from Eq. (2).

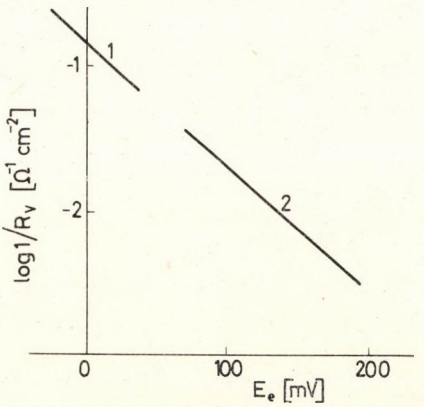


Fig. 5. Course of the reciproc resistance $1/R_V$ of the Volmer reaction in a stationary process of a palladium electrode

$$\Theta = \frac{k_-}{k_+} e^{-\frac{F}{RT}E_e} . \tag{9}$$

In this case there follows from Eq. (4):

$$1/R_V = k_+ \frac{E}{RT} a_{H^+}^z e^{-\frac{(1-\alpha)F}{RT}E_e} \tag{10}$$

or in logarithmic representation

$$\log 1/R_V = \text{const} - \frac{(1-\alpha)F}{RT} E_e \tag{11}$$

The experimental plot 1 of Fig. 5 is indeed a straight line and its slope too shows the theoretical value of 1/116 mV^{-1}.

A quite similar situation arises if, in a stationary process, there proceeds in series with the Volmer reaction — instead of the H_2 evolution reaction — a hydrogenation reaction equally eliminating atomic adsorbed hydrogen. In a previous paper [6] the possibility of measuring the Volmer overvoltage under such conditions was already treated but only with the aim of referring hydrogenation rates to potentials free of overvoltage. Kinetics of the Volmer

reaction can be derived as before from measurement of corresponding values of i, E and E_e. Plot 2 of Fig. 5 shows the result of such measurements in the case of the hydrogenation of propylene.

REFERENCES

1. TELCS, I. and JÁKY, M.: Acta Chim. Acad. Sci. Hung. **58,** 275 (1968)
2. BREITER, M.: J. Phys. Chem. **68,** 2249—2254 (1964)
3. TELCS, I. and JÁKY, M.: Acta Chim. Acad. Sci. Hung. (in the Press)
4. VETTER, KLAUS, J.: Elektrochemische Kinetik. Springer Verlag, Berlin (1961)
5. JEWETT, D. N., MAKRIDES, A. C.: Trans. Far. Soc. **61,** 932 (1965)
6. TELCS, I. and NAGY, F.: Magy. Kém. Folyóirat **73,** 143 (1967)

Iván TELCS; Budapest, II., Pusztaszeri út 57—69.

Acta Chimica Academiae Scientiarum Hungaricae, Tomus 59 (2), pp. 271—275 (1969)

KINETICS OF HYDROGEN ADSORPTION ON PLATINUM AND PALLADIUM ELECTRODES, III

THE TAFEL REACTION

I. TELCS and M. JÁKY

(Central Research Institute for Chemistry of the Hungarian Academy of Sciences)

Received December 4, 1967

It can be concluded from experimental evidence that the kinetics of the dissociative adsorption — recombination reaction of hydrogen are the same for platinum and palladium electrodes. From these kinetics follows that the kind of active sites promoting this reaction are, in the case of platinum, certainly not those known from hydrogen adsorption equilibrium, but of such a nature that hydrogen coverage on them reaches significant values only at rather negative potentials. The same seems to hold in the case of palladium electrodes, too.

In previous communications [1, 2] the adsorption of molecular hydrogen has already been discussed. On ground of various experimental evidence the possibility was excluded that the electrochemical mechanism of adsorption of molecular hydrogen, the so-called Heyrovsky reaction, should noticeably contribute to the overall process on either platinum or palladium Adsorption of molecular hydrogen, therefore, is subsequently treated only on the assumption of the dissociative or Tafel mechanism.

It was established furthermore on investigating the Volmer reaction that on charging or discharging the electrode with atomic adsorbed hydrogen, this reaction proceeds on the several kinds of active sites known from hydrogen adsorption equilibrium. If, however, the overall process is hydrogen evolution (or oxidation), *i.e.* there proceeds the Tafel reaction in series with the Volmer reaction, the latter takes place mostly or entirely on different kinds of active sites. It seems probable, therefore, that it is the Tafel reaction which can take place only on this new kind of active sites, not known from equilibrium measurements. In the present paper this assumption will be investigated in the light of further experience concerning the Tafel reaction.

On platinum electrodes, the investigation of the adsorption of molecular hydrogen is difficult, as on the only reproducible, freshly activated electrode, diffusion control only can be observed, adsorption rates thus being inaccessible to measurement. On ageing of the electrode, rate control of the adsorption process becomes a mixed one and adsorption control thus can be observed. In the sense of hydrogen evolution, *i.e.* desorption, this is not very helpful as mixed diffusion-desorption control can be observed only in a narrow potential range. Toward more negative potentials, *i.e.* higher rates, control by the

Volmer reaction is dominant. Conditions are different in the case of adsorption and oxidation. It was shown in paper [1] that on moderately aged electrodes there are found in this range rates lower than the limiting rate of diffusion which increase only weakly and monotonously with increasing potential. Here the question may be put, what these results tell about the kinetics of the Tafel reaction. The rate law of the adsorption process with diffusion and Tafel reaction in series is

$$w = k_D \sqrt{n}\,(p_0 - p_s) = k_a(1 - \Theta^2)\,p_s - k_d\,\Theta^2 \tag{1}$$

where k_D is the rate constant of diffusion, n the number of revolutions per minute of the rotating disc electrode, p_0 and p_s are the partial pressures holding equilibrium with hydrogen in the bulk of the solution (in the present experiments practically 1 atm) and in the liquid layer immediately adhering to the electrode surface, respectively; k_a and k_d are the rate constants of adsorption and desorption and Θ is the hydrogen coverage on a given kind of active sites. As in equilibrium

$$\frac{\Theta^2}{(1 - \Theta)^2} = \frac{k_a}{k_d}\,p_e\,, \tag{2}$$

where p_e is the equilibrium pressure pertaining to the given Θ, the Tafel rate law can also be written

$$w = k_a(1 - \Theta)^2\,(p_s - p_e)$$

and finally, as p_e will be always negligible besides p_0 and p_s in the range investigated, the right hand term of Eq. (1) may be omitted.

It is known from hydrogen adsorption equilibrium that there exist several states of adsorption of atomic hydrogen, *i.e.* several kinds of active sites capable of adsorbing atomic hydrogen. Most conspicuous of these are the two peaks, already known rather a long time, with equilibrium potentials $E_{0.5}$ pertaining to half coverages $\Theta = 0.5$ of about 120 and 270 mV. According to results of BREITER [3] and one of the present authors [2] the resistance of the Volmer reaction is very small in this range, so that no serious error is committed by equating the electrode potential observed in anodic oxidation of hydrogen with the equilibrium potential. The adsorption isotherm for the individual kinds of active sites is [4]

$$\Theta = \frac{e^{-\frac{F}{RT}E_e}}{e^{-\frac{F}{RT}E_e} + e^{-\frac{F}{RT}E_{0.5}}}\,. \tag{3}$$

From this it follows, that $(1 - \Theta)^2$ changes rapidly with potential near $E_{0.5}$: the values are 0.01 for $E_{0.5} - 30$ mV and 0.8 for $E_{0.5} + 30$ mV. If the adsorption of molecular hydrogen took place on these active sites, a steep rise of the rate up to 150 mV, an almost unchanged rate up to 240 mV and another rise up to 300 mV should be expected. Experiment showed nothing like this, from 60 mV, *i.e.* from the limit where neglecting of the reverse reaction in Eq. (1) is justified, the rate practically reaches a limit too, with a subsequent, insignificant rise, presumably due to secondary causes. This behaviour indicates that the active sites in question take part in the adsorption of molecular hydrogen only insignificantly, or not at all.

This conclusion can also be verified by an estimate using results of cathodic, *i.e.* desorption measurements. Let us assume that the reaction proceeds on the active sites with $E_{0.5} \approx 120$ mV. At the corresponding equilibrium pressure, $p_{0.5} \approx 10^{-4}$ atm, the rate of adsorption and desorption is equal on this kind of active sites. The maximum rate of adsorption cannot be greater than the rate of collision of gaseous hydrogen, and presumably it will be smaller by orders of magnitude. This rate of collision is given by

$$m = (p\varrho/2\pi)^{1/2}, \tag{4}$$

where m is the mass of gas striking unit surface per second, p the pressure and ϱ the density of the gas at room temperature. Introducing the actual figures

$$m \approx 3.6 \cdot 10^{-2}\ \mathrm{g/cm^2\,s}. \tag{5}$$

As electrolytic evolution of 1 g hydrogen requires a charge of 96,500 coul, the corresponding current density is

$$i \approx 3.5 \cdot 10^3\ \mathrm{A/cm^2}. \tag{6}$$

This current corresponds to half coverage, the maximum current would be four times larger. Actual measurements have been carried out at current densities up to 10^2 A/cm^2 [5] and no desorption limitation was observed. As this current approaches the one given by Eq. (6) within two orders of magnitude and the latter certainly is an overestimate, it is fairly improbable that the active sites mentioned could be the carriers of desorption. The kind of active sites with $E_{0.5} \approx 270$ mV, *i.e.* $p_{0.5} \approx 10^{-9}$ atm is ruled out without any reserve.

While on platinum electrodes conclusions were restricted to experiments in the positive and far negative potential ranges, palladium renders possible measurements in the intermediate range. In the treatment of the Volmer kinetics [2] the experiment was already introduced which permits measurement of the open circuit, or quiescent potential at the electrode surface in

the course of the hydrogen evolution reaction. As relation (3) connects hydrogen coverage and the open circuit, or equilibrium potential, this potential, under certain conditions, permits of conclusions concerning coverage. The only difficulty is that $E_{0.5}$, the equilibrium potential for half coverage is unknown in this case. On ground of the preceding findings, however, it can safely be assumed that $E_{0.5}$ is more negative than the equilibrium potential ranging down to about −30 mV. In this case, according to Eq. (3)

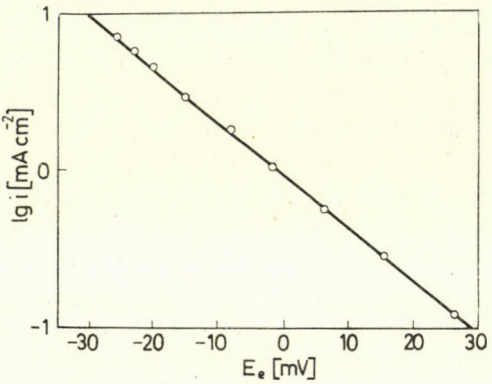


Fig. 1. Relation between the rate of hydrogen evolution and the open circuit potential on palladium electrodes

$$\Theta = \frac{e^{-\frac{F}{RT}E_e}}{e^{-\frac{F}{RT}E_{0.5}}} \ll 1. \tag{7}$$

As in these experiments the solution is flushed by inert gas and $p_0 = 0$,

$$w = -k_D \sqrt{n}\, p_s = k_a p_s - k_d \Theta^2 \tag{8}$$

or after eliminating p_S:

$$w = -\frac{k_D \sqrt{n}\, k_d \Theta^2}{k_D \sqrt{n} + k_a}. \tag{9}$$

The reaction rate at a given number n of rpm, therefore, is proportional to the square of coverage, or $e^{-\frac{2F}{RT}E_e}$. This is best visualized in the logarithmic representation. The figure shows the dependence of $\log i = \log 2Fw$ on E_e. The slope is in good agreement with the theoretical value of 1/29 mV^{-1}.

This measurement can inevitably be carried out on aged electrodes only, for charging the regenerated electrode to the potentials E_e of the range

of measurements takes a relatively long time. The fact that the process is not purely diffusion controlled ($k_D \sqrt{n} \ll k_a$) can always be verified by varying n.

REFERENCES

1. TELCS, I. and JÁKY, M.: Acta Chim. Acad. Sci. Hung. **58,** 275 (1968)
2. TELCS, I.: Acta Chim. Acad. Sci. Hung. (in the Press)
3. BREITER, M.: J. Phys. Chem. **68,** 2249, 2254 (1964)
4. TELCS, I. and JÁKY, M.: Acta Chim. Acad. Sci. Hung. **58,** 275 (1968)
5. VETTER, K. J.: Elektrochemische Kinetik, Springer Verlag, Berlin, 1961

Iván TELCS
Miklós JÁKY
Budapest II., Pusztaszeri út 57—69.

Printed in Hungary

A kiadásért felel az Akadémiai Kiadó igazgatója — Műszaki szerkesztő: Farkas Sándor

A kézirat nyomdába érkezett: 1968. XI. 4. — Terjedelem: 9,25 (A/5) ív, 32 ábra

68.66579 Akadémiai Nyomda, Budapest — Felelős vezető: Bernát György

INDEX

INORGANIC AND ANALYTICAL CHEMISTRY — ANORGANISCHE UND ANALYTISCHE CHEMIE — НЕОРГАНИЧЕСКАЯ И АНАЛИТИЧЕСКАЯ ХИМИЯ

VADOS, I., MOHAI, M. and UPOR, E.: Determination of Tantalum in Rocks by Neutron Activation Analysis 171

MÜLLER, I. and FÁY, L.: The Adsorption of Uranium Hexafluoride, II. Transport Processes in the Sorption of Uranium Hexafluoride 181

GEYER, R. und ROTERMUND, U.: Oszillopolarographische Untersuchungen zinnorganischer Verbindungen. (Oscillopolarographic Investigation of Organotin Compounds.) ... 201

ÚJHELYI, Cs.: On Solvolysis of "Alkylpyrophosphoric Acid Metal Solvent Extractants" . 211

CSÁKVÁRI, B., JENEI, S., KNAUSZ, D. and MESZTICZKY, A.: The Reaction of Dichlorogallane with Ethyl Halides (Preliminary Communication.) 225

PHYSICAL CHEMISTRY — PHYSIKALISCHE CHEMIE — ФИЗИЧЕСКАЯ ХИМИЯ

ILLÉS, V.: The Pyrolysis of Gaseous Hydrocarbons, II. The Mechanism of the Thermal Decomposition of *n*-Butane 229

AMBRÓ, I., FLÓRA, T. and BIRÓ, T.: Investigation of the Thermal Stability of the Resins Varion CH, Containing Imino Diacetic Acid Groups 249

TELCS, I.: Kinetics of Hydrogen Adsorption on Platinum and Palladium Electrodes, II. The Volmer Reaction 263

TELCS, I. and JÁKY, M.: Kinetics of Hydrogen Adsorption on Platinum and Palladium Electrodes, III. The Tafel Reaction 271

New volumes:

I. Náray-Szabó

Inorganic Crystal Chemistry

In Russian . 503 pages . 65 figures . 17×25 cm . Cloth

The results of research for more than half a century on the structure of crystals are presented in this book in terms of regular arrays of atoms, ions or molecules. The chemical formulae thought previously formalistic are represented as definite three-dimensional lattices. The structures are illustrated by a number of artistic figures. The system of elements and inorganic compounds, discussed strictly following the periodic table, gives a survey of inorganic chemistry on this basis for the first time.

L. Szepesy

Gas Chromatography

In English . Approx. 390 pages . 95 figures . 15×21 cm . Cloth

A general outline of the theoretical and practical aspects of gas chromatography including its application and trend of development is given in this book. In addition to the general survey the main features and application of preparative gas chromatography, process chromatographs as well as some special methods are treated.

Joint edition with Iliffe Books, London

Gy. Varsányi

Vibrational Spectra of Benzene Derivatives

In English . Approx. 420 pages . 17×25 cm . Cloth

This book gives a systematic survey of the vibration spectra of benzene derivatives and is also useful as regards assignation of the spectrum of benzene derivatives. It marks out what wave numbers and bands of what intensity shall be attributed to the aromatic structure — including CH bonds, i.e. it specifies the frequencies that can be ranged to the inner vibrations of the substituting groups.

Joint edition with Academic Press, New York

AKADÉMIAI KIADÓ
Publishing House of the Hungarian Academy of Sciences
Budapest

ACTA CHIMICA

ТОМ 59 — ВЫП. 2

РЕЗЮМЕ

Определение тантала в породах методом нейтронной активации

И. ВАДОШ, М. МОХАИ и Е. УПОР

Был разработан метод определения тантала в породах с помощью нейтронной активации. На основе ядерных данных для измерений был выбран фото-пик Ta^{182} с энергией 68 кэв. Выбирая за основу образец породы со средним, обычно встречающимся составом и на основе коэффициента Кларка и ядерных данных, вводилось сравнительный фактор для определения помех отдельных элементов. Исходя из этого, необходимая очистка производилась следующим образом. Вначале производилось разложение образца гидроокисью натрия и водное выщелачивание, а затем после растворения гидроокисного осадка роданид тантала экстрагировался метил-изобутилкетоном. Потери тантала незначительны, поэтому их отдельное определение нет необходимости. Конечный раствор чист с радиохимической точки зрения. Метод был применен с успехом и для анализа вольфрамовых руд. Продолжительность одного измерения составляет 30 минут.

Изучение адсорбции шестифтористого урана, II

Л. МЮЛЛЕР и Л. ФАЙ

Различные процессы диффузии-адсорбции обсуждаются на основе общего принципа классификации, т. е. известного из теории процессов и аппаратов уравнения Дамкьёлера для сохранения энергии и массы. В этом отношении процесс поглащения (выделения) может быть описан статической кинетикой адсорбции. Настоящее сообщение содержит результаты исследований кинетики адсорбции.

Описывается измерительная установка, разработанная для исследований систем UF_6-адсорбент, а также приводятся результаты измерений. На основе экспериментальных данных доказывается, что известные из литературы кинетические уравнения, содержащие условие линейности изотермы, не пригодны для описания кинетики взаимодействия UF_6 с адсорбентом. Было выведено новое кинетическое уравнение, содержащее условие изотермы типа Фрайндлиха. Полученная таким образом функция использовалась для описания кинетических кривых.

Изучение олово-органических соединений осцилло-полярографическим методом

Р. ГЕЙЕР и У. РОТЕРМУНД

С помощью осцилло-полярографического метода Хейровского и Форейта изучались следующие соединения: $BuSnCl_3$, $Bu_2Sn/OCOCH_3/_2$, Bu_3SnCl, $Bu_3SnOCOCH_3$, $Ph_3SnOCOCH_3$ и Bu_4Sn. В качестве основных растворов использовались смеси спирт–вода–HCl различного состава. Изучение этих соединений удалось осуществить вплоть до Bu_4Sn. Ацетаты ведут себя подобно хлоридам, т. к. в обоих случаях имеют место ионы типа $R_{4-n}Sn^{n+}$. Ион Bu_3Sn^+ в присутствии Bu_2Sn^{++} может быть определен вплоть до 0,005 мол.%.

Ион $BuSn^{+++}$ определяется в присутствии Bu_2Sn^{++} и Bu_3Sn^+, Bu_4Sn с помощью комплексометрического титрования в растворе уксусной кислоты и ацетата натрия и в присутствии пирокатехинового фиолета, как индикатора.

Исследование сольволиза растворителей для экстракции металлов типа алкилпирофосфорной кислоты

Ч. УЙХЕЛЬИ

При спонтанном сольволизе продуктов реакции взаимодействия окиси фосфора(V) со спиртом (н-бутанол или н-октанол) наблюдалось увеличение количества водорода сильных кислот. Увеличение количества первичного кислотного водорода объяснялось на основе алкоголиза и гидролиза присутствующей циклической алкилтрифосфорной кислоты.

Было установлено, что молярное отношение слабых (вторичных) и сильных кислотных водородов, измеренное непосредственно после окончания реакции в продукте реакции окиси фосфора(V) со спиртом, не зависит от молярного отношения $n_{спирт}/n_{P_2O_5}$ в растворе продукта реакции.

При гидролизе, т. наз., «диалкил-пирофосфорной кислоты — экстрагирующего агента», получаемого с помощью реакции окиси фосфора(V) со спиртом и используемого для приготовления экстрагирующего агента — моноалкил-ортофосфорной кислоты, образуется H_3PO_4. Образование H_3PO_4 объясняется гидролизом конденсированных алкилфосфорных кислот, содержащих более чем два атома фосфора и присутствующих в продукте реакции окиси фосфора(V) со спиртами.

Пиролиз углеводородных газов, II

Механизм термического разложения н-бутана, качественное и количественное распределение продуктов реакции

В. ИЛЛЕШ

Изучалось качественное и количественное распределение продуктов реакции при различных температурах в зависимости от конверсии н-бутана.

Из тангенса угла наклона касательных к начальному участку кривых выхода (вблизи конверсии $x = 0$) определялись стехиометрические факторы продуктов реакции, характерные для первичной реакции разложения. Полученные таким образом распределения продуктов реакции хорошо совпадают с рассчитанными на основе теории свободнорадикальных цепных реакций при условии длинных цепей.

Количественное распределение продуктов реакции значительно изменяется с увеличением конверсии и температуры. Относительное количество этилена и водорода возрастает, а относительное количество пропилена и метана уменьшается с увеличением жесткости условий пиролиза. Вышеупомянутые изменения, согласно нашим предположениям и в согласии с теорией свободнорадикальных цепных реакций, обусловлены разложением молекул пропилена и бутилена под влиянием активных радикалов растущих цепей, изомеризацией, протекающей до разложения бутильных радикалов, образующихся из исходных углеводородов в реакции расщепления водорода, а также реакциями, протекающими в двух направлениях этильных радикалов, образующихся в цепном процессе.

Было установлено, что выход продуктов реакции в зависимости от конверсии — в условиях работы промышленных реакторов пиролиза — описывается «одной кривой», независящей от температуры. Кривые выхода в зависимости от конверсии приближались полиномом третьего порядка.

Изучение термической стабильности искусственной смолы Varion-CH, содержащей группы имино-диуксусной кислоты, как ионообменники

И. АМБРО, Т. ФЛОРА и Т. БИРО

Дериватографическим методом изучались термические свойства хелатообразующей ионообменной смолы Varion-CH, отечественного производства. Изучение термического процесса проводилось с помощью ик-спектроскопии образцов, остающихся при прекращении нагрева смолы во время характерных ступеней разложения. Эти исследования проводились отдельно с модельным веществом матрицы (полистирол) и с ЭДТУ-

$NA_2 \cdot 2H_2O$, представляющим боковую цепочку. Кинетические данные термического разложения рассчитывались на основе кривых ДТГ и ТГ дериватографических измерений. Было установлено, что матрица значительно увеличивает стабильность боковой цепочки. Из данных на одной из ступеней термического разложения производились расчеты для доказательства состава.

Кинетика адсорбции водорода на платиновых и палладиевых электродах, II

Реакция Фольмера

И. ТЕЛЧ

Реакция Фольмера на платине протекает на активных центрах различных типов по уравнению 1., действительному для всех этих типов. Кинетика реакции Фольмера может быть измерена в течение заряда и разряда электродов на активных центрах с равновесным потенциалом полупокрытия $E_{0,5} > 0$, известным также из измерений адсорбционного равновесия. При выделении водорода из электрода в стационарном процессе, кинетика реакции Фольмера соответствует активным центрам с $E_{0,5} < 0$.

Проведение измерений в течение заряда и разряда палладиевого электрода менее удобно, т.к. нельзя измерить адсорбционное равновесие, и скорость адсорбции измеряется лишь приблизительно. Однако, характерная тенденция, наблюдаемая в результатах, приводит к весьма определенному выводу о существовании различных видов активных центров. В стационарных процессах реакция Фольмера протекает, согласно наблюдаемой кинетике, на других центрах, также как и в случае платины.

Кажется вполне обоснованным тот вывод, что реакция Фольмера протекает на активных центрах всех типов с константами скоростей (токами обмена) слабо отличающимися друг от друга. В процессе заряда реакция наблюдается лишь на активных центрах со значительным покрытием, т. е. $E_{0,5} > 0$. Реакция Тафеля — выделение водорода и реакции гидрирования — протекают на активных центрах с $E_{0,5} < 0$. Если эти процессы изучаются при стационарных условиях, то процесс заряда отсутствует, и реакция Фольмера находится при равновесии на активных центрах с $E_{0,5} > 0$. Таким образом, реакция Фольмера становится наблюдаемой лишь на активных центрах с $E_{0,5} < 0$, которые, с другой стороны, не принимают участия в процессе заряда.

Кинетика адсорбции водорода на платиновых и палладиевых электродах, III

Реакция Тафеля

И. ТЕЛЧ и М. ЯКИ

На основе экспериментальных данных может быть установлено, что как для платиновых, так и для палладиевых электродов, кинетика диссоциационной адсорбции — реакции рекомбинации водорода является одинаковой. Из кинетики следует, что активными центрами содействующими данной реакции, в случае платины, определенно являются не те центры, известные из адсорбционного равновесия водорода, а центры, обладающие такой природой, что покрытие водородом на них достигает значительных величин лишь в случае сильно отрицательных потенциалов. Подобная картина наблюдается и в случае палладиевых электродов.

The Acta Chimica publish papers on chemistry in English, German, French and Russian.

The Acta Chimica appear in volumes consisting of four parts of varying size, 4 volumes being published a year.

Manuscripts should be addressed to

Acta Chimica
Budapest 112/91 Műegyetem

Correspondence with the editors should be sent to the same address.

The rate of subscription is 165 forints a volume. Orders may be placed with "*Kultúra*" Foreign Trade Company for Books and Newspapers (Budapest I., Fő utca 32. Account No. 43-790-057-181) or with representatives abroad.

Les Acta Chimica paraissent en français, allemand, anglais et russe et publient des mémoires du domaine des sciences chimiques.

Les Acta Chimica sont publiés sous forme de fascicules. Quatre fascicules seront réunis en un volume (4 volumes par an).

On est prié d'envoyer les manuscrits destinés à la rédaction à l'adresse suivante:

Acta Chimica
Budapest 112/91 Műegyetem

Toute correspondance doit être envoyée à cette même adresse.

Le prix de l'abonnement est de 165 forints par volume.

On peut s'abonner à l'Entreprise pour le Commerce Extérieur de Livres et Journaux «*Kultúra*» (Budapest I., Fő utca 32. Compte-courant No. 43-790-057-181) ou à l'étranger chez tous les représentants ou dépositaires.

«*Acta Chimica*» издают трактаты из области химической науки на русском, французском, английском и немецком языках.

«*Acta Chimica*» выходят отдельными выпусками разного объема. 4 выпуска составляют один том. 4 тома публикуются в год.

Предназначенные для публикации рукописи следует направлять по адресу:

Acta Chimica
Budapest 112/91 Műegyetem

По этому же адресу направлять всякую корреспонденцию для редакции.

Подписная цена «*Acta Chimica*» — 165 форинтов за том. Заказы принимает предприятие по внешней торговле книг и газет «*Kultúra*» (Budapest I., Fő utca 32. Текущий счет № 43-790-057-181) или его заграничные представительства и уполномоченные.

42,— Ft

Reviews of the Hungarian Academy of Sciences are obtainable at the following addresses:

ALBANIA

Ndermarja Shtetnore e Botimeve
Tirana

AUSTRALIA

A. Keesing
Box 4886, GPO
Sydney

AUSTRIA

Globus Buchvertrieb
Salzgries 16
Wien I

BELGIUM

Office International de Librairie
30, Avenue Marnix
Bruxelles 5
Du Monde Entier
5, Place St. Jean
Bruxelles

BULGARIA

Raznoiznos
1, Tzar Assen
Sofia

CANADA

Pannonia Books
2, Spadina Road
Toronto 4, Ont.

CHINA

Waiwen Shudian
Peking
P. O. B. 88

CZECHOSLOVAKIA

Artia
Ve Smečkách 30
Praha 2
Poštovná Novinová Služba
Dovoz tisku
Vinohradská 46
Praha 2
Mad arská Kultura
Václavské nám. 2
Praha I
Poštová Novinová Služba
Dovoz tlače
Leningradská 14
Bratislava

DENMARK

Ejnar Munksgaard
Nörregade 6
Copenhagen

FINLAND

Akateeminen Kirjakauppa
Keskuskatu 2
Helsinki

FRANCE

Office International de Documentation et Librairie
48, rue Gay Lussac
Paris 5

GERMAN DEMOCRATIC REPUBLIC

Deutscher Buch-Export und Import
Leninstraße 16
Leipzig 701
Zeitungsvertriebsamt
Fruchtstrasse 3—4
1004 Berlin

GERMAN FEDERAL REPUBLIC

Kunst und Wissen
Erich Bieber
Postfach 46
7 Stuttgart S.

GREAT BRITAIN

Collet's Holdings Ltd.
Dennington Estate
London Rd.
Wellingborough, Northants.
Robert Maxwell and Co. Ltd.
Waynflete Bldg. The Plain
Oxford

HOLLAND

Swetz and Zeitlinger
Keizersgracht 471—487
Amsterdam C
Martinus Nijhof
Lange Voorhout 9
The Hague

INDIA

Current Technical Literature
Co. Private Ltd.
India House OPP
GPO Post Box 1374
Bombay I

ITALY

Santo Vanasia
Via M. Macchi 71
Mila
Libreria Commissionaria Sansoni
Via La Marmora 45
Firenze

JAPAN

Nauka Ltd.
92, Ikebukur O-Higashi 1-chome
Toshima-ku
Tokyo
Maruzen and Co. Ltd.
P. O. Box 605
Tokyo-Central
Far Eastern Booksellers
Kanda P. O. Box 72
Tokyo

KOREA

Chulpanmul
Phenjan

NORWAY

Johan Grundt Tanum
Karl Johansgatan 43
Oslo

POLAND

RUCH
ul. Wronia 23
Warszawa

ROUMANIA

Cartimex
Str. Aristide Briand 14—18
Bucureşti

SOVIET UNION

Mezhdunarodnaya Kniga
Moscow G—200

SWEDEN

Almquist and Wiksell
Gamla Brogatan 26
Stockholm

USA

Stechert Hafner Inc.
31, East 10th Street
New York, N. Y. 10003
Walter J. Johnson
111, Fifth Avenue
New York, N. Y. 10003

VIETNAM

Xunhasaba
19, Tran Quoc Toan
Hanoi

YUGOSLAVIA

Forum
Vojvode Mišića borj 1
Novi Sad
Jugoslovenska Knjiga
Terazije 27
Beograd

16. III. 1969

Index: 26.007

ACTA CHIMICA

ACADEMIAE SCIENTIARUM HUNGARICAE

ADIUVANTIBUS

L. ERDEY, K. POLINSZKY, G. SCHAY

AC

R. BOGNÁR, GY. BRUCKNER, Z. CSŰRÖS, T. ERDEY-GRÚZ, Z. FÖLDI, M. FREUND, Á. GERECS, GY. HARDY, J. HOLLÓ, M. KORACH, F. MÁRTA, F. NAGY, E. PUNGOR, Z. SZABÓ, P. TÉTÉNYI, L. VARGHA, K. VAS

REDIGIT

B. LENGYEL

TOMUS 59 FASCICULI 3—4

AKADÉMIAI KIADÓ, BUDAPEST

1969

ACTA CHIMICA

A MAGYAR TUDOMÁNYOS AKADÉMIA KÉMIAI TUDOMÁNYOK OSZTÁLYÁNAK IDEGEN NYELVŰ KÖZLEMÉNYEI

SZERKESZTI

LENGYEL BÉLA

TECHNIKAI SZERKESZTŐK

DEÁK GYULA és HARASZTHY-PAPP MELINDA

Az Acta Chimica német, angol, francia és orosz nyelven közöl értekezéseket a kémiai tudományok köréből.

Az Acta Chimica változó terjedelmű füzetekben jelenik meg, egy-egy kötet négy füzetből áll. Évente átlag négy kötet jelenik meg.

A közlésre szánt kéziratok a szerkesztőség címére (Budapest 112/91 Műegyetem) küldendők.

Ugyanerre a címre küldendő minden szerkesztőségi levelezés. A szerkesztőség kéziratokat nem ad vissza.

Az Acta Chimica előfizetési ára kötetenként belföldre 120 Ft, külföldre 165 Ft. Megrendelhető a belföld számára az „Akadémiai Kiadó"-nál (Budapest V., Alkotmány utca 21. Bankszámla 05-915-111-46), a külföld számára pedig a „Kultúra" Könyv- és Hírlap Külkereskedelmi Vállalatnál (Budapest I., Fő utca 32. Bankszámla: 43-790-057-181) vagy annak külföldi képviseleteinél és bizományosainál.

Die Acta Chimica veröffentlichen Abhandlungen aus dem Bereiche der chemischen Wissenschaften in deutscher, englischer, französischer und russischer Sprache.

Die Acta Chimica erscheinen in Heften wechselnden Umfanges. Vier Hefte bilden einen Band. Jährlich erscheinen 4 Bände.

Die zur Veröffentlichung bestimmten Manuskripte sind an folgende Adresse zu senden:

Acta Chimica
Budapest 112/91 Műegyetem

An die gleiche Anschrift ist auch jede für die Redaktion bestimmte Korrespondenz zu richten.

Abonnementspreis pro Band: 165 Forint. Bestellbar bei dem Buch- und Zeitungs-Außenhandels-Unternehmen »*Kultúra*« (Budapest I., Fő utca 32. Bankkonto No. 43-790-057-181) oder bei seinen Auslandsvertretungen und Kommissionären.

Acta Chimica Academiae Scientiarum Hungaricae, Tomus 59 (3—4), pp. 277—296 (1969)

THE ADSORPTION OF URANIUM HEXAFLUORIDE, III*

L. MÜLLER

(Mecsek Ore Mining Enterprise, Pécs)

Received December 21, 1967

The aim of the stationary investigation of diffusion was the selective determination of mass diffusion and molecular separation process in UF_6 adsorber systems The interpretation of convection-free diffusion processes was undertaken under utilization of the Schmith—Wakao model, and transport equations were derived for adsorbable and from the point of view of adsorption inert pairs of gases, respectively. After the description of experimental equipment, the validity of diffusion equations is proved. For columns packed with various adsorbents, the ratio of molecular separation and mass diffusion UF_6 material flow is determined in function of experimental parameters.

Investigation of stationary diffusion

In literature, mass diffusion, Knudsen diffusion, surface diffusion and "transient" diffusion are discussed in detail. Diffusion occurring in packed columns involve all the above-mentioned types of diffusion within the same operational unit, and only the ratios to each other may be questionable from the aspect of the overall diffusion current.

In this paper the diffusion in packed columns, in a stationary case, with particular respect to differentiate processes connected with the separation of molecules and with mass diffusion, respectively, is discussed. The scheme of the diffusion unit is shown in Fig. 1. In the diffusion model, the directions of the material flow of the two components are opposite to each other because

$$y_A + y_B = 1$$

and (1)

$$y_{A_1} > y_{A_2}$$

Equations describing stationary diffusion:

Fick's law cannot be directly applied to the description of the diffusion model because the diffusion in preferred direction is suppressed by the contrary flow of the other component. Let us now discuss in first approximation the diffusion of components A and B on the basis of the considerations of MAX-

* Communication II: Acta Chim. Acad. Sci. Hung. **59**, 181 (1969).

WELL and STEFAN [1, 2, 3]. Thus, in the binary mixtures various composition of components A and B, the velocity of counter-diffusion is determined by the linear progress rates of components A and B. Presuming that the concentration decrease of component $A - dc_A$, which acts as motive force of the flow of component A, is proportional to the relative linear velocity of component A related to component B, $u_A - u_B$, to the concentrations c_A and c_B and

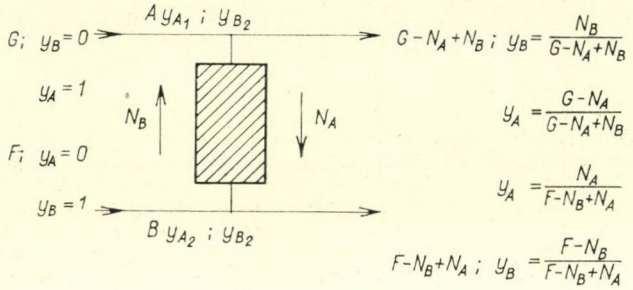


Fig. 1. Scheme of diffusion column packed with adsorbent

further to the distance dx along which diffusion actually takes place, we obtain:

$$-dc_A = \beta c_A c_B (u_A - u_B) dx \tag{2}$$

Since a binary mixture is present, molar concentrations c can be replaced by the term ϱ/M and the concentration gradient can be expressed as dp:

$$-dp_A = \beta \frac{\varrho_A \varrho_B}{M_A M_B} (u_A - u_B) dz. \tag{3}$$

Let us denote by N the number of moles passing in unit time through unit surface perpendicular to the direction of diffusion:

$$N = \frac{\varrho}{M} u \tag{4}$$

then

$$-dp_A = \beta \left(N_A \frac{\varrho_B}{M_B} - N_B \frac{\varrho_A}{M_A} \right) dz \tag{5}$$

Employing the law of ideal gases

$$\frac{\varrho}{M} = \frac{p}{RT}$$

and

$$p = p_A + p_B \text{ and } py_A = p_A;\ py_B = p_B, \tag{6}$$

further according to the definition:

$$D = \frac{R^2 T^2}{\beta p} \tag{7}$$

and applying the Bosanquet correlation:

$$\frac{1}{D} = \frac{1}{D_{AB}} + \frac{1}{D_K}$$

Thus from Eq. (5) we obtain:

$$N_A = -\frac{p}{RT} \frac{1}{\frac{(1-\alpha y_A)}{D_{AB}} + \frac{1}{D_K}} \frac{dy_A}{dx}, \tag{8}$$

where

$$\alpha = 1 + \frac{N_B}{N_A} \tag{9}$$

Eq. (8) describes the stationary diffusion of a binary gas mixture. In the case of non-sorbed pair of gases, the overall diffusion process takes place as the resultant of two components, *i.e.* of mass diffusion and Knudsen diffusion [4, 5, 6]. In respect to spheric conditions, a column packed with adsorbent behaves just as a bidisperse porous subtance with a network of channels on macro- and microscale, respectively. The network of macrochannels is represented by the free spaces between the grains of the adsorbent, while the network of microchannels by the inner pores of adsorbent grains.

Let us now consider the diffusion process on presuming the structure model suggested by SMITH and WAKAO [7] (Fig. 2). Obviously, on considering the geometrical conditions, the following possibilities exist for the diffusion of a particle.

a) Diffusion from a microchannel into a macrochannel. The substance diffuses in the free space between the adsorbent grains.

b) Diffusion from microchannel into another microchannel. The substance diffuses in the inside of the porous substance.

c) Diffusion from a macrochannel into a microchannel or reversed.

Let us presume that in the diffusion column the ratio of the cross sections of channel fractions is equal to the ratio of their volumes.

Let us denote by ε_a, ε_i and ε_s volume ratios of macropore, micropore and solid substance, respectively. Then we can write:

$$\varepsilon_a + \varepsilon_i + \varepsilon_s = 1 \tag{10}$$

If the diffusion model is intersected by a plane perpendicular to the plane of diffusion, and the obtained surfaces are fitted somehow to each other,

the new ratio of pore volumes will be, on the basis of the probability of an identical event which occurs independently:

$$(\varepsilon)\,(\varepsilon) = \varepsilon^2 \tag{11}$$

The full material transport through the "intersecting" plane consists of three terms:

a) of the diffusion term representing the diffusion which takes place in macropores and which can be characterized by the surface ε_a^2 and by the mean pore diameter, r_A;

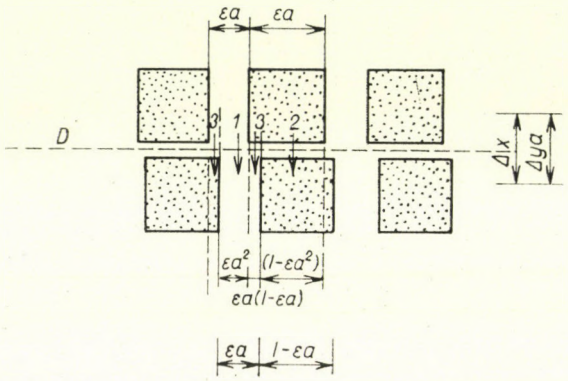


Fig. 2. Mechanism of diffusion in a bidisperse porous substance [7].
D: plane of intersection

b) of the diffusion term of intragrain micropores characterized by the surface $(1 - \varepsilon_a)^2$ and by the mean pore diameter, r_i. The real cavity surface of micropores is:

$$\frac{\varepsilon_i^2}{(\varepsilon_i + \varepsilon_s)^2} = \frac{\varepsilon_i^2}{(1 - \varepsilon_a)^2} \tag{12}$$

c) of the diffusion of macro-micro and micro-macro pore transition, respectively. The surface quotient of this process is

$$1 - \varepsilon^2 - (1 - \varepsilon_a)^2 = 2\varepsilon_a(1 - \varepsilon_a) \tag{13}$$

Let us now describe the diffusion flow of material for component A by means of Eq. (8):

$$N_A \frac{RT}{p} = -\varepsilon_a^2 D_A \frac{dy_A}{dx} - (1 - \varepsilon_a)^2 D_i \frac{dy_A}{dx} - 2\varepsilon_a(1-\varepsilon_a) \frac{2}{\frac{1}{D_A} + \frac{1}{D_i}} \frac{dy_A}{dx}$$

Mechanism 1 Mechanism 2 Mechanism 3 (14)

where D_A and D_i are the resultant diffusion constants, relating to the macro- and microregions, respectively, defined by the formulas

$$D_A = \frac{1}{\frac{1-\alpha y_A}{D_{AB}} + \frac{1}{D_{KA}}} \tag{15}$$

and

$$D_i = \frac{\frac{\varepsilon_i^2}{(1-\varepsilon_a)^2}}{\frac{1-\alpha y_A}{D_{AB}} + \frac{1}{D_{Ki}}} \tag{16}$$

In the knowledge of the mean pore radius, the Knudsen diffusion constant is calculated by the equation

$$D_K = \frac{2}{3} c_i r \tag{17}$$

At the extreme sites of the diffusion column of length L, the mole fractions of component A are y_{A1} and y_{A2}. Then the solution of Eq. (14) gives:

$$N_A \frac{RTL\alpha}{pD_{AB}} = \varepsilon_a^2 \ln \frac{1-\alpha y_{A2} + D_{AB}/D_{KA}}{1-\alpha y_{A1} + D_{AB}/D_{KA}} - \varepsilon_i^2 \ln \frac{1-\alpha y_{A2} + D_{AB}/D_{Ki}}{1-\alpha y_{A1} + D_{AB}/D_{Ki}} + \tag{18}$$

$$+ \frac{4\varepsilon_a(1-\varepsilon_a)}{1+\frac{(1-\varepsilon_a)^2}{\varepsilon_i^2}} \ln \frac{1-\alpha y_{A2} + \frac{D_{AB}}{D_{Ki}} \frac{\frac{(1-\varepsilon_a)^2}{\varepsilon_i^2} + \frac{D_{Ki}}{D_{KA}}}{1+\frac{(1-\varepsilon_a)^2}{\varepsilon_i^2}}}{1-\alpha y_{A1} + \frac{D_{AB}}{D_{Ki}} \frac{\frac{(1-\varepsilon_a)^2}{\varepsilon_i^2} + \frac{D_{Ki}}{D_{KA}}}{1+\frac{(1-\varepsilon_a)^2}{\varepsilon_i^2}}}$$

If $r_a \gg r_i$ and $\frac{D_{Ki}}{D_{KA}} \ll \frac{D_{AB}}{D_{KA}}$,

the geometric mean value can be replaced by the arithmetic mean value, in Eq. (18). Let us introduce the constant $D^\circ_{AB} = PD_{AB}$, which is independent of

the pressure. Then we obtain

$$N_A \frac{RTL\alpha}{D^0_{AB}} = \varepsilon_a^2 \ln \frac{1 - \alpha y_{A2} + \dfrac{D_{AB}{}^0}{D_{KA} P}}{1 - \alpha y_{A1} + \dfrac{D_{AB}{}^0}{D_{KA} P}} + \varepsilon_i^2 \frac{\alpha(y_{A1} - y_{A2})}{1 - \alpha \dfrac{yA_1 - yA_2}{2} + \dfrac{D_{AB}{}^0}{PD_{Ki}}} + \tag{19}$$

$$+ \frac{4\varepsilon_a(1-\varepsilon_a)}{1 + \dfrac{(1-\varepsilon_a)^2}{\varepsilon_i^2}} \frac{\alpha(y_{A1} - y_{A2})}{1 - \alpha \dfrac{y_{A1} - y_{A2}}{2} + \dfrac{\dfrac{D_{AB}{}^0}{PD_{Ki}}}{1 + \dfrac{\varepsilon_i^2}{(1-\varepsilon_a)_z}}}$$

If the diffusion model consists of a homogeneous pore structure, *i.e.* $\varepsilon_a = 0$ or, $\varepsilon_i = 0$, Eq. (14) has the following solution:

$$N_A \frac{RTL\alpha}{PD_{AB}} = \varepsilon^2 \ln \frac{1 - \alpha y_{A2} + D_{AB}/D_K}{1 - \alpha y_{A1} + D_{AB}/D_K} \tag{20}$$

In general, if one of the components of the binary gas mixture is adsorbed, the character of the non-stationary process preceding the formation of the stationary state is determined by the simultaneous diffusion and absorption. In a stationary case, the transport process is of purely diffusion character. However, on applying Eq. (14), surface diffusion must be taken into account. Surface diffusion is known to be a particular property of the adsorbed phase. The extent of diffusion depends mainly on the energetical conditions of the adsorbent-adsorbate system and on the properties of the active surface of the adsorbent. By this, also the theoretical limits of the calculation of surface diffusion have been defined. It is quite obvious that any preliminary estimation of the process is quite illusive, with the exception of one or two cases. Prior to discussing the generalization of Eq. (14), it must be noted that surface diffusion is connected with a separation according to molecular weights, and thus it is in its character, a process resembling Knudsen diffusion.

The equation describing the diffusion process for the material stream of the component to be adsorbed reads as follows:

$$N_A \frac{RT}{P} = -\varepsilon_a^2 D_A \frac{dy_A}{dx} - (1-\varepsilon_a)^2 D_i \frac{dy_A}{dx} - \varepsilon_i^2 D_F \frac{dy_A}{dx} -$$

$$- 2\varepsilon_a(1-\varepsilon_a) \frac{2}{\dfrac{1}{D_A} + \dfrac{1}{D_i + D_F^*}} \frac{dy_A}{dx} \tag{21}$$

when

$$D_F = D_a \bar{k}\, m\, y_A{}^{m-1}$$

and

$$D_F{}^* = \frac{\varepsilon_i{}^2}{(1-\varepsilon_a)^2} D_A \bar{k}\, m\, y_A{}^{m-1} \tag{22}$$

The surface diffusion constant D_A is reffered to unit surface of pore channels, for practical purposes.

The solution of Eq. (21), on integration from y_{A_1} to y_{A_2}; from $x = 0$ to $x = L$, is the following:

$$N_A \frac{RT}{P} = \frac{D_{AB}}{L\alpha} \varepsilon_a{}^2 \ln \frac{1 - \alpha y_{A2} + \dfrac{D_{AB}}{D_{KA}}}{1 - \alpha y_{A1} + \dfrac{D_{AB}}{D_{KA}}} + \frac{D_{AB}}{L\alpha} \varepsilon_i{}^2 \ln \frac{1 - \alpha y_{A2} + \dfrac{D_{AB}}{D_{Ki}}}{1 - \alpha y_{A1} + \dfrac{D_{AB}}{D_{Ki}}} +$$

$$+ \varepsilon_i{}^2 \frac{D_A \bar{k}}{L} \left(y_{A1}{}^m - y_{A2}{}^m\right) + \frac{4\varepsilon_a (1-\varepsilon_a)}{L} \cdot \tag{23}$$

$$\cdot \int_{y_{A_2}}^{y_{A_1}} - \frac{D_{AB} + D_F \left(1 - \alpha y_{A2} + \dfrac{D_{AB}}{D_{Ki}}\right)}{\left(\dfrac{1}{D_{KA}} + \dfrac{1-\alpha y_A}{D_{AB}}\right)\left[D_{AB} + D_a \bar{k} m y_A{}^{m-1}\left(1 - \alpha y_A + \dfrac{D_{AB}}{D_{Ki}}\right)\right]} +$$

$$+ 1 - \alpha y_A + \frac{D_{AB}}{D_{Ki}}$$

An approximative method is being used to perform the integration denoted in Eq. (23).

Free molecular flow and surface diffusion are the partial processes which result in the separation of molecules in the material transport unit. The efficiency of separation according to molecular weights is reduced by mass diffusion and by the process designed as Mechanism 3.

In the case when no significant physical adsorption takes place, the free molecular Knudsen flow is optimal considering the separation of molecules. This is reproduced in the industry by a separation membrane. It is, however, not practical to develop similar conditions with the investigated diffusion-adsorption model because the convectional flow caused by the pressure gradient deteriorates the separation efficiency. Therefore, the measurements were made, maintaining isobar conditions and varying the partial pressure of the component which is active in the diffusion adsorption process.

Two instruments have been employed for the diffusion experiments: in one apparatus, the porosity of the column packed with adsorbent and the

dimensions of the Knudsen diffusion channel were established, in the other one the diffusion adsorption properties of uranium hexafluoride were measured using the same column.

Apparatus

a) The parameters of the adsorption column were established with the apparatus shown in Fig. 3 [8, 9], employing N_2 and H_2 gases. The measuring system was based on a Griffin gas chromatograph of type MK II B. The column packed with the adsorbent (framed in the figure by dotted line) was placed in the air thermostat of the chromatograph. Prior to beginning the experiment, the adsorbent column was thermostated and the measuring system rinsed with nitrogen gas. The flow rate of nitrogen was adjusted by flow meter 2 by means of a reducing valve 1. The nitrogen current was allowed to part through the reference catharometer 5 into the head of the diffusion cell 6 where the gas current was enriched in the counter-diffusing component. The mixture of nitrogen and hydrogen gases were allowed to pass through

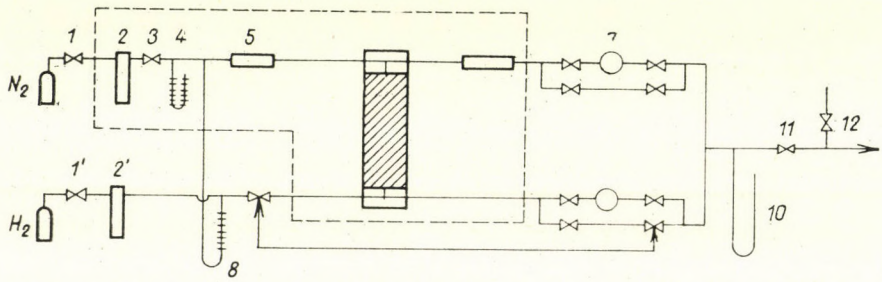


Fig. 3. Apparatus for the determination of the parameters of the diffusion column

the detector catharometer 5 into gas interferometer 7, where the composition of the gas mixture was established.

Hydrogen was introduced into the three-way head of the diffusion column through reducing valve 1' and gasometer 2', respectively; convection-free flow in the measuring systems was checked with manometer 8 and, respectively, adjusted appropriately. The mixture of nitrogen and hydrogen was analyzed after the diffusion column by a gas interferometer 7'. After the gas interferometer, the two gas streams were combined, their pressure measured and then the gases conducted. When the experiments were carried out at sub-atmospheric pressures, the desired pressure of the measuring system was adjusted by a vacuum pump built into the chromatograph. In a Zeiss gas interferometer 25- and 50-cm gas cells were applied. The reference cell contained pure nitrogen or hydrogen gas, depending on the fraction.

b) The apparatus used in the diffusion adsorption investigations performed with a gas mixture UF_6—N_2 is presented in Fig. 4.

Prior to describing the operation of this apparatus, two constructional problems of the two equipments are to be discussed.

1. *Production of a stationary uranium hexafluoride gas flow*

The solution of this problem involves the purification of uranium hexafluoride followed by the introduction of the purified substance into the gas stream at a steady rate. For this purpose, a dosing separator has been built into the apparatus (Fig. 5).

On filling up the separator constructed from copper, the apparatus was short-circuited with the aid of the taps 9 and 10, and high vacuum was established by opening tap 15. At the same time, container 8 filled with uranium hexafluoride was thermostated at 80°C, and the separator pipe heated by an electric coil until its perforated end reached a temperature of at least 20—30°C. Subsequently, tap 15 was closed, and the "freezing out" A uranium hexafluoride was started by opening the needle valve of the container 8. This operation lasted

for 2—3 hours. On closing the valve of the container, the separator was further cooled by allowing the cooling aggregate to run at its maximum capacity, and the system sucked through tap 15, in order to remove hydrogen fluoride contaminant. The separator filled up in this way was thermostated, a stream of nitrogen allowed to pass through it in order to obtain a gas stream of a steady content of uranium hexafluoride. The amount of uranium hexafluoride was variable by altering the temperature of the thermostat.

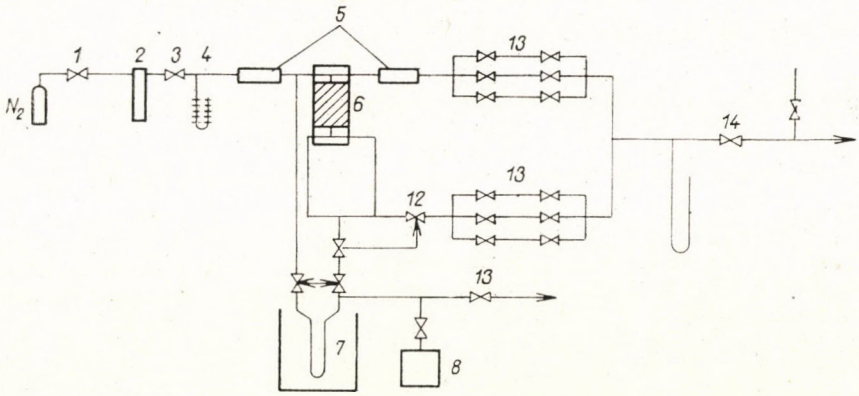


Fig. 4. Apparatus for the investigation of the diffusion adsorption properties of uranium hexafluoride

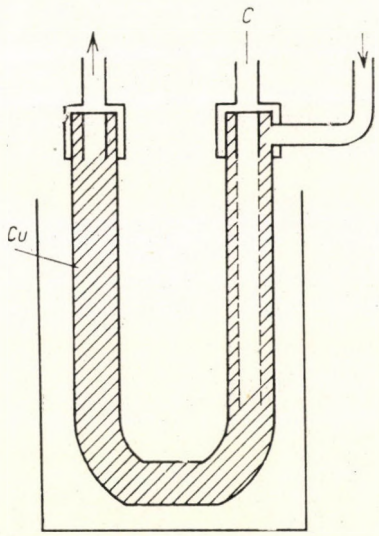


Fig. 5. Scheme of uranium hexafluoride separator, Cu: copper spiral packing; *C:* to container

2. *Excluding convection in the measuring system on applying a gas containing uranium hexafluoride*

Owing to the aggressive properties of uranium hexafluoride, no manometer can be inserted in the measuring equipment. Thus, the apparatus must exclude convection streams in the diffusion adsorption column, without any external control or intervention. Namely, from the branching after the reference catharometer to the recombination point after the

adsorbent flasks serving as traps, the system is previously measured as a gas dynamical Wheatstone bridge. The technique of this measurement is as follows. Replace column 6 by a differential manometer and select the capillary resistor or resistors in such a way that the current between end point 6 be always zero at any Δp pressure (potential) differences and convective streams (intensities). The "bridge" contains (traps) 13, on the switch sequence and on the uranium hexafluoride content of the separator, respectively. Since the resistance of these variable resistors is low (their diameter is greater by 15—20 than that of the capillaries), the changes in their resistance are negligible.

After filling up the separator and thermostating the diffusion adsorption column, the measuring equipment is ready for measurements. On switching on the nitrogen stream, rinse the apparatus. Measure the pressure and quantity of nitrogen with the aid of flow meter 2 and manometer 4, then check the uranium hexafluoride content of the nitrogen stream with the aid of taps 11 and 12 through the shunt line (switching on the taps 9 and 10), and begin the measurement by switching the gas which contains uranium hexafluoride, into the pipe of the diffusion cell. Detect the breakthrough curves and the time required for attaining equilibrium by means of catharometers 5. Fix the amount of uranium hexafluoride present in the nitrogen stream by the columns 13 packed with Nuxit Al carbon. The single columns can be lifted out separately. Measure gravimetrically the amounts of uranium hexafluoride adsorbed.

Discussion

a) *Measurements carried out with inert gas mixtures*

In the experiments carried out with nitrogen-hydrogen mixture, after attaining the stationary state, the following concentration conditions prevailed at the ends of the diffusion column (where component A was nitrogen and component B hydrogen):

molecular fractions on the side A (nitrogen)

$$y_A = \frac{G - N_A}{G - N_A + N_B}, \qquad y_B = \frac{N_B}{G - N_A + N_B} \tag{24}$$

molecular fractions on side B:

$$y_A = \frac{N_A}{F - N_B + N_A}, \qquad y_B = \frac{F - N_E}{F - N_B + N_A} \tag{25}$$

It is known [10] that the counter-diffusional material streams are reversely proportional to the square roots of molecular weights, *i.e.*

$$N_{H_2} = 3.741\ N_{N_2} \tag{26}$$

Let us examine the stationary diffusional material streams at four different adsorbents on the columns Ni II, Cu II, Pth and FO9 at various pressures and at varied molecular fractions. The experimental results are given in Table I.

Table I

Experiments with N_2—H_2 gas pairs F column surface ± 0.785 sq.cm

Adsorbent	P atm.	Nitrogen flow N_A mole/sec.	Hydrogen flow N_B mole/sec.	Nitrogen flow		Hydrogen flow		$\frac{1}{F}$	*RTL* N_A
				Y_{N_2}	Y_{N_2}	Y_{H_2}	Y_{H_2}		$(y_{A_1}-y_{A_2})D^\circ_{AB}$
Ni II	0.982	$2.239 \cdot 10^{-7}$	$8.376 \cdot 10^{-7}$	0.729	0.271	0.1200	0.880		$8.240 \cdot 10^{-2}$
	0.848	$2.382 \cdot 10^{-7}$	$8.911 \cdot 10^{-7}$	0.844	0.156	0.0523	0.547		$7.811 \cdot 10^{-2}$
	0.782	$3.726 \cdot 10^{-7}$	$13.930 \cdot 10^{-7}$	0.776	0.224	0.0891	0.911		$15.250 \cdot 10^{-2}$
	0.699	$2.605 \cdot 10^{-7}$	$9.745 \cdot 10^{-7}$	0.882	0.128	0.0362	0.964		$9.690 \cdot 10^{-2}$
Cu II	0.982	$1.173 \cdot 10^{-7}$	$4.388 \cdot 10^{-7}$	0.850	0.150	0.051	0.949		$3.292 \cdot 10^{-2}$
	0.885	$2.139 \cdot 10^{-7}$	$8.002 \cdot 10^{-7}$	0.924	0.076	0.023	0.977		$5.902 \cdot 10^{-2}$
	0.826	$2.119 \cdot 10^{-7}$	$7.927 \cdot 10^{-7}$	0.954	0.047	0.016	0.984		$6.017 \cdot 10^{-2}$
	0.755	$1.310 \cdot 10^{-7}$	$4.900 \cdot 10^{-7}$	0.965	0.035	0.010	0.990		$3.999 \cdot 10^{-2}$
	0.648	$1.273 \cdot 10^{-7}$	$4.762 \cdot 10^{-7}$	0.970	0.030	0.0084	0.991		$2.046 \cdot 10^{-2}$
Pth	0.983	$2.863 \cdot 10^{-7}$	$10.710 \cdot 10^{-7}$	0.659	0.341	0.188	0.812		
	0.884	$1.404 \cdot 10^{-7}$	$5.253 \cdot 10^{-7}$	0.849	0.151	0.051	0.948		
FO9	0.983	$0.743 \cdot 10^{-7}$	$2.782 \cdot 10^{-7}$	0.929	0.071	0.0211	0.5789		
	0.884	$1.306 \cdot 10^{-7}$	$4.887 \cdot 10^{-7}$	0.931	0.069	0.0202	0.9798		

The porosity data characteristic to the column and the mean dimensions of macro- and microchannels, respectively, required for the determination of the Knudsen diffusion constant were calculated using the data of Table I. However, for the determination of the five characteristic parameters of the packed column the experimental data of diffusion alone are not sufficient. Since ε_s is the volume of column, the correlation

$$\varepsilon_s + \varepsilon_a + \varepsilon_i = 1$$

can directly be obtained in the knowledge of the density of the adsorbent weighed. If this correlation holds, it is satisfactory to determine experimentally only one of the porosity data, practically ε_a.

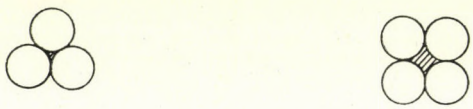


Fig. 6. Extreme cases of packing of adsorbent particles

On determining the diffusion constants let us take into account that the diffusion constant D_{Ki} of micropores had already been established on discussing the static sorption proper.

In this way, only ε_a and D_{KA} should be determined. Since under the applied experimental conditions $\frac{D_{Ki}}{D_{AB}} \sim 10^4$, the values of macro- and microporosity, respectively, fall into the same order of magnitude, and about 90 per cent of the material transport are due to mass diffusion taking place in macropores. Obviously the determination of the parameters of mass diffusion affects the accuracy of calculations carried out on the basis of Eq. (14). On the basis of the data of the measurements and of Eq. (14), let us establish the function ε- versus D_{KA}, the value range of which contains also the characteristics constants of the column. In order to select the preferred values of ε_a and D_{KA}, the following considerations are made. Let us consider the closest and widest packing, respectively, of the spherical particles of the adsorbent in the adsorbent column. For the arrangements listed in Fig. 6, a porosity value and a pore diameter characteristic of the intermediate channel system can be determined. However, a porosity value and a channel diameter belong also to all intermediate configurations. Let us now carry out the determination of the values of D_{KA} and ε_a in the two extreme cases mentioned above.

1. In the case of the closest packing, $6 \times 1/3 = 2$ free areas (denoted in Fig. 6 by stripes) pertain to each adsorbent particle.

For porosity ε_a we can write (porosity referred to surface is anyhow otherwise favourable also in respect to the considerations made on deriving Eq. (14)):

$$\varepsilon_a = \frac{\text{pore surface}}{\text{total surface}} = \frac{2R^2\left(\sqrt{3} - \frac{\pi}{2}\right)}{R^2 + 2R^2\left(\sqrt{3} + \frac{\pi}{2}\right)} = 0.0935 \tag{27}$$

2. Carrying out the same procedure for the case of the widest packing:

$$\varepsilon_a = \frac{R^2(4-\pi)}{R^2\pi + R^2(4\pi)} = 0.215 \tag{28}$$

Porosity is apparently independent of the particle radius. Let us now determine the D_{KA} values pertaining to the given porosities. The equation defining the value of D_{KA} reads [12]:

$$D_{KA} = \frac{2}{3} 14.551 \sqrt{\frac{T}{M}} \bar{R} \text{ (sq.cm per sec.)} \tag{29}$$

In the case of the closest packing, the value of R is:

$$\sqrt{\frac{R^2}{\pi}}\left(3 - \frac{\pi}{2}\right) = \bar{R} = 0.2271\, R \tag{30}$$

from that

$$D_{KA} = \frac{2}{3} 14.55 \sqrt{\frac{T}{M}} 0.2271\, R \tag{31}$$

While in the case of the widest packing

$$\sqrt{\frac{R^2}{\pi}}(4-\pi) = \bar{R} = 0.523\, R \tag{32}$$

from which

$$D_{KA} = \frac{2}{3} 14.55 \sqrt{\frac{T}{M}} 0.523\, R \tag{33}$$

On varying the particle radius, it is possible to construct a multitude of straight lines from the values D_{KA} *vs.* ε_a. The point of intersection of the straight constructed by replacing the radius of adsorbent particle and the function D_{KA} *vs.* ε_a determined by experiment affords the values of D_{KA} and

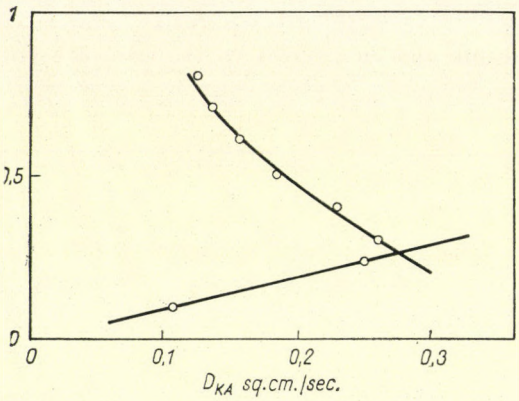


Fig. 7a

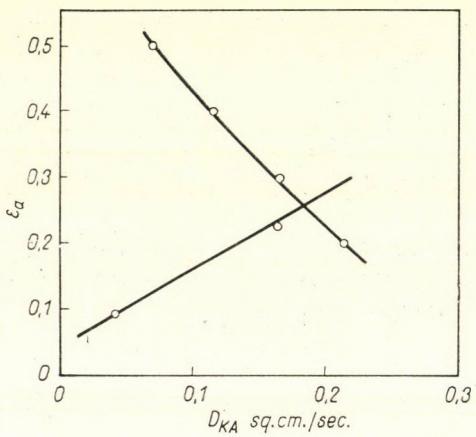


Fig. 7b

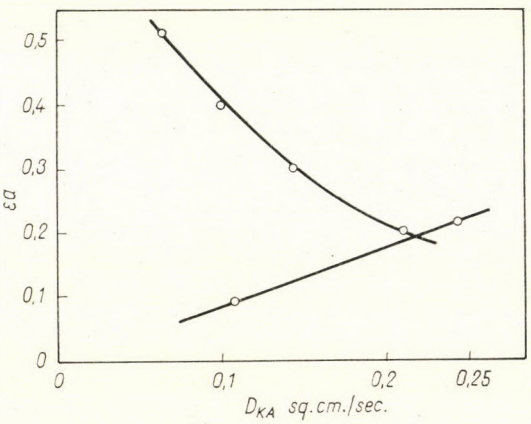


Fig. 7c

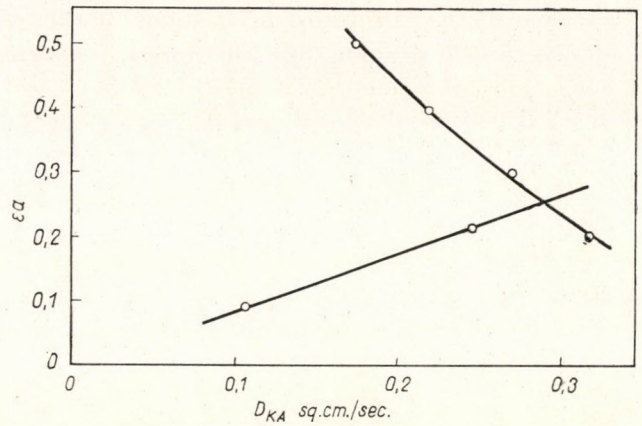


Fig. 7d

Fig. 7. Determination of the parameters of adsorbent columns by the graphical method. *a:* Ni II adsorbent, *b:* Cu II adsorbent; *c:* F 09 adsorbent; *d:* Pth adsorbent

ε_a, and through this latter also of ε_i, characteristic of the adsorbent column examined. The graphic determination of the values D_{KA} and ε_a is presented in Fig. 7.

The column characteristics calculated are summarized in Table II. Mass diffusion constants were calculated using the equation given by TIMOFEEV [17].

Table II

Characteristics of adsorbent columns

Adsorbent applied	ε_a	ε_i	ε_s	D_{KA} sq.cm/sec.	D_{Ki} sq.cm/sec.	Dimension of macropores $\bar{R}$, cm
Ni II	0.259	0.607	0.134	$0.882\sqrt{\frac{T}{M}}\cdot 10^{-1}$	$1.649\sqrt{\frac{T}{M}}\cdot 10^{-5}$	$8.48 \cdot 10^{-3}$
Cu II	0.255	0.435	0.310	$0.544\sqrt{\frac{T}{M}}\cdot 10^{-1}$	$0.970\sqrt{\frac{T}{M}}\cdot 10^{-5}$	$5.61 \cdot 10^{-3}$
FO9	0.192	0.523	0.285	$0.652\sqrt{\frac{T}{M}}\cdot 10^{-1}$	$1.940\sqrt{\frac{T}{M}}\cdot 10^{-5}$	$6.73 \cdot 10^{-3}$
Pth	0.250	0.580	0.170	$0.870\sqrt{\frac{T}{M}}\cdot 10^{-1}$	$1.164\sqrt{\frac{T}{M}}\ 10^{-5}$	$8.98 \cdot 10^{-3}$

b) *Measurements carried out with a mixture of nitrogen and uranium hexafluoride*

Uranium hexafluoride is actually adsorbed by the surface of the adsorbent. For the description of the diffusion process, Eq. (23) has been derived. The structural parameters characterizing the adsorbent columns were available on the basis of our experiments carried out with a pair of inert gases (Table II). The mass diffusion constant of the pair of gases N_2-UF_6 has been

calculated on the basis of the self-diffusion constants of the gas components. The self-diffusion constant of uranium hexafluoride *vs.* pressure and temperature can be described by the following equation [13, 14]:

$$D_{UF_6} = 0.0606 \frac{200}{p} \{1 + 6.29\,(t \cdot 10^{-3}) + \\ + 9.6\,(t \cdot 10^{-3})^2\} \qquad \text{(sq.cm per sec.)} \tag{34}$$

The mass diffusion constant $D_{UF_6-N_2}$ can be calculated using Eq. (35) [15]. (Diffusion data for nitrogen are to be found in corresponding handbooks.)

$$D_{UF_6-N_2} = 2^3 \frac{\sqrt{\frac{1}{M_A} + \frac{1}{M_B}}}{\left(\sqrt{\frac{1}{M_B D_A^2}} + \sqrt{\frac{1}{M_A D_B^2}}\right)^2} \tag{35}$$

The dependence on temperature of the diffusion constant $D_{UF_6-N_2}$ is plotted in Fig. 8.

In our diffusion adsorption studies with UF_6 and N_2 mixture, temperature was varied as an independent variable. The temperature range of the

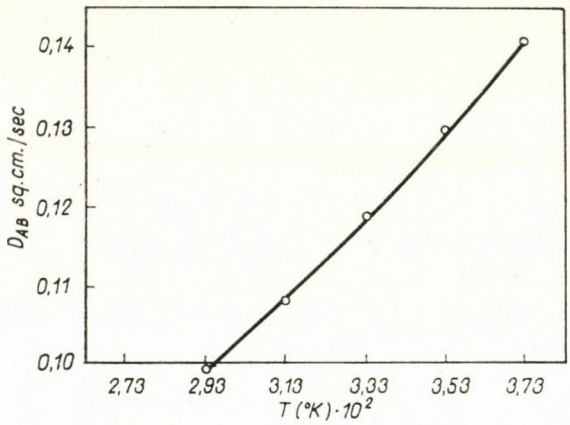


Fig. 8. Dependence on temperature of the mass diffusion constant of UF_6—N_2

experiments was determined on recognizing the properties of the adsorbents employed. In the case of Ni II as adsorbent, owing to its high sorption capacity, about 40—60 hours would be needed to attain the conditions of stationary state at room temperature. Consequently, in order to shorten the saturation period, the measurements were carried out between 60 and 127 °C while for the experiments with the adsorbent Cu II between 25 and 60 °C. In the case of the polytetrafluoroethylene adsorbent FO9 practically no temperature

requirements existed while on employing polyethylene sponge, the temperature of experiments was limited by the deterioration of the mechanical properties of the thermoplastic substance.

The data of the stationary diffusion experiments with UF_6-N_2 mixtures are presented in Table III.

The actually measured material flow is the resultant of processes denoted above by four different mechanisms such as:

a) gas diffusion material flow in micropores;

b) gas diffusion material flow in macro channels;

c) combined diffusion material flow (macro plus micro);

d) surface diffusion material flow.

The surface diffusion material flow can be determined by the resultant material flow measured experimentally and by the partial diffusion flows calculated according to Eq. (23) and denoted by the mechanisms *a)*, *b)* and *c)* (*cf.* Table III).

Now let us calculate the surface diffusion constants in the knowledge of surface diffusion data, applying Eq. (36):

$$N_{AF}\ \text{(moles per sec.)} = D_F\ \text{(sq.cm per sec.)}\ \frac{\Delta C_A\ \text{(moles/cu.cm)}}{L\ \text{(cm)}} \qquad (36)$$

referred to the unit surface of the packed column. The term ΔC_A expresses the difference in the concentrations of uranium hexafluoride present in an adsorbed phase at both ends of the column. On presuming that an equilibrium exists between the gas and the adsorbed phase, the partial pressures of uranium hexafluoride at both ends of the column are calculated by means of the measured molecular fractions of uranium hexafluoride, then the surface concentrations pertaining to given values of temperature and pressure are calculated from the isotherms. The results of these calculations are presented in Table III.

The surface diffusion constant is a function of temperature and surface coatedness [16, 17]. Increasing the temperature, the value of the "rate constant" D_F also increases. This correlation is given by the following equation [18]:

$$D_F = D_{F0}\, c^{-E/RT} \qquad (37)$$

where E is the activation energy of the process.

Since in these experiments no changes occur in the order of magnitude of surface concentration, it is possible to establish the activation energy of surface diffusion by calculation. The $\log D_F - 1/T$ plots are given in Fig. 9 while the surface activation energies are calculated from the slope of the curves (see Table IV).

Though it is not possible to draw far-reaching conclusions from the results [19, 20] the dependence of D_A on the surface-coatedness having been

Table III

Stationary diffusion investigations with $N_2 - UF_6$ gas pairs

Adsorbent	Temperature °C	Y_{A_1}	Y_{A_2}	Gas diffusion material flow				Measured overall material flow $N_A \cdot 10^9$ moles/sq. cm/sec.	Surface diff. mat. flow, N_A moles/sq.cm/sec.	ΔC_A moles/cu.cm	D_A sq.cm/sec.
				$N_A \cdot 10^9$ moles/ sq.cm/sec	Macropores	Micropores	Transient				
Ni II	60	0.0200	$2.10 \cdot 10^{-3}$	3.616	$2.136 \cdot 10^{-9}$	$3.60 \cdot 10^{-12}$	$4.84 \cdot 10^{-12}$	6.650	$3.02 \cdot 10^{-9}$	$3.48 \cdot 10^{-4}$	$0.865 \cdot 10^{-5}$
	80	0.0215	$2.25 \cdot 10^{-3}$	2.787	$2.777 \cdot 10^{-9}$	$4.04 \cdot 10^{-12}$	$5.51 \cdot 10^{-2}$	5.827	$3.14 \cdot 10^{-9}$	$3.23 \cdot 10^{-4}$	$0.973 \cdot 10^{-5}$
	100	0.0258	$1.65 \cdot 10^{-3}$	3.039	$3.029 \cdot 10^{-9}$	$4.96 \cdot 10^{-12}$	$6.76 \cdot 10^{-12}$	8.289	$5.25 \cdot 10^{-9}$	$4.33 \cdot 10^{-4}$	$1.212 \cdot 10^{-5}$
	127	0.0151	$3.50 \cdot 10^{-4}$	1.700	$1.694 \cdot 10^{-9}$	$2.91 \cdot 10^{-12}$	$3.95 \cdot 10^{-12}$	5.150	$3.43 \cdot 10^{-9}$	$2.78 \cdot 10^{-4}$	$1.237 \cdot 10^{-5}$
Cu II	25 I	0.0364	$4.56 \cdot 10^{-4}$	3.200	$3.195 \cdot 10^{-9}$	$2.42 \cdot 10^{-12}$	$2.96 \cdot 10^{-12}$	3.603	$4.03 \cdot 10^{-10}$	$4.78 \cdot 10^{-5}$	$1.450 \cdot 10^{-5}$
	25 II	0.0279	$1.98 \cdot 10^{-4}$	2.483	$2.479 \cdot 10^{-9}$	$1.86 \cdot 10^{-12}$	$2.30 \cdot 10^{-12}$	3.070	$5.87 \cdot 10^{-10}$	$3.86 \cdot 10^{-5}$	$1.520 \cdot 10^{-5}$
	38	0.0207	$2.67 \cdot 10^{-5}$	1.908	$1.905 \cdot 10^{-9}$	$1.39 \cdot 10^{-12}$	$1.91 \cdot 10^{-12}$	2.341	$4.33 \cdot 10^{-10}$	$2.78 \cdot 10^{-5}$	$1.560 \cdot 10^{-5}$
	50	0.0965	$4.16 \cdot 10^{-3}$	8.939	$8.925 \cdot 10^{-9}$	$6.14 \cdot 10^{-12}$	$8.54 \cdot 10^{-12}$	10.351	$13.92 \cdot 10^{-10}$	$7.15 \cdot 10^{-5}$	$1.950 \cdot 10^{-5}$
	60	0.0252	$2.14 \cdot 10^{-3}$	2.025	$2.022 \cdot 10^{-9}$	$1.53 \cdot 10^{-12}$	$2.12 \cdot 10^{-12}$	2.473	$4.52 \cdot 10^{-10}$	$2.61 \cdot 10^{-5}$	$1.730 \cdot 10^{-5}$
FO9	20	0.0300	$2.31 \cdot 10^{-3}$	7.910	$7.980 \cdot 10^{-9}$	$5.46 \cdot 10^{-12}$	$5.28 \cdot 10^{-12}$	8.579	$6.69 \cdot 10^{-10}$	$1.59 \cdot 10^{-5}$	$4.210 \cdot 10^{-5}$
	40	0.0298	$2.40 \cdot 10^{-3}$	1.449	$1.439 \cdot 10^{-9}$	$5.33 \cdot 10^{-12}$	$5.10 \cdot 10^{-12}$	2.089	$6.40 \cdot 10^{-10}$	$1.42 \cdot 10^{-5}$	$4.510 \cdot 10^{-5}$
	60	0.0295	$2.50 \cdot 10^{-3}$	1.522	$1.512 \cdot 10^{-9}$	$5.26 \cdot 10^{-12}$	$4.97 \cdot 10^{-12}$	2.251	$7.29 \cdot 10^{-10}$	$1.46 \cdot 10^{-5}$	$5.000 \cdot 10^{-5}$
	80	0.0290	$2.93 \cdot 10^{-3}$	1.474	$1.465 \cdot 10^{-9}$	$4.81 \cdot 10^{-12}$	$4.54 \cdot 10^{-12}$	2.046	$5.72 \cdot 10^{-10}$	$1.12 \cdot 10^{-5}$	$5.100 \cdot 10^{-5}$
Pth	20	0.0400	$5.10 \cdot 10^{-3}$	4.672	$4.660 \cdot 10^{-9}$	$5.13 \cdot 10^{-12}$	$6.83 \cdot 10^{-12}$	4.877	$2.05 \cdot 10^{-10}$	$1.27 \cdot 10^{-4}$	$0.160 \cdot 10^{-5}$
	40	0.0430	$4.90 \cdot 10^{-3}$	4.548	$4.536 \cdot 10^{-9}$	$5.48 \cdot 10^{-12}$	$7.28 \cdot 10^{-12}$	4.740	$1.92 \cdot 10^{-10}$	$1.00 \cdot 10^{-4}$	$0.192 \cdot 10^{-5}$
	50	0.0450	$3.70 \cdot 10^{-3}$	4.954	$4.940 \cdot 10^{-9}$	$5.97 \cdot 10^{-12}$	$7.66 \cdot 10^{-12}$	5.062	$2.37 \cdot 10^{-10}$	$1.08 \cdot 10^{-4}$	$0.219 \cdot 10^{-5}$

not examined, the obtained values show a good agreement with the values given in the literature [21, 22].

On the basis of the results of our experiments performed with UF_6-N_2 gas mixtures, and that with the results of our theoretical considerations, the following conclusion can be drawn:

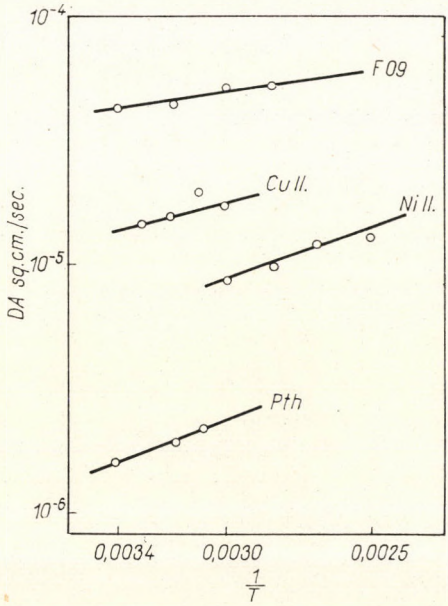


Fig. 9. Dependence on temperature of the constants of surface diffusion

Under the applied experimental conditions, surface diffusion plays a significant role in that it may amount in certain cases even to 50 per cent of the total material flow. Surface diffusion can be described appropriately by Eq. (36). The activation energy calculated from the temperature dependence of the surface diffusion constant, is 10 to 30 per cent of this mean sorption enthalpy.

Eq. (23) lends itself well to the description of stationary diffusion processes in the case of a sorbable mixtures while Eq. (18) is to be used in the case of inert gas mixtures. On utilizing the functional correlations, molecule

Table IV

Activation energy of surface diffusion on various adsorbents

Adsorbent applied	Activation energy, E cal./mole
Ni II	1800
Cu II	1000
FO9	2000
Pth	650

separation flows and mass diffusion flows can be calculated. In this way it is possible to choose adequately the pressure, temperature, pore structure and gas mixture to attain, within the operational unit of diffusion adsorption, an optimum value of molecular separation processes referred to the overall material flow.

List of symbols

c_A; c_B	concentration	moles/cu.cm
D_A; D_B	self diffusion constant	sq.cm/sec.
D_{AB}	mass diffusion constant	sq.cm/sec.
D_K	Knudsen diffusion constant	sq.cm/sec.
D_F	surface diffusion constant	sq.cm/sec.
E	activation energy of surface diffusion	cal./mole
G; F	material flow per unit surface	moles/sec. sq./cm
F	surface of column	sq. cm
k; m	constants of the Freundlich isotherm	
L	length of column	
M	molecular weight	
$N_A \cdot N_B$	material flow of components referred to unit surface	moles/sq. cm/sec.
$p_A \cdot p_B$	partial pressures of components	Torr
p	overall pressure	Torr
R	particle radius	cm
t	temperature	°C
T	temperature	°K
u_A; u_B	linear progress rate of components	cm/sec.
x	local coordinate	
y_A; y_B	molecular fractions	
α	$1 + \frac{N_B}{N_A}$	
ε_s	$1 - \varepsilon_i - \varepsilon_a$	
ε_i	microporosity	
ε_a	macroporosity	
	density	g/cu.cm

REFERENCES

1. Kinton Sherwood, T. K.: Chem. Eng. Progr. **46**, 258 (1950)
2. McAdams, E. Q.: Heat Transmission. McGraw-Hill, New York, 1942
3. Coulson, C. A., Richardson, O.: Chemical Engineering Vol. 1. Pergamon Press, 1961
4. Chennakesavan, Henry: Amer. Inst. Chem. Eng. J. **7**, 10 (1961)
5. Masamune, H., Smith, R.: Amer. Inst. Chem. Eng. J. **8**, 217 (1962)
6. Scott, R. L., Cox, J. T.: J. Chim. Phys. **57**, 1010 (1960)
7. Smith, J. M., Wakao, N.: Chem. Eng. Sci. **17**, 825 (1962)
8. Wicke, E., Kallenbach, R.: Kolloid-Z. **97**, 135 (1941)
9. Ellis, C., Ivenson, I.: Gas Chromatography (author: H. Desty) p. 30 Amsterdam, 1958
10. Hoogshager, J.: Ind. Eng. Chem. **47**, 906 (1955)
11. Eckert, G.: Teoriya teplo i massoobmena GEI, 1961
12. Dushmann, S.: A vákuumtechnika tudományos alapjai (Scientific foundations of vacuum technique). In Hungarian. Akadémiai Kiadó, Budapest, 1959
13. Report SAM A 765 (1943)
14. Ney, Armistead: Phys. Rev. **71**, 14 (1947)
15. Pallai, I., Almásy, G.: Acta Chim. Acad. Sci. Hung. 1961
16. Carman, C.: Flow of Gases through Porous Media. Butterworths, London, 1956
17. Timofeev, P.: Uspekhi Khimii **29**, 404 (1960)
18. Frenke, I.: Kinetika Teoriya Zhidkostve. Akad. Nauk. Moskva, 1945
19. Carman, C.: Proc. Roy. Soc. A **55**, 203 (1950)
20. Carman, C.: Proc. Roy. Soc. A **209**, 38 (1951)
21. Barrer, M., Barrie, A.: Proc. Roy. Soc. A **213**, 250 (1952)
22. Barrer, M.: Brit. J. Appl. Phys. **3**, 49 (1954)

László Müller, Pécs III. Páfrány u. 47, Hungary

Acta Chimica Academiae Scientiarum Hungaricae, Tomus 59 (3—4), pp. 297—302 (1969)

COULOMETRISCHE KOBALTTITRATION

G. HENZE, R. GEYER und R. HOLZBAUER

(Institut für Analytische Chemie der Technischen Hochschule für Chemie »Carl Schorlemmer« Leuna-Merseburg)

Eingegangen am 10. Februar 1968

Es wird der Aufbau einer Apparatur zur coulometrischen Titration beschrieben. Durch die Verwendung eines Schreibers zur automatischen Registrierung des Strom-Zeit-Verlaufes konnte eine wesentliche Vereinfachung in der Arbeitsweise erzielt werden. Die coulometrische Titration des 2-wertigen Kobalts ist mittels elektrolytisch erzeugten Hexacyanoferrat(III) möglich. Ein Nickelüberschuß und kleine Eisenmengen beeinflussen das Verfahren nicht.

Die Oxydation Co(II) → Co(III) lässt sich zur coulometrischen Kobalttitration nutzen. Da uns handelsübliche Geräte für diesen Zweck nicht zur Verfügung standen, entwickelten wir eine eigene coulometrische Meßanordnung.

Zur coulometrischen Bestimmung wird Kobalt nach LINGANE und PAGE [1] aus pyridinhaltiger Lösung als Metall abgeschieden. Nickel muß vorher abgetrennt werden. Die Anwesenheit von Nickel stört auch die von STEIN [2] vorgeschlagene coulometrische Titration mit elektrolytisch aus Kadmiumkomplexonat erzeugtem Komplexon, sowie das Verfahren nach PARTRIARCHE [3], der Kobalt mit einem Überschuß von 8-Oxychinolin ausfällt und das überschüssige 8-Oxychinolin mit elektrolytisch erzeugten Brom zurücktitriert. Ein anderes coulometrisches Bestimmungsverfahren beruht auf der Oxydation des 2-wertigen Kobalts mit elektrolytisch erzeugtem Kaliumoctacyanomolybdat(V) [4].

Die von uns entwickelte Apparatur besteht aus drei Baugruppen: einer elektronisch geregelten Konstantstromquelle, der Meßzelle und dem Indikationssystem (Abb. 1). Die elektronisch geregelte Stromquelle liefert einen hochkonstanten Strom, dessen Größe bei auftretenden Lastschwankungen maximal um $\pm 0{,}5\%$ vom Sollwert abweicht. Die Stromstabilisierung erfolgt über einen Regelverstärker, der durch eine dem Laststrom proportionale Spannung gesteuert wird. Der Innenwiderstand des Stabilisators beträgt 10 MΩ.

Der stabilisierte Strom wird an die Arbeitselektroden der Meßzelle angeschlossen. Zur Kontrolle und Einstellung der Stromstärke befindet sich im Elektrolysestromkreis ein Amperemeter. Als Meßzelle dient ein Becherglas von 150 ml Inhalt, welches mit einem mehrmals durchbohrten Gummistopfen verschlossen wird. In den Öffnungen des Stopfens sind zur Trennung der Elektrolyseräume ein Tondiaphragma mit einem Platindraht als Kathode und ein Platinblech mit etwa 4 cm² Oberfläche als Anode untergebracht.

Die Endpunktindizierung wird auf amperometrischem Wege durchgeführt. Dazu befinden sich in dem Gummistopfen außerdem eine Platinstiftelektrode und eine KCl-Salzbrücke, welche die Verbindung zu einer gesättigten Kalomelelektrode herstellt.

Die Rührung erfolgt mit Hilfe eines Magnetrührers. Die Polarisationsspannung für die amperometrische Indizierung wird einer Gleichstromquelle entnommen und über den Widerstand R_1 eingeregelt. Mit einem im Stromkreis befindlichen Voltmeter kann die Polarisationsspannung gemessen werden. Der im Indikationsstromkreis fließende Strom wird über einen Verstärker geleitet und von einem Kompensationsbandschreiber registriert. Der Strom kann mit Hilfe des Widerstandes R_2 reguliert werden. Durch den konstanten Papiervorschub dient der Schreiber gleichzeitig als Zeitmesser. Die coulometrische Arbeitsweise konnte durch die Verwendung des Schreibers zur Strom- und Zeitmessung stark vereinfacht werden.

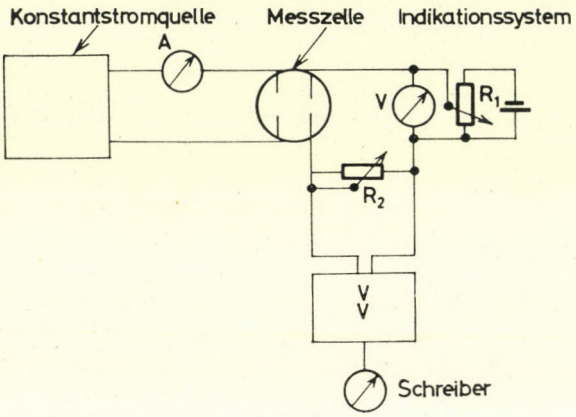


Abb. 1. Blockschema der Apparatur zur coulometrischen Titration

Das von uns entwickelte Verfahren beruht auf der Oxydation des 2-wertigen Kobalts mit elektrolytisch erzeugtem $K_3[Fe(CN)_6]$ bei pH 9,5—11,5. Die Einstellung des pH-Wertes erfolgt durch Zugabe von Kalilauge unter Kontrolle mit pH-Indikatorpapier (»Stuphan«). Um die Ausfällung von Kobalthydroxyd zu verhindern, muß der Analysenlösung ein Komplexbildner zugefügt werden. Der Kobaltkomplex soll zur Vereinfachung der Arbeitsweise gegenüber Sauerstoff beständig sein. Weiterhin ist eine hinreichend große Komplexstabilität erforderlich, um die Ausfällung von Kobalt(II) mit $K_4[Fe(CN)_6]$ zu verhindern. In ammoniakalischer und äthylendiaminhaltiger Lösung bewirkt Sauerstoff eine Oxydation des Kobalts (II). Ungeeignet erwies sich auch die Verwendung von Komplexon, da der entstehende Kobaltkomplex mit $K_3[Fe(CN)_6]$ nicht oxydiert wird. Die Komplexe, welche 2-wertiges Kobalt mit Alanin und Glutaminsäure bilden, zeigen dagegen eine zu geringe Stabilität und führen zu einer Ausfällung des Kobalts mit $K_4[Fe(CN)_6]$. Am vorteilhaftesten erwies sich die Verwendung von Glycin als Komplexbildner. Bei 80 bis 100fachem Überschuß an Glycin gegenüber der vorgelegten Kobaltmenge bilden sich keine Niederschläge und die Lösung ist gegenüber Luftsauerstoff beständig. Unter den Bedingungen der elektrolytischen Erzeugung von

$K_3[Fe(CN)_6]$ wird die alkalische, glycinhaltige Kobalt(II)lösung selbst nicht oxydiert; die Stromausbeute des Anodenprozesses erwies sich als vollständig Die Stromstärke betrug bei den Versuchen bis zu 19 mA. Die verwendete $K_4[Fe(CN)_6]$-Lösung war 0,5 *M*; sie wurde unmittelbar vor Beginn der Elektrolyse zur Analysenlösung gegeben.

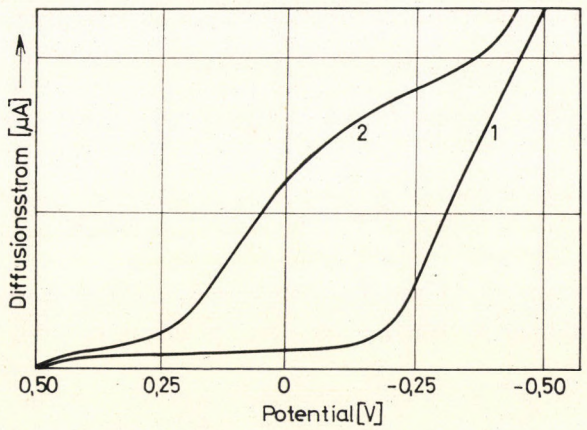


Abb. 2. Polarogramm von Hexacyanoferrat(III) in Anwesenheit von Glycin (pH = 10,5; Kurve 1: Grundlösung; Kurve 2: Kaliumhexacyanoferrat(III))

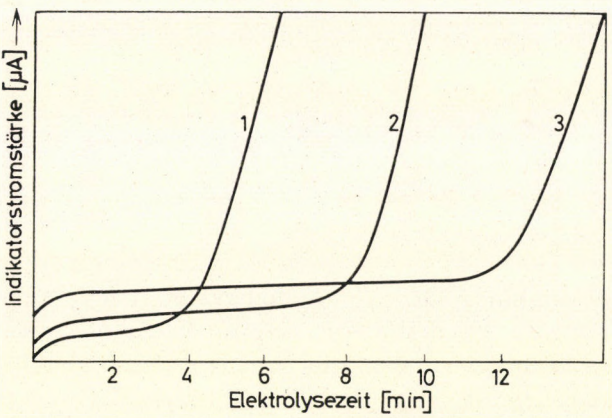


Abb. 3. Amperometrische Titration von Kobalt(II)
(Polarisationsspannung: —0,3 V; Elektrolysestrom: 19 mA; Titrationsvolumen: 100 ml; Co-Gehalte: Kurve 1 = 2,91; Kurve 2 = 5,82; Kurve 3 = 8,73 mg)

Zur amperometrischen Indizierung wird die $K_3[Fe(CN)_6]$-Konzentration während des Titrationsverlaufes verfolgt. Die erforderliche Polarisationsspannung bestimmten wir auf polarographischem Wege an einer rotierenden Platinstiftelektrode.

Das Polarogramm der $K_3[Fe(CN)_6]$-Lösung und der dazugehörigen Grundlösung ist in Abb. 2 dargestellt. Das Halbstufenpotential der polarographischen Welle liegt bei etwa Null Volt (bez. ges. Kal.-Elektrode), der Diffusionsgrenzstrom im Bereich von $-0{,}2$ bis $-0{,}4$ V.

Vorteilhaft zur amperometrischen Indizierung der $K_3[Fe(CN)_6]$-Konzentration erwies sich eine Polarisationsspannung von $-0{,}3$ V. Der unter diesen Bedingungen mit Hilfe des Kompensationsbandschreibers aufgezeichnete Strom-Zeit-Verlauf ist für verschiedene Kobaltgehalte in Abb. 3 dargestellt. Die Bandschreibergeschwindigkeit betrug bei diesen Versuchen 1200 mm/h.

Zur Berechnung der Analysenergebnisse nach der Faraday'schen Beziehung werden die Elektrolysezeiten durch Anlegen der Tangenten an die Äste der Strom-Zeit-Kurven ermittelt.

In Tabelle I sind die Analysenergebnisse für verschiedene Kobaltvorlagen zusammengefaßt. Die Standardabweichung wurde zu $s = 0{,}10$ mg berechnet. Das Titrationsvolumen betrug bei diesen Versuchen 100 ml, die Elektrolysestromstärke 19 mA.

Tabelle I

Coulometrische Titration des Kobalts mit elektrolytisch erzeugtem Kaliumhexacyanoferrat(III)
(Titrationsvolumen:100 ml; Stromstärke: 19 mA; Polarisationsspannung: $-0{,}3$ V)

Kobalt vorgelegt (mg)	2,91	5,82	8,73	11,64
Kobalt gefunden (mg)	2,82	5,81	8,67	11,80
	2,82	5,79	8,70	11,78
	3,06	5,87	8,76	11,50
	2,82	5,85	8,90	11,54
	2,83	5,81	8,70	11,58

Für die Bestimmung kleinerer Kobaltgehalte (siehe Tabelle II) betrug das Titrationsvolumen 20 ml, die Elektrolysestromstärke 10 mA und die Bandschreibergeschwindigkeit 3600 mm/h. Es errechnete sich für diese Gehalte eine Standardabweichung von $s = 0{,}02$ mg Kobalt.

Durch Nickel wird die coulometrische Kobalttitration mit Kaliumhexacyanoferrat(III) nicht gestört. Mit einem hinreichenden Überschuß an Glycin kann Nickel ebenso wie Kobalt als Komplex in Lösung gehalten werden. Damit ist die Möglichkeit gegeben, die Kobalttitration auch in Gegenwart von Nickel durchzuführen.

3-wertiges Eisen bildet im alkalischen Medium mit Glycin keinen Komplex und fällt als Hydroxyd aus. Dabei kann Kobalt adsorbiert werden. Große Eisenmengen müssen deshalb vor der Kobalttitration abgetrennt werden.

Ein häufiger Begleiter kobalthaltiger Produkte ist Mangan. Da 2-wertiges Mangan durch Kaliumhexacyanoferrat(III) oxydiert wird, stört dessen Anwesenheit die coulometrische Kobalttitration. Bei Einwirkung von Luftsauerstoff auf die alkalischen Probelösungen fällt Mangan als Braunstein aus und kann Kobalt adsorbieren.

Tabelle II

Coulometrische Titration des Kobalts mit elektrolytisch erzeugtem Kaliumhexacyanoferrat(III)
(Titrationsvolumen: 20 ml; Stromstärke: 10 mA; Polarisationsspannung: —0,3 V)

Kobalt vorgelegt (mg)	0,58	1,16
Kobalt gefunden (mg)	0.58	1,12
	0,52	1,14
	0,53	1,12
	0,56	1,12
	0,56	1,09

Tabelle III

Coulometrische Bestimmung des Kobalts
(Elektrolysestromstärke: 19 mA)

Probe	Einwaage (g)	Elektrolysezeit (sec)	Kobalt gefunden (mg)	Kobaltgehalt d. Probe	
				(mg)	%
	für 1/12,5 der Einwaage				
Kovarstahl	0,3554	453	5,26	65,8	18,5
		450	5,22	65,3	18,4
	0,3708	474	5,50	68,8	18,5
		480	5,57	69,6	18,8
	für 1/5 der Einwaage				
Nickelmetall	2,0060	206	2,39	12,0	0,60
		216	2,51	12,5	0,62
	2,0170	222	2,58	12,9	0,64
		210	2,44	12,2	0,60

Wir bestimmten den Kobaltgehalt in Nickelmetall und Kovarstahl. Die Metalle wurden in Salpetersäure gelöst, anschließend die Salpetersäure mit Salzsäure abgeraucht. Die höherwertigen Metallionen der Begleitelemente wurden durch Hydrolyse mit Bariumkarbonat von den 2-wertigen Ionen des Kobalts und Nickels abgetrennt. Die Analysenergebnisse der einzelnen Proben stimmten gut überein; einige Werte sind in Tabelle III zusammengestellt.

LITERATUR

1. LINGANE, J. J. u. J. A. PAGE: Analytica chim. Acta **13,** 281 (1955)
2. STEIN, H. H.: ref. in K. Abresch u. I. Claassen: Die coulometrische Analyse. S. 158. Verlag Chemie, Weinheim/Bergstr., 1961
3. PARTRIARCHE, G.: ref. C. A. **53,** 6528 (1959)
4. KRATOCHVIL, B. u. DIEHL, H.: Talanta **3,** 346 (1960)

Günter HENZE, Rudolf GEYER
Institut für Analytische Chemie der Technischen Hochschule für Chemie »Carl Schorlemmer«, Leuna-Merseburg
Rainer HOLZBAUER
VEB Stahlwerk Hennigsdorf/b. Berlin

Acta Chimica Academiae Scientiarum Hungaricae, Tomus 59 (3—4), pp. 303—308 (1969)

ON THE PARAMETER FORM OF FORCE CONSTANT MATRIX, VIII

CALCULATION OF ALL MEAN AMPLITUDES OF VIBRATION COMPATIBLE WITH THE NORMAL FREQUENCIES

F. TÖRÖK and GY. B. HUN

(Research Group for Inorganic Chemistry of the Hungarian Academy of Sciences, and Department of General and Inorganic Chemistry, L. Eötvös University, Budapest)

Received February 20, 1968

A computer program based on the parameter representation of force constants has been made to calculate all the mean amplitudes of vibration which are compatible with the normal frequencies of the molecule. The parameter method makes possible the determination of the matrices F which properly reproduce both the measured frequencies and the mean amplitudes of vibration. With the help of this method the sensibility of the mean square amplitudes to changes in the values of the force constants can be estimated.

The mean amplitudes of vibration are defined for atom pairs in the molecule. Let the momentary distance between two atoms be denoted by R_i, and the equilibrium distance by R_{ei}. The mean amplitude of vibration of the i-th atom pair is then given by

$$\mu_i = [\overbrace{(R_i - R_{ei})^2}]^{1/2}$$

where the wavy line designates the mean value.

The mean amplitudes of vibration can be calculated from the data of electron diffraction measurements. The first paper on this subject was published in 1949 [1]. The mean amplitudes of vibration can also be calculated with the knowledge of the geometry and force constants of a molecule, as it was pointed out by DEBYE for diatomic molecules [2] and by MORINO for polyatomic molecules [3]. Formulas were given by several authors with the help of which the mean amplitudes can be calculated from the known force constants [4—8]. Nevertheless, in the overwhelming majority of the cases the exact force constants are not known, therefore the calculated mean amplitudes are also uncertain. By comparing the calculated and measured mean amplitudes, the accuracy of the force constants can be estimated. As the parameter representation of force constants, expounded in our earlier papers [9, 10], produces all the force constants compatible with the experimental frequencies, it is obvious that by the parameter representation all mean vibrational amplitudes which are in accordance with the normal frequencies can

be calculated. With the method given in this paper and in the previous ones, all force constants reproducing both the mean amplitudes of vibration and the normal frequencies can be calculated. In the possession of these data, the reliability of the conclusions made on the basis of electron diffraction measurements can be estimated.

Let us consider a molecule having N atoms and n degrees of freedom ($n = 3N - 6$ and $n = 3N - 5$ in the case of a general molecule and a linear one, respectively). The column matrices $\boldsymbol{Q}$, $\boldsymbol{S}$, $\boldsymbol{R}$ of dimensions n have the normal coordinates, symmetry coordinates, and internal coordinates as components, respectively. In the column matrices $\boldsymbol{Q}$ and $\boldsymbol{S}$ the coordinates corresponding to the various irreducible representations follow each other in the same sequence. Let $\boldsymbol{X}$ be a column matrix of order $3N$, whose elements are the displacement Descartes coordinates. The transformation matrices are defined as follows:

$$\boldsymbol{Q} = \boldsymbol{L}^{-1}\boldsymbol{S},\ \boldsymbol{S} = \boldsymbol{O}\boldsymbol{R},\ \boldsymbol{R} = \boldsymbol{B}\boldsymbol{X}$$

The square matrix $\boldsymbol{L}^{-1}$ of dimension n is partitioned into factors corresponding to the irreducible representations of the point group of the molecule.

Let r denote the column matrix having

$$r_i = \boldsymbol{R}_i - \boldsymbol{R}_{ei}$$

as ith element. As from the N atoms of the molecule $\binom{N}{2}$ pairs of atoms can be formed, vector $\boldsymbol{r}$ has $\binom{N}{2}$ components. Let matrix P be defined as

$$\boldsymbol{P} = \overbrace{\boldsymbol{r}\boldsymbol{r}^T}$$

where $\boldsymbol{r}^T$ designates the transpose of $\boldsymbol{r}$, and the wavy line denotes the mean value again. Correspondingly, the elements of P can be obtained by computing the mean values of the matrix given by the multiplication of the column matrix $\boldsymbol{r}$ by the row matrix $\boldsymbol{r}^T$. If the matrix connecting the elements of $\boldsymbol{r}$ and $\boldsymbol{Q}$ is designated by K, *i.e.*

$$\boldsymbol{r} = K\boldsymbol{Q}$$

the following relation can be constructed:

$$P = \boldsymbol{r}\boldsymbol{r}^T = K\boldsymbol{Q}\boldsymbol{Q}^T K^T = K\,\Lambda\,K^T \qquad (1)$$

It is known that Λ is a diagonal matrix whose elements can be calculated from the normal frequencies of the molecule [11]:

$$\Lambda_{kk} = \frac{h}{8\pi^2 \nu_k} \coth \frac{h\nu_k}{2kT}$$

where ν_k is the normal frequency belonging to Q_k.

Using the matrices defined previously and the matrix B_m which transforms the elements of $\boldsymbol{X}$ into those of $\boldsymbol{r}(\boldsymbol{r} = B_m\boldsymbol{X})$, the following equation is obtained:

$$\boldsymbol{r} = K\boldsymbol{Q} = KL^{-1}\boldsymbol{S} = KL^{-1}O\boldsymbol{R} = KL^{-1}O\,B\boldsymbol{X} = B_m\boldsymbol{X},$$

and from this

$$K = B_m M^{-1} B^T G^{-1} O^T L. \tag{2}$$

Here M is a diagonal matrix whose elements are the masses of the atoms, and matrix G (defined by WILSON [12]) is constructed on the basis of internal coordinates. Formula (2) was obtained by taking into account that O is an orthogonal matrix, and the relation $\boldsymbol{X} = M^{-1}B^T G^{-1}\boldsymbol{R}$ was used.

Let the vibrational equation be written in the form:

$$G_S F_S L = L\,\Lambda, \tag{3}$$

where G_S and F_S are square matrices of n dimensions partitioned into factors corresponding to the given irreducible representations. The factors are G and F matrices belonging to symmetry coordinates [12].

It is matrix L that gives connection between Eq. (2) and (3). In our previous works [9, 10] we have expounded that all the matrices L compatible with the normal frequencies of the molecule can be written as

$$L = G_S^{1/2}\,U \tag{4}$$

Let us point out that all the matrices in Eq. (4) are partitioned, and according to this, matrix U is also a factorized orthogonal matrix whose factors of dimension n_i can be constructed by $\binom{n_i}{2}$ parameters. In this way, also matrix K can be given as a function of parameters:

$$K = B_M M^{-1} B^T G^{-1} O^T G_S^{1/2}\,U = B_M M^{-1} B_S^T G_S^{-1/2} U\,, \tag{5}$$

where B_S is a transformation matrix between the Descartes and symmetry coordinates, *i.e.* $\mathbf{S} = B_S\boldsymbol{X}$.

It follows from Eq. (5) that matrix K (and through K also the mean square of vibration) is additive in the sense that

$$K = \sum_i B_M M^{-1} B_{Si}^T G_{Si}^{-1/2} U_i,$$

where index i designates matrices belonging to the i-th irreducible representation.

Using matrix K from Eq. (5), a computer program was constructed for the calculation of the mean amplitudes of vibration [13], which gives at the same time the corresponding F matrices. In Table I the mean amplitudes of vibration and the elements of F matrices of the SO_2 molecule can be seen at some values of antisymmetric parameters [10]. $F_{11}^{(A_1)}$ and $F_{22}^{(A_1)}$ are the force constants corresponding to the S—O sym. stretching and the O\S/O angle deformational vibrations, respectively. Since only one vibration belongs to species B_1, the corresponding force constants is definite: $F^{(B_1)} = 9.996$. The zero point of the parameter was taken at such a matrix F whose elements approximate the force constants generally accepted in the literature.

The parameter method makes possible the determination of F matrices which simultaneously reproduce both the measured normal frequencies and mean amplitudes. First a matrix U must be found which reproduces the frequencies and amplitudes. Starting from this matrix U, the parameters are to be changed in such a way that the diagonal elements of matrix P should remain unchanged. In order to solve the task by iteration the partial derivatives of the mean amplitudes with respect to the parameters are needed, which can be easily calculated:

$$\frac{\partial \mu_t}{\partial \alpha_{ij}} = \frac{1}{\mu_t} (\Delta_{ii} - \Delta_{jj}) K_{ti} K_{tj}.$$

If we make small changes in parameters, using the last formula the alteration in μ_t can be given. The corresponding change in force constants can also be obtained (10). The quotient of the two changes gives information concerning the sensibility of μ_t to changes in F_{kl}:

$$\frac{\Delta \mu_t}{\Delta \partial F_{kl}} = \frac{1}{\mu_t} \sum_{i<j=2}^{n} \frac{(\Delta_{ii} - \Delta_{jj}) K_{ti} K_{tj}}{(\Delta_{ii} - \Delta_{jj})(T_{ki} T_{ej} + T_{kj} T_{ei})}.$$

We obtained for the SO_2 molecule at 0 parameter the following quotients:

$$\frac{\Delta \mu_{so}}{\Delta F_{11}^{(A_1)}} = -1.34 \cdot 10^{-4}, \quad \frac{\Delta \mu_{so}}{\Delta F_{12}^{(A_1)}} = -1.00 \cdot 10^{-4}, \quad \frac{\Delta \mu_{so}}{\Delta F_{22}^{(A1)}} = 1.99 \cdot 10^{-3},$$

$$\frac{\Delta \mu_{o\ldots o}}{\Delta F_{11}^{(A)_1}} = -4.93 \cdot 10^{-3}, \quad \frac{\Delta \mu_{o\ldots o}}{\Delta F_{12}^{(A_1)}} = -3.71 \cdot 10^{-3}, \quad \frac{\Delta \mu_{o\ldots o}}{\Delta F_{22}^{(A_1)}} = 7.37 \cdot 10^{-2}$$

Table I

The mean amplitudes and force constants of the SO_2 molecule

$F^{(B)}_1 = 9.996$

Parameter	Mean amplitudes		$F^{(A_1)}$	
	S—O	O...O		
0.4	0.040840	0.043045	9.36158	5.068 4.468
0.3	0.038872	0.043528	10.350	4.347 3.386
0.2	0.037063	0.0461831	10.877	3.218 2.437
0.15	0.036339	0.048206	10.914	2.539 2.070
0.10	0.035802	0.050555	10.785	1.815 1.802
0.08	0.035649	0.051558	10.686	1.519 1.727
0.05	0.035492	0.053104	10.489	1.077 1.650
0.04	0.035459	0.053627	10.411	0.930 1.634
0.03	0.035437	0.054152	10.326	0.785 1.623
0.02	0.035426	0.054677	10.235	0.641 1.618
0.01	0.035425	0.055203	10.138	0.498 1.617
0.00	0.035434	0.055727	10.036	0.357 1.621
—0.01	0.035453	0.056250	9.928	0.219 1.631
—0.02	0.035483	0.056770	9.815	0.082 1.646
—0.03	0.035523	0.057287	9.696	—0.051 1.665
—0.04	0.035574	0.057799	9.573	—0.183 1.690
—0.05	0.035634	0.058306	9.445	—0.311 1.720
—0.08	0.035872	0.059789	9.035	—0.675 1.837
—0.10	0.036077	0.060739	8.743	—0.898 1.939

REFERENCES

1. KARLE, I., KARLE, J.: J. Chem. Phys. **17**, 1052 (1949)
2. DEBYE, P.: J. Chem. Phys. **9**, 55 (1941)
3. MORINO, Y.: J. Chem. Phys. **18**, 395 (1950)
4. MORINO, Y., KUCHITSU, K., SHIMANOUCHI, T.: J. Chem. Phys. **20**, 726 (1952)
5. MORINO, Y., KUCHITSU, K., TAKAHASHI, A., MAEDA, K.: J. Chem. Phys. **21**, 1927 (1953)
6. MORINO, Y., HIROTA, E.: J. Chem. Phys. **23**, 737 (1955)
7. CYVIN, S. J.: Acta Chem. Scand. **13**, 2135 (1959)
8. CYVIN, S. J.: Spectrochim. Acta **15**, 828 (1959)
9. PULAY, P., TÖRÖK, F.: Acta Chim. Acad. Sci. Hung. **44**, 287 (1965)
10. PULAY, P.: Acta Chim. Acad. Sci. Hung. **47**, 49 (1967)
11. JAMES, R. W.: Physik. Z. **33**, 737 (1932)
12. WILSON, E. B., DECIUS, J. C., CROSS, P. C.: Molecular Vibrations. McGraw-Hill Book Company, Inc., New York, 1955
13. PULAY, P., HUN, GY. B., TÖRÖK, F.: J. Mol. Struct. **2**, 336 (1968)

Ferenc TÖRÖK
Györgyi B. HUN
} Budapest, VIII., Múzeum krt. 6—8.

Acta Chimica Academiae Scientiarum Hungaricae, Tomus 59 (3—4), pp. 309—318 (1969)

EQUILIBRIA OF α-AMINO ACID COMPLEXES OF TRANSITION METAL IONS, I

COMPLEXES OF GLYCINE

A. GERGELY

(Institute of Inorganic and Analytical Chemistry, L. Kossuth University, Debrecen)

Received February 24, 1968

The stability constants of the glycine complexes of d^5—d^{10} transition metal ions have been determined at 0.1 ionic strength and 25° C. A critical survey has been given on the stability constants reported in the literature. It has been pointed out that in the case of accurate measurements and appropriate choice of the method of calculation, the stability constants determined by different authors agree with one another within ~0.1 log K. In the opposite case the deviation of the constants from the accurate values may amount to 0.4—0.5 log K.

Similarly to other investigations, thorough studies on the equilibria of α-amino acids and metal ions in aqueous solutions were started in the forties, after the publication of BJERRUM's [1] pioneer work. Since then numerous, though sometimes contradictory, data have been reported for the stability constants of certain amino acid complexes [2]. In most cases summarizing tables list the constants, referring to the same equilibrium system and deviating very often from one another, without any critical comment. Very rarely there can be found remarks revising some data, *e.g.*, IRVING and ROSSOTTI [3] pointed out the inaccuracy of certain constants resulting from improperly chosen calculation methods. IZATT *et al.* [4] showed the inaccuracy of the values for thermodynamic changes in the formation of Cu(II)-glycine complexes published by LI *et al.* [5]. In the above cases inaccurate results were due to the inadequately applied experimental processes.

For some of the α-amino acid complexes, especially for the widely studied glycine and alanine chelates, accurate constants are also available. Thus IRVING *et al.* [6] determined the stability constants of Ni(II), Cu(II) and Zn(II) chelates by careful pH-metric measurements. Similarly, ANDEREGG [7] performed pH-metric determination for the Co(II), Ni(II), Cu(II) and Zn(II) complexes of glycine and, calculating with a computer, succeeded in giving the errors not greater than one hundredth of log K, too. Thus, in wiew of the fact that there are accurate constants for a part of the systems glycine-metal ion, it is even more important to make a critical survey of the data published earlier [2] and recently [8].

Contrary to data on glycine complexes, those for the metal ion complexes of hydroxyamino acids, apart from exceptional cases [4, 9], are very scarce

or they need correction [10—13]. The same holds for the metal complexes of aromatic amino acids [2]. Thus, systematic studies on the equilibria of these metal chelates are all the more significant. For several metal complexes of D-glucosaminic acid and serine, we have also reported equilibrium data [14—18]. On the basis of our experiments it turned out that, compared with glycine chelates, the IRVING—ROSSOTTI formula [19] did not hold for the hydroxyamino acid complexes studied, since the stability constants of the metal chelates did not change parallel with those of the proton complexes. This conclusion of ours, however, is not completely unequivocal, since the differences in the stabilities do not amount to more than a few tenths of log K. At least equal or sometimes even greater differences can be found in the literature in the constants determined under identical circumstances. Thus, in order to get nearer to the interpretation of the factors determining the stability constants of hydroxyamino acid complexes, it was necessary to re-determine the constants of glycine chelates, in this respect, too.

In agreement with the above-mentioned facts, the present work aims at the determination of the stability constants of the glycine complexes of d^5 — d^{10} metal ions and, at the same time, at a critical survey of the stability constants reported in the literature. Forthcoming communications will deal with the equilibria of the metal complexes of hydroxy and aromatic amino acids, as well as with the factors determining the stability constants.

Experimental

Materials and instruments

The pH-metric titrations were performed in the systems Mn(II)-, Fe(II)-, Co(II)- and Zn(II)-glycine by means of a Metrohm E 166 instrument, while for the Cu(II) and Ni(II) complexes a Radelkis Type OP 204 titriscope was used. The accuracy of the pH measurements, using the former instrument, was $\sim \pm 0.04$ pH, with the latter $\sim \pm 0.01$ pH. Temperature was maintained at a constant value, within $\pm 0.2°$ C, with a Höppler ultrathermostat.

Stock solutions containing the Mn(II), Co(II), Ni(II), Cu(II) and Zn(II) ions were prepared from the corresponding "Anal R" metal nitrates; the Fe(II) stock solution was made from Mohr salt. Concentrations of the former metal ions were checked gravimetrically, that of Fe (II) chromatometrically.

Glycine was a Merck product of analytical reagent grade.

Ionic strength was adjusted with KNO_3 solution to 0.1. For the pH-metric titrations, CO_2-free 0.2 N NaOH solution, kept under nitrogen atmosphere, was used.

Titration procedures

In the titrations, the glycine-metal ion solutions always contained glycine in $1.00 \cdot 10^{-2}$ M concentration, while the concentrations of the metal ions were $5.00 \cdot 10^{-3}$; $3.31 \cdot 10^{-3}$ and $2.00 \cdot 10^{-3}$ M.

For standardizing the pH-meter in the case of Cu(II), potassium hydrogen tartarate, while for the other metal ion–glycine systems phosphate buffers were used. Three or four parallel titrations were performed with the samples at each molar concentration.

Calculations

The formation curves were calculated from the results of the titrations, applying the following relations derived by ALBERT [20].

$$\bar{n} = \frac{T_A - [A]\left(1 + \frac{[H]^2}{K_{d_1} K_{d_2}} + \frac{[H]}{K_{d_2}}\right)}{T_M} \tag{1}$$

and

$$[A] = \frac{T_A - [NaOH] - [H] + [OH]}{2\frac{[H]^2}{K_{d_1} K_{d_2}} + \frac{[H]}{K_{d_2}}} \tag{2}$$

In Eqs (1) and (2) the square brackets denote equilibrium concentrations (for simplicity, the charges were neglected), and T_A and T_M represent the total concentrations of glycine and the metal ions, respectively. The

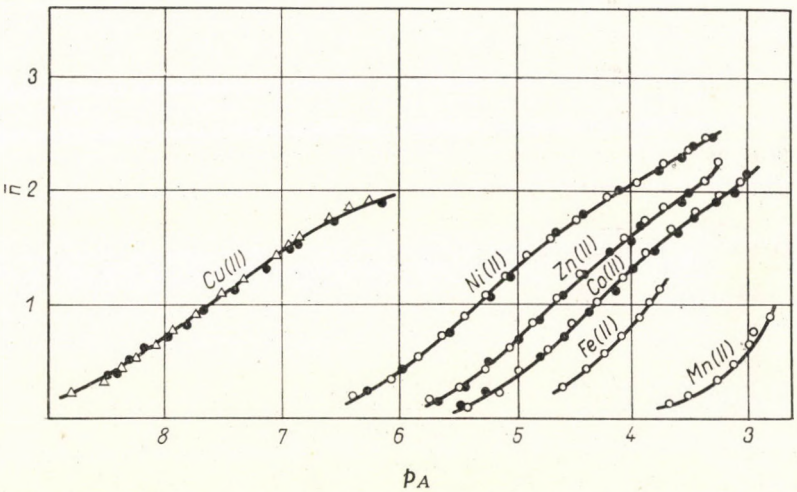


Fig. 1. Formation curves of the complexes of glycine with d^5—d^{10} metal ions. $C_{\text{glycine}} = 1.00 \cdot 10^{-2}$ *M*. Concentrations of the metal ions: △ $5.00 \cdot 10^{-3}$ *M*; ○ $3.31 \cdot 10^{-3}$ *M*; ● $2.00 \cdot 10^{-3}$ *M*; $I = 0.1$ (KNO_3); $t = 25°$ C

protonation constants of glycine are denoted with K_{d_1} and K_{d_2}. (In the calculations the values obtained by us [16] were used.) The average ligand number is denoted by $\bar{n}$, while $[A]$ represents the concentration of the free ligand. The formation curves are shown in Fig. 1.

From the figure it can be seen that the formation curve of the Cu(II)-glycine system is the only one that approximates asymptotically a determined

value. Fairly well-formed are the formation curves of the Ni(II), Zn(II) and Co(II) systems, too, though the average ligand number, owing to hydrolysis, does not reach three. With Fe(II) and Mn(II) precipitation takes place as early as $\bar{n} < 1$ (at pH ~ 7.5), therefore, their formation curves are the least accurate.

The calculation of the stability constants was made, with the pairs of values $\bar{n}$ and pA known, partly with the modified correction term method developed by the author and his co-workers [18, 21], partly with the projection strip method [22]. The maximum error of stability constants was 0.02—0.06 log K for the Co(II), Ni(II), Cu(II) and Zn(II) complexes, and 0.1—0.2 log K for the Fe(II) and Mn(II) chelates.

Evaluation of the results

The stability constants obtained for the glycine complexes of d^5 — d^{10} transition metal ions at 25°, together with data reported in the literature and determined under fairly identical conditions, are summarized in Table I.

Apart from certain cases, the values taken from the literature and listed in Table I were obtained by pH-metric measurements. Deviations as high as 0.3—0.5 log K can sometimes be found between the constants and in the log K_1/K_2 values determined by various authors, very often at identical ionic strength. As it has been mentioned above, we are in the possession of accurate values reported by ANDEREGG [7] for glycine complexes. However, he has not determined the constants of Mn(II) and Fe(II) chelates. On the other hand, an accurate thermodynamic constant is known for the system Mn(II)-glycine, which was obtained by BRANNAN *et al.* [23] under very carefully planned conditions. For Fe(II) complexes, complete data have been determined only by ALBERT [24] and in the present work. As regards the accuracy of the constants reported by various authors for the individual metal ion-glycine systems, the following details can be stated.

Mn(II) complexes

The data determined by the above-mentioned authors, with the exception of those obtained by MALEY and MELLOR [25] agree surprisingly well with one another, and with the thermodynamic constant calculated by BRANNAN *et al.* [23]. This fact alone indicates that the values reported by MALEY and MELLOR are the least accurate. It should be still considered that here the value for log K_2 can only be calculated with great uncertainty. It can be seen from Fig. 1 that the formation curve for the Mn(II)-glycine system is well defined up to $\bar{n} \cong 0.5$, only. It should be mentioned that, in the present case, the value for log K_1 too, with respect to the lesser degree

of stability as well as to the uncertain shape of the formation curve, can only be calculated from the experimental data with an error of 0.1—0.2 log K, as mentioned above.

Fe(II) complexes

The constants calculated by ALBERT [24] and according to the present work, taking into account the differences in ionic strength and temperature, agree fairly well with one another. In this case, the constants are less accurate, since there is precipitation at $\bar{n} < 1$ (at pH ~ 7.5).

Co(II) complexes

Here and in the following, in addition to the data listed in Table I, other values can also be found in the literature. Taking into consideration, however, that beginning with Co(II), we have at our disposal accurate data calculated by ANDEREGG [7], reference will be made here only to those that give possibilities to interpret the errors incidentally committed.

It is, first of all, remarkable that ALBERT [24] and SHARMA *et al.* [8] obtained 1.20 and 1.30 for log K_1/K_2, respectively. (The constants are naturally different owing to differences in ionic strength and temperature.) This can be attributed, as it will be obvious from the following, to errors committed partly in the measurements, and partly in the course of calculations.

To evaluate the results of measurements, ALBERT [20] used the relations derived by himself in 1950, namely:

$$K_1 = \frac{1}{[A]} \cdot \frac{\bar{n}}{(1 - \bar{n})} \tag{3}$$

and

$$K_2 = \frac{1}{[A]} \cdot \frac{(\bar{n} - 1)}{(2 - \bar{n})} \tag{4}$$

The ALBERT procedure does not take into account that for the complexes of glycine, where the condition $K_1/K_2 > 10^2$ is not fulfilled, the above method of calculation is not applicable.

The values obtained for log K_1/K_2 by GILBERT *et al.* [28], ANDEREGG [7] and ourselves, agree very well with one another. As to the successive constants, the data obtained for log K_1 and log K_2 by these authors agree with one another within about 0.1 log K. This can be regarded as a satisfactory result. There is, however, a greater deviation as regards the value for log K_3. This can be interpreted by inaccuracy partly in the upper section of the formation curve, partly in the calculations.

Table I

Stability constants of the glycine complexes of d^5—d^{10} metal ions as determined by different authors

I	t °C	log K_1	log K_2	log K_1/K_2	log β_2	log K_3	log K_2/K_3	log β_3	References
Mn(II)									
0.01	25	3.66	2.97	0.69	6.63	—	—	—	[25]
0.01	25	2.85	—	—	—	—	—	—	[26]
0.09	30	3.12	—	—	—	—	—	—	[27]
0.01	20	3.2	2.3	0.9	5.5	—	—	—	[24]
0.00	25	3.16	—	—	—	—	—	—	[23]
0.1	25	3.0	—	—	—	—	—	—	Present work
Fe(II)									
0.01	20	4.3	3.5	0.8	7.8	—	—	—	[24]
0.1	25	4.13	3.52	0.61	7.65	—	—	—	Present work
Co(II)									
0.01	20	5.1	3.8	1.3	8.9	—	—	—	[24]
0.15	26	4.65	3.78	0.87	8.43	2.33	1.45	10.76	[28]
0.1	20	4.684	3.792	0.892	8.476	2.645	1.147	11.121	[7]
0.2	15	4.76	3.56	1.2	8.32	—	—	—	[8]
0.1	25	4.75	3.88	0.87	8.63	2.4	1.48	11.03	Present work
Ni(II)									
0.15	25	5.97	4.95	1.02	10.92	—	—	—	[5]
0.1	20	5.73	4.76	0.97	10.49	—	—	—	[6]
0.1	25	5.86	4.73	0.93	10.59	—	—	—	[29]
0.1	20	5.824	4.803	1.021	10.627	3.773	1.030	14.400	[7]
0.2	25	5.94	4,84	1.10	10.78	—	—	—	[8]
0.1	25	5.73	4.83	0.90	10.56	3.44	1.39	14.00	Present work

Cu(II)									
0.01	20	8.50	6.90	1.60	15.40	—	—	—	[24]
0.01	20	8.34	7.05	1.29	15.39	—	—	—	[30]
0.1	25	8.38	6.87	1.51	15.25	—	—	—	[29]
0.1	20	8.12	6.91	1.21	15.03	—	—	—	[6]
0.1	20	8.188	6.900	1.288	15.088	—	—	—	[7]
0.2	25	8.46	6.83	1.68	15.29	—	—	—	[8]
0.1	25	8.23	6.96	1.27	15.19	—	—	—	Present work
Zn(II)									
0.1	20	5.16	4.34	0.82	9.50	—	—	—	[6]
0.15	25	5.42	4.52	0.90	9.94	—	—	—	[31]
0.1	25	5.03	4.27	0.76	9.30	—	—	—	[32]
0.1	20	4.995	4.230	0.765	9.225	3.108	1.112	12.333	[7]
0.2	25	5.19	4.21	0.98	9.40	—	—	—	[8]
0.1	25	4.96	4.24	0.72	9.20	2.5	1.74	11.74	Present work

Ni(II) complexes

The values calculated by IRVING *et al.* [6], BASOLO and CHEN [29], ANDEREGG [7] and ourselves, were in good agreement with one another for $\log K_1$ and $\log K_2$, within 0.1 $\log K$. A greater deviation than this ($\sim 0.2 \log K$) is only found in the data published by LI *et al.* [5].

LI *et al.* have obtained these constants partly by polarographic measurement through following competition with Cu(II) ions and partly pH-metrically. The reduction of Cu(II) ions on the dropping mercury electrode is, however, not a completely reversible process, thus the error in the constant for the Ni(II) complex is greater, too. Nor can their pH-metric data be entirely accurate, which is indicated by the relatively great values of the successive constants. As regards the calculations, reference is only made to the application of BJERRUM's [1] method (presumably the half $\bar{n}$ method). The inaccuracy of their constants is even more remarkably manifested in the erroneous values of the thermodynamic changes calculated by these authors [4, 21].

Cu(II) complexes

In the case of the Cu(II)-glycine system, the constants determined by IRVING *et al.* [6], ANDEREGG [7], and ourselves agree fairly well with one another. The values obtained by these authors for $\log K_1/K_2$ are also between 1.2—1.3. On the other hand, ALBERT in his earlier work [24], calculating with the method referred to above, obtained 1.60 for $\log K_1/K_2$. In a more recent communication [30] he corrected his earlier values and thus he got an appropriate value (1.29) for $\log K_1/K_2$, too.

It should be noted that in this transition series the formation curve of the Cu(II) complex is the best shaped of all and the value of $\log K_1/K_2$ is the greatest. In spite of this, deviation between the data determined by the different authors is rather significant, especially as regards $\log K_1/K_2$. This can be attributed, first of all, to the equations used for the calculation of the formation curve, since in Eqs (1) and (2) the squared terms may be generally negligible. In the case of the Cu(II) complex, however, the situation is different: in the $\bar{n} < 1$ portion of the formation curve the squared terms should be taken into account, while in its $\bar{n} > 1$ portion they can be neglected. In consequence of the errors in pH-measurement, the formation curve is not always symmetrical, which results in an even greater inaccuracy of the constants. To make things worse for the Cu(II)-glycine equilibrium system the pH value, corresponding to the lower portion of the formation curve, is between $\sim 2-3$, where the inaccuracy of measurement is naturally greater.

The above considerations can partly explain why BASOLO and CHEN [29] and SHARMA *et al.* [8] obtained relatively high values for $\log K_1/K_2$.

Zn(II) complexes

Data published by McKENZIE and MELLOR [32], ANDEREGG [7] and our values agree very well for log K_1 and log K_2. It is characteristic that the value obtained by these authors for log K_1/K_2 is fairly identical. On the other hand, our constant calculated for ZnA_3 is to a considerable extent different from those of ANDEREGG [7]. This circumstance, similarly to the cases of Co(II) and Ni(II), can be explained (as it has been pointed out by ANDEREGG [7]) by the fact that, owing to the low stability of the third complex, the upper portion of the formation curve is not fully shaped and so less accurate.

The constants reported by IRVING *et al.* [6] and SHARMA and MATHUR [8] also agree relatively well with the accurate data, while those determined by LI and MANNING [31] display inaccuracies amounting to $\sim$0.4—0.5 log K. The errors committed by the latter authors can be attributed to inaccuracies in the measurements and calculations, as it has been pointed out above.

In addition to the data included in Table I, constants measured at considerably different ionic strengths and temperatures can also be found in the literature. No reference has been made to these in the present work, nor have been dealt with any thermodynamic constants calculated at zero ionic strength. On the basis of the values presented, it has become clear that several constants reported in the literature are really not satisfactorily accurate. This is partly due to inadequate experimental conditions, partly to erroneously chosen methods of calculation. Therefore, it is necessary to revise critically the constants given by different authors for various systems and, in some cases to re-determine them.

*

The author's thanks are due to Mr. J. MOJZES and Mr. I. NAGYPÁL for their valuable help in the experimental work.

REFERENCES

1. BJERRUM, J.: Metal Ammine Formation in Aqueous Solutions. P. Hasse and Son, Koppenhagen, 1941
2. Stability Constants of Metal-Ion Complexes. (Special Publication No. 17. London. The Chemical Society, Burlington House W. 1.) 1964
3. IRVING, H., ROSSOTTI, H. S.: J. Chem. Soc. 1953, 3397
4. IZATT, R. M., CHRISTENSEN, J. J., KOTHARI, V.: Inorg. Chem. **3,** 1564 (1964)
5. LI, N. C., WHITE, J. M., YOEST, R. L.: J. Am. Chem. Soc. **78,** 5218 (1956)
6. IRVING, H., WILLIAMS, R. J., FERRETT, P. J., WILLIAMS, A. E.: J. Chem. Soc. **1954,** 3494
7. ANDEREGG, G.: Helv. Chim. Acta **44,** 1673 (1961)
8. SHARMA, V. S., MATHUR, H. B.: Indian J. Chem. **3,** 475 (1965)
9. PELLETIER, S.: Chim. Phys. **57,** 301 (1960)
10. SZÜCSEV, A. Ja.: Zs. Neorg. Himii **9,** 2343 (1964)
11. KRAUSE, H. W., WILCKE, F. W., MIX, H., LANGENBECK, W.: Z. Phys. Chem. **225,** 342 (1964)
12. RALEA, R., POPA, A.: Analeale Stiint Univ. "A J. Cuza" Jasi Sect. I. **6,** 391 (1960)
13. MIYAZAKI, M., SENSHU, T., TAMURA, Z.: Chem. Pharm. Bull. **14,** 117 (1966)
14. GERGELY, A., SZARVAS, P., MÁCZAY, L.: Magyar Kém. Foly. **70,** 235 (1964)
15. GERGELY, A., SZARVAS, P.: Acta Chim. Acad. Sci. Hung. **45,** 203 (1965)

16. GERGELY, A., MOJZES, J.: Magyar Kém. Foly. **72,** 292 (1966)
17. GERGELY, A., NAGYPÁL, I.: Acta Physica et Chimica Debrecina **11,** 113 (1965)
18. GERGELY, A., NAGYPÁL, I., MOJZES, J.: Magyar Kém. Foly. **72,** 506 (1966)
19. IRVING, H., ROSSOTTI, H.: Acta Chem. Scand. **10,** 72 (1956)
20. ALBERT, A.: Biochem. J. **47,** 531 (1950)
21. GERGELY, A., NAGYPÁL, I., MOJZES, J.: Acta Chim. Acad. Sci. Hung. **51,** 381 (1967)
22. ROSSOTTI, F. J. C., ROSSOTTI, H. S., SILLÉN, L. G.: Acta Chem. Scand. **10,** 203 (1956)
23. BRANNAN, J. R., DUNSMORE, H. S., NANCOLLAS, G. A.: J. Chem. Soc. **1964,** 304
24. ALBERT, A.: Biochem. J. **54,** 646 (1953)
25. MALEY, L. E., MELLOR, D. P.: J. Austral. Sci. Res. **A 2,** 579 (1949)
26. KROLL, H.: J. Am. Chem. Soc. **74,** 2034 (1952)
27. MURPHY, C. B., MARTELL, A. E.: J. Biol. Chem. **37,** 226 (1957)
28. GILBERT, J. B., OTEY, M. C., HEARON, J. Z.: J. Am. Chem. Soc. **77,** 2599 (1955)
29. BASOLO, F., CHEN, Y. T.: J. Am. Chem. Soc. **76,** 953 (1954)
30. ALBERT, A., SERJEANT, E. P.: Biochem. J. **76,** 621 (1960)
31. LI, N. C., MANNING, R. A.: J. Am. Chem. Soc. **77,** 5225 (1955)
32. MCKENZIE, H. A., MELLOR, D. P.: Austr. J. Chem. **14,** 562 (1961)

Arthur GERGELY, Debrecen 10. Hungary

Acta Chimica Academiae Scientiarum Hungaricae, Tomus 59 (3—4), pp. 319—322 (1969)

DIE EIGNUNG VON PEROWSKITPHASEN ALS REDOXINDIKATORELEKTRODEN

A. WESER* und E. PUNGOR

(KURZMITTEILUNG)

(Universität für die Chemische Industrie, Lehrstuhl für Analytische Chemie, Veszprém)

Eingegangen am 17. August 1968

Unsere Untersuchungen an Carbiden, Boriden, Nitriden und Sulfiden zeigten, daß ein Zusammenhang zwischen der Eignung eines Materials als Redoxelektrode und seiner Kristallstruktur sowie wahrscheinlich auch seiner Elektronenstruktur besteht [1, 2]. Die metallähnlichen Eigenschaften und einige Veröffentlichungen über die Eigenschaften der Wolframbronzen bewogen uns, diese Verbindungen näher zu untersuchen.

KOKSHAROV und Mitarbeiter berichteten, daß Wolframbronzen mit kubischer Struktur in einem weiten pH-Bereich eine Potentialänderung von 58 mV/pH-Einheit zeigen. Die tetragonalen Wolframbronzen zeigen dieses Verhalten nur in einem kleinen pH-Bereich. Die kubischen Wolframbronzen wurden von den gleichen Autoren als unempfindlich gegenüber Redoxmitteln gefunden [3]. Auch andere Autoren wie SEPA und Mitarbeiter stellten die elektrochemische Aktivität von kubischen Wolframbronzen bei der Reduktion von Sauerstoff fest [4, 5]. Vanadiumbronzen sollen ähnliche Eigenschaften besitzen [6].

CHARTIER und POISSON fanden, daß ReO_3 zwar eine pH-Funktion zeigt, aber nicht auf Konzentrationsänderungen von Perrhenat anspricht [7].

Eigenschaften der Wolframbronzen

Die Reduktion von Alkalipolywolframat mit H_2, Zn, Pb, Na oder W führt im Fall des Natriums zu Verbindungen mit der Formel Na_nWO_3 ($0<n\leq 1$). In Abhängigkeit von $n = 0{,}9$ bis zu $n = 0{,}3$ wechselt die Farbe von Goldgelb über Rot bis Blau.

Die Wolframbronzen sind sehr reaktionsträge Stoffe mit halbmetallischen Eigenschaften. Sie besitzen Metallglanz und Elektronenleitfähigkeit.

Die Wolframbronzen können als $NaWO_3$-Phasen mit Natriumunterschuß angesehen werden, die in Perowskitstruktur kristallisieren. Die kubische Struktur des $NaWO_3$ geht bei einem Natriumanteil von $n \sim 0{,}3$ in eine

* Zur Zeit Aspirant in Veszprém. Geschickt von der Bergakademie Freiberg, Institut für Anorganische und Analytische Chemie, DDR.

rhombische und bei noch geringerem Natriumgehalt in eine trikline Struktur über. Wolframtrioxyd besitzt als Endglied dieser Reihe eine triklinverzerrte ReO_3-Struktur.

In den Wolframbronzen besteht kein Unterschied zwischen den W^V- und W^{VI}-Atomen in Gitterverband, da alle Wolframatome kristallographisch äquivalent erscheinen. Die pro Mol WO_3 eingeführten n Überschußelektronen sind somit über das ganze Gitter verteilt, ähnlich der Elektronenverteilung in den Metallen.

Das Rheniumtrioxyd besitzt eine ähnliche Struktur und zeigt ebenfalls Metalleigenschaften. In diesem Fall wird das Leitfähigkeitselektron vom Rhenium geliefert, welches um ein Elektron mehr als das Wolfram besitzt.

Experimentelles

1. Herstellung der Wolframbronzen

Wir stellten die Wolframbronzen durch Reduktion von Schmelzen von NaCl—Na-Wolframat-Soda-Gemischen mit Wolfram oder Blei her, wobei letztere Methode größere Kristalle lieferte. Das Reaktionsprodukt wurde abwechselnd mit NaOH und HCl aufgekocht, größere Kristalle wurden ausgelesen und das feine Kristallpulver wurde durch Dekantieren abgetrennt. Wir preßten aus dem Pulver Formlinge, die anschließend 12 Stunden bei 500°C im Argonstrom gesintert wurden.

Rheniumtrioxyd stellten wir durch 5-tägiges Tempern einer entsprechenden Mischung von Re_2O_7 und Re in einer Quarzampulle her.

2. Angewandte Elektroden

Die von uns untersuchten Elektroden sind in Tabelle I zusammengestellt, wo auch einige ihrer physikalischen Eigenschaften angeführt sind. Wir stellten wieder heterogene Elektroden mit Hilfe von Silikonkautschuk (S) und homogene Elektroden (H) her, was bereits früher beschrieben wurde [1, 2].

Tabelle I

Physikalische Eigenschaften der verwendeten Elektroden

Nr.	Zeichen	Farbe	Der Farbe entsprechende Formel	Gittertyp des Hauptbestandteils	Widerstand der Elektrode 10^x Ohm x ist	Art der Elektrode
1	Wb 1	Orange	$Na_{0,8}Wo_3$	Perowskit	3—4	H*
2	Wb 2	Violett	$Na_{0,4}WO_3$	Perowskit	3—4	H*
3	Wb 3	Violett	$Na_{0,4}WO_3$	Perowskit	4—5	S
4	Wb 4	Blau	$Na_{0,3}WO_3$	tetragonal	7	S
5	Wb 8	Blau	$Na_{0,3}WO_3$	tetragonal	6	S
6	ReO_3	Rot	ReO_3	Perowskit	1	S

* Es wurden Einkristalle verwendet.

3. Die verwendete Meßkette, Meßgeräte und Redox-System

gehen aus den früheren Veröffentlichungen hervor [1, 2].

Tabelle II

Potentialmessungen in schwefelsauren Ferro-Ferricyanidlösungen

Nr.	Zeichen	Einstellzeit des Potentials	Elektrolytzusammensetzung			
			5×10^{-3} 5×10^{-2} 5×10^{-2}	5×10^{-3} 5×10^{-3} 5×10^{-2}	5×10^{-3} 5×10^{-4} 5×10^{-2}	N $K_3Fe(CN)_6$ N $K_4Fe(CN)_6$ N H_2SO_4
1	Pt	1—2 sec	189 ± 1	300 ± 1	378 ± 1	mV
2	Wb 1	2—5 sec	190 ± 1	301 ± 1	378 ± 1	mV
3	Wb 2	2—5 sec	189 ± 1	300 ± 1	378 ± 1	mV
4	Wb 3	2—5 sec	nur wenige Elektroden zeigen richt. Pot.			
5	Wb 4		keine Abhängigkeit			
6	Wb 8		keine Abhängigkeit			
7	ReO_3	2—5 sec	189 ± 1	300 ± 1	378 ± 1	mV

Tabelle III

Potentialmessungen in perchlorsauren Eisen II/III-Lösungen

Nr.	Zeichen	Einstellzeit des Potentials	Elektrolytzusammensetzung			
			$4{,}41\times10^{-2}$ $1{,}55\times10^{-3}$ 1,898	$3{,}08\times10^{-2}$ $1{,}09\times10^{-2}$ 1,434	$2{,}98\times10^{-3}$ $1{,}17\times10^{-2}$ 0,798	N Fe^{3+} N Fe^{2+} N $HClO_4$
1	Pt	1—2 sec	432 ± 1	481 ± 1	535 ± 1	mV
2	Wb 1	1—2 sec	$430 + 1$	$468 + 1$	$505 + 1$	mV
3	Wb 2	2—5 sec	$425 + 1$	$465 + 1$	501 ± 1	mV
4	Wb 3	2—5 sec	$430 + 1$	$477 + 1$	$531 + 1$	mV
5	Wb 4		keine Abhängigkeit			
6	Wb 8		keine Abhängigkeit			
7	ReO_3	2—5 sec	$430 + 1$	$481 + 1$	$534 + 1$	mV

Ergebnisse und Schlußfolgerungen

Die kubischen Wolframbronzen, welche mit Perowskitstruktur kristallisieren, eignen sich wie Platin als Material für Indikatorelektroden in verschiedenen Redoxsystemen. Wie aus den Ergebnissen der Messungen hervorgeht, bestehen nur geringe Unterschiede zwischen Einkristallen und aus Mikrokristallen aufgebauten heterogenen Membranelektroden. Mit dem Übergang der Wolframbronzen in einen Strukturtyp niederer Symmetrie, der durch eine zu große Anzahl von Leerstellen im ursprünglichen Perowskitgitter

verursacht wird, verliert sich auch die Eignung der Bronzen als Material für Indikatorelektroden.

Rheniumtrioxyd unterscheidet sich in der Kristallstruktur von den Wolframbronzen durch das Fehlen eines Kations (bei den Natriumwolframbronzen von Na^+), welches im Falle der letzteren Verbindungen in der Mitte der Elementarzelle eingeschlossen ist. Von FEINLEIB und Mitarbeitern wurde gezeigt, daß die kubischen Wolframbronzen und Rheniumtrioxyd eine gleiche Elektronenstruktur besitzen [8].

Entsprechend unserer Annahme, daß die Eignung einer Redoxindikatorelektrode in erster Linie von der Kristall- und Elektronenstruktur bestimmt wird, stellen wir auch bei den Perowskitphasen fest, daß wenn obige Bedingungen zutreffen, auch gleiches Verhalten als Indikatorelektrode zu beobachten ist.

*

Wir danken Herrn Prof. ACKERMANN (Freiberg) für die Förderung der Arbeit durch die uns überlassene Rheniumprobe.

LITERATUR

1. PUNGOR, E., WESER, A. (in Druck)
2. WESER, A., PUNGOR, E. (in Druck)
3. KOKSHAROV, A. G., UST-KACHTINTSEV, V. F.: Uch. Zap. Permsk. Gos. Univ. No. **111**, 63 (1964)
4. ŠEPA, D. B., DAMJANOVICE, A., BOCKRIS, I. O. M.: Elektroch. Acta (London) **12**, 746 (1967)
5. BROYDE, B.: J. Catal. **10**, (1) 13 (1968)
6. RHODES, D. R.: U. S. 3.367.802 (Cl. 136—120) Feb. 1968
7. CHARTIER, P., POISSON, R.: C. R. Acad. Sci. Paris Ser. C **265** (25) 1353 (1967)
8. FEINLEIB, I., SCOULER, W. I., FERRETTI, A.: Phys. Rev. Vol. **165** (3) 765 (1968)

Alexander WESER; Bergakademie, Institut für Anorganische und Analytische Chemie, Freiberg, DDR

Ernő PUNGOR; Veszprém, Schönherz Z. u. 12, Ungarn

Acta Chimica Academiae Scientiarum Hungaricae, Tomus 59 (3—4), pp. 323—349 (1969)

KINETISCHE ANALYSE EINIGER FOLGEREAKTIONEN, III

DAS KONKURRENTE FOLGEREAKTIONSSYSTEM $A + A \rightarrow C$, $A + C \rightarrow E$

T. KELEN und F. TÜDŐS*

(Forschungsinstitut für die Plastindustrie, Budapest)

Eingegangen am 23. Februar 1968

Das konkurrente Folgereaktionssystem $A + A \rightarrow C$, $A + C \rightarrow E$ wurde kinetisch untersucht und die exakte Lösung des betreffenden Differentialgleichungssystems für alle möglichen Werte des $\varkappa$-Geschwindigkeitskonstanten-Quotienten angegeben. Es wurde die Abhängigkeit der Konzentrationen der in der Reaktion teilnehmenden Stoffe voneinander und von der Zeit ausführlich behandelt und auch in Diagrammen angegeben.

In den vorangehenden Teilen unserer Mitteilung befaßten wir uns mit jenen Folgereaktionssystemen, deren primäre Schritte sog. gemischte Reaktionen zweiter Ordnung (d.h. vom Typ $A + B$) sind. So wurde im I. Teil unserer Mitteilung [1] die kinetische Behandlung der Folgereaktionen

$$A + B \rightarrow C,\ C + D \rightarrow E \tag{1}$$

und im II. Teil [2] die der Reaktionen

$$A + B \rightarrow C,\ C \rightarrow E \tag{2}$$

bzw.

$$A + B \rightarrow C,\ C + C \rightarrow E \tag{3}$$

vorgenommen und die Aufstellung der entsprechenden Differentialgleichungssysteme und deren exakte Lösung angegeben.

Eine wichtige Gruppe der Folgereaktionen bilden die sog. konkurrenten Folgereaktionen: es sind dies solche Vorgänge, in denen das im primären Schritt entstandene Zwischenprodukt (C) mit der Substanz weiterreagiert, aus welcher es entstanden ist. Die vollkommene kinetische Behandlung von Reaktionen dieses Typs wurde nocht nicht vorgenommen. Obwohl BENSON [3] sich mit dem Studium der Systeme

$$A \rightarrow C,\ A + C \rightarrow E \tag{4}$$

und

$$A + B \rightarrow C,\ A + C \rightarrow E \tag{5}$$

**Zentralforschungsinstitut für Chemie der Ungarischen Akademie der Wissenschaften, Budapest.*

befaßt (eingehend sind seine Untersuchungen in [4] beschrieben), gibt er die vollständige Lösung des Problems dennoch nicht an. Zwischen den Konzentrationen gewisser Substanzen stellt er Zusammenhänge fest, ihre Zeitabhängigkeit wird aber nicht klargestellt.

Auch FROST [5] unternimmt die Analyse des konkurrenten Folgereaktionssystems laut (5). Er behandelt jene Grenzfälle, welche zur Vereinfachung des Problems führen (z.B. $k_1 \gg k_2$, $k_1 \ll k_2$, $k_1 = 2k_2$, usw.) und befaßt sich auch mit den von verschiedenen Autoren angewandten Näherungsmethoden. So z.B. geben FROST und SCHWEMER [6] auch die Zeitabhängigkeit der Konzentrationen für die Vorgänge mit der Anfangsbedingung $A_0 = 2B_0$ an; sie fassen ihre Ergebnisse für die verschiedenen Werte des k_1/k_2 — Konstantenquotienten in Tabellen bzw. Diagrammen zusammen. Die allgemeine Lösung jedoch wird auch von FROST nicht gegeben.

In dieser Mitteilung befassen wir uns mit der kinetischen Analyse des konkurrenten Folgereaktionssystems

$$A + A \rightarrow C,\ A + C \rightarrow E. \tag{6}$$

Es wird weiters die exakte mathematische Behandlung des Systems vorgenommen und außer den Zusammenhängen zwischen den Konzentrationen der in den Reaktionen teilnehmenden Substanzen werden auch die Zeitabhängigkeiten der Konzentrationen angegeben.

1. Aufstellung des Differentialgleichungssystems

Es seien die geschwindigkeitsbestimmenden konsekutiven Schritte der untersuchten chemischen Reaktion die folgenden Prozesse zweiter Ordnung:

$$A + A \rightarrow C, \tag{7}$$

$$A + C \rightarrow E. \tag{8}$$

Die zur Entstehung von je einem Mol des Zwischenproduktes C verbrauchte Menge der Substanz A sei a_1 Mol, die zum Verbrauch von je einem Mol des Zwischenproduktes C benötigte Menge der Substanz A sei a_2 Mol, ferner sei mit e Mol die Menge der Substanz E bezeichnet, die dabei entstanden ist; die jeweiligen molaren Konzentrationen der verschiedenen Substanzen seien mit den entsprechenden großen Buchstaben (A, C, E), ihre Anfangskonzentrationen hingegen mit dem Index 0 (A_0, C_0, E_0) bezeichnet; so können die

Änderungsgeschwindigkeiten der in den Reaktionen (7) und (8) teilnehmenden Substanzen folgendermaßen aufgeschrieben werden:

$$-\frac{dA}{dt} = a_1 k_1 A^2 + a_2 k_2 AC \tag{9}$$

$$\frac{dC}{dt} = k_1 A^2 - k_2 AC \tag{10}$$

$$\frac{dE}{dt} = e k_2 AC \tag{11}$$

Zwischen diesen Geschwindigkeiten kann folgende Relation festgestellt werden:

$$-\frac{dA}{dt} = a_1 \frac{dC}{dt} + \frac{a_1 + a_2}{e} \frac{dE}{dt}, \tag{12}$$

woraus durch Integration, ferner durch Beachtung der Anfangsbedingungen (am Anfang der Reaktion ist $C_0 = E_0 = 0$) folgende stöchiometrische Relation zwischen den Konzentrationen zu gewinnen ist:

$$A_0 - A = a_1 C + \frac{a_1 + a_2}{e} E \tag{13}$$

Unser Reaktionssystem wird durch die stöchiometrische Relation laut (13) und durch die unter (9) bzw. (10) aufgeschriebenen Differentialgleichungen eindeutig bestimmt. Im Gegensatz zu den vorangehenden Teilen unserer Mitteilung ist es im Falle des gegebenen Differentialgleichungssystems nicht zweckmäßig, die Funktionen $x = x(t)$ und $y = y(t)$ zwecks Zerlegung der Zwischenprodukt-Konzentration einzuführen; es erwies sich jedoch als vorteilhaft, die Lösung als Funktion des Verhältnisses zwischen der Zwischenprodukt-Konzentration und der Konzentration des Ausgangsmaterials (C/A) zu suchen.

2. Lösung des Differentialgleichungssystems

Vereinigen wir die Differentialgleichungen (9) und (10), so gelangen wir zu folgender Differentialgleichung:

$$-\frac{dC}{dA} = \frac{k_1 A^2 - k_2 AC}{a_1 k_1 A^2 + a_2 k_2 AC} \tag{14}$$

Durch Einführung der Bezeichnung

$$\varkappa = \frac{k_2}{k_1} \tag{15}$$

und der neuen Veränderlichen

$$\psi = \frac{C}{A} \tag{16}$$

sowie unter Berücksichtigung dessen, daß auf Grund von (16) (da $C = A\psi$)

$$\frac{dC}{dA} = \psi + A\frac{d\psi}{dA} \tag{17}$$

ist, kann Gleichung (14) in folgender Form aufgeschrieben werden:

$$-\psi - A\frac{d\psi}{dA} = \frac{1 - \varkappa\psi}{a_1 + a_2\varkappa\psi} \tag{18}$$

Nach Umordnung dieser Gleichung und Trennung der Variablen gelangen wir von (18) zu folgender Relation:

$$-\frac{dA}{A} = \frac{a_1 + a_2\varkappa\psi}{a_2\varkappa\psi^2 + (a_1 - \varkappa)\psi + 1}\, d\psi \tag{19}$$

Wird die Bezeichnung

$$R(\psi) = a_2\varkappa\psi^2 + (a_1 - \varkappa)\psi + 1 \tag{20}$$

eingeführt und berücksichtigt, daß

$$\frac{dR(\psi)}{d\psi} = 2a_2\varkappa\psi + (a_1 - \varkappa) \tag{21}$$

ist, woraus

$$a_1 + a_2\varkappa\psi = \frac{1}{2}\left[\frac{dR(\psi)}{d\psi} + a_1 + \varkappa\right] \tag{22}$$

folgt, so kann die Relation (19) folgendermaßen umgestaltet werden:

$$-\frac{dA}{A} = \frac{1}{2}\frac{dR}{R} + \frac{a_1 + \varkappa}{2}\frac{d(\psi)}{R(\psi)} \tag{23}$$

Aus diesem Zusammenhang gewinnen wir durch Integration

$$\ln \delta - \ln A = \frac{1}{2} \ln R + \frac{a_1 + \varkappa}{2} \int \frac{d\psi}{R(\psi)}, \tag{24}$$

wo δ die von den Anfangsbedingungen abhängige Integrationskonstante ist. Die Relation (24) gibt in ihrer expliziten Form die Funktion $A = A(\psi)$ an:

$$A(\psi) = \delta [R(\psi)]^{-\frac{1}{2}} \exp \left[- \frac{a_1 + \varkappa}{2} \int \frac{d\psi}{R(\psi)} \right] \tag{25}$$

Auf die möglichen Werte des Integrals und der Funktion $A = A(\psi)$ in (25) kommen wir später zurück. Es soll nun untersucht werden, wie im Besitz dieser Funktion die Zeitabhängigkeit der Konzentrationen gewonnen werden kann: auf Grund der Definition von ψ laut (16) gibt der Zusammenhang

$$\frac{d\psi}{dt} = \frac{1}{A} \frac{dC}{dt} - \frac{C}{A^2} \frac{dA}{dt} \tag{26}$$

Setzt man in diesem die Relationen (9) und (10) ein und führt die Operationen durch, so nimmt (26) folgende Form an:

$$\frac{d\psi}{dt} = k_1 A [a_2 \varkappa \psi^2 + (a_1 - \varkappa) \psi + 1], \tag{27}$$

d.h. auf Grund von (20)

$$\frac{d\psi}{dt} = k_1 A(\psi) R(\psi), \tag{28}$$

bzw. nach Trennung der Variablen:

$$k_1 dt = \frac{d\psi}{A(\psi) R(\psi)} \tag{29}$$

Nach Integration wird

$$k_1 t + K(\psi_0) = \int \frac{d\psi}{A(\psi) R(\psi)}, \tag{30}$$

wo $K(\psi_0)$ die von den Anfangsbedingungen abhängige Integrationskonstante ist. Durch Einführung der Bezeichnung

$$\theta = k_1 t \tag{31}$$

kann Relation (30) in folgender Form aufgeschrieben werden:

$$\theta = \int \frac{d\psi}{A(\psi)\,R(\psi)} - K(\psi_0) \tag{32}$$

Wie zu ersehen ist, wurde die Lösung unseres Differentialgleichungssystems auf die Bestimmung der Integrale in den Relationen (25) und (32) zurückgeführt. Mit Hilfe der Relation (25) gelangen wir zur Funktion $A = A(\psi)$, und mit Hilfe von (32) zur Funktion $\theta = \theta(\psi)$: also steht uns letzten Endes die Lösung $A = A(t)$ in impliziter Form zur Verfügung, woraus mit Hilfe von (16) auch die Lösung $C = C(t)$ zu gewinnen ist.

3. Die Lösungsfunktionen

Zur Darstellung der Lösungsfunktionen muß das Integral in Relation (25)

$$\int \frac{d\psi}{R(\psi)} \tag{33}$$

bestimmt werden, ferner das Integral in Relation (32)

$$\int \frac{d\psi}{A(\psi)\,R(\psi)} \tag{34}$$

[dies geschieht mit Hilfe der aus (33) erhaltenen Funktion $A = A(\psi)$]. Die Werte beider Integrale hängen vom Charakter der Wurzeln des in den Integranden vorkommenden, durch die Relation (20) definierten Ausdruckes zweiten Grades $R(\psi)$ ab, diese hingegen wird durch die Diskriminante (Δ) von $R(\psi)$ bestimmt:

$$\Delta = (a_1 - \varkappa)^2 - 4a_2\varkappa \tag{35}$$

Es können, wie bekannt, dem Wert von Δ entsprechend, 3 Fälle unterschieden werden:

1. $\Delta > 0$, dann hat der Ausdruck zweiten Grades $R(\psi)$ zwei voneinander verschiedene reelle Wurzeln (ψ_1 und ψ_2).

2. $\Delta = 0$, dann sind die Wurzeln einander gleich ($\bar{\psi}$).

3. $\Delta < 0$, dann besitzt der Ausdruck zweiten Grades $R(\psi)$ keine reellen Wurzeln.

Im Falle von gegebenen stöchiometrischen Parametern (a_1 und a_2) hängt der Wert von Δ nur von $\varkappa$ ab, wie dies aus der Untersuchung des Ausdruckes der Diskriminanten laut (35) hervorgeht. Abbildung 1 zeigt die

Gestaltung der Δ-Werte in der Funktion von $\varkappa$. (Bei dieser und jeder anderen Abbildung sowie bei der Bestimmung der in der Publikation angegebenen Zahlenwerte haben wir für die stöchiometrischen Parameter a_1, a_2 und e bzw. für die Anfangskonzentration A_0 die Werte $a_1 = 2$, $a_2 = 1$ und $e = 1$ bzw. $A_0 = 1$ gewählt.)

Wie aus der Abbildung zu ersehen ist, müssen, den obigen drei möglichen Δ-Werten entsprechend, fünferlei Fälle untersucht werden, falls wir die

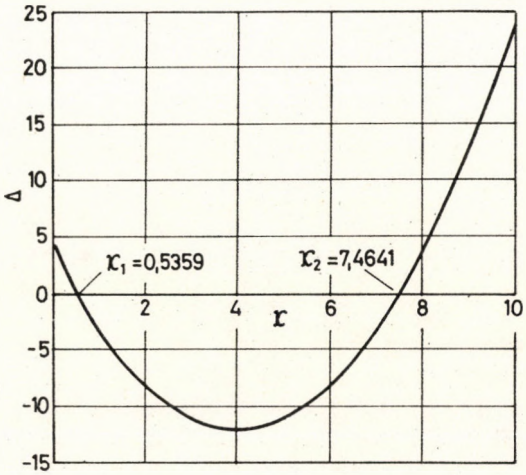


Abb. 1. Gestaltung der Δ-Werte als Funktion von $\varkappa$

Lösungsfunktionen für jeden möglichen Wert von $\varkappa$ $(0 < \varkappa < \infty)$ erhalten wollen:

$$\begin{array}{lll} 1. & 0 < \varkappa < \varkappa_1 & \Delta > 0 \\ 2. & \varkappa = \varkappa_1 & \Delta = 0 \\ 3. & \varkappa_1 < \varkappa < \varkappa_2 & \Delta < 0 \\ 4. & \varkappa = \varkappa_2 & \Delta = 0 \\ 5. & \varkappa_2 < \varkappa < \infty & \Delta > 0 \end{array} \qquad (36)$$

wo $\varkappa_1$ und $\varkappa_2$ die Wurzeln der Gleichung zweiten Grades der Diskriminanten laut (35) sind:

$$\varkappa_{1,2} = (a_1 + 2a_2) \mp 2\sqrt{(a_1 + a_2)\, a_2} \qquad (37)$$

Die Wurzeln des Ausdruckes zweiten Grades $R(\psi)$ hingegen sind die folgenden:

Im Falle von $\Delta = 0$ ist $\bar{\psi}$ die einzige Wurzel:

$$\bar{\psi} = \frac{\varkappa - a_1}{2a_1\varkappa} \qquad (38)$$

Im Falle $\Delta > 0$ sind ψ_1 und ψ_2 die verschiedenen reellen Wurzeln:

$$\psi_{1,2} = \bar{\psi} \mp \frac{\sqrt{\Delta}}{2a_2\varkappa} \tag{39}$$

In Kenntnis dieser Wurzeln kann der Ausdruck zweiten Grades $R(\psi)$ auch als Produkt aufgeschrieben werden:

Im Falle von $\Delta = 0$:

$$R(\psi) = a_2\varkappa(\psi - \bar{\psi})^2 \tag{40}$$

Im Falle $\Delta > 0$:

$$R(\psi) = a_2\varkappa(\psi - \psi_1)(\psi - \psi_2) \tag{41}$$

Die Integralwerte laut (33) und (34) und — mit deren Anwendung — die Lösungsfunktionen müssen also in fünferlei Fällen laut (36) untersucht werden.

3.1. $0 < \varkappa < \varkappa_1$; $\Delta > 0$

Der Wert des Integrals laut (33) ist in diesem Fall — bei Anwendung der Produktenform von $R(\psi)$ laut (41) — wie folgt:

$$\int \frac{d\psi}{R(\psi)} = \frac{1}{\sqrt{\Delta}} \ln \frac{\psi - \psi_2}{\psi - \psi_1}. \tag{42}$$

Die neue Veränderliche

$$\varrho = \frac{\psi - \psi_2}{\psi - \psi_1} \tag{43}$$

und die Bezeichnung

$$p = \frac{3}{2} - \frac{a_1 + \varkappa}{2\sqrt{\Delta}} \tag{44}$$

seien eingeführt, dann sind unsere Lösungsfunktionen A und C auf Grund von (16), (25), (41) und (42) folgendermaßen aufzuschreiben:

$$A(\varrho) = \frac{\delta_1\sqrt{a_2\varkappa}}{\sqrt{\Delta}} \varrho^{p-2}(1 - \varrho) \tag{45}$$

und

$$C(\varrho) = \frac{\delta_1\sqrt{a_2\varkappa}}{\sqrt{\Delta}} \varrho^{p-2}(\psi_2 - \psi_1\varrho), \tag{46}$$

wobei der Wert der Integrationskonstante δ_1

$$\delta_1 = A_0 \varrho_0^{\frac{3}{2}-p} \tag{47}$$

ist: hier bedeutet ϱ_0 den Anfangswert der laut (43) definierten Veränderlichen ϱ:

$$\varrho_0 = \frac{\psi_2}{\psi_1} \tag{48}$$

Die die Zeit enthaltende Lösungsfunktion wird auf Grund des Integrals (34) gewonnen; durch Einführung der neuen Veränderlichen (ϱ) sowie durch Anwendung von (41) und (45) wird das Integral zu

$$\int \frac{d\psi}{A(\psi)\,R(\psi)} = \frac{d\psi}{\delta_1 \sqrt{a_2 \varkappa}} \int \varrho^{p-1}(1-\varrho)^{-1} d\varrho \tag{49}$$

Der Wert des Integrals auf der rechten Seite von (49) kann mit Hilfe der unvollständigen Beta-Funktion angegeben werden:

$$\int \varrho^{p-1}(1-\varrho)^{-1} d\varrho = B_\varrho(p,0) \tag{50}$$

(bezüglich der unvollständigen Beta-Funktion s. [2, 7]). Also lautet die die Zeit enthaltende Lösungsfunktion auf Grund von (32):

$$\vartheta = \frac{1}{\delta_1 \sqrt{a_2 \varkappa}} \left[B_\varrho(p,0) - B_{\varrho_0}(p,0)\right], \tag{51}$$

da der Wert der Integrationskonstante $K(\psi_0)$ in (32) in diesem Falle

$$K(\psi_0) = \frac{1}{\delta_1 \sqrt{a_2 \varkappa}} B_{\varrho_0}(p,0) \tag{52}$$

ist.

Es kann durch die Analyse unserer Lösungsfunktionen festgestellt werden, daß die Zwischenprodukt-Konzentration im Grenzfalle ($t \to \infty$, $\theta \to \infty$, $A \to 0$) folgenden Grenzwert annimmt:

$$\lim_{t\to\infty} C(t) = \lim_{\psi\to\infty} C(\psi) = \lim_{\varrho\to 1} C(\varrho) = \frac{\delta_1}{\sqrt{a_2 \varkappa}} \tag{53}$$

Die Zwischenprodukt-Konzentration ändert sich als Funktion der Zeit gemäß einer Maximumkurve. Der zum Maximum gehörende ψ_m Wert kann auf Grund der Differentialgleichung (10) bestimmt werden: beim Maximum wird $dC/dt = 0$, also ist

$$k_1 A_m^2 = k_2 A_m C_m \tag{54}$$

und da laut (16) $C_m/A_m = \psi_m$ zutrifft, beträgt ψ beim Maximum

$$\psi_m = \frac{1}{\varkappa}. \tag{55}$$

Die Relation (55) wurde unmittelbar aus der Differentialgleichung gewonnen und somit ist sie, unabhängig von dem Wert von $\varkappa$, gültig.

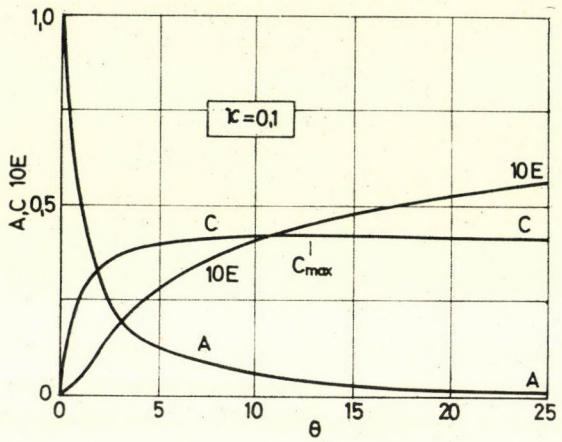


Abb. 2. Die Werte von A, C und E bei $\varkappa = 0{,}1$ in Abhängigkeit von $\theta = k_1 t$

Da $\varkappa_1 = 0{,}5359$ ist, sind die in diesem Punkt angegebenen Lösungen in dem Intervall $0 < \varkappa < 0{,}5359$ anwendbar. Abbildung 2 zeigt die Werte von A, C und E im Falle von $\varkappa = 0{,}1$: die Werte von A wurden auf Grund der Lösungsfunktion (45), jene von C auf Grund von (46), die zu ihnen gehörenden $\theta = k_1 t$ Werte auf Grund von (51) berechnet; die Werte von E hingegen wurden mit Hilfe der stöichiometrischen Relation (13) aus den Werten von A und C gewonnen.

In Abb. 3 werden die folgenden Daten in Abhängigkeit von der Reaktionskoordinate $(A_0 - A)/A_0$ (ihr Wert verändert sich im Laufe der Reaktion von 0 bis 1) im Falle von $\varkappa = 0{,}1$ veranschaulicht: ψ laut (16), ϱ laut (43) sowie C laut (46) berechnet.

3.2. $\varkappa = \varkappa_1$; $\Delta = 0$

Der Wert des Integrals laut (33) ist in diesem Falle, mit Anwendung der der Relation (40) entsprechenden Form von $R(\psi)$ wie folgt:

$$\int \frac{d\psi}{R(\psi)} = -\frac{1}{a_2 \varkappa (\psi - \overline{\psi})} \tag{56}$$

Durch Einführung der Veränderlichen

$$\omega = \frac{1}{\psi - \overline{\psi}} \tag{57}$$

und der Bezeichunng

$$\mu = \frac{a_1 + \varkappa}{2a_2\varkappa} \tag{58}$$

können unsere Lösungsfunktionen A und C auf Grund von (16), (25), (40) und (56) wie folgt aufgeschrieben werden:

$$A(\omega) = \frac{\delta_2}{\sqrt{a_2\varkappa}}\,\omega\,\exp(\mu\omega) \tag{59}$$

und

$$C(\omega) = \frac{\delta_2}{\sqrt{a_2\varkappa}}(1 + \bar{\psi}\omega)\,\exp(\mu\omega), \tag{60}$$

wobei δ_2 eine Integrationskonstante ist:

$$\delta_2 = A_0 \exp(-\mu\omega_0) \tag{61}$$

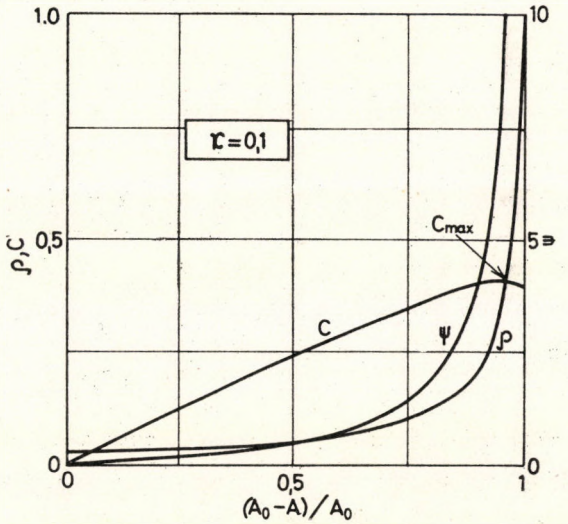


Abb. 3. Die Werte von ψ, ϱ und C bei $\varkappa = 0{,}1$ in Abhängigkeit von der Reaktionskoordinate $(A_0 - A)/A_0$

Hier ist ω_0 der Anfangswert der laut (57) definierten Veränderlichen ω:

$$\omega_0 = -\frac{1}{\bar{\psi}} \tag{62}$$

Die die Zeit enthaltende Lösungsfunktion ist auf Grund der Bestimmung des Integralwertes (34) zu gewinnen: durch Einführung der neuen Veränderlichen ω, weiters durch Anwendung von (40) und (59), verändert sich das

Integral wie folgt:

$$\int \frac{d\psi}{A(\psi)\,R(\psi)} = -\frac{1}{\delta_2\sqrt{a_2\varkappa}} \int \frac{e^{-\mu\omega}}{\omega}\,d\omega \tag{63}$$

Der Wert des Integrals auf der rechten Seite von (63) kann mit Hilfe der Integral-Exponentialfunktion angegeben werden:

$$\int \frac{e^{-\mu\omega}}{\omega}\,d\omega = Ei(-\mu\omega) \tag{64}$$

(bezügl. der Integral-Exponentialfunktion s. [7, 8]). Die die Zeit enthaltende Lösungsfunktion gestaltet sich auf Grund von (32) folgendermaßen:

$$\theta = \frac{1}{\delta_2\sqrt{a_2\varkappa}}\,[Ei(-\mu\omega_0) - Ei(-\mu\omega)], \tag{65}$$

da der Wert der in (32) vorkommenden Integrationskonstante $K(\psi_0)$ in diesem Falle

$$K(\psi_0) = -\frac{1}{\delta_2\sqrt{a_2\varkappa}}\,Ei(-\mu\omega_0) \tag{66}$$

ist.

Durch die Analyse unserer Lösungsfunktionen kann festgestellt werden, daß im Grenzfalle ($t \to \infty$, $\theta \to \infty$, $A \to 0$) die Zwischenprodukt-Konzentration folgenden Grenzwert erreicht:

$$\lim_{t\to\infty} C(t) = \lim_{\psi\to\infty} C(\psi) = \lim_{\omega\to 0} C(\omega) = \frac{\delta_2}{\sqrt{a_2\varkappa}} \tag{67}$$

Es sei bemerkt, daß alle in diesem Punkt mitgeteilten Lösungen sich auf einen konkreten Wert von $\varkappa$, auf den $\varkappa = \varkappa_1$ Wert beziehen.

3.3. $\varkappa_1 < \varkappa < \varkappa_2$; $\Delta = 0$

In diesem Falle ist der Wert des Integrals laut (33), bei Anwendung der Form von $R(\psi)$ laut (20), wie folgt:

$$\int \frac{d\psi}{R(\psi)} = \frac{2}{\sqrt{-\Delta}}\ \text{arctg}\ \frac{a_1 - \varkappa + 2a_2\varkappa\psi}{\sqrt{-\Delta}} \tag{68}$$

Mit Einführung der Veränderlichen

$$\varphi = \text{arctg}\ \frac{a_1 - \varkappa + 2a_2\varkappa\psi}{\sqrt{-\Delta}} \tag{69}$$

und der Bezeichnung

$$\sigma = \frac{a_1 + \varkappa}{\sqrt{-\Delta}} \tag{70}$$

können unsere Lösungsfunktionen A und C, auf Grund von (16), (20), (25) und (68) folgendermaßen aufgeschrieben werden:

$$A(\varphi) = \frac{2\delta_3 \sqrt{a_2 \varkappa}}{\sqrt{-\Delta}} \cos \varphi \exp(-\sigma\varphi) \tag{71}$$

und

$$C(\varphi) = \frac{\delta_3}{\sqrt{a_2 \varkappa}} (\operatorname{tg} \varphi - \operatorname{tg} \varphi_0) \cos \varphi \exp(-\sigma\varphi) \tag{72}$$

Hier ist der Wert der Integrationskonstante δ_3:

$$\delta_3 = A_0 \exp(\sigma\varphi_0) \tag{73}$$

wo φ_0 der Anfangswert der laut (69) definierten Veränderlichen φ ist:

$$\varphi_0 = \operatorname{arctg} \frac{a_1 - \varkappa}{\sqrt{-\Delta}} \tag{74}$$

Die die Zeit enthaltende Lösungsfunktion wird auf Grund der Bestimmung des Integralwertes (34) gewonnen; durch Einführung der neuen Veränderlichen (φ) sowie durch Anwendung von (20) und (71) verändert sich das Integral:

$$\int \frac{d\psi}{A(\psi) R(\psi)} = \frac{1}{\delta_3 \sqrt{a_2 \varkappa}} \int \frac{\exp(\sigma\varphi)}{\cos \varphi} d\varphi \tag{75}$$

Der Wert des Integrals auf der rechten Seite von (75) kann mit Hilfe der Integration der Taylor-Reihe des Integrandes (genommen im Punkt $\varphi = 0$) angegeben werden:

$$\int \frac{\exp(\sigma\varphi)}{\cos \varphi} d\varphi = \sum_{n=0}^{\infty} C_n \frac{\varphi^{n+1}}{(n+1)!} = S(\varphi) \tag{76}$$

wo die Werte der Koeffizienten C_n

$$C_n = \sum_{k=0}^{n} \binom{n}{2k} |E_{2k}| \sigma^{n-2k} \tag{77}$$

sind. Hier bedeuten die Werte $\binom{n}{2k}$ die binomialen Koeffizienten, die Werte

E_{2k} sind hingegen die Eulerschen Zahlen. (Bezüglich der letzteren s. [7] und [9]: ihre Werte bis E_{20} sind die folgenden:

$$\begin{aligned} E_0 &= 1 & E_{12} &= 2702765 \\ E_2 &= -1 & E_{14} &= -199360981 \\ E_4 &= 5 & E_{16} &= 19391512145 \\ E_6 &= -61 & E_{18} &= -2404879675441 \\ E_8 &= 1385 & E_{20} &= 370371188237525 \\ E_{10} &= -50521 \end{aligned} \tag{78}$$

Es sei bemerkt, daß in Formel (77) die absoluten Werte der Eulerschen Zahlen vorkommen !)

Es kann gezeigt werden, daß die in (76) definierte, mit $S(\varphi)$ bezeichnete unendliche Reihe im Falle von

$$|\varphi| < \frac{\pi}{2} \tag{79}$$

konvergent, bei $|\varphi| \geqq \pi/2$ Werten hingegen divergent ist:

$$S\left(\frac{\pi}{2}\right) = \infty \tag{80}$$

Die die Zeit enthaltende Lösungsfunktion ist also auf Grund von (32), (75) und (76):

$$\theta = \frac{1}{\delta_3 \sqrt{a_2 \varkappa}} \left[S(\varphi) - S(\varphi_0)\right], \tag{81}$$

da der Wert der in (32) vorkommenden Integrationskonstante $K(\psi_0)$ in diesem Falle

$$K(\psi_0) = \frac{1}{\delta_3 \sqrt{a_2 \varkappa}} \; S(\varphi_0) \tag{82}$$

ist.

Durch Analyse unserer Lösungsfunktionen kann festgestellt werden, daß die Konzentration des Zwischenproduktes im Grenzfalle ($t \to \infty$, $\theta \to \infty$, $A \to 0$) folgenden Grenzwert erreicht:

$$\lim_{t \to \infty} C(t) = \lim_{\psi \to \infty} C(\psi) = \lim_{\varphi \to \frac{\pi}{2}} C(\varphi) = \frac{\delta_3}{\sqrt{a_2 \varkappa}} \exp\left(-\sigma \frac{\pi}{2}\right) \tag{83}$$

Da $\varkappa_2 = 7{,}4641$ ist, können die in diesem Punkt angegebenen Lösungen im Intervall $0{,}5359 < \varkappa < 7{,}4641$ angewandt werden. Abb. 4 zeigt die Werte

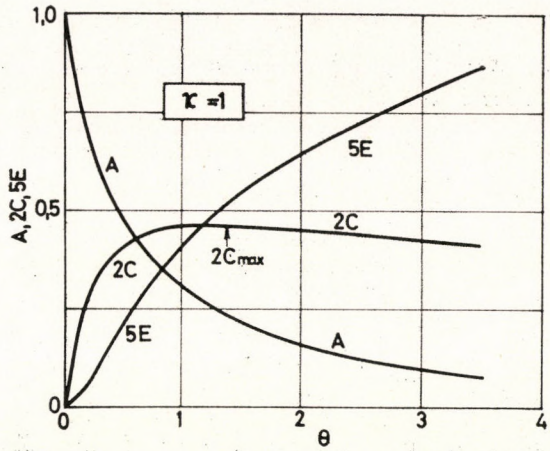


Abb. 4. Die Werte von A, C und E bei $\varkappa = 1$ in Abhängigkeit von $\theta = k_1 t$

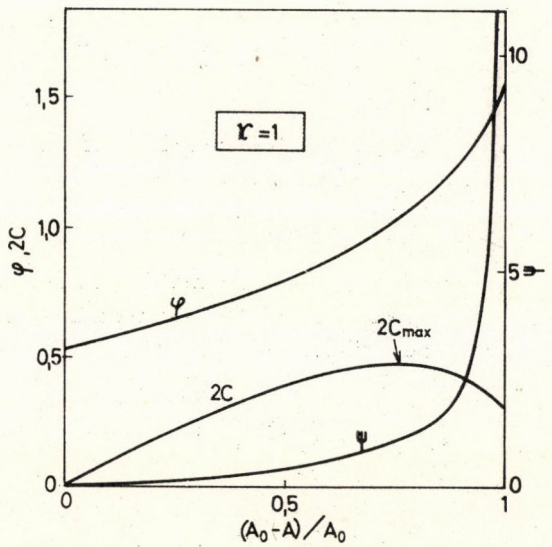


Abb. 5. Die Werte von ψ, φ und C bei $\varkappa = 1$ in Abhängigkeit von der Reaktionskoordinate $(A_0 - A)/A_0$

von A, C und E im Falle von $\varkappa = 1$; die Werte von A wurden auf Grund der Lösungsfunktion (71), jene von C auf Grund von (72) berechnet; die Werte von E hingegen wurden mit Hilfe der stöchiometrischen Relation (13) aus den berechneten A und C Werten gewonnen.

In Abb. 5 werden in Abhängigkeit von der Reaktionskoordinate $(A_0 - A)/A_0$ folgende, den Fall $\varkappa = 1$ betreffende Daten angegeben, wobei ψ laut (16), φ laut (69) und C laut (72) berechnet worden ist.

3.4. $\varkappa = \varkappa_2 \; ; \; \Delta = 0$

Die Lösungen unterscheiden sich von den im Punkt 3.2 ($\varkappa = \varkappa_1$) besprochenen nur im Vorzeichen:

$$A(\omega) = -\frac{\delta_2}{\sqrt{a_2 \varkappa}} \omega \exp(\mu\omega) \tag{84}$$

$$C(\omega) = -\frac{\delta_2}{\sqrt{a_2 \varkappa}} (1 + \bar{\psi}\omega) \exp(\mu\omega) \tag{85}$$

$$\theta = -\frac{1}{\delta_2 \sqrt{a_2 \varkappa}} [Ei(-\mu\omega_0) - Ei(-\mu\omega)] \tag{86}$$

Durch Analyse unserer Lösungsfunktionen kann festgestellt werden, daß im Grenzfalle ($t \to \infty, \theta \to \infty, A \to 0$) die Konzentration des Zwischenproduktes sich dem Wert 0 nähert:

$$\lim_{t \to \infty} C(t) = \lim_{\psi \to \bar{\psi}} C(\psi) = \lim_{\omega \to -\infty} C(\omega) = 0 \tag{87}$$

Hier soll bemerkt werden, daß diese Lösungen sich auf einen konkreten Wert von $\varkappa$, auf den Wert $\varkappa = \varkappa_2$ beziehen.

3.5. $\varkappa_2 < \varkappa < \infty \; ; \; \Delta > 0$

Die Lösungen unterscheiden sich von den im Punkt 3.1. ($0 < \varkappa < \varkappa_1$) besprochenen nur im Vorzeichen und in der Veränderlichen bzw. im Parameter der unvollständigen Beta-Funktion:

$$A(\varrho) = -\frac{\delta_1 \sqrt{a_2 \varkappa}}{\sqrt{\Delta}} \varrho^{p-2}(1 - \varrho) \tag{88}$$

$$C(\varrho) = -\frac{\delta_1 \sqrt{a_2 \varkappa}}{\sqrt{\Delta}} \varrho^{p-2}(\psi_2 - \psi_1 \varrho) \tag{89}$$

$$\theta = -\frac{1}{\delta_1 \sqrt{a_2 \varkappa}} [B_{1/\varrho}(p - 1, 0) - B_{1/\varrho_0}(p - 1, 0)] \tag{90}$$

Durch Analyse unserer Lösungsfunktionen kann festgestellt werden, daß im Grenzfalle ($t \to \infty, \theta \to \infty, A \to 0$) die Zwischenprodukt-Konzentration sich dem Wert 0 nähert:

$$\lim_{t \to \infty} C(t) = \lim_{\psi \to \psi_1} C(\psi) = \lim_{1/\varrho \to 0} C(\varrho) = 0 \tag{91}$$

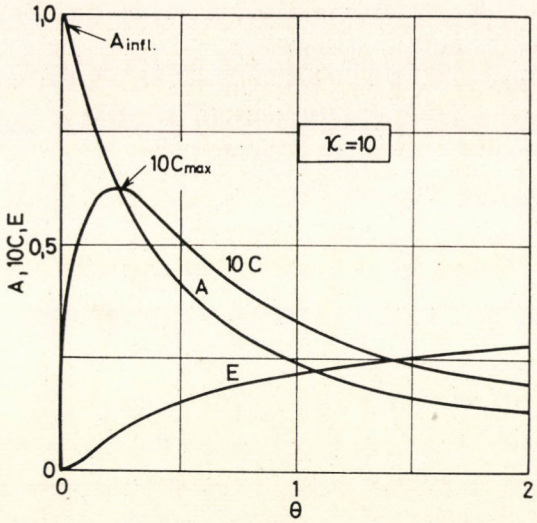


Abb. 6. Die Werte von A, C und E bei $\varkappa = 10$ in Abhängigkeit von $\theta = k_1 t$

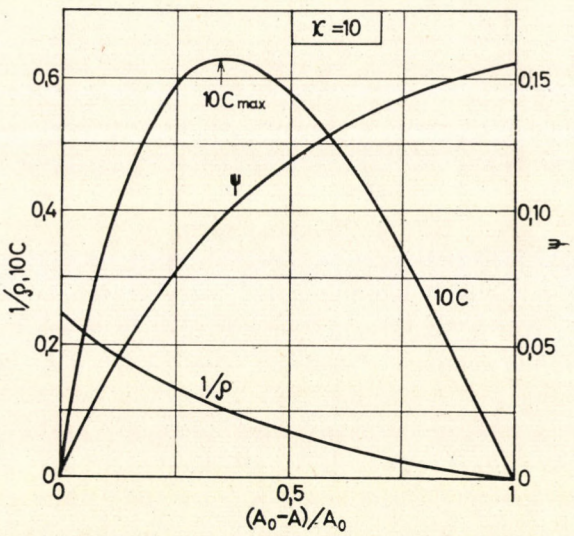


Abb. 7. Die Werte von ψ, $1/\varrho$ und C bei $\varkappa = 10$ in Abhängigkeit von der Reaktionskoordinate $(A_0 - A)/A_0$

Da $\varkappa_2 = 7{,}4641$ ist, können die in diesem Punkte angegeben Lösungen in dem Intervall $7{,}4641 < \varkappa < \infty$ angewendet werden. Abb. 6 zeigt die Werte von A, C und E im Falle von $\varkappa = 10$; die Werte von A wurden auf Grund der Lösungsfunktion (88), jene von C auf Grund von (89), die zu ihnen gehörenden $\theta = k_1 t$ Werte auf Grund von (90) berechnet; der Wert von E

hingegen wurde mit Hilfe der stöichiometrischen Relation (13) aus den berechneten Werten von A und C gewonnen.

In Abb. 7 werden in Abhängigkeit von der Reaktionskoordinate $(A_0 - A)/A_0$ folgende, den Fall $\varkappa = 10$ betreffende Daten angegeben: ψ laut (16), $1/\varrho$ laut (43) und C laut (89) berechnet.

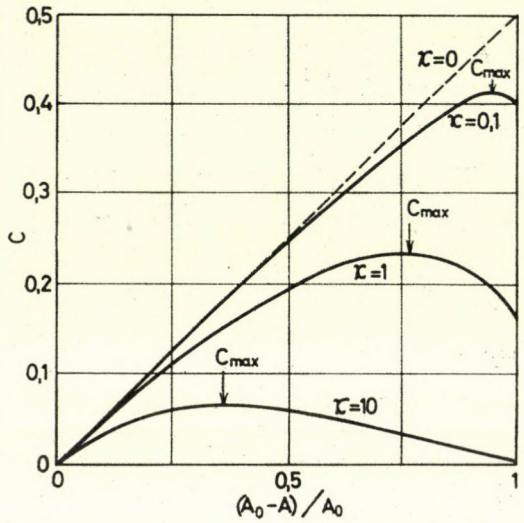


Abb. 8. Gestaltung der C-Werte als Funktion der Reaktionskoordinate $(A_0 - A)/A_0$ (der Parameter der Kurven ist $\varkappa$)

4. Bemerkungen

Die mathematische Behandlung des untersuchten konkurrenten Folgereaktionssystems wurde dadurch erschwert, daß sich im Laufe der Lösung ein Integrand ergab, der einen Ausdruck zweiten Grades enthält. Im Besitz der Lösungen hingegen kann die kinetische Analyse leicht durchgeführt werden: die Übersicht des Problems wird durch die graphische Darstellung der Ergebnisse vereinfacht. Deshalb veranschaulichen wir unsere Ergebnisse außer den schon gezeigten Abbildungen auch auf andere Weise. In allen Diagrammen sind die Werte der stöichiometrischen Parameter: $a_1 = 2$, $a_2 = 1$ und $e = 1$, der Wert von A_0 hingegen: $A_0 = 1$.

In den Abbildungen 8 und 9 werden die Konzentrationen des Zwischenproduktes C und des Endproduktes E in Abhängigkeit von der Reaktionskoordinate $(A_0 - A)/A_0$ dargestellt. Der Parameter der Kurven ist $\varkappa$.

In den Abbildungen 10, 11 und 12 werden die Konzentrationen des Ausgangsmaterials A, des Zwischenproduktes C und des Endproduktes E in Abhängigkeit von den Werten $\log \theta = \log (k_1 t)$ dargestellt. Der Parameter der Kurven ist $\varkappa$.

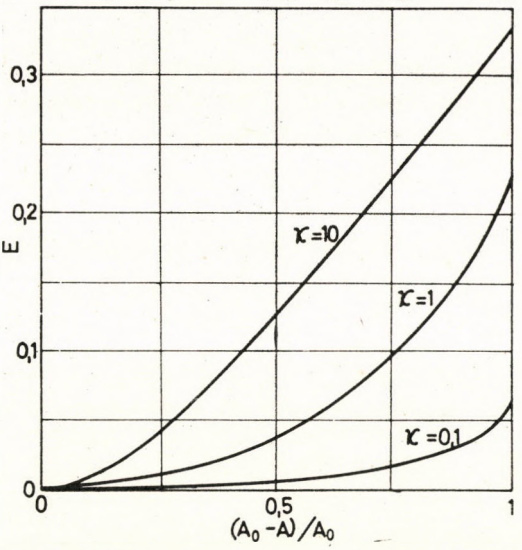


Abb. 9. Gestaltung der E-Werte als Funktion der Reaktionskoordinate $(A_0 - A)/A_0$ (der Parameter der Kurven ist $\varkappa$)

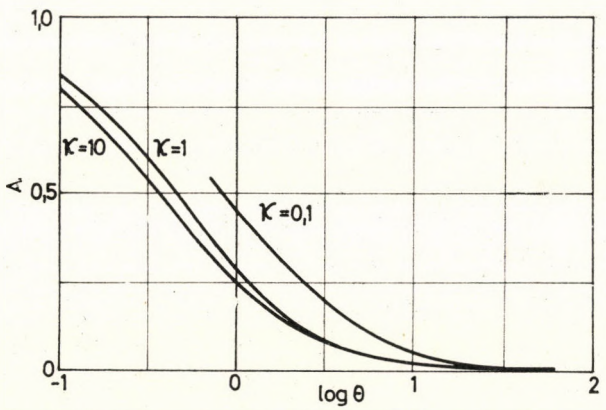


Abb. 10. Die Werte von A in Abhängigkeit von $\log \theta = \log (k_1 t)$ (der Parameter der Kurven ist $\varkappa$)

Die in Abb. 10 dargestellten $A - \log \theta$ Kurven sind mit jenen zu vergleichen, die von FROST und SCHWEMER [6] mit der Anfangsbedingung $A_0 = 2B_0$ für das einigermaßen abweichende System (5) berechnet worden sind (s. [5], Seite 169, Abb. 8).

Bei der Untersuchung des Systems (5) bezieht BENSON [3] die Konzentration des Zwischenproduktes C nicht auf die Konzentration der in beiden Reaktionen teilnehmenden Substanz A, sondern auf jene des anderen Ausgangsmaterials (B). (BENSON bezeichnet das in der ersten Reaktion teilneh-

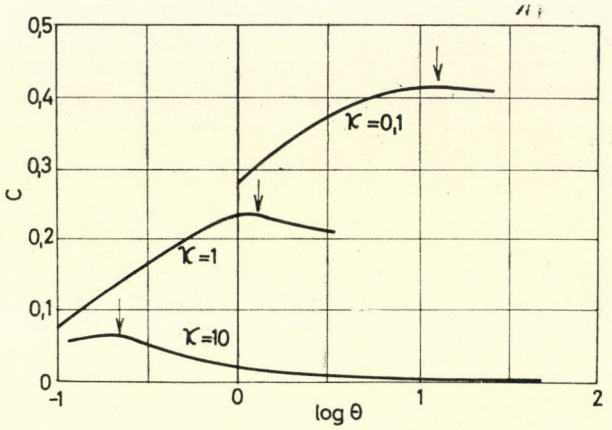


Abb. 11. Die Werte von C in Abhängigkeit von $\log \theta = \log (k_1 t)$ (der Parameter der Kurven ist $\varkappa$)

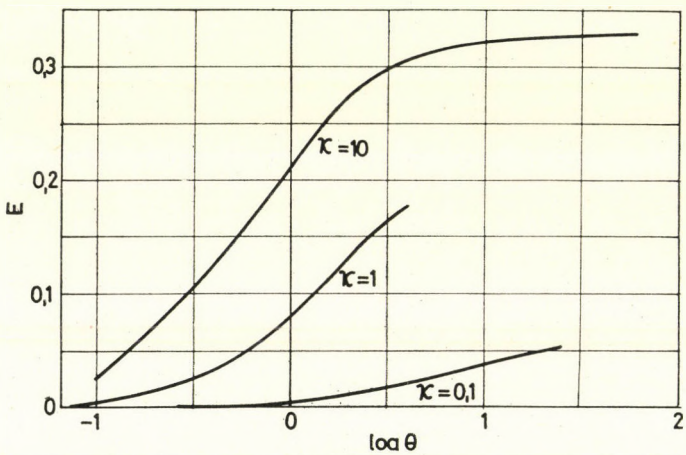


Abb. 12. Die Werte von E in Abhängigkeit von $\log \theta = \log (k_1 t)$ (der Parameter der Kurven ist $\varkappa$)

mende Material mit A, das in beiden Reaktionen teilnehmende mit B. Wir haben seine Bezeichnung zwecks Vergleichbarkeit geändert.) Er stellt das Produkt des Quotienten C/B und $\varkappa$ als Funktion der Reaktionskoordinate $(A_0 - A)/A_0$ dar (s. [3], III., Abb. 3). Zum Vergleich wird in Abb. 13 das $\varkappa$-fache des $\psi = C/A$ Quotienten als Funktion der Reaktionskoordinate $(A_0 - A)/A_0$ im Falle unseres, von (5) einigermaßen abweichenden Systems (6) dargestellt. Der Parameter der Kurven ist $\varkappa$.

Es sei auf den interessanten Umstand hingewiesen, daß der Grenzwert der Zwischenprodukt-Konzentration ($t \to \infty$, $C \to C_\infty$) nach unseren Resultaten eine Funktion des Wertes von $\varkappa$ ist. Diese Abhängigkeit wird in Abb.

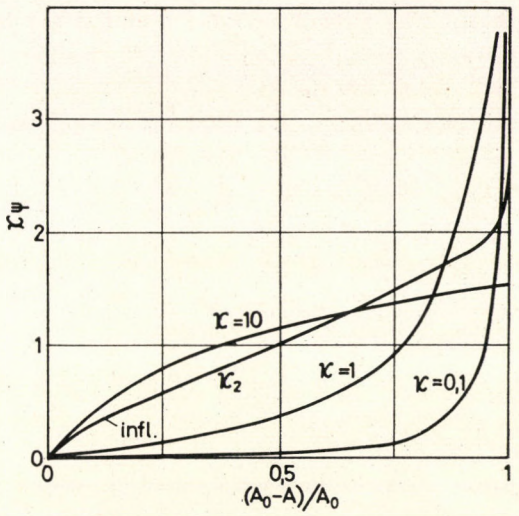


Abb. 13. Gestaltung der $\varkappa\psi$-Werte als Funktion von der Reaktionskoordinate $(A_0-A)/A_0$ (der Parameter der Kurven ist $\varkappa$)

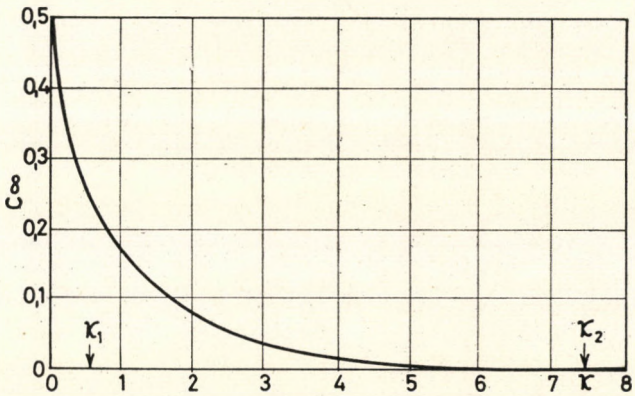


Abb. 14. Der Grenzwert ($t\to\infty$) der Zwischenprodukt-Konzentration in Abhängigkeit von $\varkappa$

14 veranschaulicht. Wie ersichtlich, ist der kleinste $\varkappa$-Wert, wo C_∞ Null wird, $\varkappa = \varkappa_2$. (Dies bedeutet gleichzeitig, daß der Wert von $\psi_\infty = \lim_{t\to\infty} C/A$ zuerst bei $\varkappa_2$ die Form 0/0 annimmt, d.h. begrenzt ist.)

Im folgenden befassen wir uns mit der Frage, welche nennenswerten Punkte sich in der Zeitabhängigkeit der Konzentration der in der Reaktion teilnehmenden Substanzen melden. Es wurde schon darauf hingewiesen, daß die Zwischenprodukt-Konzetnration C jeweils gemäß einer Maximumkurve von der Zeit abhängig ist; der zu dem Maximum gehörende ψ_m Wert laut (55) ist $\varkappa$ umgekehrt proportional. Es soll nun untersucht werden, wie sich

die Konzentrationen des Ausgangsmaterials A und des Endproduktes E in dieser Hinsicht gestalten.

Es kann gezeigt werden, daß im Fall von

$$\varkappa > \frac{2a_1^2}{a_2} = \varkappa_i \tag{92}$$

($\varkappa_i = 8$) die Kurve $A = A(t)$ eine Inflexion durchläuft (die Kurve ist S-förmig). Der zu dem Inflexionspunkt gehörende $\psi_{A_i}(t)$ Wert gestaltet sich folgendermaßen:

$$\psi_{A_i}(t) = \frac{\sqrt{(3a_1 + \varkappa)^2 + 4(a_2\varkappa - 2a_1^2)} - (3a_1 + \varkappa)}{2a_2\varkappa} \tag{93}$$

(Mit obiger Bezeichnung, $\psi_{A_i}(t)$, wollen wir andeuten, daß es sich um den zum Inflexionspunkt der Kurve $A = A(t)$ gehörenden ψ Wert handelt.)

Es lohnt sich darauf hinzuweisen, daß auch außer der bereits erwähnten Einschränkung (d.h. daß nur bei einem größerem $\varkappa$ als der in (92) eine Inflexion aufzufinden ist) die Abhängigkeit der Wendepunktlage (ψ_{A_i}) sowie des zu dem Inflexionspunkt gehörenden A_i Wertes von $\varkappa$ von Belang ist. Es kann gezeigt werden, daß $\psi_{A_i}(t)$ als Funktion von $\varkappa$ sich einer Maximumkurve entsprechend ändert; der zum Maximum gehörende $\varkappa$ Wert ($\varkappa_{i_m}$) ist wie folgt:

$$\varkappa_{i_m} = \frac{a_1^2[4a_2 + 6a_1 + \sqrt{(4a_2 + 6a_1)^2 + 2(a_2^2 + 3a_1a_2)}]}{a_2^2 + 3a_1a_2} \tag{94}$$

($\varkappa_{i_m} = 18{,}5321$). Bei diesem $\varkappa_{i_m}$ Wert erscheint ein Extremum in der $\varkappa$-Abhängigkeit sowohl von $\psi_{A_i}(t)$ als auch von A_i (der zur Inflexion gehörende Wert von A). In Abb. 15 wird die Maximumkurve der zur Inflexion der $A = A(t)$ Kurve gehörenden $\psi_{A_i}(t)$ Werte, in Abb. 16 hingegen die Minimumkurve der zur Inflexion gehörenden A_i Werte dargestellt.

Durch Vergleich der Abbildungen 2, 4 und 6 kann festgestellt werden, daß die Kurve der $A = A(t)$ Funktion in den drei dargestellten Fällen nur beim Parameterwert $\varkappa = 10$ (> 8) eine Inflexion durchläuft.

In Abb. 13 wurde außer den eingehend untersuchten drei Fällen (der $\varkappa$ Wert: 0,1; 1; 10) auch die zum Parameter $\varkappa = \varkappa_2$ gehörende Kurve dargestellt. Wie aus der Abbildung zu ersehen ist, durchläuft diese Kurve — im Gegensatz zu den anderen Fällen — eine Inflexion. Es kann gezeigt werden, daß die Funktion $\psi = \psi(A)$ nur im Wertevorrat

$$\varkappa_{i^*} = \frac{a_1^2}{a_2} < \varkappa < \varkappa_i = \frac{2a_1^2}{a_2} \tag{95}$$

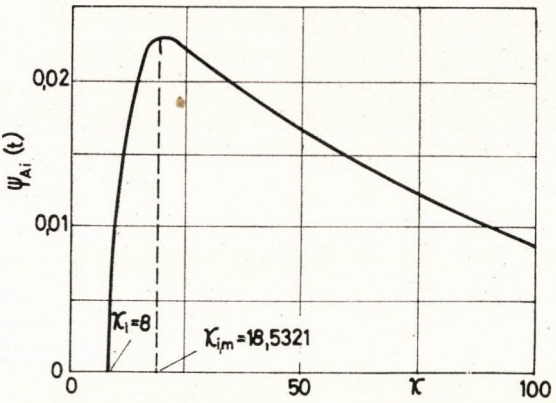


Abb. 15. Die zur Inflexion der $A = A(t)$ Kurve gehörenden ψ-Werte als Funktion von $\varkappa$

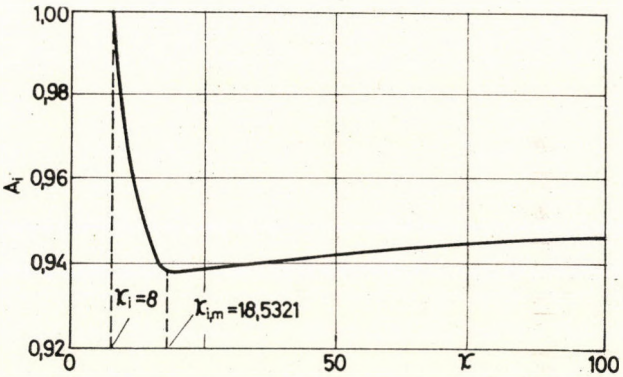


Abb. 16. Die zur Inflexion der $A = A(t)$ Kurve gehörenden A-Werte als Funktion von $\varkappa$

eine Inflexion haben kann ($\varkappa_{i*} = 4$, $\varkappa_i = 8$; letzteres stimmt mit dem laut (92) gewonnenen Wert überein). Der zum Inflexionspunkt gehörende $\psi_i(A)$ Wert gestaltet sich, vom $\varkappa$-Wert abhängig, folgendermaßen:

Im Falle von $\varkappa_{i*} < \varkappa < \varkappa_2$

$$\psi_i(A) = \frac{a_2\varkappa - a_1^2}{a_2\varkappa\,(a_1 + \varkappa)} \tag{96}$$

Im Falle von $\varkappa = \varkappa_2$

$$\psi_i(A) = \frac{\varkappa - 3a_1}{4a_2\varkappa} \tag{97}$$

Im Falle von $\varkappa_2 < \varkappa < \varkappa_i$

$$\psi_i(A) = \frac{\varkappa - 3a_1 - \sqrt{\Delta}}{4a_2\varkappa} \tag{98}$$

(Mit obiger Bezeichnung, $\psi_i(A)$, wollen wir darauf hinweisen, daß es sich um die zum Inflexionspunkt der Funktion $\psi = \psi(A)$ gehörenden ψ Werte handelt.)

Weiters kann auch festgestellt werden, daß $\psi_i(A)$, als Funktion von $\varkappa$, sich einer Maximumkurve entsprechend ändert: der zum Maximum gehörende $\varkappa$ Wert ist eben $\varkappa_2$. In Abb. 17 werden die Werte von $\psi_i(A)$ in Abhängigkeit von $\varkappa$ dargestellt.

Es sei hiermit, sowie im Zusammenhang mit Abb. 13, darauf hingewiesen, daß $\varkappa_2$ jener kleinste $\varkappa$-Wert ist, wo der Wert von ψ am Ende der Reaktion

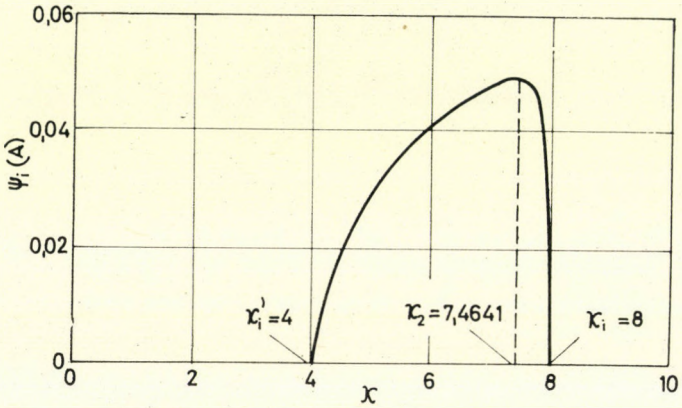


Abb. 17. Die zur Inflexion der $\psi = \psi(A)$ Kurve gehörenden ψ-Werte als Funktion von $\varkappa$

begrenzt ist. Dies bedeutet gleichzeitig, daß — wie auch aus Abb. 14 zu ersehen ist — der Wert von C_∞ zuerst bei $\varkappa_2$ gleich Null wird.

Die Konzentration des Endproduktes E ändert sich als Funktion der Zeit, unabhängig vom Wert von $\varkappa$, gemäß einer S-Kurve. Der zur Inflexion gehörende $\psi_{E_i}(t)$ Wert wird zu

$$\psi_{Ei}(t) = \frac{\sqrt{(a_1+\varkappa)^2 + 4a_2\varkappa} - (a_1+\varkappa)}{2a_2\varkappa} \tag{99}$$

(Mit obiger Bezeichnung, $\psi_{E_i}(t)$, wollen wir darauf hinweisen, daß es sich um den zum Inflexionspunkt der $E = E(t)$ Kurve gehörenden ψ Wert handelt.)

Es sei hier bemerkt, daß die $E = E(A)$ Kurve bei keinem $\varkappa$-Wert eine Inflexion aufweist (s. Abb. 9).

Zuletzt wollen wir noch auf eine interessante $\varkappa$-Abhängigkeit hinweisen. In den in Punkt 3.1 und 3.5 behandelten Fällen, also im Falle von $0 < \varkappa < \varkappa_1$, bzw. $\varkappa_2 < \varkappa < \infty$, waren unsere Lösungsfunktionen mit Hilfe des in (44) definierten Parameters p zu gewinnen. Der Wert dieses Parameters ist im Falle von $\varkappa = 0$ und $\varkappa = \infty$: $p = 1$, im Falle von $\varkappa_1$ und $\varkappa_2$ hingegen: $p = -\infty$, bei $\varkappa_1 < \varkappa < \varkappa_2$ Werten jedoch ist er nicht zu interpretieren. Es gibt zwei

solche $\varkappa$ Werte, wo $p = 0$ ist; diese sind die folgenden:

$$\varkappa_{p_1,p_2} = \frac{(5a_1 + 9a_2) \mp \sqrt{(5a_1 + 9a_2)^2 - 16a_1^2}}{4} \tag{100}$$

In Abb. 18 wird die Abhängigkeit des Parameters p von $\varkappa$ veranschaulicht ($\varkappa_{p_1} = 0{,}4416$, bzw. $\varkappa_{p_2} = 9{,}0584$).

Im Falle von $p = 0$ (dies gehört zu den speziellen $\varkappa$ Werten $\varkappa_{p_1}$ und $\varkappa_{p_2}$) wird, infolge der Vereinfachung der $A(\varrho)$ Funktion laut (45), auch das

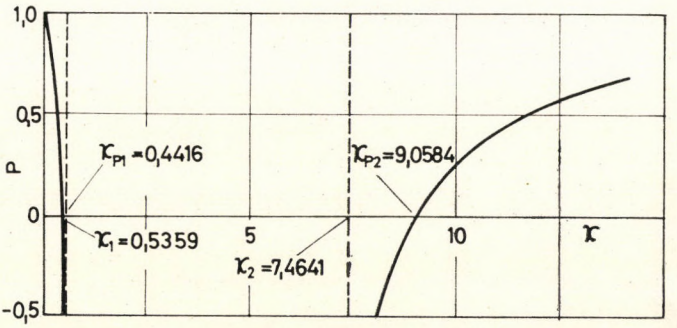


Abb. 18. Die Werte des Parameters p [s. (44)] in Abhängigkeit von $\varkappa$

Integral auf der rechten Seite von (49) vereinfacht und kann, anstatt (50), folgendermaßen aufgeschrieben werden:

$$\int \varrho^{-1} (1 - \varrho)^{-1} \, d\varrho = \ln \frac{\varrho}{1 - \varrho} \tag{101}$$

Somit, weiters durch Anwendung von (43), gewinnen wir anstatt (51) die einfache Zeitabhängigkeit:

$$\theta = \frac{1}{\delta_1 \sqrt{a_2 \varkappa}} \ln \left(1 - \frac{\psi}{\psi_2}\right) \tag{102}$$

Dieses Ergebnis bezieht sich auf den Fall $0 < \varkappa < \varkappa_1$; im Falle von $\varkappa_2 < \varkappa < \infty$ gestaltet sich die Zeitabhängigkeit anstatt (90) folgendermaßen:

$$\theta = \frac{1}{\delta_1 \sqrt{a_2 \varkappa}} \left[\frac{\psi_2 - \psi_1}{\psi_1} \frac{\psi}{\psi_1 - \psi} - \ln \left(1 - \frac{\psi}{\psi_2}\right) \right] \tag{103}$$

Die Untersuchung der Grenzwerte ($t \to \infty$) von (102) und (103) liefert richtige Ergebnisse, nämlich:
im Falle von $0 < \varkappa < \varkappa_1$ ($\lim_{t \to \infty} \psi = \infty$ und $\psi_2 < 0$)

$$\lim_{t \to \infty} \ln \left(1 - \frac{\psi}{\psi_2}\right) = \infty \tag{104}$$

im Falle von $\varkappa_2 < \varkappa < \infty$ $(\lim_{t\to\infty} \psi = \psi_1$ und $\psi_2 > \psi_1)$

$$\lim_{\psi\to\psi_1}\left[\frac{\psi_2-\psi_1}{\psi_1}\,\frac{\psi}{\psi_1-\psi} - \ln\left(1-\frac{\psi}{\psi_2}\right)\right] = \infty \qquad (105)$$

Leider sind die einfachen Zeitfunktionen laut (102) und (103) von geringer Bedeutung, wegen des zu ihnen gehörenden speziellen $\varkappa$ Wertes.

Auf Grund der obigen Ausführungen kann festgestellt werden, daß bezüglich des untersuchten konkurrenten Folgereaktionssystems zahlreiche $\varkappa$ Werte eine ausgezeichnete Rolle inne haben. Unsere Tabelle faßt unsere diesbezüglichen Feststellungen zusammen.

$\varkappa = \frac{k_2}{k_1}$	Bemerkungen
$\varkappa = 0$	nur die erste Reaktion läuft, keine Konsekution
$\varkappa_{p_1} = 0{,}4416$	eine Möglichkeit des $p = 0$ Spezialfalles; die Zeitabhängigkeit kann mit einfachen Funktionen angegeben werden
$\varkappa_1 = 0{,}5359$	Grenze zwischen den Gültigkeitsbereichen von zweierlei Lösungsfunktionen; die Zeitabhängigkeit kann im Falle von $\varkappa$-Werten kleiner als $\varkappa_1$ mit Hilfe der unvollständigen Beta-Funktion, bei $\varkappa_1$ mit Hilfe der Integral-Exponentialfunktion, im Falle von $\varkappa$-Werten größer als $\varkappa_1$ hingegen mit Hilfe einer speziellen Potenzreihe angegeben werden
$\varkappa_{i*} = 4$	die $\psi(A)$ Funktion hat nur im Falle von $\varkappa > \varkappa_{i*}$ eine Inflexion
$\varkappa_2 = 7{,}4641$	die Rolle von $\varkappa_2$ ist [illegible] von $\varkappa_1$ analog, andererseits ist die Zwischenprodukt-Konzentration am Ende der Reaktion (C_∞) nur im Falle von $\varkappa = \varkappa_2$ gleich Null, bzw. ist der Grenzwert (ψ_∞) des Quotienten C/A begrenzt; bei diesem $\varkappa$-Wert ist der Wert von $\psi_i(A)$ maximal
$\varkappa_i = 8$	die Funktion $\psi(A)$ hat nur im Falle von $\varkappa < \varkappa_i$, die Funktion $A(t)$ nur im Falle von $\varkappa > \varkappa_i$ eine Inflexion
$\varkappa_{p_2} = 9{,}0584$	seine Rolle ist jener von $\varkappa_{p_1}$ analog
$\varkappa_{i_m} = 18{,}5321$	bei diesem $\varkappa$-Wert ist der Wert von $\psi_{A_i}(t)$ maximal, der von A_i minimal
$\varkappa = \infty$	nur die zweite Reaktion läuft, keine Konsekution

LITERATUR

1. KELEN, T.: Kinetische Analyse einiger Folgereaktionen, I. Das System A + B → C, C + D → E. Z. phys. Chem. (Neue Folge) **58**, 268 (1968)
2. KELEN, T.: Kinetische Analyse einiger Folgereaktionen II. Die Systeme A + B → C, C → E und A + B →C, C + C → E. Z. phys. Chem. (Neue Folge) **60**, 191 (1968)
3. BENSON, S. W.: The Foundations of Chemical Kinetics. McGraw-Hill Book Co., Inc., New York—Toronto—London, 1960
4. BENSON, S. W.: J. Chem. Phys. **20**, 1605 (1952)
5. FROST, A. A., PEARSON, R. G.: Kinetics and Mechanism. John Wiley et Sons, Inc., New York 1953

6. FROST, A. A., SCHWEMER, W. C.: J. Am. Chem. Soc. **74**, 1268 (1952)
7. BATEMAN, H., ERDÉLYI, A.: Higher Transcendental Functions, Vol. I, McGraw-Hill Book Co., Inc., New York—Toronto—London, 1953
8. JAHNKE, R., EMDE, F.: Tafeln höherer Funktionen. B. G. Teubner Verlagsgesellschaft, Leipzig, 1952
9. GRADSTEIN, I. S., RÜSIK, I. M.: Tablizü Integralov, Sum, Rjadov i Proisvedjenij. Gos. Isd. Phys. Mat. Lit., Moskau, 1963

Tibor KELEN
Ferenc TÜDŐS
Budapest, II. Pusztaszeri út 57—69

Acta Chimica Academiae Scientiarum Hungaricae, Tomus 59 (3—4), pp. 351—358 (1969)

STUDY OF THE MOLECULAR STRUCTURE OF THIONYL CHLORIDE BY THE ELECTRON DIFFRACTION SECTOR MICROPHOTOMETER METHOD

I. HARGITTAI

(Research Laboratory for Chemical Structures of the Hungarian Academy of Sciences, Budapest)

Received March 14, 1968

The molecular structure of $SOCl_2$ was studied by the sector microphotometer electron diffraction method. Using a least-squares refinement, the following bond lengths and angles were determined: r(S—O) 1.444 ± 0.007 Å, r(S—Cl) 2.076 ± 0.006 Å, OSCl 107.3 ± 0.6° and ClSCl 96.2 ± 1.0°. Comparing the results of this investigation and those of [2] and other data, it was found that (1) tetravalent sulphur bonds are longer than the corresponding hexavalent sulphur bonds; (2) the S—O bonds are longer in compounds where chlorine atoms are substituted by CH_3 or $(CH_3)_2N$ groups both in the case of tetravalent and hexavalent sulphur.

Introduction

In the present paper the results of the molecular structure study of $SOCl_2$ by the electron diffraction sector microphotometer method are reported.*

The study of sulphur stereochemistry requires precise determination of the geometric parameters of the most simple sulphur compounds. The molecular structure of a series of sulphur compounds was studied by visual method of electron diffraction by PALMER thirty years ago [1]. In our previous work the geometric parameters of the SO_2Cl_2 molecule were re-determined [2]. The present work completes the re-investigation of the simple compounds containing sulphur-chlorine bonds, as HIROTA [3] and MORINO *et al.* [4] have dealt with the cases of S_2Cl_2 and SCl_2.

Method

The thionyl chloride used was previously distilled from linseed oil.**

As in the case of sulphuryl chloride, the electron diffraction pattern from $SOCl_2$ vapour was recorded on an apparatus developed from a Zeiss EF electron-optical unit in the Research Laboratory for Chemical Structures of the Hungarian Academy of Sciences [6]. An accelerating voltage of about

* Note added in proof: A report about the further refinement of the electron diffraction data on $SOCl_2$ and SO_2Cl_2 vapours is in the press.

** Kindly supplied by the courtesy of Mrs. E. H. VARGA (Research Institute for Experimental Medicine of the Hungarian Academy of Sciences).

Table I

sM(s) values of curve M (Fig. 2)

s, Å^{-1}	$sM(s)$	s, Å^{-1}	$sM(s)$	s, Å^{-1}	$sM(s)$
3.6	—0.009	11.0	—0.156	18.4	0.175
3.8	—0.030	11.2	—0.201	18.6	0.199
4.0	—0.011	11.4	—0.233	18.8	0.198
4.2	0.047	11.6	—0.229	19.0	0.173
4.4	0.100	11.8	—0.207	19.2	0.127
4.6	0.110	12.0	—0.158	19,4	0.077
4.8	0.085	12.2	—0.091	19.6	0.016
5.0	0.021	12.4	0.008	19.8	—0.051
5.2	—0.049	12.6	0.070	20.0	—0.082
5.4	—0.098	12.8	0.130	20.2	—0.103
5.6	—0.116	13.0	0.160	20.4	—0.110
5.8	—0.094	13.2	0.160	20.6	—0.111
6.0	—0.026	13.4	0.103	20.8	—0.095
6.2	0.043	13.6	0.057	21.0	—0.065
6.4	0.120	13.8	0.008	21.2	—0.031
6.6	0.177	14.0	—0.032	21.4	0.006
6.8	0.181	14.2	—0.066	21.6	0.037
7.0	0.153	14.4	—0.089	21.8	0.070
7.2	0.083	14.6	—0.087	22.0	0.102
7.4	0.023	14.8	—0.063	22.2	0.110
7.6	—0.095	15.0	—0.036	22.4	0.115
7.8	—0.190	15.2	0.008	22.6	0.089
8.0	—0.259	15.4	0.058	22.8	0.073
8.2	—0.283	15.6	0.104	23.0	0.030
8.4	—0.255	15.8	0.111	23.2	—0.006
8.6	—0.182	16.0	0.105	23.4	—0.051
8.8	—0.091	16.2	0.073	23.6	—0.065
9.0	—0.003	16.4	0.030	23.8	—0.065
9.2	0.078	16.6	—0.016	24.0	—0.042
9.4	0.152	16.8	—0.075	24.2	—0.010
9.6	0.203	17.0	—0.117	24.4	0.039
9.8	0.206	17.2	—0.150	24.6	0.064
10,0	0.174	17.4	—0.132	24.8	0.086
10.2	0.118	17.6	—0.081	25.0	0.086
10.4	0.062	17.8	0.000	25.2	0.076
10.6	—0.020	18.0	0.078	25.4	0.029
10.8	—0.097	18.2	0.123		

50 kV and an r^3 sector ($r_0 = 55$ mm) were used, and the two distances applied between the nozzle and photographic plate were about 285 and 230 mm. Three plates were chosen for further evaluation. Traces of the optical density of the diffraction pattern were obtained using a Zeiss GIII fast photometer equipped by a mechanism oscillating the plates [7].

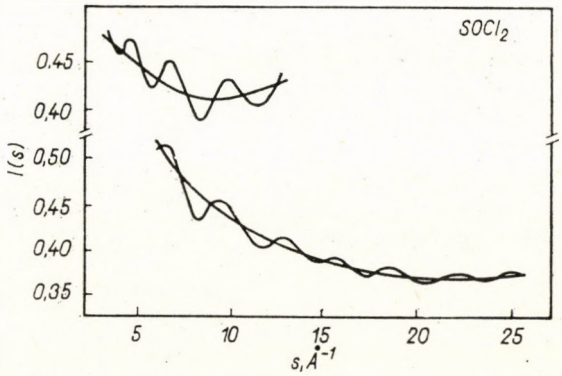


Fig. 1. Total intensities and the background lines

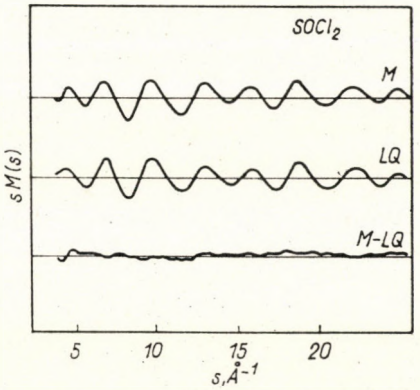


Fig. 2. $sM(s)$ molecular intensity curves. M — experimental; LQ — from the least-squares refinement

The total intensities are shown in Fig. 1. The background line was drawn in arbitrarily trying to follow the trend of the oscillating curve and to get a possibly "smooth" line. Background lines differing from those of Fig. 1 were tried, but in these cases slight increase of the error wave was observed in the inner part of the experimental $f(r)$ radial distribution curve.

The upper curve (M) of Fig. 2 is the experimental $sM(s)$ molecular intensity curve (Table I). Its Fourier-transforms obtained by different extrapolations are shown in Fig. 3. In obtaining curve $F1$ $sM(s) = 0$ values

were used in the interval of $s = 0.0$ to 3.4 Å^{-1}. The position of the maxima on curve *F 1* served as a model for calculating $sM(s)$ values used for extrapolation in a new Fourier transformation, which resulted curve *F 2* (Fig. 3). It should be mentioned that using the $sM(s)$ values calculated for a model corresponding to PALMER's data [1] in the interval $s = 0.0$ to 6.2 Å^{-1}, a further maximum appears at about $r = 3.5$ Å on the corresponding $f(r)$ curve (*F2P*, Fig. 3). This observation emphasizes the importance of examining the effect which the extrapolation has on the position of the maxima on the $f(r)$ curve.

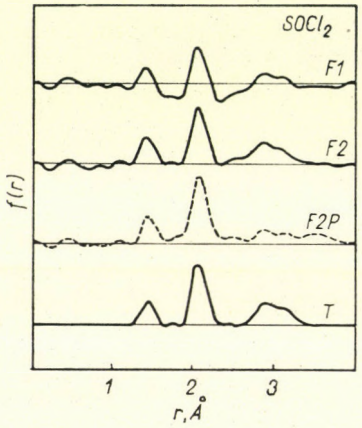


Fig. 3. $f(r)$ radial distribution curves
F 1, *F* 2, *F2P* — calculated from M using different extrapolations (see in text); *T* — calculated from the final results

Structural analysis and results

On the experimental $f(r)$ curve (*F* 2, Fig. 3) the maxima $r = 1.45_4$ Å and 2.07_5 Å were found, corresponding to the internuclear distances r(S—O) and r(S—Cl), respectively. The third compound maximum corresponds to the internuclear distances r(O...Cl) and r(Cl...Cl). Considering other data on the geometric configuration of tetravalent sulphur, *e.g.* the molecular structure of $SO(CH_3)_2$, it was assumed that r(O...Cl) is smaller than r(Cl...Cl). Correspondingly, the trial structure (Table II) was used for setting up the input data for the least-squares refinement. All internuclear distances and vibrational amplitudes were considered independent. The results of the least-squares refinement are shown in Table II. Final results including the scale error are shown in Table III. The uncertainty was determined as described previously [2]. Curve *LQ* of Fig. 2 was obtained as a result of the least-squares refinement. Curve *T* of Fig. 3 was calculated using final results (see Table III).

Discussion

Some sulphur-oxygen bond lengths are shown in Table IV. Their difference in sulphuryl chloride and thionyl chloride is in good agreement with the phenomenon observed earlier [20] that bonds of tetravalent sulphur are generally longer by some hundredths of an Å than the corresponding bonds of hexavalent sulphur.

According to data of Table IV, the S—O distance in SOF_2 is shorter by about 0.03 Å than that in $SOCl_2$, while there is no significant difference between the S—O distances in SO_2F_2 and SO_2Cl_2. The difference between the S—O distances in SO_2F_2 and SOF_2 is much less than in other cases.

CRUICKSHANK calls attention [21] to the shortening of the S—O bond in SO_2F_2 compared with sulphones, R_2SO_2, where R is a hydrocarbon residue.

A similar shortening of the S—O bond can be observed in sulphuryl chloride compared with $SO_2(CH_3)_2$ (vapour) and $SO_2ClN(CH_3)_2$ (vapour) and $SO_2[N(CH_3)_2]_2$ (crystal). Unfortunately, there is relatively great uncertainty

Table II

Results of the least-squares refinement

Trial structure		Results
r(S—O)	1.454	1.4438 ± 0.0045
r(S—Cl)	2.075	2.0758 ± 0.0021
r(O . . . Cl)	2.87	2.8601 ± 0.0101
r(Cl . . . Cl)	3.10	3.0914 ± 0.0140
l(S—O)	0.04	0.0305 ± 0.0092
l(S—Cl)	0.05	0.0524 ± 0.0036
l(O . . . Cl)	0.10	0.0753 ± 0.0084
l(Cl . . . Cl)	0.10	0.1020 ± 0.0117

Table III

Final results

	r_a Å	l, Å	Angles
S—O	1.444 ± 0.007	0.031 ± 0.010	
S—Cl	2.076 ± 0.006	0.052 ± 0.004	
O . . . Cl	2.860 ± 0.010	0.075 ± 0.008	
Cl . . . Cl	3.091 ± 0.014	0.102 ± 0.012	
OSCl			107.3 ± 0.6°
ClSCl			96.2 ± 1.0°

Table IV

Comparison of sulphur-oxygen bond lengths

	S(VI)—O, Å	Method*	Ref.		S(IV)—O, Å	Method	Ref.
$SO_2(NH_2)_2$	1.40 ± 0.01	XD	[8]				
SO_2F_2	1.405 ± 0.003	MW	[9]	SOF_2	1.412 ± 0.001	MW	[10]
$(NSOCl)_3$	1.407 ± 0.007	XD	[11]				
SO_2Cl_2	1.409 ± 0.005	SMED	[2]	$SOCl_2$	1.444 ± 0.007	SMED	see in text
$SO_2(CH_3)_2$	1.43 ± 0.02	VED	[12]	$SO(CH_3)_2$	1.47 ± 0.04	VED	[13]
	1.44 ± 0.03	VED	[12]		1.477	MW	[5]
					1.531 ± 0.005	XD	[14]
$SO_2ClN(CH_3)_2$	1.43_8 ± 0.01	SMED	[15]				
$SO_2[N(CH_3)_2]_2$	1.445 ± 0.005	XD	[16]	$SO[N(CH_3)_2]_2$	1.48	SMED	[17]
SO_2ClCCl_3	1.45 ± 0.01	SMED	[18]				
				$C_6H_4-(SO)_2-C_6H_4$	1.476 ± 0.016	XD	[19]

* XD — X-ray diffraction; MW — Microwave spectroscopy; VED — Visual method of electron diffraction; SMED — Sector microphotometer method of electron diffraction.

of the S—O distance value in $SO_2(CH_3)_2$, for it was studied by the visual method of electron diffraction. There is a remarkable difference between the S—O distances in $SO_2(NH_2)_2$ and $SO_2[N(CH_3)_2]_2$ crystals, while there is no significant difference between their S—N distances (1.61 Å [8] and 1.623 Å [16], respectively).

When the chlorine atoms in sulphuryl chloride are replaced by CH_3 or $(CH_3)_2$ N groups, the S—O distance increases by about 0.03 Å. It is therefore reasonable to expect the same effect in the case of tetravalent sulphur. Indeed, the S—O distance is shorter by 0.03 Å in thionyl chloride than in the molecules where the chlorine is substituted by CH_3 or $(CH_3)_2N$ groups (see data for $SO(CH_3)_2$ and $SO[N(CH_3)_2]_2$). The increase is much larger in $SO(CH_3)_2$ crsytal.

A similar effect can be observed if the P—O distances are compared in $POCl_3$ (1.43 Å) [22] and $PO(CH_3)_3$ (1.48 Å) [23].

The above mentioned S—O and P—O distances are much shorter than the calculated single bonds. According to CRUICKSHANK [21], the reason for this difference is the $d_\pi - p_\pi$ interaction between sulphur or phosphorus and oxygen.

The significant difference of 0.065 Å between the S—Cl distances in SO_2Cl_2 and $SOCl_2$ corresponds to the generally observed difference between the bonds of hexavalent and tetravalent sulphur. There is an even greater difference between the S—Cl distances in sulphur-nitrogen ring compounds, $(NSCl)_3$ [24] and $(NSOCl)_3$ [11].

The bond angles OSCl and ClSCl (Table III) are almost equal to the analogous angles in $SO(CH_3)_2$ gas molecules (OSC 106° 43′ and SCS 96° 23′) [5] and $SO(CH_3)_2$ crystal (OSC 106.7 ± 0.4° and CSC 97.4±0.4°) [14].

*

The author expresses his grateful thanks to Prof. S. LENGYEL and Dr. L. V. VILKOV for their assistance and the detailed discussion of the results. His thanks are also due to mathematicians Mr. J. GERGELY and Mr. G. KOSZÓ, workshop foreman Mr. J. HERNÁDI, mechanician Mr. L. HAKLIK and laboratory assistant Mrs. P. SZILÁGYI for their valuable contribution throughout the course of this work.

REFERENCES

1. PALMER, K. J.: J. Am. Chem. Soc. **60,** 2360 (1938)
2. HARGITTAI, I.: Acta Chim. Acad. Sci. Hung. **57,** 403 (1968)
3. HIROTA, E.: Bul. Chem. Soc. Japan **31,** 130 (1958)
4. MORINO, Y., MURATA, Y., ITO, T., NAKAMURA, J.: J. Phys. Soc. Japan **17,** Suppl. B—II, 37 (1962)
5. DREIZLER, H., DENDL, G.: Z. Naturforsch. **19a,** 512 (1964)
6. HARGITTAI, I., HERNÁDI, J., TREMMEL, J.: Jenaer Rundschau **13,** 3 (1968) Приборы и техника эксперимента 1968, 206
7. HARGITTAI, I., HERNÁDI, J.: Jenaer Rundschau (In the press)
8. TRUEBLOOD, K. N., MAYER, S. W.: Acta Cryst. **9,** 628 (1956)
9. LIDE, D. R., MANN, D. E., FRISTROM, R. M.: J. Chem. Phys. **26,** 734 (1957)

10. FERGUSON, R. C.: J. Am. Chem. Soc. **76,** 850 (1954)
11. HAZELL, A. C., WIEGERS, G. A., VOS, A.: Acta Cryst. **20,** 186 (1966)
12. Tables of Interatomic Distances and Configuration in Molecules and Ions. Sci. ed. Sutton, L. E., Spec. Publ. N11, London, 1958
13. BASTIANSEN, O., VIERVOLL, H.: Acta Chem. Scand. **2,** 702 (1948)
14. THOMAS, R., SHOEMAKER, C. B., ERIKS, K.: Acta Cryst. **21,** 12 (1966)
15. VILKOV, L. V., HARGITTAI, I.: Acta Chim. Acad. Sci. Hung. **52,** 423 (1967)
16. JORDAN, T., SMITH, H. W., LOHR, L. L., Jr. LIPSCOMB, W. N.: J. Am. Chem. Soc. **85,** 846 (1963)
17. HARGITTAI, I., VILKOV, L. V.: Acta Chim. Acad. Sci. Hung. (In the press)
18. Алексеев, Н. В.: Ж. структ. химии, **8,** 532 (1967)
19. HOSOYA, S.: Acta Cryst. **21,** 21 (1966)
20. TRUTER, M. R.: J. Chem. Soc. **1962,** 3400
21. CRUICKSHANK, D. W. J.: J. Chem. Soc. **1961,** 5486
22. Вилков, Л. В., Хайкин, Л. С.: Ж. структ. химии (In the press)
23. WANG, H. K.: Acta Chem. Scand. **19,** 879 (1965)
24. WIEGERS, G. A., VOS, A.: Acta Cryst. **20,** 192 (1966)

István HARGITTAI: Budapest VIII. Puskin u. 11—13

Acta Chimica Academiae Scientiarum Hungaricae, Tomus 59 (3—4), pp. 359—371 (1969)

PALLADIZED Pd-WIRE AS A HYDROGENATION CATALYST, I

RATE AND MECHANISM OF HYDROGEN TRANSPORT

F. NAGY, S. SZABÓ and I. TELCS

(Central Research Institute for Chemistry of the Hungarian Academy of Sciences)

Received December 23, 1967

Investigation of the rate of hydrogen transport from a Pd-wire initially saturated with hydrogen led to the following results:

1. Between the relative resistance (R/R_0) of the wire and the hydrogen content there exists an unambiguous linear relationship in the interval $0.08 \leq \mathrm{H/Pd} \leq 0.45$.

2. The rate of hydrogen transport from a smooth Pd-wire at 20—25° C is approximately given by Equation

$$W_M \equiv \frac{d(\mathrm{H/Pd})}{d\tau} \approx \frac{d(\Delta R/R_0)}{d\tau} \approx \frac{3.9 \cdot 10^{-5}}{d^2} (\mathrm{H/Pd}) \approx \frac{3.9 \cdot 10^{-5}}{d^2} (\Delta R/R_0)\ \mathrm{min}^{-1}$$

where d is the diameter in cm.

3. The change of $\Delta R/R_0$ with time of palladized Pd-wire can be used to determine the reaction rate W in acid aqueous solution if $W_M \geq 10\ W$.

4. In solutions containing capillary active components — in contrast with acid aqueous solutions — there has also to be considered in the case of palladized Pd-wire the rate (W_5) of hydrogen transport between wire and Pd-black particles. Correspondingly the change of $\Delta R/R_0$ with time is suited for measurements of reaction rates only if $W_M,\ W_5 \geq 10$.

It was established earlier that in hydrogenation reactions carried out in aqueous solutions on metal (Pt, Pd and Ni) catalysts, the rate determining step is in most of the cases the diffusion of hydrogen dissolved in the water to the catalyst surface [1]. Thus the true kinetics of the chemical reaction proper cannot be obtained from measurements of the rate of hydrogen consumption. As Pd dissolves considerable amounts of hydrogen, there appears a possibility of carrying out hydrogenation on palladium catalysts by hydrogen dissolved in the metal. This procedure is suited to kinetic studies if

a) the amount of hydrogen dissolved in Pd can be measured continuously during the reaction,

b) hydrogen transport is not rate determining.

As to point *a)* recourse can be taken to published results stating that the resistance of a Pd-wire changes almost linearly with the atomic ratio H/Pd. This relation is represented by Fig. 1 taken from literature [2]. As may be seen from the figure, best suited for the present purpose is the range of ratios H/Pd between 0.08 and 0.45, *i.e.* $1.08 < R/R_0 < 1.45$, where R_0 is the resistance of the wire free of hydrogen and R the resistance of the wire of

given hydrogen contents. In the region of higher ratios of H/Pd there appears a hysteresis, in the lowest region a departure from linearity occurs.

As to *b)* there are published no unambiguous data and it was therefore decided to establish the rate law of hydrogen transport in the range mentioned of $0.08 < \mathrm{H/Pd} < 0.45$ and to determine the parameters on which this rate law depends.

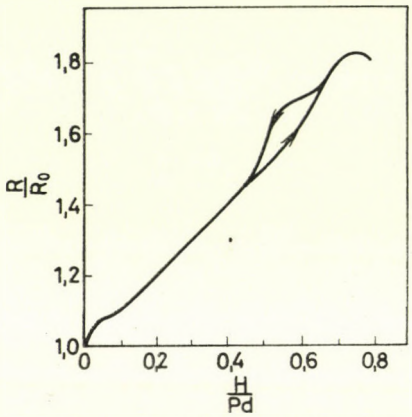


Fig. 1. Change of relative resistance of Pd-wire (R/R_0) with the hydrogen content (H/Pd)

In interpreting the rate law thus obtained there arises, of course, the question of mechanism, *i.e.* the individual steps of hydrogen transport.

In the present paper results pertaining to the above questions are treated.

A. Kinetics of hydrogen transport

In the experiments smooth or palladized wire of length $l = 6-8$ cm and 50—300 μ in diameter was used, welded to Pt-contacts. The wire thus prepared was placed in a conventional cell containing a $2M$ H_2SO_4 solution. The arrangement allowed cathodic and anodic polarization, that is charging with and stripping of hydrogen of the Pd-wire and measuring of the electrode potential (E) of the wire as referred to a hydrogen electrode in the same solution under a pressure of 1 atm. Resistance of the wire was measured in a Wheatstone bridge arrangement by taking the wire from the cell, rinsing with distilled water and placing it in doubly distilled water flushed with N_2 before measurements in order to avoid errors arising from the conductivity of the solution. (As turned out later, errors from this source are practically negligible so that they were neglected subsequently.) On the other hand a determination of the resistance during polarization would not be practical as the H/Pd—R/R_0 relations apply to equilibrium conditions only.

The first series of measurements (Table I, column A_1) was carried out with a smooth Pd-wire by subjecting the wire, initially saturated with hydrogen, to anodic polarization of varying intensity (i) for equal periods and determining the resistance of the wire in the way described. As may be seen from the table, the potential during polarization with the given current densities (I) reaches the potential of O_2 evolution. Part of the polarizing current is thus consumed by the reaction $H_2O \rightarrow {}^1/_2\, O_2 + 2H^+ + 2e$. The rate of hydrogen transport, therefore, is lower than the rate equivalent to the applied current.

The simplest assumption concerning the rate (w) of hydrogen transport is the first order rate law

$$w \equiv -\frac{d(\mathrm{H/Pd})}{d\tau} = k(\mathrm{H/Pd}) \tag{1}$$

According to Fig. 1 in the range of H/Pd applied:

$$\mathrm{H/Pd} \approx \left(\frac{R}{R_0} - 1\right) \equiv \frac{\Delta R}{R_0} \tag{2}$$

From (1) and (2)

$$-\frac{d\left(\frac{\Delta R}{R_0}\right)}{\Delta\tau} = k\left(\frac{\Delta R}{R_0}\right) \tag{3}$$

which on integrating gives

$$\frac{\Delta R}{R_0} = \left(\frac{\Delta R}{R_0}\right)_0 e^{-k\tau} \tag{4}$$

As polarization was interrupted at given intervals, the above relation can only be applied to the given intervals, *i.e.*

$$\left(\frac{\Delta R}{R_0}\right)_1 = \left(\frac{\Delta R}{R_0}\right)_2 e^{k\Delta\tau} \tag{5}$$

Plotting the values of $(\Delta R/R_0)_1$ as a function of the values of $(\Delta R/R_0)_2$ a straight line going through the origin should be obtained if (1) is fulfilled. This is represented by Fig. 2 where the individual plots are shifted on the abscissa by 0.1 unit each (*cf.* column A_1 of Table I).

From the slopes of the curves of Fig. 2 k can be computed from Eq. (5):

$$k = 4.8 \cdot 10^{-2}\ \mathrm{min}^{-1} \tag{6}$$

Table I

Change of relative resistance ($\Delta R/R_0$) of hydrogen-containing Pd-wire in the course of anodic polarization

$T = 20 - 25$ °C; $E > 1500$ mV

Sign	A_1			A_2		A_3
d_μ	300			300		150
l cm	6.0			8.0		8.0
i mA	15	20	25	30		30
I mA · cm^{-2}	26.6	35.4	44.3	39.8		79.6
$\Delta\tau$ min	5			2	5	2
$\frac{\Delta R}{R_0}$	0.377 0.282 0.228 0.188 0.158 0.134 0.112 0.094 0.077 0.066	0.501 0.351 0.268 0.217 0.178 0.150 0.124 0.103 0.088 0.069	0.468 0.306 0.240 0.194 0.165 0.137 0.117 0.099 0.081 0.066	0.480 0.428 0.372 0.313 0.274 0.246 0.225 0.205 0.188 0.179 0.159 0.149 0.136 0.127 0.118 0.110 0.102 0.096 0.087 0.079	0.415 0.290 0.230 0.190 0.162 0.135 0.115 0.100 0.085 0.072 0.061	0.420 0.265 0.200 0.158 0.123 0.095 0.070
$e^{k\Delta\tau}$	1.27	1.25	1.27	1.10	1.25	1.35
k; min^{-1}	0.048			0.049	0.045	1.151

In order to verify Eq. (1) still further, the above measurements were repeated on a different wire. Results are shown in column A_2 of Table I and Fig. 3 (in the figure the second curve is shifted along the abscissa by 0.1 unit). The values of k calculated from Eq. (5) and Fig. 3 are

$$k = 4.9 \cdot 10^{-2}\,\text{min}^{-1} \text{ for } \Delta\tau = 2\,\text{min}\,,$$
$$k = 4.5 \cdot 10^{-2}\,\text{min}^{-1} \text{ for } \Delta\tau = 5\,\text{min}\,. \qquad (7)$$

Values (6) and (7) agree within the limits of error.

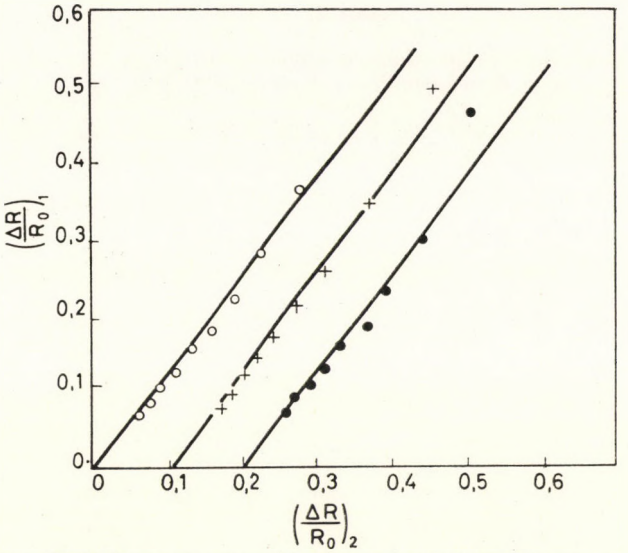


Fig. 2. Change of relative resistance of hydrogen-containing Pd-wire in the case of anodic polarization measured at equal time intervals. (Experimental series A_1 of Table I) ○: 15, +: 20, ●: 25 mA

It was investigated further whether the value of k depends on the diameter of the wire and whether hydrogen is extracted from the Pd-wire by electric current or a chemical oxidant. The corresponding results are quoted in column A_3 of Table I, columns B_1 and B_2 of Table II and Figs 4 and 5.

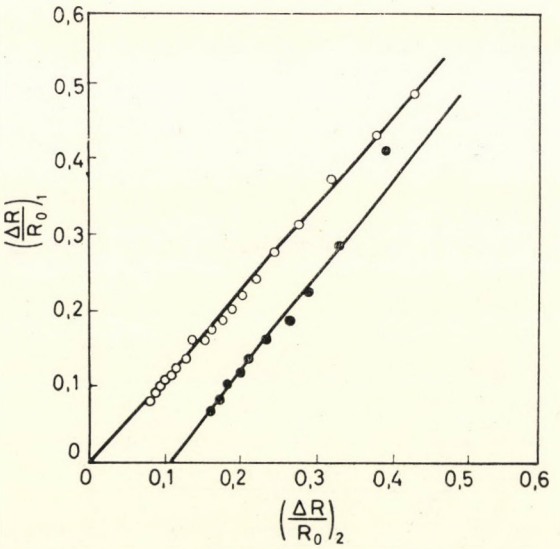


Fig. 3. Change of relative resistance of hydrogen-containing Pd-wire in the case of anodic polarization measured at equal time intervals. (Experimental series A_2 of Table I) ○: $\Delta\tau = 2$ min; ●: $\Delta\tau = 5$ min.

Table II

Change of relative resistance ($\Delta R/R_0$) of hydrogen-containing Pd-wire in H_2O_2
$t = 20—25°$ C; $E \rightarrow 750$ mV

	B_1	B_2
d_μ	150	300
l cm	8 cm	
$\Delta\tau$ min	2	5
$\frac{\Delta R}{R_0}$	0.325 0.220 0.160 0.115 0.081 0.054	0.380 0.275 0.210 0.165 0.130 0.100 0.083 0.064
$e^{k\Delta\tau}$	1.37	1.27
k; min^{-1}	0.156	0.048

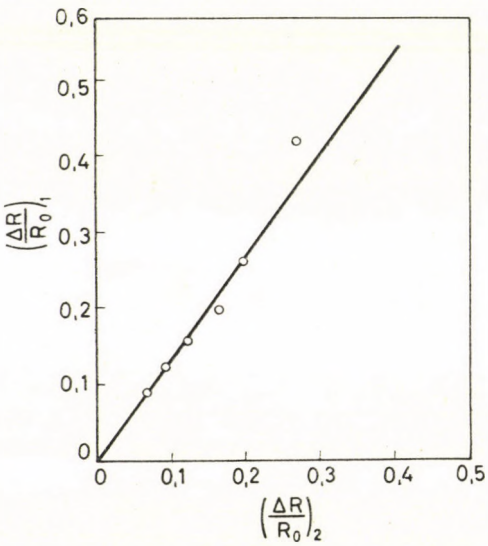


Fig. 4. Change of relative resistance of hydrogen-containing Pd-wire in the case of anodic polarization measured at equal time intervals. (Experiment A_3 of Table I)

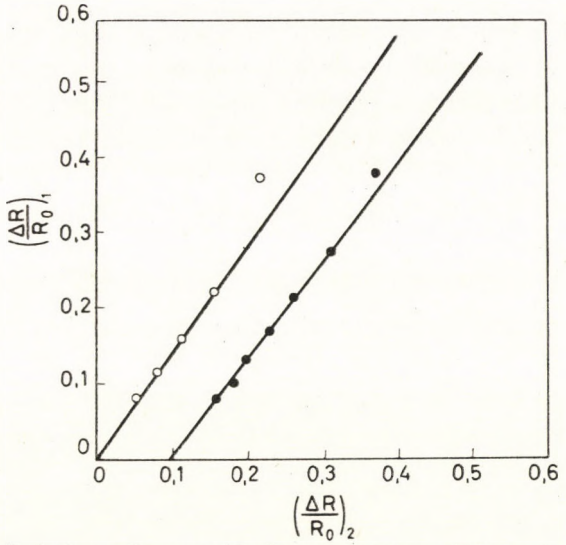


Fig. 5. Change of relative resistance of hydrogen-containing Pd-wire in sulphuric acid solution of H_2O_2. (Experiments B_1 and B_2 of Table II) ○ : $d = 150\ \mu$, $\Delta\tau = 2$ min. ●: $d = 300\ \mu$, $\Delta t = 5$ min

It is seen from the values of k in Tables I and II, that the rate of hydrogen transport depends on the diameter of the wire but does not depend on the fact whether hydrogen was eliminated by anodic polarization or chemical oxidation. It is evident, so far, that k increases with decreasing diameter of the wire. It was investigated therefore, whether the variation of k is correlated to the first or second power of the diameter. Calculations are demonstrated by Table III. The data of the table show that k is not strictly proportional to neither $1/d$ nor $1/d^2$, the latter being, however, the better fitting.

Table III

d μ	$\bar{k} \cdot 10^2$ min^{-1}	$\bar{k} \cdot d \cdot 10^4$ $\text{cm} \cdot \text{min}^{-1}$	$\bar{k} \cdot d^2 \cdot 10^6$ $\text{cm}^2 \cdot \text{min}^{-1}$	$\frac{\bar{k}d_{150}}{\bar{k}d_{300}}$	$\frac{\bar{k}d^2_{150}}{\bar{k}d^2_{300}}$	$k_H \cdot 10^5$ $\text{cm}^2 \cdot \text{min}^{-1}$
150	15.4	23.2	34.6	1.61	0.81	3.9
300	4.8	14.4	43.0			

On ground of the experimental results presented so far, the maximum rate (W_M) of hydrogen transport from the Pd-wire at 20—25 °C can approximately be expressed by the following rate equation bearing in mind Eq. (1):

$$W_M = \frac{k_H}{d^2}(\text{H/Pd}) \approx \frac{k_H}{d^2}(\Delta R/R_0)\ \text{min}^{-1} \qquad (8)$$

with $k_H = 3.9 \cdot 10^{-5}\ \text{cm}^2\text{min}^{-1}$

If it is wanted to express the maximum rate of hydrogen transport from a Pd-wire of length l and diameter d in mA (i_M), Eq. (8) is transformed as follows, taking into consideration the dimensions and density of the wire and and Faraday's law

$$i_M = k'_H l(\mathrm{H/Pd}) = k'_H l(\Delta R/R_0)\,\mathrm{mA} \tag{9}$$

with $k'_H = 5.3\ \mathrm{mAcm}^{-1}$.

B. Mechanism of hydrogen transport

The Pd-H system has been investigated by numerous authors [2]—[5]. The results of these investigations can be summarized as follows:

a) There exist two phases of Pd-H, the α phase (H/Pd) ≈ 0.03 and the β phase (H/Pd) ≈ 0.45.

b) On saturating a Pd-wire with hydrogen there can be distinguished three intervals accordingly:

I. $0 < (\mathrm{H/Pd}) \leq 0.03$; $1.00 < (R/R_0) \leq 1.06$
II. $0.03 < (\mathrm{H/Pd}) \leq 0.45$; $1.06 < (R/R_0) \leq 1.45$
III. $0.45 < (\mathrm{H/Pd})$; $1.45 < (R/R_0)$.

Interval I (the α-phase) is a solution of H in Pd.
Interval II is a mixture of phases α and β.
Interval III is a solution of H in phase β.

c) In these three intervals the electrode potential (E) of the Pd-H system shows characteristic differences.

In interval I	$E > 50-60$ mV
In interval II	$E \approx 50-60$ mV
In interval III	$E < 50-60$ mV.

In interval II there appears a hysteresis of the potential between 50 and 60 mV. On charging the wire, the equilibrium potential as referred to a hydrogen electrode of 1 atm, in the same electrolyte solution is 50 mV, on depleting the wire, the potential is 60 mV.

The experiments described in section A. were carried out in interval II, the condition $1.06 < (R/R_0) < 1.45$ prevailing according to Tables I and II. On extracting hydrogen from the Pd-wire by anodic polarization, therefore, the following elementary processes proceed:

$$\begin{aligned} &1.\ \ \mathrm{H}_\beta \rightarrow \mathrm{H}_\alpha + \mathrm{H}_{\alpha-s} \\ &2.\ \ (\mathrm{H}_{\alpha-s})_b \rightarrow (\mathrm{H}_{\alpha-s})_f \\ &3.\ \ (\mathrm{H}_{\alpha-s})_f \rightarrow (\mathrm{H})_a \\ &4.\ \ (\mathrm{H})_a \rightarrow \mathrm{H}^+ + e^- \end{aligned} \tag{10}$$

where indices α and β refer to the respective phases, index α–s refers to hydrogen dissolved in the α phase, b and f denote interior and surface, respectively, and a refers to the adsorbed state.

Process 1 is a phase transformation, Process 2 diffusion from the interior of the wire to the surface, Process 3 is migration of hydrogen from the Pd-H solution phase to the adsorption phase and Process 4 is the electrochemical oxidation of adsorbed hydrogen.

Process 4 cannot be rate controlling as its rate (W_4) is, according to the theory of ERDEY-GRÚZ and VOLMER

$$W_4 = d\pi l i_0 [H_a] e^{\frac{\alpha F}{RT} E} \tag{11}$$

where i_0 is the exchange current, $[H_a]$ the surface concentration of adsorbed hydrogen, $\alpha \approx {}^1/_2$ a constant, F the Faraday. At 25° C Eq. (11) can be expressed as

$$W_4 = d\pi l i_0 [H_a] 10^{\frac{E}{118}} \tag{12}$$

if E is given in mV.

As may be seen from (12), a change of E by 118 mV changes W_4 by an order of magnitude, all other factors being kept constant. According to Table I the same rate of depletion was obtained with current or H_2O_2 solution. The electrode potential was +1500 mV for current and +750 mV for H_2O_2. If Process 4 were rate determining, such a change in the potential would correspond to a change in the rate by 6—7 orders of magnitude. Thus rate control is reduced to steps 1, 2 and 3 of Eqs (10) .

Available experimental evidence does not permit a separation of steps 1—3 proceeding in the bulk of the Pd-wire. It can only be stated, therefore, that in the case of hydrogen depletion from smooth Pd-wire rate Eqs (8) or (9) describe the overall rate of steps 1, 2 and 3 of Eqs (10).

Smooth Pd-wire, therefore, can be used, for the investigation of contact catalytic hydrogenation reactions, if care is taken to keep the reaction rate lower by at least one order of magnitude than the limiting rate given by Eqs (8) or (9), respectively.

C. Palladized Pd-wire as hydrogenating catalyst

On smooth Pd-wire most hydrogenation reactions proceed at unmeasurably low rates. Increasing the surface of the Pd-wire by palladizing increases the rate of the catalytic reaction, too. If the amount of Pd-black deposited is negligible besides the mass of the wire — with the result that hydrogen dissolved in the Pd-black particles is far less than the amount in the interior

of the wire — the change of resistance with time can in principle still be used to determine reaction rates. The effect of palladization can — as a first approximation — be looked upon as an increase of the concentration of adsorbed hydrogen atoms as referred to the geometric surface of the wire. The reaction rate increases correspondingly. The amount of Pd-black evidently does not change the rate of hydrogen transport from the interior of the wire. The rate of the chemical reaction, however, increases proportionally with the amount of Pd-black, provided that the particle size is identic. Whether measurement of the resistance of the hydrogen-saturated Pd-wire can be used in the determination of reaction rate depends, therefore, besides the quality and concentration of the substrate also on the quantity of deposited Pd-black. If deposition of Pd-black really does not change the mechanism of hydrogen transport the statement must hold that Eqs (8) or (9), respectively, express the limiting rate and a reaction rate smaller by at least one order of magnitude must be insured. This can be achieved — as mentioned — by matching the degree of Pd-black deposition to the nature of the substrate.

Table IV represents the change of the resistance with time of differently palladized Pd-wire 50 μ in diameter, initially saturated with hydrogen and placed in a solution of acetylene-dicarboxylic acid in aqueous sulphuric acid. From the measured values the rates (W) of hydrogen depletion were calculated as quotients of differences and these rates correlated with the mean values of relative resistance of the intervals.

$$W \equiv \frac{\Delta\left(\frac{\Delta R}{R_0}\right)}{\Delta\tau}\,;\left(\frac{\overline{\Delta R}}{R_0}\right) \equiv \frac{\left(\frac{\Delta R}{R_0}\right)_1 + \left(\frac{\Delta R}{R_0}\right)_2}{2}\,. \tag{13}$$

The table also contains the quotient (W_M/W) of the maximal rate as given by Eq. (8).

$$W_M \equiv \frac{d(\Delta R/R_0)}{d\tau} = 1.56\,(\overline{\Delta R}/R_0) \tag{14}$$

and the actual rate.

The amount of deposited Pd-black increases from sample C_1 through C_5.

In previous investigations [1] it was shown, that the rate of hydrogenation of different substrates at Pt, Pd- and Ni-catalysts in aqueous solution is a function of the electrode potential. As mentioned before, the electrode potential of the system Pd/H under consideration lies between 50 and 60 mV. Correspondingly, a constant rate of hydrogenation, *i.e.*, according to Eq. (2), a constant value of W is to be expected if the change of concentration of the substrate is negligible and the chemical reaction is indeed rate controlling.

Table IV

Change of resistance of differently palladized Pd-wire in a 2% acetylene-dicarboxylic acid solution

$d = 50\,\mu$; $[H_2SO_4] = 2m$; $t = 20$—$25°$ C

C_1			C_2			C_3			C_4			C_5		
$\frac{\overline{\Delta R}}{R_0}$	$\frac{W}{\min^{-1}}$	$\frac{W_M}{W}$	$\frac{\overline{\Delta R}}{R_0}$	$\frac{W}{\min^{-1}}$	$\frac{W_M}{W}$	$\frac{\overline{\Delta R}}{R_0}$	$\frac{W}{\min^{-1}}$	$\frac{W_M}{W}$	$\frac{\overline{\Delta R}}{R_0}$	$\frac{W}{\min^{-1}}$	$\frac{W_M}{W}$	$\frac{\overline{\Delta R}}{R_0}$	$\frac{W}{\min^{-1}}$	$\frac{W_M}{W}$
0.460	0.020	35.8	0.437	0.050	13.6	0.427	0.055	12.1	0.400	0.060	10.4	0.348	0.432	1.3
0.420	0.020	32.7	0.412	0.050	12.9	0.375	0.050	11.7	0.362	0.090	6.3	0.194	0.184	1.6
0.380	0.020	29.7	0.382	0.035	17.0	0.327	0.045	11.3	0.312	0.110	4.4	0.119	0.114	1.6
0.340	0.020	26.5	0.347	0.035	15.5	0.277	0.055	7.9	0.257	0.110	3.6	0.073	0.070	1.6
0.300	0.020	23.4	0.312	0.035	13.9	0.220	0.060	5.7	0.207	0.090	3.6			
0.258	0.021	19.2	0.280	0.030	14.5	0.165	0.050	5.2	0.167	0.090	2.9			
0.216	0.021	16.0	0.245	0.040	9.6	0.117	0.045	4.1	0.132	0.070	2.9			
0.176	0.019	14.5	0.207	0.035	9.0	0.081	0.028	4.5	0.103	0.048	3.4			
0.137	0.020	10.7	0.172	0.035	7.7	0.054	0.025	3.3	0.081	0.040	3.2			
0.097	0.020	7.6	0.137	0.035	6.1				0.062	0.036	2.7			
0.059	0.019	4.7	0.102	0.035	4.6									
			0.067	0.035	3.0									

It is seen from Table IV that this is the situation in the case of the weakly palladized Pd-wires C_1 and C_2. The relation $W_M/W \geq 10$ therefore is an adequate criterion. In the case of the heavily palladized wires C_3, C_4 and especially C_5 the requirement $W_M/W \geq 10$ is fulfilled no more and the rate controlling effect of the hydrogen transport steps cannot be neglected any more. This is reflected by the result that W is not constant in these cases.

It is seen from the results shown that by moderate palladization a Pd-wire catalyst can be obtained, for which $W_M/W \geq 10$, so that hydrogen transport is not rate controlling, and thus the plot of $\Delta R/R_0$ *vs.* τ can be used to determine the rate of hydrogenation.

As mentioned before, the effect of palladization can be looked upon as a simple increase of the surface only as a first approximation. As it is, the Pd-particles on which the reaction proceeds only stick to the surface of the wire and to each other and the intervention of a new step, transport of hydrogen between the wire and the particles, should be expected. Scheme (10), therefore, should be extended by another relation regardless of the subsequent reaction of hydrogen:

$$H_\beta \xrightarrow{1,2,3} [(H)_a]_D \xrightarrow{5.} [(H)_a]_K \qquad (15)$$

where index D refers to the wire, index K to Pd-black particles and Step 5 represents transport between wire and particles.

Table V

Change of resistance of palladized Pd-wire in a 2% acetylene-dicarboxylic acid solution

$d = 50\,\mu$; $t = 20$—$25°$ C.
D_1: distilled water;
D_2: acetic acid in 0.1 N H_2SO_4;
D_3: *n*-propylic alcohol in 0.1 N H_2SO_4;
D_4: 10% acetic acid in 0.1 N H_2SO_4.

D_1			D_2			D_3			D_4		
$\frac{\Delta R}{R_0}$	$\frac{W}{\text{min}^{-1}}$	$\frac{W_M}{W}$	$\frac{\Delta R}{R_0}$	$\frac{W}{\text{min}^{-1}}$	$\frac{W_M}{W}$	$\frac{\Delta R}{R_0}$	$\frac{W}{\text{min}^{-1}}$	$\frac{W_M}{W}$	$\frac{\Delta R}{R_0}$	$\frac{W}{\text{min}^{-1}}$	$\frac{W_M}{W}$
0.334	0.057		0.412	0.024		0.470	0.075		0.407	0.022	
0.237	0.037		0.325	0.020		0.332	0.062		0.330	0.020	
0.175	0.025		0.255	0.015		0.227	0.042		0.292	0.017	
0.132	0.017	≈10	0.197	0.011	≈30	0.162	0.022	≈10	0.230	0.015	≈25
0.100	0.015		0.157	0.008		0.120	0.020		0.180	0.015	
0.074	0.011		0.132	0.006		0.089	0.012		0.155	0.010	
0.055	0.007		0.110	0.005		0.068	0.010		0.120	0.007	
			0.090	0.005					0.089	0.007	
			0.073	0.004							

The rate of Step 5 evidently depends on the contact between the wire surface and the individual particles and this is a function of the structure of the adsorption layer.

The change with time of the resistance of a palladized Pd-wire initially saturated with hydrogen under the effect of acetylene-dicarboxylic acid was therefore also investigated in solutions containing different additives. Results are shown in Table V.

It may be seen from Table V that in distilled water (D_1) W is not constant, although $W_M/W \approx 10$. The same holds for experiments D_2, D_3 and D_4. This shows that Step 5 indeed comes into play and thus $W_M/W \geq 10$ is no sufficient criterion for deciding, whether rate control by hydrogen transport can be neglected. Thus the rate of Step 5, too, has to be determined. As this is — as already mentioned — a function of the adsorption layer, a general investigation is of no avail and experimental determination has to be carried out for any given solution.

REFERENCES

1. NAGY, F.: MTA Kémiai Oszt. Közl. **25**, 237 (1966)
2. BARTON, J. C. and LEWIS, F. A.: Talanta. **10**, 237 (1963)
3. FLANAGAN, T. B. and LEWIS, F. A.: J. Electrochem. Soc. **108**, 473(1961) Z. Phys. Chem. N. F. **27**, 104 (1961)
4. KNOR, Z., POŇEC, V., ČERNI, C.: Kinetika i Kataliz **4**, 437 (1963)
5. BARTON, J. C., LEITCH, W. F. N. and LEWIS, F. A.: Trans. Far. Soc. **59**, 1208 (1963)

Ferenc NAGY
Sándor SZABÓ
Iván TELCS
Budapest II., Pusztaszeri út 57/69

Acta Chimica Academiae Scientiarum Hungaricae, Tomus 59 (3—4), pp. 373—378 (1969)

CONVERSIONS OF TOSYL AND MESYL DERIVATIVES OF THE MORPHINE GROUP, III*

PREPARATION OF AZIDO- AND AMINOCODIDES

R. BOGNÁR and S. MAKLEIT

(Institute of Organic Chemistry, L. Kossuth University, Debrecen)

Received February 5, 1968

The method of conversion of an alcoholic hydroxyl group into an amino group by means of tosylate (or mesylate) → azide → amine exchanges, being used in different fields of chemistry, has been applied in the case of morphine alkaloids. This method allowed the investigation of stereochemical problems in the morphine series and a study of further conversions of the derivatives containing a free amino group. 8-Aminocodide and the new compound 6-aminodihydrocodide have been prepared. 6-O-tosyl and 6-O-mesyl-codeine and the corresponding dihydrocodeine derivatives were prepared from codeine and dihydrocodeine. By means of azidolysis of these compounds, 8-deoxy-8-azido-pseudo-codeine- and 6-deoxy-6-azidodihydro-iso-codeine were obtained. The reaction of the azido group with lithium aluminium hydride resulted in 8-deoxy-8-amino-pseudo-codeine and 6-deoxy-6-aminodihydro-iso-codeine. The reported compounds have not been described in the literature except for 6-0-tosylcodeine and 8-aminocodide.

The structures and stereochemistry of the obtained compounds are discussed.

Until now only three compounds containing a free amino group have been isolated among aminomorphides and aminocodides.

6-Aminocodide monoacetate [1] was prepared from β-bromocodide with alcoholic ammonia solution; the free 6-aminocodide was not isolated. Since β-bromocodide contains the bromine atom in the C-8 position, the reaction must take place with allylic rearrangement, by S_N2' mechanism. The steric position of the amino group in 6-aminocodide has not yet been determined.

8-Aminocodide [2] was obtained from α-chlorocodide with liquid ammonia. The chlorine atom of α-chlorocodide is in the C-6 position, thus this reaction involves again allylic rearrangement, and occurs according to S_N2' mechanism. The steric position of the amino group is unknown.

8-Aminodihydrocodide has been prepared [2] by the catalytic reduction of 8-aminocodide.

When allylic systems of halogen derivatives undergo substitution by S_N2' mechanism, changes in the configuration must also be considered in addition to the position changes C-6 → C-8 and C-8 → C-6 [3].

We have found that reduction of the azides, prepared from tosyl and mesyl esters, is a very suitable method for the synthesis of aminomorphides and aminocodides. Using this method, the study of stereochemical problems

* Part I: BOGNÁR, R., MAKLEIT, S.: Chem. and Ind. 1956, 1239. BOGNÁR, R., MAKLEIT, S.: Arzneimittel-Forsch. **8**, 323 (1958). BOGNÁR, R., MAKLEIT, S.: Acta Univ. Debr. **5**, 225 (1958). Part II: BOGNÁR, R., MAKLEIT, S.: Acta Chim. Acad. Sci. Hung. **58**, 203 (1968).

and further conversions of the derivatives containing free amino groups is also possible.

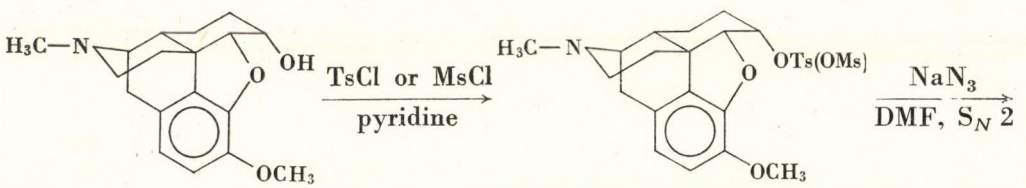
According to several authors [4], the *equatorial* tosylates and mesylates derived from *equatorial* alcohols yield *axial* azides, which give rise to axial amines. So in this reaction series it is only the tosylate (or mesylate) → azide exchange which is accompanied by a change of configuration, and the reaction is stereospecific.

In the present work, these transformations were studied on morphine, codeine, and their dihydro derivatives.

On the basis of theoretical considerations and analogies, the conformation of ring C and the steric positions of the C-6 and C-8 substituents can be described in the prepared derivatives as follows:

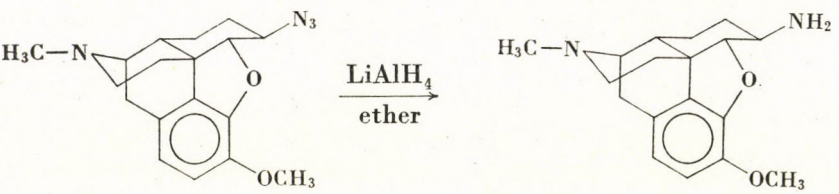
The saturated ring C of morphine and codeine derivatives has a slightly deformed chair conformation [5], and thus the hydroxyl group of C-6 hydroxy derivatives is located under the plane of ring C, *i.e.* in *axial* position. During the reactions, inversi onoccurs only in the case of the tosylate (or mesylate) → azide exchange occurring by S_N2 mechanism, thus the 6-O-tosyl and 6-O-mesyl derivatives have the same steric structures as dihydromorphine and dihydrocodeine. Their 6-amino and 6-azido derivatives however show steric structures analogous to that of dihydroisocodeine and the so-called dihydro-α-isomorphine and dihydro-α-chlorocodide; the azido and amino groups are situated above the plane of ring C.

Therefore, the products prepared from dihydrocodeine are represented in the following way:



I dihydrocodeine

IIa: 6-O-tosyldihydrocodeine
IIb: 6-O-mesyldihydrocodeine



III 6-deoxy-6-azido-dihydro-isocodeine* (6-azidodihydrocodide)

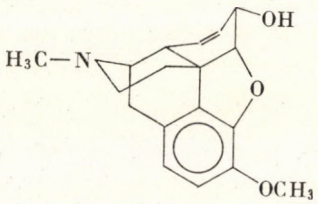
IV 6-deoxy-6-amino-dihydro-isocodeine (6-aminodihydrocodide)

* See the authors' suggestions on the nomenclature of these compounds in Part IV of this series. The names according to the former nomenclature are given in parentheses.

The reactions described in connection with dihydrocodeine can also be carried out with codeine containing an unsaturated bond in ring C. However, it is to be noted that in this case, as a result of the presence of the allylic system, the tosylate (or mesylate) → azide exchange takes place at a significantly higher rate, and the isolated products of the substitution occurring with allylic rearrangement contain the azido group at C-8. Allylic rearrangement, of course, does not occur in the azide → amine exchange, so the amino compounds derived from the azido derivatives contain the amino group at C-8, too.

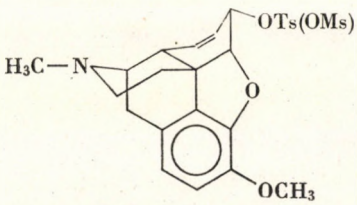
The explanation of the given representations of codeine and its derivatives is the following:

Ring C in the unsaturated morphine and codeine molecules has half-boat conformation [5] and the hydroxyl, tosyloxy and mesyloxy substituents at C-6 appear in quasi-equatorial position, below the plane of ring C. The exchange: tosyl (or mesyl) → azide in morphine and codeine derivatives occurs — as it has been mentioned — by S_N2' mechanism involving the change of the configuration [3], thus the steric position of the azido group in the resulting 8-azido derivatives corresponds to the steric structure and conformation found in pseudocodeine, γ-isomorphine and β-chlorocodide; *i.e.*, the 8-azido group, as well as the 8-amino group obtained from the former, is situated above the plane of the ring, in *quasi-equatorial* position.



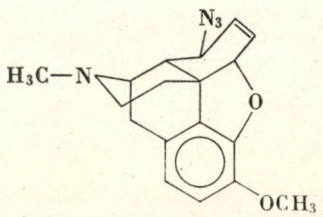
TsCl or MsCl
pyridine

V codeine

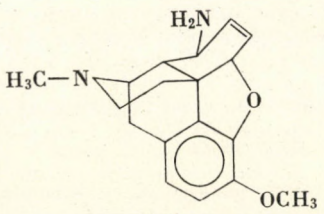


NaN_3
DMF, S_N2'

VIa: 6-O-tosylcodeine [6]
VIb: 6-O-mesylcodeine



$LiAlH_4$
ether



VII 8-deoxy-8-azido-pseudocodeine (8-azidocodide)

VIII 8-deoxy-8-amino-pseudocodeine (8-aminocodide)

It is to be noted that a substituent present in these compounds above the plane of the cyclohexene ring possesses *quasi-equatorial* position at C-8, and *quasi-axial* one at C-6; substituents situated under the plane are *quasi-equatorial* at C-6 and *quasi-axial* at C-8.

Experimental

6-O-tosyldihydrocodeine (IIa)

3.0 g of dihydrocodeine (0.01 mole) (m.p.: 114—115°) was dissolved in 12 ml of absolute pyridine, and a solution of 2.25 g (0.012 mole) of tosyl chloride in 12 ml of absolute pyridine was added by drops at 0° C. The reaction mixture was allowed to stand for 2 hrs at 0° C and for 24 hrs at room temperature. It was then poured into water (300 ml) saturated with sodium hydrogen carbonate, and extracted with 3×50 ml of ether. The ether extract was washed with 3×20 ml of water that had been saturated with sodium chloride, and dried over magnesium sulphate. The ether solution was treated with decolourizing carbon, evaporated to dryness, and the resulting pale pink oil was repeatedly rubbed with water, then dried over phosphorous pentoxyde.

The crude product was dissolved in absolute alcohol (10 ml) and a 20% solution of tartaric acid in absolute alcohol (8.5 ml) was added. The crystalline tartrate which precipitated (4.52 g; 75.3%) was recrystallized from water (15 ml) to give 3.89 g (65%) of the pure compound, m.p. 165°C; $[\alpha]_D$—67° (c = 1, in water).

$C_{29}H_{29}O_{11}NS$ (607.073). Calcd. N 2.31; S 5.28. Found N 2.32; S 5.39%.

The tartrate (3.22 g) was dissolved in water (50 ml), and the solution was made alkaline with 10% sodium hydroxide. The amorphous base which precipitated was filtered off and washed with a copious quantity of water. Drying over P_2O_5 gave 2.0 g (43.9%) of **IIa**, m.p. 64—70°C; $[\alpha]_D$—160° (c = 1, in $CHCl_3$).

$C_{25}H_{29}O_5NS$ (456.983). Calcd. N 3.09; S 7.06. Found N 3.11; S 7.03%.

6-O-mesyldihydrocodeine (IIb)

3.0 g of dihydrocodeine (0.01 mole) was dissolved in 12 ml of absolute pyridine, and a solution of 1.4 g (= 1 ml) (0.012 mole) of mesyl chloride in absolute pyridine (12 ml) was added dropwise at 0° C. The rest of the procedure was the same as for **IIa**. However, the gum obtained after evaporation to dryness rapidly crystallized on rubbing it with ether. The product was filtered off and washed with ether to obtain 0.9 g (23%) of **IIb**, m.p.: 178° C; $[\alpha]_D$—108.5° (c = 1.035, in $CHCl_3$).

$C_{19}H_{25}O_5NS$ (379.47). Calcd. N 3.71; S 8.48. Found N 3.75; S 8.46%.

6-Deoxy-6-azidodihydro-iso-codeine (6-azidodihydrocodide) (III)

a) 1.0 g of 6-O-tosyldihydrocodeine (0.002 mole) was dissolved in 32 ml of absolute dimethylformamide, and a solution of 1.4 g of sodium azide (0.02 mole) in 5 ml of water was added. The mixture was kept for 24 hrs at 100° C, then poured into 150 ml of water and extracted with 3×50 ml of ether. The ether extract was washed with 2×25 ml of water that had been saturated with sodium chloride, and dried over magnesium sulphate. Crystallization started during the evaporation of the ether solution to give finally 0.59 g (83%) of **III**, m.p.: 101° C; $[\alpha]_D$—187.1° (c = 0.31, in $CHCl_3$).

$C_{18}H_{22}O_2N_4$ (326.386). Calcd. N 17.3. Found N 17.38%.

In the IR spectrum, the azide band appeared at 2100 cm^{-1}.

b) 0.9 g (0.002 mole) of 6-O-mesyldihydrocodeine yielded 0.7 g (77%) of **III**, when the former was reacted with 1.53 g (0.02 mole) of sodium azide in 29 ml of dimethylformamide and 4.5 ml of water in the way described above. M.p. and mixed m.p. with the product prepared according to *a* : 100° C. Found: N 16.88%.

In the IR spectrum, the azide band appeared at 2100 cm^{-1}.

6-Deoxy-6-aminodihydro-iso-codeine (6-aminodihydrocodide) (IV)

0.33 g (0.001 mole) of 6-azidodihydrocodide was dissolved in 40 ml of absolute ether and the solution was added by drops to a suspension of 0.3 g of lithium aluminium hydride (0.008 mole) in 30 ml of absolute ether. The reaction mixture was gently boiled for 3 hrs. After cooling, 25 ml of ether (that had been saturated with water) and then 25 ml of water were added dropwise. The ether layer was separated and the aqueous phase was extracted with 3×25 ml of ether. The combined ethereal solutions were washed with 2×15 ml of water (saturated with sodium chloride), and dried over magnesium sulphate. The solution was evaporated to dryness and the residue dissolved again in warm absolute ether. Cooling gave crystals of **IV** (180 mg; 60%), m.p. 139° C; $[\alpha]_D$—133.3° (c = 0.6, in $CHCl_3$).

$C_{18}H_{24}O_2N_2$ (300.386). Calcd. N 9.39. Found N 9.4%. In the IR spectrum the amine band was found at 3340 cm^{-1}.

6-O-tosylcodeine (VIa)

2.0 g (0.0066 mole) of codeine was dissolved in 8 ml of absolute pyridine, and a solution of 1.5 g (0.008 mole) of tosyl chloride in 8 ml of absolute pyridine was added to it dropwise at 0° C. The mixture was allowed to stand for 2 hrs at 0° C, and for 24 hrs at room temperature. It was then poured into 200 ml of water that had been saturated with sodium hydrogen carbonate, and extracted with 3×50 ml of ether. The ether phase was washed with 3×50 ml of water and dried over magnesium sulphate. After evaporation to dryness, the residue was rubbed with absolute ether: crystallization began immediately to yield 1.74 g (58%) of **VIa**, m.p. 128° C (lit.m.p. 126—128° [6]); $[\alpha]_D$—166.6° (c = 0.6, in $CHCl_3$).

$C_{25}H_{27}O_5NS$ (454.967) Calcd. N 3.09; S 7.06. Found N 3.23; S 7.09%.

6-O-mesylcodeine (VIb)

According to the process described for **IIb**, 3.0 g of codeine gave 0.62 g (16.4%) of crystalline **VI.** m.p. 133°C; $[\alpha]_D$—178.3° (c = 0.6, in $CHCl_3$).

$C_{19}H_{23}O_5NS$ (377.46). Calcd. N 3.71; S 8.48. Found N 3.71; S 8.55%.

8-Deoxy-8-azido-pseudo-codeine (8-azidocodide) (VII)

a) 3.6 g (0.008 mole) of 6-O-tosylcodeine was dissolved in 112.5 ml of absolute dimethylformamide, and a solution of 0.7 g (0.01 mole) of sodium azide in 9 ml of water was added. The mixture was allowed to stand for 4 hrs at 100°C, it was then poured into 560 ml of water and extracted with 3×135 ml of ether. The ether phase was washed with 2×50 ml of water (saturated with sodium chloride), and dried over magnesium sulphate. Crystallization started when the ether solution was concentrated, to give 1.67 g (65%) of **VII**, m.p. 137—138° C; $[\alpha]_D$—20.4° (c = 1.076 in $CHCl_3$).

$C_{18}H_{20}O_2N_4$ (324.37) Calcd. N 17.31. Found N 17.35%. The azide band appears in the IR spectrum at 2100 cm^{-1}.

b) 0.5 g (0.0013 mole) of 6-O-mesylcodeine gave 160 mg (38%) of crystalline **VII** when reacted with 0.13 g (0.002 mole) of sodium azide in 16 ml of dimethylformamide and 2.4 ml of water, according to the method described above. M.p. and mixed m.p. with the product prepared according to *a* : 137°C. Found N 17.88%. The azide band in the IR spectrum appears at 2100 cm^{-1}.

8-Deoxy-8-amino-pseudo-codeine (8-aminocodide) (VIII)

0.93 g (0.003 mole) of 8-azidocodide was dissolved in 80 ml of absolute ether and added dropwise to a suspension of 0.5 g (0.01 mole) of lithium aluminium hydride in absolute ether. The mixture was boiled for 3 hrs, then 50 ml of ether (saturated with water) was added, followed by the addition of water. The ether phase was separated, and the water phase was extracted with 3×50 ml of ether. The combined ethereal solutions were washed with 2×30 ml of water (saturated with sodium chloride), and dried over magnesium sulphate. The extract was evaporated to dryness and the residue dissolved in ether and allowed to stand. The separated crystals 0.33 g (46%) had m.p. 128—130° C (lit.m.p. 128—129° C [2]); $[\alpha]_D$—83.3° (c = 0.6, in alcohol); (lit. $[\alpha]_D$—79.2° [2]).

$C_{18}H_{22}O_2N_2$ (298.37). Calcd. N 9.39. Found N 9.34%. In the IR spectrum the amine band was found at 3372 cm^{-1}.

N,N-diacetyl derivative of VIII

70 mg of **VIII** was allowed to stand for 18 hrs with 1 ml of acetic anhydride at room temperature. After dilution with 15 ml of ice-water, the mixture was made alkaline with sodium carbonate. The precipitated white powder was filtered off and washed with water. Recrystallization from ethyl acetate gave hexagonal crystals, m.p. 221—222° C (lit.m.p. 218—220° C [2]). $C_{22}H_{26}O_4N_2$ (382.442) Calcd. N 7.35. Found N 7.39%.

*

The authors are grateful to the Department of Chemistry of the Hungarian Academy of Sciences and to Alkaloida Chemical Works, Tiszavasvári, Hungary, for supporting this research, and to the Analytical Laboratory of the Institute for the analyses.

REFERENCES

1. Ochiai, E., Yosida, S.: J. Pharm. Soc. Japan **59,** 424 (1939)
2. Small, L. F., Palmer, F. S.: J. Am. Chem. Soc. **61,** 2186 (1939)
3. Stork, G., Clarke, F. H.: J. Am. Chem. Soc. **78,** 4619 (1956)
4. Bose, A. K., Kistner, J. F., Farber, L.: J. Org. Chem. **27,** 2925 (1962)
   Reist, E. J., Spencer, R. R., Baker, B. R., Goodmann, L.: Chem. and Ind. 1962, 1794
   Hill, J., Hough, L., Richardson, A. C.: Proc. Chem. Soc. 1963, 314
   Woodward, R. B., Heusler, K., Gosteli, J., Naegeli, P., Oppolzer, W., Ramage, R., Ranganathan, S., Vortbrüggen, H.: J. Am. Chem. Soc. **88,** 852 (1966)
   Schreiber, K., Ripperger, H.: Ann. **672,** 232 (1964)
5. Rüll, T.: Bull. soc. chim. France 1963, 586
6. Karrer, P., Widmark, G.: Helv. Chim. Acta **34,** 34 (1951)

Rezső Bognár
Sándor Makleit } Debrecen 10. Hungary

Acta Chimica Academiae Scientiarum Hungaricae, Tomus 59 (3—4), pp. 379—385 (1969)

CONVERSIONS OF TOSYL AND MESYL DERIVATIVES OF THE MORPHINE GROUP, IV*

PREPARATION OF "AZIDO- AND AMIDOMORPHIDES"

R. BOGNÁR, S. MAKLEIT and T. MILE

(Institute of Organic Chemistry, L. Kossuth University, Debrecen)

Received February 5, 1968

8-Aminomorphide and 6-aminodihydromorphide have been prepared by the exchange reactions: alcoholic hydroxyl → tosyl (or mesyl) → azide → amine. The 3-O-acetyl derivatives of morphine and dihydromorphine give, on treatment with tosyl or mesyl chloride, 3-O-acetyl-6-O-tosyl or -mesylmorphine and dihydromorphine. By the azidolysis of these compounds 8-deoxy-8-azido-pseudo-morphine and 6-deoxy-6-azido-dihydro-iso-morphine can be obtained; after acetylation of the phenolic hydroxyl group, reduction with lithium aluminium hydride yields 8-deoxy-8-amino-pseudomorphine and 6-deoxy-6-aminodihydro-iso-morphine. The compounds described — except for 3-O-acetylmorphine — have not been known so far.

A new nomenclature is suggested for morphine derivatives substituted in ring *C* accordingly proposing 8-deoxy-8-amino-pseudomorphine instead of "8-aminomorphide" and 6-deoxy-6-amino-dihydroisomorphine instead of "6-aminodihydromorphide".

Structure and stereochemistry of the compounds in question are discussed.

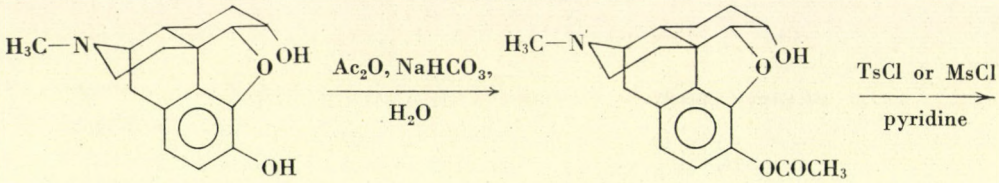
In the previous paper the preparation of 8-aminocodide and 6-aminodihydrocodide was described. The reduction of azides obtained from the tosyl and mesyl esters was found to be a very suitable method to synthesize these compounds.

Further investigations showed that the so-called 8-aminomorphide and 6-aminodihydromorphide can also be prepared in this way. The protection of the phenolic hydroxyl group of morphine by partial acetylation [2] made it possible to prepare the 6-O-tosyl and 6-O-mesyl derivatives; in this way dihydro-6-deoxymorphine-D was prepared [1].

Discussions of the reactions, explanation of the formulation of the products obtained and arranging the compounds into groups according to stereochemical analogies have been published in the previous paper of this series. The validity of those statements for the case of the present compounds is proved by the fact that 8-azidocodide and 6-azidodihydrocodide obtained by the methylation with diazomethane from 8-azidomorphide and 6-azidodihydromorphide, respectively, were identical with the corresponding products prepared from codeine or dihydrocodeine; these conversions also prove the identity of the steric course of the reactions both with morphine and codeine derivatives.

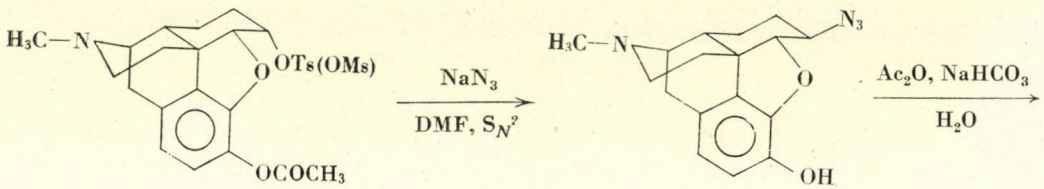
* Part III: R. BOGNÁR, S. MAKLEIT: Acta Chim. Acad. Sci. Hung. **59**, 373 (1969) and Magyar Kém. Foly. **74**, 523 (1968)

The following conversions were carried out starting from dihydromorphine:



I
dihydromorphine

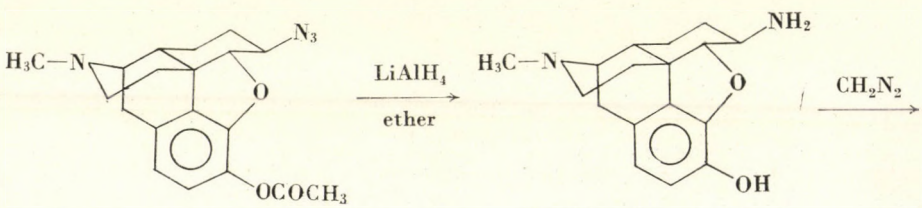
II
3-0-acetyldihydromorphine



IIIa
3-0-acetyl-6-O-tosyl-dihydromorphine

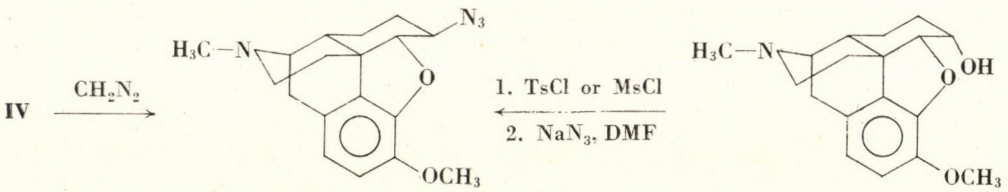
IIIb
3-0-acetyl-6-O-mesyl-dihydromorphine

IV
6-deoxy-6-azido-dihydro-iso-morphine
(6-azidodihydromorphide)



V 3-O-acetyl-6-deoxy-
6-azidodihydro-iso-morphine
(3-O-acetyl-6-azidodihydromorphide)

VI 6-deoxy-6-amino
dihydro-iso-morphine
(6-aminodihydromorphide)

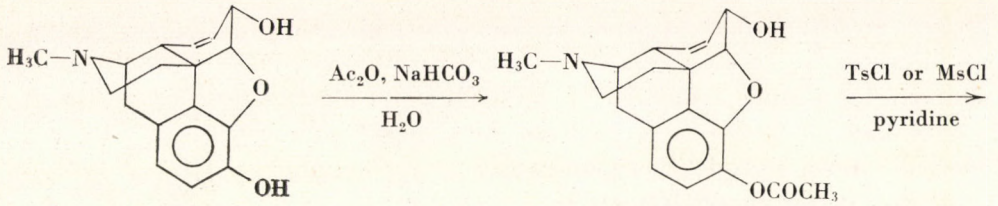


VII 6-deoxy-6-azidodihydro-iso-codeine
(6-azidodihydrocodide)

dihydrocodeine

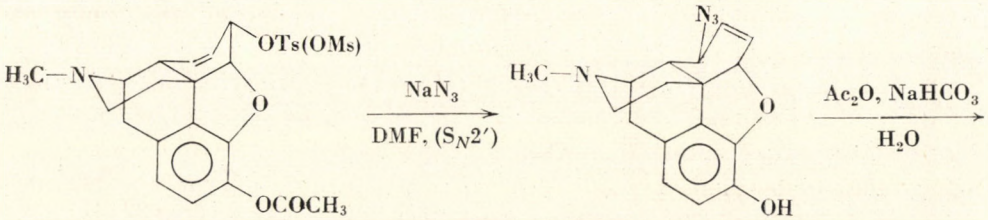
* See later the suggestions on the nomenclature of these compounds; the old names are given in parentheses.

The conversions were also carried out starting from morphine. These reactions gave the following compounds:



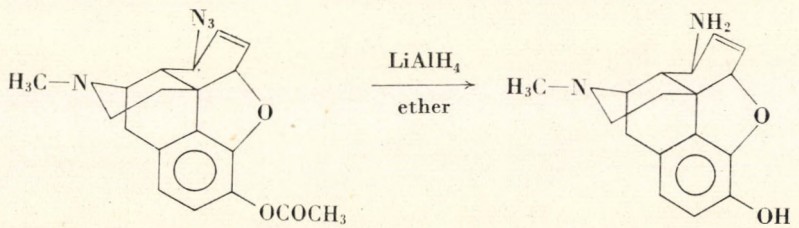
VIII morphine

IX 3-O-acetyl morphine



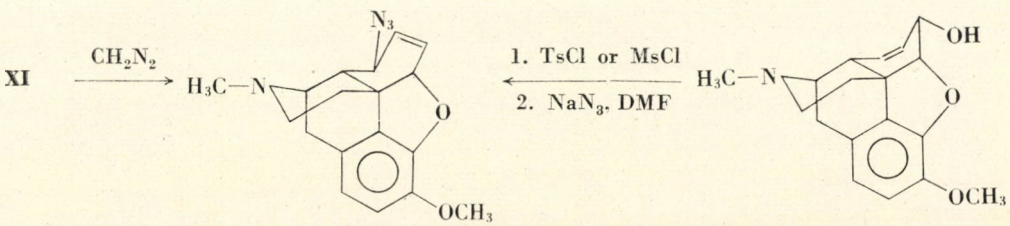
Xa 3-O-acetyl-6-O-tosyl morphine
Xb 3-O-acetyl-6-O-mesyl morphine

XI 8-deoxy-8-azido-pseudo-morphine (8-azidomorphide)



XII 3-O-acetyl-8-deoxy-8-azido-pseudo-morphine (3-O-acetyl-8-azidomorphide)

XIII 8-deoxy-8-amino-pseudo-morphine (8-aminomorphide)



XIV 8-deoxy-8-azido-pseudo-codeine (8-azidocodide)

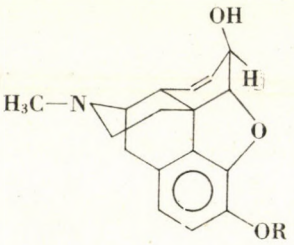
codeine

In the conversion with sodium azide, deacetylation also takes place. The deacetylated azido derivative, however, cannot be reduced with lithium aluminium hydride because of the presence of the free phenolic hydroxyl group. So compounds **IV** and **XI** were reacetylated, and the acetylated azido derivatives were reduced; in this case, although the compounds again suffer deacetylation, reduction of the azido group takes place.

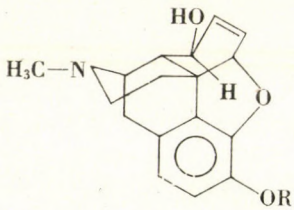
Finally, we propose a rational modification in the nomenclature of the described compounds to develop a more simple and unambiguous system of names.

(a) For the amino derivatives the name deoxy-amino is suggested. *E.g.:* 6-deoxy-6-aminodihydro-iso-codeine, instead of 6-amino-dihydrocodide; or 8-deoxy-8-amino-pseudo-codeine, instead of 6-aminocodide, etc. (This nomenclature has already been used in Part II of this series and in the present paper.)

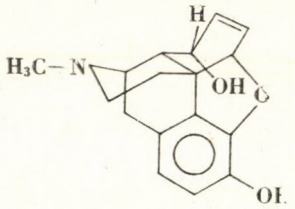
(b) For morphine isomers the nomenclature applied in the group of codeine isomers is suggested, in accordance with the codeine—morphine pair. Thus isomorphine—corresponding to isocodeine—instead of "α-isomorphine" (cf. **XVa** and **b**), pseudomorphin e — corresponding to pseudocodeine — instead of "γ-isomorphine" (cf. **XVIa** and **b**), allopseudomorphine corresponding to allopseudocodeine — instead of "β-isomorphine" are proposed. The old name "pseudomorphine" — making confusion in this nomenclature — should be changed to the rational and unambiguous name 2,2′-bimorphine [3] in the knowledge of the structure of the compound. We propose an extension of this nomenclature to derivatives containing other substituents in ring C.



XVa: R = CH_3
XVb: R = H



XVIa: R = CH_3
XVIb: R = H



XVIIa: R = CH_3
XVIIb: R = H

Experimental

3-O-acetyldihydromorphine (II)

4.96 g of **II** was obtained from 5.0 g of morphine by the method of WELSH [2].

3-O-acetyl-6-O-tosyldihydromorphine (IIIa)

6.0 g (0.018 mole) of 3-O-acetyldihydromorphine was dissolved in 24 ml of absolute pyridine, and a solution of 4.37 g (0.02 mole) tosyl chloride in 24 ml of absolute pyridine was added to it dropwise at 0°C. The mixture was allowed to stand for 2 hrs at 0°C and for 24 hrs at room temperature. Then it was poured into water (600 ml) (saturated with sodium hydrogen

carbonate) and extracted with 3×150 ml of chloroform. The chloroform solution was washed with water, dried over magnesium sulphate and evaporated to dryness. The gum which remained was rubbed with absolute ether, when crystallization started immediately. The separated crystals were filtered off and washed with absolute ether to obtain 4.65 g (55.5%) of **IIIa**, m.p. 167—169°C; $[\alpha]_D$ —130° (c = 0.6, in $CHCl_3$). $C_{26}H_{29}O_6NS$ (484.981). Calcd. N 2.9; S 6.62; acetyl 8.9. Found N 2.85; S 6.57; acetyl 9.83%.

3-0-acetyl-6-0-mesyldihydromorphine (IIIb)

It was prepared from 6.0 g (0.018 mole) of 3-O-acetyldihydromorphine and 3.0 g (2.26 ml; 0.026 mole) of mesyl chloride in pyridine solution, analogously with the process described above. After evaporating the chloroform, the residue was recrystallized from 95% ethanol to obtain 3.35 g (47.5%) of **IIIb**, m.p. 163°C; $[\alpha]_D$ —87.3° (c = 0.504, in $CHCl_3$). $C_{21}H_{25}O_6NS$ (419.478) Calcd. N 3.44; S 7.85; acetyl 10.5. Found N 3.48; S 7.77; acetyl 10.4%.

6-Deoxy-6-azidodihydro-iso-morphine (6-azidodihydromorphide) (IV)

(*a*) 4.0 g of 3-O-acetyl-6-O-tosyldihydromorphine (0.008 mole) was dissolved in 128 ml of absolute dimethylformamide, and a solution of 8.06 g (0.12 mole) of sodium azide in 19.80 ml of water was added. The mixture was heated at 100°C for 24 hrs. Then it was poured into 500 ml of water and extracted with 3×150 ml of chloroform. The chloroform solution was washed with 2×30 ml of water (saturated with sodium chloride). It was dried over magnesium sulphate and evaporated to dryness. The residue was rubbed with absolute ether, the product was filtered off and recrystallized from a mixture of 25 ml of acetone and 15 ml of water to yield 1.3 g (50.3%) of **IV**. m.p.: 192—193°C; $[\alpha]_D$ —170.6° (c = 0.504, in $CHCl_3$).

$C_{17}H_{20}O_2N_4$ (312.356). Calcd. N 17.93. Found N 18.81%; acetyl: nil.

The azide band appears in the IR spectrum at 2100 cm^{-1}

(*b*) Starting with 3.0 g of 3-0-acetyl-6-0-mesyl-dihydromorphine (0.007 mole) in 114 ml of absolute dimethylformamide and 7.18 g (0.11 mole) of sodium azide in 17.60 ml of water, and proceeding analogously as described under (*a*), 0.59 g (24.5%) of **IIIb** was obtained, m.p. and mixed m.p. with the product from (*a*): 192—193°C. The azide band appeared in the IR spectrum at 2100 cm^{-1}.

6-Deoxy-6-azidodihydro-iso-codeine (6-azidodihydrocodide) (VII)

100 mg of 6-azidodihydromorphide was dissolved in 10 ml of methanol and treated with diazomethane in ether. After evaporating to dryness, the residue was recrystallized from absolute ether. M.p. and mixed m.p. with 6-azidodihydrocodide prepared from dihydrocodeine: 100°C (see Part III of this series).

3-0-Acetyl-6-deoxy-6-azidodihydro-iso-morphine (3-0-acetyl-6-azidodihydromorphide) (V)

1.73 g of 6-azidodihydromorphide was acetylated by the method of WELSH [2], to obtain 1.45 g (73.9%) of an amorphous substance. In the IR spectrum the azide and acetyl bands were found at 2100 cm^{-1} and at 1760 cm^{-1}, respectively. ($C_{19}H_{22}O_3N_4$ (354.392)).

6-Deoxy-6-aminodihydro-iso-morphine (6-aminodihydromorphide) (VI)

A solution of 1.45 g (0.004 mole) of 3-O-acetyl-6-azidodihydromorphide in absolute ether (40 ml) was added, by drops, to a suspension of 1.4 g (0.03 mole) of lithium aluminium hydride in 150 ml absolute ether. The mixture was boiled for 3 hrs, then 50 ml of ether (saturated with water), and 50 ml of water were added to it dropwise. The water phase was acidified with glacial acetic acid, then made alkaline with ammonium hydroxyde and extracted with 3×50 ml of a mixture of chloroform and absolute ethanol (2 : 1). The solution was dried over magnesium sulphate, evaporated to dryness, and the residue was crystallized from absolute ether to obtain 0.44 g (37.5%) of **VI**, m.p.: 265°C; $[\alpha]_D$ —60° (c = 0.5, in $CHCl_3$).

$C_{17}H_{22}O_2N_2$ (286.358). Calcd. N 9.78. Found N 9.56%.

The amine band appears at 3325 cm^{-1} in the IR spectrum.

3-O-Acetylmorphine (IX)

1.79 g (78%) of 3-O-acetylmorphine was obtained from 2.0 g of morphine by the method of WELSH [2].

3-O-Acetyl-6-O-tosylmorphine (Xa)

Starting with 1.79 g of 3-O-acetylmorphine and proceeding as described for **IIIa**, 1.25 g (50%) of **Xa** was obtained m.p.: 130°C from ether; $[\alpha]_D$ —170° (c = 0.6, $CHCl_3$).

$C_{26}H_{27}O_6NS$ (482.965). Calcd. N 2.94; S 6.7; acetyl 9.01. Found N 2.84; S 6.33; acetyl 10.85%.

The ferric chloride colour reaction was negative.

3-O-Acetyl-6-O-mesylmorphine (Xb)

2.5 g of 3-O-acetylmorphine gave by the procedure used to prepare **IIIb**, 0.62 g of **Xb**, m.p. 149°C (from ether); $[\alpha]_D$ —178.3° (c = 0.6, in $CHCl_3$).

$C_{21}H_{23}O_6NS$ (417.462). Calcd. N 3.45; S 7.9; acetyl 10.62%. Found N 2.55; S 7.42; acetyl 11.15%.

The ferric chloride colour reaction was negative.

8-Deoxy-8-azido-pseudo-morphine (8-azidomorphide) (XI)

(*a*) 2.1 g (0.004 mole) of 3-O-acetyl-6-O-tosyl-morphine was dissolved in 67 ml of absolute dimethylformamide. A solution of 0.43 g (0.006 mole) of sodium azide in 10.5 ml of water was added to it and the mixture was heated at 100° for 4 hrs. It was then poured into 300 ml of water and extracted with 3×100 ml of ether. The ether solution was washed with 2×50 ml of water (saturated with sodium chloride), and dried over magnesium sulphate. Concentrating the ether solution, the product separated in crystalline form (1.04 g; 67.5%), m.p. 188°C; $[\alpha]_D$ —2.05° (c = 0.976, in $CHCl_3$).

$C_{17}H_{18}O_2N_4$ (310.340). Calcd. N 18.12. Found N 18.09%; acetyl: nil. In the IR spectrum, the azide band appeared at 2100 cm^{-1}.

(*b*) 0.8 g (0.002 mole) of 3-O-acetyl-6-O-mesyl-morphine dissolved in 25.6 ml of absolute dimethylformamide was reacted as described under (*a*) with a solution of 0.19 g (0.003 mole) of sodium azide, to obtain 0.47 g (68%) of **XI** m.p. 189° (from ether). Mixed m.p. with the product prepared according to (*a*): 188°C. (Found N, 18.05; acetyl nil.) The azide band in the IR spectrum was found at 2100 cm^{-1}.

8-Deoxy-8-azido-pseudo-codeine(8-azidocod ide) (XIV)

A solution of 100 g of 8-azidomorphide in methanol (10 ml) was mixed with diazomethane in ether, and the reaction mixture was allowed to stand. After evaporation to dryness, the residue was recrystallized from ether to obtain **XIV**, m.p. and mixed m.p. with 8-azidocodide obtained from codeine: 138°C. (See Part III of this series.)

[3-O-Acetyl-8-deoxy-8-azido-pseudo-morphine (3-O-acetyl-8-azidomorphide) (XII)

1.33 g of 8-azidomorphide gave 1.13 g (75%) of **XII** according to the method of WELSH [2], m.p.: 98—99°C (from ether).

$C_{19}H_{20}O_3N_4$ (352.376). Calcd. N 15.9; acetyl 12.21. Found N 16.24; acetyl 13.0%. IR analysis: azide band at 2100 cm^{-1}, acetyl band at 1760 cm^{-1}.

8-Deoxy-8-amino-pseudo-morphine (8-aminomorphide) (XIII)

1.13 g (0.003 mole) of 3-O-acetyl-8-azidomorphide was dissolved in 30 ml of absolute ether and added by drops to a suspension of 1.1 g (0.03 mole) of lithium aluminium hydride in absolute ether. The mixture was boiled for 3 hrs, then 50 ml of moist ether and 50 ml of water were added to it dropwise. The aqueous phase was acidified with glacial acetic acid, then

made alkaline with ammonium hydroxyde and extracted with 3×50 ml of a mixture of chloroform and absolute alcohol (2 : 1). After drying over magnesium sulphate, the solution was evaporated to dryness, and the residue was crystallized from 95% ethanol to obtain 0.43 g (48%) of **XIII**, m.p. 244—245° C; $[\alpha]_D$ —86.7° (c = 0.3, in $CHCl_3$).

$C_{17}H_{20}O_2N_2$ (284.342). Calcd. N 9.85. Found N 9.3%. The amine band was found at 3340 cm^{-1} in the IR spectrum.

*

The authors are grateful to the Department of Chemistry of the Hungarian Academy of Sciences and to Alkaloida Chemical Works, Tiszavasvári, Hungary, for supporting this research, and to the Analytical Laboratory of the Institute for the analyses.

REFERENCES

1. BOGNÁR, R., MAKLEIT, S.: Chem. and Ind. **1956,** 1239
BOGNÁR, R., MAKLEIT, S.: Arzneimittel-Forsch. **8,** 323 (1958)
BOGNÁR, R., MAKLEIT, S.: Acta Univ. Debr. **5,** 225 (1958)
2. WELSH, L. H.: J. Org. Chem. **19,** 1409 (1954)
3. BENTLEY, K. W., DYKE, S. F.: J. Chem. Soc. **1959,** 2574

Rezső BOGNÁR
Sándor MAKLEIT
Teréz MILE
Debrecen, 10. Hungary

Acta Chimica Academiae Scientiarum Hungaricae, Tomus 59 (3—4), pp. 387—388 (1969)

CONVERSIONS OF TOSYL AND MESYL DERIVATIVES OF THE MORPHINE GROUP, V*

A NEW METHOD FOR THE PREPARATION OF ISOCODEINE AND DIHYDROISOCODEINE

(SHORT COMMUNICATION)

S. MAKLEIT and R. BOGNÁR

(Institute of Organic Chemistry, L. Kossuth University, Debrecen)

Received May 3, 1968

Isocodeine(**I**), the C—6 isomer of natural codeine, can be best prepared, according to reported data, in either of the following ways:

(a) The treatment of codeine with phosphorus pentachloride gives α-chlorocodide, which, when heated in bromobenzene, is isomerized to β-chlorocodide. Upon heating with aqueous acetic acid, the latter yields a mixture of codeine isomers, from which the pure isomers may be isolated in various ways [1].

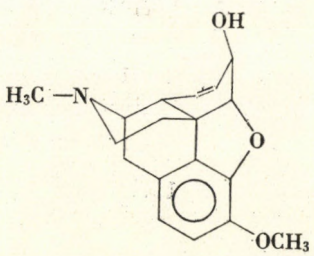
By this method, starting with 27 g of codeine, 0.5 g (1.8%) of pure isocodeine was obtained in our experiment; its homogeneity was proved by thin-layer chromatography (Silicagel G; benzene : methanol = 8 : 2).

(b) The reaction of codeine with thionyl bromide yields bromocodide, which is hydrolyzed with aqueous acetic acid, and the formed codeine isomers are separated [2].

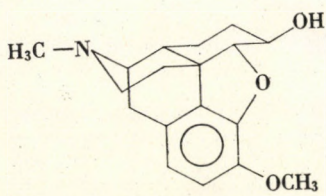
In this way 0.5 g (14.2%) of isocodeine was obtained from 3.5 g of codeine in our experiment.

Dihydroisocodeine(**II**) has been prepared by the hydrogenation of isocodeine obtained, in turn, from halogen codides [1, 2, 3].

In the course of an investigation of the reactions of the tosyl and mesyl derivatives of the morphine group [4], the epimerization of the alcoholic hydroxyl group of codeine and dihydrocodeine was attempted through the codeine-6-O-tosyl [5] and dihydrocodeine-6-O-mesyl derivatives, respectively.



I



II

* Part IV: R. BOGNÁR, S. MAKLEIT, T. MILE: Acta Chim. Acad. Sci. Hung. **79**, 359 (1969) R. BOGNÁR, S. MAKLEIT, T. MILE: Magyar Kém. Foly. **74**, 523 (1968)

For this purpose several methods were studied, such as the use of 10 or 70% acetic acid [6, 7, 8], or sodium benzoate in dimethyl formamide [9] for the treatment of 6-O-tosylcodeine, and the method of applying acetic acid, acetic anhydride and sodium acetate, when starting either from 6-O-tosylcodeine or 6-O-mesyldihydrocodeine [10].

Of these methods the following two were found suitable for the preparation of the mentioned isomers (**I, II**), being more advantageous than the syntheses starting with halogen codides:

(1) When 6-O-tosylcodeine is refluxed 4 hrs in 10% acetic acid [6, 7], isocodeine is obtained in 16.6% yield, i.e., 3.0 g of codeine gives 0.5 g of pure isocodeine. The homogeneity of the product was proved by thin-layer chromatography. M.p. 170°C; $[\alpha]_D = -156.6°$ (in $CHCl_3$, c = 0.3); lit. m.p. 171—172°C; $[\alpha]_D = -150.6°$ (in $CHCl_3$, c = 1.876) [1].

(2) 6-O-mesyldihydrocodeine was refluxed in a mixture of acetic acid, acetic anhydride and sodium acetate [9] for 31 hrs. The formed dihydroisocodeine acetate (m.p. 165°C; acetyl band in the IR spectrum at 1740 cm^{-1}; $[\alpha]_D = -151°$ (in $HCCl_3$, c = 0.51); lit. m.p. 166°C [1, 11]; analysis: Calcd. C 69.8; H 7.2; N 4.07; acetyl 12.5%. Found C 70.43, 70.60; H 7.63, 7.74; acetyl 11.14, 11.07, N 4.31, 4.34 %) was hydrolyzed. In this way 0.26 g (21.6) % of dihydroisocodeine was obtained from 1.2 g of dihydrocodeine, m.p. 201°C; $[\alpha]_D = 117.8°$ (in $CHCl_3$, c = 0.28); m.p. 199—200°C [1, 2, 3].

Further investigation of the mentioned compounds is in progress.

We wish to express our thanks of the Chemical Department of the Hungarian Academy of Sciences and to Alkaloid Chemical Factory of Tiszavasvári for supporting the above research.

REFERENCES

1. Small, L. F.: Chemistry of the Opium Alkaloids. Washington, 1932, p. 221
2. Rapoport, H., Payne, G. B.: J. Org. Chem. **15,** 1093 (1950)
3. Speyer, E., Wieters, H.: Ber. **54,** 2647 (1921)
4. Bognár, R., Makleit, S.: Chem. and Ind. **1956,** 1239
   Bognár, R., Makleit, S.: Arzneimittel-Forschung **8,** 323 (1958)
   Bognár, R., Makleit, S.: Acta Univ. Debr. **5,** 225 (1958)
   Bognár, R., Makleit, S.: Acta Chim. Acad. Sci. Hung. **58,** 203 (1968)
   Bognár, R., Makleit, S.: Acta Chim. Acad. Sci. Hung. **59,** 373 (1969)
   Bognár, R., Makleit, S., Mile, T.: Acta Chim. Acad. Sci. Hung. (In the press)
   Bognár, R., Makleit, S.: Magyar Kém. Foly. **74,** 523 (1968)
   Bognár, R., Makleit, S., Mile, T.: Magyar Kém. Foly. **74,** 526 (1968)
   Makleit, S., Bognár, R.: MTA Kém. Tud. Oszt. Közl. **30,** 289 (1968)
5. Karrer, P., Widmark, G.: Helv. Chim. Acta **34,** 34 (1951)
6. Currie, A. C., Gillon, J., Newbold, G. T., Spring, F. S.: J. Chem. Soc. **1960,** 773
7. Seki, I.: Ann. Sankyo Res. Lab. **17,** 1 (1965)
8. Kugita, H., Takeda, M., Inoue, H.: Tetrahedron Letters **14,** 1277 (1967)
9. Reist, E. I., Goodman, L., Baker, B. R.: J. Am. Chem. Soc. **80,** 5775 (1958)
10. Freudenberg, K., v. Oertzen, K.: Ann. **574,** 37 (1951)
11. Speyer, E., Krauss, W.: Ann. **432,** 233 (1923)

Sándor Makleit
Rezső Bognár
} Debrecen 10. Hungary

Acta Chimica Academiae Scientiarum Hungaricae, Tomus 59 (3—4), pp. 389—396 (1969)

SULPHUR-CONTAINING METAL CARBONYLS, X*

REACTIONS OF COBALT CARBONYLS WITH ALIPHATIC THIOETHERS AND THE INFLUENCE OF THIOETHERS ON THE CATALYTIC ACTIVITY OF COBALT CARBONYLS

L. MARKÓ

(Hungarian Oil and Gas Research Institute, Veszprém, and Institute of Organic Chemistry, University of Chemical Industries, Veszprém)

Received February 22, 1968

Labile monosubstituted derivatives are formed from $Co_2(CO)_8$ or $Co_4(CO)_{12}$ and thioethers, in a reversible reaction. Owing to the formation of these complexes, thioethers exert a slight inhibiting influence on the hydroformylation and aldehyde hydrogenation reactions catalyzed by cobalt carbonyls.

Introduction

Most sulphur compounds are poisons for cobalt carbonyl catalysts, as they convert these complexes under the conditions of hydroformylation and hydrogenation to cobalt sulphide [1—3]. The formation of cobalt sulphide takes place through various intermediate sulphur-containing cobalt carbonyl derivatives [4—9].

Satured aliphatic thioethers have been regarded so far as indifferent to cobalt carbonyl catalysts [1, 3]. We have observed, however, that even these sulphur compounds can react with dicobalt octacarbonyl at room temperature to yield new cobalt carbonyl complexes. This fact necessitated a re-examination of the problem.

Reactions of $Co_2(CO)_8$ and $Co_4(CO)_{12}$ with dialkyl sulphides

Di-*n*-butyl sulphide taken in large excess reacted with $Co_2(CO)_8$ and $Co_4(CO)_{12}$ under the evolution of approximately one mole of carbon monoxide per mole cobalt carbonyl. The infrared spectra of the dark brown liquid reaction products thus obtained showed that $Co_2(CO)_8$ or $Co_4(CO)_{12}$ was no longer present, but new bands appeared at 2083, 2040, 2035, 2018, 2004(sh), 1998(sh), 1845, 1830 cm^{-1} and at 2086, 2047, 2040, 2030, 2014, 2002, 1859(sh), 1849, 1828, 1819(sh) cm^{-1}, respectively. No uniform solid product could be isolated from these liquid mixtures.

Dimethyl sulphide reacted in a similar manner, and the dark liquid products had infrared spectra similar to those of the solutions obtained with

* Part IX: see Ref. [9].

di-*n*-butyl sulphide. Evaporation of the excess dimethyl sulphide in vacuum gave black crystalline products, which had, in the cases of both cobalt carbonyls, the approximate composition $Co_4(CO)_{11}(SMe_2)$, and were found to be identical by their infrared spectra.

The reactions between dimethyl sulphide and $Co_2(CO)_8$ or $Co_4(CO)_{12}$ were found to be reversible. Using *n*-heptane as the solvent and bubbling carbon monoxide through the liquid reaction products, which — according to their infrared spectra — did not contain $Co_2(CO)_8$ or $Co_4(CO)_{12}$ any more, dimethyl sulphide, the component with the highest vapour tension, could be removed, and the regeneration of $Co_2(CO)_8$ and $Co_4(CO)_{12}$ could be proved by infrared spectrometry. The above facts can be explained by assuming that saturated aliphatic thioethers react with $Co_2(CO)_8$ and $Co_4(CO)_{12}$ as "regular" monodentate ligands effecting the reversible substitution of one carbon monoxide ligand [Reactions (1) and (2)]:

$$Co_2(CO)_8 + R_2S \rightleftharpoons Co_2(CO)_7(R_2S) + CO \quad (1)$$

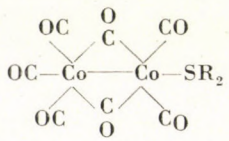
$$Co_4(CO)_{12} + R_2S \rightleftharpoons Co_4(CO)_{11}(R_2S) + CO \quad (2)$$

The formation of $Co_4(CO)_{11}(SMe_2)$ from $Co_2(CO)_8$ and dimethyl sulphide after evaporation of the excess thioether is probably due to the partial decomposition of the primary product $Co_2(CO)_7(SMe_2)$, present in solution.

Even the complex $Co_4(CO)_{11}(SMe_2)$ is rather labile and an attempted purification by recrystallization failed.

Thioether derivatives of dicobalt octacarbonyl

The dicobalt heptacarbonyl thioether complexes show two absorption bands in the region characteristic for bridging carbonyl groups and thus obviously have the following structure:



The frequency shifts of both the terminal and the bridging C—O stretching bands towards lower values are in good agreement with those to be expected for a compound with an L : CO ratio of 1 : 7 on the basis of the regularities observed for some triphenylphosphine derivatives of metal carbonyls (*cf.* Fig. 7 in Ref. [10]), considering that the C—O frequency lowering effects of $(C_6H_5)_3P$ [11] and $(C_2H_5)_2S$ [12] are about equal.

These complexes are thought to be the first reported monosubstituted derivatives of the dicobalt octacarbonyl isomer containing bridging carbonyl groups [13, 14].

Thioether-substituted simple metal carbonyls are rather rare, the only examples reported up till now being the molybdenum derivatives $Mo(CO)_nL_{6-n}$ (L = Me_2S, Et_2S and tetrahydrothiophene) [12, 15] and the nickel complex $Ni(CO)_3SEt_2$ [12] which latter, however, was observed only in solution. This is obviously caused by the labile character of these complexes, in agreement with the cases just reported. This is in sharp contrast to the stability of the somewhat similar tertiary phosphine derivatives of metal carbonyls. The case, with which carbon monoxide was observed to replace the thioether ligand is also quite unusual in metal carbonyl chemistry.*

The formation of $Co_2(CO)_7(SR)_2$ type complexes is strongly influenced by steric factors: under similar conditions a slow and incomplete substitution of $Co_2(CO)_8$ was observed with di-*sec*-butyl sulphide and no reaction occurred with di-*tert*-butyl sulphide. In the case of dimethyl sulphide, the infrared spectrum of the reaction product showed further bands at 2062, 2020*, 2002, 1989, 1820* and 1806 cm^{-1} [*overlapping with the corresponding bands of $Co_2(CO)_7(SMe_2)$], indicating the formation of a disubstituted derivative, $Co_2(CO)_6(SMe_2)_2$, also exemplifying the predominant role of steric factors in these substitution reactions.

The monosubstituted dicobalt octacarbonyl derivatives show very similar infrared absorption spectra in the C—O stretching region. The observed values are collected in Table I.

Table I

Infrared absorption spectra in the C—O stretching region of $Co_2(CO)_7(SR)_2$ complexes in hexane solution

Thioether	ν_{CO}, cm^{-1}		
Me_2S	2086 (m),	2042 (s),	2037 (s),
	2022 (vs),	2007 (m, sh),	
	1999 (m, sh),	1848 (m),	1828 (m)
$(n\text{-Bu})_2S$	2083 (m),	2040 (s),	2035 (s),
	2018 (vs),	2004 (m, sh),	
	1998 (m, sh),	1845 (m),	1830 (m)
$(sec.\text{-Bu})_2S$*	2086 (w),	1999 (s),	1842 (m),
	1830 (m)		

* In the case of this complex, the presence of unchanged $Co_2(CO)_8$ in the reaction mixture prevented the detection of some bands.

* The substitution of PR_3 ligands by CO has been observed so far only in bi- or poly-substituted derivatives to yield the monosubstituted products [16, 17] but, to our knowledge, no case has been reported in which a single phosphinic ligand was replaced by carbon monoxide to yield an unsubstituted carbonyl.

Thioether derivatives of tetracobalt dodecacarbonyl

As already mentioned, the complex containing dimethyl sulphide was obtained both from $Co_4(CO)_{12}$ or $Co_2(CO)_8$ when the excess thioether was evaporated from the liquid reaction product. The correctness of the formulation $Co_4(CO)_{11}(SMe_2)$ was evidenced, besides the elemental analysis, by the striking

Table II

Infrared absorption spectra in the C—O stretching region of $Co_4(CO)_{11}(SR_2)$ complexes in hexane solution

Thioether	ν_{CO}, cm^{-1}
Me_2S	2087 (m), 2043 (vs), 2036 (s,sh), 2011 (m), 1998 (m), 1860 (w), 1850 (m), 1831 (m), 1804 (vw)
$(n\text{-}Bu)_2S$	2086 (m), 2047 (s), 2040 (vs), 2030 (s), 2014 (m), 2002 (m), 1859 (vw, sh), 1849 (m), 1828 (m), 1819 (vw, sh)

similarity of its IR spectrum in the C—O stretching region to those of the compounds $Co_4(CO)_{11}PR_3$ ($R = C_6H_5$, $n\text{-}C_4H_9$) [18].

As to our knowledge, this dimethyl sulphide complex is the first isolated monosubstituted derivative of tetracobalt dodecacarbonyl to be reported.* The complex yielded metallic cobalt and dimethylsulphide on thermal decomposition and not cobalt sulphide, in contrast to the complexes obtained from cobalt carbonyls and mercaptans [6]. This observation shows the coordinative sulphur-cobalt single bond to be rather weak.

The formation of an analogous di-*n*-butyl sulphide derivative in solution was evidenced by infrared spectroscopy: the two thioether derivatives of tetracobalt dodecacarbonyl show similar infrared spectra in the C—O stretching region, as can be seen from Table II.

Influence of dialkyl sulphides on the catalytic effect of cobalt carbonyls

The formation of thioether-substituted cobalt carbonyls obviously can also take place under the conditions of catalytic reactions, although the high carbon monoxide pressures used in these cases strongly shift substitution equilibria in favour of the unsubstituted carbonyl complexes. In principle,

* Note added in proof: recently some complexes of type $Co_4(CO)_{11}L$ ($L = PPh_3$, $AsPh_3$, $SbPh_3$) have been reported [CETINI, G., GAMBINO, O., ROSSETTI, R., STANGHELLINI, P. L.: Inorg. Chem. 7, 609 (1968)].

however, an influence of saturated aliphatic thioethers on the catalytic activity of cobalt carbonyls cannot be excluded. The problem is of interest, because the mechanisms proposed for hydroformylation [19] and aldehyde hydrogenation [20] do not exclude the participation of thioether-substituted cobalt carbonyls [*e.g.*, $Co_2(CO)_7(SR_2)$, $HCo(CO)_3(SR_2)$ etc.] in these reactions. A similar case is encountered in the presence of tertiary phosphines, for which the participation of similar phosphine-substituted cobalt carbonyl derivatives in the hy-

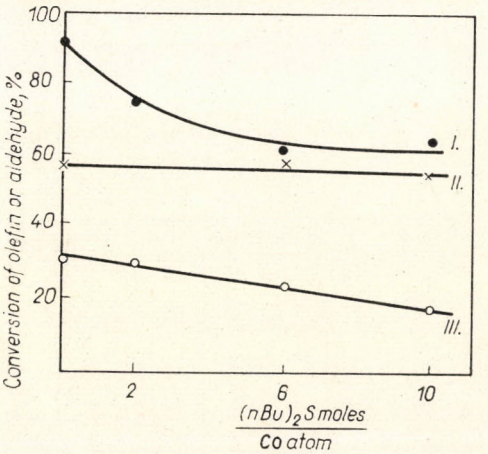


Fig. 1. Effect of di-*n*-butyl sulphide on olefin hydroformylation and aldehyde hydrogenation with cobalt carbonyl catalysts. I: Hydroformylation of cyclohexene, 100°C; carbon monoxide partial pressure: 20 atm. II: Hydroformylation of cyclohexene, 110°C; carbon monoxide partial pressure: 100 atm. III: Hydrogenation of butyraldehyde, 150°C; carbon monoxyde partial pressure: 80 atm.

droformylation reaction has been proved [21]; these ligands exert a pronounced-modifying influence on the catalytic properties of cobalt carbonyls [22—27].

The effect of thioethers, however, must be much smaller than that of tertiary phosphines, sinc eotherwise the experiments performed up till now in this direction would not have yielded negative results. Conditions were therefore chosen which ensured only a partial conversion of olefins (or aldehydes) in the absence of any sulphur compound, thus enabling the observation of much smaller effects than under conditions leading to almost total conversions, used in the previous investigations [1, 3].

The results of three series of experiments are shown in Fig. 1. It can be seen, that di-*n*-butyl sulphide has a small, but definite retarding effect both on hydroformylation and hydrogenation. This retarding effect, however, is not caused by cobalt sulphide formation as in the cases of most sulphur compounds [1—3], since the cobalt content of the reaction products is not affected by using even relatively high (10 : 1) S : Co ratios. The thioether exerts its influence obviously through the formation of the $Co(CO)_7(SR_2)$ complex.

This conclusion is supported by the infrared spectra of the products obtained at high S : Co ratios, which show, besides the absorption bands of $Co_2(CO)_8$, those of the monosubstituted di-*n*-butyl sulphide derivative. The retarding effect of the thioether can be compensated by raising the carbon monoxide partial pressure, which is in accordance with the reversibility of Reaction (1).

The results show that the $Co_2(CO)_7(SR_2)$ complexes are either inactive, or at least less active catalysts for hydroformylation and hydrogenation, than unsubstituted $Co_2(CO)_8$. The data available up till now are not sufficient to distinguish which step of the whole catalytic cycle is actually inhibited by substituting one carbon monoxide with a thioether ligand. In general, the use of ligands which can reversibly substitute carbon monoxide must have the same effect as an increase of the carbon monoxide concentration, *i.e.* its partial pressure. Since this latter is known to retard practically all reactions catalyzed by metal carbonyls, the observed retarding effect of di-*n*-butyl sulphide is just a special case of this general phenomenon.

Experimental

Reaction of $(n\text{-Bu})_2S$ with $Co_2(CO)_8$ and $Co_4(CO)_{12}$

Crystalline dicobalt octacarbonyl (0.25 g; 0.73 mmole) was placed in a Schlenk tube that had been flushed with carbon monoxide, and di-*n*-butyl sulphide (3.5 g; 24 mmoles) was added to it. $Co_2(CO)_8$ rapidly dissolved in the thioether and gas was evolved from the reaction mixture. The gas evolution stopped after 90 min.; the total quantity of gas evolved was 17.4 Nml (0.78 mmole). This corresponds to 1.07 mole of carbon monoxide per mole dicobalt o.tacarbonyl.

In a similar experiment with tetracobalt dodecacarbonyl, 1.06 moles of carbon monoxide were evolved per mole of the metal carbonyl used.

Reversibility of the reaction between Me_2S and $Co_2(CO)_8$

In a Schlenk tube flushed with carbon monoxide, dicobalt octacarbonyl (0.50 g; 1.46 mmoles) was dissolved in *n*-heptane (14.4 ml) and dimethyl sulphide (6.1 g; 98 mmoles) was added. The evolution of gas gradually slowed down, the infrared spectrum of a sample taken after 30 min. showed only the bands attributed to $Co_2(CO)_7(SMe_2)$ and $Co_2(CO)_6(SMe_2)_2$.

Subsequently carbon monoxide was bubbled through the reaction mixture for 90 min. The infrared spectrum of a sample taken after this time showed only bands characteristic for $Co_2(CO)_8$ at 2067, 2059, 2042, 2031, 2023, 1866 and 1857 cm^{-1}.

Reversibility of the reaction between Me_2S and $Co_4(CO)_{12}$

This experiment was conducted under the same conditions as those described above for dimethyl sulphide and dicobalt octacarbonyl, with the exception that the reaction time required for the formation of the thioether-substituted complex, $Co_4(CO)_{11}(SMe_2)$, was found to be 2 hrs.

During the bubbling of carbon monoxide into the reaction mixture, black crystals separated on the gas inlet tube, which rapidly became plugged. These crystals were sparingly soluble in hexane and the infrared spectrum of this hexane solution showed bands characteristic for $Co_4(CO)_{12}$ at 2063, 2055 and 1867 cm^{-1}. The liquid part of the reaction product had the same spectrum.

Preparation of $Co_4(CO)_{11}(SMe_2)$ from $Co_4(CO)_{12}$ and dimethyl sulphide

Tetracobalt dodecacarbonyl (0.57 g; 1 mmole) was mixed in a Schlenk tube with dimethyl sulphide (4.0 g; 64 mmoles) and the mixture was allowed to stand at room temperature for 2 hrs. After this time, gas evolution stopped and a dark brown liquid product was obtained. The excess dimethyl sulphide was evaporated at room temperature in vacuum to obtain a black crystalline material (0.45 g; 74%, based on tetracobalt dodecacarbonyl). $C_{13}Co_4H_6O_{11}S$. Calcd. Co 38.91; C 25.75; H 1.00; S 5.29. Found Co 38.8; C 25.5; H 1.33; S 4.85%.

Formation of $Co_4(CO)_{11}(SMe_2)$ from $Co_2(CO)_8$ and dimethyl sulphide

Dicobalt octacarbonyl (6.3 g; 21.5 mmoles) and dimethyl sulphide (17.8 g; 290 mmoles) were reacted in a Schlenk tube for 2 hrs. After this time, gas evolution ceased and a dark brownish-red liquid product was obtained. This product showed the infrared absorption bands attributed to $Co_2(CO)_7SMe_2$ and $Co_2(CO)_6(SMe_2)_2$.

After evaporation of the excess dimethyl sulphide in vacuum at room temperature, a black crystalline material was obtained, which showed in hexane solution the infrared absorption bands characteristic of $Co_4(CO)_{11}(SMe_2)$. This solid product had approximately correct analysis for $Co_4(CO)_{11}(SMe_2)$. $C_{13}Co_4H_6O_{11}S$. Calcd. Co 38.91; C 25.75; H 1.00; S 5.29. Found Co 36.8; C 23.1; H 1.27; S 6.19%.

Thermal decomposition of $Co_4(CO)_{11}(SMe_2)$

$Co_4(CO)_{11}(SMe_2)$ (0.3881 g) was heated in a Schlenk tube to 150C° for 45 min. In the receiver, connected to the Schlenk tube and cooled to —78°C, a few drops of a colourless liquid condensed. This liquid was identified by G. L. C. as dimethyl sulphide. The solid which remained in the Schlenk tube was practically insoluble in hexane; it contained 89.4% cobalt and only 1.08% sulphur.

Hydroformylation of cyclohexene

Toluene (225 g), dicobalt octacarbonyl (0.50 g; 4.25 mmoles) and di-*n*-butyl sulphide (12.4 g; 85 mmoles) were placed in a 1-litre autoclave. The autoclave was flushed and pressurized to 140 atm. with synthesis gas ($CO + H_2$), heated to 150°C, held at this temperature for 1 hr., and then cooled to 110°C. (This technique was used to eliminate any occasional detrimental effect of oxygen or other impurities, by reducing them to inert compounds.) Following this, cyclohexene (25 g; 305 mmoles) was injected, and the reaction conditions (110°C and 200 atm.) were maintained for additional 3 hrs by feeding synthesis gas at a rate necessitated by the gas absorption due to hydroformylation.

After this period the autoclave was cooled to room temperature, and the brownish-red liquid product [cobalt content 0.18%, infrared spectrum showing the presence of $Co_2(CO)_8$ and $Co_2(CO)_7(SMe_2)$] was heated in a closed vessel to 200°C to decompose the dissolved cobalt carbonyl complexes. The cobalt-free product was analyzed for functional groups (aldehyde, olefinic double bond) by the conventional methods.

Hydrogenation of *n*-butyraldehyde

In these experiments hexane (200 g), *n*-butyraldehyde (57.6 g; 0.78 moles) and dicobalt octacarbonyl (0.51 g; 8.7 mmoles) were used in the presence of varying amounts of di-*n*-butyl sulphide. The reaction conditions were: 150°C, 200 atm. ($CO + H_2$), and 1 hr.

Work-up and analysis of the products were made in the same way as in the hydroformylation experiments.

Infrared spectra were obtained with a UR—10 instrument, Carl Zeiss Jena, with LiF prism. The recorded wave numbers are correct within ± 2 cm^{-1}.

*

The author gratefully acknowledges a pleasant cooperation and valuable discussions with Dr. G. Bor and Mr. J. Laky, and his thanks are due for the skilful technical assistance of Mrs. Z. Nagy-Magos and Mr. P. Szabó.

REFERENCES

1. MACHO, V.: Chem. Zvesti (Bratislava) **15,** 181 (1961)
2. FREUND, M., MARKÓ, L.: Brennstoff-Chem. **46,** 100 (1965)
3. LAKY, J., SZABÓ, P., MARKÓ, L.: Acta Chim. Acad. Sci. Hung. **46,** 247 (1965)
4. MARKÓ, L., BOR, G., KLUMPP, E., MARKÓ, B., ALMÁSY, G.: Chem. Ber. **96,** 955 (1963)
5. MARKÓ, L., BOR, G., KLUMPP, E.: Angew. Chem. **75,** 248 (1963)
6. KLUMPP, E., MARKÓ, L., BOR, G.: Chem. Ber. **97,** 926 (1964)
7. KHATTAB, S. A., MARKÓ, L., BOR, G., MARKÓ, B.: J. Organometal. Chem. **1,** 373 (1964)
8. KLUMPP, E., BOR, G., MARKÓ, L.: Chem. Ber. **100,** 1451 (1967)
9. KLUMPP, E., BOR, G., MARKÓ, L.: J. Organometal. Chem. **11,** 207 (1968)
10. BOR, G.: Proc. Symp. Coord. Chem., Tihany, Hungary p. 361. Akadémiai Kiadó, Budapest, 1964
11. POILBLANC, R., BIGORGNE, M.: Bull. soc. chim. France **1962,** 1301
12. BOUQUET, G., BIGORGNE, M.: Bull. soc. chim. France **1962,** 433
13. BOR, G.: Spectrochim. Acta **19,** 1209, 2065 (1963)
14. NOACK, K.: Spectrochim. Acta **19,** 1925 (1963); Helv. Chim. Acta **47,** 1064, 1555 (1964)
15. COTTON, F. A., ZINGALES, F.: Chem. Ind. (London) **1960,** 1219; Inorg. Chem. **1,** 145 (1962)
16. MERIWETHER, L. S., FIENE, M. L.: J. Am. Chem. Soc. **81,** 4200 (1959)
17. SZABÓ, P., FEKETE, L., NAGY-MAGOS, Z., BOR, G., MARKÓ, L.: J. Organometal. Chem. **12,** 245 (1968)
18. SZABÓ, P., BOR, G., MARKÓ, L.: Unpublished results
19. BRESLOW, D. S., HECK, R. F.: Chem. Ind. (London) **1960,** 467
20. MARKÓ, L.: Proc. Chem. Soc. (London) **1962,** 67
21. PIACENTI, F., BIANCHI, M., BENEDETTI, E.: Chim. Ind. (Milano) **49,** 245 (1967)
22. SLAUGH, L. H., MULLINEAUX, R. D.: Belg. Pat. 606 408, 621 662, 621 833 (1962); French Pat. 1 300 404 (1962)
23. EISENMANN, J. L., YAMARTINO, R. L.: Ger. Pat. 1 146 485 (1963)
24. CANNELL, L. G., SLAUGH, L. H., MULLINEAUX, R. D.: D. P. Auslegeschrift 1 186 455 (1965)
25. Brit. Pat. 988 941 (1965)
26. GREENE, C. R., MEEKER, R. E.: D. P. Auslegeschrift 1 212 953 (1966)
27. PALM, C.: D. P. Auslegeschrift 1 230 010 (1966)

László MARKÓ; Veszprém, Schönherz Z. u. 12. Hungary

Acta Chimica Academiae Scientiarum Hungaricae, Tomus 59 (3—4), pp. 397—400 (1969)

DARSTELLUNG UND EIGENSCHAFTEN VON δ-OXOGERANIUMSÄURE

I. ALKONYI und A. SÁNDOR

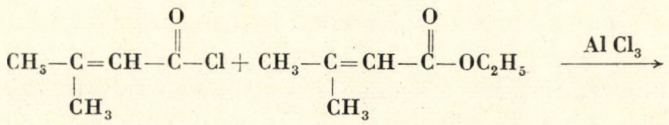
(Aus dem Biochemischen Institut der Universität Pécs)

Eingegangen am 15. März 1968

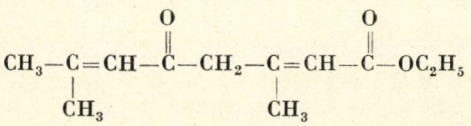
Eine früher bereits beschriebene Methode der Verfasser wurde zur Synthese des δ-Oxogeraniumsäureäthylesters angewendet. Der Dimethylacrylsäureäthylester kann an seiner endständigen Methylgruppe unter Friedel—Crafts-Bedingungen mit dem Chlorid der eigenen Säure acyliert werden, wobei eine monoterpenartige Verbindung mit 10 Kohlenstoffatomen erhalten wird. Die freie δ-Oxogeraniumsäure und ihr Äthylester wurden auf Grund ihrer spektralen Eigenschaften und durch Herstellung verschiedener Derivate identifiziert.

ββ-Dimethylacrylsäureäthylester **2** wird durch Acetylchlorid in Gegenwart von wasserfreiem Aluminiumchlorid glatt acetyliert [1]. Die Substitution erfolgt an der endständigen Methylgruppe. Wir haben diese Reaktion als eine ungewöhnliche Acylierung beschrieben, und die darin liegenden synthetischen Möglichkeiten gezeigt. LOHAUS, FRIEDRICH und JESCHKE haben später in einer umfangreichen Publikation [2] diese Acylierung mit einer größeren Anwendungsbreite formuliert und mit vielen Beispielen belegt. Wir wollen nun in der vorliegenden Arbeit die Darstellung von δ-Oxogeraniumsäureäthylester nach dieser Acylierungsmethode beschreiben.

ββ-Dimethylacrylsäureäthylester **2** kann auf Grund seines Kohlenstoffskeletts (wenn man von der Äthoxygruppe absieht) als isoprenoide Einheit angesehen werden. Wir versuchten daher, ββ-Dimethylacrylsäurechlorid **1** als Acylierungsmittel anzuwenden und damit zwei isoprenoide Einheiten zu verknüpfen.



1 **2**



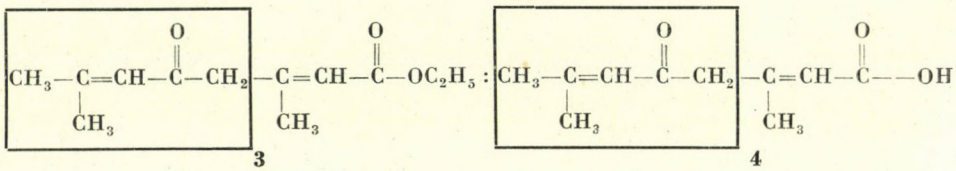
3

Die geplante Reaktion verläuft unter starker Wärmeentwicklung; mit mäßiger Ausbeute (36%, bezogen auf umgesetztes **2**) entsteht der δ-Ketogeraniumsäureester **3**.

3 ist stereochemisch warscheinlich nicht einheitlich, da es kein Semicarbazon bildet und mit 2.4-Dinitrophenylhydrazin nur eine ölige Abscheidung liefert.

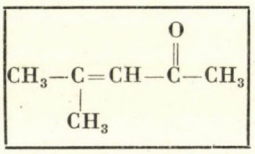
Zum Strukturbeweis für **3** seien folgende Argumente angeführt:

a) Die spektralen Eigenschaften des Oxoesters **3** und der freien Säure **4** sind denen des Mesityloxyds **5** sehr ähnlich:



3 **4**

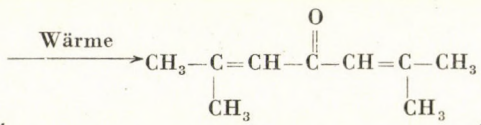
λ_{max} 243 mμ (Wasser) λ_{max} 245 mμ (Wasser)



5

λ_{max} 244,5 Mμ (Wasser)[4]

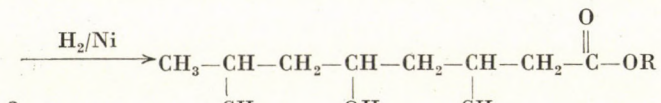
b) Die freie Säure **4** wird leicht in das wohlbekannte ungesättigte Keton (Phoron) **6**, umgewandelt:



4 **6**

6 wurde UV-spektrometrisch, sowie durch Analyse, Schmp. und Misch-Schmp. seines 2,4-Dinitro-phenylhydrazons identifiziert. Die Decarboxylierung von **4** erfolgt bei 100°C in 2 Stdn. mit fast quantitativer Ausbeute.

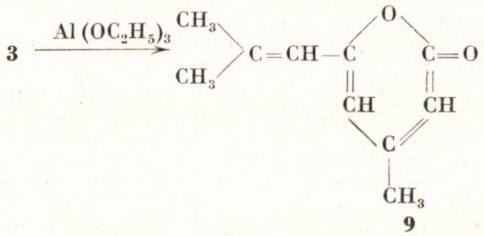
c) Reduziert man **3** in Gegenwart von Raney-Nickel, so gewinnt man den 4-Hydroxy-2.6-dimethyloctansäure -(8)-äthylester **7**, der nach Verseifung die ölige Hydroxysäure **8** liefert.



3 **7** : R = C_2H_5 **8** : R = H

Die Hydroxysäure **8** überführten wir in das kristallisierte p-Toluidid [5].

Erhitzt man den Oxoester **3** mit Aluminiumäthylat, so bildet sich ein flüssiges Lacton, dessen Konstitution **9** die Analyse und das spektrale Verhalten belegen.



9

Beschreibung der Versuche

Alle Schmelzpunkte sind unkorrigiert. Die Spektren wurden mit dem Gerät »Spektronom 202« aufgenommen.

δ-Oxogeraniumsäureäthylester, 3

In einem Kolben mit Rückflußkühler, Tropftrichter und mechanischem Rührer wurden zur Suspension von 124,8 g (0,93 Mol) wasserfreiem Aluminiumchlorid in 300 ml trockenem Schwefelkohlenstoff tropfenweise 70,0 g (0,54 Mol) ββ-Dimethylacrylsäurechlorid 1 und 63,08 (0,50 Mol) ββ-Dimethylacrylsäureäthylester in 80 ml Schwefelkohlenstoff gegeben. Nach Zugabe von einigen Tropfen wurde die Reaktion durch gelindes Erwärmen in Gang gesetzt und dann ohne weitere Wärmezufuhr die Lösung mit einer Geschwindigkeit eingetragen, die gerade genügte, die Suspension in gelindem Sieden zu halten und eine allzu stürmische Entwicklung von Chlorowasserstoff zu vermeiden. Nach Beendigung des Zutropfens wurde 2 Std. gerührt.

Drei solche Ansätze wurden vereinigt, die obere Schwefelkohlenstoff-Schicht wurde abgegossen und die untere braune ölige Phase vorsichtig in Ammoniumchlorid enthaltendes Wasser gegossen. Nach Ausziehen mit Äther wurde die Ätherlösung mit 150 g Chinolin und etwas wasserfreiem Natriumsulfat versetzt, über Nacht stehen gelassen, nach Abtreiben des Äthers wurde der Rückstand 8 Std. auf dem Dampfbad erhitzt, dann auf 90 g konz. Schwefelsäure und Eisstücke enthaltendes Wasser gegossen und abermals mit Äther ausgeschüttelt. Nach der üblichen Aufarbeitung und Vakuumdestillation wurden 114 g Ausgangssubstanz **2** (Sdp.$_2$ 40° C, n_D^{20} 1,347) zurückgewonnen. Nach viermaliger Vakuumdestillation erhielten wir 56,2 g **3** (36%) Sdp.$_2$ 96—98°, n_D^{20} 1,493, λ_{max} 243 mμ (Wasser). ε_{max} 13,150. $C_{12}H_{18}O_3$ (210,3) Ber. C 68,57 H 8,63 Gef. C 68,90 H 8,73.

Bildung von Phoron, 6

Zu einer Lösung von 0,92 g (40 mg-Atom) Na in 100 ml absol. Äthanol wurden 8,2 g (39 m Mol) δ-Oxogeraniumsäureester **3**, dann 0,72 g (40 m Mol) Wasser gegeben. Die Lösung färbte sich rot und wurde 24 Std. bei Raumtemperatur stehen gelassen. Das Äthanol wurde bei 50° C Badtemperatur i. Vak. abgedampft, der Rückstand in 50 ml Wasser aufgenommen und mit Äther dreimal (je 30 ml) gewaschen. Nach der üblichen Aufarbeitung wurden 6 g ölige Säure 4 erhalten, die ohne Reinigung 2 Std. bei 100°C gehalten, dann in 50 ml Äther aufgenommen und einmal mit 20 ml *n* NaOH und dreimal mit 30 ml Wasser gewaschen wurden. Nach einmaligem Destillieren 3 g 6: λ_{max} 270 mμ ε_{max} 22 000 (Wasser). Ein authent. Präparat zeigte ebenfalls λ_{max} 270 mμ (Wasser). Lit. [6]: λ_{max} 273,5 mμ (Wasser). Das 2,4-Dinitrophenylhydrazon wurde an Al_2O_3, Talcum (70 : 30) chromatographiert, nach Elution (untere, rote Zone) mit Benzol eingedampft und aus Äthanolum kristallisiert. Schmp. 112,8° C. Misch-Schmp. mit einem authentischen Präparat. 113 °C. Lit. Schmp. 109 °C [7].

4-Hydroxy-2,6-dimethyloctansäure-(8)-äthylester, 7

10 g **3** in 100 ml Äthanol wurde in Gegenwart von 10 g Raney-Nickel bei 110 at. Anfangsdruck hydriert. Die übliche Aufarbeitung lieferte 5,6 g 7 Sdp.$_2$ 100—105°, n_D^{20} 1,435.
$C_{12}H_{24}O_3$ (216,3) Ber. C 66,64 H 11,18 Gef. C 67,00 H 10,95.

4-Hydroxy-2,6-dimethyloctansäure, 8

Verseifung von 5,5 g 7 erbrachte 2,8 g 8 als ölige Säure. Sie wurde nach KORTE und MACHLEIDT in das *p*-Toluidid überführt, Schmp. 104,4°C (aus Petroläther).
$C_{17}H_{27}NO_2$ (277,4) Ber. C 73,61 H 9,81 Gef. C 73,53 H 9,79.

4-Methyl-6-isobutenyl-α-pyron, 9

7,0 g 3 wurde mit 3,5 g Aluminiumäthylat in 50 ml abs. Äthanol 40 Std. gekocht. Die Aufarbeitung, wie im Falle des 4,6-Dimethyl-α-pyrons [1], erbrachte 2,53 g 9 λ_{max} 330 mμ ε_{max} 3750.
$C_{10}H_{12}O_2$ (164,2) Ber. C 73,15 H 7,36 Gef. C 73,00 H 7,26.

LITERATUR

1. ALKONYI, I.: Chem. Ber. **98,** 3099 (1965)
2. LOHAUS, G., FRIEDRICH, W., JESCHKE, J. P.: Chem. Ber. **100,** 658 (1967)
3. Man verfuhr dabei wie in SHRINER, R. L. und FUSON, R. C.: The Systematic Identification of Organic Compounds. New York, John Wiley and Sons Inc., London, Chapman and Hall, Ltd., 1948. S. 171.
4. JAFFÉ, H. H. und ORCHIN, M.: Theory and Applications of Ultraviolet Spectroscopy. John Wiley and Sons, Inc., New York—London, 1962. S. 260.
5. KORTE, F., MACHLEIDT, H.: Chem. Ber. **88,** 141 (1955)
6. SCHEIBE, G.: Ber. dtsch. chem. Ges. **58,** 595 (1925)
7. WILEY, R. H., ESTERLE, J. G., HUSSUNG, K. F., DESILVA, C. L. und SLAYMAKER, S. C.: J. Org. Chemistry **22,** 1737 (1957)

István ALKONYI
Attila SÁNDOR
Pécs, Rákóczi út 2. Ungarn

Acta Chimica Academiae Scientiarum Hungaricae, Tomus 59 (3—4), pp. 401—410 (1969)

NITRATION IN THE PRESENCE OF BORON FLUORIDE CATALYST

Z. CSŰRÖS GY. DEÁK, L. FENICHEL and A. TÖRÖK-KALMÁR

(Department of Organic Chemical Technology, Technical University, Budapest)

Received May, 15 1968

The catalytic effect of boron fluoride and its complexes $BF_3 \cdot H_2O$, $BF_3 \cdot 2H_2O$ and $BF_3(CH_3COOH)_2$, has been studied in the reaction of *o*-nitrotoluene and fuming nitric acid. These compounds strongly promote, or bring to completion, the reaction of mono-nitration. The influence of the concentration of BF_3 and its complexes, as well as that of the reaction time, on the yield has been investigated.

The kinetic results for the nitration of toluene with nitric acid indicate first order dependence of the rate on both the toluene and BF_3 concentrations. The results prove that nitration is catalyzed by boron fluoride, and they support the reaction mechanism involving nitronium ion.

The nitrating properties of a mixture of nitric acid-boron fluoride have been studied by THOMAS *et al.* [1]. The mixture has been found to be an efficient nitrating agent for aromatic compounds which show reduced activity in electrophilic substitution, such as nitrobenzene; nitration occurs according to the equation:

$$ArH + HNO_3 + BF_3 \rightarrow Ar{-}NO_2 + BF_3 \cdot H_2O. \qquad (1)$$

On the basis of spectroscopic studies GERDING *et al.* [2] assumed that nitric acid with boron fluoride gives nitronium ion in a reversible reaction:

$$HNO_3 + BF_3 \rightleftharpoons NO_2^+ + BF_3OH^- \qquad (2)$$

In the present paper we report a study of the effect of boron fluoride and its complexes on the nitrating power of nitric acid and on the product composition. Nitrotoluene has been selected as a substrate, because if offers a possibility for determing the ratio of isomeric products, and at the same time, it is sufficiently deactivated for electrophilic substitution to allow comparison of the strengths of nitrating agents. First, nitration was studied in preparative experiments; 0.25 mole of *o*-nitrotoluene was mixed with 0.33 mole of fuming nitric acid. The mixture was saturated under cooling and stirring with gaseous boron fluoride and thereafter heated for 30 min. Approximately 0.25 mole of boron fluoride was absorbed. The mixture was poured into water, washed free of acid, and dried. The product consisted mainly of isomeric dinitrotoluenes accompanied by some trinitrotoluene and a small

amount of unreacted *o*-nitrotoluene. Trinitrotoluene was identified by HALFTER's chromatographic method [3]. No trinitrotoluene was found among the products, if after saturation with boron fluoride the reaction temperature did not exceed 60°C.

In order to determine the isomeric composition of the product, 2,3-, 2,4-, 2,5-, 2,6-, and 3,4-dinitrotoluene have been prepared or purchased, and

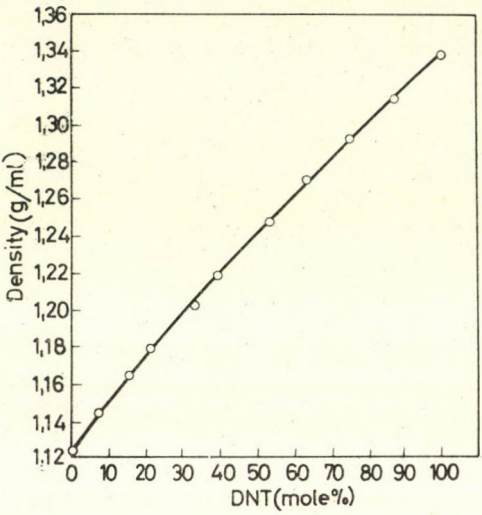


Fig. 1. Densities of *o*-nitrotoluene-dinitrotoluene mixtures at 60 °C as a function of the composition (ratio of 2,4- to 2,6-dinitrotoluene: 66 : 34)

their IR-spectra recorded [4]. According to GIBSON *et al.* [5], these are the isomers formed during the nitration of nitrotoluene.

The IR spectrum of the nitration product obtained in the presence of boron fluoride showed that it consisted of 2,4- and 2,6-dinitrotoluene almost exclusively, as it contained 66% and 34% of 2,4- and 2,6-dinitrotoluene, respectively. This is almost identical with the 66.6 : 33.3 isomer ratio [5] obtained with $HNO_3 - H_2SO_4$ nitrating mixtures, indicating that nitration takes place *via* the nitronium ion, similarly to the known mechanism of the reaction with mixed acid.

The 66 : 34 mixture of the 2,4- and 2,6-dinitrotoluene isomers was mixed with varying amounts of *o*-nitrotoluene, and the densities were determined at 60°C.

The density *vs.* composition curve was used to determine the conversion during reaction (Fig. 1).

In order to elucidate the effect of the added quantity of boron fluoride on the nitration, yields after 30 min. at 40° have been determined as a function of the amount of BF_3. The results shown in Fig. 2 indicate that the yields

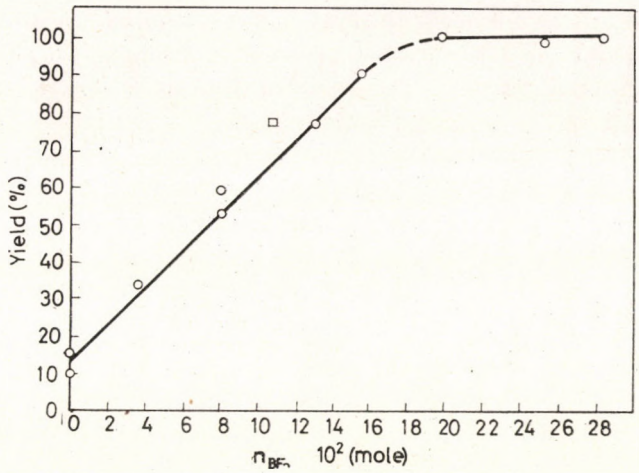


Fig. 2. Nitration of *o*-nitrotoluene with HNO_3 in the presence of BF_3 (0.25 mole of *o*-nitrotoluene, 0.33 mole of HNO_3; ○ — heating at 40 °C for 30 min.; □ — for 60 min.)

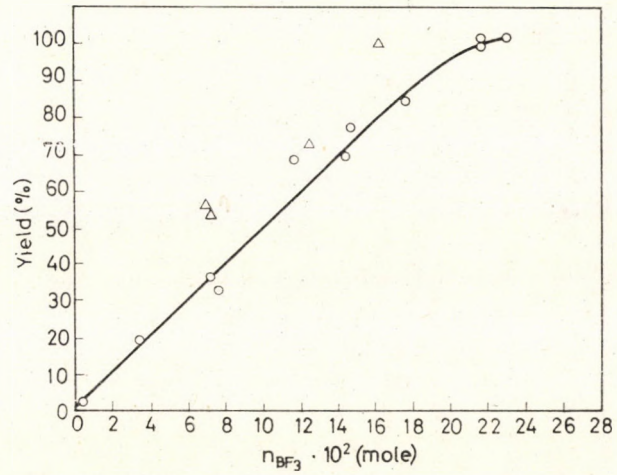


Fig. 3. Nitration of *o*-nitrotoluene with HNO_3 in the presence of BF_3 in nitromethane; ○ — 0.25 mole of *o*-nitrotoluene (0.33 mole of HNO_3; heating at 40 °C for 30 min.); △ — the same except that 100 g of $CaSO_4$ was added

(up to 90%), and presumably the rates of the reactions, are proportional to the amount of boron fluoride added. In the absence of BF_3 the yield is only 12%, while the use of 0.192 mole of boron fluoride for 0.25 mole of *o*-nitrotoluene gives yields as high as 100%.

o-Nitrotoluene is soluble in nitric acid, but two separate phases appear when BF_3 is introduced. Since it was desirable to carry out the reaction in homogeneous solution, the experiments were repeated in nitromethane as a solvent (Fig. 3). The results are similar to those obtained without solvent, the yields (up to 80%) being proportional to the amount of the boron fluoride

added. The yield at a given amount of BF_3 is lower than in the nitration without solvent, but the decrease is smaller than it would be expected on the basis of dilution by the solvent. The effect of dilution is partly compensated by a faster reaction in the homogeneous medium.

Boron fluoride may play a dual part in nitration being a catalyst and/or a dehydrating agent.

If boron fluoride would act only as a dehydrating agent, inert drying agents would obviously be capable of performing the same function. Anhydrous calcium sulphate (Drierite) is a strong dehydrating agent and it does not interact with any of the components in the mixture. According to Fig. 3, calcium sulphate alone is unsuitable to replace boron fluoride, as practically no nitration takes place in the absence of BF_3. However, if $CaSO_4$ and BF_3 are used together, the yield is higher than in the absence of a dehydrating agent. These results prove the catalytic effect of BF_3, but do not preclude a dual function.

If the nitration is carried out without a solvent, introduction of BF_3 gives rise to the formation of a lower aqueous and an upper organic layer. The lower layer probably consists of an equilibrium mixture of boron fluoride and nitric acid, and of the aquo-complexes formed with the water released during nitration. As regards the efficiency and capacity of BF_3 as a catalyst for nitration, it is an important question whether the aquo-complexes, $BF_3 \cdot H_2O$ and $BF_3 \cdot 2H_2O$, are catalytically active. The experimental results concerning nitration experiments in the presence of boron fluoride aquo-complexes are shown in Table I.

It can be concluded from the Table that the aquo-complexes of boron trifluoride also promote nitration. An equimolar mixture of $BF_3 \cdot H_2O$ with nitrotoluene gives rise to almost complete nitration. If the complex is added in excess, even 100% yield can be achieved. Although much less effective, the $BF_3 \cdot 2H_2O$ complex still has a promoting effect on nitration. Low yields are obtained in nitromethane solvent, but they are higher in the presence of anhydrous calcium sulphate.

In order to show that $BF_3 \cdot H_2O$ is formed as a by-product of the reaction in the presence of BF_3, the spent acid was separated after nitration and added to a mixture of *o*-nitrotoluene and nitric acid. A yield of 82% was obtained by carrying out the nitration, as described above, but without adding fresh $BF_3 \cdot H_2O$; this yield is fairly close to the 91% obtained with the $BF_3 \cdot H_2O$ complex.

Since it is difficult to handle gaseous boron fluoride in the laboratory, the liquid $BF_3 \cdot 2CH_3COOH$ complex has also been used. The 2,4- to 2,6-dinitrotoluene isomer ratio was found to be 66 : 34, in agreement with the results obtained previously. Thus, the fact that instead of pure BF_3 an acetic acid complex is used, does not change the ratio of the isomers in the nitration

product, obviously leaving the reaction mechanism unaltered, too. The catalytic effect of $BF_3 \cdot 2CH_3COOH$ in the nitration is illustred in Fig. 4. The curve is not as steep as with gaseous BF_3. The effectivities of BF_3 and its complexes are compared in Table II.

Table I

Nitration of o-nitrotoluene in the presence of the aquo-complexes of boron fluoride at 40 °C
(0.25 mole of *o*-nitrotoluene, 0.33 mole of fuming nitric acid; heating time: 30 min.)

Complex			Yield (%)	Note
Formula	g	mole		
$BF_3 \cdot H_2O$	42.6	0.496	100	
	42.9	0.500	100	
	20.9	0.243	91	
	21.3	0.248	91	
	11.8	0.137	55	
	11.6	0.135	54	
	20.9	0.243	55	*a*
	22.7	0.264	59	*a*
	21.1	0.246	74	*a, b*
	21.7	0.253	78	*a, b*
	21.0	0.244	69	*a, b*
$BF_3 \cdot 2H_2O$	52.9	0.509	47	
	51.8	0.498	42	
	26.1	0.251	36	
	24.0	0.231	35	
	25.7	0.247	10	*a*
	26.2	0.252	5	*a*

a: in 50 ml of nitromethane as solvent
b: in the presence of 100 g of $CaSO_4$ (Drierite)

Table II

The efficiency of BF_3 and its complexes in the nitration of o-nitrotoluene

Reagent	Yield (%)	
	BF_3/*o*-nitrotoluene molar ratio: 1 : 1	BF_3/*o*-nitrotoluene molar ratio: 1 : 2
BF_3	100	76
$BF_3 \cdot H_2O$	91	54
$BF_3 \cdot 2H_2O$	36	—
$BF_3 \cdot 2CH_3COOH$	76	54
without BF_3	12	

It is remarkable that no really great difference can be observed between the catalytic activities of BF_3 and $BF_3 \cdot H_2O$, especially considering the fact that BF_3 is converted to its aquo-complex in the reaction. $BF_3 \cdot 2CH_3COOH$ is a less effective catalyst for nitration than $BF_3 \cdot H_2O$. This is partly due to dilution effects: the aquo-complex contains 79%, while the acetic acid complex only 36.1% of boron fluoride. To demonstrate the dilution effect of acetic acid, it was added in various amounts to reaction mixtures containing identical amounts of $BF_3 \cdot 2CH_3COOH$ (Fig. 5). The nitration yield has been found to decrease in a direct proportion to the amount of acetic acid added. However, while the addition of 11 g of acetic acid to 64.6 ml of the reaction mixture

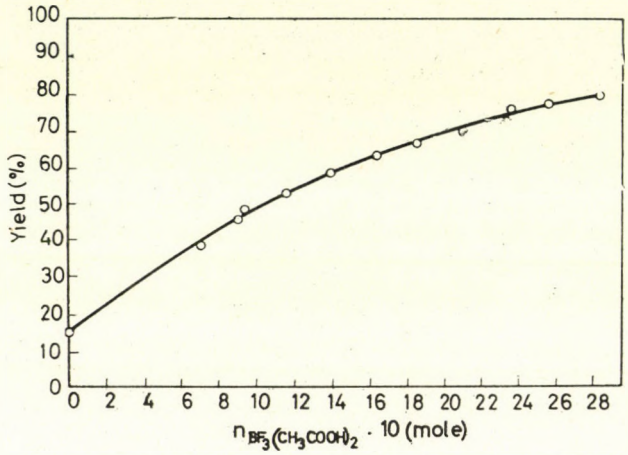


Fig. 4. Nitration of *o*-nitrotoluene with HNO_3 in the presence of 93% $BF_3(CH_3COOH)_2$ (0.25 mole of *o*-nitrotoluene, 0.33 mole of HNO_3; heating at 40° C for 30 min.)

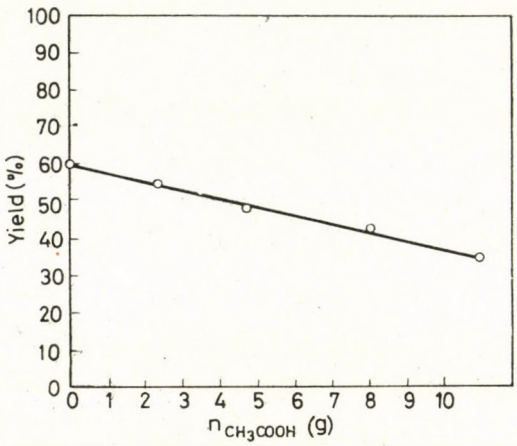


Fig. 5. Nitration of *o*-nitrotoluene with HNO_3 in the presence of 93% $BF_3(CH_3COOH)_2$, as a function of the amount of acetic acid added [0.25 mole of *o*-nitrotoluene, 0.33 mole of HNO_3, 0.140 mole of $BF_3(CH_3COOH)_2$; heating at 40 °C for 30 min.]

brings about a dilution by 17 (v/v), the yield drops from 58.5% to 36%, which is a 38.6% decrease relative to the conditions with no dilution. This means that acetic acid not only dilutes the mixture but, being a Lewis base, it probably causes a redistribution of BF_3, resulting in a slower reaction:

$$BF_3 \cdot H_2O + 2\ CH_3COOH \rightleftharpoons BF_3 \cdot 2CH_3COOH + H_2O. \qquad (3)$$

A study of the time-course of the reaction (Fig. 6) shows that after about 1.5 hr. of heating an equilibrium is attained and the yield levels off. (In all cases we started to measure the time of heating after a 10-min. period of

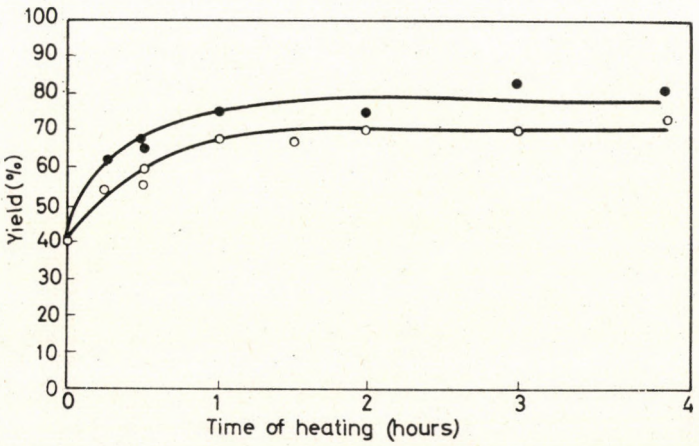


Fig. 6. Nitration of *o*-nitrotoluene with HNO_3 in the presence of 0.21 mole of 93.3% $BF_3(CH_3COOH)_2$ (0.25 mole of *o*-nitrotoluene, 0.33 mole of HNO_3; ○ — 40 °C; ● — 60 °C)

adding the acetic acid complex. This is the reason why relatively high yields are given for zero time.) A 20 °C increase in temperature brings about a 10% increase in yield.

In order to elucidate the mechanism of nitration, an accurate kinetic study was carried out. The originally selected substrate, o-nitrotoluene, was found inadequate for kinetic measurements because, being a deactivated compound, it practically did not undergo nitration in dilute solutions. Suitable reaction rates were obtained with toluene. Acetic acid was used as a solvent, and the boron fluoride was also added in acetic acid solution. The amount of the formed nitrotoluene mixture was determined by UV spectroscopy, after the reaction had been stopped by pouring the mixture into water. The nitration was first carried out on a preparative scale, and the UV spectra of the produced *o*-nitrotoluene mixtures were recorded. An absorption maximum was detected at 275 nm ($\varepsilon = 5400$). At this wavelength toluene absorbs negligibly.

The kinetic experiments were performed with an acetic acid solution containing 0.01 mole/l of toluene, 0.158 mole/l of HNO_3, and 0.1 mole/l

of $BF_3 \cdot 2CH_3COOH$. Samples were withdrawn at 10 min. intervals and, after pouring them into water, the optical densities were measured at 275, 280, and 285 nm. The concentrations of nitrotoluene and toluene were then calculated using the known molar absorptivities (5400, 5250, and 5000, respectively) at the above wavelengths. The yields after 1 hr. was about 56%. (No nitrotoluene formed in the absence of boron fluoride—acetic acid complex.) The logarithm of the toluene concentration plotted against time gave straight lines, indicating a first order reaction with respect to toluene. Similar results were obtained at other toluene concentrations. The pseudo-first order behaviour is due to the fact that boron fluoride and nitric acid were present at least in a ten-fold excess over toluene, therefore, their concentrations practically did not change during the reaction.

The rate law for the reaction is:

$$-\frac{dc}{dt} = k_1 c_{\text{toluene}} \tag{4}$$

The pseudo-first-order rate constants (k_1) were calculated for different times from the integrated rate equation

$$k_1 = \frac{2.3}{t} \log \frac{c_o}{c} \tag{5}$$

and the average of the results was taken. The value of k_1 was also determined from the slopes of the $\log c_{\text{toluene}}$ *vs.* time straight lines (Table III).

Since the concentrations of $BF_3 \cdot 2CH_3COOH$ are slightly different in the individual reaction solutions, the pseudo-second order rate constant (k_2) was also calculated. It was assumed, and subsequently proved, that the rate of nitration also depends on the concentration of $BF_3 \cdot 2CH_3COOH$. The rate equation, disregarding the effect of nitric acid present in excess, can now be written as follows:

$$-\frac{dc}{dt} k_2 c_{\text{toluene}} c_{\text{complex}} \tag{6}$$

On comparison with Eq. (4) one obtains

$$k_2 = \frac{k_1}{c_{\text{complex}}}. \tag{7}$$

The values for k_2 calculated from different runs agree to a good approximation (Table III). (A slightly different value was obtained for the concentration of 0.02018 mole/l, where HNO_3 and $BF_3 \cdot 2CH_3COOH$ were present in

a less than tenfold excess.) It can be concluded from the results that the rate of reaction is directly proportional to the concentration of toluene.

A series of experiments was made to study the influence of the $BF_3 \cdot 2CH_3COOH$ concentration on the value of k_1, and to test whether k_2 really remains constant. On the basis of Table IV it can be concluded that the rate of nitration catalyzed by the acetic acid complex of BF_3 is directly

Table III

Nitration of toluene with HNO_3 in the presence of $BF_3(CH_3COOH)_2$ at 25° C: kinetic measurements ($c_{HNO_3} = 0.158$ mole/l)

$c_{toluene} \times 10^2$ (mole/l)	$c_{complex} \times 10$ (mole/l)	$k_1 \times 10^2$ (min^{-1})	$k_{1,\,graph} \times 10^2$ (min^{-1})	$k_2 \times 10$ (l/mole.min)
1.009	1.003	1.48	1.41	1.47
2.018	0.957	1.21	1.31	1.26
0.505	0.957	1.33	1.28	1.39

Table IV

Nitration of toluene with HNO_3 in the presence of $BF_3(CH_3COOH)_2$ at 25° C: kinetic measurements ($c_{HNO_3} = 0.158$ mole/l)

$c_{toluene} \times 10^2$ (mole/l)	$c_{complex} \times 10$ (mole/l)	$k_1 \times 10^2$ (min^{-1})	$k_{1,\,graph} \times 10^2$ (min^{-1})	$k_2 \times 10$ (l/mole.min)
1.092	0.501	0.379	0.38	0.76
1.092	1.006	1.17	1.09	1.16
1.092	1.503	1.80	1.75	1.19
1.092	2.012	2.36	2.26	1.17

proportional to the concentration of this complex. The calculated second order rate constants are in good agreement with one another, with the exception of the 0.501 mole/l $BF_3 \cdot 2CH_3COOH$ solution, where the toluene to $BF_3 \cdot 2CH_3COOH$ ratio was only 1 : 5.

The above results support the assumption expressed in Eq. (2), based on spectroscopic evidence, according to which boron fluoride promotes nitronium ion formation, and thus assists nitration.

According to our present state of knowledge, nitration in the presence of boron fluoride catalyst involves the following reactions:

$$HNO_3 + BF_3 \rightleftharpoons NO_2^+ + BF_3OH^-$$

$$NO_2^+ + Ar{-}H \rightarrow Ar{-}NO_2 + H^+.$$

Experimental

Materials

Nitric acid was an analytical grade Merck product. HNO_3 content 94.6%; $d_4^{15} = 1.50$.

Boron fluoride. A BASF product supplied in a cylinder was used; it was purified in a B_2O_3-saturated sulphuric acid scrubber.

o-Nitrotoluene. A crude Hichson—Welch product was purified by distillation. 98% of the substance distilled over at 98—99°C/10 mm Hg.

Toluene was an analytical grade Reanal product dried over metallic sodium.

$BF_3 \cdot 2CH_3COOH$. Absolute acetic acid was saturated with gaseous BF_3, then distilled. The BF_3 content was determined [6].

$BF_3 \cdot H_2O$ and **$BF_3 \cdot 2H_2O$.** Distilled water was saturated with boron fluoride and after the amount of absorbed BF_3 had been determined, the solution was diluted with a known amount of water.

All organic solvents were absolutized before use.

Nitration of o-nitrotoluene. In a 250-ml 3-necked round-bottomed flask, equipped with a mercury-sealed stirrer, thermometer, and a calcium chloride tube, 34.3 g (29.4 ml) of *o*-nitrotoluene was mixed with 19 g (12.7 ml) of fuming nitric acid. The flask was weighed and, under stirring, gaseous BF_3 was introduced above the surface of the liquid. When the acetic acid- and aquo-complexes of BF_3 were used, they were added from a dropping funnel. The flask was cooled in ice-water to prevent the temperature from rising above 40°C. After saturation, the mixture was stirred at 40°C for 30 min. The flask was weighed again to determine the amount of BF_3 absorbed. The reaction mixture, which separated into two layers, was poured into 150 ml of water. The separated solid was melted after decanting water, and washed with 3×100 ml of hot water. The product was dried over P_2O_5 in vacuum, and its density determined in a pyknometer at 60°C.

Nitration of toluene (kinetic measurements). The required volumes of a 0.1 mole/l toluene solution in acetic acid, and of a 1.0 mole/l acetic acid solution of $BF_3(CH_3COOH)_2$, were pipetted into a 10-ml volumetric flask. Anhydrous acetic acid was added to bring the level a little below the mark, and the flask was placed into a 25 ± 0.01 °C ultrathermostat for 30 min. After thermal equilibrium had been reached, the flask was filled up with 25°C acetic acid to the mark. Fuming nitric acid (0.07 ml) was then added from a pipette, and the content of the flask was mixed by shaking. 1-ml samples were withdrawn at 10 min. intervals and added into 100 ml of distilled water. The optical density of the solution was measured on a Spectromom 201 spectrophotometer in a 10-mm quartz cell. The reference solution was prepared in an identical way but without toluene.

REFERENCES

1. THOMAS, R. J., ANZILOTTI, W. F., HENNION, G. F.: Ind. Eng. Chem. **32,** 408 (1940); U. S Pat. 2 314 212 (1943)
2. GERDING, H., HEERTJES, P. M., REVALLIER, L. J., STEEMAN, I. W. S.: Rec. Trav. Chim. Pays-Bas **71,** 501 (1952)
3. HALFTER, I.: Z. für das ges. Schieß- u. Sprengstoffwesen **38,** 173 (1943)
4. VARSÁNYI, GY., HOLLY, S., FENICHEL, L.: Acta Chim. Acad. Sci. Hung. **41,** 309 (1964)
5. GIBSON, W. H., DUCKHMAN, R., FAIRBANC, R.: J. Chem. Soc. **121,** 270 (1922)
6. CSŰRÖS, Z., DEÁK, GY., FENICHEL, L., KALMÁR, A.: Periodica Polytechnica, Chem. Ing. **8,** 1 (1964)

Zoltán CSŰRÖS
Gyula DEÁK
László FENICHEL
Anna TÖRÖK-KALMÁR

Budapest, XI. Műegyetem rkp. 3.

Acta Chimica Academiae Scientiarum Hungaricae, Tomus 59 (3—4), pp. 411—415 (1969)

PHENYLETHANOLAMINE DERIVATIVES, I

^{14}C-LABELLING OF 1-(*m*-AMINOPHENYL)-2-CYCLOPROPYL-AMINOETHANOL DIHYDROCHLORIDE, A MONOAMINOOXIDASE BLOCKING AGENT

J. ENGLER, D. BÁNFI and A. HAJÓS

(Research Institute for Pharmaceutical Chemistry, Budapest)

Received December 19, 1967

For the purpose of radioisotope indication studies and pharmacological tests, as well as for an investigation of the mechanism of action, the ^{14}C-labelling of 1-(*m*-aminophenyl)-2-cyclopropyl-aminoethanol dihydrochloride, a strong monoaminooxidase blocking agent, was performed. The synthesis started from $Ba^{14}CO_3$, involved 9 steps, and almost 10% radiochemical yield was obtained. The endproduct was homogeneous both from the chemical and radiochemical points of view and possessed a high specific activity.

1-(*m*-Aminophenyl)-2-cyclopropyl-aminoethanol dihydrochloride was first synthesized by HAJÓS *et al.* [1]. The compound was found to possess intense monoaminooxidase blocking effect. For the purpose of radioisotope indication studies and pharmacological tests, and in order to investigate the mechanism of action, the ^{14}C-labelling of the compound was performed. In the synthesis of the labelled compound, the preparative experiences obtained in the preparation of the inactive derivative were utilized.

The ^{14}C-isotope labelling procedure was based on the acetophenone intermediate labelled in its carbonyl group [2]. This compound was prepared by reductive alkylation with dimethylcadmium of benzoyl-^{14}C-chloride [3]. In this reaction the observations of CASON [4] concerning the preparation of carbonyl-labelled propiophenone were used. The radioactive acetophenone (**IV**) was nitrated with a mixture of fuming nitric acid and concentrated sulphuric acid, and the product, *m*-nitroacetophenone (**V**), was brominated in the ω-position. Subsequently, the carbonyl group of *m*-nitro-ω-bromoacetophenone (**VI**) was reduced with sodium borohydride. *m*-Nitrophenyl-bromomethyl-carbinol (**VII**) thus obtained was allowed to react with cyclopropylamine, and finally the nitro group of the product, 1-(*m*-nitrophenyl)-2-cyclopropyl-aminoethanol (**VIII**), was reduced with hydrogen in the presence of Raney Ni catalyst to an amino group. The reduced derivative (**IX**) was isolated as the dihydrochloride and purified in this form. In this way a chromatographically homogeneous 1-(*m*-aminophenyl)-2-cyclopropyl-aminoethan-1-^{14}C-ol dihydrochloride (**X**) preparation could be synthesized in about 10% radiochemical yield, based on $Ba^{14}CO_3$.

The chemical and radiochemical purity of the endproduct was checked by thin-layer chromatography. The chromatograms were evaluated radio-

autographically and radiometrically, using a Packard M 7201 type instrument.

The activities of the radioactive intermediary products and the end-product were determined, after transformation of the carbon content of the

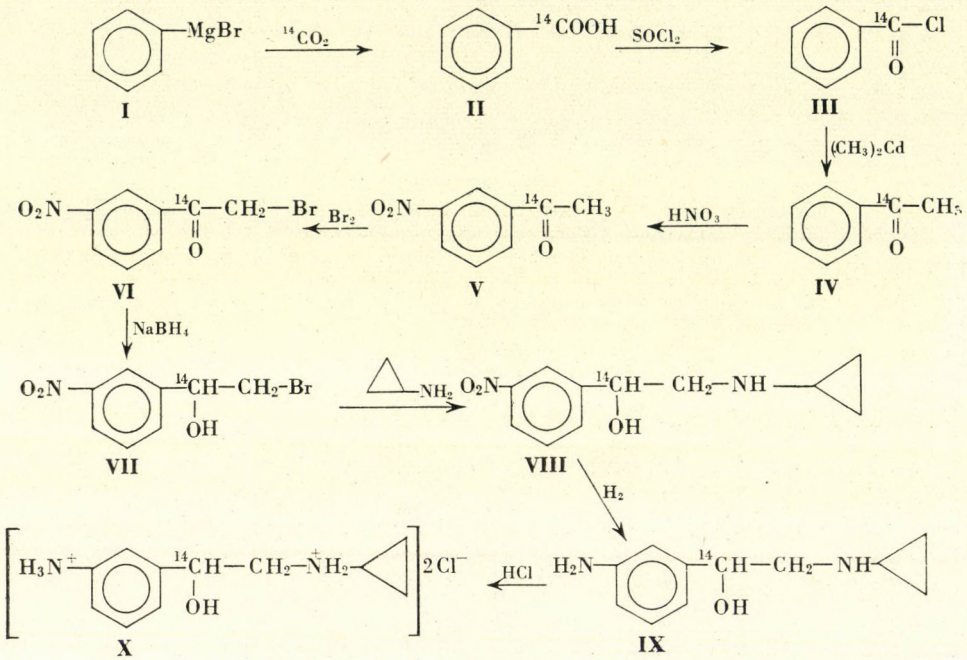


Fig. 1. Synthesis of the radioactive product

samples to $^{14}CO_2$, in an ionization chamber with a vibrocondensator electrometer (type Dynacon 6000).

Fig. 1 shows the scheme of the synthesis of the radioactive product.

Experimental

Benzoic acid-^{14}C (II)

Radioactive benzoic acid was prepared by the procedure of DAUBEN *et al.* [5]; starting with 7.48 g (37.9 mmoles) of $Ba^{14}CO_3$ (23.6 mCi/g; 4.6 mCi/mmole), 3.66 g (30.0 mmoles) of benzoic acid was obtained.

Radiochemical yield: 140 mCi (38.0 mCi/g, 4.46 mCi/mmole); 79.1% based on $Ba^{14}CO_3$.

Benzoyl-^{14}C-chloride (III)

3.66 g (30.0 mmoles) of **II** was transformed to the acid chloride, according to the procedure of HEIDELBERGER [3], with thionyl chloride. The crude product (3.88 g; 27.6 mmoles) was purified by vacuum distillation, the material being diluted with 0.40 g (2.8 mmoles) of inactive benzoyl chloride. Yield: 3.65 g (26.0 mmoles).

Radiochemical yield: 114.4 mCi (31.4 mCi/g, 4.4 mCi/mmole); 81.7% based on **II**.

Acetophenone-carbonyl-^{14}C (IV)

0.90 g (37.0 mmoles) of magnesium turnings and 80 ml of abs. ether were placed in a 250-ml three-necked round-bottomed flask equipped with a stirrer, a reflux condenser, a double gas-inlet tube and a thermometer. Dry nitrogen gas was introduced in one of the gas inlet tubes and passed through the apparatus in a slow stream, while the other gas inlet tube, which extended as low as the bottom of the flask and was provided with an absorption tube filled with potassium hydroxide, was connected to a vessel containing 180 g of methyl bromide cooled to —20° C. The reaction mixture was kept in boiling (40—45° C) and the methyl bromide was distilled into it in a steady stream, over a period of 2—3 hours, with continuous stirring. The progress of the reaction was indicated by the decrease in the amount of magnesium turnings. After the introduction of methyl bromide had been completed, the mixture was refluxed, with stirring, for 1 hr., cooled to 5° C, and 3.55 g (19.4 mmoles) of finely ground cadmium chloride was added carefully in small portions. The mixture was stirred at 5° C for 10 min., at 40° C for 20 min., and at room temperature for 12 hrs. The ether was removed by distillation in vacuum and 50 ml of dry benzene was added to the residue. 20 ml of benzene was distilled off, and the mixture diluted with 20 ml of fresh benzene. The mixture was cooled to 10° C, and a solution of 3.65 g (26.0 mmoles) of **III** in 30 ml of dry benzene was added dropwise in nitrogen atmosphere, over a period of 2 minutes. The mixture was stirred at 10° C for 10 min. and at 80—85° C for 90 min., cooled to 5° C, and 25 ml of 2*N* H_2SO_4 was added with stirring. The two layers were separated, and the aqueous one was extracted with 3×20 ml of benzene. The combined benzene phases were washed with 2×20 ml of H_2O, 15 ml of 5% Na_2CO_3 and 25 ml of saturated NaCl solution, dried over anhydrous Na_2SO_4 and concentrated in vacuum. The oily residue was purified by fractionation to yield 2.46 g (20.5 mmoles) of **IV.**

Radiochemical yield: 91.0 mCi (37.0 mCi/g; 4.4 mCi/mmole); 79.5% based on **III.**

m-Nitroacetophenone-carbonyl-^{14}C (V)

2.46 g (20.5 mmoles) of **IV** obtained in the preceding step was diluted with 3.54 g (29.5 mmoles) of inactive acetophenone to 6.0 g (50.0 mmoles; 15.2 mCi/g, 1.8 mCi/mmole; 91.0 mCi). The activity data of the product were determined using its phenylhydrazone (m.p. 105°C).

15 ml of conc. H_2SO_4 was placed in a 50-ml three-necked round-bottomed flask equipped with a stirrer, a dropping funnel and a thermometer, and the apparatus was cooled to 0—5°C. The radioactive acetophenone was added in portions into the flask, with continuous stirring. The mixture was cooled to —5° C and a mixture of 4 ml of conc. HNO_3 (sp. gr. 1.52) and 6 ml of conc. H_2SO_4 was added with stirring and cooling (bath temperature —20° C) over a period of 40 min. The mixture was stirred at —5° C for 10 min. and poured into ice-water (75 g of ice and 150 ml of water). The material which precipitated was collected by filtration, washed with a little cold water and dissolved in 10 ml of hot 95% ethanol. 150 ml of water was added to the hot solution and it was cooled to 0—5°C. The crystals deposited were filtered off, washed with 15 ml of cold water and recrystallized from 10 ml of 95% ethanol to obtain 4.26 g (25.8 mmoles) of **V**, m.p. 80—82° C.

Radiochemical yield: 48.0 mCi (11.3 mCi/g; 1.8 mCi/mmole); 52.7% based on **IV.**

m-Nitro-ω-bromoacetophenone-carbonyl-^{14}C (VI)

The 4.26 g (25.8 mmoles) of **V** obtained in the preceding step was diluted with 2.14 g (12.9 mmoles) of inactive substance to 6.4 g (38.7 mmoles; 7.5 mCi/g; 1.2 mCi/mmole; 48.0 mCi), dissolved in 52 ml of chloroform and treated with 2.0 ml (38.0 mmoles) of bromine, added dropwise, with stirring, at 40° C. The reaction mixture was stirred for a further 1 hr., washed with 3×20 ml of water in a separatory funnel, and the organic phase was dried over anhydrous Na_2SO_4 and concentrated in vacuum. The solid residue was dried at room temperature in an exsiccator over phosphorus pentoxide, to obtain 9.27 g (38.0 mmoles) of **VI**, m.p. 94—96° C. Radiochemical yield: 47.0 mCi (5.1 mCi/g, 1.2 mCi/mmole); 98.0% based on **V.**

1-(m-Nitrophenyl)-2-bromoethan-1-^{14}C-ol (VII)

9.27 g (38.0 mmoles) of **VI** obtained in the preceding experiment was dissolved in 240 ml of abs. ethanol in a 500-ml three-necked round-bottomed flask equipped with a mechanical stirrer, thermometer, a $CaCl_2$ tube and a feeding adapter. 1.89 g 98% sodium borohydride was

added with stirring in portions to the solution at 4° C over a period of about 1 hr., the mixture was stirred for a further 1 hr. at 4° C, kept at room temperature for 12 hrs. After the addition of 4.5 ml of glacial acetic acid, the mixture was concentrated in vacuum, the residue taken up in 40 ml of water and extracted with 3×25 ml of chloroform. The organic phase was washed with 2×10 ml of water, dried over anhydrous Na_2SO_4, and the solvent was removed in vacuum to leave a pale yellow oil. According to experiences obtained in earlier experiments with inactive material, this crude product may be used in the following step without purification.

Yield: 7.49 g (30.4 mmoles).

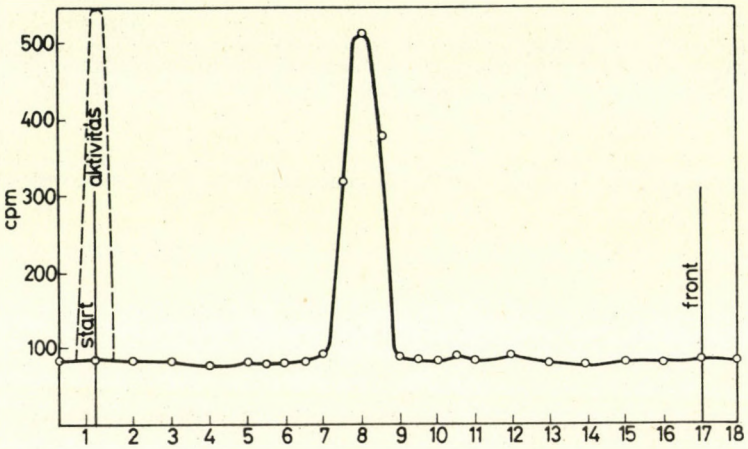


Fig. 2. Radiochromatogram of 1-(*m*-aminophenyl)-2-cyclopropyl-aminoethan-1-^{14}C-ol dihydrochloride

1-(m-Nitrophenyl)-2-cyclopropyl-aminoethan-1-^{14}C-ol (VIII)

7.49 g (30.4 mmole) of **VII** obtained in the preceding step was dissolved in abs. ethanol, and 11.5 ml of freshly distilled cyclopropylamine was added to the solution. The mixture was refluxed for 6 hrs. and the solvent removed in vacuum. The residue was mixed with 10 ml of abs. ether and kept in a refrigerator for 12 hrs. The crystalline product was filtered off, washed with abs. ether and dried in an exsiccator over phosphorus pentoxide at room temperature, to obtain 4.46 g (20.1 mmole) of **VIII**, m.p. 117—118° C. Radiochemical yield: 23.0 mCi (5.2 mCi/g; 1.1 mCi/mmole); 49% based on **VI**.

1-(m-Aminophenyl)-2-cyclopropyl-aminoethan-1-^{14}C-ol (IX)

4.46 g (20.1 mmoles) of **VIII** was hydrogenated in 50 ml of abs. ethanol in the presence of Raney Ni catalyst (2 g). Reduction took place in 2.5—3 hours (H_2 uptake 1330 ml). The catalyst was filtered off and the solvent removed in vacuum. 20 ml of abs. ether was added to the residual oil, and the mixture was kept in a refrigerator for 12 hrs to deposit crystals, which were filtered off and washed with 2×3 ml of cold abs. ether. Yield: 2.56 g (13.3 mmoles); m.p. 83—84°C. Radiochemical yield: 15.0 mCi (5.8 mCi/g, 1.1 mCi/mmole); 65% based on **VIII**.

1-(m-Aminophenyl)-2-cyclopropyl-aminoethan-1-^{14}C-ol dihydrochloride (X)

2.56 g (13.3 mmoles) of **IX** was dissolved in 5 ml of abs. ethanol and 6 ml of 25% hydrochloric acid in ethanol was added at 5°C. The mixture was allowed to stand in a refrigerator for 12 hrs, and the deposited crystals were collected, washed with 2—3 ml of abs. ether and dried in a vacuum exsiccator over KOH at room temperature, to obtain 2.89 g (10.9 mmoles) of **X**, m.p. 208—209°C. Radiochemical yield: 12.6 mCi (4.3 mCi/g; 1.15 mCi/mmole); 84% based on **IX**, and 7.1% based on $Ba^{14}CO_3$.

Thin-layer chromatographie analysis of the end-product

Adsorbent:	Kieselgel G
Solvent:	Chloroform — methanol 3 : 1
Quantity applied:	10 γ
Time:	1.5 hrs
Chemical detection:	a brown spot in iodine vapour
Autoradiography:	Forte X-ray film, 24 hr. contact exposition
R_f:	0.45

The authors are indebted to Dr. T. Szarvas (Isotope Institute of the Hungarian Academy of Sciences) for the isotope-analytical measurements.

REFERENCES

1. Hajós, A., Huszti, Zs., Fekete, M., Borsi, J., Elek, S., Polgári, I.: Biochem. Pharm. (In the Press)
2. Dauben, W. G., Reid, J. C., Yankwich, P. E., Calvin, M.: J. Am. Chem. Soc. **72,** 121 (1950)
3. Heidelberger, C., Rieke, H. S.: Cancer Research **11,** 640 (1951)
4. Cason, J.: J. Am. Chem. Soc. **68,** 2078 (1946)
5. Dauben, W. G., Reid, J. C., Yankwich, P. E.: Anal. Chem. **19,** 828 (1947)

József Engler
Dezső Bánfi
Andor Hajós
Budapest, IV., Szabadságharcosok útja 47—49

Acta Chimica Academiae Scientiarum Hungaricae, Tomus 59 (3—4), pp. 417—418 (1969)

PREPARATION OF LEAD COBALT CARBONYL AND ITS TRIPHENYLPHOSPHINE DERIVATIVE

(PRELIMINARY NOTE)

A. VIZI-OROSZ, G. BOR* and L. MARKÓ

(University of Chemical Industries, Institute of Organic Chemistry and Research Group for Petrochemistry of the Hungarian Academy of Sciences, Veszprém)

Received July 29, 1968

Two unsuccessful attempts for the preparation of $Pb[Co(CO)_4]_2$ are reported in the literature [1, 2]. This complex, however, would be of theoretical interest, since to our knowledge no derivatives of two-coordinate lead are known in which lead is bonded to a transition metal. The organolead derivatives of metal carbonyls prepared up till now [3] all contain four-coordinate lead.

When 15 ml of a n-hexane solution of cobalt-carbonyl hydride (0.36 mmoles) was added to metallic lead (about 5 g), and was stirred in an atmosphere of carbon monoxide, the light yellow solution turned over olive-green rapidly to the deep-violet. This violet solution contains $Pb[Co(CO)_4]_2$, the presence of which is indicated by its infrared absorption bands at 2073 (vs), 2030 (m), 2016 (vs) and 1994 (vw) cm^{-1}. This infrared spectrum shows a close similarity to that of $Hg[Co(CO)_4]_2$ [4]. Attempts to isolate $Pb[Co(CO)_4]_2$ from the solution failed owing to its extreme sensibility towards oxygen, by which it is transformed to dicobalt octacarbonyl.

Adding triphenylphosphine (0.90 mmoles) in 10 ml n-hexane to the above obtained solution of $Pb[Co(CO)_4]_2$ and stirring until the evolution of carbon monoxide gas ceased a finely divided black precipitate was formed. After filtration the product was washed with ether, and dried under nitrogen. (Yield 52 mg, 28% calculated on cobalt carbonyl hydride.) The analysis confirmed the formula $Pb[Co(CO)_3\,PPh_3]_2$. (Found: Co, 11.3; Pb, 20.0, calcd.: Co, 11.59; Pb, 20.37%.) The compound is relatively stable in air.

The infrared spectrum of this solid product in KBr pellet has bands at 2020 (w), 1998 (m), 1946 (broad, vs) and 1899 (vw) cm^{-1}. Comparing these frequencies with those of $Hg[Co(CO)_3\,PPh_3]_2$ presents further evidence for the given structure of the lead compound. A sample of the phosphine substituted mercury cobalt carbonyl was prepared by the method of HIEBER and BREU [5] and found to show in a KBr pellet the following absorption bands: 2022 (w), 1991 (m), 1950, 1938 (double, vs) and 1910 (vw) cm^{-1}.**

* Hungarian Oil and Gas Research Institute M.Á.F.K.I. Veszprém, Hungary.

** Both samples of $Pb[Co(CO)_3\,PPh_3]_2$ and $Hg[Co(CO)_3\,PPh_3]_2$ did show one additional weak absorption band at 2060 and 1074 cm^{-1}, respectively, which has to be attributed to some contamination by the monosubstituted derivatives $[(CO)_4Co]Pb[Co(CO)_3\,PPh_3]$ and $[(CO)_4Co]Hg[Co(CO)_3\,PPh_3]$ [6].

The formation of the violet lead cobalt carbonyl has been observed even in the cells of the IR spectrometer having lead spacing rings, if hexane solutions of $HCo(CO)_4$ were kept for several hours in the cell. Furthermore $Pb[Co(CO)_4]_2$ is formed also from finely dispersed $Pb(OOCCH_3)_2$ and $HCo(CO)_4$ dissolved in hexane, as evidenced by infrared spectroscopy.

Recently metal exchange reactions between compounds of type $M[Co(CO)_4]_2$ (M = Hg, Cd, Zn) were reported [7]. Analogously, $Pb[Co(CO)_4]_2$ in hexane solution could be transformed by metallic mercury to $Hg[Co(CO)_4]_2$ as shown by the colour change and the infrared spectrum of the reaction mixture. Moreover, if cobalt carbonyl hydride (dissolved in hexane) was kept in contact with lead amalgam, first the here reported lead compound was formed which then transformed to the more stable mercury cobalt carbonyl. This sequence of reactions could be followed by infrared spectra.

Based on the great similarity between the infrared spectra of $Hg[Co(CO)_4]_2$ [4] and $Pb[Co(CO)_4]_2$ it can be assumed that the latter compound has the structure $(CO)_4Co\text{-}Pb\text{-}Co(CO)_4$ with linear arrangement of the metal atoms and has D_{3d} symmetry as shown by IR [4] and RAMAN [8] spectroscopy and recently by X-ray diffraction [9] studies for $Hg[Co(CO)_4]_2$.

REFERENCES

1. HIEBER, W., TELLER, U.: Z. anorg. allg. Chem. **249,** 43 (1942).
2. KRUMHOLZ, P., BRIL, S.: Proc. Chem. Soc. (London) 116 (1960).
3. HEIN, F., POBLOTH, H.: Z. anorg. Chem. **248,** 84 (1941); HEIN, F., HEUSER, E.: Z. anorg. Chem. **254,** 138 (1947); **255,** 125 (1947); HEIN, F., KLEINERT, P., JEHN, W.: Naturwiss. **44,** 34 (1957); GORSICH, R. D.: J. Am. Chem. Soc. **84,** 2486 (1962); NESMEYANOV, A. N., ANISIMOV, K. N., KOLOBOVA, N. E., KHANDOZHKO, V. N.: Dokl. Akad. Nauk SSSR **156,** 383 (1964); HEIN, F., JEHN, W.: Ann. Chem. **684,** 4 (1965); KAHN, O., BIGORGNE, M.: Comp. rend. **261,** 2483 (1965); **263,** 973 (1966); J. Organometal. Chem. **10,** 137 (1967); PATMORE, D. J., GRAHAM, W. A. G.: Inorg. Chem. **6,** 981 (1967).
4. BOR, G., MARKÓ, L.: Spectrochim. Acta **16,** 1105 (1960).
5. HIEBER, W., BREU, R.: Chem. Ber. **90,** 1259 (1957).
6. BOR, G., MARKO, L.: Chem. Ind. (London) 912 (1963).
7. BURLITCH, J. M.: J. Organometal. Chem. **9,** P9 (1967).
8. STAMMREICH, H., KAWAI, K., SALA, O., KRUMHOLZ, P.: J. Chem. Phys. **35,** 2175 (1961).
9. SHELDRICK, G. M., SIMPSON, R. N. F.: Chem. Comm. 1015 (1967).

Anna VIZI-OROSZ, László MARKÓ — Veszprém, Schönherz Z. u. 12. Hungary
György BOR, Veszprém, Wartha W. u. 2. Hungary

Acta Chimica Academiae Scientiarum Hungaricae, Tomus 59 (3—4), pp. 419—424 (1969)

ABBAU UND REAKTIONEN VON ONSÄUREAZIDEN, II*

AUSDEHNUNG DER CURTIUS-REAKTION AUF DAS OCTAACETYL-CELLOBIONSÄUREAZID

I. FARKAS, I. F. SZABÓ und R. BOGNÁR

(Institut für Organische Chemie, L. Kossuth Universität, Debrecen)

Eingegangen am 3. April 1968

Das Octaacetyl-cellobionsäureazid kann mit Essigsäureanhydrid zu dem amorphen, jedoch einheitlichen N-[D-Gluco-1,2,3,5-tetraacetoxy-4-(tetraacetyl-β-D-glucopyranosyl)-pentyl]-acetamid **(I)** umgesetzt werden. Die Struktur des Produkts wird durch seine Reaktionen bestätigt: nach Verseifen mit Natriummethylat wird die Verbindung durch 1 *n* Schwefelsäure zu Glucose und Arabinose hydrolysiert, während eine Behandlung mit konzentriertem Ammoniak 3-β-D-Glucopyranosyl-D-arabinosebisacetamid **(II)** mit einer Ausbeute von 51% liefert. Demzufolge scheint es, daß der Curtius-Abbau bei Disacchariden wesentlich vorteilhafter ist, als die Wohlsche Reaktion.

Bereits früher haben wir darüber berichtet, daß es uns gelungen ist, geeignete Varianten des Curtius-Abbaus erfolgreich bei Monosacchariden anzuwenden und auf diese Art Pentaacetyl-D-gluconsäureazid zu D-Arabinose [1], Pentaacetyl-D-galactonsäureazid zu D-Lyxose und Tetraacetyl-D-arabonsäureazid zu D-Erythrose [2] abzubauen. Besonders bemerkenswert ist die auf der Reaktion von Carbonsäureazid und Essigsäureanhydrid beruhende Variante des Curtius-Abbaus [3], die bei der Zuckerreihe zu einem bisher unbekannten, acyclischen N-(Polyacetoxyalkyl)-acetamidderivat führt. Diese Verbindung konnte aus dem Pentaacetyl-D-galactonsäureazid in einheitlichem kristallinem Zustand erhalten werden [2]. Auf Grund ihrer Reaktionen paßt die Verbindung gut als Intermediärprodukt in den Mechanismus des Wohlschen Abbaus [4—8], wodurch dieser auch von einer anderen Seite her experimentell unterstützt werden konnte [2].

Da wir das Octaacetyl-cellobionsäureazid bereits früher hergestellt hatten [1], schien die Frage, zu welchem Ergebnis der Curtius-Abbau bei Disacchariden führt, der Untersuchung wert. Dieses Interesse ist umsomehr begründet, als die Ausdehnung des analogen Wohlschen Abbaus auf Disaccharide bisher begreiflicherweise nur wenig untersucht worden ist, da das abgebaute Disaccharid aus **II** nicht hergestellt werden kann. ZEMPLÉN [9] berichtete zwar 1926, daß bei der Ammonolyse des Octaacetyl-cellobionsäurenitrils ein stickstoffhaltiges amorphes Produkt entsteht; er prüfte jedoch das Produkt nicht eingehender. Die Frage wurde durch DEFERRARI und Mitarbeiter geklärt, die beim

* I. Mitteilung: siehe Literaturangabe [2].

Wohlschen Abbau des Octaacetyl-cellobionsäurenitrils — unter Anwendung einer chromatographischen Reinigung — 3-β-D-Glucopyranosyl-D-arabinose-bisacetamid (**II**) mit einer Ausbeute von 24,2% und 3-β-D-Glucopyranosyl-N-acetyl-D-arabinofuranosylamin (**III**) mit einer Ausbeute von 4,2% erhielten [10]. Bei der Aufarbeitung wurde auch eine geringe Menge (0,38%) Disaccharid (3-β-D-Glucopyranosyl-D-arabinose) isoliert.

Analoge Ergebnisse wurden auch beim Wohlschen Abbau des Octaacetyl-lactobionsäurenitrils erhalten [11]: die analogen Verbindungen von **II** und **III** wurden mit Ausbeuten von 17,6% bzw. 4,4% isoliert.

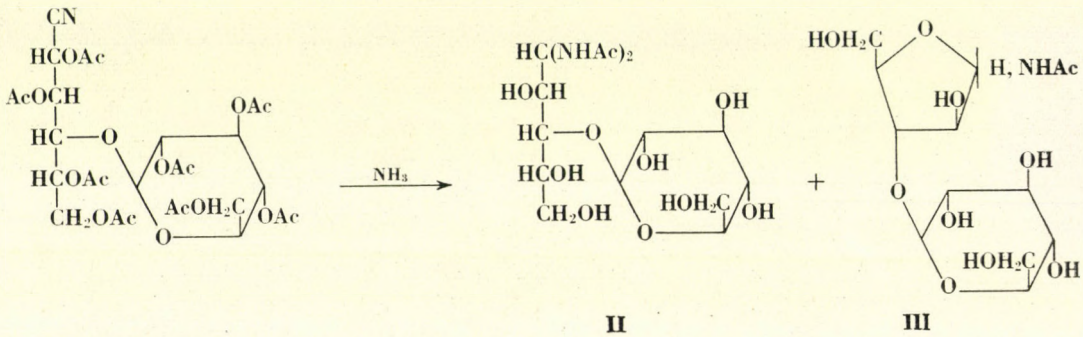


Abb. 1

Beim Erhitzen von Octaacetyl-cellobionsäureazid mit Essigsäureanhydrid erhielten wir erwartungsgemäß eine acetylierte geminale Oxyaminverbindung, N-[D-Gluco-1,2,3,5-tetraacetoxy-4-(tetraacetyl-β-D-glucopyranosyl)-pentyl]-acetamid (**I**) mit einer Ausbeute von 81%. Verbindung ist zwar amorph, jedoch einheitlich, wie auch aus ihren Analysenergebnissen ersichtlich ist. Die Struktur von **I** wird auch durch ihr infrarotes Spektrum bestätigt. Bei 3360 cm^{-1} tritt die ausschließlich für primäre Säureamidderivate charakteristische NH-Bande auf, bei 1700 cm^{-1} die Amid-I-Bande, bei 1525 cm^{-1} die Amid-II-Bande. Im Spektrum sind natürlich auch die charakteristischen Absorptionsbanden der Acetatester (bei 1750 und 1370 cm^{-1}) vorhanden. Aus den angeführten Befunden kann eindeutig auf die substituierte primäre Säureamid-Struktur geschlossen werden.

Die Struktur von **I** wird auch durch ihre Reaktionen bestätigt: die Verbindung wird durch Behandlung mit konzentrierter Ammoniaklösung zu 3-β-D-Glucopyranosyl-D-arabinose-bisacetamid (**II**) mit der hohen Ausbeute von 51% umgesetzt. Die Verseifung von **I** mit Natriummethylat und die anschließende Hydrolyse mit Säure liefert ein Hydrolysat, in dem papierchromatographisch [12] nur D-Glucose und D-Arabinose nachgewiesen werden konnte.

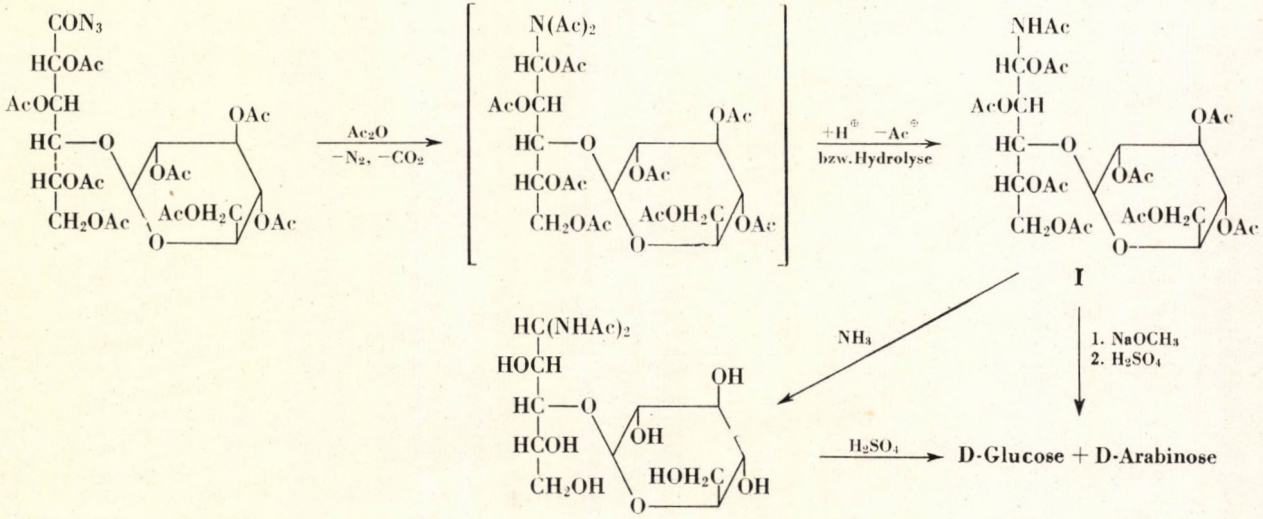

CON3
HCOAc
AcOCH
HC—O
HCOAc
CH2OAc
OAc
OAc
AcOH2C
OAc
O
Ac2O
−N2, −CO2
N(Ac)2
HCOAc
AcOCH
HC—O
HCOAc
CH2OAc
OAc
OAc
AcOH2C
OAc
O
+H⊕ −Ac⊕
bzw. Hydrolyse
NHAc
HCOAc
AcOCH
HC—O
HCOAc
CH2OAc
OAc
OAc
AcOH2C
OAc
O
I
NH3
1. NaOCH3
2. H2SO4
HC(NHAc)2
HOCH
HC—O
HCOH
CH2OH
OH
OH
HOH2C
OH
O
H2SO4
D-Glucose + D-Arabinose
II

Abb. 2

Die Struktur von **II** konnte auch durch Oxydation mit Perjodsäure [13] bestätigt werden. In Übereinstimmung mit DEFERRARI und seinen Mitarbeitern wurde ein Verbrauch von 3 Mol Perjodsäure festgestellt (Abb. 3).

Endlich wurde auch das Acetat von **II** hergestellt, dessen Schmelzpunkt um etwa 10 °C höher lag (82—84 °C), als der in der Literatur [10] angegebene Schmelzpunkt (74—75 °C).

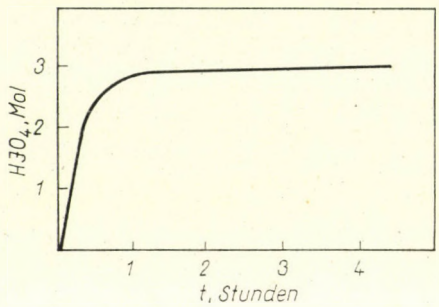


Abb. 3. Oxydation des 3-β-D-Glucopyranosyl-D-arabinose-bisacetamids (II) mit Perjodsäure

Da wir die Reaktionsprodukte mit einfachen präparativen Methoden in einheitlicher, reiner Form isolieren konnten und unser Verfahren eine mehr als doppelte Ausbeute für **II** ergibt, scheint der Curtius-Abbau bei Disacchariden wesentlich vorteilhafter zu sein, als die Wohlsche Reaktion.

*

Unsere Arbeit wurde durch die Ungarische Akademie der Wissenschaften unterstützt, wofür wir auch an dieser Stelle unseren Dank aussprechen möchten. Für ihre wertvolle Mitwirkung in der experimentellen Arbeit sei Fräulein phil. M. OROSZ, für die Durchführung der Mikroanalysen dem mikroanalytischen Laboratorium unseres Instituts (Laboratoriumsleiter: Frau Dr. É. R. DÁVID), für die Aufnahme der infrarot Spektren Herrn Dr. S. SZABÓ gedankt.

Experimenteller Teil

N-[D-Gluco-1,2,3,5-tetraacetoxy-4-(tetraacetyl-β-D-glucopyranosyl)-pentyl]-acetamid (I)

1,64 g Octaacetyl-cellobionsäureazid [1] werden mit 11 ml Essigsäureanhydrid 1 Stunde lang auf dem siedenden Wasserbad erhitzt. Die klare Lösung wird auf 50 ml Eiswasser gegossen, mit festem $KHCO_3$ neutralisiert und anschließend dreimal mit insgesamt 100 ml Chloroform ausgeschüttelt. Die Chloroform-Schicht wird mit $KHCO_3$-Lösung ausgeschüttelt, über wasserfreiem Na_2SO_4 getrocknet und im Vakuum eingedampft. Der sirupartige Rückstand erstarrt auf Zugabe von warmem abs. Äther zu einem weißen amorphen Pulver. Nach einigen Stunden wird abgesaugt, mit abs. Äther gewaschen und das Produkt im Vakuum über Paraffin — P_2O_5 aufbewahrt.

Ausbeute: 1,3 g (81%). Schmelzpunkt: erweicht bei 80° C, schmilzt ohne scharfen Meniskus bei 85 °C. $[\alpha]_D = +17{,}5°$ ($c = 0{,}97$, Lösungsmittel: Chloroform). Analyse ($C_{29}H_{41}O_{19}N$, 707,6): Berechnet C 49,22, H 5,84, N 1,98%. Gefunden C 49,19, H 5,85, N 2,01%.

Hydrolyse von I

0,1 g **I** wird in 3 ml abs. Methanol gelöst, 0,3 ml einer 1 *n* Natriummethylatlösung in abs. Methanol werden zugefügt und das Gemisch wird 3 Stunden bei 20 °C stehen gelassen. Danach wird mit Eisessig neutralisiert, die Lösung eingedampft, der sirupartige Rückstand in 1 *n* Schwefelsäure gelöst und auf dem siedenden Wasserbad 5 Stunden lang hydrolysiert. Die papierchromatographische Prüfung der Lösung [12] zeigt nur die Gegenwart von Glucose und Arabinose an.

3-β-D-Glucopyranosyl-D-arabinose-bisacetamid (II)

2,3 g Octaacetyl-cellobionsäureazid wird mit 15 ml Essigsäureanhydrid auf dem siedenden Wasserbad 1 Stunde erhitzt. Das Reaktionsgemisch wird wie bei **I** weiterverarbeitet. Zum sirupartigen Rückstand aus der Vakuumeindampfung der chloroformischen Lösung werden 25 ml konzentriertes Ammoniak zugefügt und auf dem Wasserbad wird bei 50 °C bis zur Auflösung des Sirups erwärmt. Die klare Lösung wird 4 Stunden lang bei Zimmertemperatur stehen gelassen und danach im Vakuum eingedampft. Um die letzten Wasserspuren zu entfernen, werden zweimal je 5 ml Alkohol vom Rückstand abdestilliert. Das Acetamid wird aus dem festen Rückstand mit zweimal 10 ml warmem Äthylacetat herausgelöst und das zurückbleibende Bisacetamidderivat zweimal aus heißem Alkohol umkristallisiert.

Ausbeute: 0,68 g (51%). Schmelzpunkt: 217—218 °C (Zersetzung). $[\alpha]_D = +24{,}2°$ ($c = 1{,}15$, Lösungsmittel: Wasser).

Literaturangaben [10]: Schmelzpunkt 214—215 °C, $[\alpha]_D = +25.2°$ (Lösungsmittel: Wasser).

Analyse* ($C_{15}H_{28}O_{11}N_2$, 412,4): Berechnet C 43,68, H 6,84, N 6,79%. Gefunden C 43,39, H 6,80, N 6,63%.

Auf dem Papierchromatogramm der Verbindung wurde nur ein einziger Fleck gefunden (Entwickler: Silbernitrat/Natriummethylat) [14].

Nach der sauren Hydrolyse (1 *n* Schwefelsäure 5 Stunden auf dem siedenden Wasserbad) zeigte die papierchromatographische Prüfung der Lösung [12] ausschließlich die Gegenwart von D-Glucose und D-Arabinose an.

3-β-D-Glucopyranosyl-D-arabinose-bisacetamid-heptaacetat

0,4 g **II** wird mit einem Gemisch aus 7 ml wasserfreiem Pyridin und 7 ml Essigsäureanhydrid auf dem siedenden Wasserbad bis zur Auflösung (45 Minuten) erhitzt. Die Lösung wird 24 Stunden bei Zimmertemperatur stehen gelassen und danach auf 100 ml Eiswasser gegossen. Die wäßrige Lösung wird dreimal mit insgesamt 40 ml Chloroform ausgeschüttelt, die Chloroform-Schicht mit Eiswasser, mit eiskalter $KHCO_3$-Lösung und wiederum mit Eiswasser gewaschen, über wasserfreiem $MgSO_4$ getrocknet und im Vakuum eingedampft. Der feste Rückstand wird zweimal aus Benzol umkristallisiert.

Ausbeute: 0,48 g (70%). Schmelzpunkt: sintert bei 82 °C, schmilzt ohne scharfem Meniskus bei 84 °C. $[\alpha]_D = +55{,}6°$ ($c = 0{,}47$, Lösungsmittel: Chloroform).

Literaturangaben [10]: Schmelzpunkt 74—75 °C, $[\alpha]_D = +55.3°$ (Lösungsmittel: Chloroform).

Analyse ($C_{29}H_{42}N_2O_{18}$, 706,6): Molekulargew. gef. 701**. Berechnet C 49,26 H 5,98 N 3,96%. Gefunden C 49,54 H 6,10 N 4,02%

LITERATUR

1. Bognár, R., Farkas, I., Szabó, I. F. und Szabó, G. D.: Chem. Ber. **96**, 689 (1963); Magyar Kém. Foly. **69**, 450 (1963)
2. Bognár, R., Farkas, I. und Szabó, I. F.: Liebigs Ann. Chem. **680**, 118 (1964); Magyar Kém. Foly. **71**, 382 (1965)

* Für die Analyse wurde das Produkt 24 Stunden lang bei 100 °C im Vakuum (20 Torr) über P_2O_5 getrocknet.

** Das Molekulargewicht wurde mit einem thermistorisierten Osmometer bestimmt. Lösungsmittel: Aceton.

3. SMITH, P. A.: Org. Reactions **3,** 337 (1947). HOUBEN—WEYL: Methoden der organischen Chemie **11/1,** 868—869. Georg Thieme Verlag, Stuttgart, **1957**
4. ISBELL, H. S. und FRUSH, H. L.: J. Amer. Chem. Soc. **71,** 1579 (1949)
5. HOCKETT, R. C., DEULOFEU, V. und DEFERRARI, J. O.: J. Amer. Chem. Soc. **72,** 1840 (1950)
6. ALLERTON, R. und OVEREND, W. G.: J. Chem. Soc. (London) **1952,** 35
7. GROS, E. G., ONDETTI, M. A., SPROVIERO, J. O., DEULOFEU, V. und DEFERRARI, J. O.: J. Org. Chem. **27,** 924 (1962)
8. LEZEROVICH, A., GROS, E. G., SPROVIERO, J. F. und DEULOFEU, V.: Carbohyd. Res. 4 (1967) 1
9. ZEMPLÉN, G.: Ber. **59,** 1254 (1926)
10. DEFERRARI, J. O., GELPI, M. E. und CADENAS, R. A.: J. Org. Chem. **30,** 2328 (1965)
11. GELPI, M. E., DEFERRARI, J. O. und CADENAS, R. A.: J. Org. Chem. **30,** 4064 (1965)
12. NÁNÁSI, P., BOGNÁR, R., PUSKÁS, M., TEICHMANN, F. und Frau J. ECSÉDI: Acta Univ. Debr. III, 95 (1956)
13. RAPPAPORT, F., REIFER, J. und WEIDMANN, H.: Mikrochim. Acta **1,** 290 (1937)
14. CADENAS, R. A. und DEFERRARI, J. O.: Analyst **86,** 132 (1961)

István FARKAS
Ilona F. SZABÓ
Rezső BOGNÁR
Debrecen 10. Ungarn

Acta Chimica Academiae Scientiarum Hungaricae, Tomus 59 (3—4), pp. 425—429 (1969)

APPLICATION OF GAS-LIQUID CHROMATOGRAPHY TO THE STRUCTURAL ELUCIDATION OF NATURAL FLAVONES

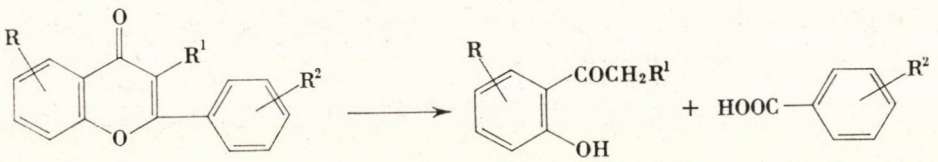
S. BÉKÁSSY* and M. NÓGRÁDI

(Institute of Organic Chemistry, Technical University, Budapest)

Received May 6, 1968

Polymethoxy-*o*-hydroxyacetophenones, which are the characteristic degradation products of fully methylated flavones, may conveniently be identified and separated by gas-liquid chromatography. The GLC-behaviour of 11 acetophenones in four systems has been investigated.

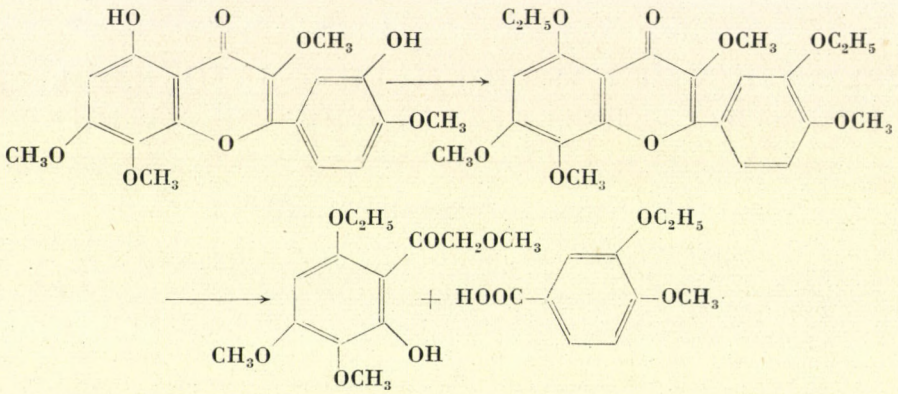
Alkaline degradation is one of the oldest and most frequently used method for the structural elucidation of natural polyhydroxyflavones. In this procedure, the flavone skeleton is broken down to an aromatic carboxylic acid reflecting the structure of ring *B* and to an *o*-hydroxyacetophenone representing the benzopyrone part of the molecule [1].



As free phenolic hydroxyls, particularly those in vicinal position, may cause extensive oxidative degradation under the several conditions employed, the degradation is conveniently carried out with the fully methylated derivative of the parent flavone. In this case the separation of the *o*-hydroxyacetophenone and aromatic acid is very simple, as the latter can be selectively extracted from an ethereal solution of the degradation products with aqueous bicarbonate.

Partially methylated derivatives of polyhydroxyflavones are widely distributed in nature. As in this case alkaline degradation of the fully methylated derivatives gives only information about the oxygenation pattern of the molecule and does not reveal the original distribution of the methyl groups, the procedure is often carried out using the totally ethylated compounds. In this case, identification of the degradation products allows the unambiguous elucidation of the original structure, *e.g.* [2].

* Present address: Institute for Organic Chemical Technology, Technical University, Budapest



A serious disadvantage of the alkaline degradation is that, in the majority of cases, the only fragment that can be identified by preparative methods, is the aromatic acid. Polyalkoxyacetophenones are namely predominantly low-melting solids or liquids, requiring the use of a considerable quantity of the starting material to allow identification.

The analysis of aromatic carboxylic acids by gas-liquid chromatography (GLC) has been investigated by several authors, *e.g.* [3—6]; the problem of separation and identification (in the form of esters) can be considered a solved problem. This prompted us to investigate the separation and identification of the other products, the *o*-hydroxy-polymethoxyacetophenones.

In view of their physical properties, the suitability of this class of compounds to GLC-analysis could be anticipated. Further, the variability of the quality, number and position of the substituents on the acetophenone skeleton offered ample possibilities to examine intramolecular interactions and interactions between the substrate and the partition liquid.

Method and results

The compounds chosen first of all were those, which could possibly result from the degradation of natural flavones, *i.e.* 2'-(or 6'-)hydroxyacetophenones (**I—IV**) and 2'-(or 6'-)-hydroxy-2-methoxyacetophenones (**V—VIII**). This series has been completed by some of the fully methylated derivatives of these compounds (**IX—XI**).

The instrument used was a Carlo Erba Model P gaschromatograph, with a tungsten-filament heat conductivity detector. For the analysis packed stainless steel columns were used at 170° (evaporator 210°, detector 200°). The carrier gas was hydrogen. The characteristics of the individual columns were as follows:

Column (a): ⌀5×1000 mm, 20% Silicone Oil 550 on Chromosorb W (60—80 mesh). Inlet pressure 1.1 att., flow rate 540 ml/min.

Column (b): ⌀6×1000 mm, 8% Apiezon L on Chromosorb G (60—80 mesh). Inlet pressure 1.1 att., flow rate 736 ml/min.

Column (c): ⌀10×1000 mm, 8% Methyl Silicone Polymer SE 30 on Chromosorb G (60—80 mesh). Inlet pressure 0.6 att., flow rate 824 ml/min.

Column (d): ⌀5×1000 mm, 8% Epikote 728 on Chromosorb G (60—80 mesh). Inlet pressure 2 att., flow rate 1250 ml/min.

The liquid samples were injected without dilution, the solids in acetone solution. Retention data are summarized in Table I.

Table I

Retention times of acetophenones

Acetophenone		Column							
		(a) Silicone Oil 550		(b) Apiezon L		(c) Silicone Polymer SE 30		(d) Epikote 728	
		Retention data							
No.	Substitution	t'_R	r	t'_R	r	t'_R	r	t'_R	r
I	2'-OH-4'-OCH_3	1.59	0.274	1.35	0.327	1.35	0.334	2.95	0.282
II	6'-OH-2',3'-OCH_3	2.07	0.356	1.67	0.404	1.75	0.432	3.43	0.328
III	6'-OH-2',3',4'-OCH_3	5.82	1.00	4.15	1.00	4.07	1.00	10.45	1.00
IV	2'-OH-3',4',6'-OCH_3	9.56	1.64	6.45	1.56	6.45	1.58	26.2	2.50
V	2'-OH-2,4',6'-OCH_3	12.76	2.19	9.40	2.27	8.37	2.06	—	—
VI	6'-OH-2,2',3',4'-OCH_3	14.75	2.54	9.73	2.34	9.40	2.32	—	—
VII	2'-OH-2,3',4',6'-OCH_3	26.4	4.56	18.0	4.28	15.8	3.88	—	—
VIII	2'-OH-2,3',4',5',6'-OCH_3	17.5	3.00	10.70	2.58	11.80	2.90	—	—
IX	2',4'-OCH_3	4.70	0.810	3.82	0.924	3.43	0.844	9.74	0.932
X	2',3',4',6'-OCH_3	5.74	0.987	2.71	0.654	3.82	0.943	13.40	1.28
XI	2,2',3',4',6'-OCH_3	13.40	2.30	5.82	1.41	8.05	1.96	42.1	4.03

t'_R = retention time, min.
r = relative retention, based on the t'_R of compound **III.**

Discussion

The retention data recorded in the Table and those shown in Figs 1 and 2 clearly indicate that GLC provides an efficient and simple means to identify acetophenones that may be produced in the course of the alkaline degradation of fully methylated natural flavones.

Each of the eleven different compounds investigated could be readily separated on a column of appropriate composition. The best separation was achieved with Silicone Oil 550 on Chromosorb W *(a)*. Though Apiezon L *(b)*

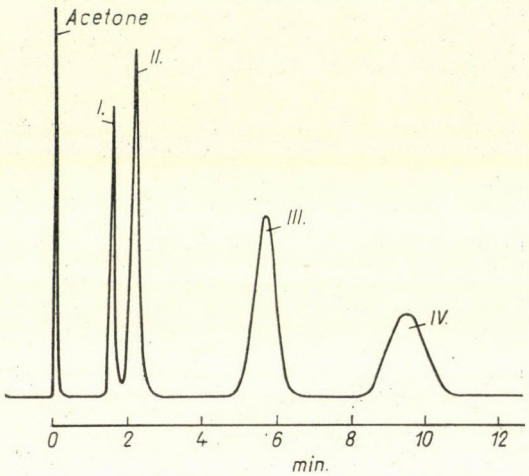


Fig. 1. Separation of 2'-(or 6'-)hydroxyacetophenones on a column of Silicone Oil 550/Chromosorb W

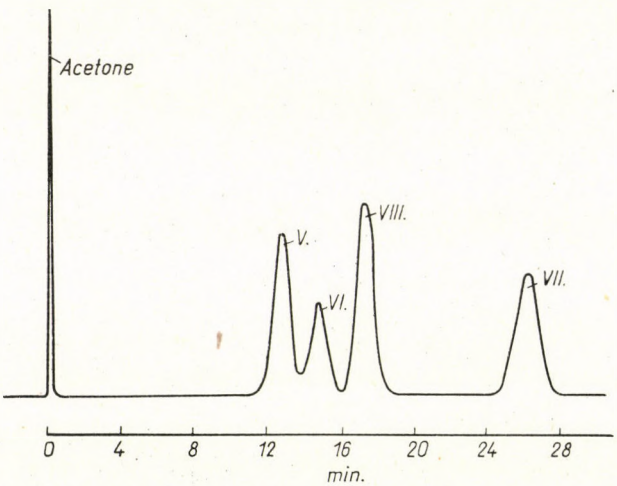


Fig. 2. Separation of 2'-(or 6'-)hydroxy-2-methoxyacetophenones on a column of Silicone Oil 550/Chromosorb W

or SE 30 *(c)* were slightly inferior, only one non-resolvable pair was found on either of them. Strong retention on Epikote 728 *(d)* prevented the ω-substituted acetophenones (**V**—**VIII**) to pass through the column.

Despite the relatively small number of the models analyzed, a comparison of the retention times indicates some interesting regularities.

A considerable increase in the retention time results if a methoxy group is introduced into position 3′ (*e.g.* **V** → **VII**). It may be assumed that chelation between the carbonyl and *o*-hydroxyl groups is disturbed by the steric repulsion of the adjacent methoxy group. The retention times are also notably increased by methoxy substitution in the side chain (**III** → **IV**, **IV** → **VII** and **X** → **XI**).

The correlations between the retention times are, however, far from being consistent, and the analysis of additional models is intended to clarify some of the contradictions. Investigations with ethoxylated compounds are in progress.

*

Thanks are due to the Hungarian Academy of Sciences for financial support, and to Prof. L. FARKAS for his interest in this work.

REFERENCES

1. VENKATARAMAN, K.: Methods for Determining the Structures of Flavonoid Compounds in GEISMANN, T.A., ed.: The Chemistry of Flavonoid Compounds, p. 83. Pergamon Press, Oxford, 1962
2. HENRICK, C.A., JEFFERIES, P.R.: Aust. J. Chem. **17**, 934 (1964)
3. WILLIAMS, C.N.: Anal. Biochem. **11**, 224 (1965)
4. WILLIAMS, C.N., SWEELEY, C.C., in SZYMANSKI, H.A.: Biomedical Application of Gas Chromatography, pp. 225—259. Plenum Press, New York, 1964
5. HEDIN, P.A., MINYARD, J.P. Jr., THOMPSON, A.C.: J. Chromatog. **30**, 43 (1967)
6. MENDEZ, J., STEVENSON, F.J.: J. Gas Chromatog. **4**, 483 (1966)

Sándor BÉKÁSSY; Budapest XI. Műegyetem rkp. 3.
Mihály NÓGRÁDI; Budapest XI. Gellért tér 4.

N. I. SHEVERDINA, K. A. KOCHESKOV: *Methods of Elemento-Organic Chemistry — Vol. 3 — The Organic Compounds of Zinc and Cadmium.* North-Holland, 1967, pp. 252

In an earlier issue of this journal the reviewer had already the opportunity to praise the first two volumes of this excellent series which is edited by A. N. NESMEYANOV and K. A. KOCHESKOV and published in English by North-Holland, to avoid repetitions, he will therefore not indulge here in statements and descriptions characteristic of the entire series. A single feature may nevertheless be pointed out again, namely — as apparent from its title — the series is primarily concerned with methodical-synthetic problems, and in its compilation other aspects, as *e.g.* the structure and physical chemistry of compounds, though mentioned, were therefore considered of secondary importance only.

Zinc organic chemistry has a long history; its origin goes back to 1849 when the Englishman FRANKLAND published his first dialkyl zinc synthesis, nevertheless within metallo-organic chemistry zinc organic chemistry is perhaps the most "Russian" of all. In this respect it may be enough to mention BUTLEROV, ZAITSEV and VAGNER who were the first to apply extensively zinc organic syntheses, or REFORMATSKII who inscribed his name on the pages of organic chemistry by the zinc organic reaction which still bears his name. In the solution of their task the authors were aware of the general — for them, however, quite specific importance of their subject. In this respect it should be mentioned — as stressed also by the authors — that this is the first independent monograph on the two groups of compounds. The book will convince the reader that this field of organic chemistry has been neglected for a long time without good reason, and this disregard may perhaps be explained sooner with the success of the magnesium organic reactions, that is of the Gridnard syntheses, than with the nature of the zinc and cadmium organic compounds. The authors very aptly compare in every chapter of the zinc and cadmium organic chemistry the same with the organic chemistry of magnesium, and this comparison reveals more than once the practical advantages of the first two. In this way the expediency of zinc organic reagents is pointed out in the synthesis of secondary and tertiary alcohols, of compounds with quaternary carbon atoms, of ketones, ketoesters, organic hydroperoxides, etc. It may perhaps be sufficient to mention the fact that contrary to the Gridnard reaction, the zinc organic reaction stops at the ketone.

Some quite up-to-date aspects of the chemistry of zinc organic compounds are also included in the discussion, such as the complexes which are important polymerization catalysts of the bimetallo-organic compounds with alkali metals whose theoretical importance is now on the increase. The volume includes the most important pretaining results of structure chemistry.

It should be mentioned further that the authors deal in a special section of three chapters, over 28 pages with the REFORMATSKII synthesis in its broader sense and this section is highly important not only from the aspect of metallo-organic chemistry, but also from that of entire organic chemistry.

The 149 pages devoted to zinc organic chemistry offer a good survey of the syntheses of compounds and of their reagent solutions including the characteristic reactions of each group of compounds.

The six chapters dealing with the chemistry of cadmium organic compounds are by nature somewhat overshadowed by the chemistry of the zinc compounds, as substantially less data are available on the first than on the second. Nevertheless, the authors succeeded in presenting a good survey of the advantageous properties of these compounds from the aspect of the research chemist, and I believe that we may agree with their statement concerning the future of cadmium organic syntheses, as the cadmium organic solutions are easy to handle with and to prepare, the cadmium salts resist hydrolysis and their protection against moisture is

therefore easier. Contrary to the Grignard reagent cadmium organic reagents in general do not react with the carbonyl group, but react with acid chlorides, so that ketones and diketones are formed in a satisfactory yield by a selective relation; the ketones and diketones do not enter into further reactions and neither do they undergo condensation. Characteristically neither alkoxy substitution nor chlorination on the α-carbon atom will alter the reactivity of the acid chlorides.

In this volume many allusions may be found to problems yet hardly answered in fields where there is still much to do, such as *e.g.* the reactions between cadmium organic compounds and nitrogen containing molecules. These references also indicate that many new results and serious development are to be expected — may be in the near future — in the field of cadmium organic chemistry both from the preparative and theoretical aspect.

This volume sums up over 252 pages original publications on zinc organic chemistry (433 papers), on the REFORMATSKII reaction (417 papers) and on cadmium organic compounds (285 papers).

Editing and presentation of the book are of the same high standard as those of the preceding volumes.

T. SZÉKELY

Standardmethoden der Praktischen Chemie. Hauptgruppe: *Präparative Methoden der Organischen Chemie.* Lieferung 6: Grundverbindungen, III. Bearbeitet von Jürgen GÖMANN, Dieter HOPPE und Ernst POULSEN NAUTRUP. Friedr. Vieweg & Sohn GmbH, Braunschweig, 1968.

Nach einer ziemlich langen Pause ist nun die Lieferung 6 der Präparativen Methoden von POULSEN NAUTRUP — es ist dies die achte der geplanten insgesamt 14 Lieferungen — erschienen*.

Über die Zielsetzung und die Anlage des Werkes wurde bereits in der Besprechung der als erste erschienenen Lieferung 2 berichtet, wobei auch betont wurde, daß nach Meinung des Rezensenten die diesbezüglichen Gedanken des Herausgebers (E.P.N.) durchaus zu begrüßen sind. Um eine Wiederholung zu vermeiden, seien hier daher lediglich die in der vorliegenden Lieferung behandelten Verbindungsklassen aufgezählt: Chloralkane, Aromatische Jod- und Bromverbindungen, Phenole, Ketone (aus β-Ketoestern), Aldehyde und Ketone (aus Acetalen bzw. Ketalen), Aldehydacetale, Aromatische Aminosulfonsäuren, Hydroxyazoverbindungen.

Eine bedeutende Schwierigkeit bei der (wenn nicht Hindernis für die) Benutzung der »Präparativen Methoden« ergibt sich daraus, daß das Werk noch immer nicht komplett ist, obwohl die erste Lieferung bereits 1963 vorlag. Die einzelnen Lieferungen folgen einander in immer größeren Abständen; so ist zwischen dem Erscheinen der vorletzten und der letzten Lieferung mehr als ein Jahr vergangen, obwohl ursprünglich eine Frist von 2 Monaten zwischen dem Erscheinen zweier Lieferungen vorgesehen wurde.

Wenn alsbald nicht dafür gesorgt wird, daß die einzelnen Lieferungen rascher aufeinander folgen, kann es leicht vorkommen, daß zur Zeit des Erscheinens der letzten Lieferungen die ersten durch die stürmische Entwicklung der neuen präparativen Methoden bereits größtenteils überholt sein werden.

K. LEMPERT

K. BURGER: *Modern Experimental Methods in Coordination Chemistry* Akadémiai Kiadó, Budapest, 1967 pp. 287.

Kálmán BURGER's "Modern experimental methods in coordination chemistry" is a valuable contribution to the Hungarian chemical literature. In recent years research work on coordination chemistry has been taken up in several institutions in Hungary. BURGER's

* Besprechungen der früheren Lieferungen s. Acta Chim. Acad. Sci. Hung. **40**, 475, 476 (1964); **43**, 445 (1965); **44**, 459 (1965), **51**, 436 (1967).

book is intended primarily for those specialized in this field, however, it is a valuable help and an important source of information to research work in various fields of inorganic, organic and physical chemistry.

In this book, the author does not deal with all the testing methods known at present, but selecting those of greatest importance, outlines for each the theoretical fundamentals, then discusses them on numerous examples together with the experimental techniques.

The book is divided into ten chapters. In the introduction, some basic concepts of complex chemistry are elucidated, and a short description is given of the methods to be discussed. The second chapter deals with the electron excitation spectra of complexes, and discusses within this connection the electrostatic crystal field and ligand field theories, and the molecular orbital method. As compared to its importance, this chapter is brief, and illustrated by relatively few examples. Contrary to the other chapters, a short description experimental techniques is missing. The next chapter, on the infrared and Raman spectra of complexes, is the best part of the book, furnishing a wide range of information. The vibrational spectra of the bonds which occur most frequently in coordination chemistry, are discussed in detail, and presented to the reader in a very logical concept, illustrated by a number of examples. A part of this chapter (Subchapter 3.5) reporting about infrared spectrophotometric studies on some problems of coordination chemistry, is of particular interest. The next chapter of the book, the Mössbauer spectra of complexes, is one of the author's principal fields of research. It is, therefore, understandable and even natural that more emphasis is laid upon this chapter, and the subject is discussed more fully than would be otherwise justified in a book of such dimensions. In the reviewer's opinion this is not a disadvantage: this chapter may be regarded as an independent monograph, in which all results, important from the chemical point of view are discussed, such as problems pertinent to spinel oxides and iron-containing silicate minerals, the inclusion of which in coordination chemistry would seem otherwise rather forced. Indeed, this chapter is the first monograph in this field compiled from the aspect of coordination chemistry.

The fifth chapter describes the magnetic properties of complexes. Here the theoretical part, the survey of applications in coordination chemistry and description of experimental techniques are very well balanced. The same holds true for the next chapter, dealing with the applications of NMR spectroscopy in complex chemistry. The seventh chapter gives a short summary on the use of ESR and nuclear quadrupole resonance spectroscopical methods in coordination chemistry.

The eight chapter deals with X-ray diffraction studies, a field rather neglected by Hungarian coordination chemists. In this chapters, very laudably, the author discusses in detail both theoretical principles and experimental methods. What is only missing is the presentation of examples for X-ray diffraction structural investigations in solutions.

In the ninth chapter, the measuring techniques and the complex-chemical importance of two more rarely used, nevertheless important methods, optical rotation and circular dichroism, are described.

In the last chapter the author present his own research methods to the reader, and shows how different techniques may complement each other. This is a very though-provoking part of the book.

A detailed list of references completes each chapter. This bibliography includes literature up to the end of 1966.

It may be considered a minor fault of the book that the author does not always use the IUPAC nomenclature for the naming of complexes (*e.g.* "silver(I) dicyanide" and "platinum(II) dithiooxalate" instead of dicyano argentate(I) and dithiooxalato platinate(II), respectively). Furthermore, the mode of presentation of the spectra in the infrared chapter is not consistent, and some of the infrared spectra in this chapter afford little information (3.23—3.26).

The tables and figures facilitate better understanding of the topics discussed. The attractive presentation of the book does credit to the publisher.

E. KŐRÖS

INDEX

INORGANIC AND ANALYTICAL CHEMISTRY – ANORGANISCHE UND ANALYTISCHE CHEMIE – НЕОРГАНИЧЕСКАЯ И АНАЛИТИЧЕСКАЯ ХИМИЯ

MÜLLER, L.: The Adsorption of Uranium Hexafluoride, III 277

HENZE, G., GEYER, R. und HOLZBAUER, R.: Coulometrische Kobalttitration (Cobalt Titration by Coulometry) 297

TÖRÖK, F. and HUN, B. GY.: On the Parameter Form of Force Constant Matrix, VIII. Calculation of all Mean Amplitudes of Vibration Compatible with the Normal Frequencies 303

GERGELY, A.: Equilibria of α-Amino Acid Complexes of Transition Metal Ions, I. Complexes of Glycine 309

WESER, A. und PUNGOR, E.: Die Eignung von Perowskitphasen als Redoxindikatorelektroden. (On the Use of Perowskite Phases as Redox Indicator Electrodes) (Kurzmitteilung) 319

PHYSICAL CHEMISTRY – PHYSIKALISCHE CHEMIE – ФИЗИЧЕСКАЯ ХИМИЯ

KELEN, T. und TÜDŐS, F.: Kinetische Analyse einiger Folgereaktionen. III. Das konkurrente Folgereaktionssystem $A + A \rightarrow C$, $A + C \rightarrow E$. (Kinetical Discussion of a Few Consecutive Reactions, III. The Concurrent Consecutive Reaction System $A + A \rightarrow C$, $A + C \rightarrow E$) 323

HARGITTAI I.: Study of the Molecular Structure of Thionyl Chloride by the Electron Diffraction Sector Microphotometer Method 351

NAGY, F., SZABÓ, S. and TELCS, I.: Palladized Pd-Wire as a Hydrogenation Catalyst, I. Rate and Mechanism of Hydrogen Transport 359

ORGANIC CHEMISTRY – ORGANISCHE CHEMIE – ОРГАНИЧЕСКАЯ ХИМИЯ

BOGNÁR, R. and MAKLEIT, S.: Conversions of Tosyl and Mesyl Derivatives of the Morphine Group, III. Preparation of Azido- and Aminocodides 373

BOGNÁR, R., MAKLEIT, S. and MILE, T.: Conversions of Tosyl and Mesyl Derivatives of the Morphine Group, IV. Preparation of Azido- and Amidomorphides 379

MAKLEIT, S. and BOGNÁR, R.: Conversions of Tosyl and Mesyl Derivatives of the Morphine Group, V. A New Method for the Preparation of Isocodeine and Dihydroisocodeine (Short Communication) 387

MARKÓ, L.: Sulphur-containing Metal Carbonyls, X. Reactions of Cobalt Carbonyls with Aliphatic Thioethers and the Influence of Thioethers on the Catalytic Activity of Cobalt Carbonyls 389

ALKONYI, I. und SÁNDOR, A.: Darstellung und Eigenschaften von δ-Oxogeraniumsäure. (The Preparation and Properties of δ-ketogeranic Acid) 397

CSŰRÖS, Z., DEÁK, GY., FENICHEL, L. and TÖRÖK-KALMÁR, A.: Nitration in the Presence of Boron Fluoride Catalyst 401

ENGLER, J., BÁNFI, D. and HAJÓS, A.: Phenylethanolamine Derivatives, I. ^{14}C-Labelling of 1-(*m*-Aminophenyl)-2-Cyclopropyl-Aminoethanol Dihydrochloride, a Monoaminooxidase Blocking Agent 411

VIZI-OROSZ, A., BÓR, G. and MARKÓ, L.: Preparation of Lead Cobalt Carbonyl and its Triphenylphosphine Derivative (Preliminary Note) 417

FARKAS, I., SZABÓ, I. F. und BOGNÁR, R.: Abbau und Reaktionen von Onsäureaziden, II. Ausdehnung der Curtius-Reaktion auf das Octaacetyl-Cellobionsäureazid. (Decomposition and Reactions of Onic Acid Azides, II. Extension of the Curtius Reaction to Octaacetylcellobionic Acid Azide) 419

BÉKÁSSY, S. and NÓGRÁDI, M.: Application of Gas-Liquid Chromatography to the Structural Elucidation of Natural Flavones 425

Book Reviews — Buchbesprechungen — Рецензии книг 431

Preliminary Announcement:

RADIOCHEMICAL AND RADIOANALYTICAL LETTERS

A **New** International Journal
Distributed to Subscribers by **Airmail**
Delay Between Receipt and Publication of Contributions Reduced to **Eight Weeks**

Subject Coverage: Radiation Detection and Measurement - Radiochemical and Radioanalytical Techniques - Radionuclide Production - Separation Techniques - Syntheses of Labelled Compounds - Nuclear Chemistry - Chemistry of Radioactive Elements - Radio-Tracer and Radiation Chemistry - Activation Analysis - Analysis by Radiation Absorption and Backscattering - Isotope Dilution Analysis - Radioreagent Analysis and Radiometric Titration - Instruments, Equipment and Controls

Editors: Dr. J. Tölgyessy, Bratislava and Dr. T. Braun, Budapest

Publishers: Elsevier Sequoia S. A., Lausanne and Akadémiai Kiadó, Budapest

Subscription rates: Vols 1 & 2, 1969 (400 pages in 6 to 9 issues per volume): Swiss Francs 215. — (approx. US $ 50.00 or £ 21.10.0), including airmail postage.

For further information and sample copies please apply to:

Elsevier Sequoia S.A.
P.O. Box 851
1001 Lausanne 1, Switzerland

Printed in Hungary

A kiadásért felel az Akadémiai Kiadó igazgatója — Műszaki szerkesztő: Farkas Sándor

A kézirat nyomdába érkezett: 1968. XI. 29. — Terjedelem: 14,25 (A/5) ív, 56 ábra

68.66718 Akadémiai Nyomda, Budapest — Felelős vezető: Bernát György

ACTA CHIMICA

ТОМ 59 — ВЫП. 3—4

РЕЗЮМЕ

Изучение адсорбции шестифтористого урана, III

Л. МЮЛЛЕР

Целью стационарных диффузионных исследований было селективное определение процессов массовой диффузии и молекулярного разделения в системах UF_6-адсорбент. Диффузионные процессы без конвекции интерпретируются на основе использования модели Смис—Вакао, в которой уравнение транспорта выводится для случая пары адсорбируемого и инертного, с точки зрения поглощения, газов. Приводится описание опытной установки. Доказывается справедливость уравнений диффузии и определяется зависимость между экспериментальными параметрами и отношением массовых потоков UF_6 в процессах молекулярного разделения и массовой диффузии на столбцах, заполненных различными адсорбентами.

Кулометрическое титрование кобальта

Г. ХЕНЗЕ, Р. ГЕЙЕР и Р. ХОЛЦБАУЭР

В работе описывается прибор для кулометрического титрования. Способ намного упрощен с помощью устройства записывающего автоматически зависимость силы тока от времени. Кулометрическое титрование кобальта(II) возможно с помощью электролитически приготовленного гекса-цианоферрата(III). Избыток никеля и следы железа не оказывают влияния на данный метод.

Параметрическое определение F-матрицы силовых постоянных, VIII

Определение всех возможных средних амплитуд колебаний в соответствии с нормальными частотами

Ф. ТЁРЁК и ДЬ. Б. ХУН

На основе метода параметрического определения силовых постоянных, была разработана программа для счетной машины, позволяющая рассчитывать все серии средних амплитуд, которые согласуются с измеренными нормальными частотами молекулы. Параметрический метод позволяет также построение тех F-матриц, которые правильно отражают, как измеренные частоты, так и измеренные средние амплитуды колебаний. С помощью данного метода могут быть определены частные производные средних амплитуд колебаний по силовым постоянным, что и, в свою очередь, позволяет удобно оценить в данных случаях чувствительность величин силовых постоянных к изменениям средних амплитуд колебаний.

Условия равновесия в комплексах переходных металлов с α-аминокислотами, I

Комплексы глицина

А. ГЕРГЕЙ

Были определены константы стабильности комплексов ионов переходных металлов (с электронной структурой d^5 — d^{10}) с глицином при ионной силе 0,1 и при температуре 25° С. Константы стабильности, приводимые в литературе обсуждались критически. Было установлено, что в случае точного измерения и хорошего метода расчета, константы стабильности, измеренные различными авторами, совпадают в пределах 0,1 log K. В обратном случае расхождение последовательных констант может достигать 0,4 — 0,5 log K от точных значений.

Кинетический анализ некоторых последовательных реакций, III

Система конкурирующих последовательных реакций: $A + A \rightarrow C$, $A + C \rightarrow E$

Т. КЕЛЕН

Производился кинетический анализ системы конкурирующих последовательных реакций $A + A \rightarrow C$, $A + C \rightarrow E$. Приводятся точные решения для соответствующей системы дифференциальных уравнений и все возможные значения для отношения констант. Подробно обсуждаются и приводятся в диаграммах зависимости концентраций веществ, принимающих участие в реакции, друг от друга и от времени.

Электронографическое сектор-микрофотометрическое исследование строения молекулы $SOCl_2$

И. ХАРГИТТАИ

Электронографическим сектор-микрофотометрическим методом было исследовано строение молекулы $SOCl_2$. Следующие длины связи и валентные углы были получены с помощью метода наименьших квадратов: r(S—O) 1,444 ± 0,007 Å, r (S — Cl) 2,076 ± ± 0,006 Å, OSCl 107,3 ± 0,6° и ClSCl 96,2 ± 1,0°. Сопоставляя результаты исследования строения молекулы $SOCl_2$ и SO_2Cl_2 с другими данными можно делать следующие выводы: 1) Связи четырёхвалентного атома серы являются длиннее чем соответствующие связи шестивалентного атома серы. 2) Связи S — O удлиняются если атомы хлора заменяются на CH_3 или $(CH_3)_2N$ группы.

Палладированная Pd-проволока как катализатор гидрирования, I

Ф. НАДЬ, Ш. САБО и И. ТЕЛЧ

На основе исследований скорости извлечения водорода из Pd-проволоки, насыщенной водородом, было установлено:

1. Между относительным сопротивлением проволоки (R/R_0) и содержанием водорода, в интервале $0{,}08 \leq H/Pd \leq 0{,}45$, наблюдается однозначная линейная зависимость.

2. В случае гладкой проволоки скорость извлечения водорода приблизительно может быть описана следующим уравнением (t = 20 — 25° C):

$$W_M \equiv \frac{d(H/Pd)}{d\tau} \approx \frac{d(\Delta R/R_0)}{d\tau} \approx \frac{3{,}9 \cdot 10^{-5}}{d^2}\,(H/Pd) \approx \frac{3{,}9 \cdot 10^{-5}}{d^2}\,(\Delta R/R_0)\ \mathrm{min}^{-1}$$

где d — диаметр проволоки в см-ах.

Отщепление азидов оновых кислот и их реакции, II.

Распространение реакции Курциуса на азид октаацетил-целлобиновой кислоты

И. ФАРКАШ, Ф. И. САБО и Р. БОГНАР

Азид октаацетил-целлобионовой кислоты под действием уксусного ангидрида превращается в аморфный, но однородный N-[D-*глюко*-1,2,3,5-тетраацетокси-4-(тетраацетил-β-D-глюкопиранозил)пентил]-ацетамид (1). Структура соединения 1 была доказана следующими реакциями: после омыления метилатом натрия с помощью 1 н. серной кислоты вещество гидролизуется в глюкозу и арабинозу, а при обработке концентрированной гидроокисью аммония образуется 3-β-D-глюкопиранозил-D-арабиноза-бисацетамид с выходом 51%. Поэтому отщепление по Курциусу кажется значительно более удобным по сравнению с реакцией Вола.

Метод газовой хроматографии для определения строения природных флавонов

Ш. БЕКАШИ и М. НОГРАДИ

Орто-гидрокси-полиметокси-ацетофеноны, образующиеся в результате щелочного расщепления полностью метилированных флавонов, легко разделяются и идентифицируются с помощью метода газовой хроматографии. На 4 различных набив как изучалось поведение 11 производных ацетофенона; наилучшее разделение было получено на столбце, содержащем силиконовое масло—550.

3. В случае палладированной Pd-проволоки в кислом водном растворе изменение отношения $\Delta R/R_0$ во времени может быть использовано для определения скорости реакции (W) лишь, если $W_M \geq 10W$.

4. В случае растворов, содержащих капиллярноактивные вещества, в противоположность случаю палладированной Pd-проволоки в кислых водных растворах, необходимо принять в расчет и скорость транспорта водорода между проволокой и частицами палладиевой черны на поверхности (W_5). Согласно этому, изменение $\Delta R/R_0$ во времени можно использовать для определения скорости реакции лишь в том случае, если W_M, $W_5 \geq 10W$.

Реакции тозилокси- и мезилокси-производных в серии морфина, III

Получение азидо- и амино-кодидов

Р. БОГНАР и Ш. МАКЛЕЙТ

Метод замещения спиртовой гидроксильной группы на аминогруппу с помощью обмена тозилата (или мезилата) — через азид на амин— применяемый в различных областях химии, был использован для случая морфиновых алкалоидов. Этот метод позволяет изучение стереохимических проблем в серии морфина и превращений его производных, содержащих свободную аминогруппу. Были получены 8-аминокодид и новое соединение — 6-аминодигидрокодид. 6-Тозил- и 6-мезилпроизводные кодеина и дигидрокодеина были приготовлены за счет взаимодействия кодеина и дигидрокодеина с хлористыми тозилом и мезилом. При азидолизе этих соединений образуются 6-дезокси-8-азидокодеин и 6-дезокси-6-азидо-дигидрокодеин. Взаимодействие азидной группы с литий-алюмогидридом приводит к образованию 6-дезокси-8-амино-кодеина и 6-дезокси-6-аминодигидрокодеина. Полученные соединения — за исключением 6-тозил-кодеина и 8-аминокодида — не описаны в литературе.

Обсуждается строение и стереохимия полученных соединений и интерпретируются их формулы.

Реакции тозилокси- и мезилокси-производных в морфиновой серии, IV

Получение азидо- и амино-морфинов

Р. БОГНАР, Ш. МАКЛЕЙТ и Т. МИЛЕ

Неизвестные до сих пор соединения — 8-аминоморфид и 6-аминодигидроморфид были получены серией реакций обмена: спиртовый гидроксил — тозил (или мезил) — азид — амин. При обработке 3-ацетилпроизводных морфина и дигидроморфина хлористыми тозилом или мезилом были получены 3-ацетил-6-тозил- или -мезил-производные морфина и дигидроморфина. Азидолизом этих соединений могут быть получены 6-дезокси--8-азидо-морфин и 6-дезокси-6-азидо-дигидроморфин; после ацетилирования фенольной гидроксильной группы в результате их восстановления литий-алюминийгидридом, были получены 6-дезокси-8-амино-морфин и 6-дезокси-6-амино-дигидроморфин. Описанные соединения — за исключением 3-ацетил-морфина — до сих пор еще не были известны.

Обсуждается строение и стереохимия этих соединений и интерпретируются приводимые формулы.

Предлагается новая номенклатура для производных морфина, замещенных на углероде кольца.

Серосодержащие карбонилы металлов, X

Взаимодействие карбонилов кобальта с алифатическими тиоэфирами и влияние тиоэфиров на каталитическую активность карбонилов кобальта

Л. МАРКО

При обратимом взаимодействии тиоэфиров с $Co_2(CO)_8$ или с $Co_4(CO)_{12}$ образуются нестабильные монозамещенные производные. Образование этих комплексов в небольшой степени уменьшает каталитическую активность карбонилов кобальта в гидрировании альдегидов и в гидроформировании.

Получение и свойства δ-оксо-гераниевой кислоты

И. АЛКОНИ и А. ШАНДОР

Ранее описанный авторами метод использовался для синтеза этилового эфира δ-оксо-гераниевой кислоты. Ацилирование на крайней метиловой группе этилового эфира диметил-акриловой кислоты в условиях реакции Фриделя—Крафца, с помощью хлорида собственной кислоты приводит к образованию соединения монотерпенового типа, содержащего 10 углеродных атомов. Эфир упомянутой в заглавии кислоты и сама свободная кислота были идентифицированы на основе их спектральных свойств, а также получением их различных производных.

Нитрование, катализированное трехфтористым бором

З. ЧЮРЁШ, ДЬ. ДЕАК, Л. ФЕНИХЕЛ и А. ТЁРЁК-КАЛМАР

Изучалось влияние трехфтористого бора и его комплексов с составом $BF_3 \cdot H_2O$, $BF_3 \cdot 2H_2O$ и $BF_3(CH_3COOH)_2$ на реакцию взаимодействия *о*-нитро-толуола с дымящей азотной кислотой, и было установлено, что эти соединения катализируют и благоприятствуют полному завершению реакции мононитрования. Проводились исследования для изучения зависимости выхода продуктов от концентрации трехфтористого бора и его комплексов, а также от времени реакции.

Проводились кинетические исследования реакции нитрования толуола азотной кислотой, в безводной уксусной кислоте и в присутствии трехфтористого бора. Было установлено, что скорость реакции возрастает пропорционально, как увеличению концентрации толуола, так и увеличению концентрации трехфтористого бора. Это доказывает каталитическое влияние трехфтористого бора в реакции нитрования, а также подтверждает механизм реакции, протекающей через ион нитрования.

Изучение производных фенилэтаноламина, I

Мечение 1-(м-аминофенил)-2-циклопропил-аминоэтанол-дигидрохлорида, препарат для блокирования моноаминооксидазы изотопом C^{14}

Й. ЭНГЛЕР, Д. БАНФИ и А. ХАЙОШ

Как для целей радиоактивной индикации и фармакологических исследований, так и для изучения механизма действия был приготовлен препарат сильно блокирующий моноаминооксидазу-1-(м-аминофенил)-2-циклопропил-аминоэтанол-дигидрохлорид, меченный изотопом C^{14}. Исходным веществом для синтеза был $BaC^{14}O_3$, синтез состоял из 9 ступеней, и был достигнут почти 10%-ный радиохимический выход. Продукт гомогенен, как с химической, так и с радиохимической точек зрения, и обладает высокой удельной активностью.

The Acta Chimica publish papers on chemistry, in English, German, French and Russian.

The Acta Chimica appear in volumes consisting of four parts of varying size, 4 volumes being published a year.

Manuscripts should be addressed to

Acta Chimica
Budapest 112/91 Műegyetem

Correspondence with the editors should be sent to the same address.

The rate of subscription is 165 forints a volume. Orders may be placed with "*Kultúra*" Foreign Trade Company for Books and Newspapers (Budapest I., Fő utca 32. Account No. 43-790-057-181) or with representatives abroad.

Les Acta Chimica paraissent en français, allemand, anglais et russe et publient des mémoires du domaine des sciences chimiques.

Les Acta Chimica sont publiés sous forme de fascicules. Quatre fascicules seront réunis en un volume (4 volumes par an).

On est prié d'envoyer les manuscrits destinés à la rédaction à l'adresse suivante:

Acta Chimica
Budapest 112/91 Műegyetem

Toute correspondance doit être envoyée à cette même adresse.

Le prix de l'abonnement est de 165 forints par volume.

On peut s'abonner à l'Entreprise pour le Commerce Extérieur de Livres et Journaux «*Kultúra*» (Budapest I., Fő utca 32. Compte-courant No. 43-790-057-181) ou à l'étranger chez tous les représentants ou dépositaires.

«*Acta Chimica*» издают трактаты из области химической науки на русском, французском, английском и немецком языках.

«*Acta Chimica*» выходят отдельными выпусками разного объема. 4 выпуска составляют один том. 4 тома публикуются в год.

Предназначенные для публикации рукописи следует направлять по адресу:

Acta Chimica
Budapest 112/91 Műegyetem

По этому же адресу направлять всякую корреспонденцию для редакции.

Подписная цена «*Acta Chimica*» — 165 форинтов за том. Заказы принимает предприятие по внешней торговле книг и газет «*Kultúra*» (Budapest I., Fő utca 32. Текущий счет № 43-790-057-181) или его заграничные представительства и уполномоченные.

64,— Ft

Reviews of the Hungarian Academy of Sciences are obtainable at the following addresses:

ALBANIA
Ndermarja Shtetnore e Botimeve
Tirana

AUSTRALIA
A. Keesing
Box 4886, GPO
Sydney

AUSTRIA
Globus Buchvertrieb
Salzgries 16
Wien I

BELGIUM
Office International de Librairie
30, Avenue Marnix
Bruxelles 5
Du Monde Entier
5, Place St. Jean
Bruxelles

BULGARIA
Raznoiznos
1, Tzar Assen
Sofia

CANADA
Pannonia Books
2, Spadina Road
Toronto 4, Ont.

CHINA
Waiwen Shudian
Peking
P. O. B. 88

CZECHOSLOVAKIA
Artia
Ve Směčkách 30
Praha 2
Poštovná Novinová Služba
Dovoz tisku
Vinohradská 46
Praha 2
Mad'arská Kultura
Václavské nám. 2
Praha I
Poštová Novinová Služba
Dovoz tlače
Leningradská 14
Bratislava

DENMARK
Ejnar Munksgaard
Nörregade 6
Copenhagen

FINLAND
Akateeminen Kirjakauppa
Keskuskatu 2
Helsinki

FRANCE
Office International de Documentation et Librairie
48, rue Gay Lussac
Paris 5

GERMAN DEMOCRATIC REPUBLIC
Deutscher Buch-Export und Import
Leninstraße 16
Leipzig 701
Zeitungsvertriebsamt
Fruchtstraße 3—4
1004 Berlin

GERMAN FEDERAL REPUBLIC
Kunst und Wissen
Erich Bieber
Postfach 46
7 Stuttgart S.

GREAT BRITAIN
Collet's Holdings Ltd.
Dennington Estate
London Rd.
Wellingborough. Northants.
Robert Maxwell and Co. Ltd.
Waynflete Bldg. The Plain
Oxford

HOLLAND
Swetz and Zeitlinger
Keizersgracht 471—487
Amsterdam C.
Martinus Nijhof
Lange Voorhout 9
The Hague

INDIA
Current Technical Literature
Co. Private Ltd.
India House OPP
GPO Post Box 1374
Bombay I

ITALY
Santo Vanasla
Via M. Macchi 71
Milano
Libreria Commissionaria Sansoni
Via La Marmora 45
Firenze

JAPAN
Nauka Ltd.
92, Ikebukur O-Higashi 1-chome
Toshima-ku
Tokyo
Maruzen and Co. Ltd.
P.O. Box 605
Tokyo-Central
Far Eastern Booksellers
Kanda P. O. Box 72
Tokyo

KOREA
Chulpanmul
Phenjan

NORWAY
Johan Grundt Tanum
Karl Johansgatan 43
Oslo

POLAND
RUCH
ul. Wronia 23
Warszawa

ROUMANIA
Cartimex
Str. Aristide Briand 14—18
Bucureşti

SOVIET UNION
Mezhdunarodnaya Kniga
Moscow G—200

SWEDEN
Almquist and Wiksell
Gamla Brogatan 26
Stockholm

USA
Stechert Hafner Inc.
31, East 10th Street
New York, N. Y. 10003
Walter J. Johnson
111, Fifth Avenue
New York, N. Y. 10003

VIETNAM
Xunhasaba
19, Tran Quoc Toan
Hanoi

YUGOSLAVIA
Forum
Vojvode Mišića broj 1
Novi Sad
Jugoslovenska Knjiga
Terazije 27
Beograd

8. V. 1969

Index: 26.007